Determining the Enantioselectivity of Chiral Catalysts – Mass Spectrometry as a Mechanistic and Screening Tool

Inauguraldissertation

zur

Erlangung der Würde eines Doktors der Philosophie

vorgelegt der
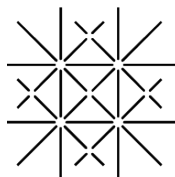
Philosophisch-Naturwissenschaftlichen Fakultät

der Universität Basel

von

Florian Bächle

aus Bad Säckingen, Deutschland

Basel, 2014

UNI
BASEL

Genehmigt von der Philosophisch-Naturwissenschaftlichen Fakultät
auf Antrag von

Prof. Dr. Andreas Pfaltz
Prof. Dr. Dennis Gillingham

Basel, den 20.05.2014

Prof. Dr. Jörg Schibler
Dekan

für Anja

"Our greatest glory is not in never failing,
but in raising up every time we fail."

Ralph Waldo Emerson

This thesis was supervised by Prof. Dr. Andreas Pfaltz from April 2010 to May 2014 at the University of Basel, Department of Chemistry.

Parts of this work have been previously published:

"*Organocatalytic Asymmetric Conjugate Addition of Aldehydes to Nitroolefins: Identification of Catalytic Intermediates and the Stereoselectivity-Determining Step by ESI-MS*"
F. Bächle, J. Duschmalé, C. Ebner, A. Pfaltz, H. Wennemers, *Angew. Chem. Int. Ed.* **2013**, *52*, 12619-12623.

Acknowledgement

Ich möchte mich bei meiner ganzen Familie und allen meinen Freunden bedanken. Ganz besonders möchte ich mich bei meiner Oma, meiner Mutter und meinem Vater bedanken die immer für mich da waren und mich in allen Lebensbereichen so unglaublich unterstützt haben und mich zu der Person gemacht haben die ich heute bin. Ohne euch wäre all dies nicht möglich gewesen.

Zu guter Letzt möchte ich mich bei der wichtigsten Person in meinem Leben bedanken. Danke Schatz für deine Liebe, deine Geduld, dein Rückhalt und deine uneigennützige Unterstützung über all die Jahre.

TABLE OF CONTENTS

I

IV

CHAPTER 1

INTRODUCTION

1.1 Mass Spectrometry & High-Throughput Screening in Asymmetric Catalysis

Asymmetric catalysis is an important tool to selectively create new stereogenic centers starting from prochiral molecules.[1] However, the identification of effective, highly selective catalysts is often a costly, time intensive and material demanding process. Each new catalyst, even with small structural modifications, and every optimization of the reaction parameters (solvents, temperatures, additives) usually needs to be applied repeatedly to a benchmark reaction. This complex optimization process is illustrated in Figure 1 and is associated with multiple reaction set-up, long reaction times, product purification steps and product analyses to determine the enantioselectivity.
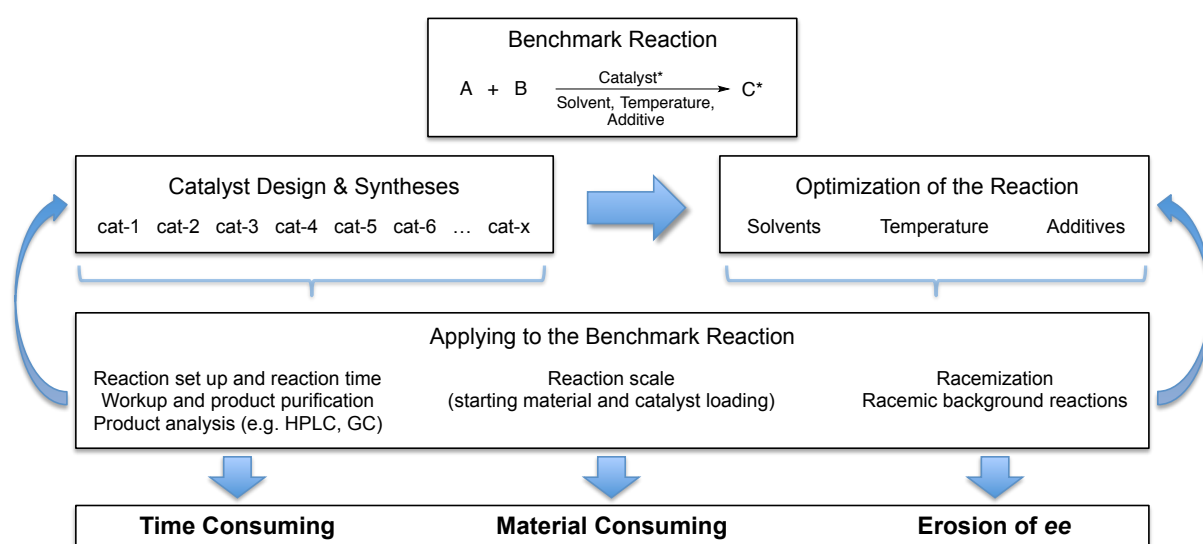
Figure 1: Typical screening process of chiral catalysts for an asymmetric reaction.

With the introduction of combinatorial methods and automated systems in modern synthesis,[2] the development of new high-throughput screening methods has received increased attention in recent years, as they accelerate the process of product analysis, which usually remains the bottleneck of high-throughput catalyst screenings.[3] Routinely, determination of the enantioselectivity relies on chromatographic methods such as high performance liquid chromatography (HPLC) or gas chromatography (GC) analysis with a chiral stationary phase. However, common drawbacks of these analytical methods are time consuming identification of suitable separation conditions and the associated elution times, as well as the required pre-treatment of the sample and the waste amount of solvent.

Additionally, for GC analysis the analyte needs to be volatile and thermal stable, thus limiting the scope of this method. In recent years, new optical methods for a rapid determination of the enantioselectivity have been reported.[3a] For example, REETZ applied infrared thermography to monitor the different levels of heat output from lipase-catalyzed acylations of (R)- and (S)-alcohols.[4] MAHMOUDIAN used the same reaction to generate calibration curves for the subsequent estimation of the enantioselectivity of catalysts for the Corey-Bakshi-Shibata reduction of ketones.[5] Other examples are found in the application of supramolecular sensors (host) interacting with an analyte (guest) in combination with UV-vis, fluorescence or circular dichroism spectroscopy.[3a] However, thus far these methods are seldom applicable for a quantitative determination of the enantiomeric excess (ee) and are usually considered as preselective screening methods to identify promising reactions, which are then analyzed more thoroughly by standard chromatography techniques.

In addition to the optical methods mentioned above, mass spectrometry has also become an important tool for the evaluation of enantiomer discriminating systems.[6] However, mass spectrometric methods suffer from their inability to distinguish between enantiomers and diastereoisomers, due to the identical mass of the compounds. In 1990, HOREAU introduced an elegant and simple method to overcome this limitation (Figure 2).[7] An equimolar mixture of enantiomeric anhydrides 1, where enantiomer 1b was mass-labeled by deuteration (so called quasienantiomers[8]), were reacted in a kinetic resolution with an optically active alcohol of unknown configuration. The diastereomeric products 2 differ in the mass-label and therefore become distinguishable by mass spectrometry. The absolute configuration of various alcohols were assigned according to the relative peak heights of the two fragmentation products determined by electron ionization mass spectrometry (EI-MS). Later, FINN further elaborated HOREAU′S method allowing for a quantitative determination of the enantioselectivity of optically active alcohols by electrospray ionization mass spectrometry (ESI-MS).[9]
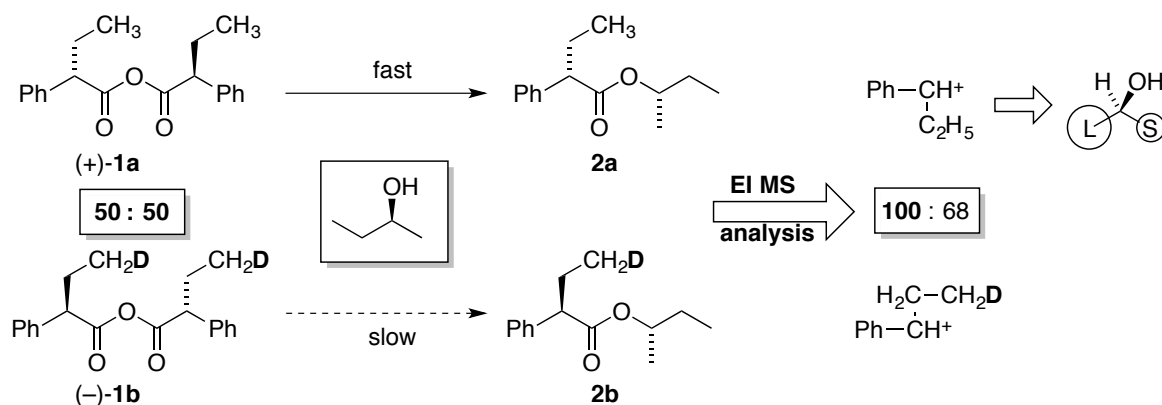
Figure 2: HOREAU′S method to determine the absolute configuration of optical active alcohols.[6a]

REETZ *et al.* applied a similar concept of mass-labeled quasienantiomers for lipase-catalyzed kinetic resolutions and asymmetric transformations of prochiral substrates bearing enantiotopic groups.[3f, 10] Recently, SPERANZA reported an alternative procedure to determine the enantioselectivity based on ESI-MS.[11] The method relies on analysis of the reaction kinetic of a diastereomeric proton bound complex with a reactant in the gas phase. This approach avoids any "wet" chemical transformation of the enantiomerically pure compound in solution prior to ESI-MS analysis and eliminates conceivable sources of error (such as formation of supramolecular aggregates with an excess of the chiral reagent) in the ESI nanodrops.

Thus far, the determination of the enantioselectivity by mass spectrometry for an investigated reaction relied on analysis of the composition of reaction products, residual starting materials or further derivatized products. In 1999, CHEN introduced a straightforward method to identify the activity of Brookhard-type polymerization catalysts out of catalysts mixtures by means of ESI-MS/MS studies.[3d, 12] Therein, charged reaction intermediates derived from eight catalysts were directly monitored by ESI-MS, whereupon the most active catalyst was represented by the intermediate bearing the longest chain (i.e. highest mass). To simplify the complex spectra, the signal patterns with highest mass were subjected to Xe-collision induced β-hydride elimination in the gas phase to afford the signal of the most active catalyst as single peak (Figure 3).
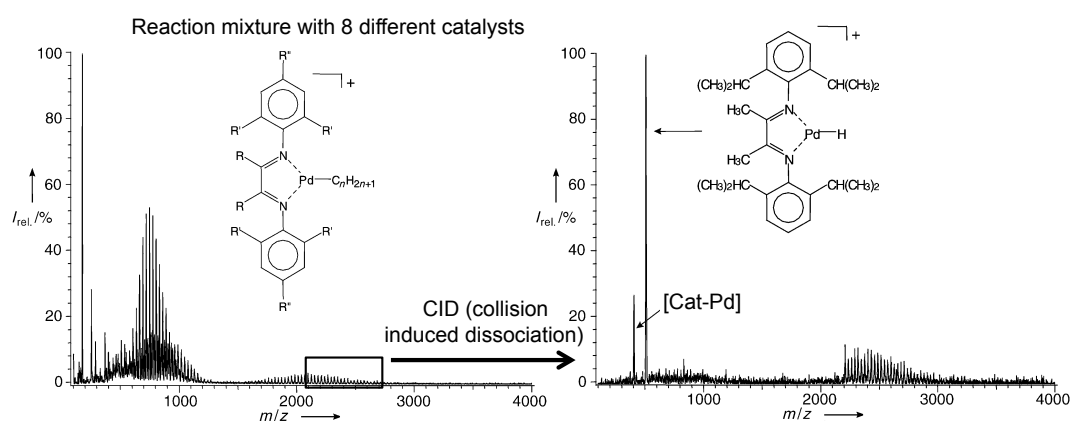
Figure 3: ESI-MS spectrum of the quenched reaction mixture of 8 catalysts (left) and the spectrum after β-hydride elimination of the polymeric ions *m/z* >2200 (right).[3d]

Another simple approach to estimate the activity of a catalyst by monitoring reaction intermediates was reported by BICKELHAUPT and REEK in 2010.[13] In their principle of the *"survival of the weakest"* the least abundant Pd-allyl intermediate represents the most active catalyst. The proposed trend was confirmed by ESI-MS screening of the Pd-catalyzed allylic

alkylation reaction with a set of various ligands present in the reaction mixture and was validated by measuring the turnover frequencies (TOF) of the corresponding reactions with the single ligand (Figure 4). However, this application is very restricted to special kinetic scenarios.
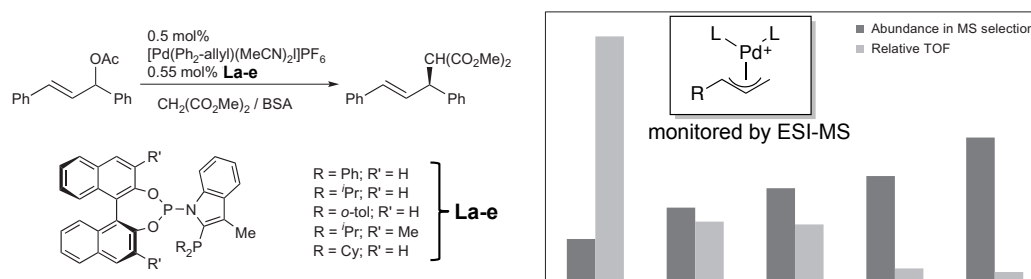
Figure 4: Inverse correlation between the ESI-MS intensity of the Pd-allyl intermediates and the turnover frequency (TOF) for the Pd-catalyzed allylic alkylation reaction.[13]

Inspired by the work of CHEN,[3d] the PFALTZ research group approached the demand for a more efficient analysis of enantioselective reactions by the development of a high-throughput screening method to determine the enantioselectivity of chiral catalysts for the Pd-catalyzed allylic substitution reaction.[6a, 14] This methodology relies on quantification of intensity ratios of charged reaction intermediates monitored by ESI-MS. These intermediates become distinguishable by mass spectrometry due to the installation of a mass label on a remote position on the individual enantiomers of the substrate (quasienantiomers). The mass labels used are not necessarily based on an isotope-labeling strategy as initially introduced by HOREAU (Figure 2). For example, in all previous studies examined in the PFALTZ group, alkyl-derived mass labels in the *para*-position of an aryl substituent far away from the reaction center were identified to be suitable for the ESI-MS screening (Figure 5). Molecules that differ in such mass labels are usually more easily accessible in perfect enantiopurity and were found to be chemically similar enough to have no influence on the selectivity outcome of the catalyst and therefore behave identically in terms of their electrospray ionization efficiency.

Initially, the kinetic resolution of allylic esters was investigated by ESI-MS leading to the identification of new, highly selective ligands for the Pd-catalyst.[14b, 14c] The subsequent extension of this ESI-MS methodology to a back reaction screening gave access to selectivity determination of catalysts for enantioselective transformations of prochiral substrates, which considerably broadened the scope of this method.[14a] In accordance with the principle of microscopic reversibility, the analysis of the ratio of the intermediates of the back reaction reflects the enantioselectivity induced by the catalyst in the corresponding forward reaction

for the same transformation. This principle can be applied to ESI-MS screenings provided that a reaction is reversible allowing for a screening of the back direction through intermediates, which are detectable by ESI-MS and are involved in the selectivity-determining step. Although the scope of the screening method is limited, the requirements described above are still given for many catalytic processes and reactions. Besides Pd-catalyzed allylic substitution reactions, this method was successfully applied to Cu- and organocatalyzed Diels-Alder reactions[15] and organocatalyzed Michael additions (Figure 5).[16] Even more exciting and worthwhile, the ESI-MS methodology was successfully extended to multi-catalyst screenings. Here, a catalysts' selectivity can be determined directly from a mixture of several catalysts by monitoring the corresponding catalyst-intermediate signals by ESI-MS analysis. In a further application, a slight modification of the ESI-MS screening protocol allowed for an estimation of the enantioselectivity of Pd-catalysts bearing *racemic* PHOX-ligands for the Pd-catalyzed allylic substitution reaction.[17] In general, the ESI-MS screening methodology is characterized by its short reaction and analysis times as well as its operational simplicity, as no workup, isolation or purification steps are required.
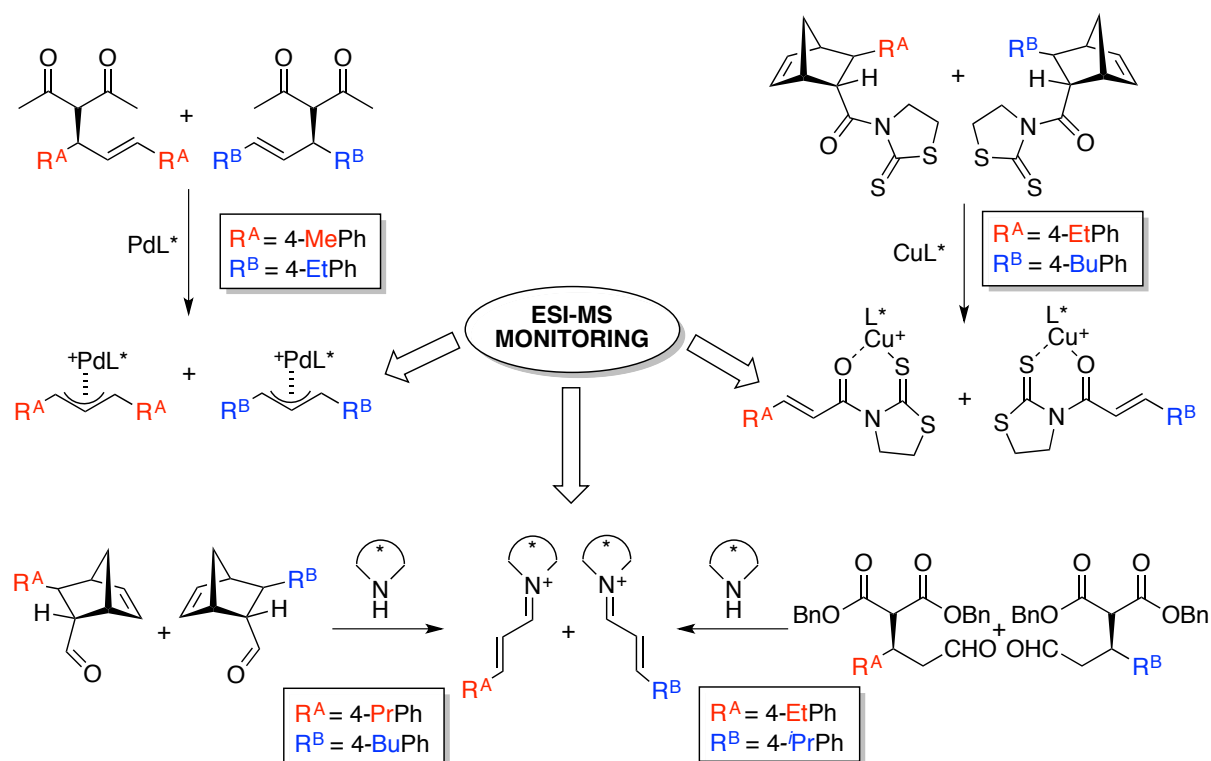
Figure 5: Previously studied back reactions, applied quasienantiomers and key intermediates monitored by ESI-MS therein.

1.2   Thesis Outline

In all previous studies cationic metal complexes or iminium ions were the key intermediates to be detected by ESI-MS analysis (Figure 5). Due to the high sensitivity of ESI-MS for ionic species these intermediates were easily detected even at the very low concentrations (10^{-5}-10^{-2} M) commonly present in a catalytic cycle. However, processes with neutral intermediates are of course very common, especially in organocatalysis,[18] and therefore we started to focus on such reactions to further broaden the scope of our screening method. The organocatalyzed aldol reaction represents a very interesting process in this context, as this transformation proceeds *via* neutral enamine intermediates in the selectivity-determining step. These intermediates could be protonated in solution to allow for ESI-MS monitoring. Within this thesis, the synthesis of suitable mass-labeled, quasienantiomeric aldol products is shown in CHAPTER 2. As expected, ESI-MS detection of enamine intermediates proved to be significantly more challenging. Unforeseen complications, encountered with the ESI-MS screening of neutral intermediates are discussed in detail. Though, a general ESI-MS screening protocol for the organocatalyzed aldol reaction was still successfully developed. For the first time, additives were applied to the screening to overcome certain limitations. Moreover, screening of additive effects was elaborated, which further extends the reaction portfolio.

Another transformation for the ESI-MS screening of enantiopure catalysts is the phosphine-catalyzed Morita-Baylis-Hillman reaction. For this process, not only are new selective catalysts still required, the reaction also proceeds *via* zwitterionic phosphorus intermediates, which were not investigated by ESI-MS thus far. The preliminary ESI-MS results and the identification of potential mass-labeled Morita-Baylis-Hillman products are presented in CHAPTER 3.

The potential of the ESI-MS back reaction screening to answer mechanistic questions is highlighted in CHAPTER 4. Catalytic intermediates and the enantioselectivity-determining step were identified in the secondary amine-catalyzed conjugate addition of aldehydes to form nitroolefins.

The ESI-MS-based determination of the enantioselectivity of racemic catalysts is further elaborated in CHAPTER 5. A screening protocol and a straightforward synthesis of racemic pyrrolidine and isoindoline-based organocatalysts were developed and applied to organo-catalyzed Michael additions.

CHAPTER 2

ESI-MS Screening of Organocatalyzed Aldol Reactions

2.1 Introduction

2.1.1 Historical Overview

The aldol reaction was discovered by Wurtz in 1872 during his investigation of the dimerization of acetaldehyde in the presence of water and hydrochloric acid to form 3-hydroxybutanal, an **ald**ehyde-alcoh**ol** (*aldol*).[19] Independently, Borodin described the formation of an aldol condensation product when treating valeraldehyde with sodium.[20]

"Man mischt zuerst das Aldehyd mit Wasser von 0 °C (...) und fügt allmählich auf –10° abgekühlte Salzsäure hinzu. (...) Destilliert man dieses Produkt im Vacuum, so geht zuerst Aether, dann Wasser, endlich zwischen 90° und 105° bei einem Quecksilberdruck von 20 Mm. eine ganz farblose Flüssigkeit über, welche beim Erkalten consistent wird und wie concentrirtester Zuckersyrup aussieht. Dieser Körper ist der Aldehyd-Alkohol, den ich kurz Aldol nennen will"; adapted from Wurtz, *Über einen Aldehyd-Alkohol*, Journal für Praktische Chemie, 1872.[19]

Since then, the aldol reaction has become a powerful tool for C–C bond forming reactions in organic synthesis.[21] To enhance control of the chemo-, regio-, diastereo- and enantio-selectivity of the reaction, various Lewis acid mediated transformations of preformed enols and enolates have been developed (indirect aldol reaction). Perhaps the most well known among them is the Mukaiyama aldol reaction applying enol silanes as substrates.[22] Although a variety of catalysts and broad applicability is known for Mukaiyama-type reactions, for reasons of practicality and atom economy, protocols for selective direct aldol reactions between two unmodified carbonyl compounds are also of great importance.[23] In recent years, organocatalyzed direct aldol reactions have become a reliable and versatile alternative to indirect aldol reactions.[18c, 24] The concept of today's organocatalysis (involving an enamine mechanism) is inspired by three fundamental roots.[18c]

(1) *Stork´s enamine chemistry*

(2) *Natures approach for C–C bond forming reactions (e.g. class I aldolases)*

(3) *The Hajos-Parrish-Eder-Sauer-Wiechert reaction*

The Wieland-Miescher ketone **6** and its 5-membered ring analogue **5** are important building blocks for the total synthesis of steroids such as cortisone. Driven by the need for an efficient

asymmetric synthesis of these intermediates, HAJOS and PARRISH at Hoffmann La Roche (Figure 6, left) and EDER, SAUER and WIECHERT at Schering (Figure 6, right) discovered the intramolecular proline catalyzed aldol reaction in the early 1970s.[24f]
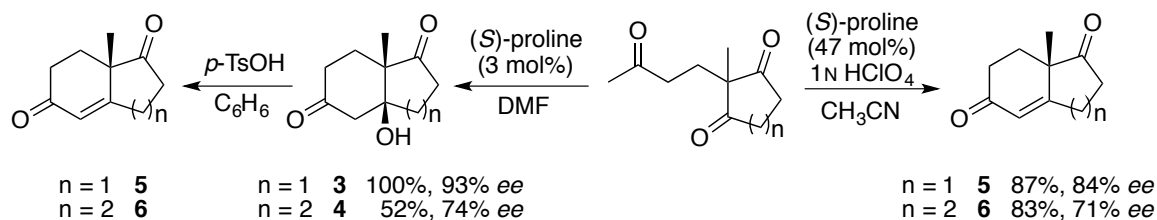
Figure 6: Hajos-Parrish-Eder-Sauer-Wiechert reactions.

Despite these remarkable results for the intramolecular version, it took almost three decades until LIST and BARBAS developed in 2000 the first amine catalyzed asymmetric intermolecular direct aldol reaction (Figure 7a).[25] Independently, MACMILLAN reported the first highly enantioselective amine-catalyzed Diels-Alder reaction based on iminium activation (Figure 7b).[26] These two publications could be considered as the birth of a new research field, *organocatalysis* (Figure 7c).[27]
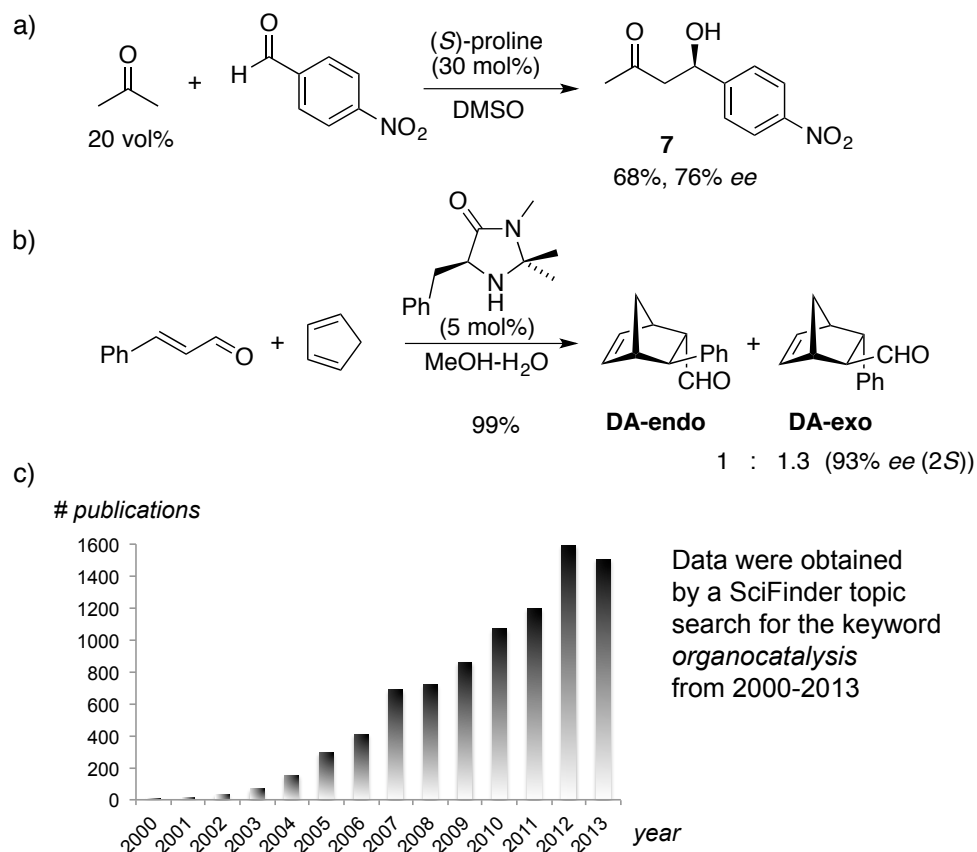
Figure 7: a) First proline-catalyzed aldol reaction. b) First asymmetric organocatalyzed Diels-Alder reaction. c) The explosion on the number of publications on the topic of organocatalysis during the last decade.

2.1.2 Mechanism of the Proline-catalyzed Aldol Reaction

Since the initial reports of the Hajos-Parrish-Eder-Sauer-Wiechert reaction, elucidation of the mechanism of proline-catalyzed aldol reactions is of particular research interest. Initially, HAJOS proposed a nucleophilic attack of an enol on the side chain carbonyl group to a carbinolamine intermediate of one of the enantiotopic ring carbonyl groups eliminating proline as the leaving group (Figure 8, left).[28] However, LIST et al. conducted ^{18}O-incorporation experiments using [18]O enriched water and found approximately 90% incorporation into the side chain carbonyl group giving strong evidence for an iminium formation and hydrolysis occurring at that position.[29] Kinetic studies for inter- and intramolecular aldolizations indicate that only one proline molecule is involved in the transition state, excluding an activation of the ketone by a second, protonated proline molecule as proposed by AGAMI (Figure 8, middle).[18c, 30] Finally, N-methylproline as catalyst proved to be completely inactive. These findings support an enamine mechanism in line with quantum chemical calculations conducted by CLEMENTE and HOUK (Figure 8, right).[31]
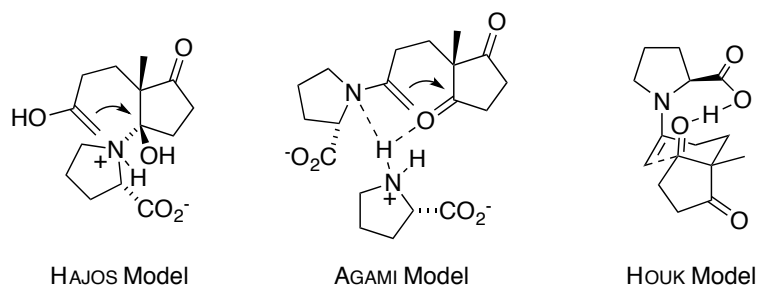
Figure 8: Mechanistic models proposed for the Hajos-Parrish-Eder-Sauer-Wiechert reaction.

In nature, an enamine mechanism is commonly accepted for asymmetric aldol reactions catalyzed by class I aldolases.[32] Recently, an enamine was directly observed as the intermediate in amine catalysis of an aldolase antibody binding site reacting with a 1,3-diketone hapten.[33] Inspired by nature, an enamine mechanism was also initially proposed for intermolecular aldol reactions (LIST-HOUK model, Figure 9, outer circle).[18c, 25, 34] Intermediates **II**, **III** and especially the enamine **En** of this catalytic cycle were identified by METZGER when performing tandem ESI mass spectrometry.[35] The results of the MS/MS studies gave clear evidence for an enamine and not the mass isomeric oxazolidinone **Oxa-I**. However, this was in conflict to several NMR studies where only the oxazolidinones were observed as intermediates.[29, 36] It might be that enamines monitored by ESI-MS were formed during the transformation and ionization of the solution molecules into the gas phase, therefore this experiment does not necessarily reflect the situation in solution. The role of oxazolidinones

remained ambiguous for a long time. Initially, the formation was considered as a rate diminishing "parasitic equilibrium". Though, GSCHWIND *et al.* monitored in real time NMR studies for the self aldolization of propionaldehyde in DMSO for the first time enamine intermediates.[36a] The spectroscopic data revealed the *E*-configuration of the enamine double bond and s-*trans* conformation of the molecule. Even more, according to NMR exchange spectroscopy the enamine **En** is directly formed from the oxazolidinone **Oxa-I** giving evidence that oxazolidinones are real catalytic intermediates and not off-cycle products (Figure 9, inner circle). For such a transformation of oxazolidinones into enamines a concerted E2 mechanism, where proline or the oxazolidinone itself acts as base, was reported by SEEBACH.[36b] Nevertheless, the selectivity-determining step of the aldol reaction remains the attack of the enamine to the aldehyde. Kinetic studies conducted by BLACKMOND *et al.* gave evidence that aldehyde addition is also the rate-determining step in contrast to intramolecular aldolizations were the enamine formation was found to be rate-limiting.[37]
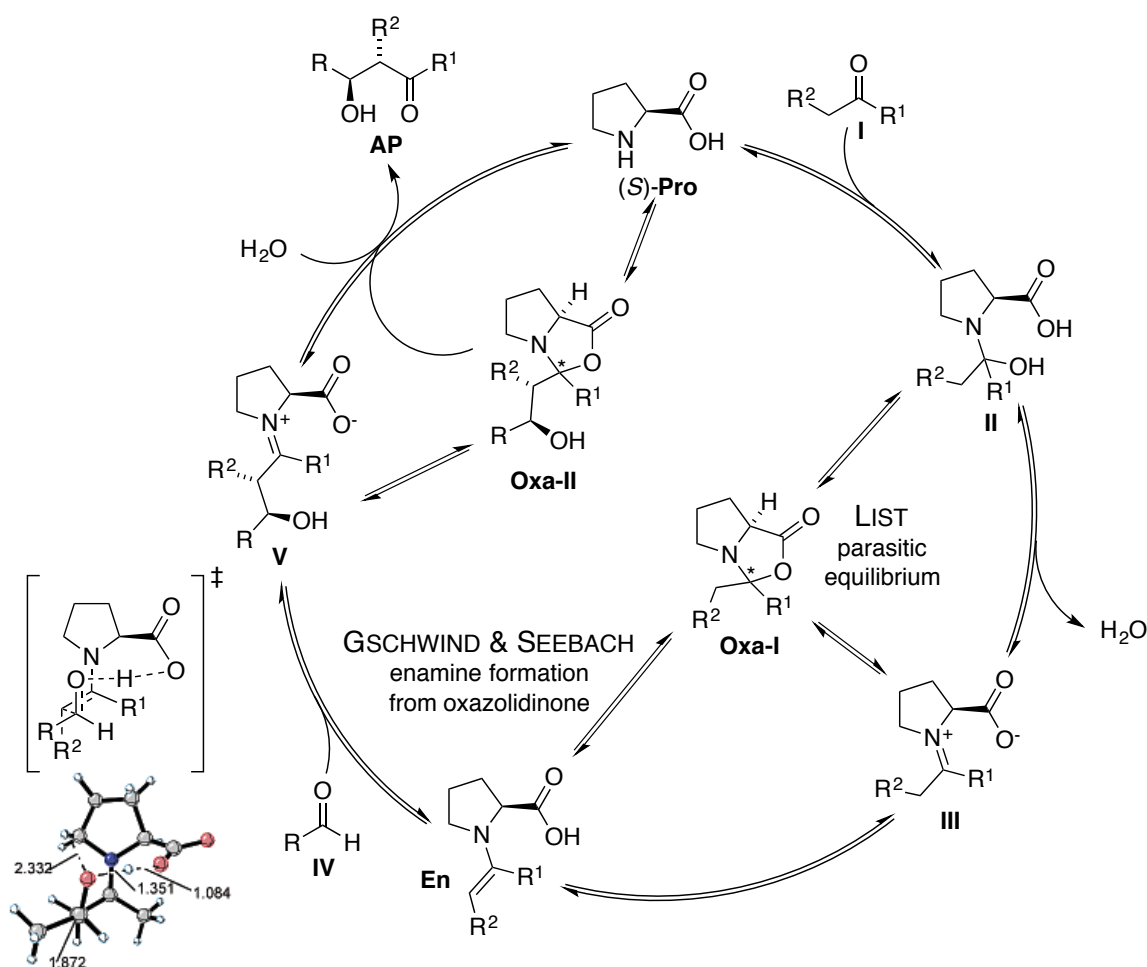
Figure 9: Potential mechanistic pathways for the proline-catalyzed aldol reaction. Calculated transition state adapted from HOUK and LIST.[34]

It is worth to mention that SEEBACH proposed a pathway where oxazolidinones are even actively participating as intermediates affecting the selectivity outcome of the reaction.[36b] Here the oxazolidinone **Oxa-I** reacts to an enamine-carboxylate followed by *trans* addition (in s-*cis* conformation) with electrophile-induced lactonization to the alcoholate of oxazolidinone **Oxa-II**. The configuration of the product for the more stable s-*cis* oxazolidinone isomer would match the configuration observed experimentally. However, calculations conducted by SHARMA and SUNOJ revealed that the activation barrier for the enamine pathway is lower in energy.[38] Additionally, although the oxazolidinone derived from the s-*cis* conformer is indeed lower in energy, the associated barrier for its formation is higher, implying a kinetic preference for the oxazolidinone leading to the wrong stereochemical outcome.

2.1.3 Proline Amide-based Organocatalysts for the Aldol Reaction

Proline itself proved to be a versatile catalyst for a variety of substrates.[24d] Nevertheless, to further improve the substrate scope and reduce drawbacks such as high catalyst loadings, large excesses of ketones, long reaction times and low solubility in various reaction media, new catalyst structures for direct aldol reactions were developed over the last decade (Figure 10).[24c, 24d, 39]
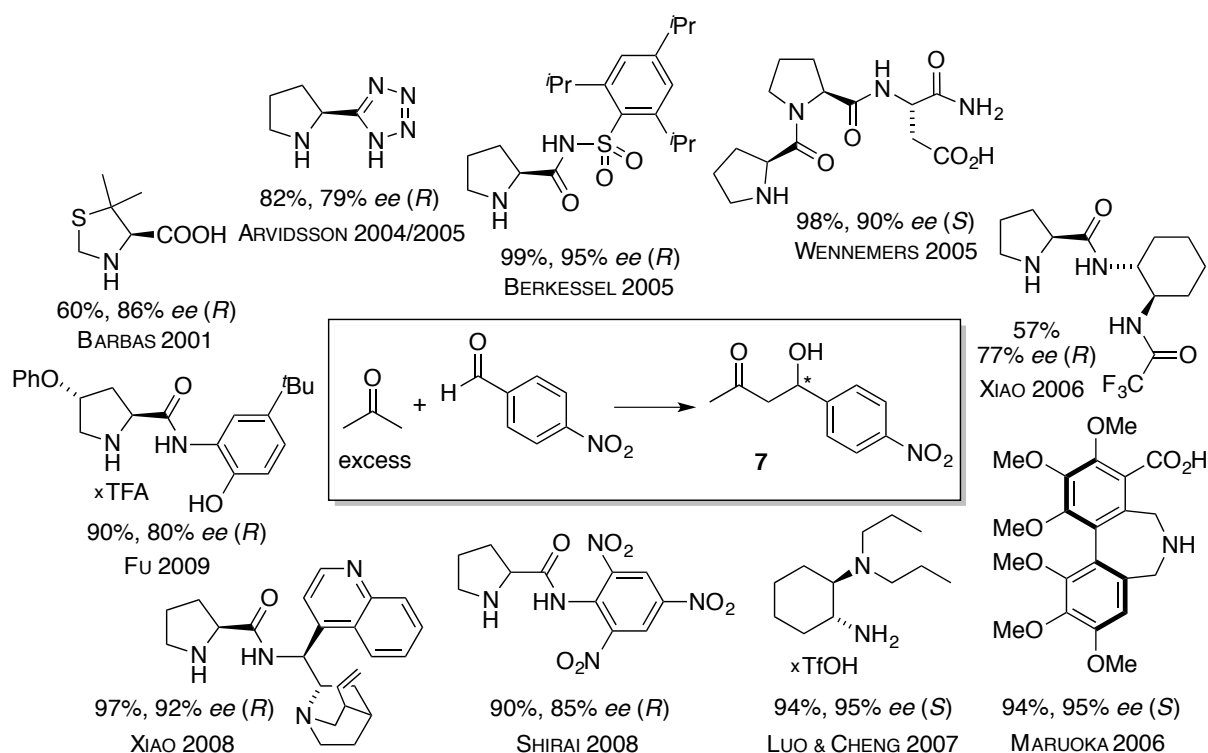
Figure 10: Selected proline and non-proline derived organocatalyst for the acetone aldol reaction as a benchmark system.[24d]

Among these new organocatalysts, particular attention has been paid to proline-based amide derivatives. The amide functional group allows for a simple tuning of the catalyst and to insert new structural diversity (selected examples are illustrated in Figure 10). Variations such as modification of the hydrogen bond donor strength of the amide nitrogen,[40] increased lipophilicity or steric bulk as well as additional stereogenic centers, functional groups and hydrogen bond donors are easily accessible by a modification of the amine as a coupling partner for proline. Additionally, for coupling reactions of acids with amines a variety of reagents and methods are established in the literature.[41]

GONG and WU developed readily available proline amide catalysts derived from proline and α,β-hydroxyamines.[42] These structures showed enhanced catalytic activity and enantio-selectivity compared to the parent proline amide **8** (Figure 11). For the catalyst structure (*S,S,S*)-**10** containing the (*S,S*) configured α,β-diphenyl substituted aminoalcohol, a superior enantioselectivity of 93% *ee* was observed at –25 °C in the benchmark reaction with acetone and *para*-nitrobenzaldehyde.[42a] The configuration of the stereogenic center at the α-carbon of catalyst **10** seemed to be of higher importance for a match case with the configuration of the proline than the configuration at the β-carbon. Moderate to good yields and good to excellent enantioselectivities were obtained for the acetone aldol reaction with different aldehydes. In 2005, GONG *et al*. reported further improved selectivities using modified catalyst-derivatives bearing electron-withdrawing groups at the stereogenic centers in the side chain such as **12**. In contrast, electron-donating substituents (**11**) led to a considerable decrease in selectivity (Figure 11).[43]

8	**9**	**10**	**11**	**12**
80%, 30% *ee*	(*S*) 75%, 48% *ee*	(α*R*,β*S*) 63%, 49% *ee*	53%, 15% *ee*	85%, 87% *ee* (2 mol%)
	(*R*) 84%, 46% *ee*	(α*R*,β*R*) 77%, 44% *ee*		62%, 99% *ee*
		(α*S*,β*R*) 76%, 64% *ee*		(2 mol%, –25 °C)
		(α*S*,β*S*) 89%, 69% *ee*		
		66%, 93% *ee* (–25 °C)		
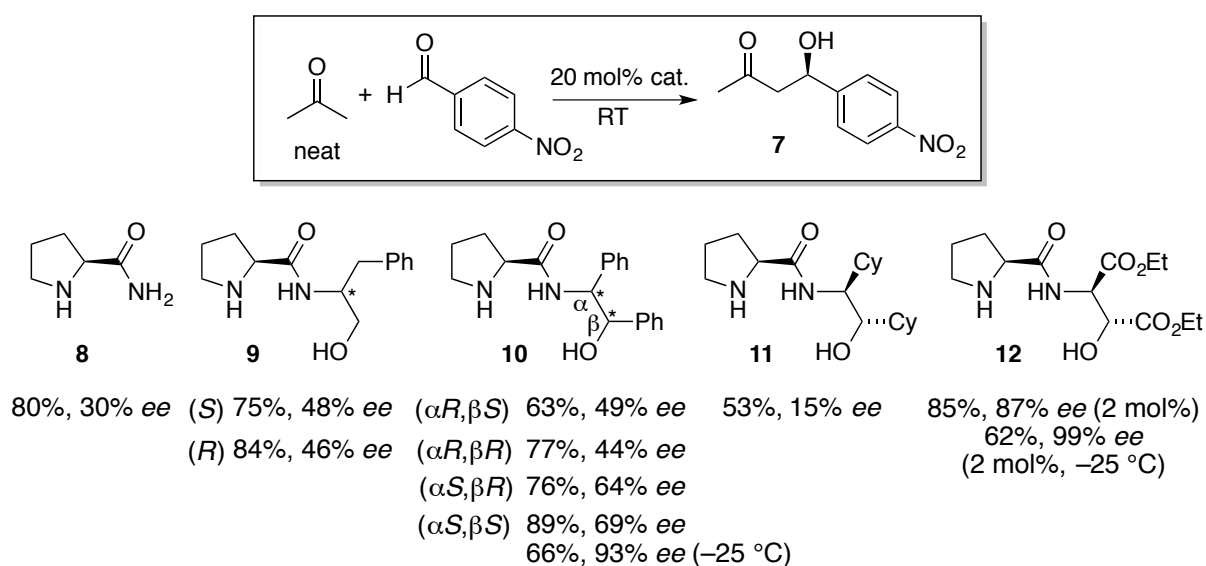
Figure 11: Selected results with organocatalysts bearing aminoalcohols in the side chain.

Mechanistic investigations for aldol reactions using proline amides are rare compared to proline-catalyzed reactions. Experiments to elucidate the structure-selectivity relationships for a set of proline amides were conducted by GONG and WU.[24c, 42b] They also calculated transition states and activation energies for aldol reactions catalyzed by proline amides **8** and **10** assuming an enamine mechanism as established for proline catalyzed reactions (see Chapter 2.1.2). For a derivative of catalyst **8** bearing a diethyl substituted amide-nitrogen the observed selectivity dropped to 18% *ee*. On the other hand, mono substituted *para*-trifluoromethyl phenyl amide gave a slightly enhanced selectivity of 45% *ee* compared to 30% *ee* with the parent proline amide **8**. Thus, the amide N-H group was supposed to be directly involved in the transition state of the stereoselectivity determining step through hydrogen bonding to the aldehyde substrate in line with the accepted transition state for proline-catalyzed aldolizations.[34] The same observations that more electron withdrawing substituents induce higher selectivities due to an increased hydrogen-bond donor strength were made for the α,β-hydroxyamine-derived catalysts described above (Figure 11). Furthermore, methylation of the amide and/or the alcohol function led to a decrease in the selectivity (Figure 12), thus providing further evidence for the hydrogen-bond network present in the transition state.
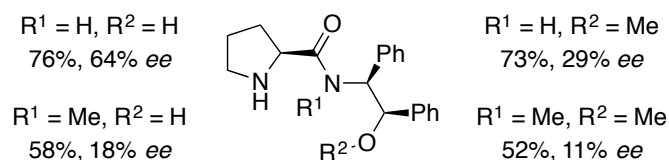
Figure 12: Influence of methylation of hydrogen-bond donor positions on the selectivity.

As depicted in Figure 13, calculations of the transition state with proline amide **8** revealed higher stability of the *anti* compared to the *syn* enamine. The second hydrogen bond of the terminal hydroxyl group of catalyst (*S,S,S*)-**10** considerably decreases the activation barrier. Attack of the enamine to the *si* face of the aldehyde is less favored due to steric interactions of aryl hydrogens with the hydroxy group, in line with the experimentally observed selectivity outcome. However, the predicted selectivity should be higher than actually determined in preparative experiments. The authors rationalized this due to an over-estimate of the hydrogen bond strength in the gas phase model or competitive background reactions leading to lower selectivities. It is worth mentioning that unsubstituted aminoalcohols gave comparable activation energies as diphenyl-substituted derivatives, however the substituents are essential for the conformation of the molecule leading to higher energy gaps between the (*R*) and the (*S*) transition states. These calculations and experimental results support the influence and

beneficial effect of the hydrogen-bonding network and in particular the importance of the terminal hydroxyl group on the selectivity and activity of the catalyst.

ΔE_a = 10.0 kcal/mol
anti enamine, *re* face, (*R*)-product

ΔE_a = 15.6 kcal/mol
syn enamine, *re* face, (*R*)-product

ΔE_a = 7.0 kcal/mol
re face, (*R*)-product

ΔE_a = 12.1 kcal/mol
si face, (*S*)-product
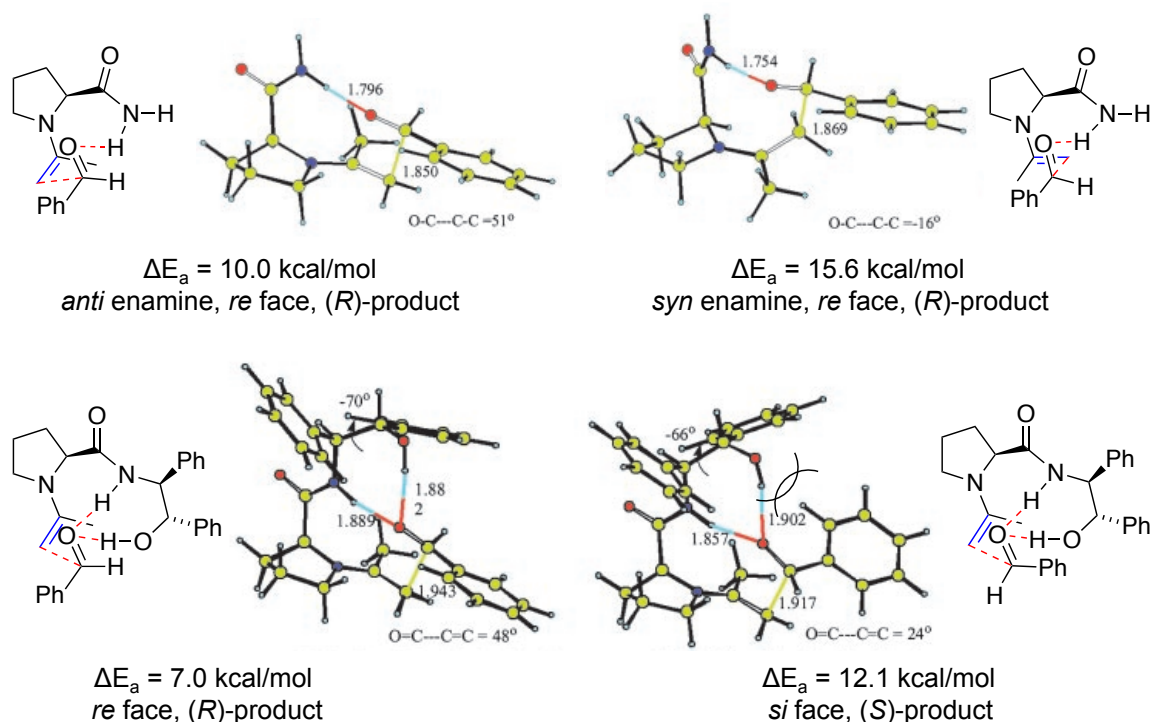
Figure 13: Transition state calculations conducted by GONG and WU.[42b]

Inspired by the work of GONG, the SINGH group developed a new set of proline amides bearing geminal diphenyl substituted aminoalcohols (Figure 14).[44] The enantiopure aminoalcohols are easily available from various amino acid esters *via* Grignard reactions. Comparable transition states to those presented in Figure 13 were proposed for these catalysts, where the geminal diphenyl group should restrict the conformation and increase the hydrogen-bond donor potency of the hydroxyl group. L-Leucine-derived catalyst **13** (SINGH'S catalyst) has emerged to catalyze the aldol reaction of acetone and benzaldehyde smoothly affording the aldol product in >99% *ee* and 52% yield in 48 h even at low temperatures of –40 °C. For various aldehydes, yields of 52-70% and selectivities of 97-99% *ee* were reported at –40 °C reaction temperature. Moreover, a substituent at the α-position seems to be essential to achieve these higher selectivities. Again, the (*S,S*) configuration was superior over the (*S,R*) derivative, as demonstrated using the two diastereomers of catalyst **8**. Modifications at the terminal quaternary carbon atom of catalyst **16**, such as ethyl or electron-rich aryl substituents, also led to a considerable drop in selectivity.

In the following years several applications of SINGH's catalyst were reported. DUAN and WANG found catalyst **13** to be suitable for aldol-lactonization reactions of various ketones with 2-formylbenzoic methyl ester to form biologically active 3-phthalides.[45]
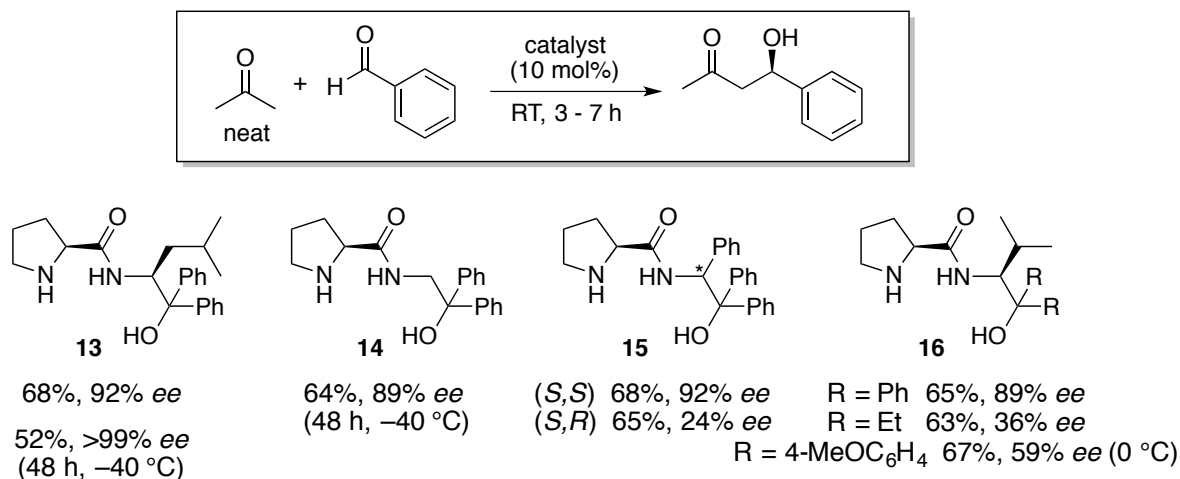
Figure 14: Selected results reported by SINGH.

In 2009, the BERKESSEL group reported an interesting application of SINGH's catalyst **13** in combination with asymmetric biocatalysis. A sequential one pot procedure of an organocatalyzed aldol reaction of acetone with various aldehydes followed by enzymatic reduction of the ketone afforded all four stereoisomers of 1,3-diols in high enantio- and diastereo-selectivity.[46] Moreover, the groups of SINGH[44a, 47] and BERKESSEL[48] identified amine **13** as active and selective organocatalyst for asymmetric aldol reactions in aqueous media. In more detailed studies Berkessel *et al*. observed an interesting effect of the catalyst loading on the enantioselectivity of the aldol reaction (Figure 15).[48b] This effect was attributed to a switch-over from a kinetically to a thermodynamically controlled reaction with increasing catalyst loadings. The impact of the *retro*-aldol reaction increased and therefore a thermodynamically favored racemate was the product of the reaction. Whereas at 0.5 mol% catalyst loading the selectivity remained almost constant over a 48 h period, the *ee* dropped significantly from 90% to 47% using 5 mol% catalyst loading. To further support this hypothesis they mixed enantiomerically enriched aldol product **17** with 0.5 mol% and 5.2 mol% of SINGH's catalyst **13**.[48a] Indeed, in the presence of 0.5 mol% of catalyst only a slight decrease of the enantiomeric purity was observed after 24 h, in contrast to a strong erosion of the *ee* induced by 5.2 mol% catalyst. To prove the reversibility of the aldol reaction, crossover ^{1}H NMR investigations of the back reaction were conducted. A mixture of aldol product **17** as starting material, 5.2 mol% catalyst **13** and an excess of deuterated acetone in brine revealed an incorporation of deuterated acetone after 24 h indicating the *retro* reaction. In contrast,

incorporation was negligible at 0.5 mol% catalyst loading. Although, in general enamine-iminium formation could lead to a deuterium scrambling under these conditions the authors claimed that no partially deuterated products were observed.[48a] The potential observation of the aldehyde signal, which would be unambiguous evidence for the back reaction, was not described.
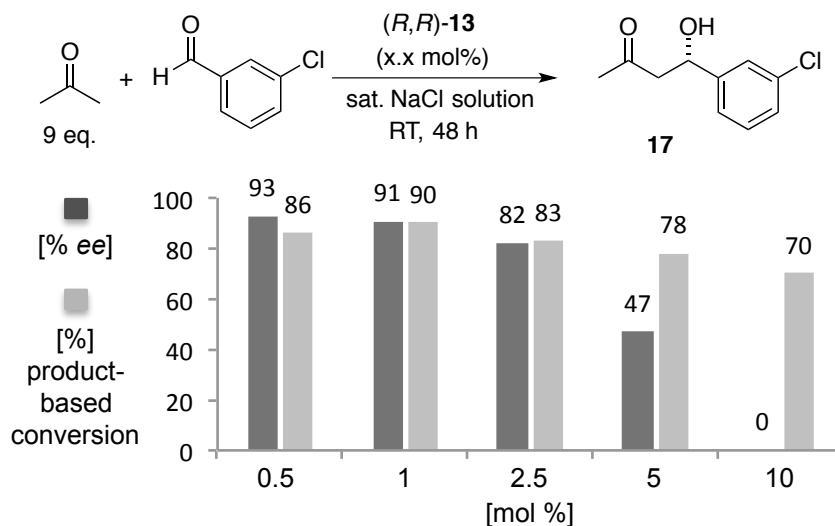
Figure 15: Decreasing enantioselectivity with increasing catalyst loading.

In 2012, BERKESSEL described the synthesis of aldol products containing a CF_3-subsituted quaternary stereogenic center derived from the reaction of acetone with 2,2,2-trifluoro-acetophenones using SINGH'S catalyst **13**.[49] Although the reaction was carried out in neat acetone, again a depletion of the enantiomeric purity of the product, as observed for aldol reactions in brine, was determined for high catalyst loadings. However, the erosion in organic media was slower than in brine. In addition, they noticed that slightly acidic additives such as hexafluoro-2-propanol led to a dramatically faster racemization. Even NH_4Cl solution, added to quench the reaction, gave a decrease of the enantiopurity of the aldol product. Therefore, it was crucial to identify and avoid potential racemization conditions for this reaction type.

The observations made by the BERKESSEL group described above demonstrate the high value and benefit of a catalyst screening, such as the ESI-MS screening developed in the PFALTZ group,[6a] allowing for a monitoring of the intrinsic enantioselectivity of a catalyst. Thus, problems related to convenient product analysis, such as potential racemizations caused during workup or product purification and/or background reactions are eliminated.

2.2 Principle of the ESI-MS Screening of Aldol Reactions

The reversibility of organocatalyzed aldol reactions and the proposed participation of an enamine in the selectivity-determining step makes this transformation to a particularly suitable target for ESI-MS screening. In addition, a screening protocol for reactions proceeding *via* neutral intermediates such as enamines considerably broadens the scope of the ESI-MS screening methodology.

The general concept of the ESI-MS methodology is illustrated in Scheme 1. As already presented in Chapter 1, ESI-MS back reaction screening is a method for the determination of the enantioselectivity induced by a catalyst in the corresponding forward reaction. For that purpose, an organocatalyst is reacted in the *retro* aldol reaction starting from a 1:1 mixture of mass-labeled quasienantiomeric aldol products M_A and M_B. If the initial iminium ions (**Im-M_A** and **Im-M_B**) are formed in a fast pre-equilibrium, the ratio of the enamine intermediates **En-M_A**/**En-M_B**, determined by ESI-MS analysis of the back reaction mixture should correlate to the ratio of the rate constants for the rate determining C–C bond cleavage (Curtin-Hammett conditions). In accordance with the principle of microscopic reversibility, the stereoselectivity of the forward and the back reaction is controlled by the same transition states.[50] Therefore, given that the C–C bond formation is the selectivity-determining step of the forward reaction, the enantioselectivity of the catalyst (s = k_A/k_B) is reflected by the ratio of the enamine intermediates (**En-M_A**/**En-M_B**) formed in the back reaction.

$$s = k_A/k_B \sim Int(\textbf{En-}M_A)/Int(\textbf{En-}M_B)$$
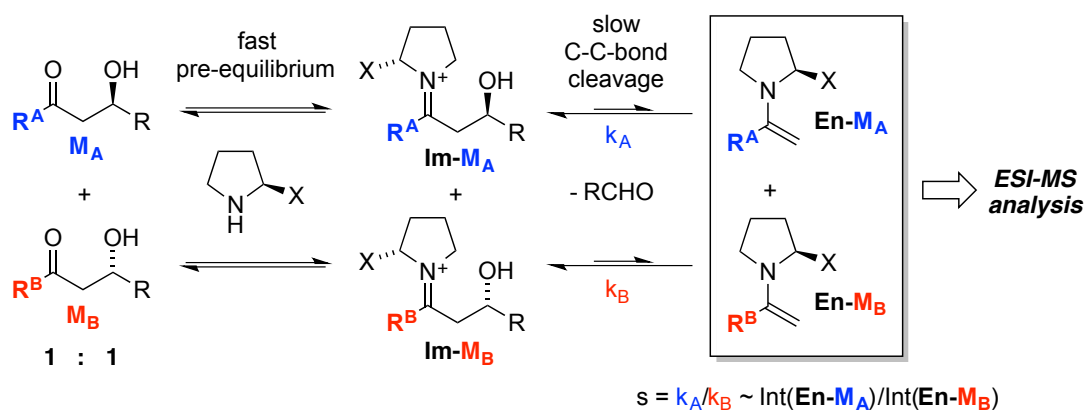
Scheme 1: Concept of the ESI-MS back reaction screening related to the organocatalyzed aldol reaction.

2.3 Preliminary Experiments

In Scheme 1 enamines are presented as key intermediates employed to ESI-MS analysis. However, for ESI-MS detection a proton source in the system is required to transform the neutral enamines formed in the process into positively charged iminium ions. If this protonation does not occur efficiently, the enamine might still be formed to a significant extent but cannot be detected by ESI-MS. Additionally, protonation is the first step of enamine hydrolysis and thus the iminium species is even more prone to decay to the carbonyl compound and the free catalyst. This could even lower the amount of detectable intermediates formed in the back reaction. Therefore, ESI-MS back reaction screening involving neutral catalytic intermediates was considered to be more challenging than the investigations previously performed in our group monitoring positively charged catalytic intermediates.

2.3.1 Identification of Aldol Products Suitable for the Back Reaction Screening

The first aim of the project was an evaluation of suitable aldol products and reaction conditions for a back reaction screening affording enamine intermediates in acceptable ESI-MS intensities. To avoid problems and limitations due to the solubility and potential formation of zwitterionic intermediates with L-proline, the commercially available catalyst (*S,S,S*)-**10** was applied in initial experiments. This catalyst system was known to be active in aldolizations presumably involving an enamine mechanism and allows for simple modifications for further potential catalysts to be screened (see Chapter 2.1.3).
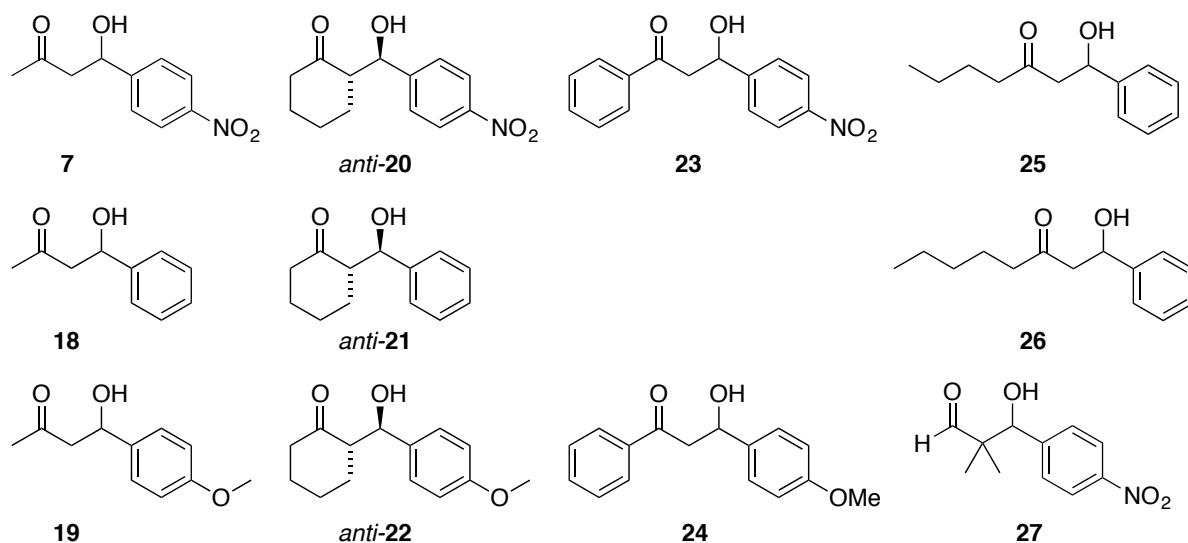
Figure 16: Aldol products applied in preliminary ESI-MS test experiments.

The enamine[i] signal was detected clearly as a base peak for the forward reaction of cyclohexanone with three different substituted benzaldehydes and catalyst **10**. MeOH was used as both reaction and diluting solvent prior to ESI-MS analysis. It is worth mentioning that the absolute intensity of the enamine signal in the forward direction was considerably higher with benzaldehyde and anisaldehyde as an aldol acceptor, which reveals the increased reactivity using the more electrophilic *para*-nitrobenzaldehyde. Several racemic aldol products were synthesized and subjected to ESI-MS back reaction analysis (Figure 16). For the back reaction screening the *anti* aldol products of cyclohexanone **20**, **21** and **22** were used exclusively to avoid potential mismatch scenarios of the catalyst with non-favored *syn*-products.[43] With DMSO as reaction solvent and MeOH for sample dilution no enamines were detected. However, performing the reaction in pure MeOH, an enamine was observed in acceptable signal-to-noise ratios after 30 min. The intensity was found to increase with longer reaction times for the cyclohexanone derivatives.

By far the highest intensities among the explored aldol products were found for acetone derivatives **7**, **18** and **19** (Figure 17). Although an acceleration of the back reaction was expected with electron donating substituents, no significant influence of the electronic properties of the aryl moiety were observed. The ratio of free catalyst to enamine was further optimized by addition of acetic acid (AcOH) to the diluted analyte mixture in MeOH (Figure 17, box). The initially formed iminium ion was generally not detected by ESI-MS analysis of the back reaction mixture. Since the *retro* aldol reaction obviously occurred, this indicates that once the iminium ion is formed it either undergoes fast hydrolysis back to the free catalyst, isomerizes to the neutral product enamine or the C–C bond cleavage takes place therefore leaving only negligible quantities of product iminium ions present in the catalytic cycle. Water (10 µL, 10 vol.-%) present in the reaction mixture induced a complete extinction of the enamine intermediates. Nevertheless, reactions could be performed under air with non-dried solvents, as in the presence of minor amounts of water the enamine intensity did not drop significantly. However, solvents of crown-cap quality were usually applied for the reaction and dilution to maintain reproducible conditions.

Acetophenone derivatives **23** and **24** were considered as ideal test compounds, since an easy mass-labeling in *para*-position of the aryl group of the ketone derived part of the molecule is possible. However, organocatalyzed aldol reactions using acetophenones as enamine

---

[i] Within the scope of the thesis the intermediate signals formed in the back reaction after C–C bond cleavage will be described as enamines, although its clear that the signals monitored by ESI-MS are positively charged species such as for example the corresponding iminium ion.

precursors are rare.[51] On the one hand, this would allow for a benchmark system screening new active catalysts for this transformation, but on the other hand only the less known active organocatalysts for this transformation would complicate the setup of a general screening protocol for proof-of-principle studies. Unfortunately, this substrate class turned out not be suited to the described purposes. Even in the forward direction no enamine signals of acetophenone and a pyrrolidine sulfonamide, known to catalyze this reactions,[51a] were observed. For aldehyde aldol product **27** the enamine signal was observed in the back reaction, albeit with a very poor signal-to-noise ratio.
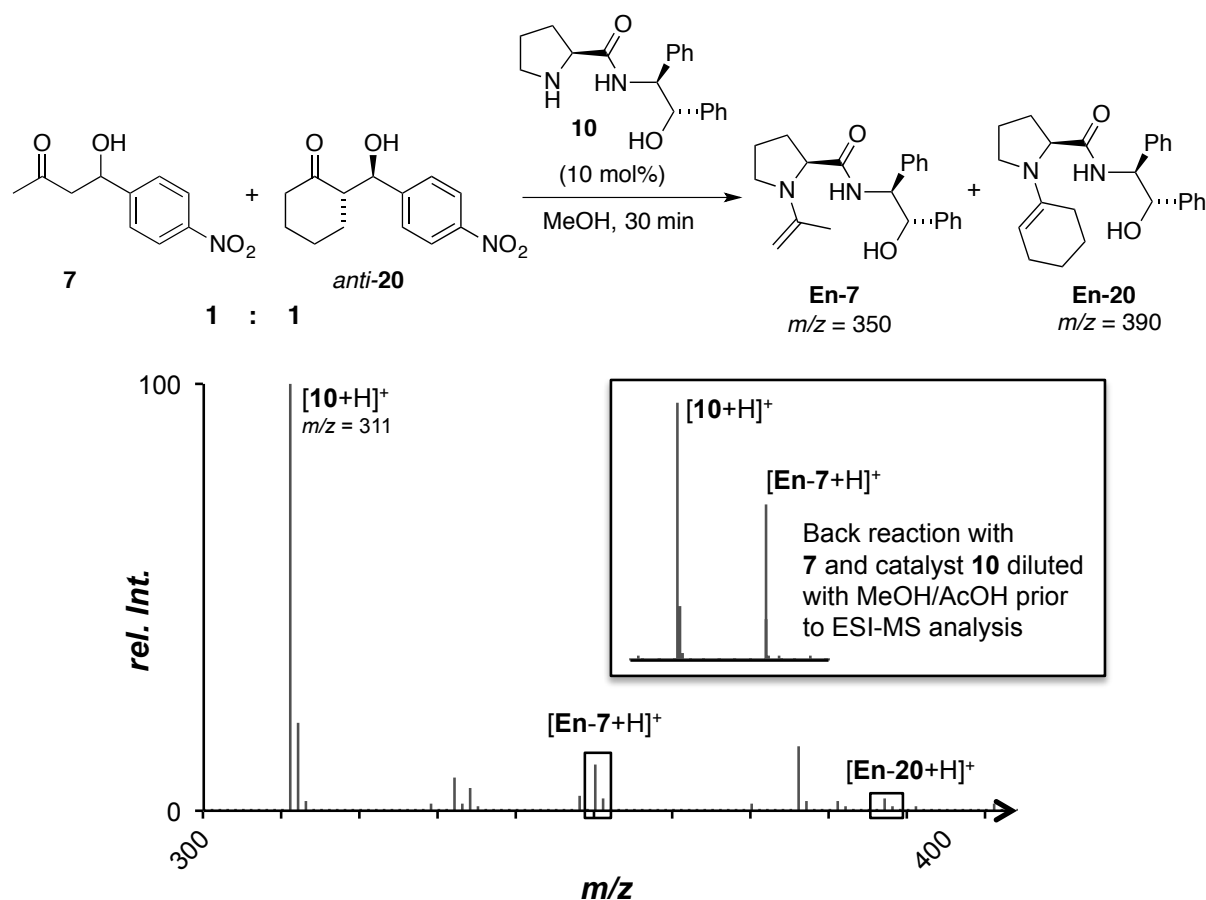
Figure 17: Competitive enamine formation in the back reaction with aldol products **7** and **20**. Box: Increased enamine intensity after dilution with MeOH/AcOH in an independent back reaction with aldol product **7**.

Furthermore, the influence of the reaction solvent was explored. Back reactions were conducted in different solvents and then diluted with MeOH and AcOH (10 μL/mL). Interestingly, among the investigated solvents the signal intensity of the enamine intermediates was found to be superior in MeOH, but also in other protic solvents such as EtOH and ^{i}PrOH excellent intensities were detected. Aprotic solvents such as CH_2Cl_2, CH_3CN and toluene proved to be suitable as well, whereas for DMSO, DMF, $CHCl_3$ and THF

only poor signal-to-noise ratios were found (Figure 18).
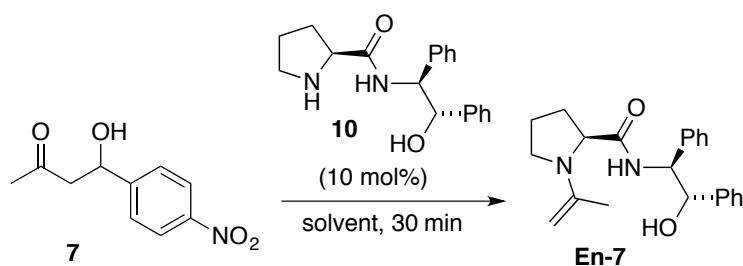
MeOH > EtOH > ^{i}PrOH ≈ CH$_2$Cl$_2$ ≈ CH$_3$CN ≈ toluene > DMSO, DMF, CHCl$_3$, THF

Figure 18: Dependency of the intensity of **En-7** in various reaction solvents.

Since acetone-based enamines gave the best results in terms of intermediate ratios a potential mass-labeling of the acetone moiety was investigated. Elongation of the terminal chain was one possibility. To examine the influence of chain length a 1:1 mixture of racemic hexanone- and heptanone-derived aldol products (**25** and **26**) were subjected to the back reaction catalyzed by amine **10**. ESI-MS analysis revealed an enamine intermediate ratio of 54:46 in favor for the hexanone enamine both in lower intensities compared to an acetone enamine. Therefore, the additional methylene group has either an influence on enamine stability, an impact on the transition state and/or a difference in the electrospray ionization efficiency of the different intermediates.

2.4 Synthesis of Isotope-labeled Quasienantiomeric Aldol Products

Based on the above mentioned results, it was decided to keep the acetone enamine framework constant. Therefore, an isotope-labeling strategy was investigated next to provide chemical similarity (Figure 19). For that purpose commercially available deuterated or ^{13}C-labeled acetone was considered as the precursor. Aldol acceptor *para*-nitrobenzaldehyde was chosen as in many cases the aldol reaction of acetone and *para*-nitrobenzaldehyde is commonly reported in the literature as a benchmark reaction in literature.[18c, 24c, 24d] Even more important, the preparative forward reaction with an activated aldehyde should be more feasible for a broader range of organocatalysts, and allow for a simpler validation of the back reaction screening results.
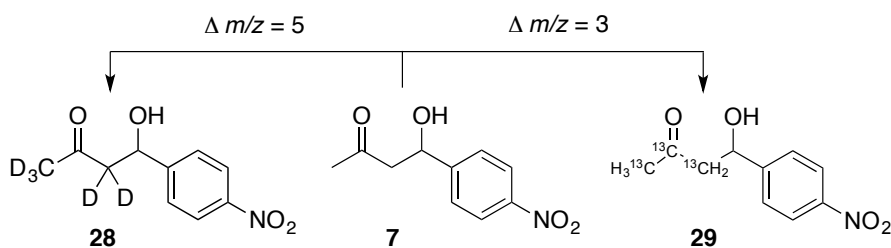
Figure 19: Potential mass-labeled acetone aldol products (syntheses are presented in the following sections).

2.4.1 Synthesis of the Unlabeled Aldol Product

The aldol products for the back reaction screening were required in an enantiopure fashion. Organocatalysis was chosen as the method of choice for their synthesis. SINGH'S catalyst **13** was reported to induce high selectivities.[44b] However, the synthesis of this catalyst according to the original procedure (Scheme 2a) did not prove reliable and led to purification problems. Especially, deprotection of the Boc-group did not afford the product in the reported purity. Later, similar problems with the original procedure were also described by the BERKESSEL group, which developed a more elegant and straightforward route to this catalyst (Scheme 2b).[52] At that time an alternative synthesis for catalyst **13** was applied, according to a coupling procedure of NAKANO and KABUTO starting from Cbz-protected proline (Scheme 2c, see also Scheme 12).[53] The poor yield obtained over that pathway is probably caused by the quality of the coupling reagents used. Nevertheless, a sufficient amount of material for ESI-MS studies was generated. In addition, catalyst **13** became recently commercially available from Sigma-Aldrich making an improved synthesis unnecessary.

a)

b)

one-pot procedure

c)
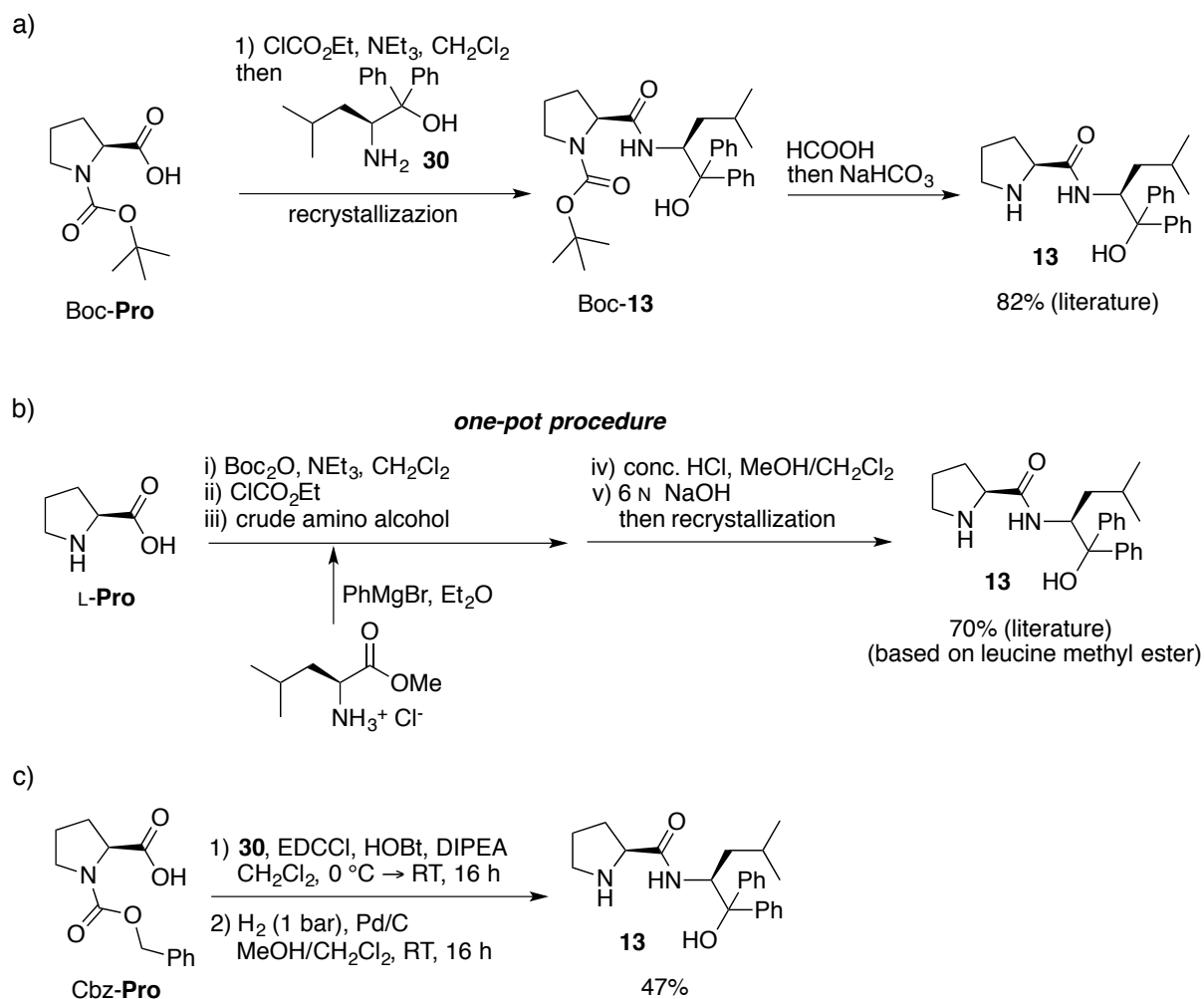
Scheme 2: a) Original synthesis and yield reported by SINGH in 2006. b) New straightforward "one-pot procedure" reported by BERKESSEL *et al.* in 2012. c) Applied synthesis starting from Cbz-protected proline.

However, due to the initial problems to synthesize a sufficient amount of SINGH'S catalyst **13**, we moved our focus to an alternative catalyst for substrate synthesis. BERKESSEL'S sulfonamide catalyst **31** was reported to catalyze the aldol reaction efficiently.[54] This catalyst was also thought to be more convenient for the synthesis of aldol products as it is based on cheap *para*-toluenesulfonamide as side chain and contains only one stereogenic center at the proline site. Therefore, switching from L- to D-proline without additional modification of the side chain stereoisomers gives access to both enantiomers of the aldol products. The original procedure was slightly modified and worked well without purification of the intermediates after the individual steps (Scheme 3).
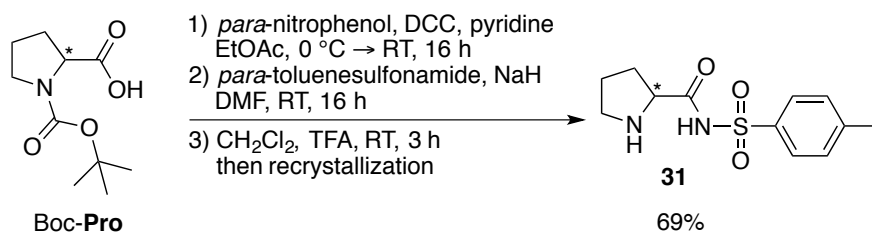
Scheme 3: Synthesis of BERKESSEL'S sulfonamide.[54]

BERKESSEL'S catalyst **31** was successfully applied for the synthesis of both enantiomers of the non-labeled aldol products in 85-88% *ee*. Starting from this *ee* two subsequent recrystallizations (rec.) afforded the required enantiomeric purity of the aldol product (Scheme 4).
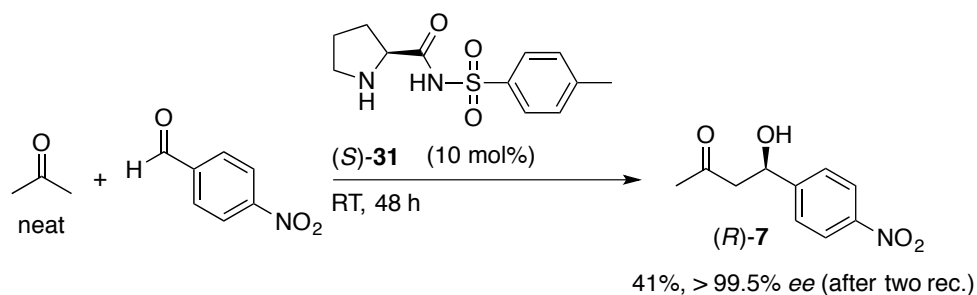
Scheme 4: Representative procedure for the synthesis of the (*R*)-aldol product **7**.

2.4.2 Synthesis and Application of the Deuterated Aldol Product

For the deuterated aldol product issues regarding a potential deuterium scrambling *via* an enamine-iminium mechanism appearing during the synthesis had to be considered, in particular for the back reaction screening (Scheme 5). Therein, a scrambling of the deuterated enamine could lead to an overlay with the corresponding non-labeled enamine. However, since a C-H bond should be cleaved faster then a C-D bond and if isomerization is slow, ESI-MS screening might be possible even in the presence of a proton source.
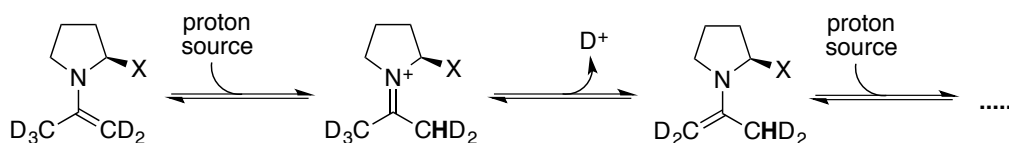
Scheme 5: Deuterium scrambling *via* enamine-iminium isomerization.

The major advantage of the deuterated aldol product is the availability of comparatively cheap deuterated acetone, which was again directly used as neat solvent for the organocatalyzed

reaction (Figure 20). After recrystallization, only trace amounts of partially H-substituted product were observed by ^{1}H NMR analysis. This amount should not considerably influence first ESI-MS measurements.
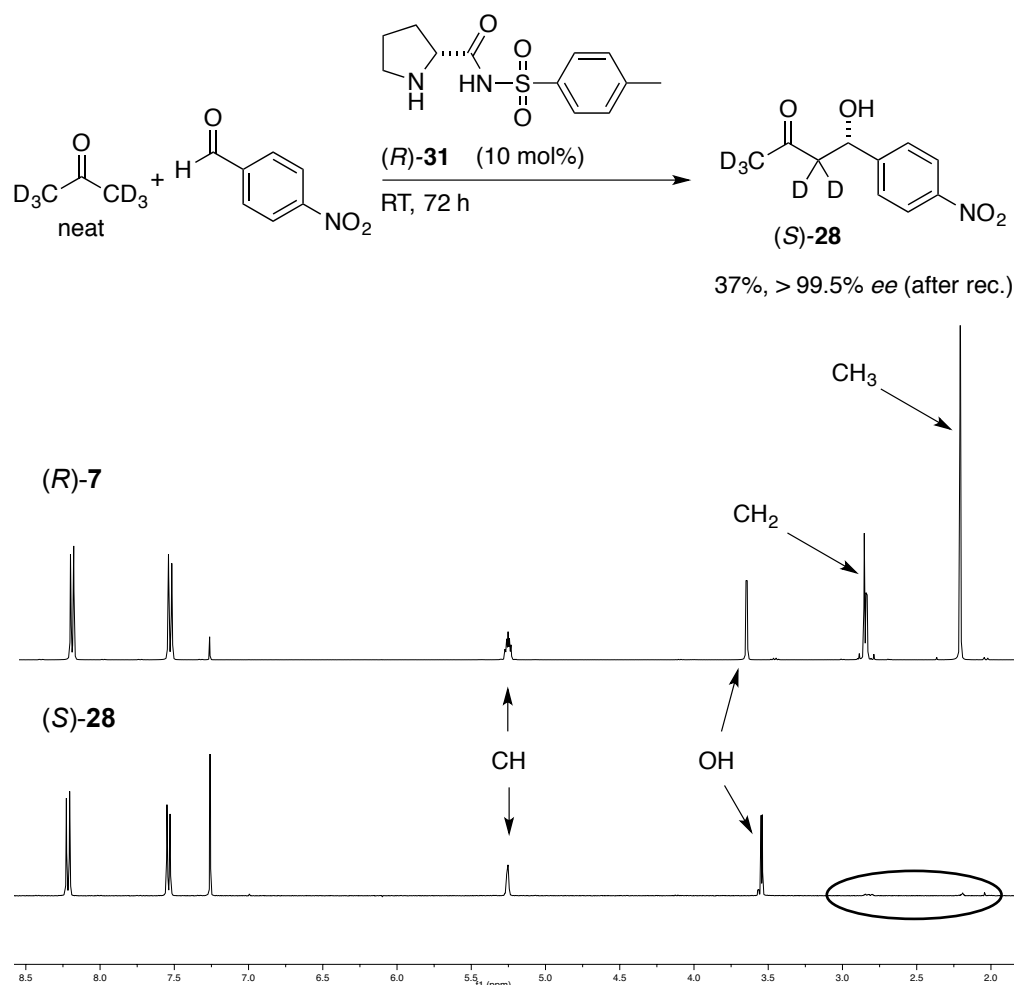
Figure 20: Synthesis and purity of the deuterated aldol product.

For the optimized ESI-MS screening conditions in MeOH with AcOH as dilution additive a complete scrambling of all five deuterium substituents was found and only trace amounts of the original completely deuterated enamine remained (Figure 21, left). Similar observations were made for shorter reaction times, lower temperatures and reactions in CH$_3$CN with MeOH or CH$_3$CN/AcOH as dilution solvents. Since the enamine intermediate needed to be transformed into a positively charged species the use of KI as additive after dilution was investigated. KI is a commonly applied additive and has a high solubility in many polar aprotic solvents.[55] Indeed, the potassium adduct of the enamine was visible in the ESI-MS back reaction analysis, albeit in lower intensities. However, even under anhydrous conditions[i]

---

[i] KI was dried for several hours in HV at 160 °C. The back reaction was conducted in anhydrous solvents under argon. Minor amounts of water in the ESI-MS and air contact of the diluted reaction

scrambling of up to five deuterium atoms occurred. Moreover, under conditions lacking a sufficient amount of proton sources in the system a scrambling of the enamine residue and acidic catalyst protons was observed by ESI-MS clearly apparent from the isotope pattern of the catalyst signal (Figure 21, right). This led to the assumption that similar scramblings could also occur between the non-labeled and deuterated enamine in back reaction experiments which would considerably broaden both isotope patterns. Therefore, even under carefully conducted back reaction experiments under anhydrous and aprotic conditions, a practical application of the deuterated aldol product **28** as mass-labeled quasienantiomer was found not to be suitable.
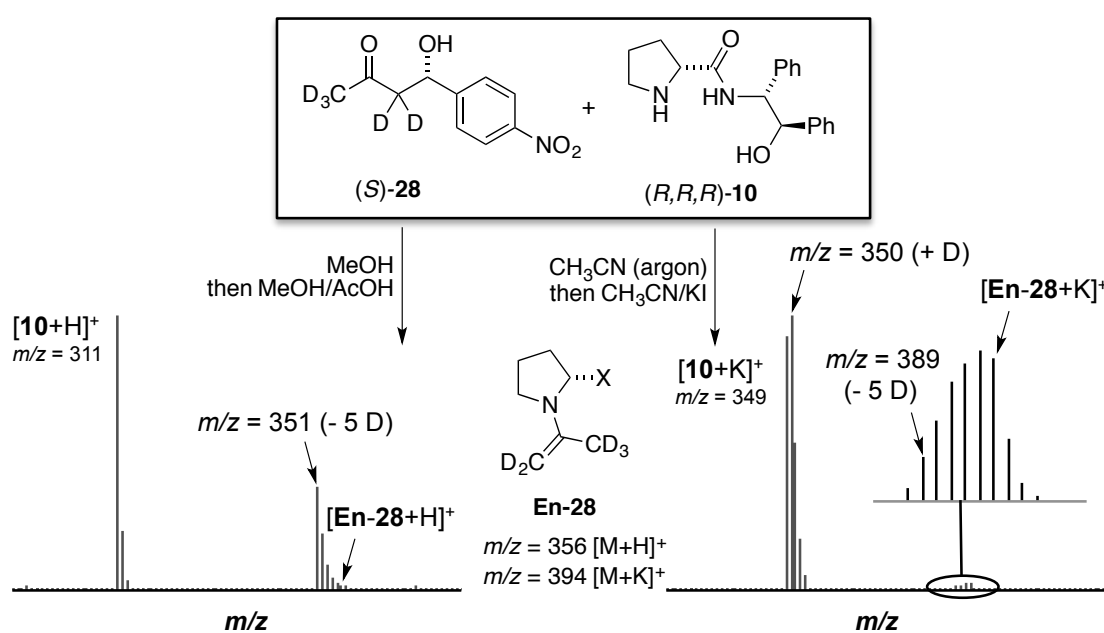
Figure 21: ESI-MS back reaction analysis using deuterated aldol product **28**. Left: back reaction under protic conditions. Right: back reaction under aprotic conditions.

2.4.3 Studies Towards the Synthesis of ^{13}C-labeled Aldol Products with Unlabeled Acetone as Test Substrate

The combination of non-labeled aldol product **7** and ^{13}C-labeled aldol product **29** differ by three mass units, affording the corresponding enamine signals sufficiently separated. The intensity of the third isotope peak (M+3) of the non-labeled intermediates considered for the screening is in general ≤1%. Drawbacks such as isotope scrambling are not existent for the ^{13}C-labeled aldol product. However, the ^{13}C-labeled acetone is rather expensive, which makes a synthesis of the product using the ketone in large excess unfeasible. Usually excess of the

mixture prior to injection could not be excluded.

aldol donor is required to avoid side reactions such as formation of a di-aldol product.

Initially, several test reactions were performed with non-labeled acetone. An organocatalyzed synthesis similar to the procedure depicted in Scheme 4 in DMSO as solvent using 2 eq. of acetone afforded the aldol product in 36% yield in 95% *ee* in 8 d. Although the selectivity was high the yield was not considered as reasonable for an excess of 2 eq. of the expensive ^{13}C-acetone. An ideal synthesis of the aldol product would employ only 1 eq.
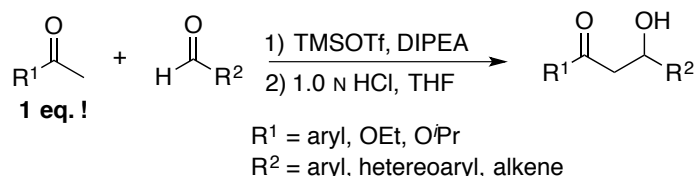
Scheme 6: Tandem enol silane formation-Mukaiyama aldol reaction.

Downey reported in 2007 a simple racemic Mukaiyama aldol reaction with *in situ* enol silane formation mediated by TMSOTf (Scheme 6).[56] This protocol was also applicable for acetone as enol precursor giving the *para*-nitrobenzaldehyde substituted aldol product **7** in excellent yield (Scheme 7). For optimal results, acetone was freshly distilled over Drierite® prior to use. It was then envisaged to obtain enantiomericly enriched products by semi-preparative HPLC separation of the racemate on a chiral stationary phase. Even partial separation of the racemate providing the enantiomers in >80% *ee* would be sufficient, since the final enantiopure aldol products could be obtained by recrystallization. Unfortunately, besides a low solubility in the HPLC eluent, no significant separations of the enantiomers were found on the available chiral columns (AD, OD). Similar separation problems were observed for *para*- (**33**) or *ortho*-chloro (**34**) substituted and benzaldehyde-derived (**18**) aldol products. A narrow baseline-separation was obtained for *ortho*-substituted aldol product (**32**). Still, broad peaks due to the polarity of the aldol product appeared in the HPLC-spectrum, which proved problematic for semi-preparative HPLC separation due to excessive signal broadening. Furthermore, under standard conditions the yield when applying *ortho*-nitro substituted benzaldehyde dropped significantly (Scheme 7).

7	R = *p*-NO$_2$	96%
32	R = *o*-NO$_2$	22%
33	R = *p*-Cl	quant.
34	R = *o*-Cl	quant.
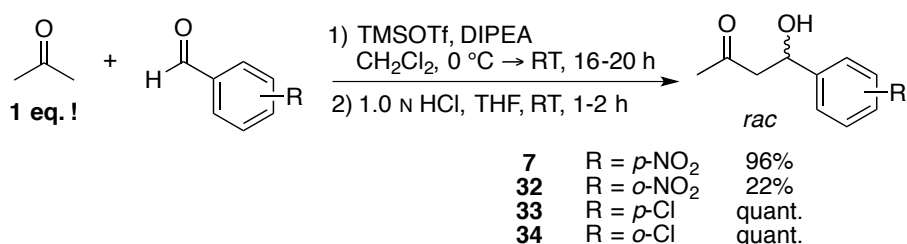
Scheme 7: Synthesis of aldol products according to the procedure of Downey.

Another separation approach was based on derivatization of the product into diastereosiomers. The alcohol function was supposed to be suitable for ester formation with (1*S*)-(−)-camphanic acid chloride (Scheme 8). ^{1}H NMR analysis of the product revealed formation of the expected 1:1 mixture of diastereosiomers. However, separation was not possible by column chromatography or various HPLC conditions. Furthermore, a parasitic elimination of the ester, destroying the stereogenic center, to form aldol condensation product **36** was observed as a side reaction and during purification by flash column chromatography on silica gel.
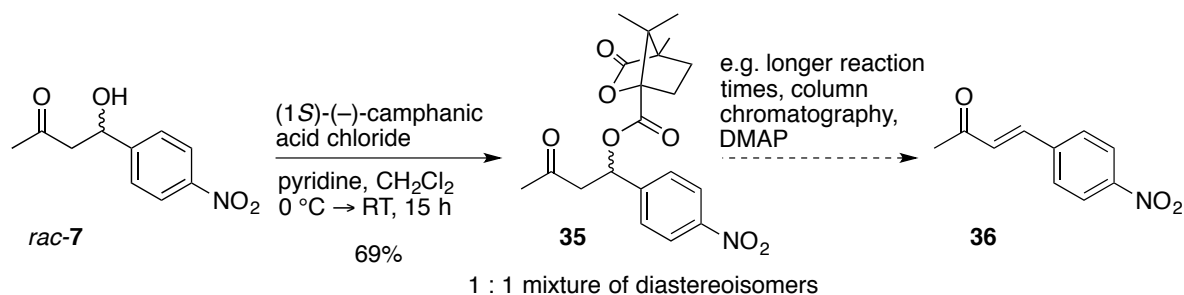
Scheme 8: Formation of diastereomers with (1*S*)-(−)-camphanic acid chloride and side reaction to the aldol condensation product.

Since the comparatively high polarity of the aldol products was one reason for the poor HPLC separations, derivatization into less polar compounds was considered as an alternative. The use of silyl-protecting groups, which can be readily introduced and removed should also significantly decrease the polarity of the molecule. During the course of the Mukaiyama aldol reaction the TMS-ether is formed. However, this intermediate appeared not to be stable as partial deprotection already occurred during the reaction and/or isolation of the compound. Additionally, under the conditions used for HPLC the separation did not significantly improve, although sharper peaks where observed. Aldol products **7** and **33** were derivatized with TBSCl and TBDPSCl. The *ortho*-substituted derivatives **32** and **34** were not used due to a low yield in the Mukaiyama aldol reaction or a low melting point of the aldol product, which would complicate a final recrystallization, respectively. An *in situ* TBS-protection by using TBSOTf instead of TMSOTF as a reagent in the Mukaiyama aldol reaction was not considered, since a significant rate deceleration was reported by DOWNEY providing low yields even after 72 h reaction time.[56] Sharp peaks and an acceptable separation were finally found for the TBS-ether of **7**. A protection protocol adopted from DIAS with silver nitrate[i] as activator emerged to be well suited affording the product in good yield.[57]

---

[i] Only moderate yields were obtained applying a protection procedure with imidazole and DMAP.
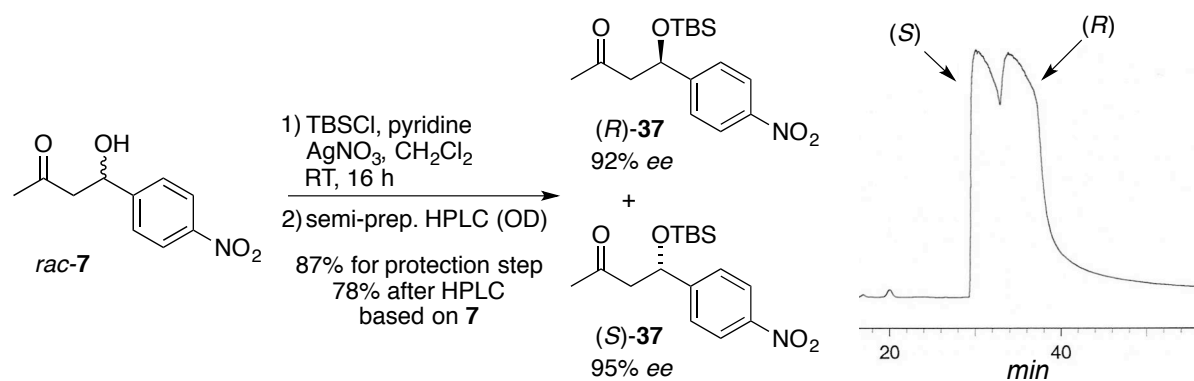
Figure 22: Synthesis and semi-preparative HPLC separation of the TBS-protected aldol product (semi-preparative HPLC trace, Chiralcel OD, hexane/^{i}PrOH 99:1, 6 mL/min, 265 nm, 20 °C).

For the subsequent deprotection it was important to prevent formation of the aldol condensation product **36**. TBAF and *in situ* HCl formation from AcCl in MeOH[58] emerged as too harsh. Again conditions described by DIAS proved superior, providing full conversion with formation of only a small amount of the side product **36** (Table 1, entry 5).[57]

Table 1: TBS-deprotection of the test substrate **37**.
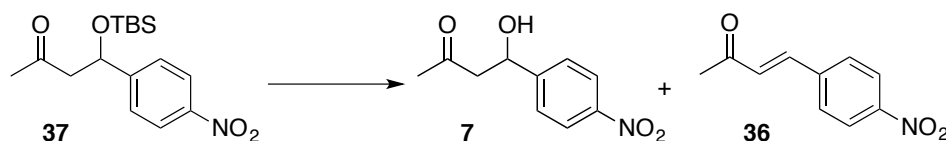
entry	solvent	reagent	T	t [h]	yield [%] 7	yield [%] 36
1	THF	TBAF 4.0 eq.	RT	2	decomposition	
2	THF	TBAF 1.5 eq.	0 °C	0.5	17	n.d.[a)]
3	MeOH	AcCl 2 x 0.15 eq.	RT	16	43	n.d.[a)]
4	MeOH	AcCl 0.2 eq.	0 °C → RT[b)]	30	60 (7:3)[c)]	
5	CH$_3$CN/CH$_2$Cl$_2$ 4:1	HF$_{(aq)}$ 6 eq.	0 °C → RT	30	94	6[c)]

a) Not determined. b) Incomplete conversion at 0 °C, formation of the condensation product at higher temperatures. c) Overall yield. Ratio determined by ^{1}H NMR analysis of the crude product.

2.4.4 Preparation of ^{13}C-labeled Aldol Products

The synthesis of the enantiopure ^{13}C-labeled racemic aldol product **29** was performed by applying the reaction conditions optimized for the non-labeled acetone derivatives presented in Chapter 2.4.3 (Scheme 9). Surprisingly, for the corresponding Mukaiyama aldol reaction only a poor yield of 46% was obtained with the commercially available isotope-labeled acetone. As described above, the acetone was freshly distilled over DRIERITE® prior to use. The same treatment was not possible with an amount of 250 mg ^{13}C-acetone. However, with molecular sieves as reaction additive a similar improvement in the yield was observed and the racemic ^{13}C-labeled aldol product **29** was again isolated in 92% yield. Careful separation of the enantiomers by semi-preparative HPLC on a chiral stationary phase (OD) gave both enantiomers of the TBS-protected product **38** in even higher enantiomeric purity as that initially obtained for the non-labeled product. Using an immobilized version of the OD column (IC column)[i] allowed for further improvement of the separation. Thus, the enantiomer eluting first was obtained in perfect enantiopurity of >99.5% *ee*. (Scheme 9, blue path). Deprotection and recrystallization afforded both enantiomers in >99.5% *ee*. The side product formation during the deprotection step was reduced by slower warm-up from 0 °C to room temperature.
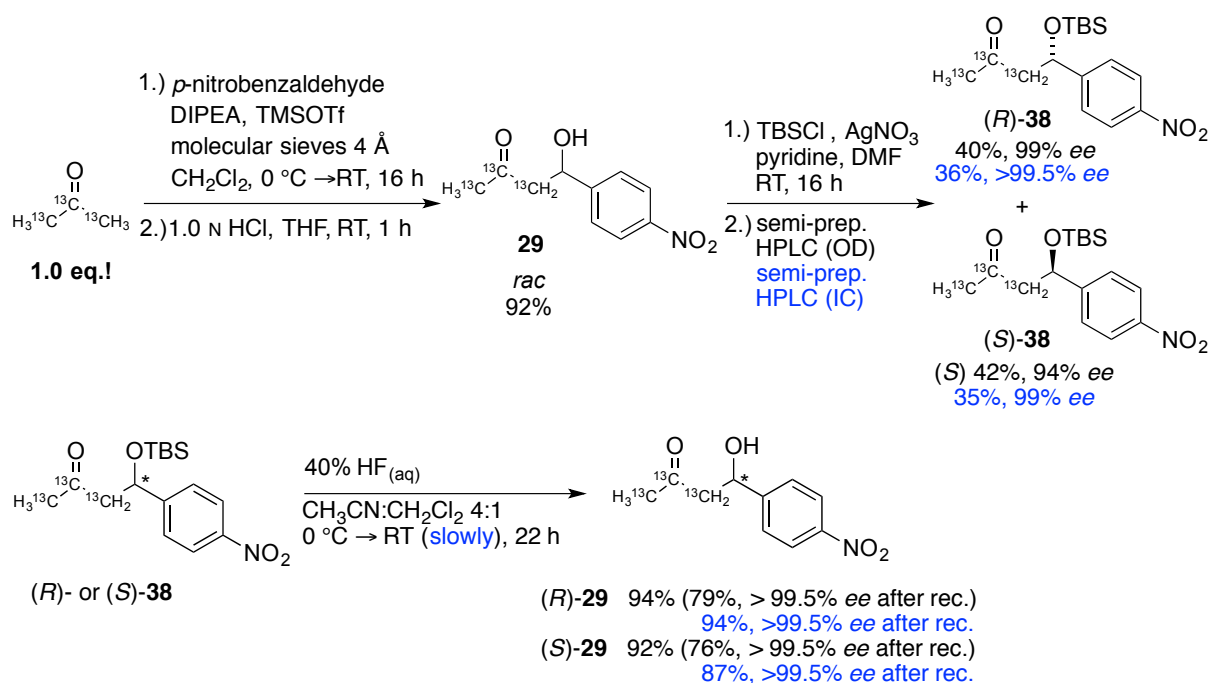
Scheme 9: Synthesis of both enantiomers of the ^{13}C-labeled aldol product **29** starting from 1 eq. of ^{13}C-labeled acetone. Semi-preparative HPLC initially conducted with **OD** column (**black path**). Later, improved separation of the enantiomers was achieved with a new available **IC** column (**blue path**).

---

[i] The IC column was purchased after a first separation of ^{13}C-labeled material.

In summary, the synthesis of the enantiopure aldol products (>99.5% *ee*) was achieved in 57-59% overall yield. Starting from 250 mg ^{13}C-acetone (approx. 300 CHF) an amount of quasienantiomers was isolated sufficient for more then 400 ESI-MS screening experiments (back reaction scale: 5 μmol of each quasienantiomer), making this protocol feasible for the synthesis of ^{13}C-labeled aldol products in >99.5% *ee*.

2.5 Elaboration of a General ESI-MS Screening Protocol

2.5.1 Influence of the Mass-Label

With a pair of potential mass-labeled substrates in hand the influence of the ^{13}C-tag on the signal intensity and selectivity was investigated (Figure 23).
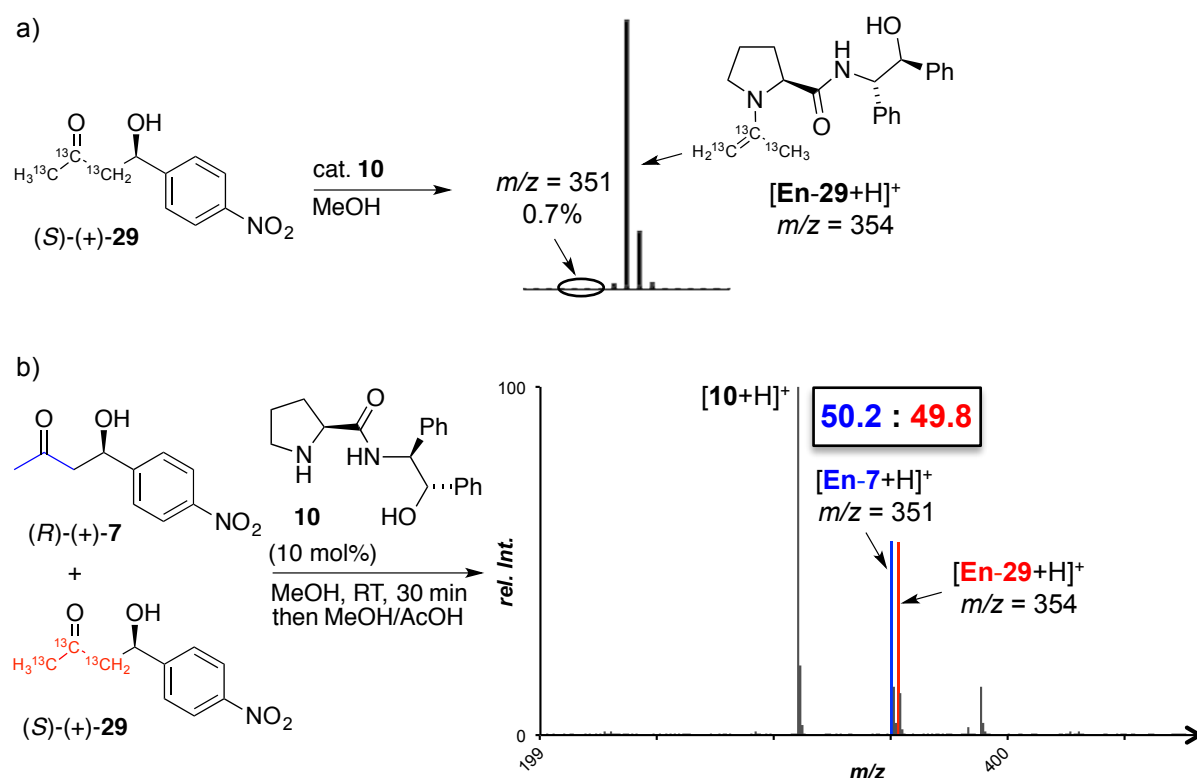
Figure 23: a) Enamine isotope pattern derived from the back reaction with aldol product **29**. b) Back reaction applying an equimolar mixture of the quasienantiomeric (+)-aldol products.

The enamine from aldol product **29** was clearly formed in the back reaction and the intensity of a non-labeled enamine signal (*m/z* = 351) at 0.7% was negligible and only slightly higher then the noise of the spectra (Figure 23a). The back reaction was conducted with an equimolar

mixture of aldol products **7** and **29** having the same configuration of the stereogenic center.[i] As the isotope-labeling was supposed to have no influence on the selectivity and electrospray ionization efficiency a **50**:**50** ratio of the enamine intermediates **En-7** and **En-29** was expected as the catalyst should not distinguish between labeled and unlabeled (+)-enantiomers. And indeed, a ratio of **50.2**:**49.8** was found for the reaction intermediates (Figure 23b) proving that the mass-label has no influence.

2.5.2 First Results, Influence of Dilution Conditions and an Unexpected Additive Effect

Having identified suitable quasienantiomers, initial back reaction experiments were performed with organocatalysts **10** and **13** in MeOH. For this purpose, a 1:1 mixture of the quasienantiomers ((+)-**7**/(–)-**29** or the inverse labeled combination (–)-**7**/(+)-**29**) in MeOH was stirred with the organocatalyst (Figure 24). To validate the screening results, the enantioselectivity of each catalyst was determined by conventional HPLC analysis of the products obtained in corresponding preparative forward reactions with 10 eq. of acetone in 24 h reaction time to ensure sufficient conversions but otherwise under identical conditions as applied in the back reaction experiment (Figure 24c). HPLC conditions were identified that allowed for a direct determination of the enantioselectivity from the crude product after filtration of the reaction mixture through a short pad of silica. Alternatively, an aliquot of the reaction mixture was purified by preparative TLC prior to HPLC analysis, which was found to be a preferable method, especially for catalysts forming the product in low conversions.

Both catalysts applied to the back reaction screening showed a clear preference for the (+)-quasienantiomer forming the corresponding enamine as the major intermediate (Figure 24a and b). Moreover, an excellent agreement between the enamine ratios (**En-7**/**En-29**) monitored by ESI-MS and the enantioselectivities induced in the forward reaction were obtained. Finally, the same intermediate ratio was observed for both combinations of quasienantiomers ((+)-**7**/(–)-**29** and (–)-**7**/(+)-**29**). Again, this provided clear evidence that the mass-label has no influence on the selectivity of the catalyst and additionally demonstrates the reproducibility of the protocol.

---

[i] According to the CIP nomenclature the ^{13}C-isotope is higher in priority then the ^{12}C-isotope. Therefore, a (R)-^{12}C (S)-^{13}C combination reflects a pair of quasienantiomeric products bearing the same configuration of the stereogenic centers. To avoid confusion the sign of the optical rotation is used in following denotations.
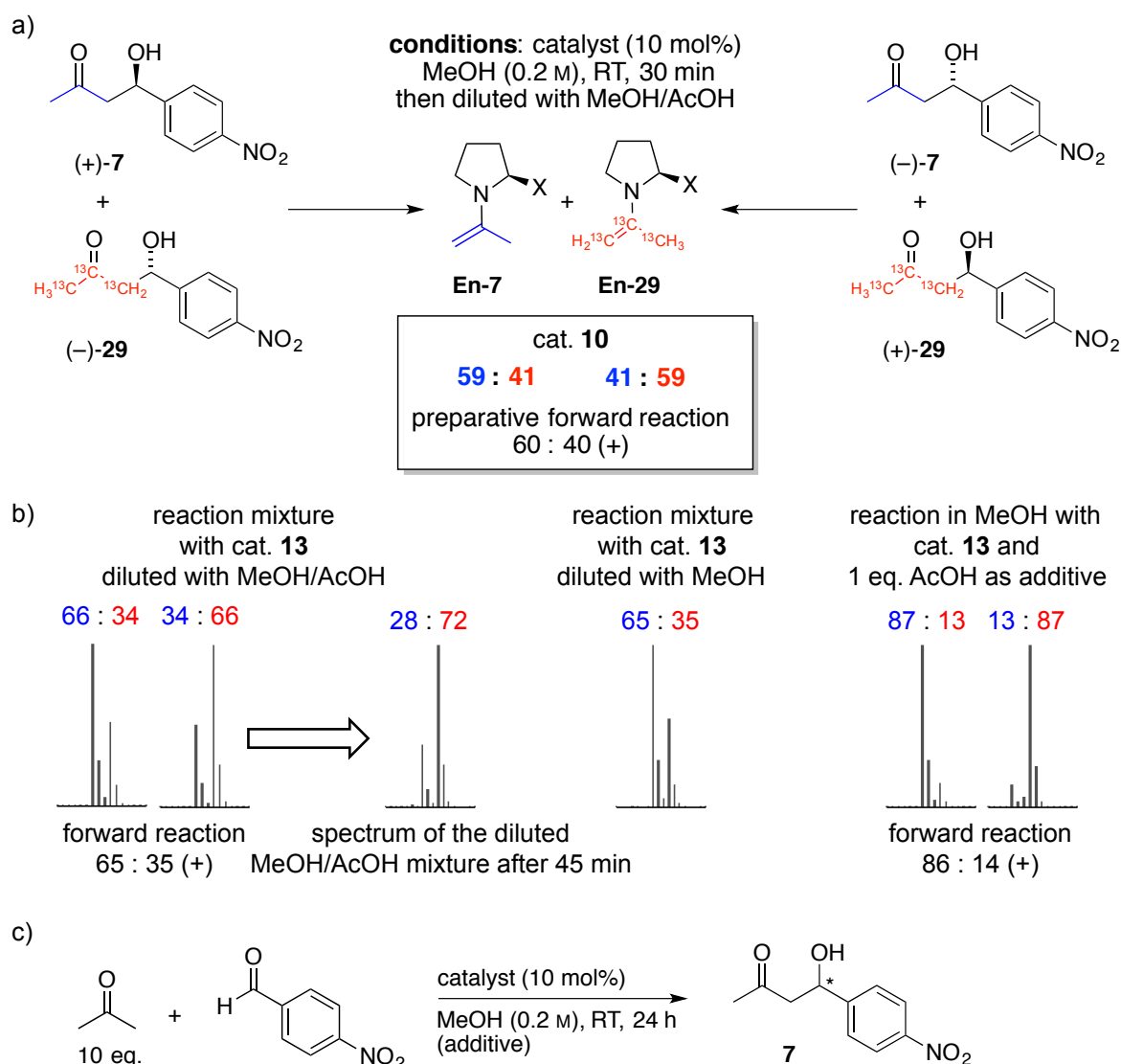
Figure 24: a) General scheme of the ESI-MS back reaction screening and results obtained with organocatalyst **10**. b) ESI-MS intermediate ratios for the back reaction with SINGH'S catalyst **13** under different dilution conditions and with acetic acid as reaction additive. c) General scheme for the preparative forward reaction for a validation of the screening results.

In order to probe whether the dilution agent influences the intermediate ratio initially formed in the reaction mixture during the back reaction, the diluted reaction mixture was again subjected to ESI-MS analysis after 45 min standing at room temperature. Surprisingly, a slight increase of the signal ratio to 28:72 was detected. This suggests that AcOH, present in the dilution solvent, might influence the enamine ratio. However, in the time scale of the measurement (1-3 min) the influence seems to be negligible. This was further proven in an independent experiment applying pure MeOH without AcOH for the dilution whereupon a comparable ratio of 65:35 was found (Figure 24b, middle). Therefore, AcOH is an acceptable dilution additive for screenings in MeOH as long ESI-MS analysis is fast.

The results mentioned above indicate that even in the diluted mixture a back reaction takes place forming enamine intermediates reflecting the selectivity of the catalyst under these "new" conditions. Since the ratio increased after dilution, AcOH was supposed to have a beneficial effect on the catalysts' selectivity. Indeed, conducting an ESI-MS back reaction experiment with 1 eq. of AcOH as additive for the reaction the enamine ratio increased to 87:13 (Figure 24b, right). The same effect of AcOH was observed in the preparative forward reaction with 1 eq. AcOH as additive giving an enantioselectivity of 86:14, confirming the ESI-MS results. This highlights very nicely that the ESI-MS screening protocol is not only a suitable method for catalyst screening, it also allows to study the influence of reaction additives on the selectivity of the catalyst.

2.5.3 CH$_3$CN as Solvent for the ESI-MS Screening

Having established conditions that allowed proof of concept of the ESI-MS screening, reaction conditions should be applied allowing for induction of higher enantioselectivities. Presumably, MeOH as a protic solvent prevents an efficient hydrogen-bonding framework leading to low energy differences between the stereo-discriminating transition states, therefore complicating a determination of the impact of the structure-selectivity relationships among the investigated catalysts. Thus, the ESI-MS screening was performed in CH$_3$CN as aprotic solvent. The aldol reaction was not only supposed to afford higher selectivities in CH$_3$CN, this solvent was already identified to be a suitable solvent regarding enamine formation in the back reaction (see Chapter 2.3.1, Figure 18). Additionally CH$_3$CN is applicable for ESI-MS injection and therefore it is a suitable solvent for dilution of the reaction mixture. However, due to the lack of a proton source in the system an acid additive is still necessary in order to obtain ESI-MS detectable positively charged species by protonation of the intermediate enamine. KI as additive failed to produce consistent enamine-potassium adducts in acceptable signal-to-noise ratios.

The main intention of the ESI-MS screening is first and foremost the identification of the most selective catalyst rather than an exact determination of the selectivity value. For that purpose, a third aminoalcohol derived organocatalyst **9** was synthesized according to a procedure reported in the literature.[42a] Together with amines **13** and **10** a set of three different selective organocatalysts was available to prove whether their selectivity trend is also reflected by ESI-MS analysis (for reported results in neat acetone see Chapter 2.3.1,

Figure 11 and Figure 14). With those catalysts in hand the ESI-MS back reaction screening was initially performed with 10 µmol of each quasienantiomer in 200 µL CH_3CN (0.1 M). The reaction mixture was stirred for 30 min and then diluted with 1 mL CH_3CN and 10 µL AcOH (Table 2, entry 1, 6 and 8). For all catalysts the determined enamine ratios demonstrated an increased selectivity in CH_3CN compared to MeOH in favor of the (+)-enantiomer, which is in line with the preparative reactions. Furthermore, again for both combinations of quasienantiomers the same enamine ratio was observed, proving that also in CH_3CN the mass-label has no influence. However, whereas the ESI-MS results reflected only minor differences between the selectivities for the different catalysts (73:27 → 79:21) a stronger trend was found for the preparative reactions (62:38 → 88:12).

The question arose why the ESI-MS results differ from the preparative results and do not reflect the selectivity trends. A similar behavior was found for back reactions in CH_2Cl_2 after dilution with MeOH/AcOH. Dilution with CH_2Cl_2 and AcOH as an additive was not suitable for ESI-MS analysis. Whereas for catalyst **13** an excellent agreement with the preparative result was found (88:12 ESI; 88:12 prep.) a considerable mismatch scenario without maintaining the selectivity trend was observed for catalyst **10** (68:32 ESI; 76:24 prep.) and **9** (76:24 ESI; 61:39 prep.). To avoid additional parameters that could influence signal ratios, the focus was kept on back reactions in CH_3CN where dilution with the same solvent as applied for the reaction was possible. Expecting the enamine to be involved in the stereoselectivity-determining step of the forward reaction, two major problems were assumed to be responsible for this discrepancy. First, the acetic acid added to the diluted mixture could influence the enamine ratio to a greater extent than observed in MeOH. In the preparative reaction no such effect would occur as no acid is added which could lead to a deviation in the observed selectivity. Even more problematic, the initial product iminium formation in the back reaction could be slower in aprotic solvents and therefore the back reaction might no longer follow the crucial Curtin-Hammett scenario with the initial fast pre-equilibrium as described in section 2.2.

Table 2: ESI-MS back reaction screening in CH$_3$CN under various dilution conditions.

entry	catalyst	dilution protocol	ESI-MS screening (En-7/En-29)		*e.r.* (+) preparative reaction[a)]
			(+)-**7**/(−)-**29**	(−)-**7**/(+)-**29**	
1		CH$_3$CN AcOH (10 μL)	79 : 21	22 : 78	
2		CH$_3$CN AcOH (3 μL)	81 : 19	18 : 82	88 : 12
3	**13**	CH$_3$CN[b)] AcOH (3 μL)	81 : 19	19 : 81	89 : 11[e)]
4		CH$_3$CN (N$_{2(l)}$)[b,c)] AcOH (3 μL)	82 : 18	n.d.[d)]	
5		MeOH	82 : 18	n.d.	
6	**10**	CH$_3$CN AcOH (10 μL)	74 : 26	26 : 74	80 : 20
7		MeOH	n.d.	39 : 61	
8		CH$_3$CN AcOH (10 μL)	74 : 26	27 : 73	
9		CH$_3$CN AcOH (3 μL)	72 : 28	n.d.	
10	**9**	CH$_3$CN (N$_{2(l)}$)[c)] AcOH (3 μL)	72 : 28	n.d.	62 : 38
11		CH$_3$CN	n.d.	45 : 55[f)]	
12		MeOH	n.d.	48 : 52	

a) Preparative forward reaction was conducted with 10 eq. acetone and 10 mol% catalyst in CH$_3$CN (0.1 M) at RT for 24-48 h. *E.r.* was determined by HPLC on a chiral stationary phase. b) Back reaction was stirred for 5 min at RT. c) The dilution solvent was frozen in liquid nitrogen prior to addition to the reaction mixture. d) Not determined. e) Forward reaction conducted with 2 eq. of acetone. f) Poor signal-to-noise ratio.

To gain further insight into the mismatch of ESI-MS and preparative results the effect of dilution on the ESI-MS ratios was further evaluated. The influence of AcOH on signal ratio alterations seemed to be higher than observed under screening conditions in MeOH. By reducing the amount of AcOH added after dilution the ratio of enamine intermediates improved slightly when applying catalyst **13**. Reducing the reaction time to 5 min and dilution with pre-cooled CH$_3$CN or MeOH did not further influence the signal ratio (Table 2, entry 2-

5). Especially with MeOH as the diluting solvent fast signal alteration was observed even in the time scale of the measurement (1-3 min). Bearing in mind that the selectivity of catalyst **13** was significantly lower in MeOH (66:34), this again provides clear evidence for a proceeding back reaction even after dilution, adjusting a new enamine ratio correlating to the selectivity under dilution conditions.[i] In an extreme case, the enamines formed in the back reaction are immediately hydrolyzed during the dilution process followed by generation of signal ratios dominated completely by the new environment. This was further supported for ESI-MS screenings of catalysts **10** and **9**. When these reaction mixtures were diluted with MeOH, significantly lower signal ratios of 39:61 and 48:52 (Table 2, entry 7 and 12) were detected compared to the standard protocol (26:74 and 27:73). Moreover, for catalyst **9** the enamine intermediate ratio after dilution with pure CH_3CN (45:55, Table 2, entry 11) supported the value obtained from the MeOH solution, although an exact determination of the ratio was not possible due to the poor signal-to-noise ratio. Additionally, the signal ratios were relatively stable without significant change over time. This led to the assumption that for these systems the enamine ratio is indeed completely dominated by the dilution conditions, in contrast to the ESI-MS ratios derived from catalyst **13**.[ii] The different behavior could be explained by higher intermediate concentrations due to faster back reactions and/or improved stability of the enamine intermediate leading to a decreased extent of hydrolyzation of this intermediate when diluting the reaction mixture. In fact, the enamine signal intensity of catalyst **13** was found to be higher than for catalyst **9** by ESI-MS analysis of the back reaction.[iii] However, the ESI-MS observation does not allow for a conclusive result if higher intensities are based on the concentration of reaction intermediates or a better ionization efficiency. Therefore, the back reaction was also analyzed by ^{1}H NMR after different reaction times (Figure 25). The formation of *para*-nitrobenzaldehyde demonstrated that C–C bond cleavage took place in NMR detectable amounts already after 5 min reaction time. In addition, after 120 h complete decomposition of the catalyst was observed. A comparison of the aldehyde intensity for catalyst **13** and **9** revealed that amine **13** catalyzes the *retro* reaction more efficiently. Due to hydrolysis and the different stability of the enamines, their concentration is not directly reflected by the aldehyde concentration. Nevertheless, a more efficient back reaction should also lead to higher enamine concentrations and therefore, for catalyst **13** indeed more enamine intermediates should be available in the reaction mixture

---

[i] Nevertheless, higher dilutions would also reduce the amount of reaction intermediates in the analyte leading to problems with the detection limits.

[ii] Clear evidence was found in further studies with acid additives discussed in the following Chapter.

[iii] This fact became especially obvious in later experiments with *tert*-BNP as additive.

subjected to ESI-MS analysis. Although the back reaction was found to be slower for catalyst **9** it could not be excluded that a cooperative stability effect is also contributing. The sterically less hindered primary and secondary hydroxyl group in catalyst **10** and **9** could potentially participate in the hydrolysis process and accelerate this step.
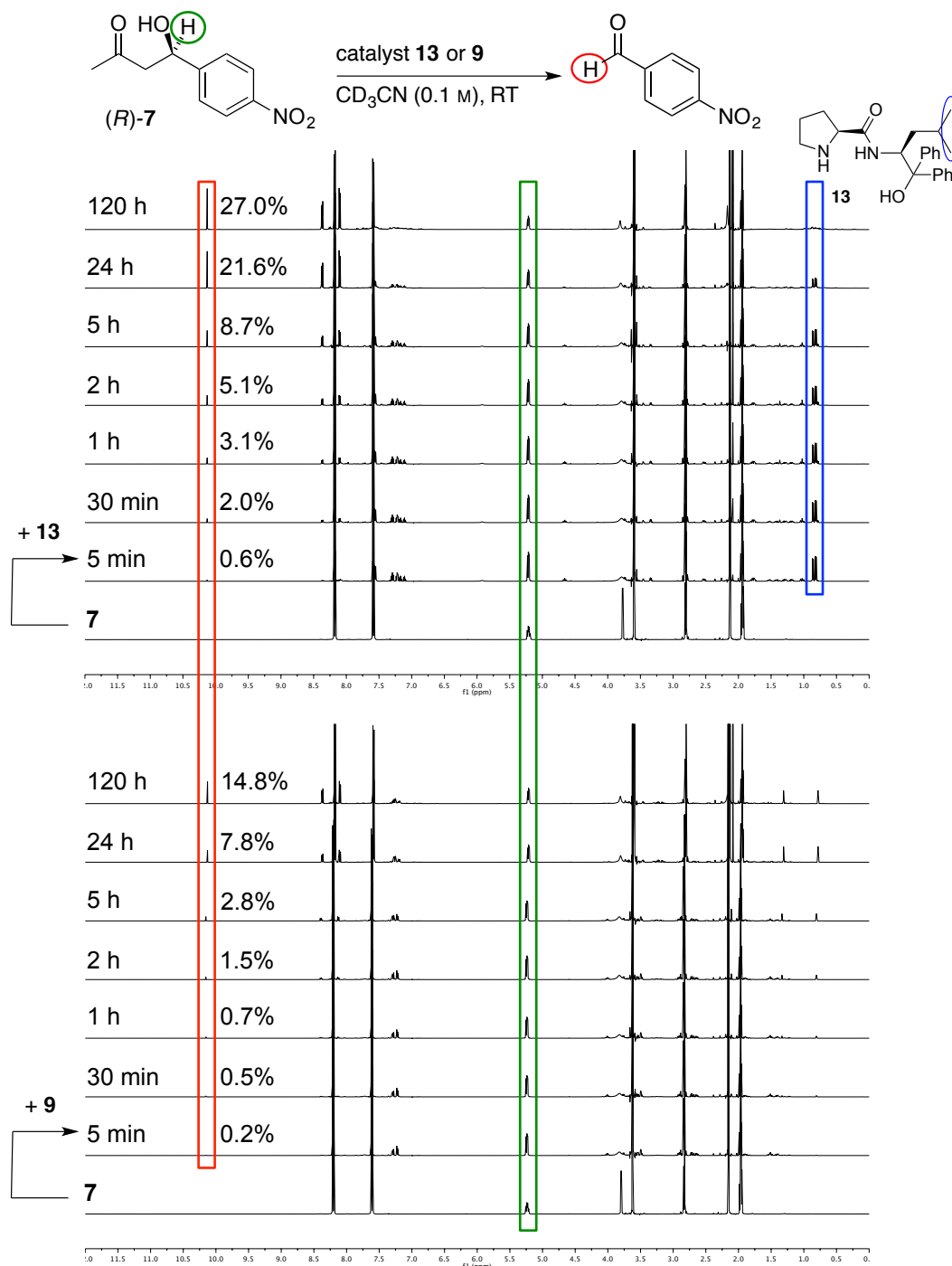
Figure 25: ^{1}H NMR analysis of the *retro* aldol reaction under ESI-MS screening conditions catalyzed by organocatalyst **13** (top) and **9** (bottom) with dioxane as internal standard.

2.5.4 Acids as Reaction Additives for the ESI-MS Back Reaction Screening in CH₃CN

The findings discussed in the previous section provide clear evidence for the influence of dilution conditions on the signal ratios. However, an ineffective pre-equilibrium might still contribute to further discrepancies between the ESI-MS results and the preparative enantioselectivities. In either case, by conventional ESI-MS analysis it is hard to distinguish and assign the disagreement to either one or the other effect. Addition of acid additives not during the dilution process, but instead already as additive to the reaction mixture was assumed to solve both problems simultaneously. Under acidic conditions the iminium formation should be accelerated and no further additive to protonate the enamine during the dilution is necessary. The influence of acidic additives on the forward and the back reaction is depicted in Table 3 and Figure 26.

During the investigations of the back reaction screening in MeOH it was already found that the ESI-MS method is capable of monitoring the influence of AcOH as an additive on the selectivity of the catalyst. Therefore, the ESI-MS additive screening was initially conducted with 1 eq. (100 mol%) of AcOH (Table 3, entry 1, 6 and 9). As predicted, for all three catalysts the enamine ratio matched perfectly the enantioselectivity of the forward reaction, which was also conducted with 1 eq. of the acid additive. In general this shows that the use of AcOH as reaction additive eliminates both potential sources of errors, a slow pre-equilibrium and/or negative effects of other dilution conditions than those present in the reaction. This approach would provide a working screening protocol for organocatalyzed aldol reactions. However, as displayed in Figure 26, with AcOH as additive the explored catalysts no longer differed considerably in their enantioselectivity. Moreover, the selectivity trend of the catalysts changed compared to the reaction without additive. Thus, such an ESI-MS screening protocol would not allow for an identification of the most selective catalyst under more general conditions.

Table 3: ESI-MS back reaction screening with acidic reaction additives.

entry	catalyst	additive	ESI-MS screening (En-7/En-29)		e.r. (+) preparative reaction[a]
			(+)-7/(−)-29	(−)-7/(+)-29	
1		AcOH (1 eq.)	73 : 27	27 : 73	74 : 26
2		AcOH (0.1 eq.)	76 : 24	n.d.[b]	76 : 24
3	13	*tert*-BNP (0.1 eq.)[c]	**87 : 13**	**12 : 88**	**88 : 12**
4		*tert*-BNP (0.1 eq.)[d]	81 : 19	17 : 83	
5		**39**[e] (0.1 eq.)	78 : 22[f]	n.d.	78 : 22
6	10	AcOH (1 eq.)	79 : 21	23 : 77	77 : 23
7		*tert*-BNP (0.1 eq.)	59 : 41	40 : 60	75 : 25
8		*tert*-BNP (0.1 eq.)[d]	73 : 27	25 : 75	
9	9	AcOH (1 eq.)	77 : 23	24 : 76	76 : 24
10		*tert*-BNP (0.1 eq.)	52 : 48	49 : 51	68 : 32
11		*tert*-BNP (0.1 eq.)[d]	72 : 28	28 : 72	
12		*tert*-BNP (0.2 eq.)	52 : 48	n.d.	69 : 31
13		*tert*-BNP (0.2 eq.)[d]	73 : 27	29: 71	

a) Preparative forward reaction was conducted with 10 eq. acetone and 10 mol% catalyst and the illustrated amount of additive in CH_3CN (0.1 M) at RT for 24-48 h. *E.r.* was determined by HPLC on a chiral stationary phase. b) Not determined. c) 2,6-Di-*tert*-butyl-*para*-nitrophenol (*tert*-BNP). d) Additional AcOH was added to the diluted mixture prior ESI-MS analysis. e) 3,5-Di-*tert*-butylbenzoic acid **39**. f) Reaction stirred for 2 min.

Next, it was assumed that more sterically hindered and less coordinating acids might simply act as a proton shuttle and should have less influence of the transition state of the stereo-selectivity-determining step. The hydroxyl group of a bulky 2,6-di-*tert*-butyl substituted *para*-nitrophenol was supposed to be well shielded and therefore avoid a tremendous participation in the transition state *via* a hydrogen-bonding framework. Furthermore, the less acidic[i] 2,6-di-*tert*-butyl-*para*-nitrophenol (*tert*-BNP) was found to be similarly effective as AcOH as additive in the back reaction, giving the enamine intermediates in excellent intensities.

---

[i] For a more acidic co-catalyst such as *para*-TsOH no enamines were monitored in the back reaction.

Moreover, the enantioselectivities induced in the forward reaction with *tert*-BNP as additive were of a similar order of magnitude to those obtained under non-additive conditions (Figure 26). Interestingly, with Singh's catalyst **13** the ESI-MS results were in excellent accordance with the preparative results, whereas for catalyst **10** and **9** a discrepancy was still observed (Table 3). A closer look revealed that the signal ratios are similar to those obtained for the back reaction in CH$_3$CN without additive but after dilution with MeOH (Figure 26). Obviously, ESI-MS screening failed to predict the right enantioselectivity of the catalyst for these structures in the presence of *tert*-BNP or without additive. Using twice the amount of the additive did still not show a match effect (Table 3, entry 12). Application of more then 20-30 mol% of *tert*-BNP was not practical, since the additive was hard to wash out from the ESI-MS instrument, therefore the more nitrophenol that was injected the more extensive cleaning was necessary. When the back reaction mixture with *tert*-BNP as additive was diluted with a CH$_3$CN/AcOH mixture the same ratios as previously found for the screening experiment without reaction additive but AcOH as dilution additive was observed. Moreover these were in the same range as the corresponding results with AcOH as reaction additive (Figure 26). This once more proved the fact that the enamine ratios for catalyst **10** and **9** are exclusively governed by the dilution process (as soon as additional acid is used) and not from the initial ratio present in the reaction mixture. Further discussion will follow in Chapter 2.7 on the basis of additional catalyst structures applied to the back reaction screening.

In further experiments using *para*-nitrophenol as additive for the forward reaction a considerable impact on the stereoselectivity of the catalysts was observed, without any clear selectivity-trend visible (Figure 26). These results demonstrate that with the shielding *tert*-butyl substituents the selectivity outcome of the reaction is less affected. Additionally the back reaction screening results did not agree with the forward reaction.
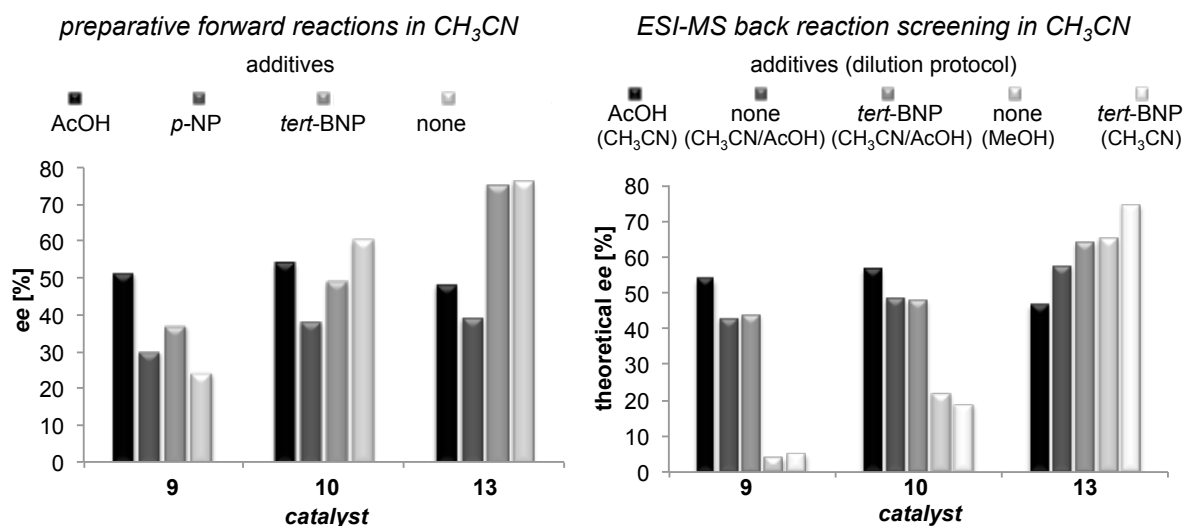
Figure 26: Influences of reaction additives on the enantioselectivity of organocatalysts **9**, **10** and **13** (*p*-NP = *para*-nitrophenol) in preparative forward reactions (left). Selectivity determined by ESI-MS screening with various additive and dilution protocols (right).[i]

Another acid investigated was 3,5-di-*tert*-butylbenzoic acid **39**, having a similar pK_a value to AcOH. The back reaction was efficient and after 2 min reaction time an excellent agreement with the forward reaction was found however with a similarly low selectivity as obtained with AcOH (Table 3, entry 5). For longer reaction times lower ratios were observed probably due to a fast racemization of the aldol products over the back and subsequent forward reaction providing the products in lower *ee* (Figure 27). In contrast, for *tert*-BNP even after 5 h back reaction time only a negligible decrease of the of the enamine ratios was measured by ESI-MS.
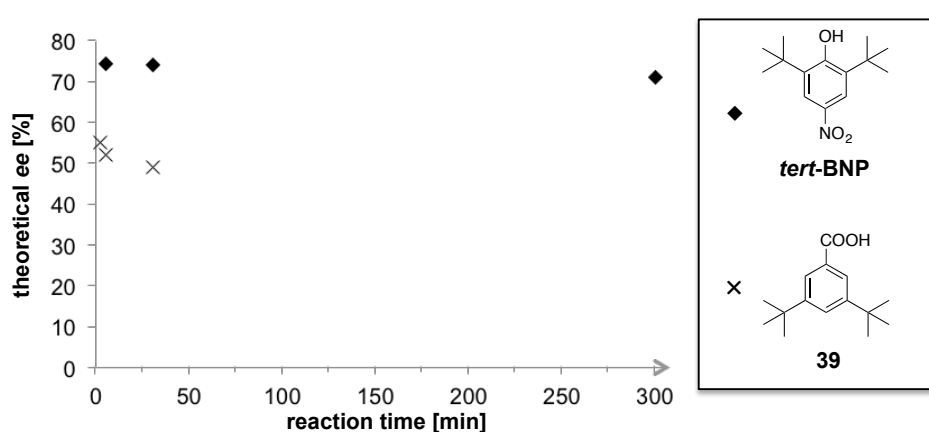
Figure 27: Decrease of enamine ratios with increasing reaction time in the back reaction.

---

[i] The theoretical *ee* was calculated as average value from the ESI-MS signal ratios derived from both combinations of quasienantiomeric aldol products.

Even though for catalysts **10** and **9** a discrepancy was observed, the correct selectivity trend of the catalysts was reflected by ESI-MS analysis of the back reaction. Therefore, the screening procedure with *tert*-BNP in CH₃CN could act as a versatile and general ESI-MS protocol. The induced selectivities are similar to those found under non-additive conditions. In addition no further manipulation of the reaction conditions during the dilution is required, in contrast to a dilution with MeOH as a source for enamine protonation. Finally, even with a reduced reaction scale of 5 μmol of each aldol product (instead of 10 μmol) the enamine intermediates were detected in good signal-to-noise ratios allowing for a suitable detection of the minor peak even for highly selective catalysts (Figure 28).
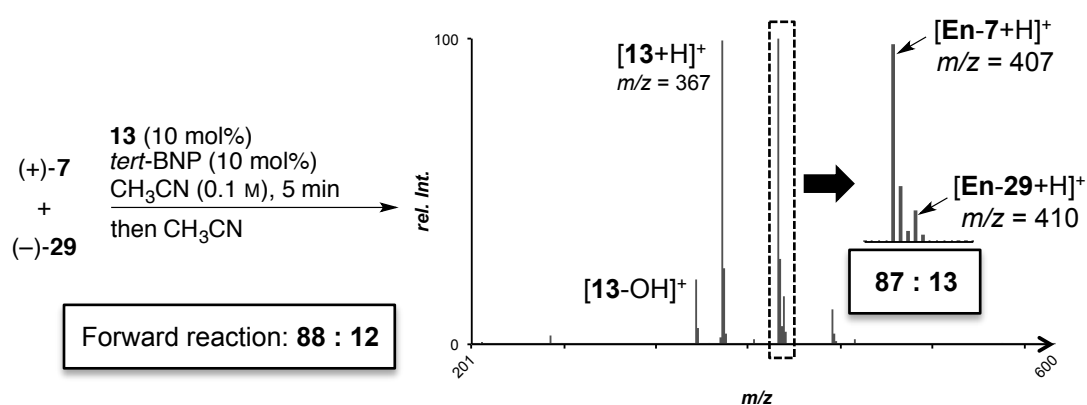
Figure 28: Selected ESI-MS spectra of the back reaction with catalyst **13** and *tert*-BNP as additive (**Table 3**, entry 3).

2.6   Catalyst Synthesis

Having identified and elaborated promising screening conditions, which work extraordinarily well for structures such as SINGH'S catalyst **13**, a small set of known and also new catalysts for further proof-of-principle studies was synthesized based on this framework. Although several modifications of this catalyst structure were already reported and applied in organocatalyzed reactions in organic and aqueous media, the disadvantages of low reaction temperatures of –40 °C necessary for aldol reactions in neat acetone (see Figure 14 for details), but also its remarkable catalytic activity in aqueous systems made this structure still to an interesting target.[44a] Catalyst structures based on the 2nd and 3rd generation were mainly applied in aqueous medium and were not found to be significantly superior compared to the best catalysts identified initially. Therefore, the focus was maintained on the 1st generation catalyst framework developed by the SINGH group (Figure 29).
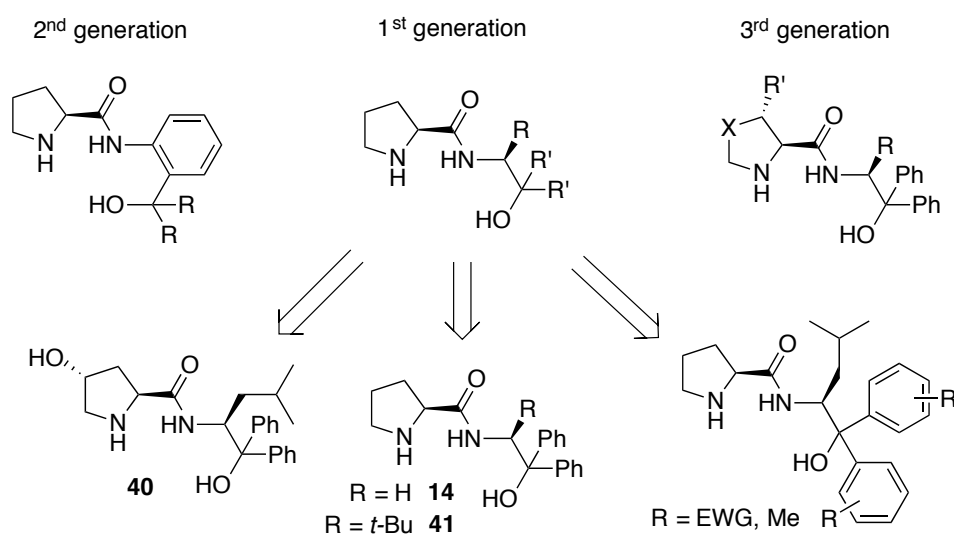
Figure 29: Potential catalysts structures derived from 1st generation SINGH type catalysts.

Catalyst **40** derived from *trans*-hydroxy proline was already applied by NAKANO and KABUTO in aldol reactions of acetone and benzaldehyde but showed no catalytic activity for this reaction.[53] It would be interesting to evaluate the behavior of such a catalyst in the ESI-MS screening. In addition, the influence of a sterically less hindered hydroxy group could be further investigated. Catalyst **14**, which was already tested in aldol reactions by the SINGH group[44b] is a perfect test compound to evaluate the influence of the side chain in ESI-MS analysis. To obtain further insight into structure-selectivity relationships, so far unknown compounds such as the *t*-Bu substituted catalyst **41** and catalysts modified at the aryl substituents, such as increasing sterical bulk or different electronic nature, are interesting candidates. In the literature only electron-donating substituted aryl groups of 1st generation

catalysts were applied leading to a drop of the enantioselectivity (see Figure 14). In contrast, an electron-withdrawing substituent at the aryl group could further increase the hydrogen-bond donor strength of the hydroxy-group, which may lead to enhanced selectivity. Such effects were observed for aldol reactions catalyzed by 2nd generation organocatalysts in aqueous medium.[44a]

The catalysts were synthesized from the Cbz- or Boc-protected proline or hydroxy proline and the corresponding aminoalcohols. The latter are available from the corresponding amino acid esters (Figure 30).
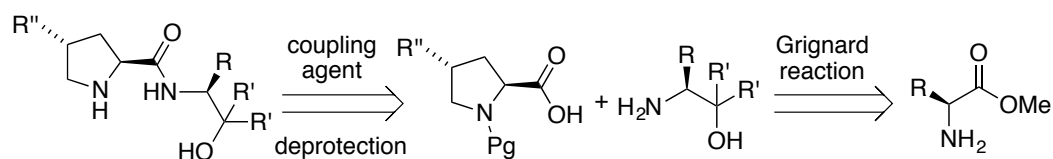
Figure 30: Retrosynthetic analysis of SINGH type catalysts.

2.6.1 Synthesis of Aminoalcohols

In order to install different aryl groups at the aminoalcohol unit bearing an iso-butyl side chain the L-leucine methyl ester hydrochloride was chosen as a commercially available precursor. *tert*-L-Leucine methyl ester hydrochloride salt **42** was synthesized starting from the corresponding amino acid using thionyl chloride in MeOH. However, under these conditions *tert*-L-leucine was considerably less reactive than the transformation of valine as described in the literature.[59] Repetitive addition of thionyl chloride finally afforded the methyl ester, containing about 7% of unreacted acid hydrochloride as an impurity in the otherwise quantitative yield after 60 h. Since a high excess of Grignard reagent was necessary the product could simply be used without further purification, as it was possible to remove the side product after the subsequent Grignard addition.
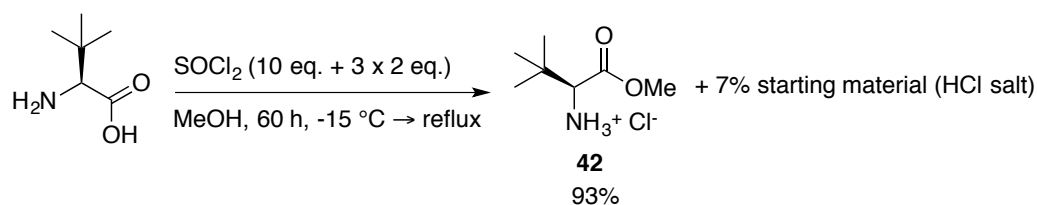
Scheme 10: Synthesis of the *tert*-L-leucine methyl ester hydrochloride.

With the amino acid precursor in hand the aminoalcohols were synthesized by *in situ* formation of the Grignard precursor from the corresponding aryl bromides (Table 4). In general 6-10 eq. of the Grignard reagent were necessary for sufficient conversions. Individual workup and purification afforded the products in good to moderate yields. Initially, 2-bromomesitylene was used as a Grignard precursor to increase the steric bulk in the final organocatalyst. For the reaction in Et$_2$O a quantitative isolation of defunctionalized mesitylene after workup indicated the successful formation of the aryl magnesium bromide. However, the activation barrier for the subsequent addition to the ester appeared to be too high. A survey of the literature revealed the problems encountered in the addition of this sterically hindered Grignard reagent. Even addition to the less hindered acetone proceeds only slowly in 22% yield.[60] Since lithiation of the arylbromide did not afford any product traces either, 5-bromo-*m*-xylene was used for the synthesis of a sterically more demanding aryl substituent, where the Grignard reaction worked again smoothly to form the desired aminoalcohol **44**. The synthesis of CF$_3$-aryl-substitued aminoalcohol also worked well, even though after coupling with proline the formation of diastereomers gave evidence for a racemization of the aminoalcohol. This will be discussed in more detail in section 2.6.2.

Table 4: Synthesis of aminoalcohols by double Grignard additions to the ester.
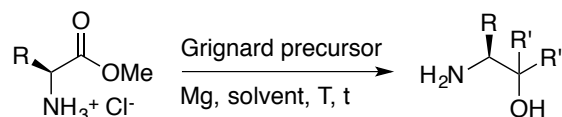
entry	R	Grignard precursor	solvent	T	t	yield (product)
1	iso-Bu	◯—Br	THF	RT	4 h	41% (**30**)
2	*tert*-Bu	◯—Br	Et$_2$O	RT	overnight	70% (**43**)
3	iso-Bu	◯—Br	Et$_2$O	RT	20 h	n.c.[a)]
4	iso-Bu	◯—Br	THF	reflux	18 h	n.c.
5	iso-Bu	◯—Br	THF	reflux	3 h	52% (**44**)
6	iso-Bu	F$_3$C—◯—Br	THF	0 °C → RT	4 h	68% (**45**)

a) No conversion.

The aminoalcohol **46** bearing no side-chain was synthesized from commercially available aminoacetophenone hydrochloride in good yield (Scheme 11).
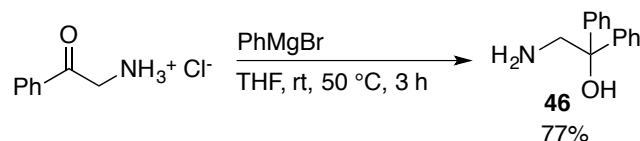
Scheme 11: Synthesis of aminoalcohol **46**.

2.6.2 Synthesis of Pyrrolidine-based Organocatalysts

Having synthesized a small library of aminoalcohols, efficient coupling reactions based on common reagents were elaborated. Hydroxy-proline derived catalyst **40** was synthesized according to a literature known procedure,[53] without purification of the protected intermediate (Scheme 12). The secondary hydroxy group was selectively protected using silyl chlorides. Blocking the secondary alcohol function was of interest to evaluate its effect on the ESI-MS screening. Although as mentioned above, the parent catalyst was reported to be not active in aldol reactions, possibly protection of the alcohol could increase the reactivity. If this position also influences the selectivity, this would allow for an easy synthesis of catalyst mixtures for the multi-catalyst ESI-MS screening.
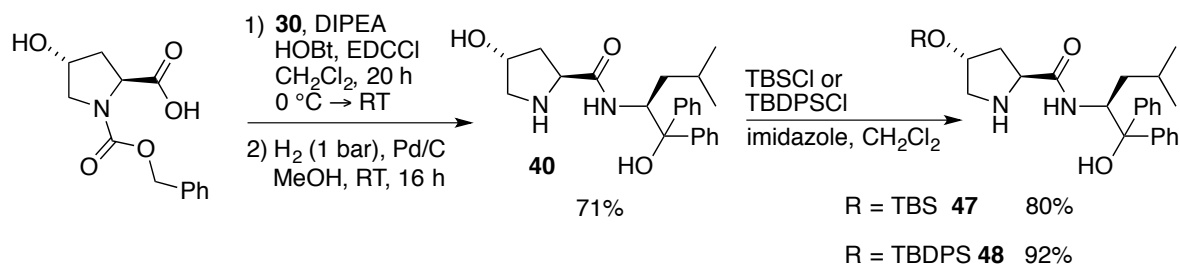
Scheme 12: Performed synthesis of organocatalyst **40** and subsequent TBS and TBDPS-protection to its analogs.

The same protocol failed to afford the coupling product for proline and the *tert*-butyl substituted amine **43**. Activation of the acid with ethyl chloroformate also afforded less then 5% of the organocatalyst. Finally, a protocol using HATU and DIPEA in DMF was found to be a suitable coupling method for amid formation. After simple filtration of the protected amine intermediate through a short plug of silica gel, subsequent Cbz-deprotection afforded organocatalyst **41** in good yield over two steps (Scheme 13). With the same protocol, the yield of amine **49** after coupling of proline and aminoalcohol **44** was considerably improved

from 45% with HOBt up to 90% with HATU. This procedure generally worked well for several catalysts. The embedded purification step involving filtration of the Cbz-protected intermediate performed well, removing more polar impurities, which would have complicated a purification of the final catalyst. However, Cbz-protected intermediate **41** was hardly soluble in the eluent and was therefore first adsorbed onto silica gel prior to filtration and eluted with the a threefold quantity of solvent. Catalyst **49** was isolated as a colorless foam. Although treatment with hexane afforded a solid, solvent traces were not completely removed even after several days in high vacuum. Recrystallization under several conditions was not successful for this catalyst.

R = *tert*-Bu, R' = Ph **41**   75%
R = iso-Bu, R' = 3,5-diMe-C_6H_3 **49**   90%
R = H, R' = Ph **14**   58% (after rec.)
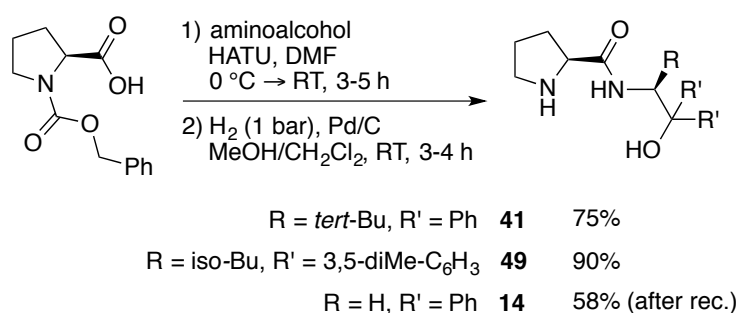
Scheme 13: HATU-mediated synthesis of organocatalysts **41, 49** and **14**.

During the synthesis of the CF_3-substituted catalyst under HOBt or HATU coupling conditions the formation of a 6:1 mixture of two diastereomers was observed (Scheme 14).[i] Only partial separation of the isomers was possible by flash column chromatography, however the pure major diastereomer was still obtained after recrystallization (>20:1).

R' = 4-CF_3-C_6H_4 73% combined yield (6 : 1)
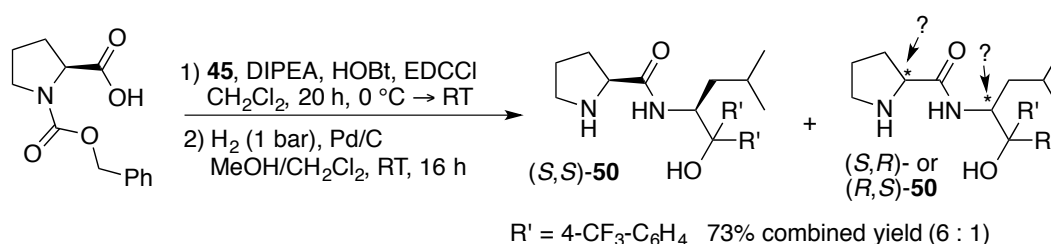
Scheme 14: Synthesis of the CF_3-substituted catalyst **50** using HOBt as coupling reagent.

Since the initially applied starting materials contained both a (*S*)-configured stereogenic center, the major diastereomer was expected to be the (*S,S*)-organocatalyst as depicted in Scheme 14. This raised the question whether an epimerization occurred at the α-carbon of proline under coupling conditions or at the stereogenic center of the side chain during the

---

[i] A clear integration of the signals in the ^{1}H NMR spectra of the crude product was not possible. The diastereomeric ratio was determined based on ^{1}H NMR analysis and quantification of the isolated and purified product fractions.

Grignard reaction. An epimerization at the α-carbon was not observed for similar couplings and the applied aminoalcohols investigated should not differ dramatically in their behavior as a potential base. Therefore, the minor diastereomer was assumed to be more likely the (*S*,*R*)-catalyst with an inverted stereogenic center in the side chain. This was further supported by the performance of the minor and major diastereomer in acetone aldolizations (Scheme 15). Both catalyzed the reaction in preference for the (*R*)-product. The stereoselectivity outcome is usually controlled by the stereogenic center at the proline moiety and indicates a (*S*)-configuration. Additionally, the selectivity was lower for the minor diastereomer suggesting a mismatch (*S*,*R*)-combination as it was observed for a similar catalyst structure (see Figure 14, Chapter 2.1.3)
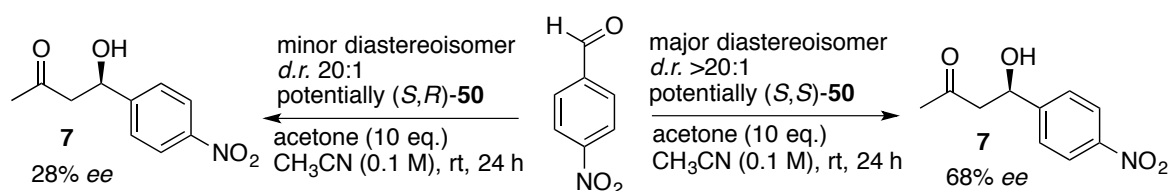
Scheme 15: Organocatalyzed aldol reactions under ESI-MS screening conditions conducted with the major and minor diastereomer of catalyst **50**.

The minor catalyst isomer was synthesized independently starting from D-leucine methyl ester hydrochloride. After the corresponding Grignard reaction, with both enantiomeric amino-alcohols in hand, HPLC conditions were established verifying the proposed racemization. For aminoalcohol (*S*)-**45** a decreased *ee* of 73% was determined (Scheme 16). This value is in excellent agreement with the monitored 6:1 ratio of the diastereomers **50** after coupling and allow for an unambiguous assigning of the absolute configuration of major and minor **50** as (*S*,*S*) and (*S*,*R*). Performing the Grignard addition with D-leucine methyl ester hydrochloride at lower temperatures of −78° → RT the racemization was not minimized and aminoalcohol (*R*)-**45** was isolated in even slightly lower *ee* of 65% (Scheme 16). Later, it was envisaged to apply organocatalyst (*S*,*R*)-**50** in an ESI-MS screening of crude catalyst mixtures. Since the method would not distinguish between the mass isomeric diastereomers, it was necessary to increase the *ee* of aminoalcohol (*R*)-**45**. Since this was not possible by recrystallization, the enantiomers were separated by semi-preparative HPLC affording the (*R*)-enantiomer in >98% *ee*.
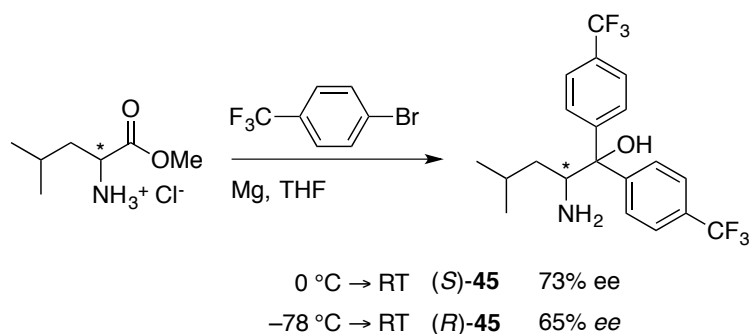
Scheme 16: *Ee* of aminoalcohol **45** after Grignard addition starting from enantiopure L- or D-leucine methyl ester hydrochloride.

The enantiomerically enriched aminoalcohol (*R*)-**45** was applied to the synthesis of organocatalyst (*S,R*)-**50** adopting a new protocol of BERKESSEL, first reported in 2012 (see Chapter 2.4.1, Scheme 2b).[52] The one-pot procedure starting from Boc-protected proline afforded the catalyst in excellent purity of the crude product and 85% yield after purification by flash column chromatography (Scheme 17). The solution of HCl in MeOH was prepared *in situ* by stirring of AcCl in dry MeOH for 30 min prior to direct addition into the reaction mixture.
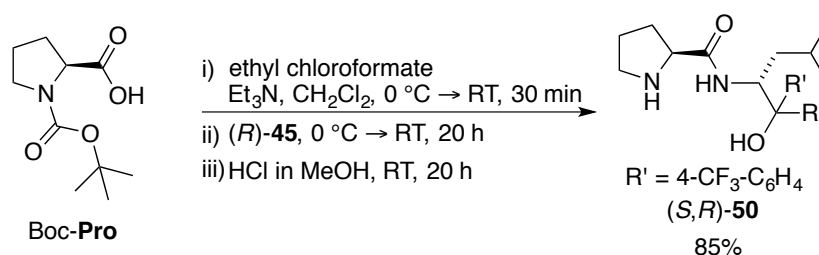
Scheme 17: One-pot synthesis of organocatalyst (***S,R***)-**50**.

To gain further insight into the influence of structural changes on the ESI-MS screening a simple proline amide **51** was synthesized bearing no additional hydroxy groups for the supporting hydrogen-bonding network. *tert*-Butylaniline was chosen as the amine coupling partner instead of aniline to improve the solubility of the catalyst in the screening solvent.
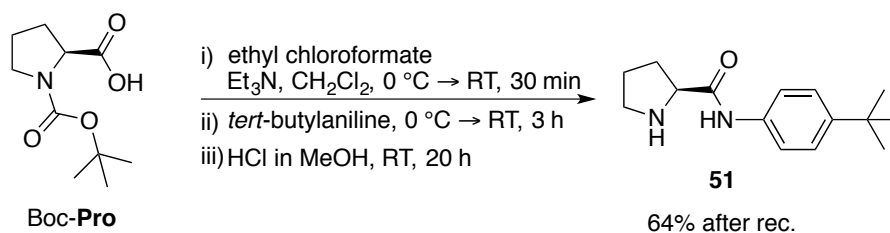
Scheme 18: One-pot synthesis of proline amide **51**.

Additionally, the secondary hydroxy group of Gong's catalyst **10** was TMS-protected to study the effect in the ESI-MS back reaction screening.
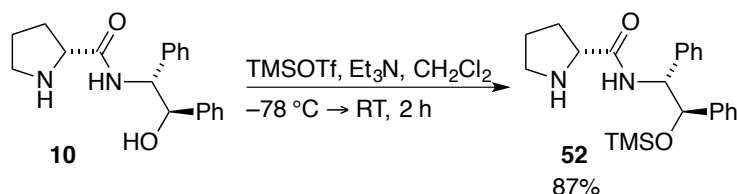
Scheme 19: Synthesis of TMS-protected catalyst **52**.

2.6.3 Synthesis of Primary Amines as Organocatalysts

The main focus on amine mediated aldol reaction relies on proline derived secondary amines. Nevertheless, primary amines were also successfully applied as catalysts for aldolizations.[24c] Therefore, primary amines were included as catalyst candidates for ESI-MS.

A primary amine catalyst similar to the structural type already studied by ESI-MS analysis was found in a literature survey (Scheme 20). Since the aminoalcohol was already available this structure was easily accessible. Moreover, in the literature amine **53** was identified as being an active catalyst with nitrophenols as additives.[61]
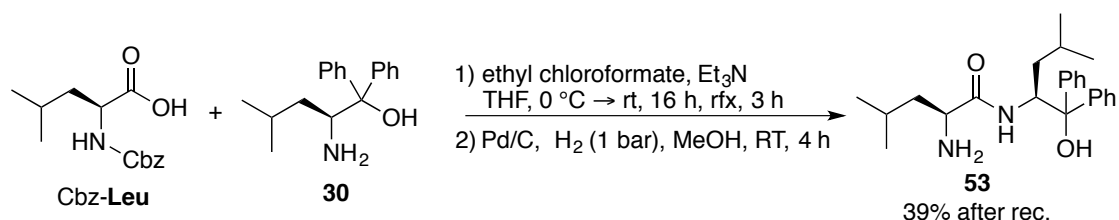
Scheme 20: Synthesis of primary amine **53** based on Cbz-**Leu** and aminoalcohol **30**.

The group of CHEN applied the triflic acid salt of diamine **55** as catalyst for *retro-* and transfer aldol reactions.[62] Since this structure was known to catalyze the back reaction it was selected as a potential candidate for the ESI-MS screening as well. The catalyst was synthesized in accordance to the literature *via* a monoprotection and reductive alkylation strategy (Scheme 21). ESI-MS analysis of the crude product **55** revealed the formation of a side product with a mass of *m/z* = 241. This mass could potentially be assigned to two reasonable structures, an over-alkylated side product **56** or the acylated reaction intermediate **57**. For the latter product no NMR evidence was found. In the original procedure the catalyst was synthesized in multi-gram scale and purified by distillation, which was not possible with the smaller amounts synthesized for the ESI-MS screening. Due to an overlay of the first isotope peak of the

impurity signal with the ^{13}C-enamine peak (m/z = 242), higher purity of the catalyst was required for the ESI-MS screening. Bulb-to-bulb distillation did not afforded the product in perfect purity, but purification by flash column chromatography gave a small amount of product in sufficient purity.
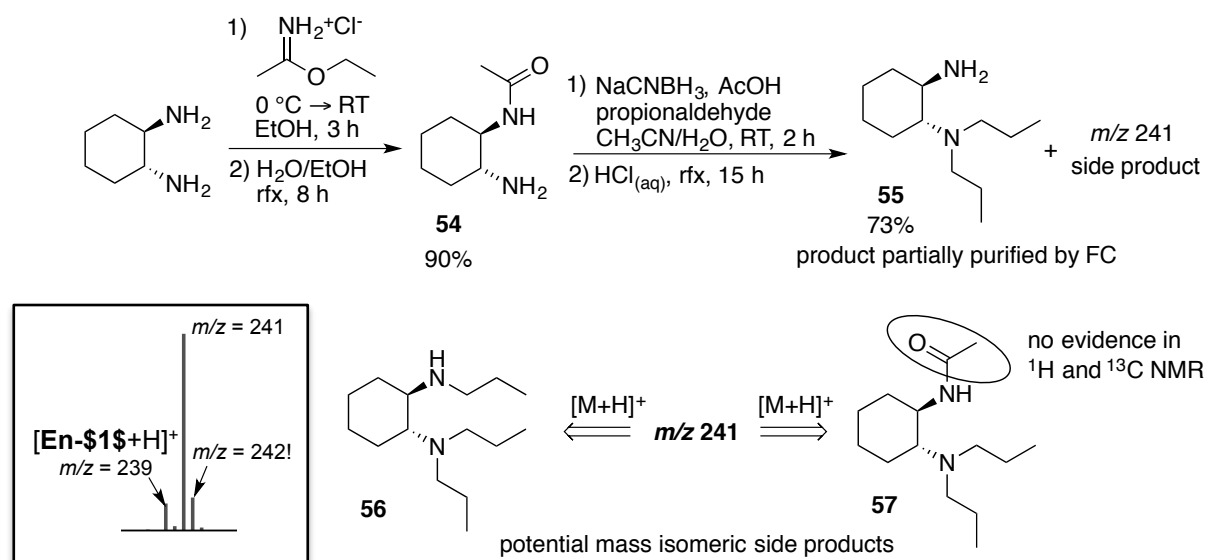
Scheme 21: Synthesis of primary-tertiary amine **55**.

2.7 ESI-MS Screening of Single Catalysts

2.7.1 ESI-MS Screening of Single Catalysts in MeOH

The developed ESI-MS protocol for screening in MeOH was applied to the synthesized catalysts. All results were validated with corresponding forward aldol reactions with acetone and *para*-nitrobenzaldehyde. As illustrated in Figure 31, the enamine ratios derived from the back reaction after C–C-bond cleavage and monitored by ESI-MS analysis (blue bars) matched the enantioselectivity of the catalyst determined by conventional methods (red bars) very well.
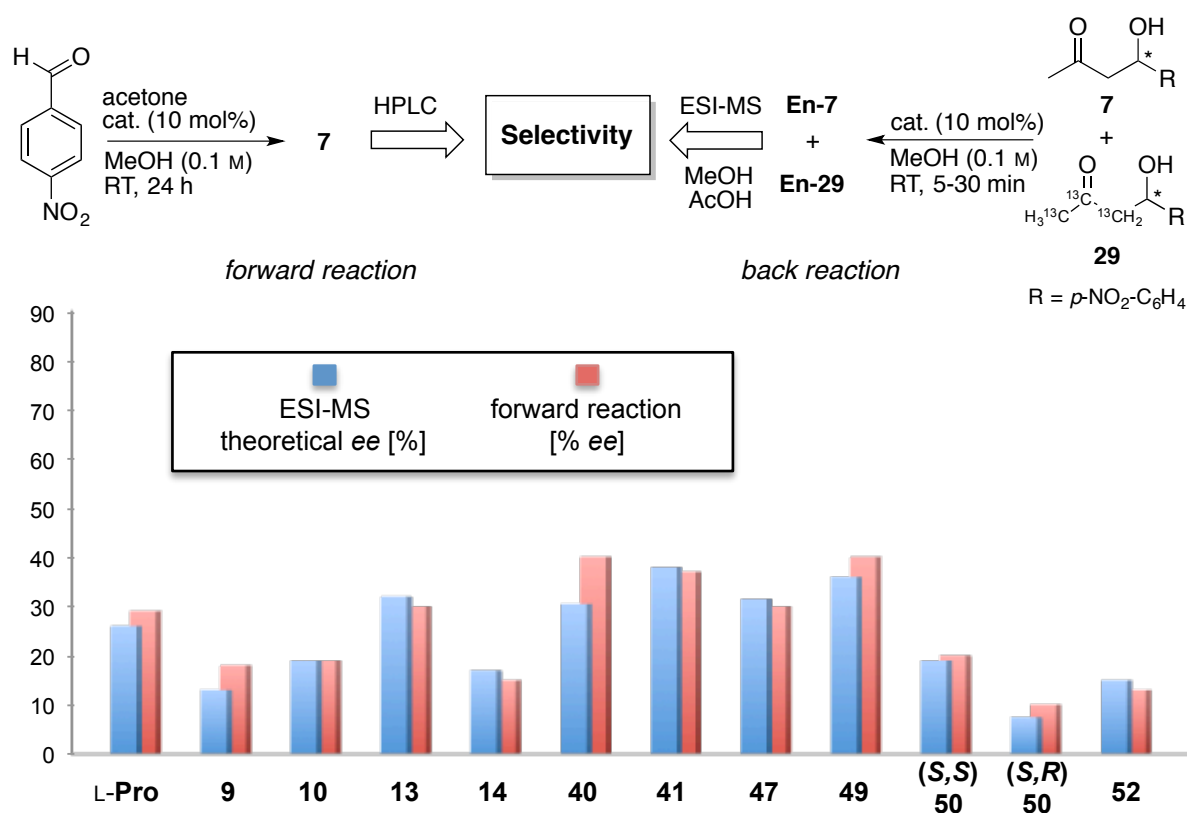
Figure 31: ESI-MS screening results in MeOH.

Due to the low enantioselectivities in MeOH this protocol was not further elaborated. However, a few observations are worth mentioning. L-Proline worked well in the back reaction screening affording intermediate enamines in good signal-to-noise ratios, although proline was expected to be able to form a non-detectable zwitterionic iminium-carboxylate species. It might indeed be possible that such a species is formed, which reacts to the isomeric oxazolidinone (see section 2.1.3, Figure 9) and then is protonated and detected by ESI-MS. For the highly polar and acidic sulfonamide catalyst **31** the enamine intermediates were also observed by ESI-MS. However, a reaction time of at least 30 min was necessary to obtain

suitable intensities. For this catalyst a disagreement was found with ratios of about 61:39 compared to a preparative selectivity of 73:27. Curiously, the enamine ratios increased with longer reaction times (e.g. 68:32 after 16 h). In addition, already after 30 min, a formation of α,β-unsaturated iminium products were observed (Figure 32). This is problematic for an ESI-MS screening since formation of the condensation product is a dead end for the back reaction and alters the initial equimolar ratio of aldol substrates **7** and **29**. Since the preference of the iminium ion was found to be for the same quasienantiomer as the major enamine signal this provided no explanation for the increasing intermediate ratios with longer reaction times. This species was not detected for any other catalyst, aside from tripeptide H-Pro-Pro-Asp-NH$_2$ bearing a carboxylic acid in the side chain. A plausible formation of these intermediates could proceed through water elimination assisted by the acidic amide proton of catalyst **31** (pK_a = 9.5 in DMSO; in contrast amide acidity of catalyst **10** pK_a = 25.5; AcOH pK_a = 12.6).[40]
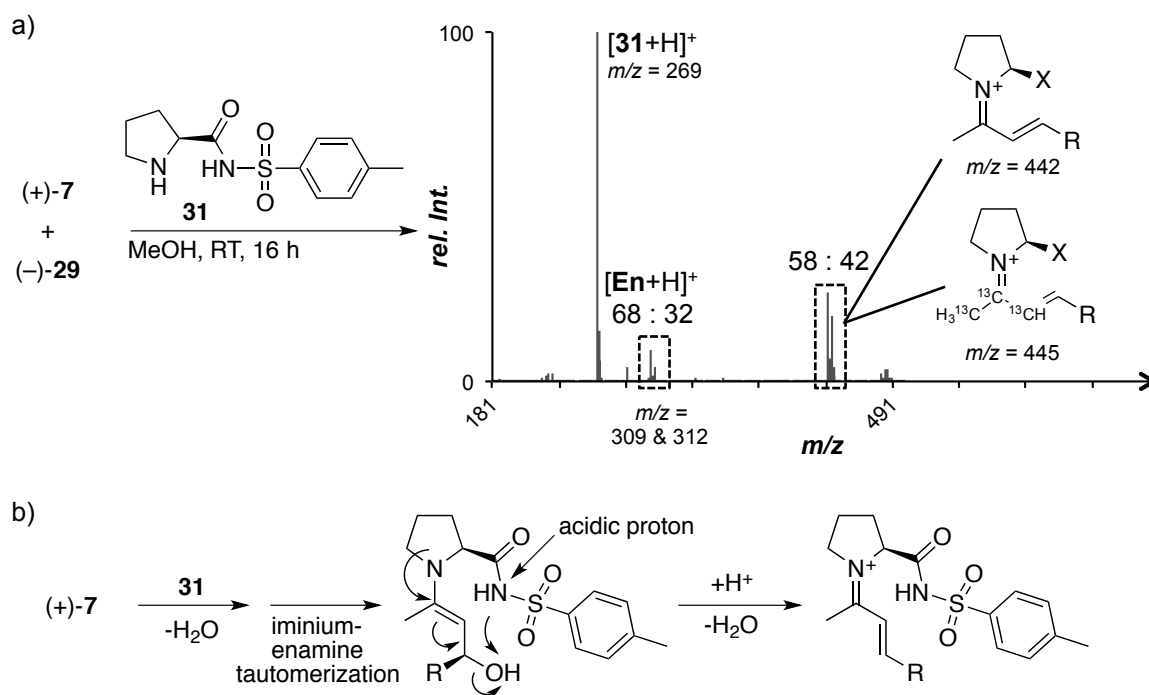
Figure 32: a) ESI-MS back reaction experiment and spectrum after 16 h reaction time. b) Plausible formation the α,β-unsaturated iminium ion.

The application of simple *tert*-butyl phenyl proline amide **51** led to another intriguing result. The ESI-MS result of 45:55 was even in slight favor of the "wrong" (−)-quasienantiomer. Although the catalyst displayed low activities in the preparative reaction a ratio of about 65:35 in favor of the expected (+)-enantiomer was determined by HPLC analysis. Using AcOH as reaction additive in MeOH the signal ratios were again found be in favor for the enamine intermediate derived from the (+)-aldol product and in good agreement with the

forward reaction. It has to be mentioned that under these conditions TLC monitoring of the reaction indicated not only low conversions but also formation of several side products. In the literature it was reported that in particular such simple proline amides tend to behave differently. In analogy to the observation of oxazolidinones, MORÁN reported the formation of imidazolidinones of acetone **59** and the aldol product **60** during the reaction of aniline proline amide **58** with *para*-nitrobenzaldehyde in neat acetone (Scheme 22).[63] The authors also described back reaction experiments in deuterated MeOH where intermediates **59** and **60** were also observed. According to these results, they concluded that imidazolidinones could influence the reaction enantioselectivity and that under neutral conditions the hydrolysis of imidazolidinone **60** is at least partially rate-limiting, whereas acidic conditions prevent their formation. Imidazolidinone formation could also play a major role in the kinetic profile of the aldol reaction under ESI-MS conditions (with 10 mol% catalyst in 0.1 M solution in MeOH) and thus the intermediate ratio would no longer reflect the enantioselectivity of preparative reactions. By ESI-MS, signal with masses consistent with a protonated "enamine" dimer and their sodium adducts, were monitored respectively, which reflected the different reaction modes of this catalyst. In addition, dimer formation of an enamine or an isomeric species was never observed for other catalysts. However, more detailed studies with such catalyst structures would be necessary in order to elucidate the role of imidazolidinones in the ESI-MS screening.
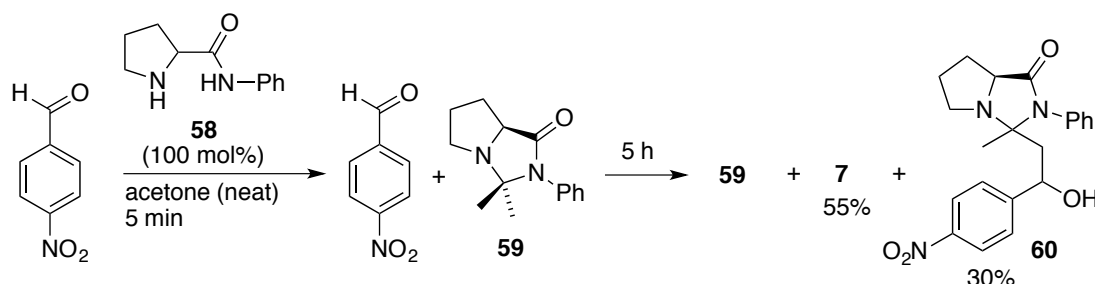
Scheme 22: Imidazolidinone formation observed by MORÁN *et al.* with 100 mol% of proline amide **58** in neat acetone in ^{1}H NMR studies.

In the majority of cases the enamine ratio derived from a pair of quasienantiomers is in perfect agreement with the ratio obtained from the inversely labeled combination. This was a basic requirement for the usability of ^{12}C and ^{13}C acetone as a mass-label. Still, in very few examples, exclusively observed in MeOH, this requirement was violated. For catalyst **52** the difference was remarkably high with signal ratios of 48:52 ((+)-**7**/(–)-**29**) and 63:37 ((–)-**7**/(+)-**29**). In this special case, the discrepancy was caused by background noise overlapping with the corresponding enamine peak of the non-labeled acetone, supported by a back

reaction applying catalyst **52** with aldol product **29** (Figure 33). A background signal with the mass of **En-7** (m/z = 423) was found in significant quantities, although the non-labeled aldol product **7** was not present in the reaction mixture. As both signal ratios were determined, the signal overlay was partially eliminated for these low selectivities by the average value of 48:52 and 63:37 (theoretical *ee* 15%, forward reaction 13% *ee*). Mass-isomeric impurity signals might be problematic especially for higher selectivities, however for ESI-MS screenings performed in CH_3CN and even with crude mixtures of catalysts, problems in this dimension have so far not been encountered.
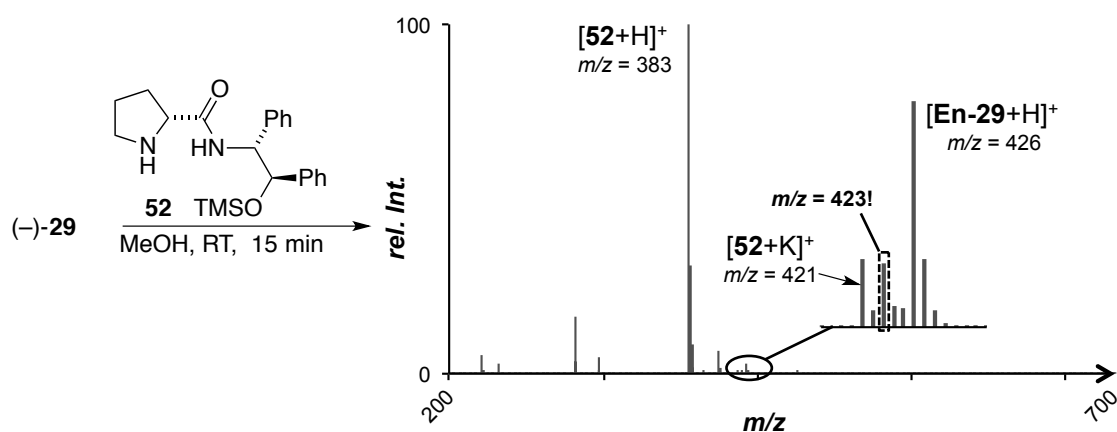
Figure 33: Observation of a signal impurity leading to a misleading result.

2.7.2 ESI-MS Screening of Single Catalysts in CH_3CN with *tert*-BNP as Additive

As mentioned above, the main focus of this work was set on a screening of catalysts in CH_3CN where higher selectivities are induced. For this purpose back reactions were performed under the optimized conditions described in section 2.5.4, with 10 mol% of *tert*-BNP as additive. All results were validated by performing corresponding forward aldol reactions under identical conditions with acetone, *para*-nitrobenzaldehyde and 10 mol% of *tert*-BNP as additive. Unless noted otherwise the selectivity presented in Figure 34 is in favor of the (+)-enantiomer. The theoretical selectivities determined by ESI-MS were again calculated from the ratios of the intermediates derived from both combinations of quasienantiomers (see appendix). In general, an excellent agreement of the enamine ratios determined by ESI-MS monitoring (blue bars) and the enantioselectivities of the preparative forward reaction (red bars) was found. This was consistently the case for SINGH-type catalysts where no mismatch case was observed. In addition, in the majority of cases *tert*-BNP indeed showed only a minor influence on the enantioselectivities of the catalysts in the forward

reactions. Thus, the most selective catalysts under the optimized screening conditions using *tert*-BNP (red bars) were also the most selective species under the best preparative conditions without the additive (green bars). Unfortunately, for more polar catalysts such as proline and sulfonamide **31** no enamine intermediates were observed in CH₃CN.
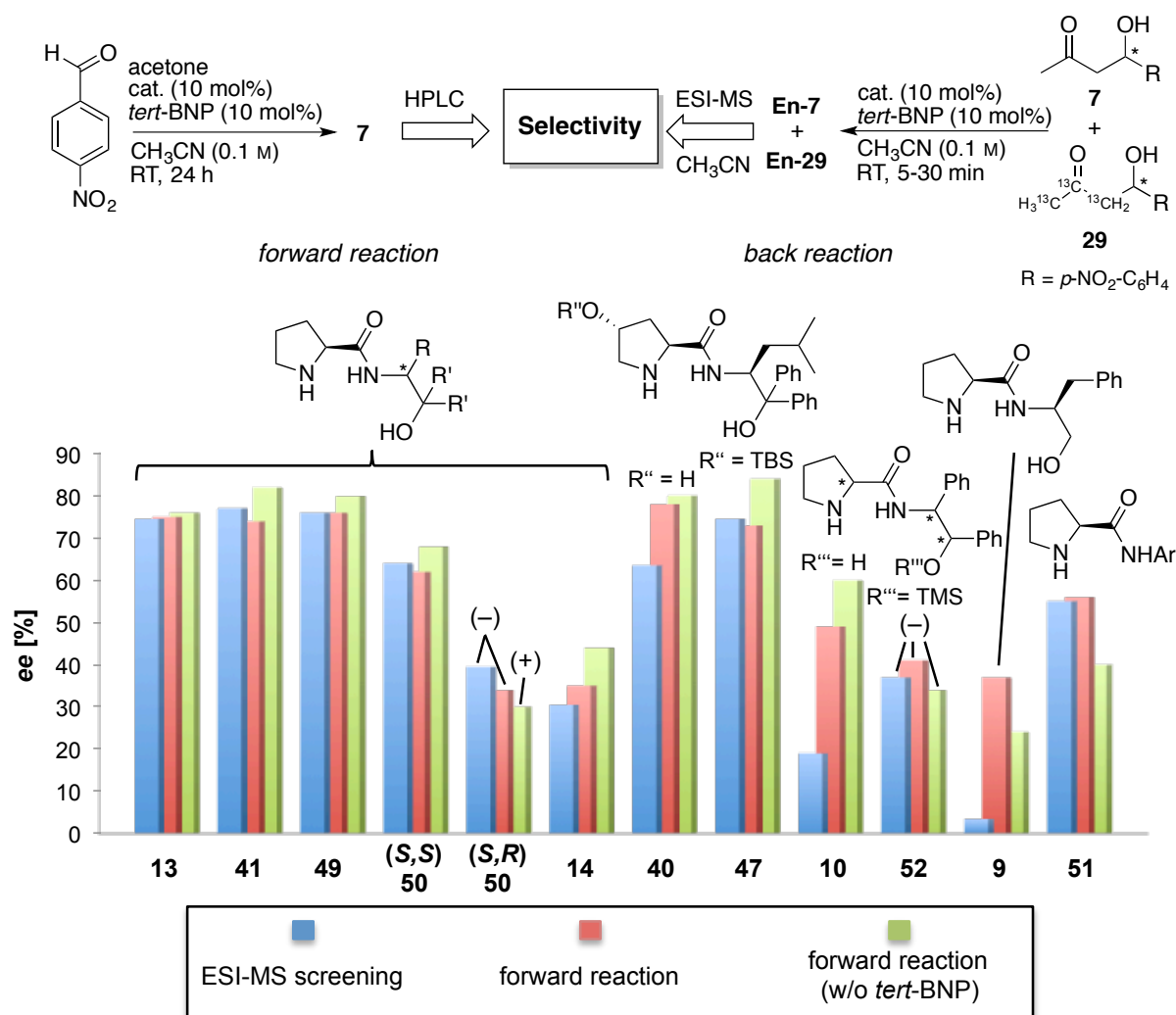
Figure 34: Results of the ESI-MS screening in CH₃CN and the correlation with the forward reactions with and without *tert*-BNP.

Although catalyst **40** was reported to not be active in benzaldehyde aldol reactions,[53] a validation of the screening was possible in CH₃CN with the more reactive *para*-nitrobenz-aldehyde, although only low conversions were observed. Remarkably, for catalyst **40** with a less hindered secondary hydroxyl group at the pyrrolidine moiety, a discrepancy between the ESI-MS results and the preparative reaction was again found. This is in common with catalysts **9** and **10**, both of them bearing a primary or secondary hydroxyl group at the side chain. TBS-protection of the free hydroxy group of catalyst **40** did not only improve the activity of the catalyst, but moreover the ESI-MS results matched again perfectly, as it was

the case for all catalysts bearing a tertiary alcohol function. TMS-protection of the secondary hydroxy group of catalyst **10** also led to a better agreement, but the enamine intensities derived from **52** were low and not stable and therefore hard to analyze. In the corresponding forward reactions the catalyst also showed low activity. On one hand the increased sterical hindrance from the silyl protecting group could minimize enamine formation in both directions. On the other hand, the loss of the second hydrogen bond donor is known to reduce the activity of the catalyst. Similar results were also observed for *tert*-butyl aniline proline amide **51** where poor conversions in the forward reaction as well as low enamine intensities in back direction were observed. However, in the latter case the low intermediate intensities could also be based on the inferior basicity of a potential imidazolidinone and therefore a reduced ability to be transferred into a detectable positively charged species compared to the related enamine.

The problems encountered with primary or secondary hydroxy groups are hard to rationalize based on the available data. As described during the preliminary studies, back reactions with AcOH as additive led to a good agreement with the preparative results, independent of the catalyst structure applied. It can be assumed that without additive and the less acidic nitrophenol, pre-equilibria prior to the C–C-bond cleavage at least partially influences the overall back reaction rate and therefore the signal ratio monitored by ESI-MS analysis. Since this was conspicuous for catalysts bearing sterically less hindered alcohols the hydroxy-group might change the kinetic profile by participating in the ongoing process in an intra- and/or intermolecular fashion. The addition of acetic acid might prevent or accelerate such pathways. Fragmentation studies of enamine intermediates derived from catalysts **13** and **9** when performing ESI-MS/MS experiments provided no further insight. ^{1}H NMR experiments of the back reaction with 10 mol% of catalyst did not reveal any difference between the two catalysts except for the slower formation of the aldehyde peak for catalyst **9** (see Chapter 2.5.3, Figure 25, essentially the same spectra were recorded with and without *tert*-BNP as additive). For both catalysts decomposition occurred with proceeding reaction time and only a small amount of the catalyst seemed to be involved in the catalytic cycle in the back reaction. This seems reasonable, especially when bearing in mind that the equilibrium of aldol product and its iminium ion should be on the side of the free catalyst, which is in accordance with ESI-MS spectra where no product iminium species was detected, except the condensation products derived from sulfonamide **31**.

Interestingly, for catalyst **50** with a mismatch (*S,R*)-configuration the opposite (−)-enantiomer was preferred in the preparative reaction with *tert*-BNP as additive. The reversal in stereochemical outcome was unique for *tert*-BNP conditions. In MeOH, CH$_3$CN and with AcOH as additive a slight preference of the (+)-enantiomer was found both by ESI-MS and under preparative conditions. This demonstrates once more the suitability of the ESI-MS screening for the identification of additive effects as the alteration of the favored enantiomer was also determined by ESI-MS in perfect agreement with the forward reaction (Figure 35). As discussed in Chapter 2.5.3, enamines derived from SINGH-type catalysts were expected to be present in higher concentrations or/and have superior stability compared to enamines derived from catalysts such as **9** or **10**. The influence of AcOH present in the dilution mixture on the signal ratio was nicely shown for catalyst (*S,R*)-**50** due to the preference of the opposite quasienantiomer with either *tert*-BNP or AcOH as reaction additive. Upon dilution of the back reaction mixture containing *tert*-BNP, aldol products **(+)-7** and (−)-**29** and catalyst (*S,R*)-**50** with a CH$_3$CN/AcOH mixture the preference of the (−)-quasienantiomer is still reflected by the enamine ratio, albeit in slightly lower ratios than without addition of AcOH during the dilution. However, when the diluted reaction mixture was subjected a second time to ESI-MS analysis after 15 min standing at room temperature the ratio was now in favor for the enamine derived from the (+)-quasienantiomer, as it was the case for the back reaction conditions with AcOH as reaction additive (Figure 35). After 15 min no change was observed any longer.
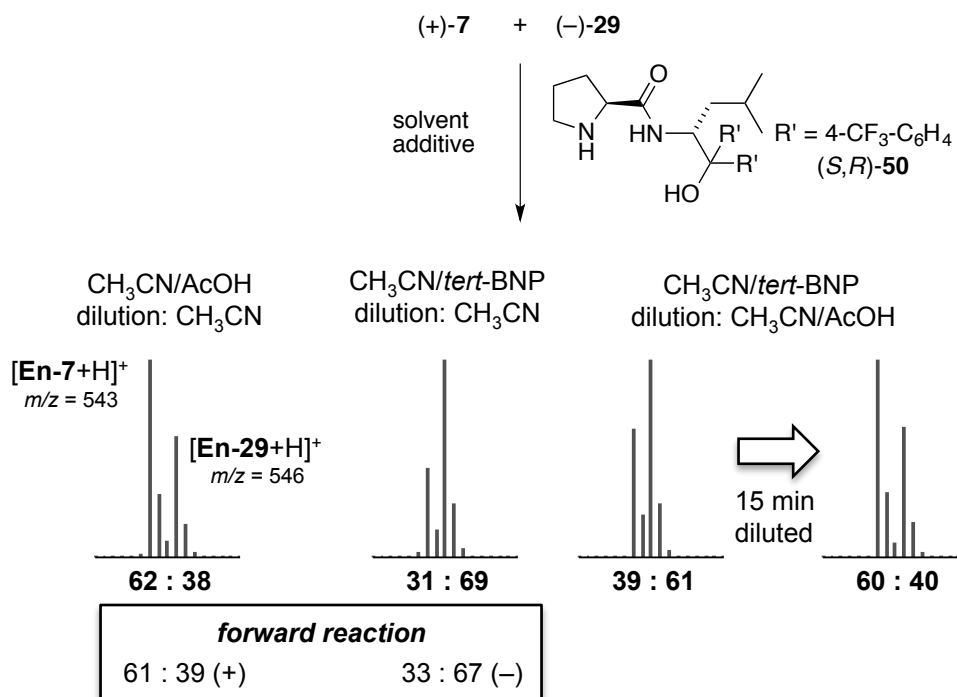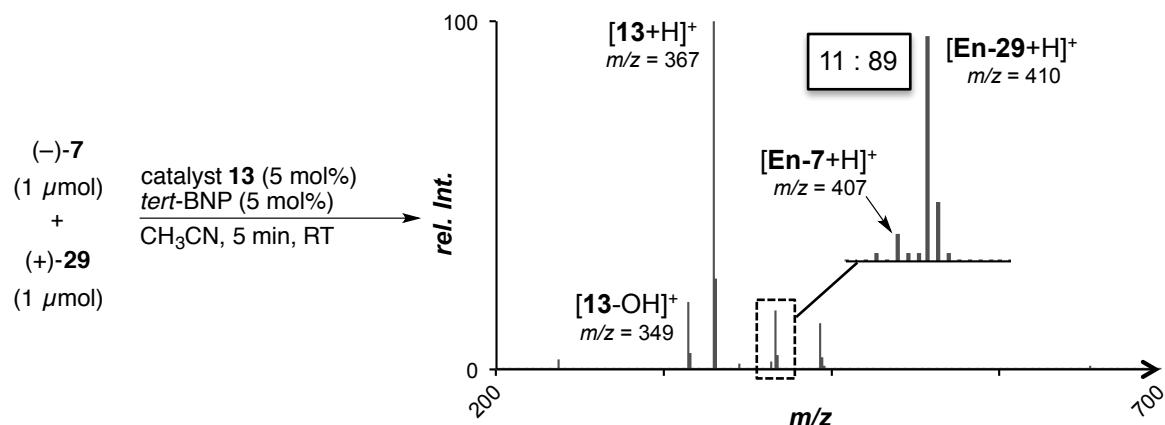

Figure 35: ESI-MS screening of catalyst (*S,R*)-**50** under various conditions.

The influence of AcOH as dilution additive was observed for all investigated SINGH-type catalysts, where the signal ratios of enamine intermediates were lower than expected. Since at least 1 min is necessary from dilution to the first ESI-MS detection, signal alteration could be minimized for such systems, but not avoided. This was even more obvious for back reaction screening in CH$_3$CN without a reaction additive, where a proton source was essential to transform the intermediates into ESI-MS detectable species. For catalyst screenings of such a system where the side chain or aryl groups were modified, the influence of the structural diversity on the selectivity in the preparative forward reaction was much better reflected and also more reliable and reproducible by the ESI-MS screening with *tert*-BNP as reaction additive than with AcOH as dilution additive (Figure 36). Whereas, under additive conditions catalysts **13**, **41** and **49** were identified as a group of the most selective catalysts (green bars), the selectivity difference to amine (*S,S*)-**50** was not reflected in an ESI-MS screening without *tert*-BNP (blue bars).
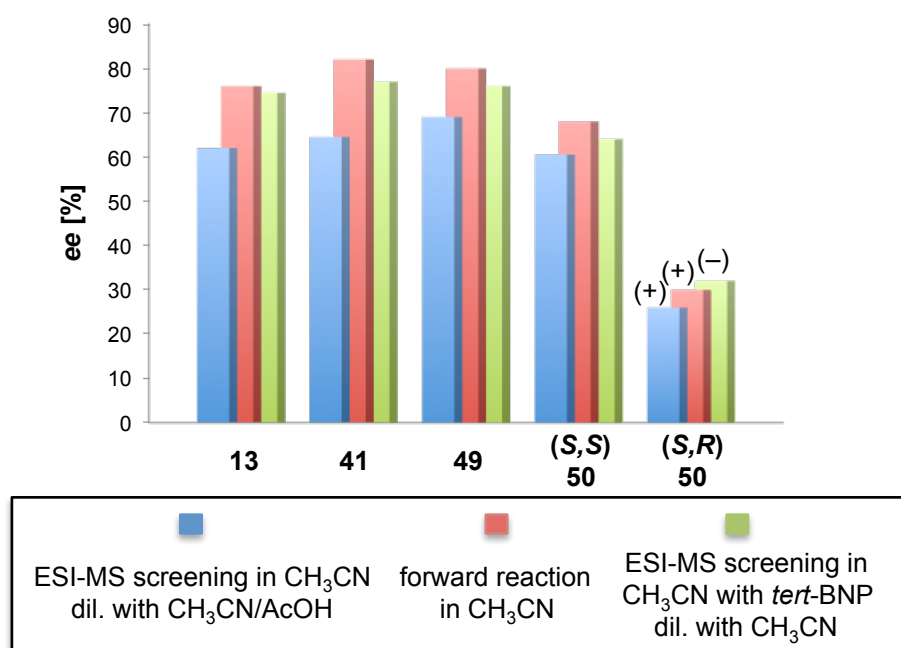
Figure 36: Improved correlation of the selectivity trend determined by ESI-MS screening for SINGH-type catalysts and the preparative forward reaction without additive.

Finally, the amount of aldol products applied to the back reaction screening was successfully reduced to 1 μmol corresponding to approximately 0.2 mg of each substrate (Figure 37). With 5 mol% of catalyst **13** and *tert*-BNP the enamine intermediates were still monitored in excellent signal-to-noise ratios. Further, the determined ratio of 11:89 (**En-7**/**En-29**) was in excellent agreement with the experiment on a larger scale (12:88).

Figure 37: ESI-MS back reaction screening of catalyst **13** on a low scale of 1 μmol.

2.7.3 ESI-MS Monitoring of Temperature Effects for Aldol Reactions in CH₃CN

It would be interesting to know whether the ESI-MS screening methodology also allows for monitoring temperature effects on the selectivity of the catalyst. For this purpose, forward reactions at 0 °C were performed with catalyst **13** and **41** in CH_3CN with and without *tert*-BNP as additive (Table 5). Under these preparative conditions the selectivity of the catalysts was indeed found to increase. The most beneficial effect of decreased reaction temperatures was observed for catalyst **13** without additive (Table 5, brackets). Back reaction experiments were also conducted in CH_3CN and diluted with a CH_3CN/AcOH mixture and with *tert*-BNP as reaction additive followed by dilution with pure CH_3CN. For the corresponding ESI-MS screenings it was important to pre-freeze the dilution solvent and the reaction mixture prior to dilution. A fast spectrum collection was needed as signal alteration was observed to be fast for reaction mixtures diluted with a CH_3CN/AcOH mixture.[i] However, under these conditions the increased selectivity was reflected well by ESI-MS analysis. This was particularly apparent for catalyst **41**.

---

[i] In contrast, with *tert*-BNP as reaction additive and without a dilution additive, the signal ratio was stable over a 2 min measurement time.

**Table 5:** Effects of the reaction temperature on the ESI-MS screening.
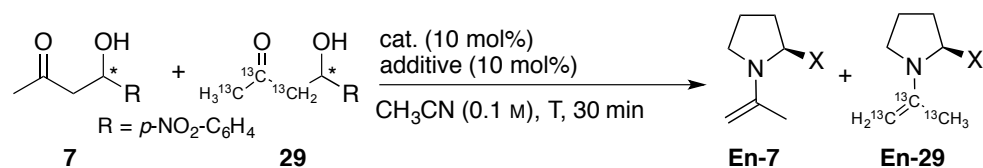
entry	catalyst	additive dilution	T [° C]	ESI-MS screening (En-7/En-29)		e.r. (+) preparative reaction[a)]
				(+)-7/(−)-29	(−)-7/(+)-29	
1			RT	81 : 19	19 : 81	88 : 12
2		CH₃CN/AcOH	0	86 : 14	15 : 85	94 : 6
3	**13**	tert-BNP	RT	87 : 13	12 : 88	88 : 12
4		CH₃CN	0	88 : 12	12 : 88	89 : 11
5			RT	81 : 19	16 : 84	91 : 9
6		CH₃CN/AcOH	0	90 : 10	7 : 93	94 : 6
7	**41**	tert-BNP	RT	88 : 12	11 : 89	87 : 13
8		CH₃CN	0	91 : 9	10 : 90	90 : 10

a) Preparative forward reaction was conducted with 10 eq. acetone and 10 mol% catalyst in CH₃CN (0.1 M) at 0 °C for 48 h. *E.r.* was determined by HPLC on a chiral stationary phase.

2.7.4 *tert*-BNP as Dilution Additive for the ESI-MS Back Reaction Screening

Next, it was investigated whether *tert*-BNP could merely be used as a generally applicable dilution additive allowing for the determination of the selectivity of the catalyst in CH₃CN without an additional reaction additive. This could be possible, provided that the nitrophenol simply acts as a proton source for the formation of an ESI-MS detectable species and the induction of the signal alteration after dilution is slow, as generally observed with AcOH as proton source. Catalyst (*S*,*R*)-**50** was supposed to be optimal for studies of the effect of the dilution solvent containing *tert*-BNP since with this reaction additive, formation of the opposite enantiomer was preferred (see Chapter 2.7.2, Figure 34). Starting from aldol products (+)-**7** and (−)-**29** it would be expected that the formation of the enamine derived from **7** is favored by the same extent as observed in the forward reaction in CH₃CN (65:35

(+)). This would imply that *tert*-BNP simply acts as a proton source and the intermediate signals are stable. On the other hand, if signal alteration is fast and a new ratio is immediately established under dilution conditions due to the proceeding back reaction dominated by the new environment, the enamine intermediate derived from **29** should be observed as the major intermediate by ESI-MS analysis. Performing the back reaction experiment with catalyst (*S*,*R*)-**50** an enamine ratio of 56:44 in favor for **En-7** was monitored by ESI-MS after diluting the reaction mixture with CH$_3$CN/*tert*-BNP (Figure 38). However, the observed ratio still differed by about 20% *ee* from the preparative results. Moreover, when the diluted reaction mixture was reinjected after 10 min and 20 min to ESI-MS analysis the signal alteration was found to be much slower than that observed when AcOH was present in the dilution mixture. Thus, the discrepancy between ESI-MS and preparative result seemed to not only be generated by the dilution conditions. More likely, this result demonstrates that *tert*-BNP does not simply act as a proton source for enamine transformation into the ESI-MS detectable species but also plays an important role as reaction additive, for example by accelerating the pre-formation of the iminium intermediate of the aldol product prior to C–C bond cleavage.
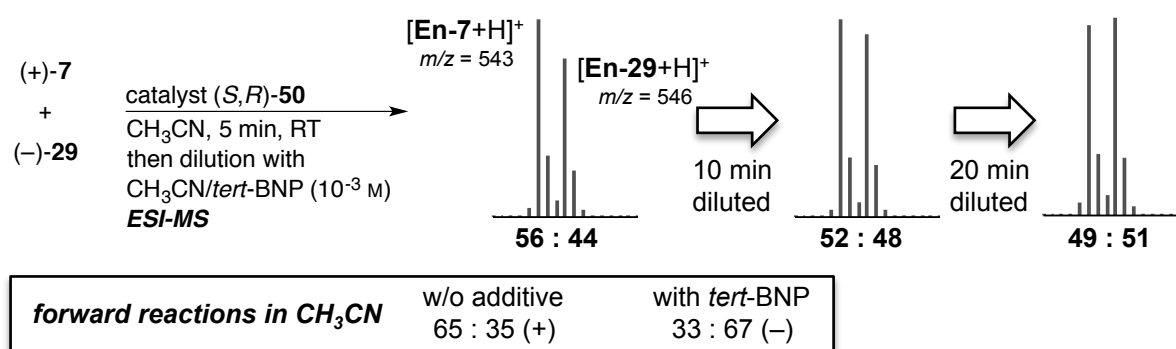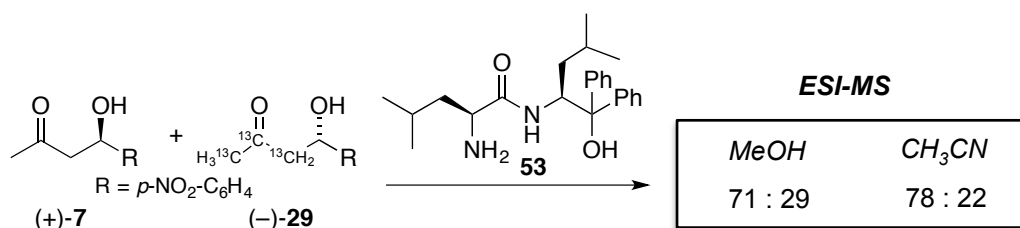

Figure 38: ESI-MS back reaction experiment diluted with a mixture of *tert*-BNP in CH$_3$CN (10^{-3} M).

For most of the other SINGH-type catalysts the selectivity differences between additive free and *tert*-BNP conditions were not large enough to draw clear conclusions from the experiment with *tert*BNP as dilution additive. TBS-protected hydroxy-proline catalyst **47** differed by 11% *ee*, which could be sufficient to monitor the influence of the *tert*-BNP as a dilution additive. Indeed, a slightly higher enamine ratio was found applying the new protocol (87:13 → 89:11 **En-7**/**En-29**). The new intermediate ratio was still lower than the preparative results without additive (92:8 (+)). Although *tert*-BNP was found to be essential for a prediction of the correct selectivities, the extension of the screening protocol using the nitrophenol simply as a dilution additive could emerge as a valuable additional experiment to determine whether *tert*-BNP considerably influences the selectivity outcome of the catalyst compared to additive

free conditions or not.

### 2.7.5 ESI-MS Screening of Primary Amines as Organocatalysts for Aldol Reactions

To evaluate the scope of the ESI-MS methodology primary amines were included in the screening. With amine **53** the back reaction was conducted in MeOH and CH$_3$CN. In both solvents the enamine intermediates were detected in ratios of 71:29 and 78:22, respectively (Scheme 23).

Scheme 23: ESI-MS back reaction experiment with primary amine **53** in MeOH and CH$_3$CN.

A validation of the screening results was not possible due to the low activity of the catalyst in the forward direction under the ESI-MS screening conditions in MeOH and CH$_3$CN and also with *tert*-BNP as additive. However, the intermediate ratios are in a similar range to the reported selectivity of the aldol reaction in neat acetone (Table 6, entry 1).[61]

Table 6: Selected results for the acetone aldol reaction with catalyst **53** reported by DA *et al.*[61]
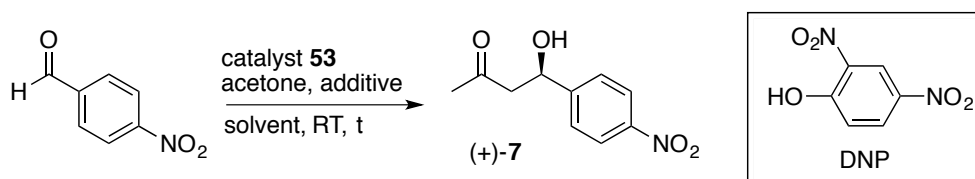
entry	additive	solvent	t [h]	yield [%]	ee [%]
1	-	acetone	50	n.d.[a)]	56
2	DNP	acetone	7	82	93
3	DNP	CH$_3$CN	132	50	86
4	DNP	MeOH	90	59	86

a) Not determined.

In order to obtain a validation of the screening, back reaction experiments were performed in CH$_3$CN and MeOH with DNP as additive (Figure 39). As already observed for the reaction where benzoic acid was the additive, the enamine ratio was considerably lower after 30 min

reaction time than after just 5 min using DNP in CH₃CN. Moreover, again, the enamine ratio was found to be unstable after dilution leading to fast signal changes even within the time frame of the measurement. This increase of selectivity was clearly detected compared to the screening in pure CH₃CN, albeit with a slightly lower value of 86% *ee* (Table 6, entry 3), than was previously published. In MeOH the intermediate signals were found to be much more stable, although a factor of ten less intensive (absolute intensity), but still with an excellent signal-to-noise-ratio. Moreover, the ESI-MS result (94:6 (average), **En-7**/**En-29**) was in perfect agreement with the preparative reaction under the same conditions (93:7 (+), 87% *ee*) and the published selectivity of 86% *ee* (Table 6, entry 4). This example demonstrates another benefit of the ESI-MS methodology. With two experiments of about 30 min each (including reaction time and set-up) using the DNP additive in two different solvents, the general improvement of the selectivity over the reaction without additive was monitored. In contrast, reaction times of 7 h up to 132 h in preparative reactions were necessary, which does not even include product purification and analysis. Of course, conditions identified by ESI-MS analysis need to be optimized in corresponding preparative reactions, since ESI-MS analysis does not reveal any information about activity. This fact was also recognized for the current example, where under non-additive conditions the back reaction was observed by ESI-MS, however no conversion was found in the forward reaction. Still, the pre-identification of promising parameters could already considerably shorten the catalyst and additive screening process.
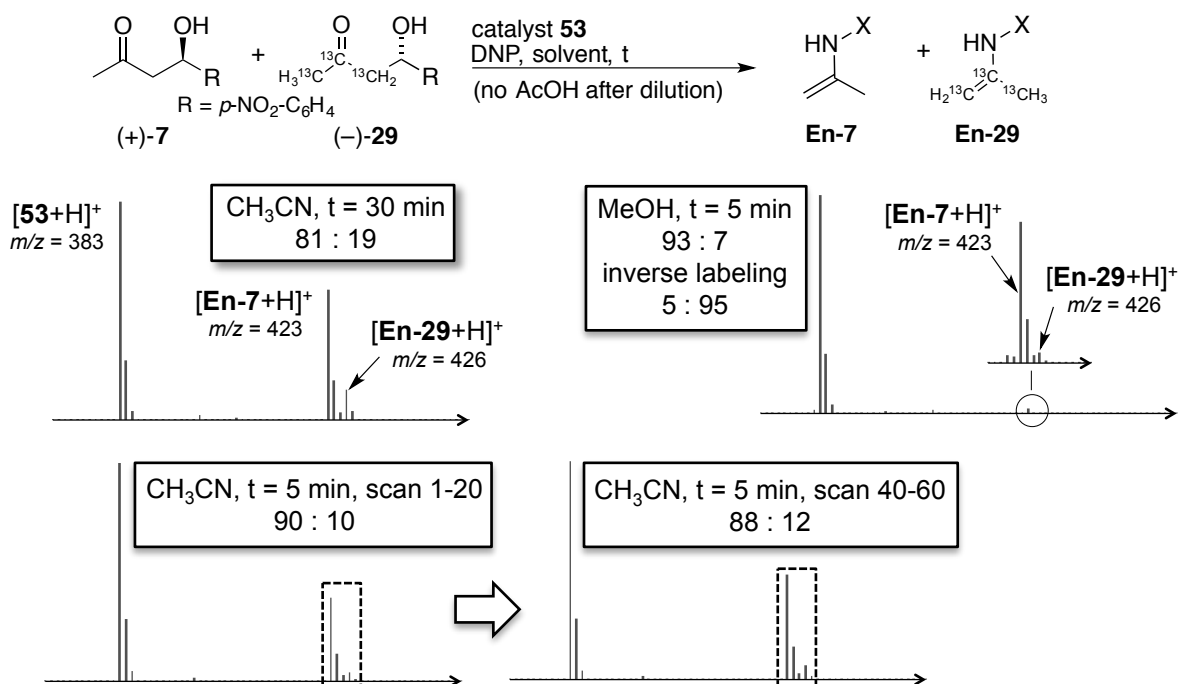
Figure 39: ESI-MS back reaction experiment with primary amine **53** in MeOH or CH₃CN with DNP as additive. The average over different scan ranges (scan/2s) of the same measurement reflects the signal alteration during the ESI-MS analysis in CH₃CN.

Substantial problems were encountered in the ESI-MS screening when the triflic acid salt of diamine **55** was used. The excellent enantioselectivities of 92-94% *ee* in CH_3CN and even MeOH obtained in preparative reactions were not reflected by the ESI-MS screening. Under various conditions a maximum ratio of 84:16 was monitored (Figure 40). The preference of the (*S*)-enantiomer was also found by ESI-MS analysis applying standard conditions and instrument parameters (50 V detector voltage). Interestingly, higher detector voltages considerably influenced the signal intensities even up to the point where a reversal of the ratios was observed. Such a behavior was unexpected because the electrospray ionization efficiency for either a ^{12}C- or ^{13}C-enamine should be identical. Although the initially observed side product (*m/z* = 241) was partially removed from the catalyst by flash column chromatography, Et_3N applied as chromatography additive was not completely removed from diamine **55**. However, to elucidate details of the signal alteration problems with side products or background signals should be excluded and therefore the catalyst must be perfectly pure. Since the ESI-MS results were not promising an optimization of the synthesis and purification was not further pursued.
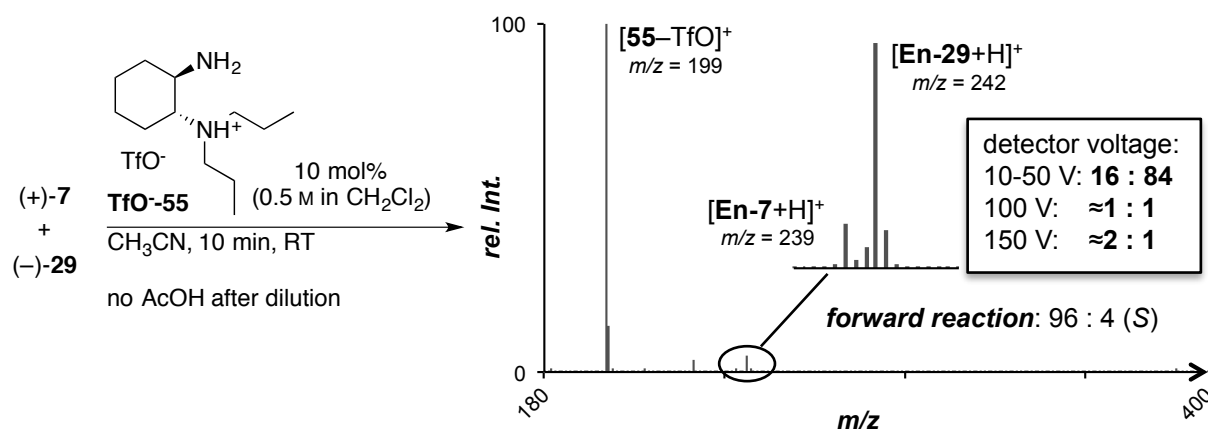
Figure 40: ESI-MS back reaction experiment with triflic acid salt **TfO⁻-55** in CH_3CN. Unexpected dependency of the intermediate ratio and the detector voltage of the ESI-MS (box).

2.8   Multi-Catalyst Screening

In contrast to a classical determination of the enantioselectivity, which relies on product analysis, the monitored enamine ratio reflects the intrinsic enantioselectivity of a catalyst. Therefore, it should be possible to apply crude catalysts to the ESI-MS screening. Here, potential catalytically active impurities, which could lead to an erosion of product enantioselectivity in preparative reactions, should not considerably influence the signal ratio of intermediates formed in the back reaction. Since catalyst-substrate intermediates are monitored, it should be possible to extend the ESI-MS protocol to a multi-catalyst screening, if the catalyst differ sufficient in molecular mass. This would allow to determine the enamine ratios from a mixture of several catalysts simultaneously and to identify the most selective catalysts directly from the crude mixture.
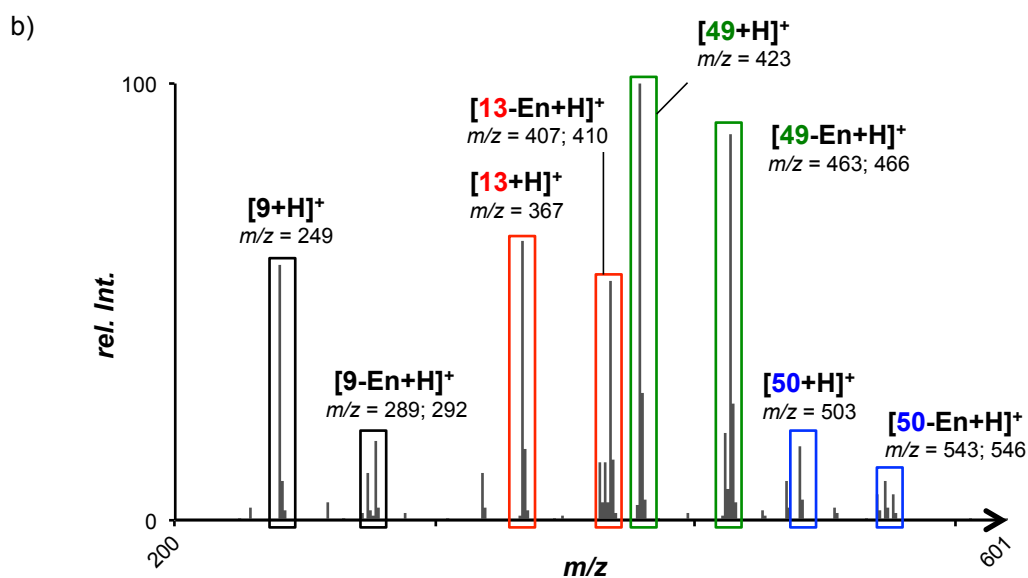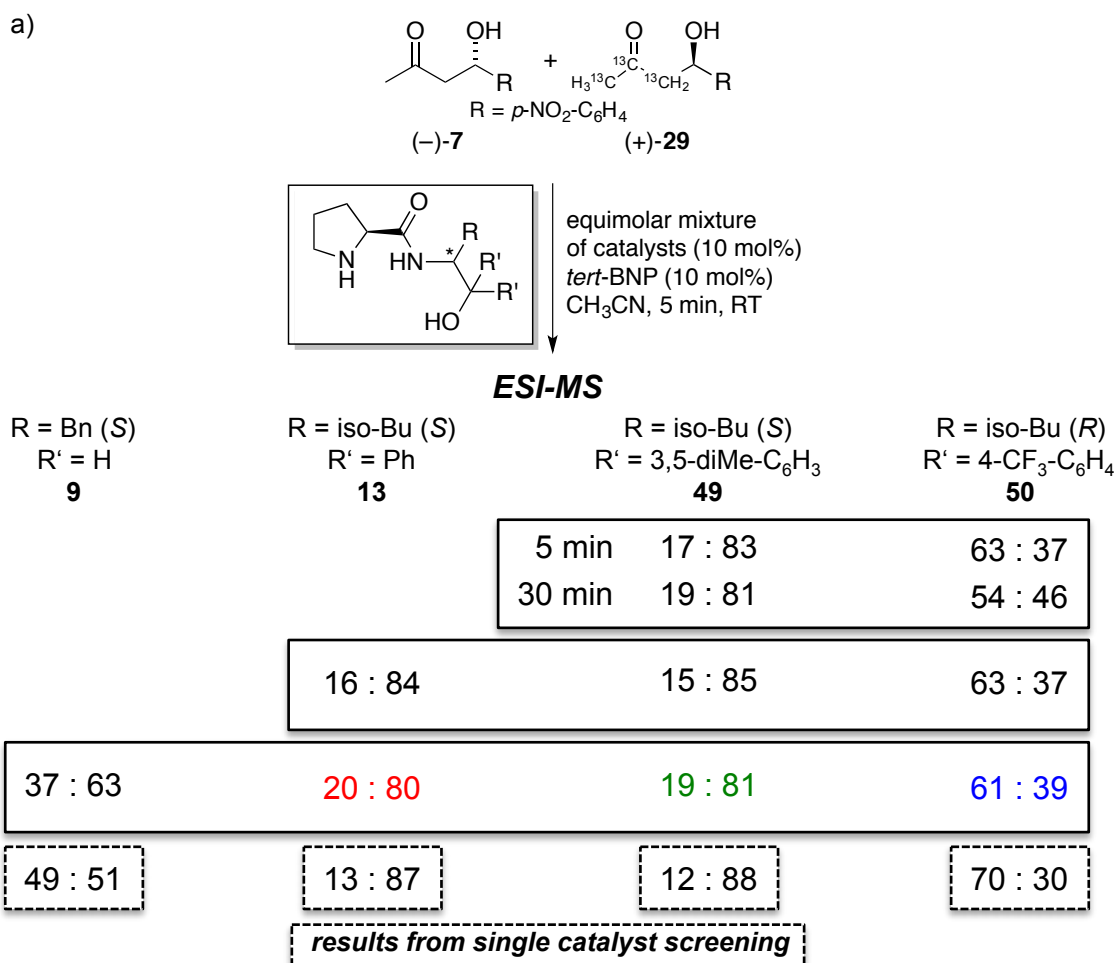
Initially, the hydroxy group at the pyrrolidine moiety introduced by coupling of *trans*-hydroxy proline was chosen as reactive site for catalyst modification. For example, mixtures of catalysts with different masses can be easily synthesized employing commonly used protection conditions with different silyl chlorides. However, most common silyl-protecting groups would lead to an overlay of catalyst and enamine signals. The structure of the silyl-group did not notably influence the selectivity of the catalyst as the same signal ratio of 87:13 was found for the TBS- and TBDPS-protected catalysts (**47** and **48**) in the ESI-MS screening. Therefore, the focus was laid on the identification of coupling conditions allowing for amid formation of proline in the presence of a mixture of several aminoalcohols. A variety of catalysts can be prepared in this way, which should differ sufficiently in mass and selectivity for proof of concept studies.

2.8.1   Multi-Catalyst Screening of Equimolar Mixtures of Purified Catalysts

First, it was probed whether the standard ESI-MS screening protocol with *tert*-BNP as additive in CH_3CN is applicable to a screening of catalyst mixtures. For that purpose up to four purified catalysts were mixed in an equimolar ratio and subjected to ESI-MS back reaction analysis (Figure 41). A mixture of catalyst **49** and (*S,R*)-**50** should be suited for initial proof-of-principle studies since these catalysts show opposite selectivity toward the opposite quasienantiomers under the applied screening conditions. They also should differ enough in their mass to avoid signal overlay of the catalyst and enamine signals. After 5 min reaction time ESI-MS analysis clearly revealed the preference for the opposite enantiomer. Moreover,

the enamine ratios were in a good agreement with the results from single catalyst screening. This result is remarkable since it shows that even in a mixture where catalyst-catalyst interactions could occur, the effect of the additive on the selectivity is clearly reflected by ESI-MS analysis. After 30 min reaction time the intermediate ratio had decreased, but the enamine signal derived from catalyst (*S,R*)-**50** and aldol product (–)-**7** was still slightly favored, demonstrating that scrambling of the enamine moiety by hydrolysis and reformation of the enamine of ^{13}C-labeled acetone and free catalyst takes place but is slow during the process. Nevertheless, the reaction was stopped after 5 min for subsequent experiments to minimize scrambling.
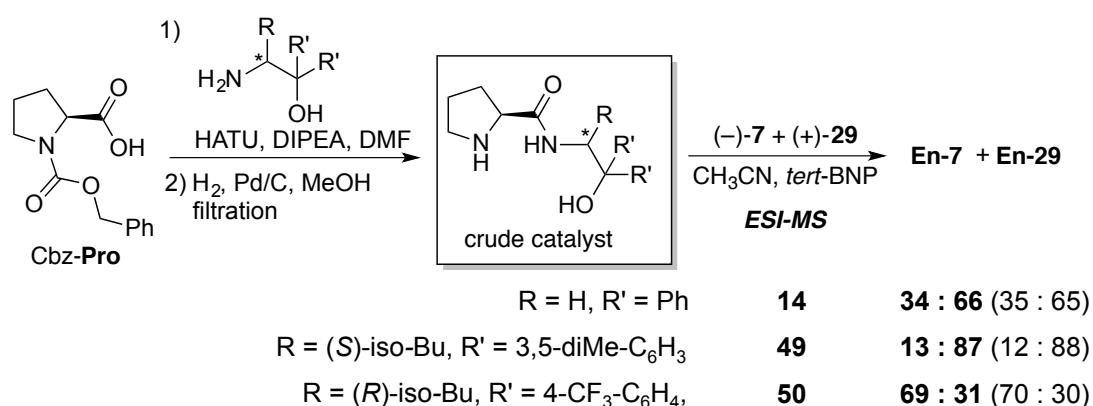
Next, we investigated a mixture of three catalysts (**13**, **49** and **50**). Also the second catalyst present in the reaction mixture favored the opposite enantiomer compared to (*S,R*)-**50**. Here too the enamine ratio determined from the back reaction mixture was found to closely match the results from the single catalyst screening. For a mixture of four catalysts larger deviations were note especially for catalyst **9** for which the formation of less stable intermediates was assumed based on dilution experiments in the single catalyst screening. Nevertheless, the most selective catalysts and the preference of the opposite enantiomer of catalyst **50** was clearly reflected by ESI-MS analysis. To reduce potential catalyst-catalyst interactions, which might lead to selectivity alterations, the back reaction was conducted in a highly diluted reaction environment (x5). However, the signal ratios did not change under these conditions. Since the overall amount of catalyst was kept constant at 10 mol% the amount of a single catalyst in a reaction mixture of four catalysts is reduced to 2.5 mol%. A catalyst screening with 2.5 mol% of catalyst **49** and a slight excess of *tert*-BNP related to the catalyst was performed to determine whether lower catalyst loadings and an excess of additive affect the signal ratios. However, the determined ratio of 89:11 was comparable to the enamine ratio monitored with 10 mol% (88:12).

a)

R = Bn (*S*) R' = H **9**

R = iso-Bu (*S*) R' = Ph **13**

R = iso-Bu (*S*) R' = 3,5-diMe-C₆H₃ **49**

R = iso-Bu (*R*) R' = 4-CF₃-C₆H₄ **50**

		5 min 17 : 83	63 : 37
		30 min 19 : 81	54 : 46

	16 : 84	15 : 85	63 : 37

37 : 63	20 : 80	19 : 81	61 : 39

| 49 : 51 | 13 : 87 | 12 : 88 | 70 : 30 |

results from single catalyst screening

b)

Figure 41: a) ESI-MS screening applying an equimolar mixture of up to four separately purified catalysts. b) ESI-MS back reaction spectra with four different catalysts.

### 2.8.2 Synthesis of Catalyst Mixtures Using HATU as Coupling Reagent

Having established screening conditions for multi-catalyst screening, it was decided to synthesize a catalyst mixture directly from protected proline and a mixture of aminoalcohols and subject it in crude form to ESI-MS analysis. Initially, HATU was applied as coupling reagent. To investigate whether impurities present in the crude product under these conditions influence the screening, crude products of single catalysts synthesized according to the standard coupling protocol were subjected to ESI-MS screening. As illustrated in Scheme 24, the enamine ratios determined from the crude products were in excellent agreement with the values obtained from the purified catalysts (in brackets).

R = H, R' = Ph	**14**	**34 : 66** (35 : 65)
R = (*S*)-iso-Bu, R' = 3,5-diMe-C$_6$H$_3$	**49**	**13 : 87** (12 : 88)
R = (*R*)-iso-Bu, R' = 4-CF$_3$-C$_6$H$_4$,	**50**	**69 : 31** (70 : 30)

Scheme 24: Synthesis of catalysts and analysis of the crude product by ESI-MS. The intermediate ratios from the purified catalyst are given in brackets.

The synthesis protocol depicted in Scheme 24 was also applied for the preparation of a crude mixture containing up to three catalysts. For this purpose an equimolar mixture of the corresponding aminoalcohols was added either simultaneously or stepwise to the activated Cbz-protected proline. The protected intermediates were filtrated through silica gel. After deprotection of the Cbz-group, Pd/C was filtered-off and the solvent evaporated. Finally, 10 mol% of the solid crude mixture was then subjected to ESI-MS analysis assuming full conversion and removal of the coupling reagents during the filtration step. The protocol worked well for a synthesis of a mixture of catalysts **13** and **49**. The subsequent ESI-MS back reaction experiment revealed a ratio of about 82:19 for both catalysts. However, the first problems were encountered with a crude mixture of catalyst **14** and **49** wherein the enamine intermediates derived from catalyst **14** were about a factor of 80 less intensive than those from catalyst **49** (Figure 42a). The ratio of the enamine signals with lower intensity seemed to be considerably altered. In addition, due to a rather noisy spectrum, overlay with background signals was observed, which further complicated analysis. Increasing the amount of aminoalcohol **46** for the synthesis of the crude mixture did not improve the signal-to-noise-

ratio. In the corresponding back reaction experiment with a 1:1 mixture of the separately purified catalysts the signal of catalyst **14** was also considerably lower in intensity, probably due to its lower electrospray ionization efficiency. Nevertheless, the relative intensity of the enamine signals compared to the catalyst signal indicated that the concentration of these enamines also seemed to be lower compared to the enamines from catalyst **49**. The synthesis of a mixture of three catalysts and subsequent back reaction screening gave even more contra-dictory results. The theoretical selectivities determined by ESI-MS of catalyst **13** and **49** where significantly lower than those obtained from the single catalyst screening (Figure 42b). Moreover, the enamine ratio for catalyst (*S,R*)-**50** was in favor of the wrong quasienantiomer. Since comparable problems were not observed for the equimolar mixture of pure catalysts it is assumed that impurities present in the reaction mixture either influence the catalyst selectivity determined by the back reaction screening or accelerate the scrambling of the acetone moieties.
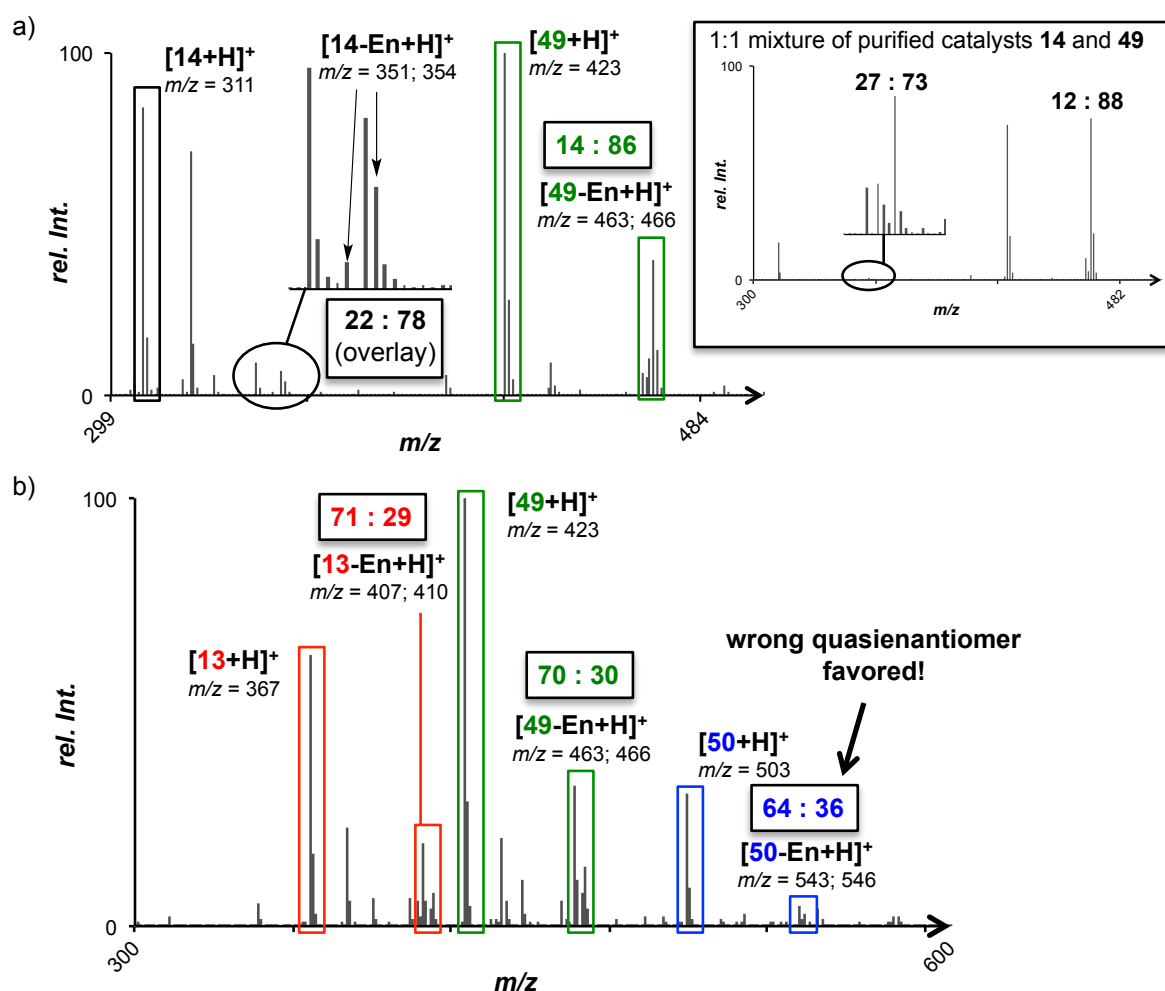
Figure 42: a) Back reaction experiment applying a crude mixture of catalysts **14** and **49**. In contrast, ESI-MS spectra and ratio of enamine intermediates recorded with an equimolar mixture of the purified catalysts (frame). b) ESI-MS back reaction experiment applying a crude mixture of three catalysts (for ESI-MS results with the single catalyst see Scheme 24 and Figure 41).

### 2.8.3 Synthesis of Catalysts Mixtures Applying BERKESSEL'S Protocol

The synthesis of SINGH-type catalysts according to the elegant one-pot procedure developed by BERKESSEL[52] was already found to afford crude products in very high purity. This procedure offers a route to catalyst mixtures. ESI-MS analysis of the crude product after synthesis of catalyst (S,R)-**50** again revealed an excellent agreement with the selectivity of the purified catalyst (Scheme 25).

R = (R)-iso-Bu, R' = 4-CF$_3$-C$_6$H$_4$ **50**   **71 : 29** (70 : 30)
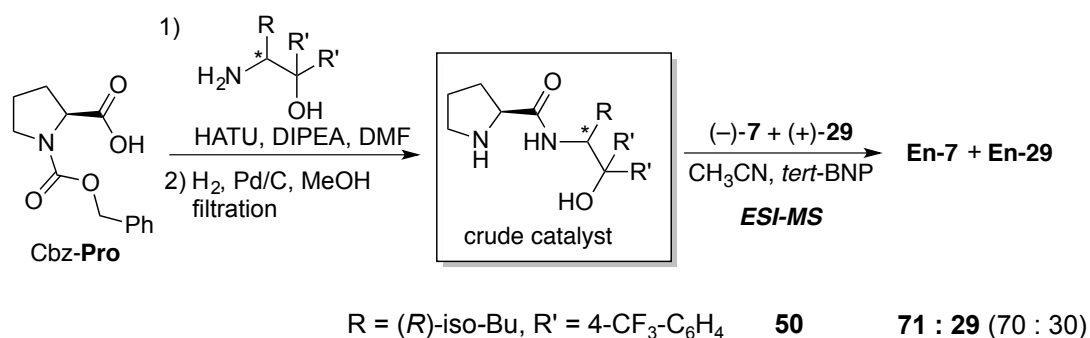
Scheme 25: One-pot synthesis of catalysts and analysis of the crude product by ESI-MS. The intermediate ratio of the purified catalyst is given in brackets.

The one-pot synthesis illustrated in Scheme 25 was successfully applied for the preparation of crude mixtures containing up to three catalysts. For that purpose, an equimolar mixture of the corresponding aminoalcohols was dissolved in CH$_2$Cl$_2$ and added dropwise to the solution of the active ester of proline. After deprotection of the Boc-group and workup, the crude products were obtained as colorless solids or foams, which showed high purity by ^{1}H NMR analysis. Applying the crude products to the back reaction screening, the resulting ESI-MS spectra were cleaner than the spectra obtained from crude products prepared with HATU as coupling reagent. The initial ESI-MS results of a two-catalyst crude mixture of **49** and (S,R)-**50** were very promising, clearly reflecting the preference for the opposite quasienantiomers in similar ratios to those obtained in the single catalyst screenings. The crude mixture of three catalysts was also successfully synthesized and subjected to ESI-MS analysis with aldol products (+)-**7** and (−)-**29**. Although changes of the signal ratios were observed, it was still possible to identify most selective catalysts out of the mixture (Figure 43).
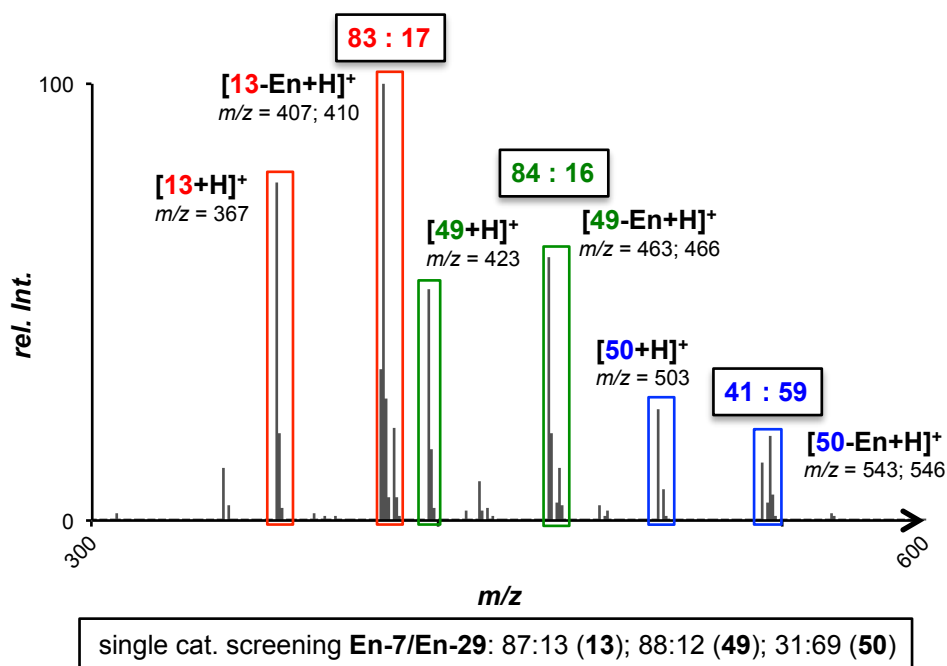
Figure 43: ESI-MS back reaction screening applying a crude mixture of three different catalysts synthesized according to the protocol illustrated in Scheme 25.
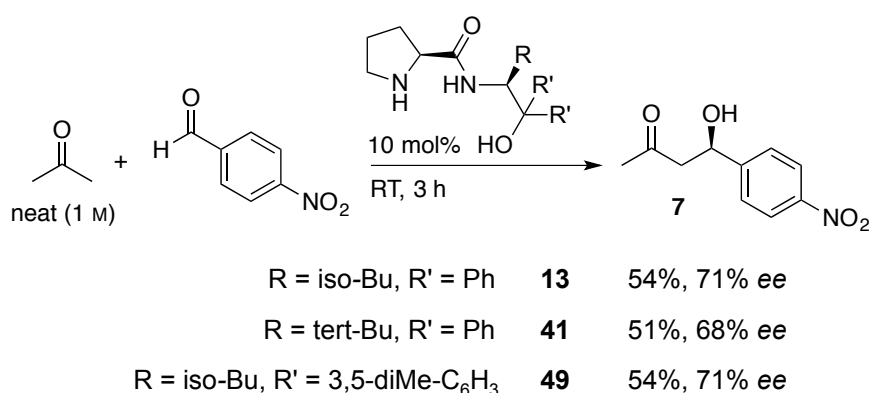
Since the applied synthesis protocol worked well affording crude products in high purity, only a small amount of background and impurity signals were present in the ESI-MS spectra. Moreover, enamine scrambling was considerably minimized compared to that observed for the crude products synthesized with HATU as coupling reagent. Therefore, ESI-MS screening of a mixture containing a catalyst providing the enamine in low intensities such as amine **14** was thought to be possible. Indeed, in the spectrum obtained from the catalyst mixture prepared from aminoalcohols **44** and **46** the enamine intermediates derived from **14** could be clearly analyzed and matched well with the ratio obtained from the purified catalyst (Figure 44). Besides the catalyst signal from **49** a third signal of high intensity was detected and identified as the condensation product **61** derived from catalyst **49**. For these catalyst structures elimination of the hydroxy group was frequently observed by ESI-MS. However, here also, the related enamine signals were found for this peak, which provides evidence that species **61** was already present in the catalyst mixture, resulting from a side reaction during deprotection of the Boc-group. According to the corresponding intermediate ratio, such a catalyst bearing an enamide moiety would induce almost no selectivity. This appears reasonable bearing in mind that a supporting hydrogen bond network is no longer possible.
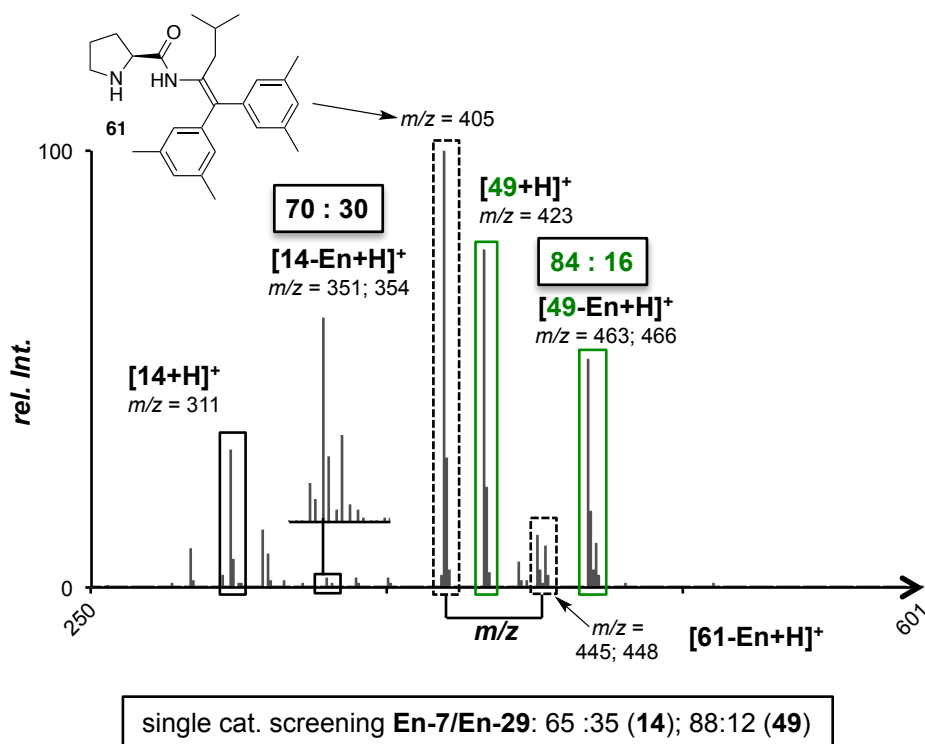
Figure 44: ESI-MS back reaction screening applying a crude mixture of catalysts derived from aminoalcohols **44** and **46** according to the protocol illustrated in Scheme 25.

2.9 Optimization of Preparative Aldol Reactions

Finally we were interested in how some of the new catalysts behave in preparative aldol reactions compared to Singh's catalyst **13** under reported optimized conditions.[44b] The general procedure for the aldolizations reported by the Singh group was first applied at room temperature (Scheme 26). The selectivities in neat acetone were found to be slightly lower, but still close to those obtained in the forward reactions under ESI-MS screening conditions in CH₃CN. However, the structural influence of the modified catalysts on the enantioselectivity and yield in acetone at room temperature is not high. Further improvement compared to the original catalyst was not achieved by this modifications.

R = iso-Bu, R' = Ph	**13**	54%, 71% *ee*
R = tert-Bu, R' = Ph	**41**	51%, 68% *ee*
R = iso-Bu, R' = 3,5-diMe-C₆H₃	**49**	54%, 71% *ee*

Scheme 26: *para*-Nitrobenzaldehyde aldol reaction at room temperature according to the original procedure reported by Singh.

The aldol reaction with *para*-nitrobenzaldehyde and catalyst **13** was only performed at –40 °C by the Singh group. Aldol product **7** was obtained in 70% yield and 99% *ee* in 24-48 h reaction time (Figure 46). Nevertheless, the result for catalyst **13** at room temperature is in excellent agreement with an independent investigation conducted by the Berkessel group (48%, 71% *ee*).[46] Applying this slightly modified protocol with only 5 mol% of catalyst **13**, the reaction proceeded in almost full conversion after 3 h reaction time with an *ee* of 73% for product **7** as was also observed under Singh's conditions. A closer look into the reaction by ¹H NMR analysis revealed considerable formation of the di-aldol product under these conditions, which resulted in the lower yields (Figure 45).
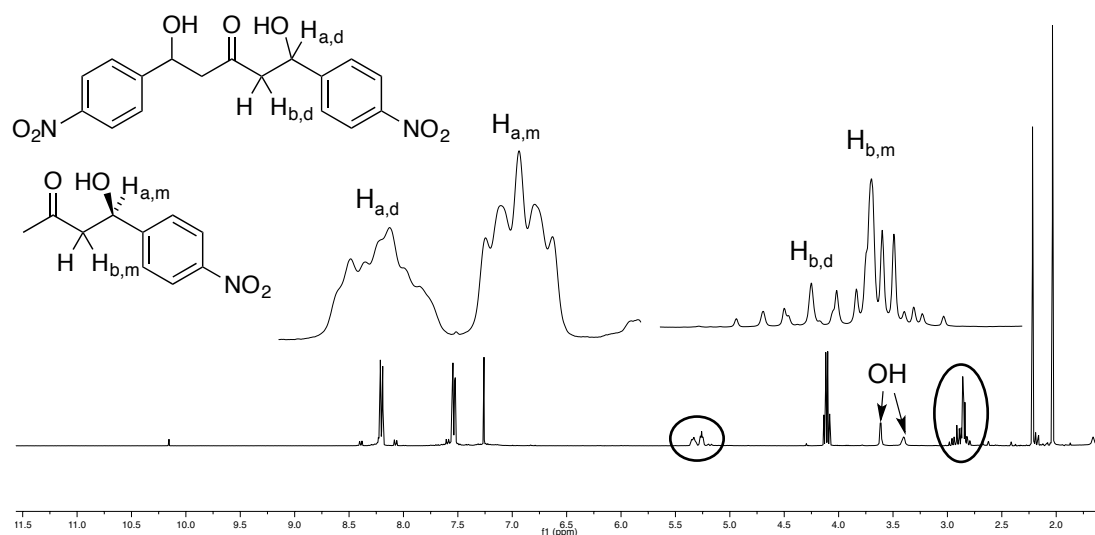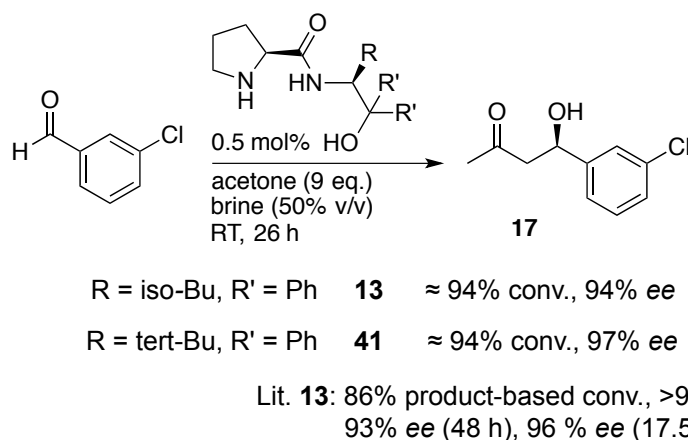
Figure 45: ^{1}H NMR spectra of the crude product of the aldol reaction of acetone and *para*-nitrobenzaldehyde catalyzed by **13**. The signals of the di-aldol product were assigned according to the literature data.[64]

Aldolization experiments to compare the *tert*-butyl substituted catalyst **41** to SINGH′S catalyst **13** under the reported optimized conditions at –40 °C were carried out (Figure 46).[44b] However, the reported results with catalyst **13** could not be reproduced. Even after 6 d reaction time almost no conversion took place with a maximum of 92% *ee* of the product when applying various conditions (Figure 46). For catalyst **49** the conversions were also extremely low, albeit the *ee* was slightly higher (94%) but still lower than the reported 99% *ee* for catalyst **13**. To identify potential sources of error the catalyst purity was verified by elemental analysis. Recently, catalyst **13** became commercially available from Sigma-Aldrich. Applying this catalyst charge still did not improve the results. The acetone quality also did not play an important role. The acetone was used without further treatment ("wet"), purchased as anhydrous solvent, freshly distilled over DRIERITE® prior to use or dried over Na_2SO_4 or K_2SO_4 (as reported in the literature) without seeing considerable enhancement of the conversion or the selectivity. Even at –15 °C the conversion was low. Since at low temperature the reaction mixture was found to be a suspension the mixture was further diluted. With a 0.1 M reaction mixture the best selectivity was observed so far was 92% *ee* still in low conversions. Direct purification by preparative TLC was found to give slightly higher selectivity values than the work-up described in the original procedure including NH_4Cl addition and extraction. It can be assumed that due to the extremely low conversions a slight racemization takes place during the work-up and/or reaction. This could be one explanation for the lower *ee* which did not further improve by decreasing the reaction temperature from 0 °C to –40 °C.
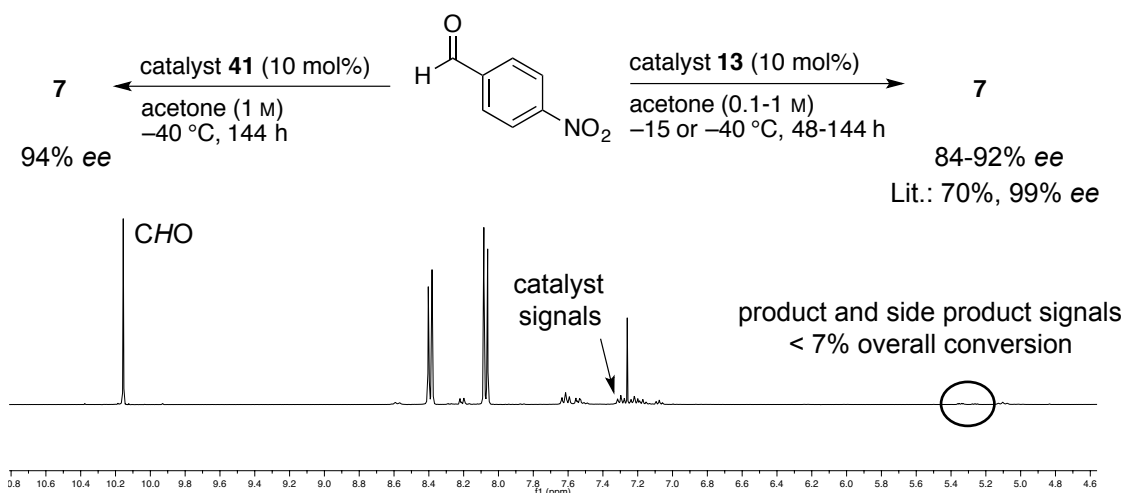
Figure 46: Aldol reactions at low temperatures applying SINGH'S conditions. ^{1}H NMR spectrum of the crude product after 48 h applying catalyst **13**.

In contrast to the reaction in an organic medium, aldol reactions in brine at room temperature according to a procedure of BERKESSEL were found to be reproducible when applying catalyst **13** (Scheme 27).[48a] The modified *tert*-butyl catalyst **41** was even found to induce slightly higher selectivities with comparable conversion.

| R = iso-Bu, R' = Ph | **13** | ≈ 94% conv., 94% *ee* |
| R = tert-Bu, R' = Ph | **41** | ≈ 94% conv., 97% *ee* |

Lit. **13**: 86% product-based conv., >95% overall
93% *ee* (48 h), 96 % *ee* (17.5 h)

Scheme 27: Aldol reaction in aqueous medium according to the procedure established by BERKESSEL.

The ESI-MS screening of catalysts for the aldol reaction was primarily investigated to demonstrate the generality of the principle of ESI-MS screening and not as a tool for the identification of new highly selective catalysts for aldol transformations. In addition, due to the fact that in an organic medium the catalyst system was found to be highly inactive under the conditions applied and given that optimal results were already reported in the literature, further optimization studies were not performed. Although in aqueous medium the results looked promising, high enantioselectivities and product-based conversions were already achieved with the now commercially available catalyst of SINGH. Moreover, such aqueous

conditions were suitable for ESI-MS screening since no enamine intermediates were detected even with only a small amount of water present in the reaction mixture.

2.10   Conclusion

In summary, an extension of the ESI-MS high-throughput screening methodology to organocatalyzed aldol reactions, monitoring formal neutral enamines as key intermediates, was developed. An isotope mass-labeling strategy was applied that allowed for a screening of acetone derived enamines which gave in preliminary experiments superior intensities compared to aldol products derived from other ketones such as cyclohexanone or acetophenone. In addition to different solvents and temperatures, for the first time the influence of additives was investigated and successfully monitored by ESI-MS analysis. Moreover, acids and in particular *tert*-BNP were found to be suitable additives to overcome measurement issues related to insufficient enamine protonation, deviation from the ideal Curtin-Hammett scenario, or dilution induced signal scrambling. Especially for catalysts derived from the basic framework of SINGH'S catalyst bearing a geminal di-aryl substituted tertiary hydroxy group, ESI-MS screening allowed for a perfect prediction of the enantioselectivity of the catalyst in its corresponding forward reaction. Since the additive showed only a minor influence on the selectivity, an efficient determination of the most selective catalysts in CH_3CN was possible despite the fact that the screening conditions did not exactly match the optimized preparative conditions. The benefit of the ESI-MS screening methodology is characterized by its short reaction and analysis times as well as low quantities of material consumed. In addition, no catalyst purification and workup of the reaction sample was required prior to analysis. Thus, simultaneous screening of crude mixtures of several catalysts becomes possible. Here the most selective catalysts were clearly identified by monitoring the corresponding enamine ratios in a single screening experiment.

CHAPTER 3

# ESI-MS Screening of Phosphines as Catalysts for Morita-Baylis-Hillman Reactions

3.1 Introduction

Organic molecules functionalized with one or more phosphorus atoms play a major role in asymmetric catalysis. Commonly, they are involved as chiral ligands in metal complexes for a vast range of synthetic transformations.[65] However, with the growing impact of organocatalysis in the 21st century, nucleophilic phosphines found also increasing application as organocatalysts.[66] The first groundbreaking phosphine-catalyzed C–C bond formation reactions were already reported in the 1960s when RAUHUT and COURIER and later MORITA investigated the catalytic influence of trialkylphosphines for the dimerization of acrylates and their reactions with aldehydes, respectively (Scheme 28).[67]

a) Rauhut-Currier reaction (vinylogous Morita-Baylis-Hillman)

b) MORITA's work

EWG = CN, CO$_2$CH$_3$
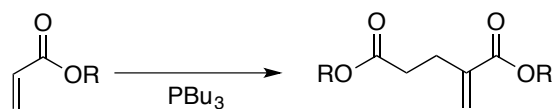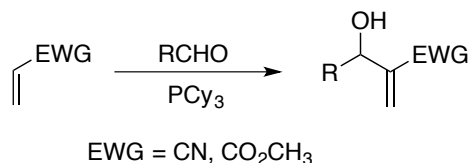
Scheme 28: Early work of RAUHUT and CURRIER in 1963 (a) and MORITA in 1968 (b).

3.1.1 Morita-Baylis-Hillman Reaction

In analogy to the early work of MORITA, BAYLIS and HILLMAN reported in 1972 a similar reaction catalyzed by tertiary amines.[67] The α-functionalization of activated olefins with a broad variety of carbonyl electrophiles or activated imines are nowadays commonly referred to as the Morita-Baylis-Hillman (MBH) and aza-MBH reaction, respectively (Scheme 29).[67-68] Several advantages attributed to the MBH reaction made this process to a powerful tool for C–C bond forming reactions in recent years. The process is operationally simple and occurs in general under mild reaction conditions and with perfect atom economy. Usually the starting

materials are commercially available or easily accessible and the reaction is suitable for upscaling. The required nucleophilic organocatalytic system avoids heavy-metal pollution in the final product and makes this process interesting for example for the synthesis of active pharmaceutical ingredients. Finally, the MBH reaction gives access to a variety of products bearing functional groups, which can be further transformed into many synthetically interesting products or starting materials.[67-68, 69]
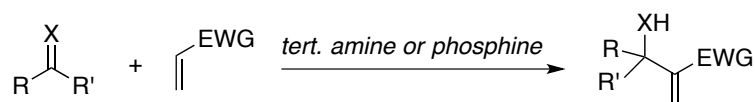
R = aryl, alkyl, hetereoaryl; R' = H, CO$_2$R", alkyl, *etc.*
X = O, NCO$_2$R", NSO$_2$Ar, *etc.*
EWG = COR", CHO, CN, CO$_2$R", PO(OEt)$_2$, SO$_2$Ph, SO$_3$Ph, SOPh, *etc.*

Scheme 29: Substrate scope of the MBH and aza-MBH reaction.

3.1.2 Bifunctional Phosphine Catalysts

The synthetic value of MBH-products as building blocks for further transformations was outlined above. To overcome limitations such as low yields, long reaction times and/or low induced selectivities new efficient catalysts are needed for this transformation. Besides tertiary enantiopure amines, multifunctional chiral phosphine catalysts, which contain a Lewis basic phosphorus atom and an additional Brønsted acidic reaction site were found to provide good to excellent reactivities and stereoselectivities in asymmetric aza-MBH and MBH reactions.[68a, 68b, 70] However, especially for the less reactive acrylates, only few examples of reactive and selective bifunctional phosphine catalysts are known. In 2009, WU developed a thiourea catalyst **62** which was found to induce low to good selectivities in excellent yields (Scheme 30).[71] Although in recent years several reports on similar catalysts followed after this promising result, there is still an enormous potential to be explored with these multifunctional catalyst structures.
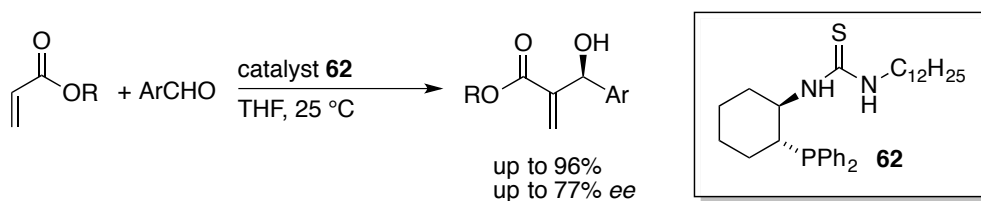
Scheme 30: Bifunctional phosphine-thiourea catalyst MBH reaction.

In 2011, our group reported new Ir-catalysts for asymmetric hydrogenation of trisubstituted alkenes bearing proline-derived P,O ligands.[72] Besides the common tertiary phosphine moiety some of the ligands are substituted with an additional urea moiety. The Brønsted acidic urea NH is capable of forming hydrogen bonds as illustrated for ligand **63** (Figure 47). Such phosphines could act as a potential bifunctional organocatalyst for MBH reactions.
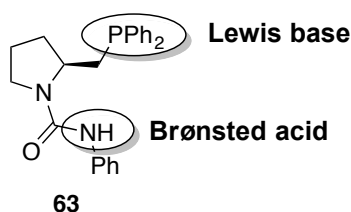

Figure 47: Proline-derived P,O ligand as potential bifunctional organocatalyst for MBH reactions.

3.1.3 Mechanism of the Morita-Baylis-Hillman Reaction

The mechanism of the amine-catalyzed version is illustrated in Figure 48a and is based on four key steps. A conjugate addition of a tertiary amine to an activated olefin forms a zwitterionic intermediate **I**, which can then undergo nucleophilic C–C bond formation at the α-position with the electrophile in an aldol-like reaction. A subsequent proton transfer and elimination generates MBH product **V** and releases the catalyst for the next cycle. Intermediates **I**, **II**, **III** and **V** using DABCO, acrylate and *para*-nitrobenzaldehyde were monitored and identified by ESI-MS/MS analysis.[73] However, recent theoretical and kinetic studies revealed that the proton transfer is more complex than initially proposed.[68a, 74] Two competing mechanism are discussed and illustrated in Figure 48. MCQUADE proposed a rate-determining proton transfer *via* a hemiacetal intermediate involving a second aldehyde. AGGARWAL also found a proton transfer step to be rate-determining, however only at the beginning of the reaction. For conversions >20% when a sufficient amount of product **V** is formed, the proton transfer becomes accelerated due to the autocatalytic properties of the MBH product **V** and the C–C bond cleavage should be rate-limiting. In general, both mechanisms are accepted and might occur in parallel depending on the reaction conditions.[68c] It has also been proposed that the selectivity is not necessarily introduced during the C–C bond formation. For example, depending on the reaction conditions the diastereomeric composition of intermediate **II** could erode the final enantioselectivity.[68a, 68c] AGGARWAL proposed that during the course of the reaction all four alkoxide diastereoisomers of intermediate **II** are formed. Applying bifunctional catalysts the origin of enantioselectivity

might than be caused by a subsequent fast proton transfer preferred with only one of these diastereoisomers due to the suitable positioned hydrogen-bond donor, whereas the other diastereoisomers react back to intermediate **I** (Figure 48b).[74a]
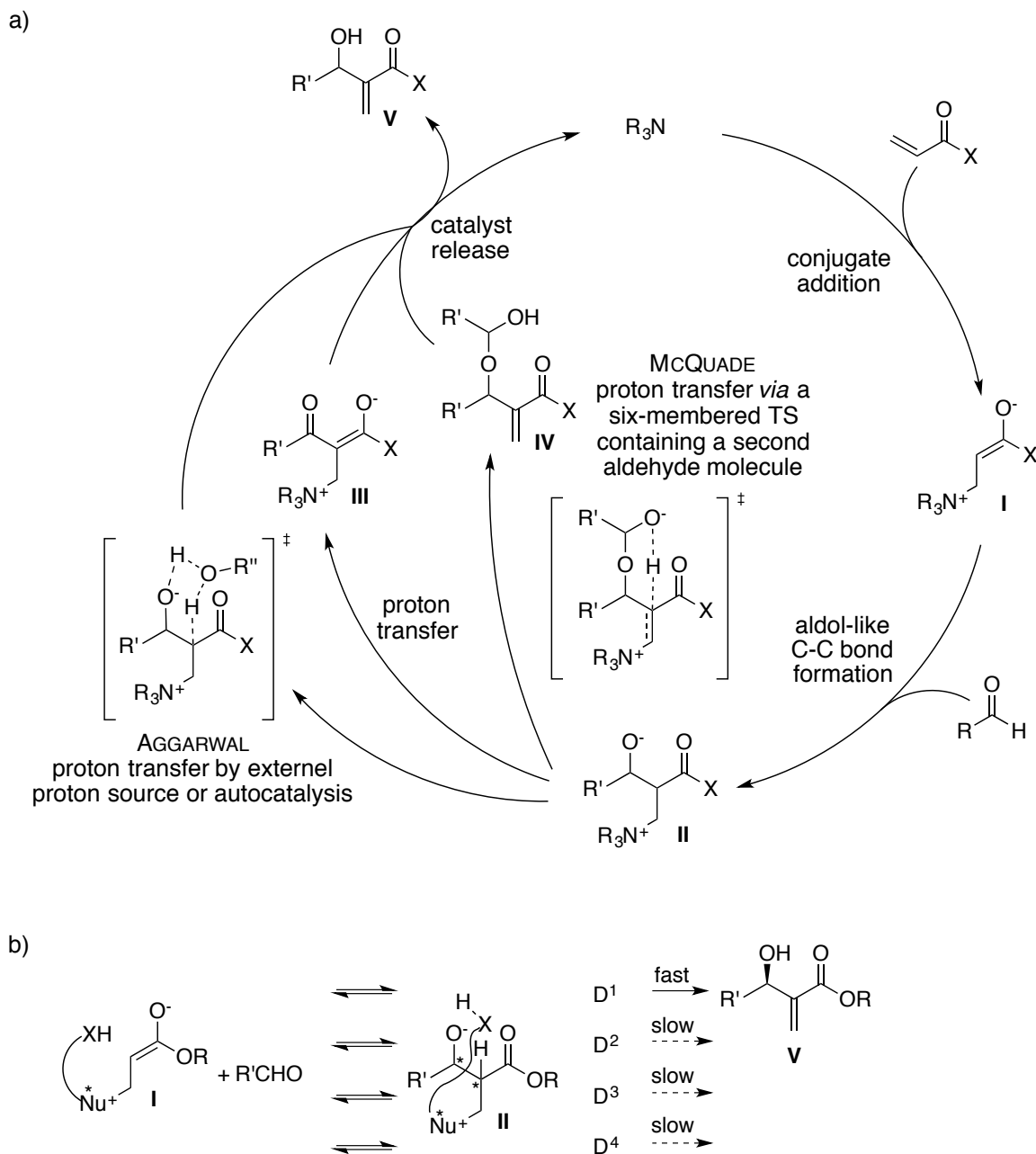
Figure 48: a) Proposed mechanistic pathways for the MBH reaction catalyzed by tertiary amines. The equilibrium arrows are omitted for clarity reasons. b) AGGARWAL proposal for the origin of enantioselection in the MBH reaction. D^{1-4} represents the four diastereoisomers of intermediate **II**.

3.2 ESI-MS Screening of Phosphine Catalysts

The ESI-MS screening method was so far successfully applied to organocatalyzed reactions proceeding *via* positively charged iminium ions or neutral enamines as key intermediates for ESI-MS analysis. The detection of phosphonium species as active catalytic intermediates was seen as a suitable opportunity to further broaden the scope of the ESI-MS methodology. Thus, the phosphine-catalyzed MBH reaction was chosen as a potential benchmark system for such a screening. Moreover, the need for new selective catalysts as well as the availability of phosphorus-containing ligands for Ir-catalyzed hydrogenations that could also act as potential organocatalysts provided additional incentive to develop an ESI-MS screening protocol for MBH reactions. In initial experiments potential reaction conditions and substrates that might enable an ESI-MS back reaction screening had to be identified.

3.2.1 Screening Methodology

Although most mechanistic studies had been carried out for amine-mediated MBH reactions, the mechanism for phosphines is commonly accepted to proceed through the same elemental steps (Scheme 31).[68a] For reasons of simplicity the proton transfer is not illustrated in full detail in this scheme. The same ESI-MS screening concept as illustrated for the aldol reaction in Chapter 2 was also applied to the MBH reaction (Scheme 31). Due to the full reversibility of the reaction the corresponding quasienantiomeric MBH products, bearing a mass-label X_A and X_B at the acrylate or ketone moiety, should react with the phosphine catalyst in a conjugate addition followed by a proton shift to form intermediate **II**. Subsequent C–C bond cleavage forms the phosphonium intermediates **I**, the targets for ESI-MS analysis. The intermediate ratio of **I** (M_A/M_B) should again correlate to the selectivity of the catalyst in forward direction, provided that the formation of **II** over the pre-equilibria in the back direction is fast and the C–C bond formation is the enantioselectivity-determining step of the reaction. However, both requirements could significantly complicate the back reaction screening. The complex proton transfer pathways could cause problems in the back reaction regarding the rate of equilibration of intermediates prior to C–C bond cleavage. In addition, the induction of enantioselectivity is not fully understood yet, but might not simply be governed by the C–C bond formation as illustrated in Figure 48b in the last section. If C–C bond formation is not the selectivity-determining step, then the intermediate ratios measured by ESI-MS should not match with the enantioselectivity determined in the preparative

forward reaction. Although this would prevent the use of ESI-MS for enantioselectivity determination, the results could provide valuable mechanistic information. It should be mentioned that ratio of intermediates related to the proton transfer step could not be monitored by ESI-MS screening of the back reaction due to the same mass of alkoxide **II** and intermediate **III** and hence the inability to distinguish between both by ESI-MS analysis.
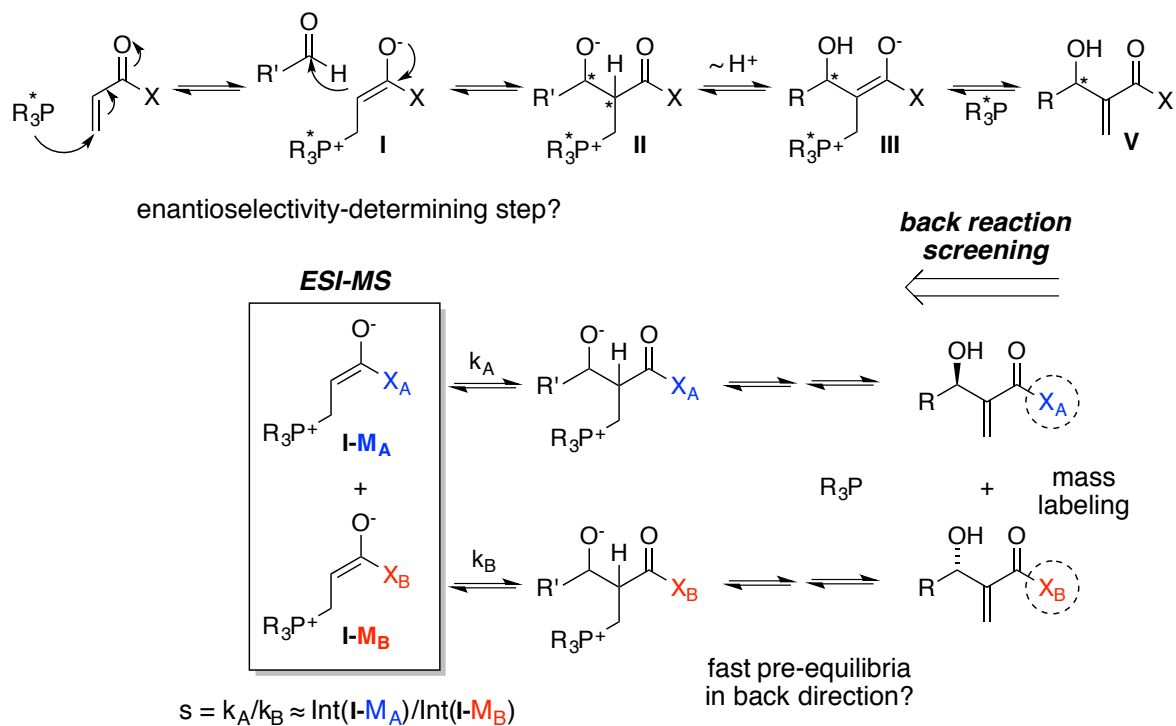
Scheme 31: Simplified mechanism for phosphine-catalyzed MBH reactions and a screening of the corresponding back reaction applying mass-labeled quasienantiomeric MBH products.

3.2.2 Synthesis of MBH Products

To introduce a mass-label into the MBH products, acryloyl esters or alkyl vinyl ketones were supposed to be suitable and easily accessible precursors, either by Grignard additions of vinyl magnesium bromide to aldehydes and subsequent oxidation or esterification reactions of acryloyl chlorides with the corresponding alcohols (Scheme 32).
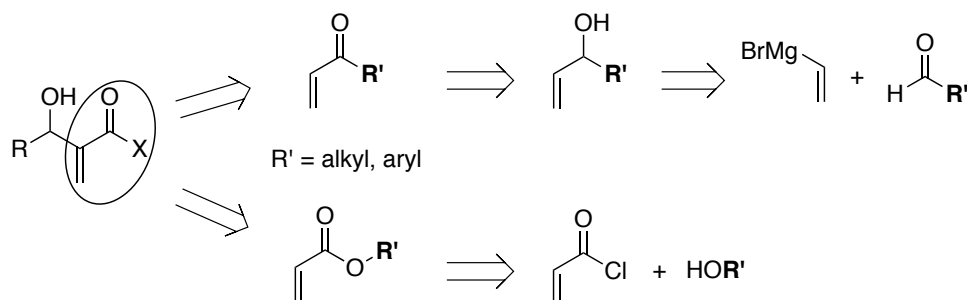
Scheme 32: Retrosynthetic analysis of MBH products with various residues (**R'**) for a final mass-labeling of the MBH products.

For the initial synthesis MBH products derived from acryloyl esters were chosen. These substrates were already reported to undergo *retro*-MBH reactions, which makes them to ideal substrates for the initial ESI-MS experiments (Scheme 33).[75]
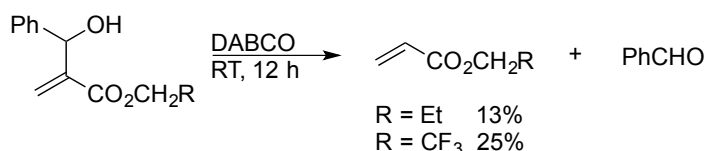
Scheme 33: Previously reported *retro*-MBH reactions.

The synthesis of MBH product **69** derived from methyl acrylate and *para*-nitrobenzaldehyde catalyzed by DABCO afforded the desired product in poor yields. Therefore, for a more effective application a Lewis acid catalyzed MBH reaction reported by Aggarwal was applied as a general procedure for substrate synthesis (Table 7).[76] The synthesis of the alkyl acrylates as proposed in Scheme 32 from acryloyl chloride worked as predicted. For sterically more demanding substrates, longer reaction times showed a beneficial effect on the conversions in the subsequent Lewis-acid mediated MBH reaction. For most of the MBH products suitable HPLC conditions were found allowing for a fast separation of the racemic compound into its enantiomers on the available chiral columns. Therefore, for the synthesis of later required enantiopure quasienantiomers, further derivatization, as described in Chapter 2 for the aldol products, or an asymmetric transformation inducing high enantioselectivity, is not necessary for this substrate class.

Table 7: Synthesis of alkyl acrylates and MBH products.[i]
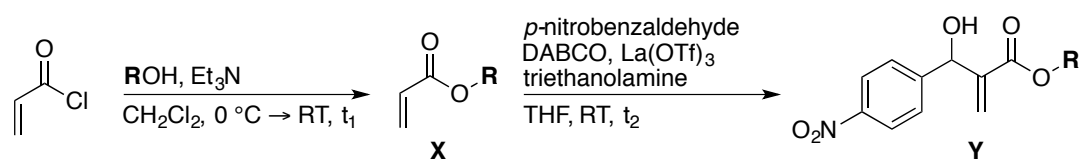
entry	R	t_1 [h]	X (yield [%])	t_2 [h]	X (yield [%])
1	methyl	-	-[a)]	3	**69** (75)
2	ethyl	-	-[a)]	3	**70** (69)
3	iso-propyl	8	**64** (69)	5	**71** (20)
4	*tert*-butyl	16	**65** (24)	6	**72** (10)
5	*tert*-pentyl	16	**66** (24)	20	**73** (25)
6	octyl	16	**67** (52)	48	**74** (86)
7	*p*-methylphenyl	16	**68** (74)	20	**75** (7)

a) Product **X** is commercially available.

3.2.3 Preliminary ESI-MS Results

In a first set of experiments it was tested for a proof of concept whether it is possible to monitor key intermediate **I** under standard ESI-MS parameters in the forward direction. For this purpose, *para*-nitrobenzaldehyde was reacted with methyl acrylate in the presence of PPh_3 as catalyst. MeOH was applied as reaction solvent and proton source to transfer the zwitterionic intermediates into ESI-MS detectable positively charged species. After dilution of an aliquot of the reaction mixture with MeOH, ESI-MS analysis showed clear formation of the key intermediate **I** and already after 30 min reaction time trace amounts of the isomeric intermediates **II** and **III** generated after C–C bond formation were detected (Figure 49). A third signal with a mass of [cat+31], also measured for other catalysts in MeOH, was assigned to an oxidized catalyst-MeOH adduct.

---

[i] P. ISENEGGER synthesized further MBH products as potential mass-labeled quasienantiomers derived from alkyl acrylates and alkyl vinyl ketones during his master thesis.
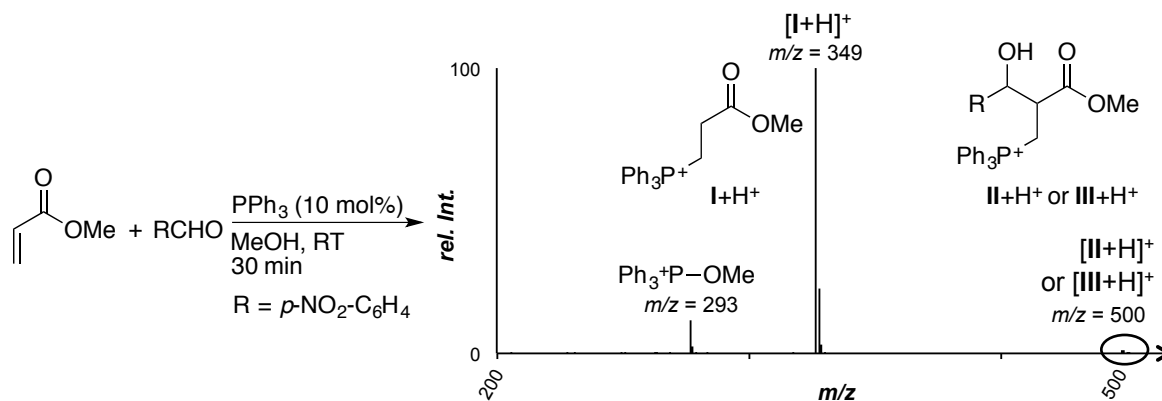
Figure 49: ESI-MS analysis of the forward MBH reaction.

Although the spectrum looked more crowded in the back reaction using substrate **69**, intermediate **I** was formed in good intensities even with PPh$_3$, a rather poor catalyst for this transformation. Applying the bifunctional proline derived catalyst **63**[i] the back reaction proceeded smoothly with almost exclusive formation of intermediate **I**. The low intensities of intermediates **II** and **III** monitored with catalyst **63** compared to those obtained with PPh$_3$ led to the assumption that a more effective back reaction, or at least C–C bond cleavage, takes place with the bifunctional catalyst.
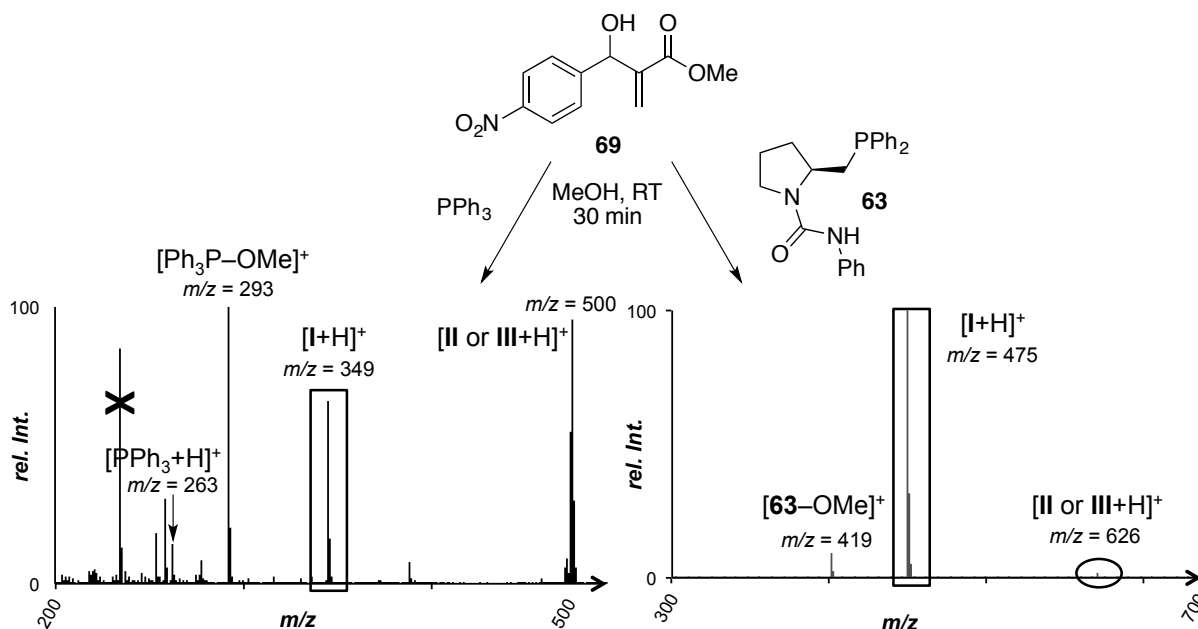
Figure 50: ESI-MS analysis of the back reaction with MBH product **69** mediated by PPh$_3$ (left) or bifunctional phosphine **63** (right).

---

[i] Catalyst **63** was kindly provided by D. RAGEOT.

Being active in the back direction, catalyst **63** was also examined for its activity and selectivity in the forward reaction of methyl acrylate and *para*-nitrobenzaldehyde. Although, good conversion was observed after 24 h in CH_2Cl_2, the catalyst induced no enantioselectivity and product **69** was isolated as a racemate.

The back reactions were performed for several MBH products in MeOH with PPh_3 or catalyst **63**. The reaction mixture or an aliquot was subsequently diluted and analyzed by ESI-MS. Several observations became apparent:

(i)   For all investigated products signals of intermediate **I** isomeric intermediates **II** and **III** were monitored.

(ii)   Throughout the measurements with PPh_3 as catalysts, the signal of intermediates **II** or **III** was more intensive than that of intermediate **I**. In contrast, catalyst **63** in the majority of cases led to the formation of **I** as the major intermediate.

(iii)   Elongation of the chain on the ester moiety and especially an increasing sterical bulk led to a considerable decrease of the signal intensity of the intermediates.

(iv)   In preliminary experiments equimolar mixtures of racemic mass-labeled substrates were reacted with the corresponding catalysts. If the mass-label has no influence a 50:50 ratio of the intermediates is expected. However, the results obtained for various combinations of mass-labeled substrates, which differ in the ester moiety indicated that the side chain showed a strong influence on the ratio of key intermediate **I**. Interestingly the influence was even different depending on the nature of catalyst being investigated (Figure 51).

(v)   Longer reaction times in MeOH, applying MBH products other than methyl ester **69**, led to the formation of a considerable amount of the transesterification product.

(vi) CH_2Cl_2 as a reaction solvent followed by dilution with CH_2Cl_2 and AcOH showed promising results in the back reaction. In an initial experiment with bifunctional catalyst **63** and MBH product **75** intermediate **I** was still formed as base peak.

An example for the influence of the side chain moiety and the catalyst dependency is illustrated in Figure 51. Further investigations conducted by P. ISENEGGER during his master thesis with longer linear aliphatic chains also revealed an influence of the mass label.[77]
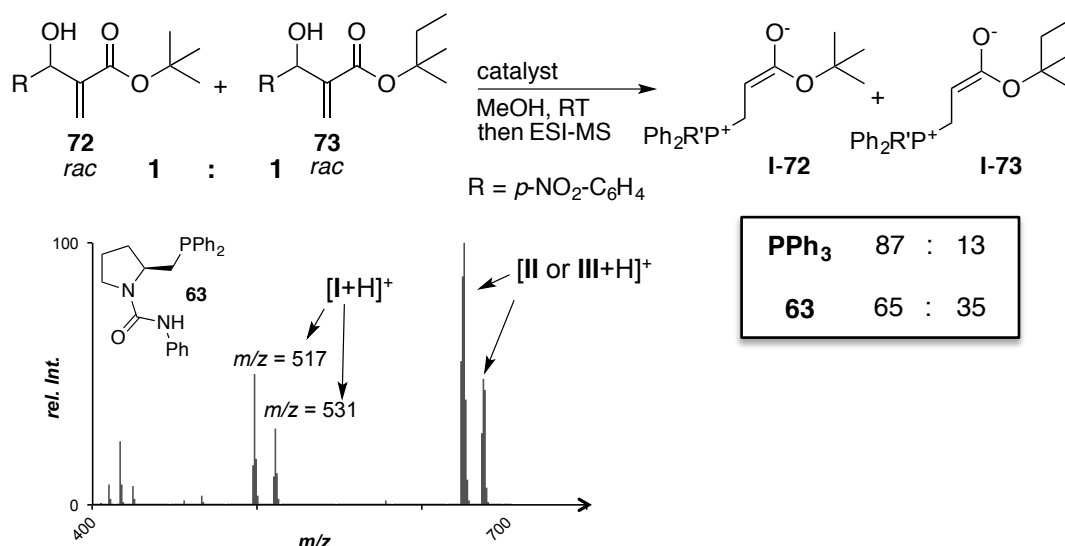
Figure 51: ESI-MS back reaction analysis starting from a mixture of racemic MBH products (broad signal patterns caused by insufficient ESI-MS tuning).

In several experiments a transesterification was observed by ESI-MS especially after longer reaction times (Figure 52a). For octyl-MBH product **74** all four intermediates bearing either a methyl- or an octyl-group were detected by ESI-MS after 45 min whereas after 120 min only the methyl-labeled intermediate **I** was left in the spectrum. During initial ESI-MS screenings performed in the PFALTZ group aryl groups that differ in a mass-label in *para*-position were usually applied as quasienantiomers. However, for the corresponding MBH aryl ester **75** transesterification was even completed after 30 min in MeOH, probably due to the phenol which acts as a better leaving group. The same process was observed even when the back reaction was conducted in CH$_2$Cl$_2$ and the reaction mixture was diluted with MeOH prior to analysis. This also indicated a scrambling during the ESI-MS ionization process. One plausible mechanism for the transesterification could involve formation of a ketene intermediate, however the mass of such a species was only observed in one ESI-MS spectrum in very low intensities. To eliminate transesterification as a side reaction using CH$_2$Cl$_2$ as both reaction and dilution solvent with AcOH as a proton source was investigated and proved to be promising.
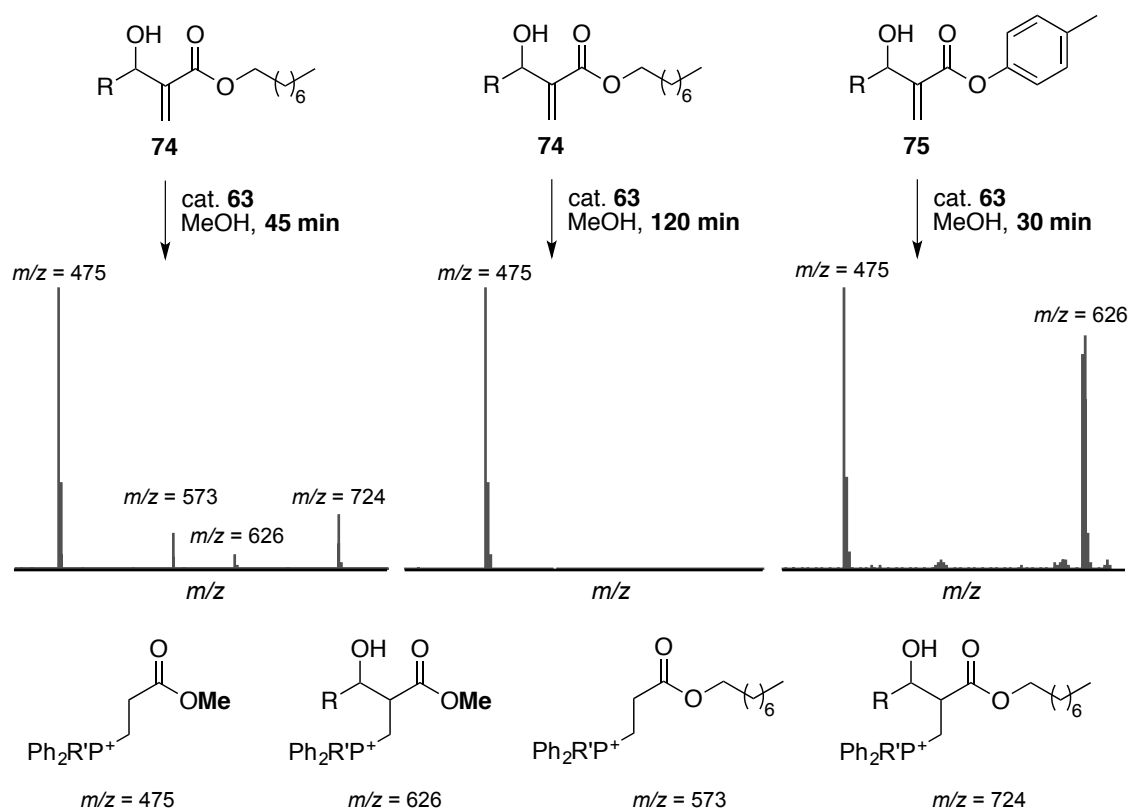
Figure 52: Transesterification in back reaction experiments in MeOH.

3.3   Conclusion and Current Research Progress

The aim of these preliminary experiments was the identification of potential reaction conditions and substrates that might enable an ESI-MS back reaction screening of the MBH reaction. For a variety of acrylate derived MBH products the desired phosphonium species **I** was detected in good to excellent intensities with two different catalysts. However, the ester moiety showed a considerable influence on the intermediate intensity, which decreased with increasing bulk and chain length and thus gave a first indication of limitations for potential mass-labels.

After these promising initial results, this work was continued by P. Isenegger during his master thesis and is currently still an ongoing research project within our group.[77] During these investigations CH_2Cl_2 was indeed identified as a suitable screening solvent for a broad variety of new bifunctional thiourea and squareamide derived phosphine catalysts. A combination of a deuterated and a non-labeled MBH product **69** was identified as a suitable pair of quasienantiomers having no influence on the selectivity of the catalyst (Figure 53). The deuterium label was easily introduced by the standard reaction procedure illustrated in Table 7. Moreover, screening new bifunctional catalysts in the back reaction, in the majority of the cases the intermediate ratios monitored by ESI-MS were in an excellent agreement with the preparative forward reaction. This provides evidence that the C–C bond formation is indeed the selectivity-determining step under the conditions investigated.
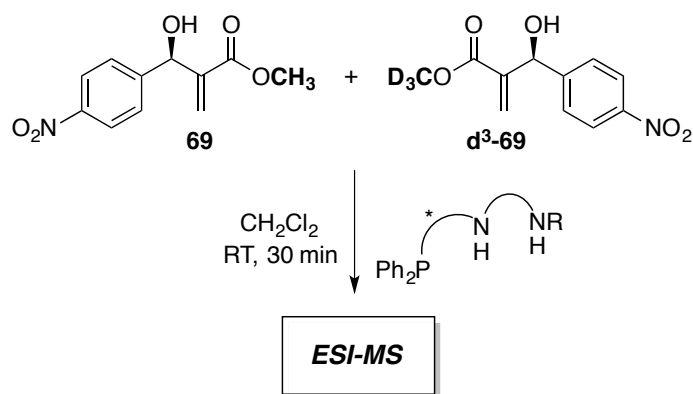
Figure 53: Optimized ESI-MS back reaction screening in CH_2Cl_2 applying a pair of quasienantiomers differ in the deuterated ester moiety as mass-label.

CHAPTER 4

ORGANOCATALYTIC ASYMMETRIC CONJUGATE ADDITION OF ALDEHYDES TO NITROOLEFINS: MECHANISTIC INVESTIGATIONS BASED ON ESI-MS STUDIES OF THE BACK REACTION

4.1 Introduction

4.1.1 Organocatalytic Asymmetric Conjugate Addition of Aldehydes to Nitroolefins

Addition reactions of enolizable carbonyl compounds to electrophiles are among the most widely used organocatalytic reactions. In particular, nitroolefins have emerged as prominent acceptor molecules for conjugate addition reactions due to their high reactivity and useful functionalities allowing for further synthetic transformations.[18c, 78] The first example of an organocatalyzed conjugate addition of unmodified aldehydes to nitroolefins was reported in 2001 by BARBAS employing pyrrolidine-type diamine catalysts. Although long reaction times were required for sufficient conversions, good to excellent yields and diastereoselectivities as well as enantioselectivities of up to 78% *ee* were generated using morpholine-pyrrolidine **76** as catalyst (Scheme 34).[79]
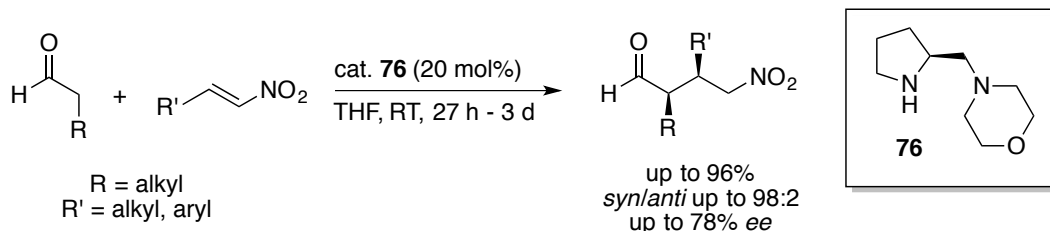
Scheme 34: First organocatalyzed conjugate addition of aldehydes to nitroolefins.

A few years later HAYASHI introduced a new catalyst system for asymmetric conjugate additions based on silyl-protected diarylprolinols (Scheme 35).[80] Independently, the same catalyst was applied by JØRGENSEN for enantioselective α-sulfenylations of aldehydes.[81] These two findings could be considered as another milestone in organocatalysis, as the TMS-protected diphenylprolinol **77a**, now commonly referred to the Hayashi-Jørgensen catalyst, has become a privileged catalyst for a variety of organocatalyzed transformations.[82]
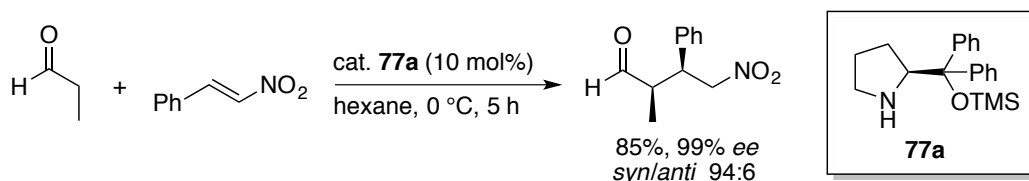
Scheme 35: Organocatalytic conjugate addition of aldehydes to nitroolefins mediated by Hayashi-Jørgensen catalyst **77a**.

101

Although the reported procedure of HAYASHI afforded addition products in excellent yields and selectivities, high catalyst loadings of 10 mol% were required for a sufficient reactivity. When the catalyst loading was reduced to 5 mol%, a reaction time of 38 h at room temperature was required to achieve comparable results.[80] A few years later, the group of WENNEMERS identified tripeptides of the structural motif Pro-Pro-Xaa (Xaa = acidic amino acid) to catalyze the conjugate addition smoothly, affording disubstituted γ-nitroaldehydes (**80**) in excellent yields and stereoselectivities using ≤1 mol% of catalyst loading (Scheme 36a).[83] A related tripeptide with an acidic side chain was found to mediate efficiently the addition of aldehydes to more challenging α,β-disubstituted nitroolefins affording synthetically useful γ-nitroaldehydes (**81**) bearing three consecutive stereogenic center (Scheme 36b). A dipeptide, functionalized at the C-terminus with an amine lacking a carboxylic acid and amide residue, was a suitable catalyst for β,β-disubstituted nitroolefin acceptors and even allowed for the construction of quaternary stereogenic center (**82**, Scheme 36c).[84]
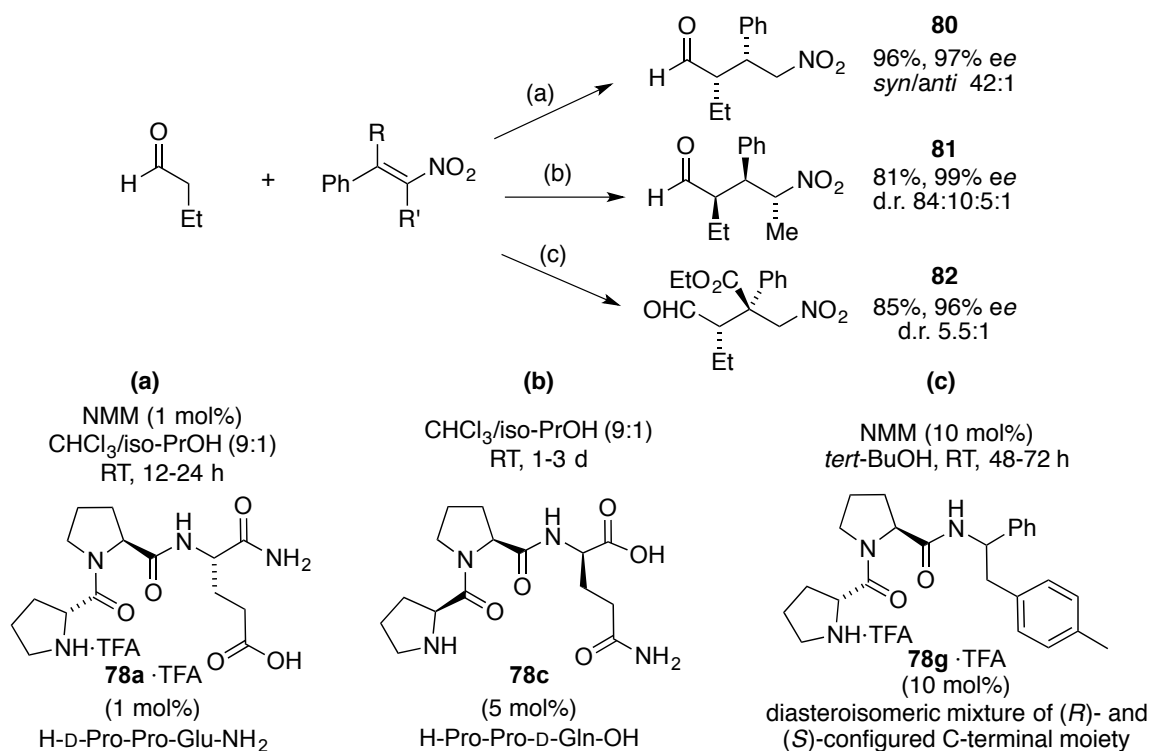
Scheme 36: Selected examples for peptide catalyzed conjugate addition of aldehydes to nitroolefins. The depicted products represent the major diastereoisomer.

4.1.2 Current Mechanistic Considerations of Conjugate Addition Reactions – ESI-MS Back Reaction Analysis as Mechanistic Tool

A plausible mechanism for the reaction of carbonyl compounds with electrophiles mediated by secondary amines involves formation of a nucleophilic enamine intermediate. This is discussed in detail in Chapter 2 for organocatalyzed aldol reactions. Besides ^{1}H NMR studies with proline[36a] the GSCHWIND group was also able to monitor enamine intermediates for aldehydes with prolinol-type amines and Hayashi-Jørgensen catalyst **77a**. Superior enamine concentrations where observed in DMSO, in particular for catalyst **77a**, which is, in contrast to prolinol, not able to form oxazolidines.[85] METZGER found enamine evidence within ESI-MS studies on the α-halogenation of aldehydes.[86] Although an enamine mechanism has been widely accepted, an alternative mechanism involving non-covalent activation by enol formation is still discussed (Figure 54). In studies conducted by the group of TSOGOEVA, evidence for an enol mechanism was found by computational and labeling experiments in a primary amine-thiourea catalyzed Mannich-type reaction.[87] Computational work of WONG revealed that for several C–C and C-X bond forming reactions catalyzed by amine **77a** an enol mechanism would fully account for the experimentally observed enantio- and diastereo-selectivity.[88] ALEXAKIS and KRAUSE found evidence for an enol mechanism by ^{18}O-incorporation experiments on the 1,4-addition of aldehydes to nitrodienes. The obtained results suggested that both an enamine and an enol pathway was active. However, the reaction was carried out in aqueous media where enamine formation should be disfavored.[89]
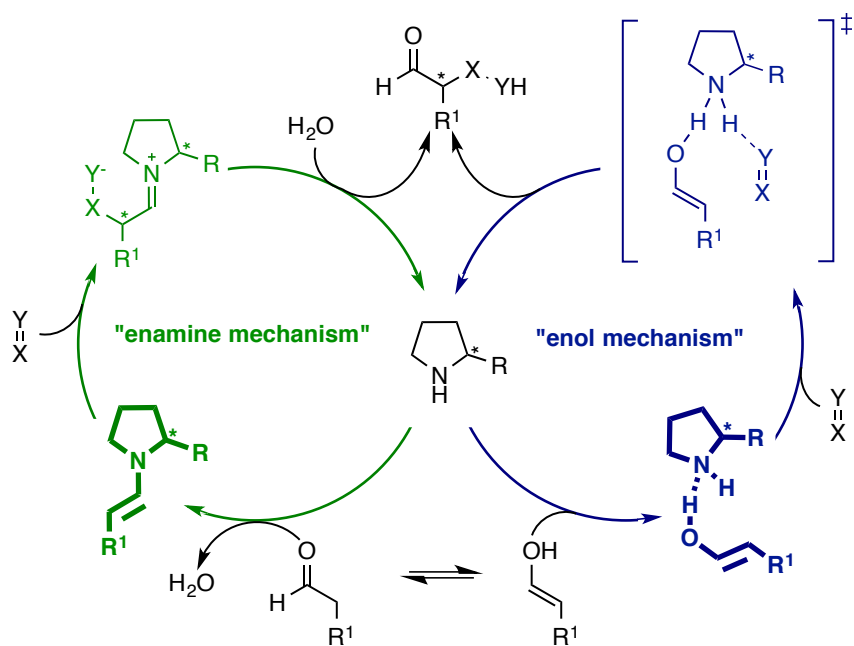
Figure 54: Enamine *vs.* enol mechanism for amine-catalyzed reactions of aldehydes with electrophiles.

103

The concept of the ESI-MS screening methodology introduced in previous chapters was envisioned to be ideally suited to examine whether conjugate addition reactions between aldehydes and nitroolefins proceed *via* an enamine or enol intermediate. Standard ESI-MS based mechanistic investigations solely rely on the detection of species formed in the reaction mixture,[90] however the back reaction screening method also provides information on the enantioselectivity-determining step and the intermediates involved. Applying a pair of mass-labeled quasienantiomeric conjugate addition products **79** and **79'** to the back reaction catalyzed by tripeptides of the type Pro-Pro-Xaa **78**, enamine intermediates **En** and **En'** should be formed and monitored by ESI-MS (Figure 55).[i] If the reaction of the enamine with the nitroolefin is rate-determining in the forward reaction, the stereoselectivity **79/79'** (= k_1/k_2) is determined by the energy difference $\Delta\Delta G^{\ddagger}$ of the transition states of this step leading to **Im** and **Im'**. In this case, according to the principle of microscopic reversibility, the same transition states would also control the stereoselectivity of the back reaction, which is characterized by a pre-equilibrium to form iminium ions **Im** and **Im'** and a slow rate-determining C–C bond cleavage (Curtin-Hammett conditions). Thus, a enamine ratio (**En**/**En'**) measured in the back reaction by ESI-MS that matches the enantioselectivity determined for the preparative forward reaction would provide strong evidence for the involvement of the enamine rather than the enol intermediate in the enantioselectivity-determining step. On the other hand, a signal ratio (**En**/**En'**) that deviates from the stereoselectivity of the preparative reaction does not necessarily rule out an enamine mechanism. It only shows that C–C bond formation is not the enantioselectivity-determining step.

---

[i] The signals correspond to the protonated cationic forms.
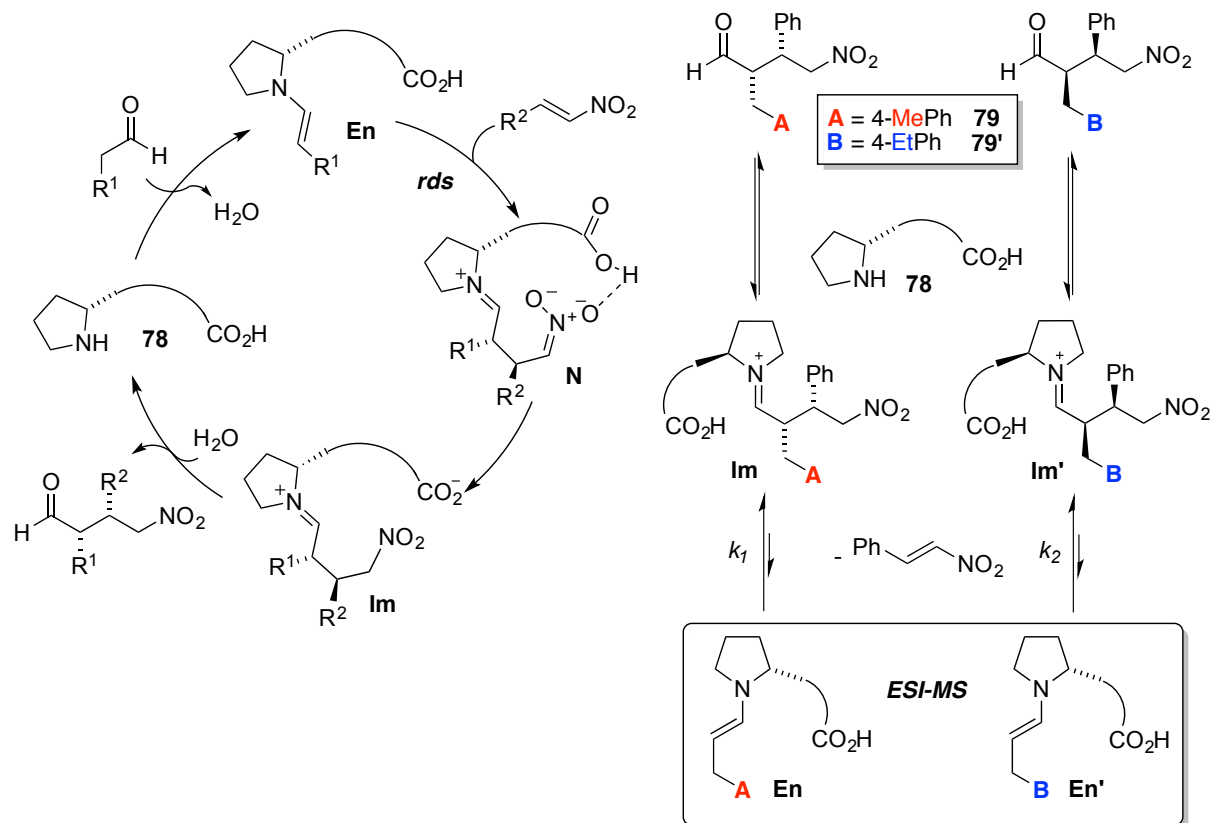
Figure 55: Proposed mechanism for catalysts bearing an acidic side chain (left). Principle of the ESI-MS back reaction screening applying quasienantiomeric nitroaldehydes (right).

Recent mechanistic studies revealed that the reaction proceeds *via* alternative pathways with different rate-determining steps for catalysts either bearing or lacking a carboxylic acid moiety (compare catalytic cycles Figure 55 and Figure 56).[91] WENNEMERS *et al.* studied in more detail the addition of butanal to nitrostyrene catalyzed by tripeptides of type **78** with a free acid or an ester group in the side chain.[91a] Indeed, these catalysts were found to react different in their reaction kinetics. For catalysts bearing a suitably positioned intramolecular carboxylic acid moiety the reaction proceeded faster and the conversion-time profile showed a fast reaction in the beginning, which slows down after the starting materials are consumed. This indicates a dependence of the reaction rate on the concentration of at least one reactant. In contrast, for the peptide bearing the ester a sigmoidal shape was found where the reaction is slow in the beginning and becomes faster with proceeding conversion. Furthermore, for higher concentrations of butanal or nitrostyrene the reaction profile did not change. Both findings indicate that for the ester catalyst the reaction rate does not depend on the substrate concentrations. Further, addition of an external acid additive had no influence on the reaction rate for peptides with an incorporated acid, whereas for the peptide ester significant rate acceleration was observed. ^{1}H NMR studies of the stoichiometric reaction of tripeptides with the reagents revealed immediate formation of a cyclobutane intermediate **C** (Figure 56) as the

only observable new species for the catalyst lacking a carboxylic acid. In contrast, only formation of the γ-nitroaldehyde product was monitored for the identical reaction with the acid bearing catalyst. The findings described above for the tripeptide ester, such as the independence of the reaction rate on the concentration of applied substrates, the rate acceleration in the presence of acid and cyclobutane formation as a resting state are in line with observations made with the Hayashi-Jørgensen catalyst **77a**.[91c, 91f] In general, for catalysts bearing a suitably positioned intramolecular acid the protonation of the nitronate **N** to generate the iminium ion (**Im**) is proposed to be fast and C–C bond formation is rate limiting (Figure 55). Thus, the reaction rate depends on the enamine concentration and the nitroolefin but not on external proton sources. On the other hand, for catalysts lacking a covalently attached acid the intermediates are stabilized by C–C bond formation to the cyclobutane **C** or dihydrooxazine oxides **OO** and protonation of these intermediates becomes the rate limiting step (Figure 56).[91a] The different rate-determining steps in the catalytic cycles of acidic and non-acidic catalysts suggest that the enantioselectivity-determining steps may also differ. In fact, BLACKMOND proposed for reactions catalyzed by the Hayashi-Jørgensen catalyst that the stereoselectivity depends on the relative stability and reactivity of the diastereomeric cyclobutanes.[91c] Hence, the application of the ESI-MS screening for an identification of intermediates involved in the enantioselectivity-determining step, was supposed to give further insights about the mechanism of catalysts bearing or lacking a covalently attached acid. Whereas in the first case ESI-MS monitored enamine ratios should match the selectivities determined in the preparative forward reaction, for latter catalysts a mismatch case was expected where the C–C bond formation is not the selectivity-determining step.
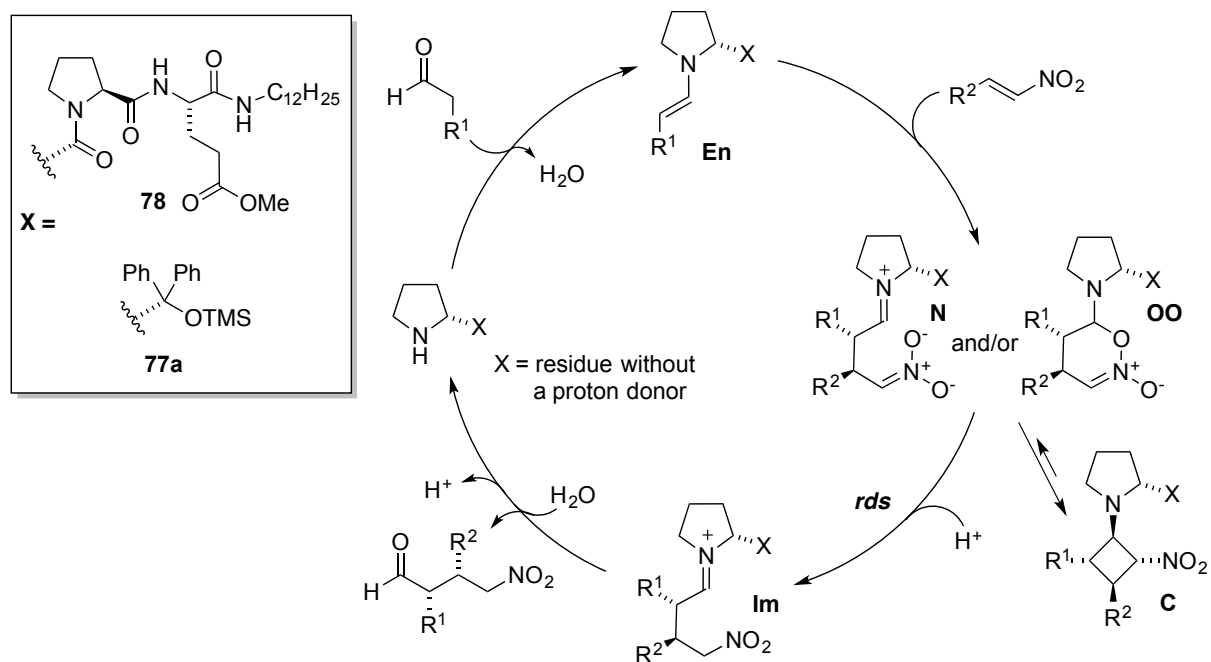
Figure 56: Proposed mechanism for catalysts lacking a covalently attached proton donor (**C** = cyclobutane intermediate).

4.2 ESI-MS Back Reaction Experiments on the Conjugate Addition Reaction

4.2.1 Preparative Reactions

The results presented were acquired in collaboration with the research group of H. WENNEMERS.[92] Mass labeled quasienenatiomeric substrates **79** and **79'** were synthesized by J. DUSCHMALÉ starting from ethyl- and methyl-substituted iodobenzene by a Heck reaction. In the subsequent organocatalyzed addition reaction catalyzed by H-D-Pro-Pro-Glu-NH$_2$ **78a** and its enantiomer, respectively, both substrates were obtained in 97% *ee*,[i] confirming that the mass labels do not affect the stereoselectivity of the reaction (Scheme 37). The organocatalyzed reaction under identical conditions employing commercially available 3-phenylpropanal also afforded the product in 97% *ee*. Therefore, in order to validate the ESI-MS screening results the unsubstituted aldehyde was used for preparative reactions, which were conducted by J. DUSCHMALÉ. The group of H. WENNEMERS provided the peptide catalysts, which were applied for ESI-MS investigations.
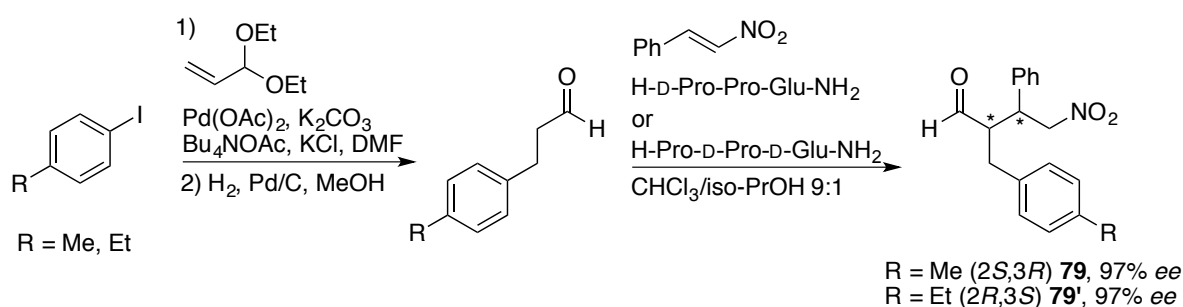
Scheme 37: Synthesis of mass-labeled quasienantiomeric conjugate addition products.

The reversibility of the conjugate addition reaction was confirmed by cross-over experiments conducted by J. DUSCHMALÉ. γ-Nitroaldehyde 2-ethyl-3-(4-methoxyphenyl)-4-nitrobutanal was reacted with H-D-Pro-Pro-Glu-NH$_2$ **78a** in the presence of one equivalent of *trans*-β-nitrostyrene in a 9:1 mixture of CDCl$_3$/iso-PrOH d-9. Examination of the reaction mixture by ^{1}H NMR spectroscopy showed the release of approximately 20% of *trans*-4-methoxynitro-styrene within 2 weeks. This finding demonstrated that the conjugate addition reaction is reversible, although the back reaction proceeds slowly.

---

[i] The enantiopurity of 97% of the quasienantiomeric substrates was sufficient for the subsequent mechanistic studies.

4.2.2 Initial ESI-MS Experiments

Preliminary ESI-MS experiments were conducted by C. EBNER.[92-93] First, the forward reaction of 3-phenylpropanal and *trans*-β-nitrostyrene catalyzed by tripeptide H-D-Pro-Pro-Glu-NH$_2$ **78a** in the protic solvent mixture of CHCl$_3$/iso-PrOH was examined by ESI-MS. Both intermediates (**En** and **Im**) proposed for the enamine pathway (Figure 55, left) were identified by ESI-MS analysis (Figure 57, left). Nevertheless, although the enamine signal was clearly detected in the reaction mixture, it does not unambiguously rule out an enol mechanism. Having observed enamine signals in the forward direction, the back reaction was performed with an equimolar mixture of quasienantiomeric substrates **79** and **79'** and 10 mol% of catalyst **78a**. Under these conditions only signals related to the free catalyst and the iminium ions (**Im** and **Im'**) were observed in the corresponding ESI-MS spectrum (Figure 57, right).
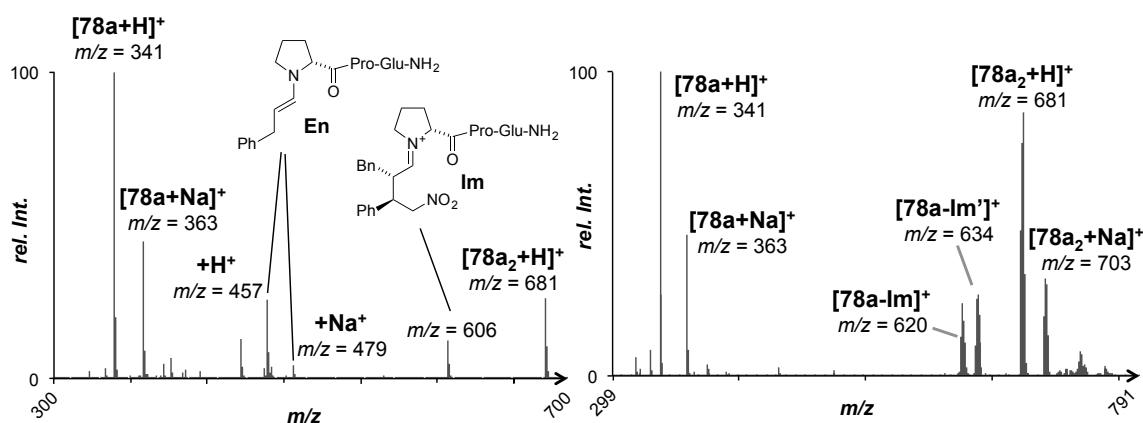
Figure 57: ESI-MS analysis of the forward reaction (left) and the back reaction using quasi-enantiomeric substrates **79** and **79'** (right) in CHCl$_3$/iso-PrOH.

The enamine intermediate is most likely formed only in low quantities in the back reaction, which is in line with the observation that C–C bond cleavage is slow, as demonstrated by the crossover experiments described in the previous section. In addition, as already described in Chapter 2 the neutral enamine intermediate needs to be protonated in order to form an ESI-MS detectable species. However, the resulting iminium ion is even more prone to be hydrolyzed to the free catalyst and the aldehyde. Therefore, the enamine intermediate might be formed in the back reaction but not in a sufficient amount to exceed the detection limits due to a proceeding hydrolysis *via* its iminium ion.

Attempts to trap the enamine intermediate with Eschenmoser's salt failed. Also an approach using a catalyst bearing an imidazolium residue as charged tag in the side chain was not successful. Due to the positive charge attached to the catalyst the neutral enamine signals should be more easily detected as protonation can be avoided. However in the back reaction screening using this catalyst bearing a charged tag, only the catalyst signals were observed.

Inspired by ^{1}H NMR studies where enamine intermediates derived from aldehydes were found to be more stable in aprotic solvents and in particular in DMSO,[85] these solvents were applied for the back reaction screening. And indeed, in DMSO for the first time the enamine signal of catalyst **78a** was detected in the back reaction in low but acceptable signal to noise ratios. With toluene as the reaction solvent the intensity of the enamine signal was slightly lower. Nevertheless, the major signal was clearly assigned to the quasienantiomer also formed as the preferred enantiomer in the preparative reaction. As the catalyst induced an excellent selectivity of 97% *ee* the minor signal disappeared in the noise and a maximum ratio of approximately 5:1 could be assumed. This revealed another advantage of DMSO as the selectivities are considerably lower and thus the signal corresponding to the minor enantiomer of the putative enamines **En** and **En'** was expected to be more easily detectable. In fact, the enamine ratio (**En**/**En'**) measured in the back reaction matched perfectly the enantiomeric ratio (73:27) determined in the preparative reaction (see Chapter 4.2.3).

4.2.3 ESI-MS Back Reaction Screening of Tripeptides Bearing an Acidic Side Chain

With DMSO as a promising reaction solvent, the reaction conditions and parameters were further optimized in order to improve the signal-to-noise ratio of the enamine intermediate.

i) The intensity of enamine intermediates was found to increase, by up to 10 min reaction time, after which no further significant improvement was observed anymore.

ii) Partially better signal-to-noise ratios were monitored with higher concentration of catalyst and quasienantiomers present in the reaction mixture.

iii) The enamine signal disappeared after a few minutes in the diluted mixture (MeOH as dilution solvent).

iv) Other dilution conditions (MeOH/NaOAc, CH$_3$CN/AcOH, CH$_3$CN/KI) led to a decrease of the intensity of the intermediates.

In general, the back reaction was conducted with 5 μmol of each quasienantiomer, 10 mol% catalyst and 10 min reaction time in DMSO prior to direct dilution with MeOH and ESI-MS analysis. For catalyst **78a** the substrate amount was increased to 10 μmol to obtain more stable signals, particularly of the enamine intermediate derived from the minor quasi-enantiomer. Under these conditions the relative intensity of these signals was measured to be 73:27, a ratio that correlates perfectly with the enantiomeric ratio observed for the preparative forward reaction (Figure 58).
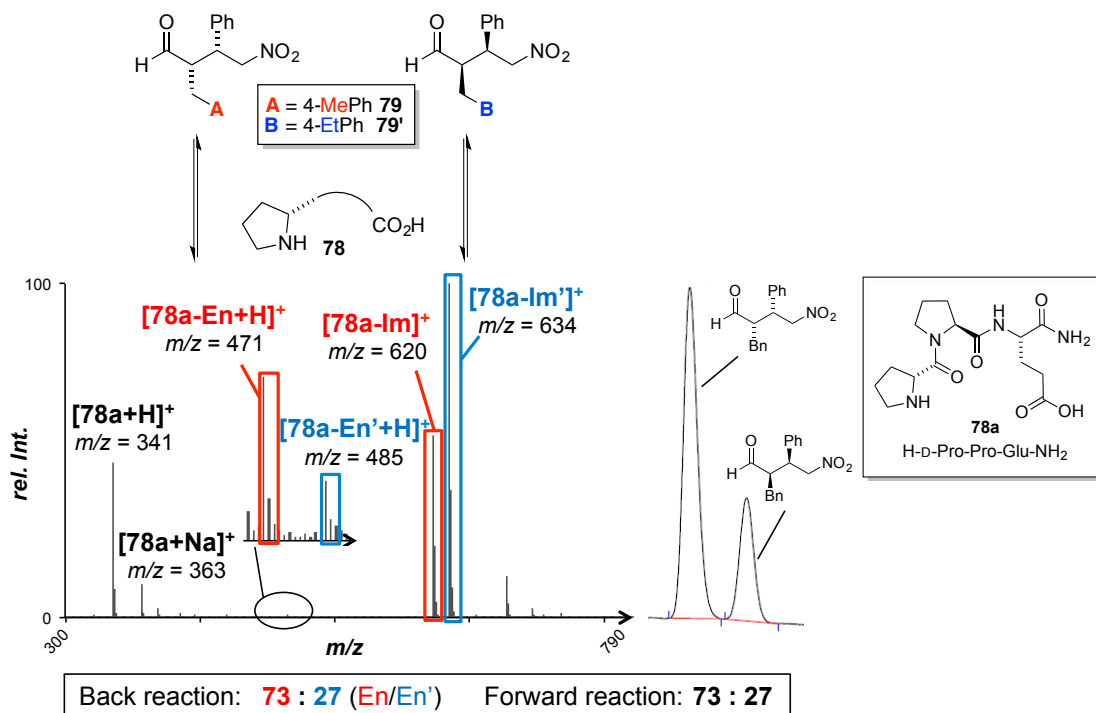
Figure 58: Back reaction screening and enantioselectivity of the forward reaction in DMSO employing H-D-Pro-Pro-Glu-NH$_2$ **(78a)**.

Further back reaction screenings were also performed with diastereomeric peptide H-Pro-Pro-D-Glu-NH$_2$ **(78b)** and regioisomer H-Pro-Pro-D-Gln-OH **(78c)** having the free acid group directly adjacent to the proline amide. In addition, these two peptides bear L-Pro instead of D-Pro residues at their N-termini, and therefore provide the opposite enantiomer as the major conjugate addition product compared to **78a**. The preference for the other quasienantiomer was reflected in the ESI-MS screening. Furthermore, these catalysts also provided a signal ratio (**En**/**En'**), which was in excellent agreement with the preparative results (Figure 59a and b).

111
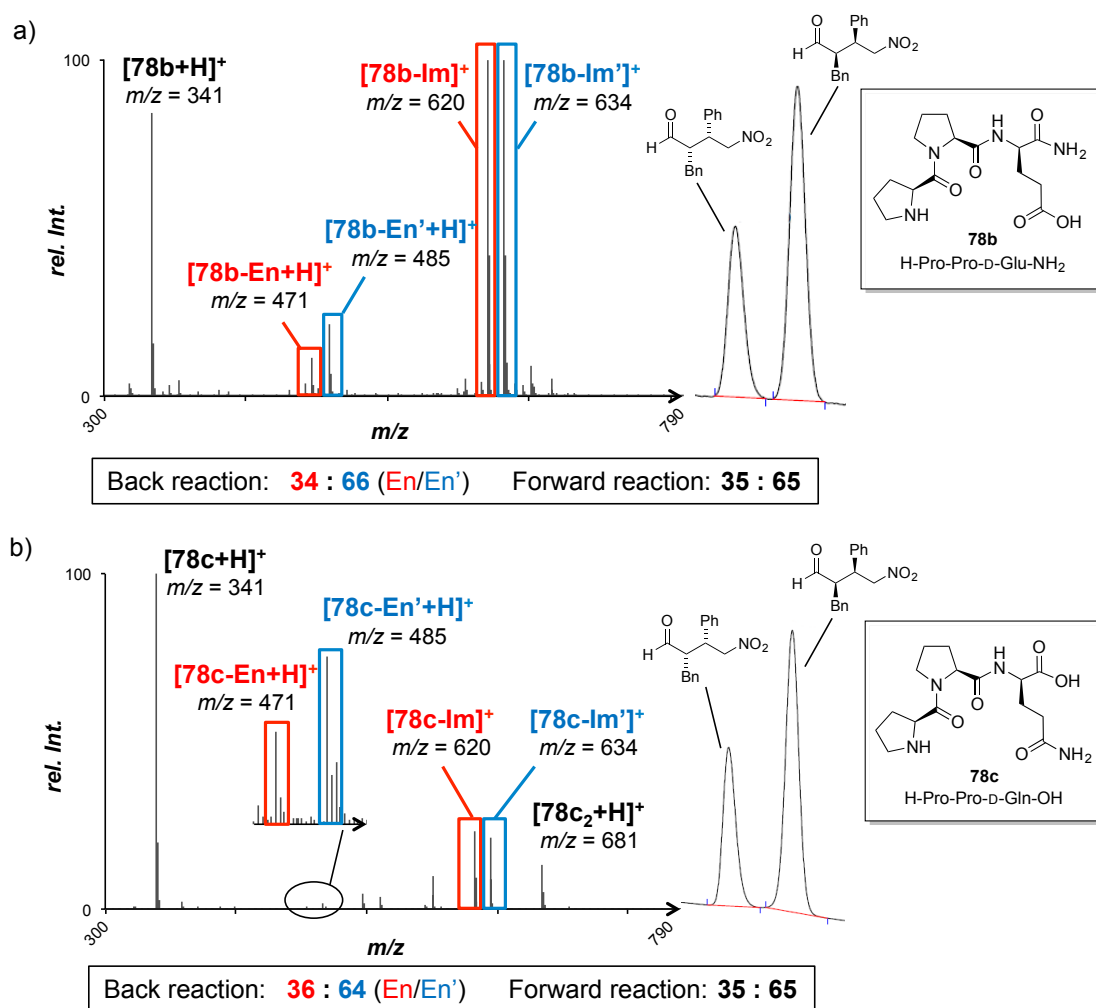
Figure 59: Back reaction screening and enantioselectivity of the forward reaction in DMSO. a) H-Pro-Pro-D-Glu-NH$_2$ (**78b**), b) H-Pro-Pro-D-Gln-OH (**78c**).

When the enantiomer of peptide **78b** was applied to the back reaction screening the same signal ratio was measured, but of course in favor of the opposite enantiomer. This proved again that the mass-label had no influence on the selectivity of the catalyst (Figure 60). However, both the enamine and iminium intermediates were considerable less intensive most likely due to an older catalyst charge used for the experiment. Finally, catalyst H-Pro-Pro-Asp-NH$_2$ (**78f**) was examined in the back reaction by ESI-MS. For the first time a slight discrepancy was observed after 10 min back reaction time. A higher theoretical selectivity in better agreement with the preparative result was found after shorter reaction times of 5 min (Figure 61). A potential explanation could be a racemization of the addition products **79** and **79'** *via* the forward reaction in low selectivity. Indeed, in previous studies the catalyst was identified as rather reactive.[83d] Further reduction of the reaction time (1 min) no longer afforded the enamine signal in acceptable signal-to-noise ratios.
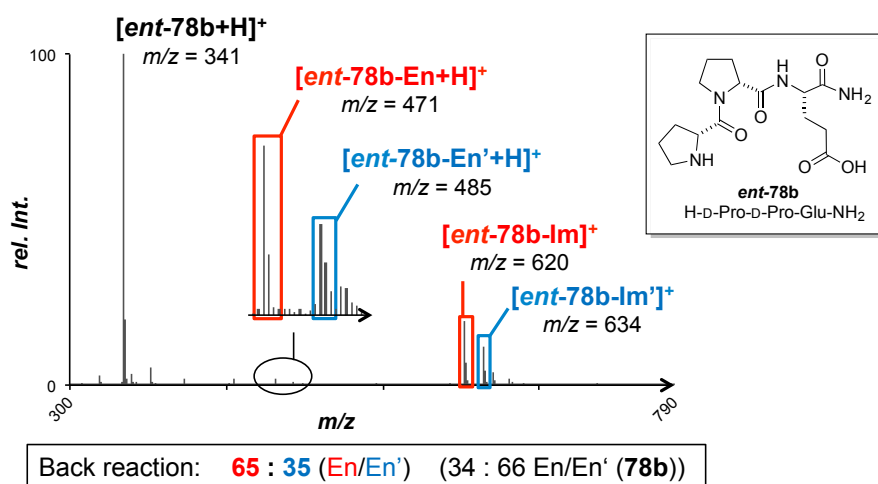
Figure 60: Back reaction screening of enantiomeric catalyst H-D-Pro-D-Pro-Glu-NH$_2$ (**ent-78b**).
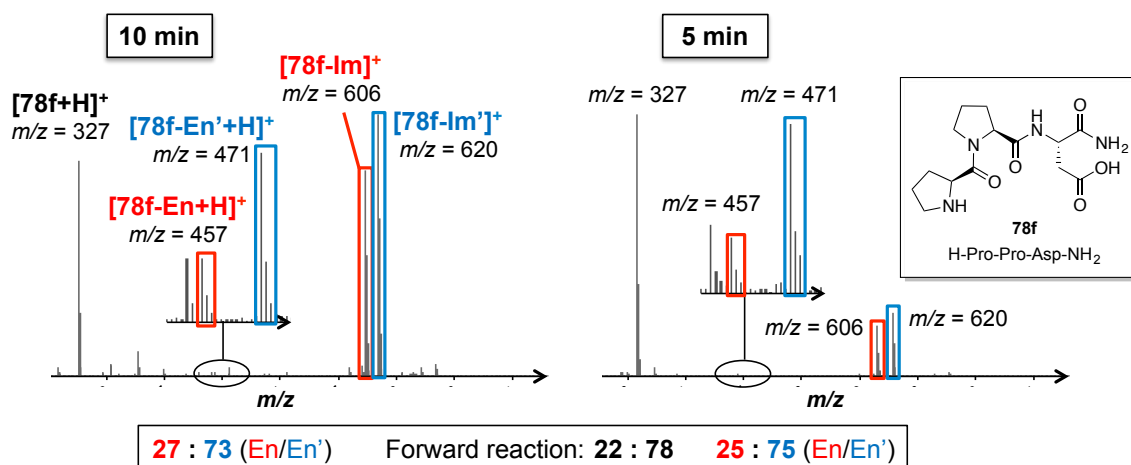
Figure 61: ESI-MS analysis of the back reaction after 10 min (left) and 5 min (right) employing peptide H-Pro-Pro-Asp-NH$_2$ (**78f**).

It should be noted that the ratios of the enamine intermediates determined by screening the back reaction were not related to the ratio of the corresponding iminium intermediates. **78b-Im** and **78b-Im'** as well as **78c-Im** and **78c-Im'** were formed in a ratio of ~ 1:1 (Figure 59b and c) whereas iminium ions derived from catalyst **78f** were in slight favor for the same product species as also observed for the enamine intermediates (Figure 61). In contrast, **78a-Im** and **78a-Im'** were even present in an approximately 1:2 ratio with the major species corresponding to the minor product enantiomer obtained in the forward reaction (Figure 58). Thus, the concentration of initially formed iminium ions had no influence on the signal ratio of enamine intermediates formed in the back reaction.

113

In general, for all investigated catalysts bearing an intramolecular proton donor the signal ratio (**En/En'**) were in excellent agreement with the enantioselectivity obtained from the preparative forward reaction. Thus, the intrinsic selectivity of the attack of the enamine onto the nitroolefin determined by ESI-MS matches the stereoselectivity of the preparative reaction. These results provide clear evidence that the reaction proceeds *via* an enamine rather than an enol intermediate. In addition they show that the C–C bond formation is the enantioselectivity-determining step of the reaction.

4.2.3 ESI-MS Back Reaction Screening of Catalysts Without an Intramolecular Proton Donor

In previous mechanistic studies it was proposed that in the absence of an appropriately positioned proton donor within the catalyst, the protonation step and not the C–C bond forming is the rate- and even enantioselectivity-determining step (see Chapter 4.1.2). Therefore, it was investigated how catalysts that lack an intramolecular proton donor such as peptide **78d**, bearing a methyl ester instead of a carboxylic acid moiety, or the Hayashi-Jørgensen catalyst **77a** would perform in back reaction screenings. Thus, the same back reaction experiments as described in the previous section were conducted with ester **78d** and its free acid analogue **78e** for comparison to the induced enantioselectivities in the preparative reaction. For the first time, a clear disagreement of a theoretical *ee* of about 20% was found (Figure 62a). In contrast, with acid bearing peptide **78e** the signal ratio again perfectly matched the preparative enantiomeric ratio (Figure 62b). Although the enamine intermediate was monitored with a poor intensity, the ratio was reproducible in five independent measurements (75:25±2.5). The observed mismatch between preparative and ESI-MS result was even more dramatic for Hayashi-Jørgensen catalyst **77a**, where enamine intermediates **77a-En** and **77a-En'** were formed in the back reaction in a ratio of 88:12 in favor of the quasienantiomer, which is the minor product enantiomer in the forward reaction (Figure 62c).
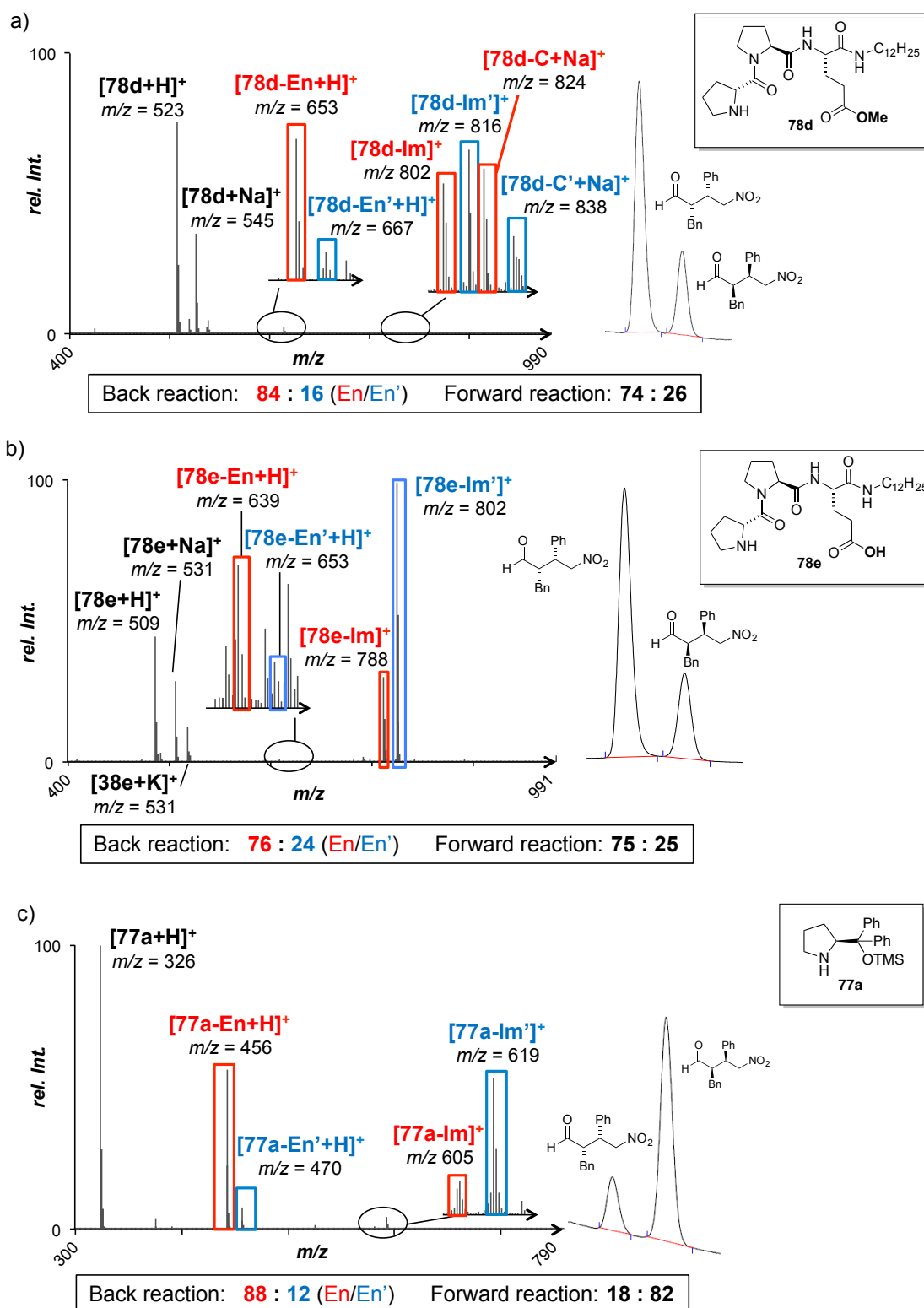
Figure 62: Back reaction screening of a) ester **78d**, b) its free acid analogue **78e** and c) the Hayashi-Jørgensen catalyst **77a** in DMSO.

The recorded spectra of these three catalysts revealed some interesting details worth mentioning (Figure 62). First, the enamine intermediates based on ester catalyst **78d** and in particular Hayashi-Jørgensen catalyst **77a** are more intensive than these derived from catalyst **78e** bearing an intramolecular acid donor. Most likely due to the acid group, the enamine

intermediates are destabilized and more prone to decay to the free catalyst and the aldehyde. Even more obvious is the considerable intensity difference of iminium ions **Im** and **Im'** formed from the catalysts and quasienantiomers **79** and **79'**. In addition, for peptide **78d** the sodium adducts of these signals were observed. The lower intensity and in particular the observation of sodium signals suggests that the original intermediates in solution are neutral and correspond to a potential cyclobutane intermediate **78d-C**, which would be in line with recent NMR studies.[91a] Also for Hayashi-Jørgensen catalyst **77a** the iminium species was much less intensive. The lack of the sodium signals are most likely based on the fact that sodium ions are considerably better coordinated to a tripeptide catalyst than to the prolinol silyl ether, which is supported by the signal of the free catalyst where only for tripeptides the signal pattern correlating to their sodium adducts were observed.

The mismatch in the enantioselectivity of the forward reaction with the enamine ratio determined in the back reaction provides strong evidence that C–C bond formation between the enamine and the nitroolefin is not the enantioselectivity-determining step for catalysts lacking an intramolecular proton donor. In preparative reactions a significant rate acceleration is observed applying an external acid as additive for such catalyst systems.[91a, 91f, 91g] Therefore, the potential influence of acid additives on the back reaction screening was also examined. For that purpose, 10 mol% of ester **78d** or Hayashi-Jørgensen catalyst **77a** were reacted with the quasienantiomeric substrates (**79** and **79'**) in the presence of either 10 mol% or 100 mol% of the corresponding acid (Table 8). For the acid screening with catalyst **77a**, reaction times of 2 min were generally sufficient for producing excellent signal intensities. However, with increasing acid strength the intensity of the enamine intermediates was found to decrease. Using 100 mol% of chloroacetic acid and ester **78d** no enamine signals were observed and even with only 5 mol% of acid the signals were detected in poor signal-to-noise ratios even after 30 min (Table 8, entry 6). This could be explained assuming that stronger acids might induce irreversible protonation and therefore reduce the overall back reaction rate and therefore the quantities of enamine intermediates present in the reaction mixture. Remarkably, even in the presence of 100 mol% AcOH the sodium adducts of putative cyclobutane intermediates were visible (Figure 63). Moreover, the initially formed reaction adducts showed considerably higher intensity with an external acid than without the additive (see Figure 62a). This might be due to a shift of the equilibrium of cyclobutane **C** and protonated iminium **Im** towards the positively charged species, which is on the one hand better detected by ESI-MS, but also reduces the amount of nitronate **N** or dihydrooxazine oxides **OO** from which C–C bond cleavage to the enamine intermediate would occur. As

these intermediates are detected, suggesting that a back reaction takes place, the enamine intermediate might also be less stable and shows a stronger tendency to hydrolyze in the protic environment.

**Table 8:** Back reaction screening employing external acid additives.
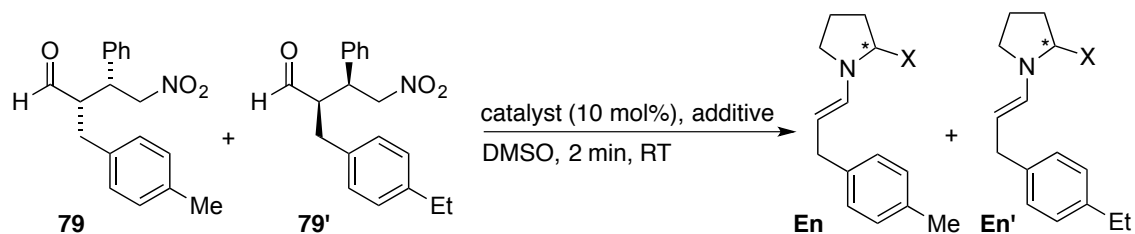
entry	catalyst	additive	ESI-MS En/En'	e.r.[a] preparative rct.
1	**78d**	-	84 : 16	74 : 26
2	**78d**	*para*-nitrophenol (10 mol%)	88 : 12	80 : 20
3	**78d**	*para*-nitrophenol (100 mol%)	87 : 13	82 : 18
4	**78d**	AcOH (10 mol%)[b]	87 : 13	80 : 20
5	**78d**	AcOH (100 mol%)[b]	79 : 21	81 : 19
6	**78d**	ClCH$_2$CO$_2$H (5 mol%)[c]	>66 : 34[d]	n.d.[e]
7	**77a**	-	88 : 12	18 : 82
8	**77a**	*para*-nitrophenol (10 mol%)	67 : 33	11 : 89
9	**77a**	*para*-nitrophenol (100 mol%)	57 : 43	3 : 97
10	**77a**	AcOH (10 mol%)	73 : 27	14 : 86
11	**77a**	AcOH (100 mol%)	61 : 39	10 : 90
12	**77a**	ClCH$_2$CO$_2$H (10 mol%)	84 : 16	10 : 90
13	**77a**	ClCH$_2$CO$_2$H (100 mol%)	76 : 24	4 : 96

a) Determined in preparative forward reaction with phenylpropanal and *trans*-β-nitrostyrene. b) Back reaction time: 10 min. c) Back reaction time: 30 min. d) Poor signal-to-noise ratio. e) Not determined.

117
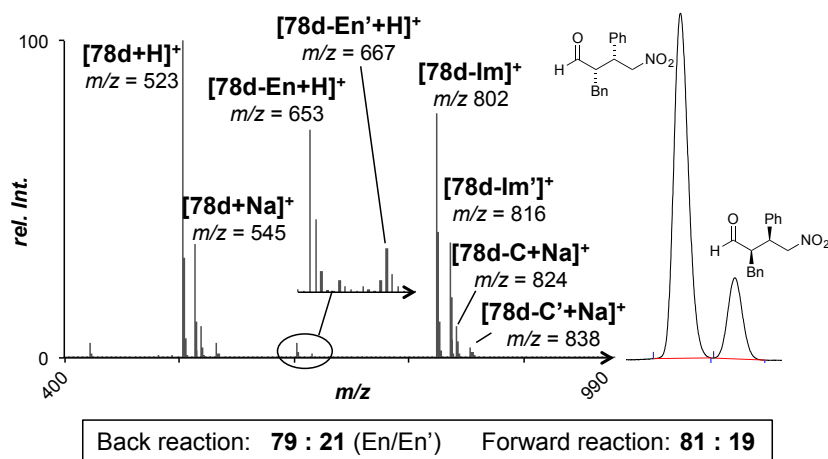
Figure 63: Back reaction screening of peptide ester **78d** in DMSO in presence of 100 mol% AcOH. Spectrum recorded after 10 min reaction time.

In preparative reactions, addition of acid commonly led to an increase of the enantioselectivity in particular for catalyst **77a**. Due to the similar signal ratios and selectivities for catalyst **78d** the results were not conclusive (Table 8, entry 1-6). However, the acid's influence on enamine ratios derived from catalyst **77a** was clearly observed (Table 8, entry 7-13). The most obvious alteration was observed with 100 mol% *para*-nitrophenol as additive (Table 8, entry 9), but still the ratio was in favor for the "wrong" quasienantiomer. Remarkably, screening of Hayashi-Jørgensen catalyst **77a** in 2,2,2-trifluoroethanol as an acidic solvent the measured signal ratio of 35:65 (**En**/**En'**) was for the first time reversed, with the major quasienantiomer now corresponding to the major enantiomer formed in the forward reaction. However, this ratio still deviated strongly from the e.r. of the preparative reaction (Figure 64). Interestingly, 2,2,2-trifluoroethanol seemed to stabilize the enamine intermediates or led to the formation of higher quantities, as even in the highly protic environment the signals were well detected (in contrast in aprotic solvent mixture CHCl$_3$/iso-PrOH where no enamine intermediates were detected for acid containing catalysts in the back reaction, Figure 57b). In general, signal intensities of the enamine derived from catalysts lacking an intramolecular proton donor in an acidic environment were more intensive than enamine signals derived from catalysts bearing a covalently attached acid. This demonstrates that the acid is not only suitably positioned to accelerate protonation of intermediates such as the nitronate **N** but also to destabilize the enamine more than external acid additives.
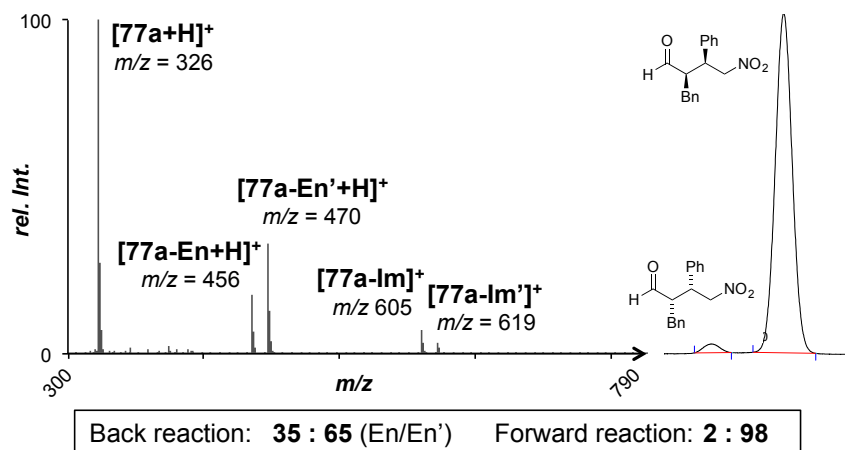
Figure 64: Back reaction screening of Hayashi-Jørgensen catalyst **77a** in 2,2,2-trifluoroethanol.

The results discussed above for Hayashi-Jørgensen catalyst **77a** demonstrate that acidic additives influence the enantioselectivity of the forward as well as the ratio of enamine intermediates formed in the back reaction. But even at relatively high acid concentration, the enantiomeric ratio seemed to still not be governed by the addition reaction between the enamine and the nitroolefin when catalysts lacking a proton donor are used. Only with an ideally positioned acidic group in the catalyst, protonation of nitronate **N** or dihydrooxazine oxides **OO** becomes so fast that the enantioselectivity is completely determined in the C–C bond formation step.

4.3   Summary

In collaboration with J. DUSCHMALÉ, C. EBNER and H. WENNEMERS, the ESI-MS back reaction screening was successfully applied as a mechanistic tool for a distinct identification of enamines as active intermediates in the conjugate addition of aldehydes to nitroolefins. Thus an enol mechanism can be ruled out for this reaction. Moreover, it could be demonstrated that C–C bond formation between the enamine and the nitroolefin is the enantioselectivity-determining step of this transformation using tripeptide catalysts of the type Pro-Pro-Xaa bearing a suitably positioned intramolecular acid. Furthermore, the results of the ESI-MS screening of non-acidic catalysts such as ester **78d** and in particular Hayashi-Jørgensen catalyst **77a** revealed that a different mechanistic pathway is active, where most-likely the protonation step of the intermediate generated after C–C bond formation is rate- and selectivity-determining, in line with recent mechanistic studies.[91c]

CHAPTER 5

ESI-MS SCREENING OF RACEMIC ORGANOCATALYSTS FOR THE MICHAEL ADDITION

5.1 Introduction

In an asymmetric transformation the chiral catalyst has to be employed in high enantiomeric purity. The synthesis of chiral catalysts often relies on a chiral pool strategy to avoid time consuming and expensive methods for racemate separations (e.g. kinetic resolution, co-crystallization with chiral additives). This approach is particularly used for the synthesis of organocatalysts, which are commonly derived from the chiral pool, e.g. from naturally occurring amino acids (Figure 65). Despite the availability and convenience, this strategy also represents a limitation in the development of new catalysts. Scaffolds, which are not derived from the chiral pool or other readily available chiral building blocks, are usually harder to obtain in an enantiopure manner. Hence, a screening method allowing determination of the selectivity of a catalyst by applying its racemic form would provide fast access to a significantly broader range of catalysts.
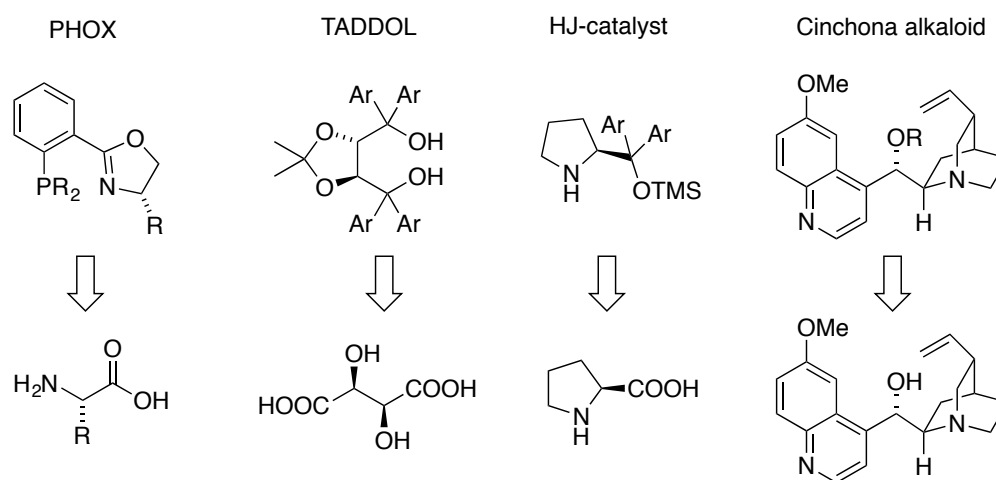
Figure 65: Selected examples of catalysts and ligands derived from the chiral pool.[65]

5.1.1 Approaches to Determine or Induce Enantioselectivity Employing Racemic Chiral Catalysts

Historically, racemic chiral catalysts have been applied in the area of polymerization in order to control the relative (e.g. tacticity in polypropylene) and not the absolute configuration in the propagation of the polymerization.[94] Early examples of an application of racemic catalysts to induce enantioselectivity are based on the so-called chiral poisoning approach.[95] In an ideal case one enantiomer of the racemic catalyst selectively binds to a chiral modifier that either increases its activity or, more commonly, deactivates (poisons) this enantiomer (Figure 66). MARUOKA and YAMAMOTO applied this concept already in 1989 in a Diels Alder reaction catalyzed by a racemic Lewis acid.[96] A chiral ketone was identified to bind with high selectivity to the (R)-BINOL aluminium complex. This mixture afforded the Diels Alder product in 82% *ee*. In contrast, the enantiopure (S)-BINOL derivative induced an enantioselectivity of 95%.
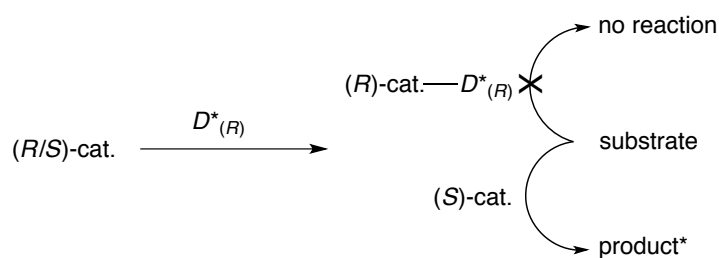
Figure 66: Ideal case of a 100% selective chiral poison for the (R)-enantiomer (D = chiral deactivator).[95]

MIKAMI and NOYORI developed a protocol for the Ru-catalyzed transfer hydrogenation where two enantiomerically pure diamines were applied to simultaneously activate one and deactivate the other enantiomer of the catalyst bearing a racemic ligand.[97] This strategy led to a considerable improvement of catalyst activity and selectivity. Without modifiers the hydrogenation product was obtained in poor yield and enantioselectivity, when using the enantiopure (R)-ligand. However, applying the racemic catalyst in combination with the activator and deactivator, the product was formed with full conversion in excellent stereoselectivity (Figure 67). Although this protocol could emerge as a powerful tool for the development of highly selective catalysts, it suffers from a rather limited scope. For example, a chiral poison and activator are not necessarily available for every catalyst. In addition, the chiral modifier needs to bind with high affinity to the catalyst, which could make the identification of a suitable additive labor and cost intensive.
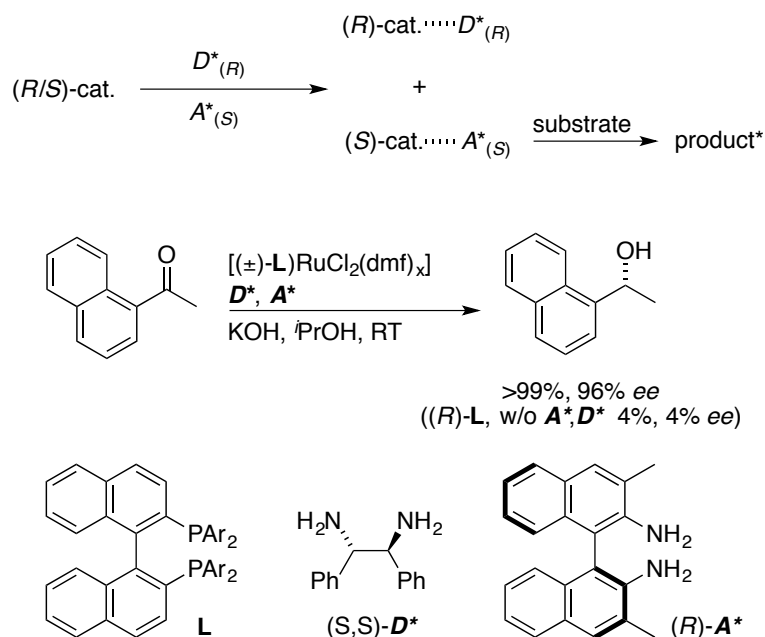
Figure 67: Activation-deactivation strategy employing a racemic ligand and enantiopure diamines as selective deactivator (**D***) and activator (**A***) in the Ru-catalyzed transfer hydrogenation.[94, 97]

An approach to estimate the enantioselectivity of a racemic catalyst for prochiral substrates was reported by KAGAN.[98] There, the diastereoselectivity determined in a sequential two step transformation of a substrate bearing two remote prochiral centers was used to calculate the catalyst enantioselectivity. The borane-mediated reduction of a diketone with racemic oxazaborolidines as catalysts was used as a model system (Figure 68). Under limiting conditions, in which the stereoselectivity of both steps is identical and the catalyst does not dissociate from the substrate between step 1 and step 2,[94] the enantioselectivity (ee_1), that would be induced by the chiral catalyst can be calculated according to the equation illustrated in Figure 68 by simply determining the *de* of the homoproduct ((S,S) and (R,R), respectively). Indeed, a *de* of 83% determined from the racemic catalyst indicated an enantioselectivity of 91%, which was in reasonable agreement with an *ee* of 83% obtained from the enantiopure catalyst and the phenyl-pentyl-substituted ketone as model substrate. Although this approach allows a simple and fast estimation of the stereoselectivity of a racemic catalyst, the strict requirements only met a narrow substrate and reaction range. For example, KAGAN described additional catalytic systems such as the Rh-catalyzed hydrosilylation and the Ru-catalyzed transfer hydrogenation.[98] However, these systems failed, as no diastereoselectivity was observed with the racemic catalyst, probably due to significant catalyst scrambling.
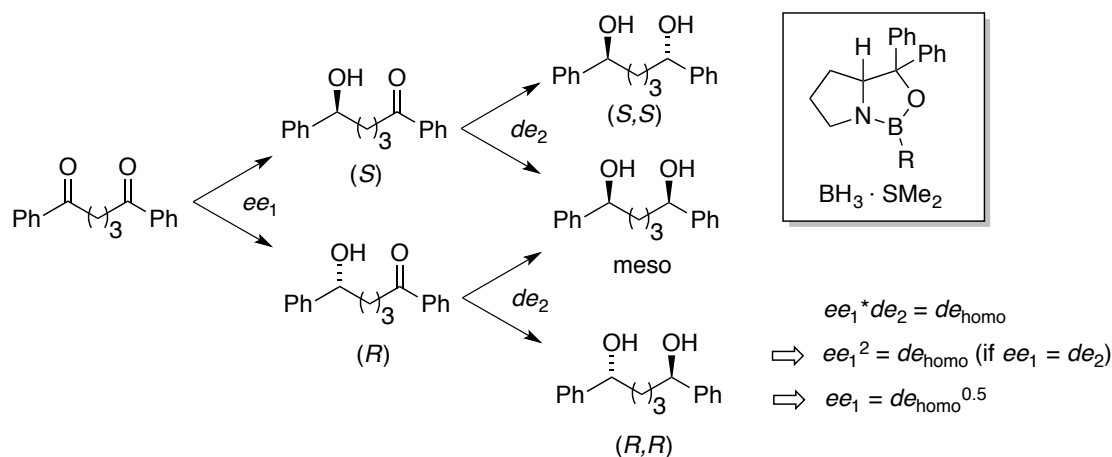
Figure 68: KAGAN'S method to estimate the enantioselectivity of a racemic catalyst in two consecutive borane-mediated ketone reductions.

In 2001 LLOYD-JONES and coworkers developed a new concept to estimate the selectivity of a racemic catalyst in a kinetic resolution under pseudo zero-order conditions with respect to the substrate.[94, 99] For a proof-of-concept study they chose the Pd-catalyzed kinetic resolution of allylic substrates. There, a scalemic allylic acetate (S)-**83** (60% ee) reacts with a Pd-catalyst bearing a racemic ligand under a pseudo zero-order regime (Figure 69). If the catalyst induces selectivity the initial 60% ee of the substrate increases. In extreme case if the catalyst is perfectly enantioselective (selectivity factor $s = \infty$) each catalyst enantiomer only reacts with one substrate enantiomer in equal amounts until all of the minor enantiomer is converted into the product (R)-**84** and the ee of the unreacted acetate (S)-**83** is raised to 100%. On the other hand, an unselective catalyst ($s = 1$) does not distinguish between the substrate enantiomers and the ee of the acetate is constant throughout the reaction. Thus, the increase of the initial 60% ee of the allylic acetate with progressing conversion upon reaction with a racemic Pd-catalyst was recorded. Although the shape of the experimentally established curves (Figure 69, top right) considerably differ from ideality validation experiments revealed a correct prediction of the selectivity trends for the experimentally obtained curves from the racemic catalyst.
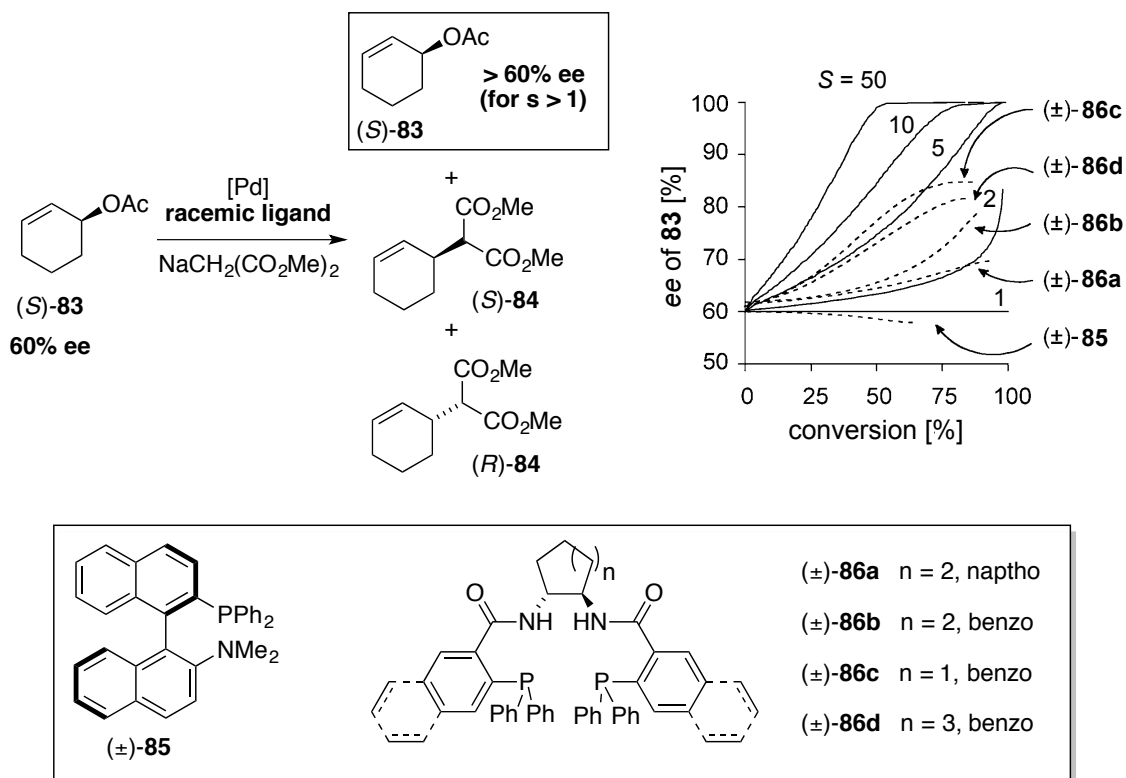
Figure 69: Method of LLOYD-JONES to estimate the selectivity of a racemic catalyst. Change of *ee* values of scalemic acetate ((*S*)-**83**) as a function of the conversion upon reaction with Pd-catalysts bearing racemic ligands (dashed lines: experimentally obtained data; solid lines: ideal curves for various selectivity factors (*s*)).[94]

The same concept was applied to the Jacobsen-Katsuki epoxidation of scalemic allylic alcohols. Although the method did not allow conclusive distinction between catalysts with similar selectivity factors (*s* = 9 and *s* = 6) this system behaved closer to ideality demonstrating the potential of this approach.[94] However, a labor intensive collection of many data points was needed to establish a graph for each racemic catalyst and in particular the limitation to kinetic resolutions in combination with a pseudo zero-order dependency of the substrate are particular drawbacks of this methodology.

127

5.1.2 ESI-MS Screening of Racemic Pd-Catalysts for the Allylic Substitution Reaction

Inspired by the work of LLOYD-JONES, the PFALTZ group combined this approach with the ESI-MS back reaction screening in order to develop a method to determine the enantio-selectivity of racemic catalysts for asymmetric reactions with prochiral substrates.[17] Initially, the ESI-MS screening of racemic catalysts was applied to Pd-catalyzed allylic substitutions starting from a scalemic mixture (75:25) of quasienantiomeric substrates (**87** and **87'**) monitoring positively charged Pd-allyl intermediates bearing various racemic PHOX-Ligands (Figure 70).
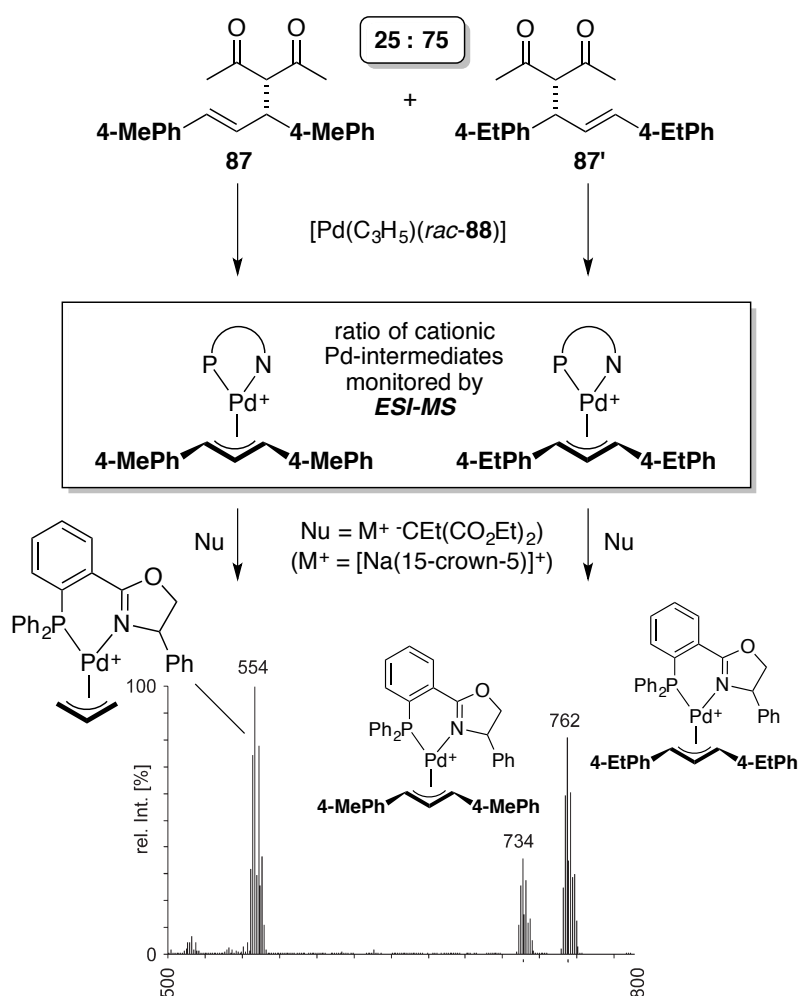
Figure 70: a) ESI-MS screening of racemic Pd-catalysts with a scalemic mixture of quasienantiomers monitoring cationic Pd-allyl intermediates. Representative spectrum measured for the back reaction employing ligand **88c**.[17]

Based on the intermediate ratio the most selective catalysts were clearly identified screening their racemic form. Moreover, from the signal ratio of the mass-labeled Pd-allyl intermediates the selectivity factor *s* and therefore the theoretical enantioselectivity provided by the catalyst could be calculated (Figure 71, the principle and the equation for the calculation will be

discussed in more detail in section 5.2.2, related to the screening of racemic Michael catalysts). For more selective catalysts a deviation between the calculated enantioselectivity and the actual *ee* obtained from the enantiopure catalyst was observed. However, an excellent linear correlation between these two data sets was found, which allowed for a correction of the racemate screening results to more reliably predict the theoretically induced enantioselectivities. Thus, this method not only allowed for an estimation of the selectivity trend of racemic catalysts, but even a prediction of the actual enantioselectivity was possible.
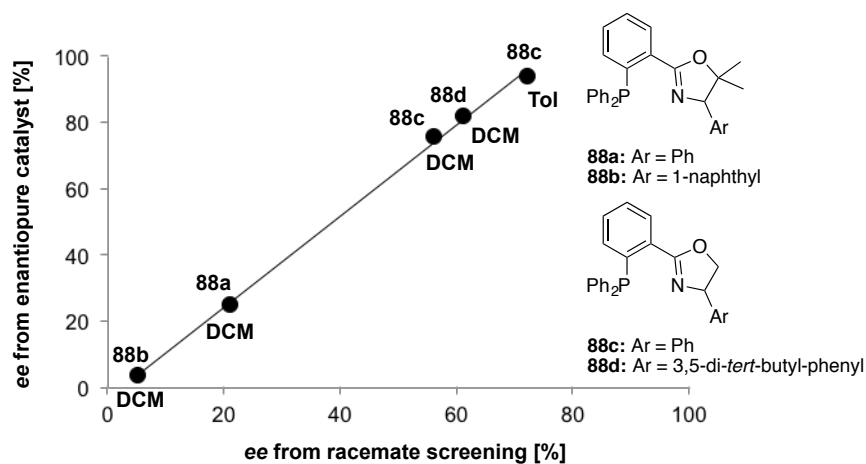
Figure 71: Linear correlation between the screening results obtained with the racemate and actual *ee* determined from the corresponding enantiopure Pd-catalysts.[17]

5.2 ESI-MS Screening of Organocatalysts for the Michael Addition

5.2.1 ESI-MS Screening of Enantiopure Organocatalysts

Within this thesis the scope of the screening of racemic catalysts was further extended to organocatalyzed reactions. The Michael addition of malonates to cinnamaldehyde mediated by secondary amines was chosen for proof-of-principle studies. Recently, for this reaction an ESI-MS screening of enantiopure catalysts monitoring iminium ions was successfully developed by I. FLEISCHER (Figure 72).[16] Here, the same screening methodology was applied as discussed in previous sections for other organocatalyzed reactions. An equimolar mixture of the quasienantiomeric mass-labeled addition products **89** and **89'** was reacted with a chiral secondary amine based catalyst (Figure 72a). In the back reaction the two mass spectrometric distinguishable iminium intermediates (**Im** and **Im'**) were formed upon condensation, isomerization and C–C bond cleavage. According to the principle of microscopic reversibility the C–C bond formation (selectivity determining step in the forward reaction) and the C–C bond cleavage (reverse direction) proceed through the same transition state. Thus, assuming a fast pre-equilibrium of the condensation and isomerization in the back reaction (Curtin-Hammett conditions), the iminium ratio **Im/Im'** reflects directly the intrinsic enantio-selectivity of the catalysts in the forward reaction. Indeed, an excellent agreement between the signal ratio **Im/Im'** determined by ESI-MS and the enantioselectivity induced in the preparative forward reaction was found (Figure 72b).
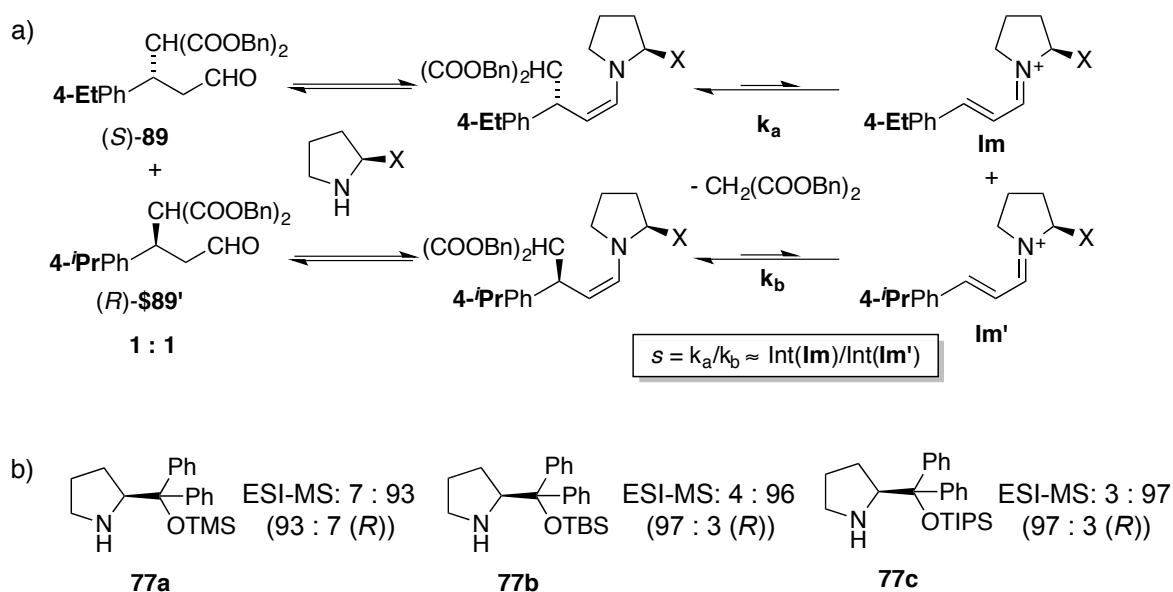
Figure 72: a) Principle of the ESI-MS back reaction screening employing mass-labeled quasi-enantiomeric Michael products **89** and **89'**. b) Selected results of the back reaction screening. Enantiomeric ratios determined from the corresponding preparative reactions are given in brackets.

5.2.2 Principle of the ESI-MS Screening of Racemic Organocatalysts

In contrast to the ESI-MS screening of enantiopure catalysts, the mass-labeled quasi-enantiomeric substrates ((S)-**89** and (R)-**89'**) were applied in a scalemic instead of an equimolar ratio (Figure 73). A 75:25 ratio of the quasienantiomeric substrates was identified during the ESI-MS studies on the Pd-catalyzed allylic substitution as suitable compromise between sensitivity of the method and detection limits of the minor peak formed after the back reaction.[100] Starting with the 75:25 ratio, under pseudo-zero order conditions, each enantiomer of a perfectly enantioselective, racemic catalyst (selectivity factor $s \rightarrow \infty$) only reacts with its preferred substrate enantiomer (e.g. the (R)-enantiomer of the catalyst reacts exclusively with the (S)-quasienantiomer and the (S)-enantiomer of the catalyst with the (R)-quasienantiomer). Furthermore, under pseudo zero-order conditions the concentration of the Michael products does not affect the rate and therefore both catalyst enantiomers react equally fast to form iminium ions, providing a signal ratio (**Im/Im'**) of 50:50. On the other hand, a non-selective catalyst ($s = 1$) shows no preference for any substrate enantiomer resulting in the statistical ratio of 75:25, derived from the initial ratio of the quasienantiomers. Thus, the more selective the catalyst is, the closer iminium ratios monitored by ESI-MS to 50:50 should be.
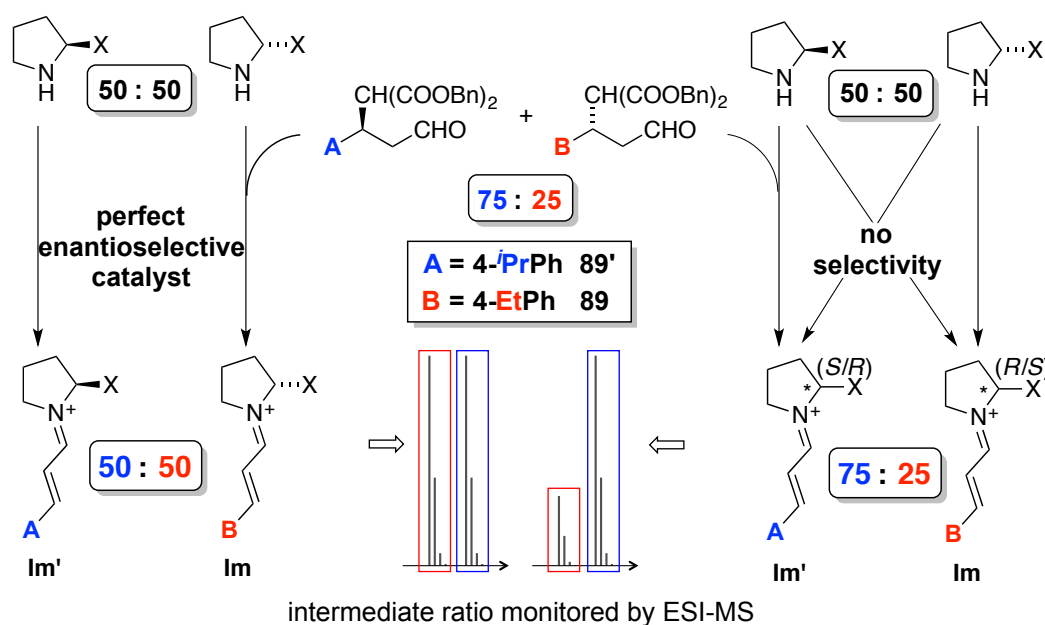
Figure 73: Principle of the ESI-MS screening of racemic catalysts.

On the basis of the reaction kinetics under pseudo zero-order conditions an equation can be derived (**Eq. 2**, I = signal intensity (**Im/Im'**); Q = [**89**]/[**89'**]) that allows calculation of the selectivity factor s from the signal ratio (R) of the iminium intermediates monitored by ESI-MS. Thus a prediction of the enantioselectivity (theoretically induced by the enantiopure catalyst) becomes possible. The derivation of **Eq. 1** and **Eq. 2** from the reaction kinetics was previously reported in connection with the studies on Pd-catalyzed allylic substitution with racemic catalysts.[17]

$$\frac{I_{Et}}{I_{iPr}} = R = \frac{\frac{s*Q}{s*Q+1} + \frac{Q}{Q+s}}{\frac{1}{s*Q+1} + \frac{s}{Q+s}} \qquad \textbf{Eq. 1}$$

$$\implies \quad s = \frac{Q^2 - R + \sqrt{(R-Q^2)^2 - (R\times Q - Q)^2}}{R\times Q - Q} \qquad \textbf{Eq. 2}$$

5.2.3 Preliminary Experiments

In the ESI-MS studies on the screening of enantiopure catalysts for the organocatalyzed Michael addition, TBS protected prolinol **77b** was found to generate the Michael product **89** in a high enantiomeric ratio of 97:3. I. FLEISCHER chose this catalyst for initial experiments.[101] According to **Eq. 1** an enantiomeric ratio of 97:3 (s = 32) corresponds to an intermediate ratio of 54:46 in the racemate screening with a scalemic 3:1 mixture (Q = 3) of quasienantiomers (**89'/89**). However, under established reaction conditions for the ESI-MS back reaction screening with 10 mol% of catalyst **77b** (9.38 µmol/3.13 µmol **89'/89**), a signal ratio of 74:26 was observed for the iminium intermediates (**Im'/Im**). This reflected the initial ratio of substrates and implied that the required pseudo zero-order regime is not achieved under these conditions with high catalyst loadings. Indeed, in further experiments increasing the substrate concentration and therefore reducing the catalyst loading, I. FLEISCHER found a beneficial effect (1 mol%: **Im'/Im** = 70:30). However, even with 0.25 mol% of catalyst **77b** (30 µmol/10 µmol **89'/89**) the iminium ratio of 66:34 (**Im'/Im**) differed considerably from the expected ratio of 54:46. In addition the spectrum was obtained in poor signal-to-noise ratios. Different reaction temperatures or freezing of the intermediates (–78 °C) during dilution prior to ESI-MS injection was attempted without any success.[101]

Also during the investigation of the Pd-catalyzed allylic substitutions screening racemic catalysts, the observed signal ratio determined by ESI-MS differed from the expected results.

However, an excellent linear correlation was found to correct the selectivities obtained from the racemate screening (Figure 71). In addition, a correct prediction of the actual *ee* is not necessary as long as the selectivity trend is clearly reflected by the iminium ratios, which allows for the identification of the most selective catalysts. Therefore, the initial results collected by I. FLEISCHER where sufficiently promising for further elaboration of this methodology. First the reaction and screening parameters were further investigated. To avoid large amounts of material present in the injection solution the catalyst concentration was reduced in order to minimize the catalyst loading, instead of using increased quantities of quasienantiomers. Interestingly, when slightly changing the dilution protocol, already with 1 mol% of catalyst **77b** (3.13 μmol/9.38 μmol **89/89'**) the iminium ions were generated in a ratio of 35:65 (**Im/Im'**) in excellent signal intensities. These optimized conditions were used as a standard procedure for all screening experiments presented below.
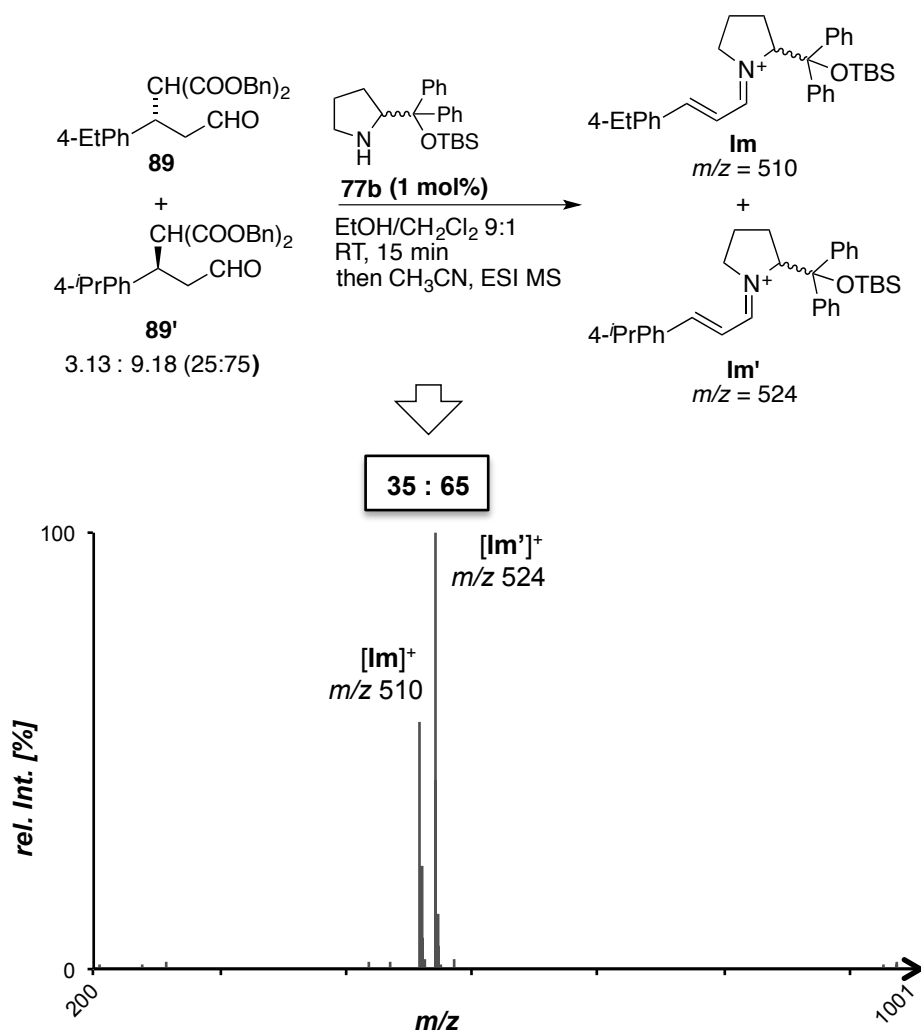
Figure 74: ESI-MS back reaction screening with 1 mol% of racemic catalyst **77b**. Below, typical ESI-MS spectra obtained under screening conditions.

5.3 Catalyst Synthesis

To prove the concept further racemic catalyst structures were synthesized in order to investigate whether it might be possible to identify the selectivity trend by screening the racemic catalyst. To validate the screening results, the enantiopure catalyst was either synthesized or obtained by separation of the racemate by means of semi-preparative HPLC on a chiral stationary phase. For preliminary ESI-MS experiments catalysts structures, for which the enantiopure catalyst is easily accessible or even commercially available, were chosen to accelerate the validation experiments.

5.3.1 1st Generation Catalyst Synthesis

The racemic TBS-protected catalyst **77b**, was synthesized according to the procedure reported in the literature for the enantiopure catalyst with racemic proline as a starting material (Scheme 38).[80, 102] This approach permitted reliable and fast access to the catalyst for initial ESI-MS experiments. Ester formation and protection of proline is completed in a single step using ethyl chloroformate. Subsequent Grignard reaction afforded the tertiary alcohol **91**. Basic deprotection *via* an oxazolidinone intermediate **95** (see Scheme 40) afforded the aminoalcohol **92**, which was TBS-protected without further purification. The enantiopure catalyst was synthesized starting from commercially available (*S*)-diphenylprolinol **92** in 61% yield.
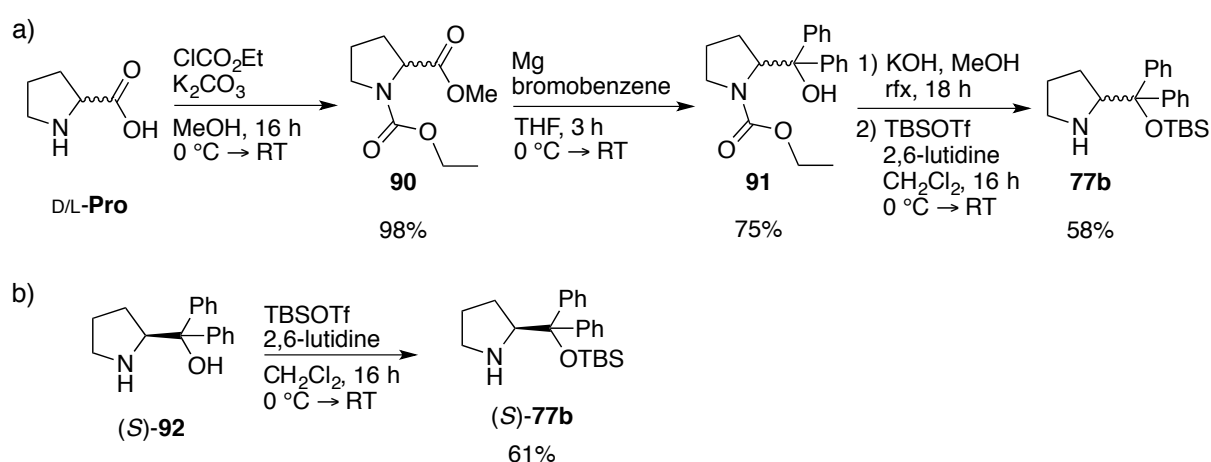
Scheme 38: a) Synthesis of racemic catalyst **77b** starting from racemic proline. b) Synthesis of the enantiopure catalyst (*S*)-**77b**.

5.3.2   2nd Generation Catalyst Synthesis

The synthesis described above afforded the TBS-protected catalyst **77b** in good overall yield. However, a more reasonable approach for the racemic catalysts avoids an application of the racemic amino acid, which is even more expensive than the enantiopure derivative. As an alternative procedure a lithiation of Boc-protected pyrrolidine should form the nucleophilic carbon next to the nitrogen, which could be trapped by a variety of electrophiles or even subjected to cross coupling reactions. Several lithiation procedures are reported, although usually applied as asymmetric deprotonations using sparteine as an additive (Scheme 39).[103]
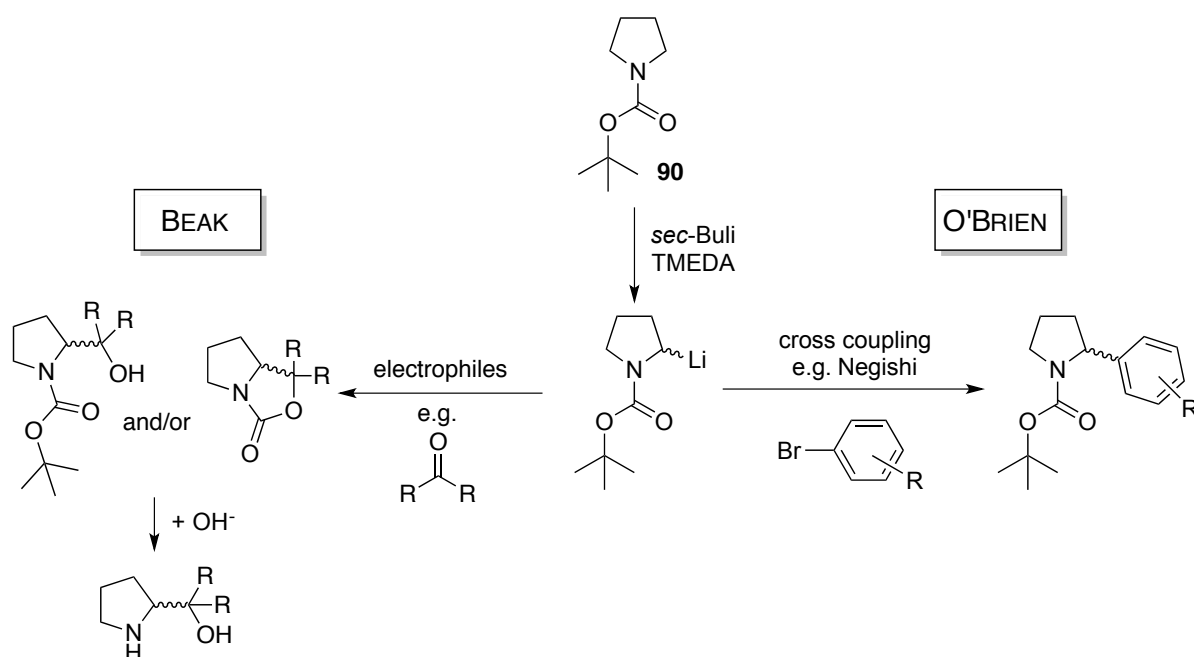
Scheme 39: Synthesis of racemic catalysts *via* α-lithiated Boc-pyrrolidines.

In a first experiment it was investigated if this procedure is applicable for the straightforward synthesis of racemic diphenylprolinol **92**. Under similar conditions formation of both, the alcohol and the oxazolidinone as major product, was independently reported using benzophenone as the electrophile.[103c, 103d] When performing the experiment with TMEDA as additive for the lithiation, the Boc-protected alcohol **94** was formed besides approximately 10% of the oxazolidinone **95** (Scheme 40a). As the oxazolidinone **95** is an intermediate in the subsequent deprotection of the carbamate (Scheme 40b, its formation could be clearly monitored by ¹H NMR and TLC), the oxazolidinone **95** was also isolated. However, for both, the combined and separate isolation, perfect purification of the mixture and the oxazolidinone **95** species was not possible. Therefore, it was investigated whether the crude product after reaction workup could be directly applied to the deprotection conditions. Indeed, the alcohol **92** was isolated in 56% yield and excellent purity after recrystallization (Scheme 40c).
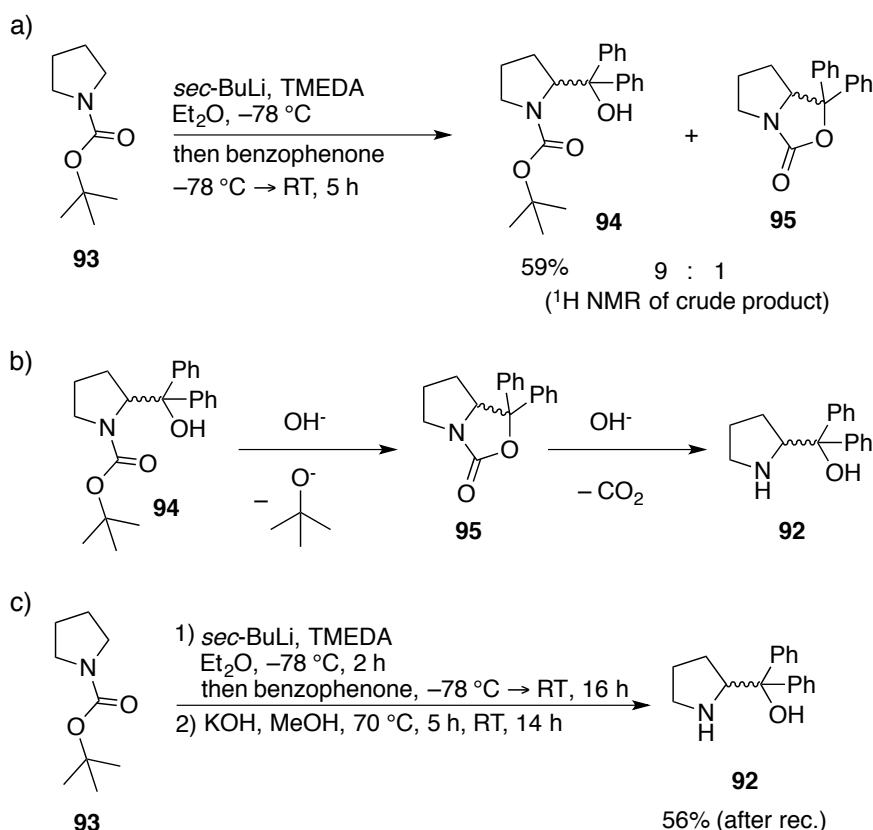
Scheme 40: a) Lithiation and trapping of the lithiated intermediate with benzophenone. b) Oxazolidinone formation during the deprotection of Boc-alcohol **94** under basic conditions. c) Direct deprotection of the crude product after lithiation.

With the racemic alcohol **92** in hand, the racemic Hayashi-Jørgensen catalyst **77a** was synthesized according to the reported procedure for the enantiopure catalyst (Scheme 41).[81] The latter one is commercially available.
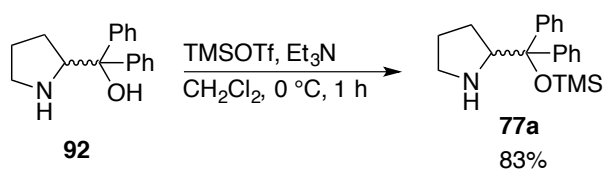
Scheme 41: Synthesis of racemic Hayashi-Jørgensen catalyst **77a**.

During the studies of the enantiopure catalyst screening, TIPS-protected catalyst **77c** was already identified to induce high selectivities.[16] For the synthesis it was essential to use lutidine instead of Et_3N as base and long reaction times. Still, after stirring overnight with an excess of TIPSOTf (5 eq.) only 2% of the racemic catalyst was isolated. However, the isolated amount was sufficient for the ESI-MS screening despite in this low yield. An increased yield of 26% for the enantiopure catalyst **77c** was obtained after longer reaction times of 72 h (Scheme 42).
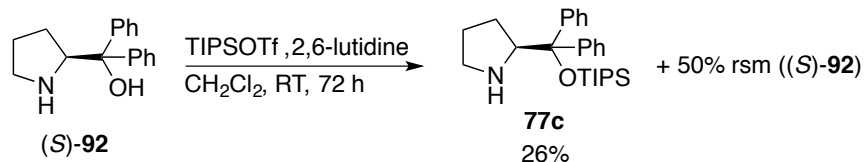
Scheme 42: Synthesis of TIPS-protected catalyst **77c**.

Methyl-protected diphenlyprolinol **77d** was another commercially available enantiopure catalyst. In addition this catalyst structure was supposed to induce only moderate selectivities, which would provide a useful additional data point in the racemate screening. In contrast to the silylation, formation of the OMe-ether needs to be conducted prior to the deprotection to avoid *N*-methylation. The methylation of Boc- and TBS-protected *trans*-hydroxy diphenylprolinol in neat MeI with NaH was reported by the GELLMAN group (Scheme 43).[104]
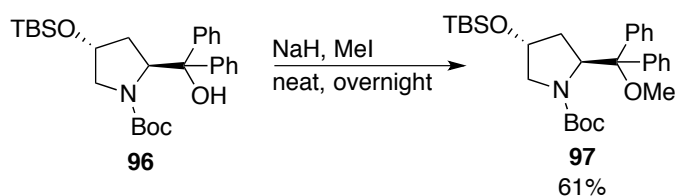
Scheme 43: Methylation of the tertiary alcohol reported by GELLMAN *et al*.

However, the additional substituent at the pyrrolidine moiety seemed to be essential for such a methylation. Without this substituent the ring closure to the oxazolidinone was observed for both, the ethyl carbamate **90** synthesized during the 1st generation synthesis and the Boc-protected aminoalcohol **94** obtained in the lithiation reaction (Scheme 44).
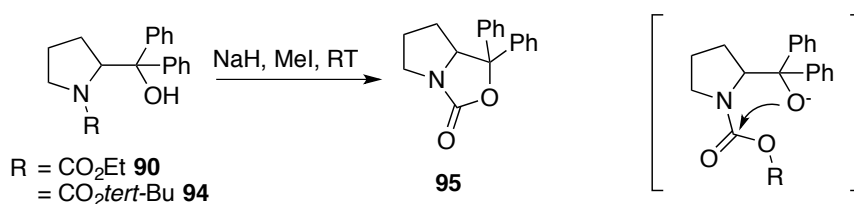
Scheme 44: Observed ring closure to the oxazolidinone under methylation conditions.

A more reactive methylating agent such as Meerwein's reagent failed to give any product. Using ethyl carbamate **90** and methyl triflate in the presence of 2,6-di-*tert*-butylpyridine the desired product was obtained in 41% yield. Subsequent deprotection under basic conditions failed, which is reasonable bearing in mind that oxazolidinone formation cannot occur with the methylated tertiary hydroxy group. Using Boc-protected alcohol **94** might be more promising as a variety of acidic deprotection procedures are known. However, at this point a new approach was chosen, which was less straightforward, but more reliable and less expensive. Following a procedure from ENDERS the synthesis of the methylated racemic catalyst **77d** was obtained in 64% overall yield by methylation of *N*-benzylated diphenylprolinol **98** (Scheme 45).[105]
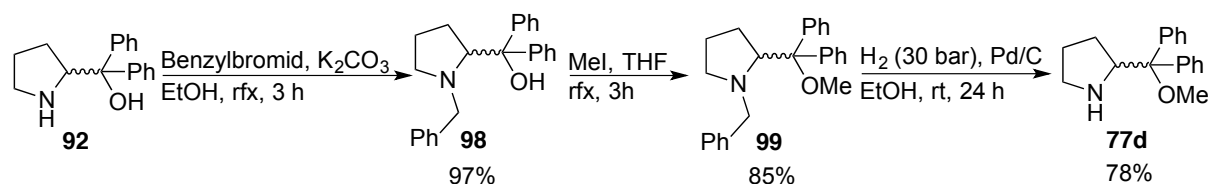
Scheme 45: Synthesis of the racemic methylated organocatalyst **77d**.

Further organocatalysts bearing a cyclic backbone instead of the diphenyl group at the side chain were thought to be suitable for ESI-MS analysis (Figure 75). The racemic derivative should be accessible by trapping lithiated Boc-pyrrolidine **93** with the corresponding cyclic ketone. The enantiopure catalyst could be obtained by double Grignard addition of a dibromide precursor to proline ester **90**, which was synthesized according to the procedure used for the racemic compound (see Scheme 38).
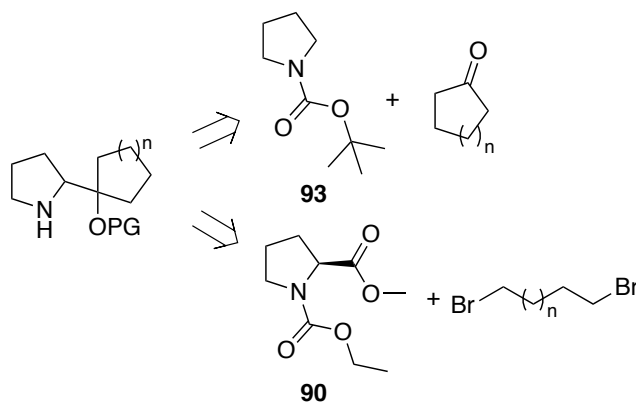
Figure 75: Retrosynthetic analysis of racemic and enantiopure catalysts having a cyclic backbone in the side chain.

The six- and the five- membered ring analogues were chosen as targets, as here the enantiopure catalysts should be more easily accessible due to a more favored intramolecular ring formation during the Grignard addition compared to other ring sizes. However, for the catalyst bearing a cyclohexane ring, in both reactions, the lithiation and the Grignard reaction, the formation of a complex product mixture was observed. Separation by flash column chromatography only gave poor isolated yields of the desired product. During the lithiation process besides oxazolidinone formation, an aldol condensation occurred as the major side reaction (Scheme 46a). During the Grignard addition more than 10 by-products were monitored by GC-MS analysis of the crude product. Reducing the reaction time to 3 h afforded the product in about 21% yield, but still considerably unpure (Scheme 46b).
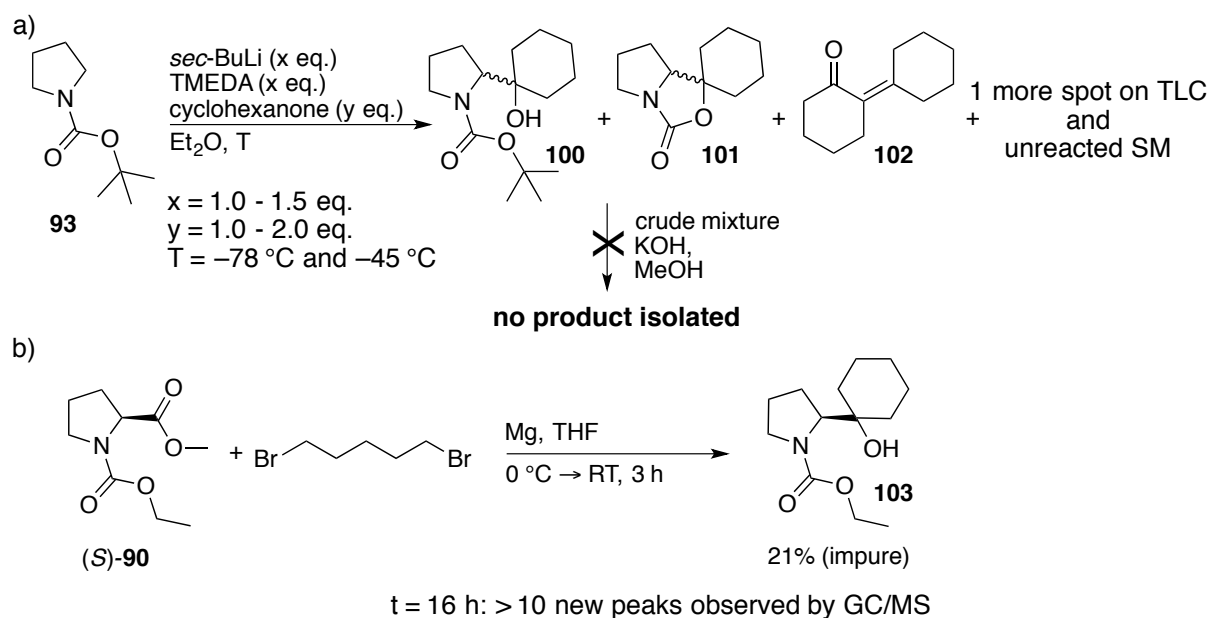
Scheme 46: a) Initial experiments with cyclohexanone as electrophile in the lithiation reaction. b) Grignard addition using dibromopentane as precursor to form the six-membered ring.

As both reactions seemed to proceed more cleanly to the corresponding five-membered ring, further investigations for these reactions were carried out with cyclopentanone as the electrophile for the lithiation and 1,5-dibromobutane for the Grignard addition. For the lithiation the product **104** was formed in 30% yield and 66% of unreacted starting material (sm) **93** was recovered. Again formation of the aldol condensation product of cyclopentanone was observed, indicating that an enolate of cyclopentanone is formed under these conditions. To prove whether the lithiation is not complete and excess *sec*-BuLi deprotonates the cyclopentanone an aliquot of the lithiation mixture prior to the addition of cyclopentanone was quenched with CD$_3$OD and analyzed by GC/MS (Scheme 47a). An incorporation of deuterium of about 77% was found. As the quench was not performed under perfect air and

139

moisture exclusion this indicates that the *sec*-BuLi is mainly consumed and is not responsible for the formation of the high quantities of the aldol product **106** (GC/MS analysis[i] of the crude product revealed an intensity of similar order of magnitude as observed for the substrate). In combination with the 66% of re-isolated starting material mentioned above, this clearly demonstrates that the lithiated species is responsible for the deprotonation of the ketone, as a competitive reaction to the nucleophilic addition (Scheme 47b).
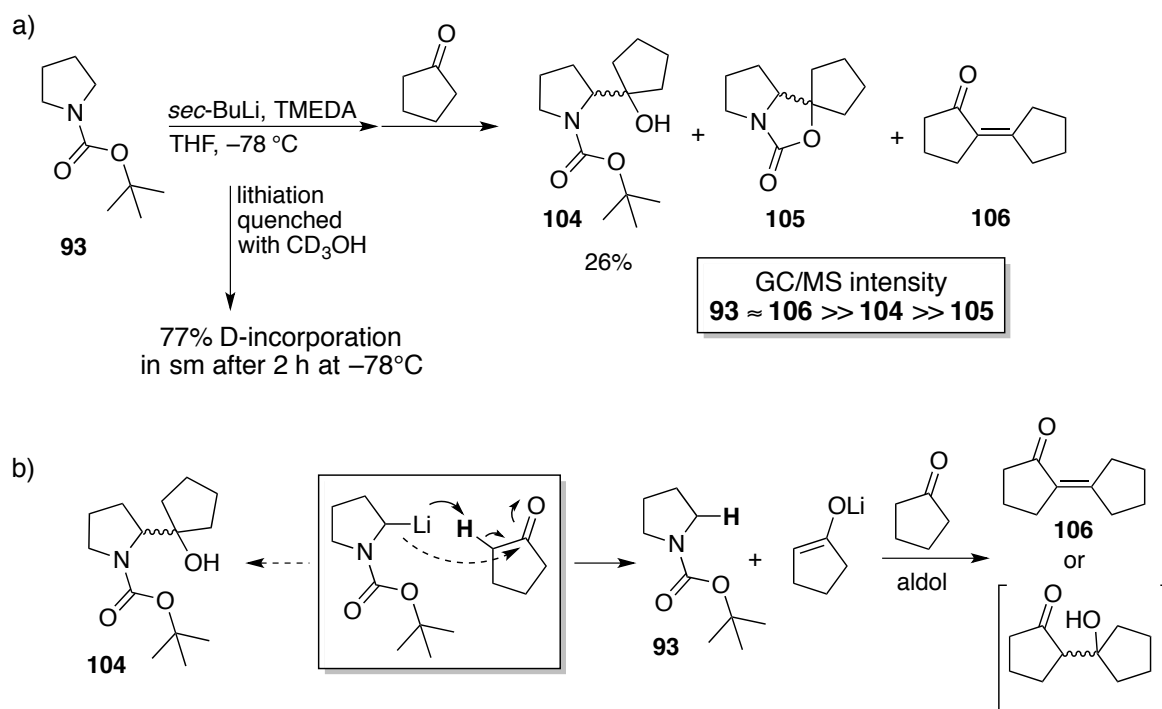
Scheme 47: a) Initial experiments with cyclopentanone as electrophile in the lithiation reaction. b) Nucleophilic addition (dashed arrows) *vs.* deprotonation, enolate formation and subsequent aldol reaction (solid arrows).

Variation of the parameters such as equivalents of the ketone or reaction temperature did not considerably inhibit enolate formation. An optimized yield of 35% of isolated alcohol **104** in high purity was obtained when cyclopentanone dissolved in THF was added slowly keeping the internal temperature below −50 °C (Scheme 48). Since the isolated quantities were sufficient for further catalyst synthesis, optimizations such as addition of an external Lewis acid to increase the electrophilicity of the ketone were not investigated.

---

[i] As no internal standard was applied the GC/MS analysis only allowed for a qualitative interpretation of the quantities.
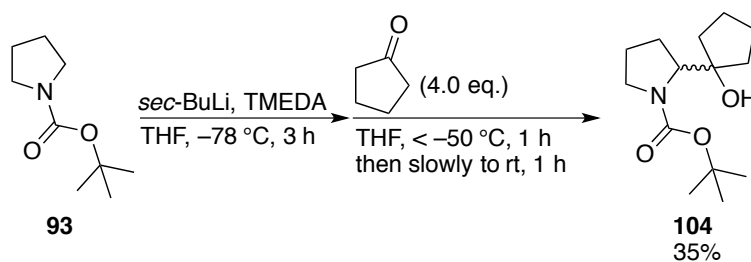
Scheme 48: Final synthesis of racemic alcohol **104**.

Although the synthesis of the five membered enantiopure analogue **107** worked more smoothly than the reacton to six-membered ring derivative **103**, the product was isolated in only 38% yield (Scheme 49). ESI-MS indicated complete consumption of the ester **90** after 1.5 h. With increasing reaction time the major product shifted from alcohol **107** to oxazolidinone **105**. In addition crystals, which precipitated from the crude product were identified as the deprotected alcohol **108**. Unfortunately, when using the crude product for deprotection isolation of pure aminoalcohol **108** became difficult (purification and TLC-monitoring of low quantities by column chromatography caused problems).
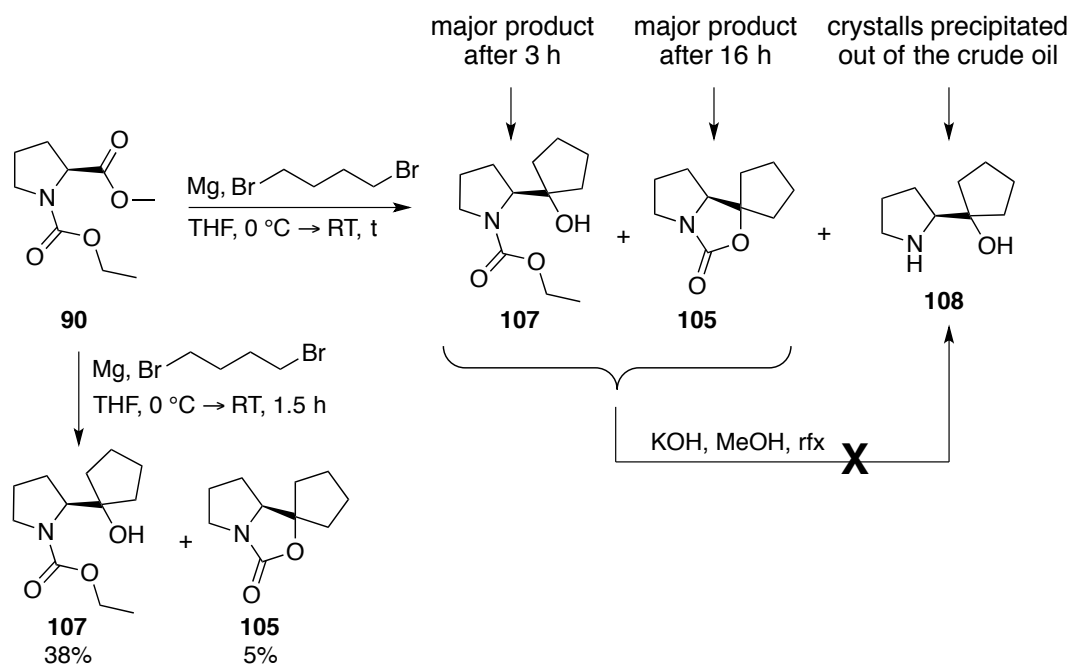
Scheme 49: Synthesis of the enantiopure alcohol **107** by Grignard addition to enantiopure ester **90**.

Acidic deprotection of the Boc-group worked smoothly affording the racemic aminoalcohol in quantitative yields and excellent purity without further purification. In contrast, deprotection of ethyl carbamate **107** under basic conditions appeared to need more harsh conditions and a purification (Scheme 50a). Subsequent TBS-protection under identical conditions as applied for diphenylprolinols **92** afforded the corresponding cyclopentyl TBS-alcohols **109** in lower

yields. On one hand this might be due to the increased steric hindrance in the more rigid system, on the other hand due to purification problems, which appeared during flash column chromatography. Nevertheless, a sufficient quantity for ESI-MS screening experiments was isolated.
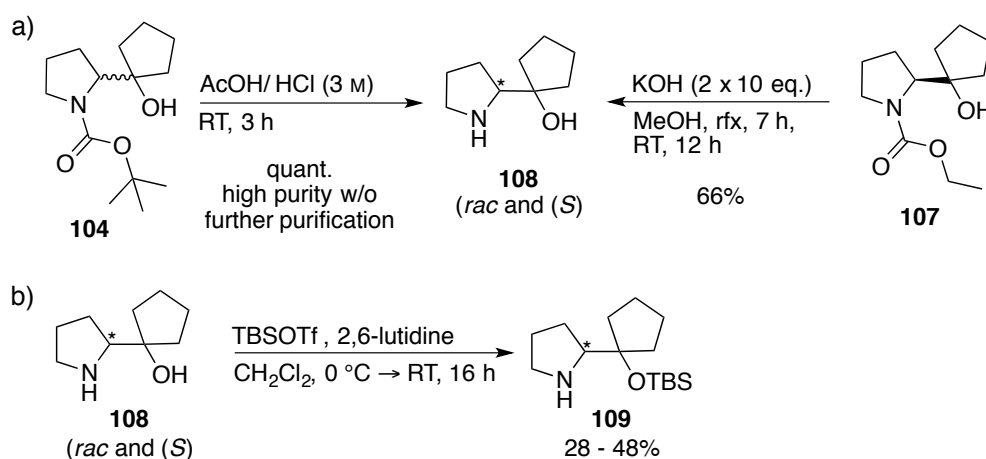
Scheme 50: a) Deprotection to aminoalcohol **108** under acidic and basic conditions. b) TBS-protection of the tertiary alcohol.

The group of SEEBACH was able to obtain x-ray suitable crystals for enamine and iminium intermediates based on silyl-protected diphenylprolinols.[106] In both solid state structures the two phenyl groups were oriented opposite to the pyrrolidine ring, whereas the silyl group blocks an approach from the top of the reactive site (Figure 76).
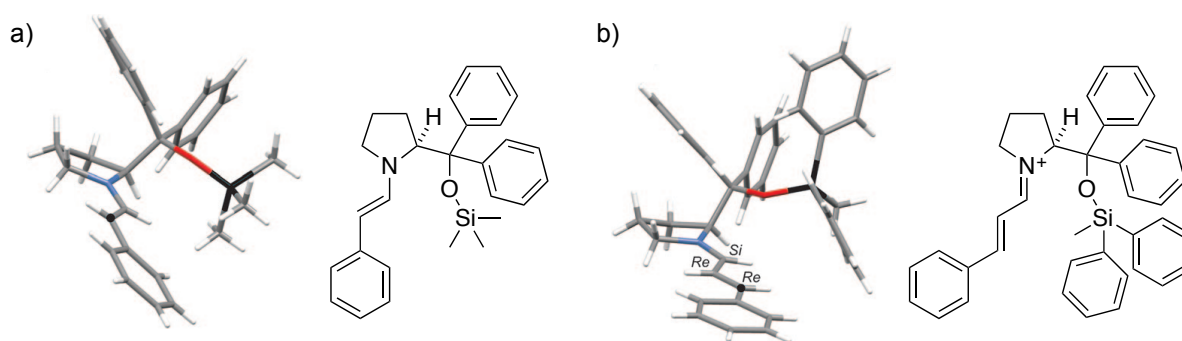
Figure 76: Reported x-ray structures derived from diphenylprolinols for a) an enamine intermediate and b) an iminium ion.[106]

So far unknown structures applied as organocatalysts were silyl-protected mono-phenyl substituted prolinols. Here, two diastereomeric forms are possible. The x-ray structures depicted in Figure 76 demonstrate the importance of the phenyl groups for the conformation of the intermediate and therefore the effective shielding of one reactive site. Investigations of such structures could give further insight into the structure-selectivity relationship. In line with such studies isoindoline derivatives were also synthesized.

The enantiopure diastereomeric alcohols ((*S,S*)- and (*S,R*)-112) were easily accessible from (*S*)-Boc-prolinol after Swern oxidation and subsequent Grignard addition. As the x-ray structure of the (*S,R*)-diastereomer was reported, the relative configuration of the diastereomeric products could be clearly assigned according to the ¹H NMR data.[107]
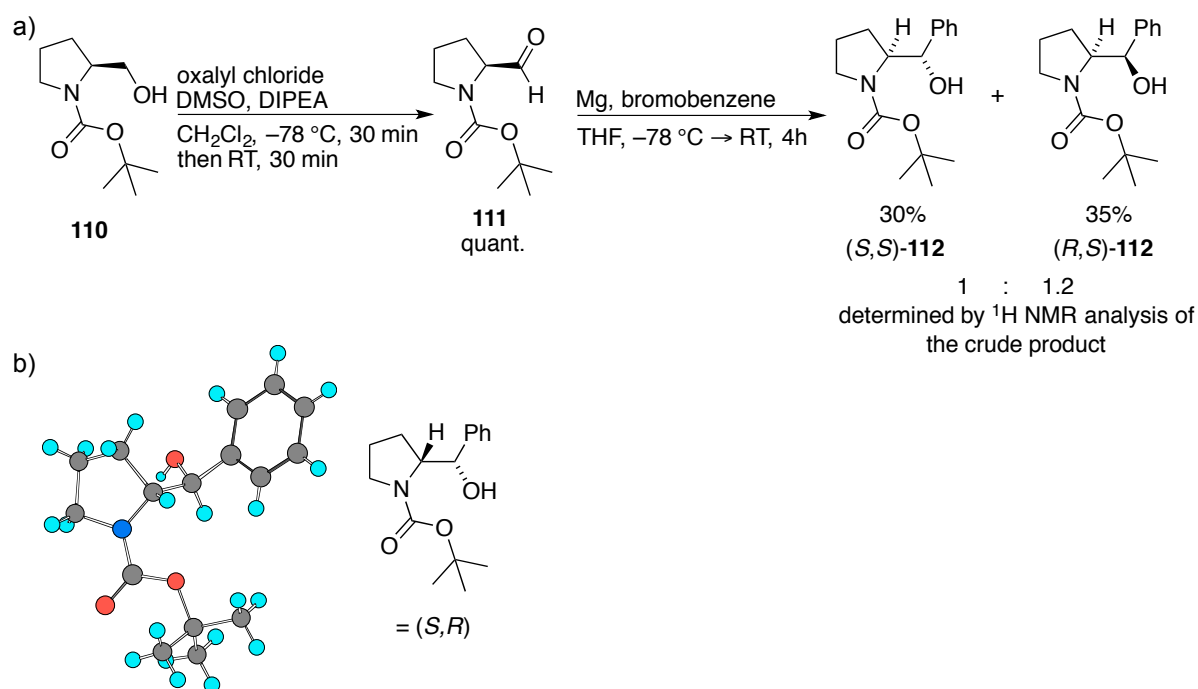
Scheme 51: a) Synthesis of the enantiopure diastereomeric Boc-protected alcohols ((*S,S*)- and (*S,R*)-112). b) Reported x-ray structure of the (*S,R*) diastereomer.

Again, the racemic alcohol was synthesized *via* lithiated Boc-pyrrolidine with benzaldehyde as the electrophile. In contrast to the procedures described above with benzophenone or cyclohexanone the reaction worked smoothly in 98% overall yield of a 2:1 mixture of diastereomers. Formation of an oxazolidinone intermediate was not observed. This demonstrates that two phenyl groups or a cyclic backbone have a distinct influence on the conformation, locating the hydroxy group in closer proximity to the carbamate and therefore simplify oxazolidinone formation.
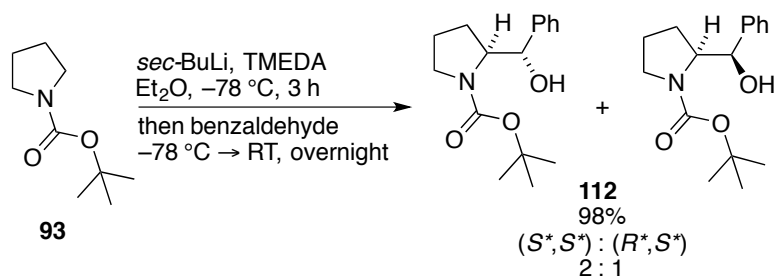
Scheme 52: Synthesis of racemic alcohol **112**. The diastereomers were partially separated by flash column chromatography.

With the Boc-protected alcohols **112** in hand the same deprotection procedure as described above for the cyclopentanone-derivative **104** was applied. Interestingly, with these substrates longer reaction times were required for high conversions. Nevertheless, the aminoalcohols **113** were isolated in high purity and were used without further purification (Scheme 53). The longer reaction times are caused by the decreased solubility in the aq. HCl/AcOH mixture of the more non-polar phenyl-substituted alcohol **112**. Boc-protected diphenylprolinols **94** were insoluble in such a reaction mixture and were no longer deprotected under these conditions. Subsequent protection with TBSOTf in the presence of Et$_3$N instead of lutidine, which also simplified the final product purification, afforded the desired racemic and enantiopure organocatalysts **114** (Scheme 53).
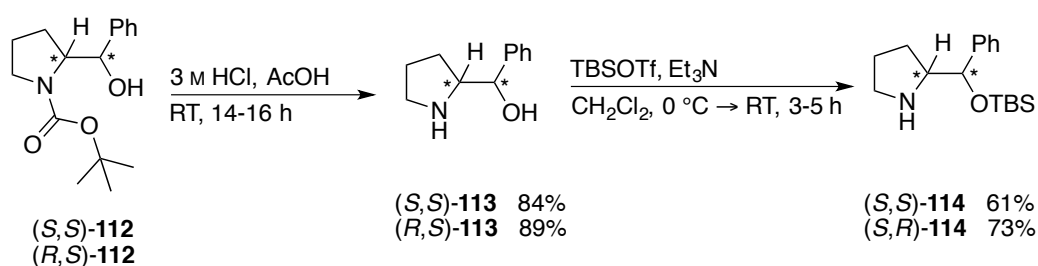
Scheme 53: Synthesis of enantiopure TBS-protected organocatalysts **114**. The racemic analogues were synthesized according to the same procedure.

5.3.3 Synthesis of Further Pyrrolidine-based Catalysts

In order to investigate how catalysts that induce low selectivity perform in the ESI-MS screening of racemic catalysts, TBS-protected prolinol **116** was synthesized. In previous studies this catalyst provided the Michael product **89** in about 20% *ee*.[16] Both the racemic and enantiopure aminoalcohol precursor were commercially available. Applying a reported procedure with TBSCl in DMF,[108] the *N*-formylated species **117** was formed as the major product (Scheme 54). Most likely, TBSCl activated DMF under formation of the Vilsmeier-Haack formylation species. It is worth mentioning that under these and similar conditions the amine was isolated as hydrochloride. The NMR data of this hydrochloride matched very well the literature data although the free amine was reported.[108]
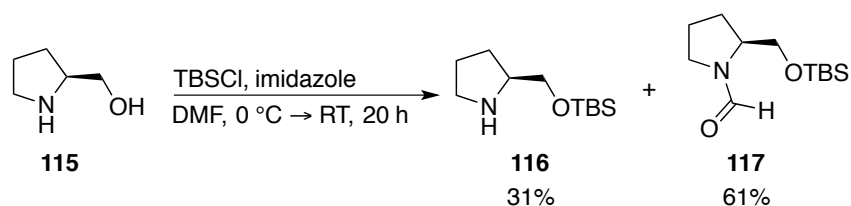
Scheme 54: Attempted synthesis of TBS-prolinol according to the procedure of Peng.

As DMF was supposed to be the formylation agent, changing the solvent to CH_2Cl_2 should avoid the side reaction. Indeed, after bulb-to-bulb distillation and filtration through basic alox the desired product was isolated in excellent purity without formation of the side product (Scheme 55).
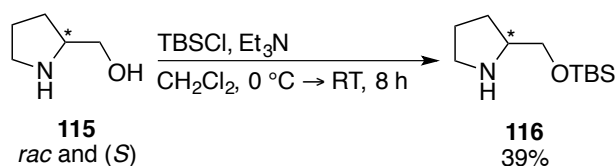
Scheme 55: Synthesis of TBS-prolinol in CH_2Cl_2.

As discussed in the previous section, lithiation of Boc-pyrrolidine **93** and a subsequent Negishi coupling with aryl halides could give access to α-aryl substituted organocatalysts. To prove whether such structures are active in the back reaction and selective in the forward reaction, commercially available racemic α-phenyl pyrrolidine **118** was initially applied to the ESI-MS screening. To validate the result the racemic catalyst was separated into its enantiomers by semi-preparative HPLC conditions. Sufficient quantities of the (*R*)-enantiomer, which eluted first, were isolated in 99% *ee*. As no baseline separation was obtained under HPLC conditions, the final *ee* was determined by GC analysis after derivatization of the amine into the trifluoroacetamide. The absolute configuration was assigned according to the optical rotation value of (*R*)-**118**.[109]
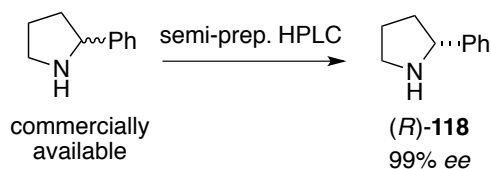
Scheme 56: Separation of racemate **118** into its enantiomers by semi-preparative HPLC.

5.3.4 Synthesis of Isoindoline-derived Catalysts

The isoindoline framework was chosen as a new structure-type for ESI-MS investigations for several reasons. First of all, with unsubstituted isoindoline **119** the iminium ion **Im** was detected in the back reaction after 15 min reaction time in acceptable signal intensities in the ESI-MS. In addition, such structures were not evaluated as organocatalysts so far and the starting material for this framework is not available from the chiral pool, thus making these catalysts more difficult to obtain in an enantiopure manner. Finally, in line with the conformational studies mentioned in the previous section (see Figure 76), isoindoline bears, in contrast to pyrrolidine-derived catalysts, an annulated phenyl ring that makes the pyrrolidine ring planar. In combination with the different steric interactions between the phenyl protons and the side chain moieties the facial selectivity of the catalyst could be further improved but also decreased compared to the pyrrolidine analogues (Figure 77).
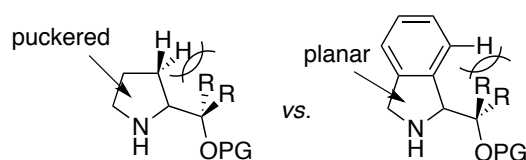
Figure 77: Different conformation and steric interaction of organocatalysts based on a pyrrolidine *vs.* an isoindoline framework.

For a comparison of the isoindoline derived catalyst with the parent prolinol derivatives the same TBS- and TMS-protected diphenyl derivatives and the diastereomeric TBS-protected monophenyl derivatives were synthesized. For the racemic catalysts the above applied lithiation strategy was envisioned to afford the corresponding catalysts.
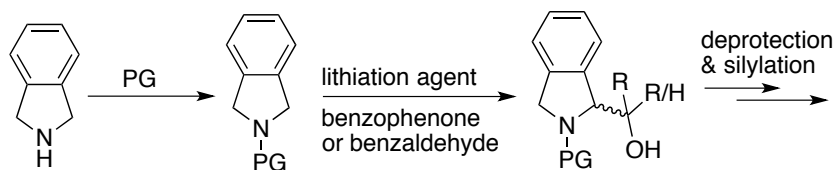
Scheme 57: General scheme for the synthesis of racemic isoindoline-based organocatalysts.

As conducted for the pyrrolidine derivative, the Boc-protecting group was chosen for initial experiments (Scheme 58). Although isoindoline **119** tends to decompose and needs to be stored at low temperatures, the Boc-protected compound was isolated as a bench stable solid. However, in the subsequent lithiation reaction under standard conditions only the signals of benzophenone were observed by NMR analysis of the crude product after reaction workup. This provides clear evidence for a decomposition of the starting material **120**. Also using

further lithiation agents, GC/MS analysis of the starting material after quenching the reaction mixture with a deuterium source indicated either decomposition or no D-incorporation (Scheme 58).

lithiation agent	D-incorporation
sec-BuLi, TMEDA	decomposition
sec-BuLi	decomposition
n-BuLi, TMEDA	decomposition
n-BuLi	no incorporation
LiTMP	no incorporation
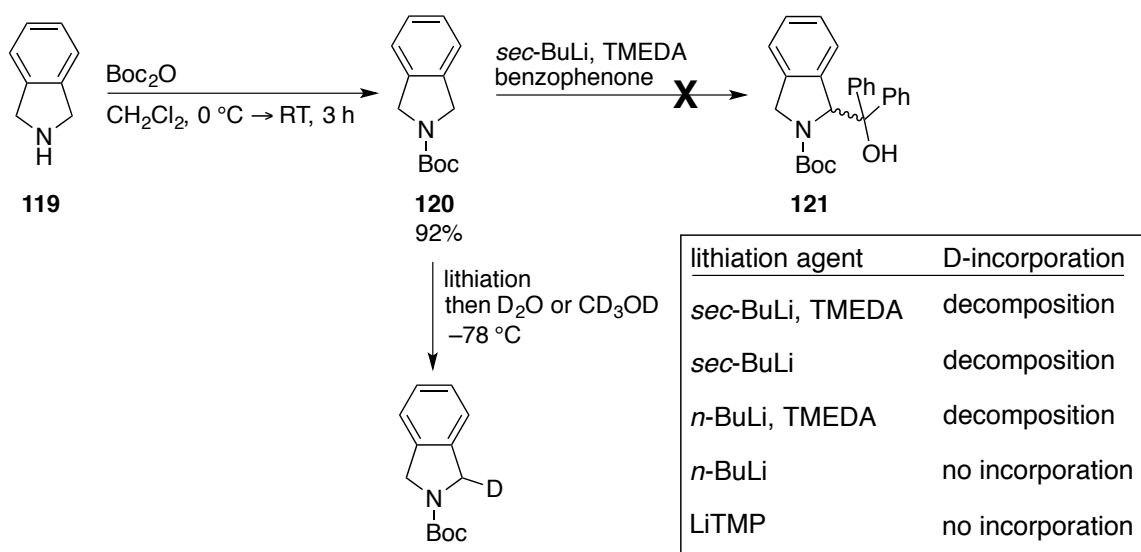
Scheme 58: First attempt to α-functionalize Boc-protected isoindoline **119** *via* lithiation.

The purity of commercially available isoindoline was poor. A potential synthesis of this compound employed benzylamine and 1,2-bis(bromomethyl) benzene and generates the benzylated species **122** (Scheme 59). As expected, attempts to lithiate the benzyl isoindoline with *sec-* and *tert*-BuLi failed. However, even in the case of a successful deprotonation, the *N*-benzyl protons are of a similar electronic nature as the CH$_2$ protons in the isoindoline core, which could also cause regioselectivity problems.
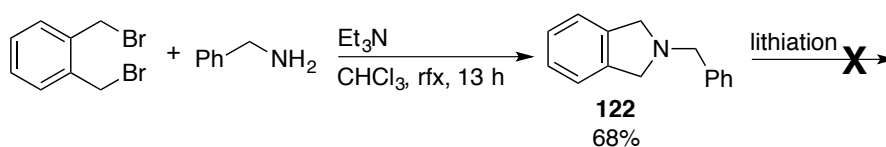
Scheme 59: Synthesis of *N*-benzyl isoindoline **120** and subsequent lithiation attempts.

An alternative approach for an α-functionalization could encompass *N*-oxide formation followed by SmI$_2$-mediated C–C bond formation with electrophiles as reported by CHAVANT for pyrrolidines with ketones.[110] However, a similar procedure for *N*-oxide formation with methyl trioxorhenium and urea hydrogen peroxide failed to form the *N*-oxide of isoindoline. This is in line with literature reports where formation of *N*-oxide of "naked" isoindoline was reported to be unsuccessful. The only literature examples for *N*-oxides of isoindolines were found when the isoindoline aryl part was substituted with an electron-donating substituent.[111]

In a literature survey, one procedure for an α-alkylation of isoindolines in moderate to good yields was found.[112] In 1990, ROCKELL and BEELEY used a formamidine protected isoindoline and *sec*-Buli for deprotonation. The lithiated intermediates were trapped with alkyl halides and benzaldehyde. This procedure was adopted and indeed found to work very well also for benzophenone as an electrophile (Scheme 60). For the installation of the protection group (Scheme 60, step a) the amount of *N'*-*tert*-Butyl-*N*,*N*-dimethylformamidine was increased compared to the reported procedure for sufficient conversion. Isoindoline was freshly distilled prior to use and lithiation was conducted with *sec*-BuLi without diamine additive (Scheme 60, step b). After addition of the electrophile, the reaction mixture was slowly allowed to warm to room temperature in the cooling bath, as for lithiation experiments at temperatures higher than –40 °C decomposition of the starting material was observed. The addition of benzaldehyde as electrophile led to the formation of diastereomers (1.3:1 (*S**,*S**)/(*S**,*R**)), which were successfully separated by flash column chromatography. The assignment of the relative configuration will be discussed below. Finally, reductive deprotection was performed with LiAlH$_4$ (Scheme 60, step c (1)) affording aminoalcohols **126** and **127**. Conducting FIESER`S workup, the aminoalcohols were isolated as black or red foams, but in good NMR purity. Further purification steps were found to be complicated due to the polarity and instability of the intermediates and therefore the crude products were used without further treatment in the subsequent silylation with TMSOTf and TBSOTf, respectively (Scheme 60, step c (2)). The deprotection prior to the silylation was important, as TMS-protection of formamidine **124** resulted in low yields probably due to even higher steric hindrance between the *N*-protecting group and the tertiary alcohol. Even after two purifications by column chromatography (silica gel or alox) the silylated products were isolated as black and red oils. Nevertheless, NMR analysis showed an acceptable purity allowing for an application in the ESI-MS screening. Analytically pure products were obtained after purification by semi-preparative HPLC on an achiral silica column. However, after drying in high vacuum overnight under exclusion of light, the initially colorless solid **128a** or pale red oils (**129**) became dark red. Also in solution decomposition was observed by repeated HPLC analysis of the catalyst solution. The low stability of these compounds is a clear disadvantage for their application as organocatalysts. On the other hand this highlights one advantage of the ESI-MS screening, as here the intrinsic selectivity is determined, the catalyst did not need to be applied in perfect purity for a determination of its enantioselectivity. For an alternative purification, catalyst **128b** was precipitated as its HBF$_4$ salt (HBF$_4$-**128b**). Black crystals were formed, which became pale grey after three subsequent

recrystallizations. Under identical precipitation conditions TMS cleavage was observed for catalyst **128a**.
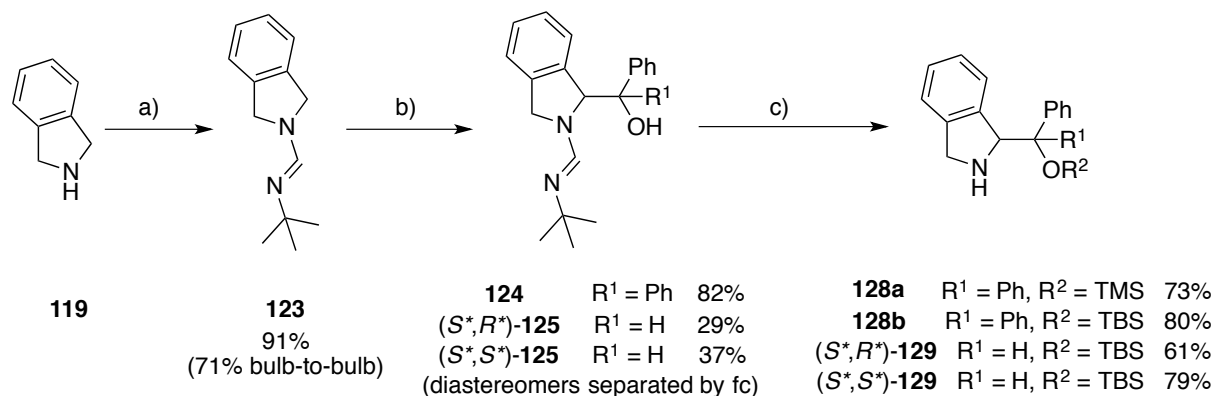
Scheme 60: Synthesis of racemic organocatalysts **128** and **129** starting from isoindoline. Conditions: N'-*tert*-Butyl-N,N-dimethylformamidine, $(NH_4)_2SO_4$, toluene, rfx. (b) For **124**: *sec*-BuLi, THF, −78 °C; then benzophenone, −78 °C to RT. For **125**: *sec*-BuLi, THF, −78 °C; then benzaldehyde, −78 °C to RT. (c) (1) LiAlH₄, THF, rfx. (2) For **128a**: TMSOTf, NEt₃, DCM, 0 °C to RT. For **128b**: TBSOTf, NEt₃, DCM, 0 °C to RT. For **129**: TBSOTf, NEt₃, DCM, −78 °C to RT.

The relative configuration was assigned by ^{1}H NMR experiments according to 2D NOE correlations. Moreover, the proposed relative configuration was confirmed by a x-ray structure obtained for the hydrochloride of the final racemic catalyst (R^*,R^*)-**129** (Figure 78). The x-ray structure also highlights the planar conformation of the five membered ring due to the annulated phenyl group. A few NMR observations regarding these structures are worth mentioning. For the (R^*,R^*)- or (S^*,S^*)-diastereomer, respectively, a characteristic high field shift of the isoindoline-aryl proton was observed (Figure 78). This suggests a structure where the phenyl substituent lies partially over this proton inducing the high field shift due to the aromatic ring current. Such a shift was also observed for the diphenyl substituted derivative **124** but not for the (S^*,R^*)-diastereomer of **125**. Furthermore, as soon the nitrogen group is deprotected in every structure the high field shift was no longer monitored in line with the conformation found in the solid state (Figure 78). The structure of the amidine moiety of **124** and **125** is similar to that of the pyrrolidine derived enamines and iminium ions reported by Seebach (see Figure 76).[106] The conformation of **125** as depicted in Figure 78, which explains the high field shift, would support the findings from the x-ray structures reported by Seebach that the hydroxy substituent points towards the residue bound to the nitrogen atom. However, it has to be admitted, that here the additional hydrogen bond between the hydroxy group and the amidine nitrogen might further fix this structure into this particular conformation. More insight might be given by OTMS-protected analogues. However, TMS protection of compound **124** did not work well and gave no clear insight from the

corresponding NMR spectrum.
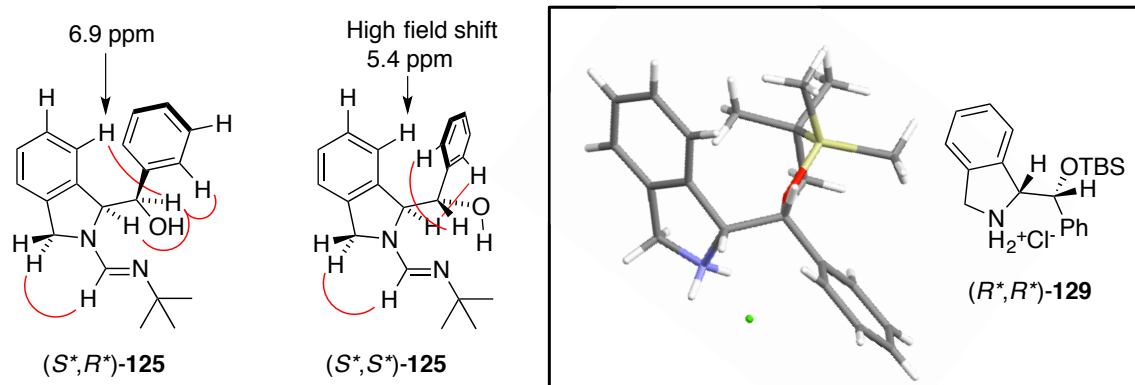
Figure 78: Selected representative NOE correlations for the diastereomers **125** formed after lithiation and reaction with benzaldehyde. X-ray structure of the hydrochloride of the final racemic catalyst **129**.

In order to validate the ESI-MS screening results the synthesized isoindoline derived catalysts were required in enantiopure form. To our delight, for all catalysts, separation conditions by means of semi-preparative HPLC on a chiral stationary phase were identified affording at least one of the enantiomers in perfect enantiopurity. The assignment of the optical rotation sign to the enantiomers obtained after separation of racemate (S*,R*)-**129** was not possible due to a very small and unstable value (< 1°).

R^1 = Ph, R^2 = TMS	**128a**	(+) >99.5%; (−) >99.5%
R^1 = Ph, R^2 = TBS	**128b**	(+) >99.5%; (−) >99.5%
R^1 = H, R^2 = TBS	(S*,R*)-**129**	>99.5%; 98%
R^1 = H, R^2 = TBS	(S*,S*)-**129**	(+) >99.5%; (−) >99.5%
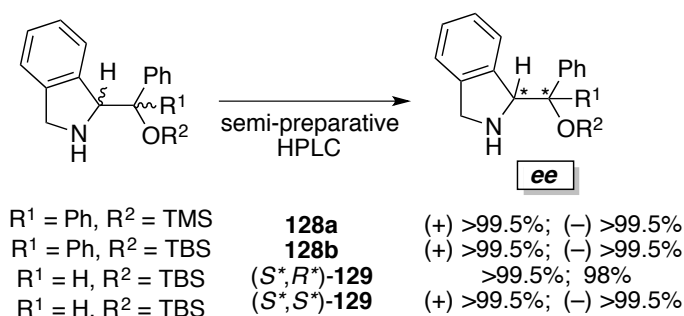
Scheme 61: HPLC separation of the racemate into its enantiomers.

The α-ester of isoindoline was intended to be a versatile precursor for further catalyst structures such as isoindolinols after reduction to the primary alcohol or isoindoline α-amides after saponification and coupling with various amines. However, a reaction of the lithiated species with methyl chloroformate failed to generate the monoester **131**. Instead, formation of a mixture with the diester **130** as the major product (di:mono approx. 8:1) in very low yields was observed, accompanied by decomposition of the starting material. This is reasonable bearing in mind that the acidity of the residual CH_2-group of the monoester (electron withdrawing substituent) is increased and could therefore be deprotonated by the lithiated species. Variation of the reaction parameters and addition procedures (e.g. slow addition of

the lithiated species to a solution of methyl chloroformate) did not significantly enhance the reaction outcome (Scheme 62). The isoindoline catalysts described above were already prone to decompose. An electron withdrawing ester substituent was even supposed to decrease the stability of the isoindoline derivate, which is in line with the first observations made for the ester formation and therefore no further synthetic efforts were made.
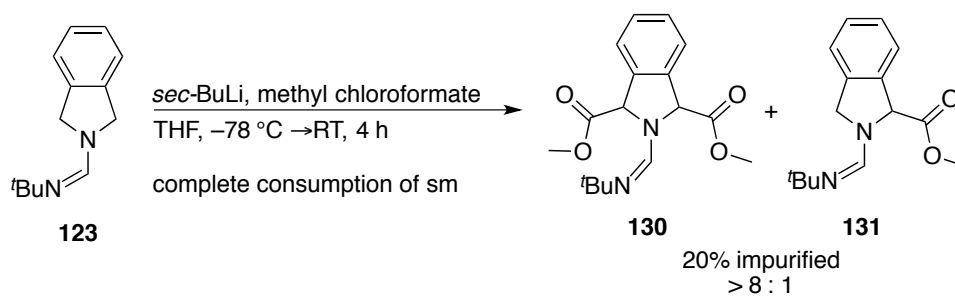
Scheme 62: Attempt to introduce an ester functionality at the α-position of isoindoline.

5.4 ESI-MS Screening

5.4.1 Development and Validation of a Screening Protocol

In preliminary experiments promising conditions for a racemate screening were identified, where a clear effect on the iminium ratio was observed using 1 mol% of catalyst **77b**. It should be noted that variation of reaction and also ESI-MS parameter led to partially different ratios of iminium ions. As no clear trend was visible, consistent conditions were chosen which gave stable signals for a variety of catalysts. Therefore, a 75:25 mixture of quasienantiomers **89** and **89'** and 1 mol% of catalyst was stirred for 15 min in EtOH/CH$_2$Cl$_2$ (9:1), then directly diluted with CH$_3$CN and subjected to ESI-MS analysis. For all measurements ESI-MS parameters (e.g. drying gas temperature, detector voltage) were kept constant.

Initially, four Hayashi-Jørgensen type catalysts inducing different selectivities were applied to prove whether under the described conditions their selectivity trend is reflected by ESI-MS screening of the racemic catalyst. Their actual *ee* was determined by screening of the enantiopure form under identical conditions with 1 mol% of catalyst (Figure 79).[i] The obtained results for catalyst **77a-c** matched very well the previously reported *ee* (ESI-MS and preparative forward reaction) using 10 mol% of catalyst (see also Figure 72, section 5.2.1).[16] This also demonstrates that ESI-MS screening of the enantiopure catalyst is an adequate method to validate the results of the racemate screening.

	d: R = Me	a: R = TMS	b: R = TBS	c: R = TIPS
	88 : 12 (76% *ee*)	91.5 : 8.5 (83% *ee*)	96.5 : 3.5 (93% *ee*)	97 : 3 (94% *ee*)
preparative results (e.r.) (10 mol% catalyst)	n.d.	93 : 7	97 : 3	97 : 3

increasing selectivity
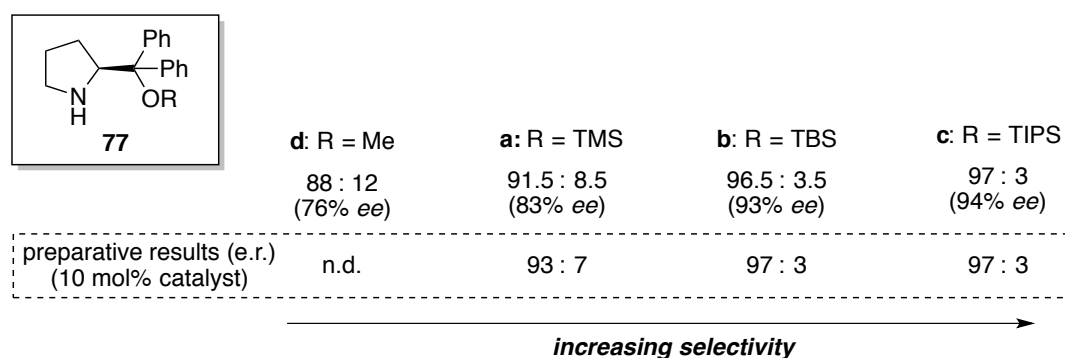
Figure 79: Iminium ratio and the related theoretical enantioselectivity determined by ESI-MS screening using 1 mol% of the enantiopure catalysts. The enantiomeric ratio was determined in the preparative reaction with 10 mol% catalyst.[16]

---

[i] Depending on the catalyst the signal ratio was slightly fluctuating. To minimize the resulting error four independent measurements were conducted. The depicted ratio and *ee* is the average value from these four measurements (see appendix).

Next, the corresponding racemic catalysts were subjected to the ESI-MS screening under the conditions described above. Having identified a selectivity trend for the enantiopure catalysts **77** (R = Me < TMS < TBS < TIPS), a signal ratio closer to 50:50 was expected in the same order. And indeed, when screening the racemic catalysts exactly this trend was found for the iminium ratios **Im/Im'**, from 28:72 for **77d** up to 38:62 for **77c** (Figure 80).[i] Moreover, as already discussed for the Pd-catalyzed allylic substitution, **Eq. 2** (see also section 5.2.2) allowed for a calculation of the theoretical enantioselectivity (in brackets) *via* the selectivity factor *s* from the monitored signal ratio. The selectivity trend is clearly reflected by monitoring the iminium ratios, although for practical reasons the ratios of quasienantiomers **89'** and **89** were not exactly 75:25. However, these small deviations were corrected by calculating the theoretical selectivity using **Eq. 2**, which includes the ratio of quasienantiomers (Q = [**89**]/[**89'**]) used in the specific experiment.
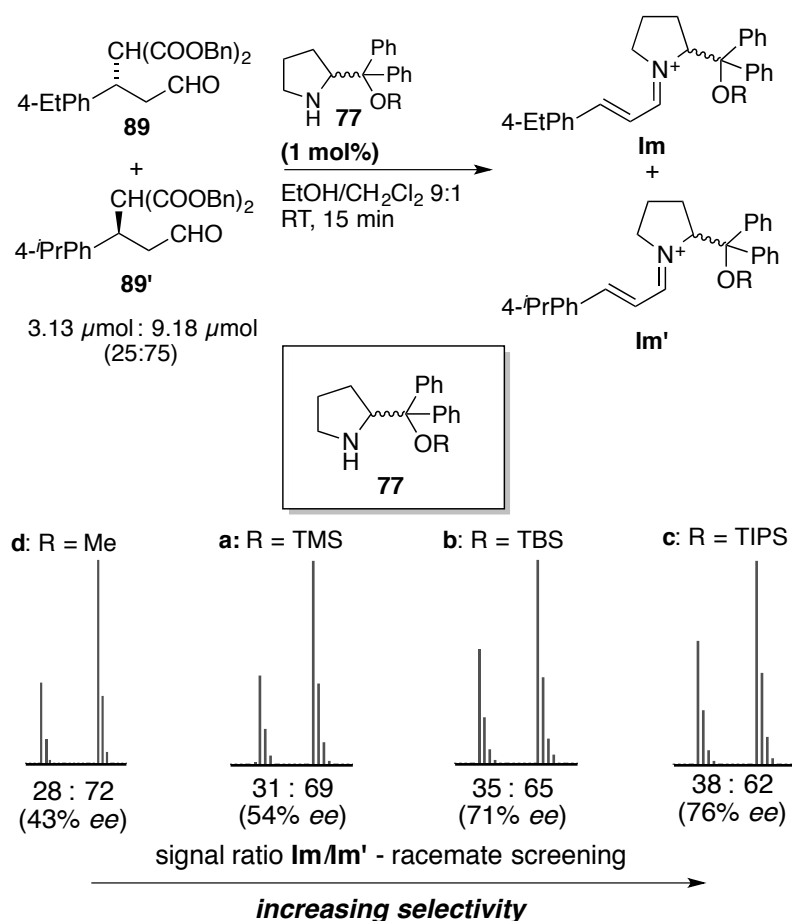
Figure 80: Monitored signal ratio **Im/Im'** by ESI-MS screening the back reaction using the racemic catalyst. In brackets: calculated stereoselectivity derived from the corresponding intermediate ratio according to **Eq. 2** for catalysts **77a-d**.

---

[i] The depicted ratio and *ee* is the average value from four independent measurements (see appendix).

$$s = \frac{Q^2 - R + \sqrt{(R - Q^2)^2 - (R \times Q - Q)^2}}{R \times Q - Q} \qquad \textbf{Eq. 2}$$

The screening results demonstrated that an identification of the most selective catalysts is possible by screening the racemic form. Nevertheless, as already indicated in preliminary experiments, the calculated enantioselectivity deviated significantly from the actual *ee* determined with the enantiopure catalyst (Figure 81, left). Most likely, the applied 1 mol% catalyst loading did not ensure an ideal pseudo zero-order regime providing an explanation for the deviation of the results. These findings are in line with the results of the racemic catalyst screening for the Pd-catalyzed allylic substitution, where a similar deviation was observed.[17] As observed in this case, an excellent linear correlation between the determined *ee* from the enantiopure and the racemic catalyst was found (see Figure 71), which allowed for a correction of the racemate screening results. In the Michael addition, a linear trend line with an R^2 value of 0.99 was found when the *ee* obtained from the racemate screening was plotted against the *ee* from the enantiopure catalyst (Figure 81, right). Provided that the linear correlation is generally applicable, the associated mathematical function y = 0.56x + 52.43 (**Eq. 3**, with y = *ee* from enantiopure catalyst, x = *ee* from racemate screening, m = 0.56 (slope), b = 52.43 (y-intercept)) can be used as a correction function to transform the theoretical selectivities obtained from the racemate screening into the actual *ee* of newly investigated catalysts.
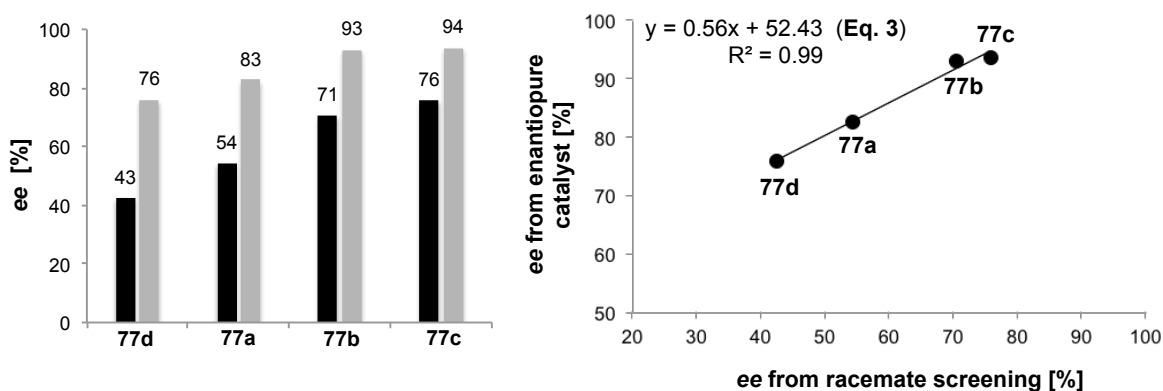
Figure 81: Left: Calculated enantioselectivity obtained from the racemic (black bars) and the enantiopure (grey bars) catalysts. Right: Linear correlation between the racemate screening results and the actual *ee* of the catalysts.

A few limitations regarding this linear regression are worth mentioning. A slope (m) of 0.56 ($0 < m < 1$) with a y-inercept of 52 was found for the mathematical function (Figure 81, **Eq. 3**). This slope ($0 < m < 1$) of the linear regression arises from a decreasing deviation between the selectivities obtained from the racemate screening and those of the corresponding enantiopure catalyst with increasing catalyst selectivity (Figure 81, left). Due to the y-intercept $\gg 0$, the correction function is inapplicable for catalysts inducing low enantioselectivity (< 50-60% *ee*). For example, for a catalyst inducing no selectivity (0% *ee* = x) the correction function would predict an *ee* of 52%. In addition, this screening methodology is considerably more accurate for highly selective catalysts, where a broad range of the iminium ratios covers a comparably small difference in the related theoretical *ee* (Figure 82). In contrast, for less selective catalysts, small changes in the measured signal ratio lead to large errors in the calculated *ee* values (e.g. an intermediate ratio of **Im/Im'** of 25:75 (0.33) to 28:72 (0.39) correspond to a theoretical enantioselectivity area of approximately 0-40% *ee*). However, because the primary goal is to identify the most selective catalysts, a correct prediction for low selective catalysts is not essential, as long as they are still identified as less selective.

One potential explanation for the slope ($0 < m < 1$) of the correction function (**Eq. 3**) is provided by two opposing trends. As mentioned above, the applied 1 mol% catalyst loading did not ensure an ideal pseudo zero-order regime providing iminium ratios closer to the 3:1 ratio of quasienantiomers **89'** and **89**. This effect should lead to an increased deviation between the *ee* obtained from the racemate screening and the actual *ee* induced by the enantiopure catalyst with increasing catalysts selectivity. On the other hand, the flattening shape of the curve in Figure 82 for signal ratios approaching 50:50 is an opposing trend. A deviation from the iminium ratio of a highly selective catalyst (e.g. 60:40 instead of 55:45), leads to a difference of 10% *ee* in the calculated enantioselectivity (92% *ee* to 82% *ee*). However, the disagreement in the calculated selectivity of a moderately selective catalyst (e.g. 70:30 instead of 65:35) is with 19% *ee* difference (69% *ee* to 50% *ee*) almost twice as high as the deviation of the more selective one. This could explain the observed decreasing difference of the theoretically calculated enantioselectivity with increasing catalyst selectivity, which results in the slope of the correction function of ($0 < m < 1$).
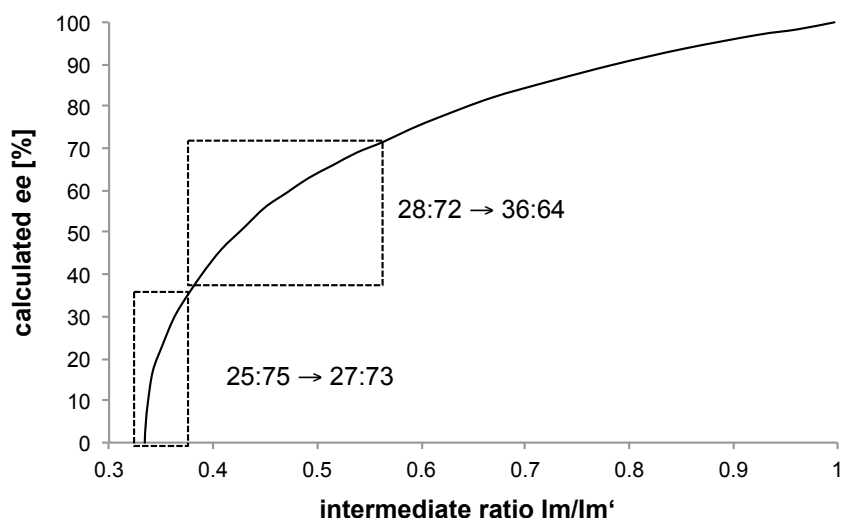
Figure 82: Dependency (according to **Eq. 2**) between the calculated theoretical enantioselectivity and the signal ratio (**Im/Im'**) in the racemate screening (with Q = 1/3).

In the initial experiments only catalysts with enantioselectivities >76% *ee* were applied to the racemate screening. As mentioned in the previous paragraph, a determination of the exact selectivity of low selective catalysts is not of interest. Still, it needs to be proved that low selective catalysts do not lead to misleading results. For that purpose TBS-protected prolinol **116** was analyzed in the back reaction screening. With 1 mol% of enantiopure catalyst in the back reaction screening an iminium ratio of 55:45 was found, which is in the same order of magnitude as the previously reported ratio of 59:41 with 10 mol% of catalyst and an e.r. of 62:38 determined in the preparative reaction.[16] Indeed, when applying the racemic catalyst to the back reaction with the scalemic (25:75) mixture of quasienantiomers, signal ratios that only slightly deviate from the initial ratio of quasienantiomers starting from where observed. This clearly indicated that the catalyst has a low selectivity (Figure 83).
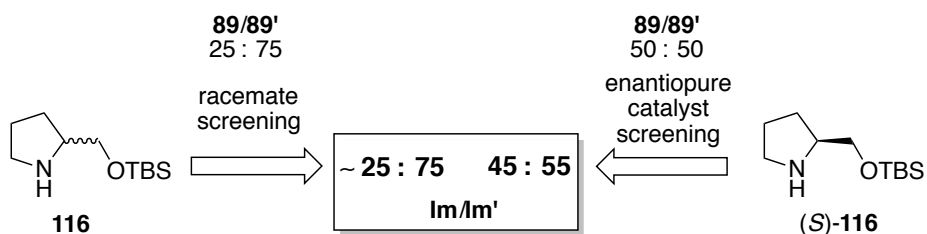
Figure 83: ESI-MS screening of enantiopure and racemic low selective TBS-prolinol **116**.

5.4.2 ESI-MS Screening of New Catalysts

In order to examine the utility and viability of the methodology new organocatalysts based on different frameworks were applied in the racemate screening. The first catalyst structure, was TBS-protected cyclopentyl derivative **109**. ESI-MS screening of the racemate indicated no or only low selectivity, whereas for the enantiopure catalyst an iminium ratio of 16:84 (**Im/Im'**) was found. This e.r. is slightly lower than the selectivity which is induced by the O-methyl substituted Hayashi-Jørgensen type catalyst **77d**. For the latter a signal ratio of approximately 28:72 (43% calc. theo. *ee*) was observed in the racemate screening, which clearly reflected the selectivity trend. Also from the perspective of later studies with further catalysts, a signal ratio for **109** of approximately 27:73 would be expected. The iminium ratio obtained from the enantiopure catalysts was also verified in a preparative forward reaction using unsubstituted cinnamaldehyde as the Michael acceptor and 10 mol% of the catalyst (e.r. 85:15). Several attempts to optimize the racemate screening failed and resulted approximately in the initial 25:75 ratio (Figure 84). Although a plausible explanation for the different behavior in the racemate screening of this catalyst's structure was not found, the deviation of the expected ratio of 27:73 and the finally observed 25:75 is small due to the narrow screening range for catalysts with moderate selectivity. A slight alteration of the signal ratio due to minor effects, which are not entirely clear, could be responsible for such a discrepancy.
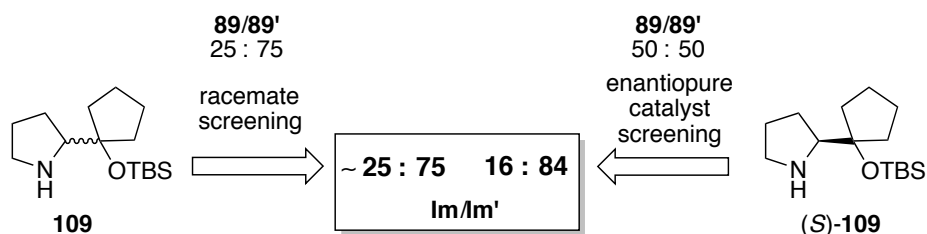
Racemic catalyst screening: Im/Im' ~ 25:75 for:

- Variation of back reaction times: 10 sec, 1 min, 5 min, 15 min, 30 min

- Addition of catalyst: vigorous stirring or no stirring

- Variation of reaction concentrations (x2; x1/2)

- 0.5 mol% catalyst loading

- Different ESI-MS parameters (detector voltage, temperature)

- Applying an eqimolar 1:1 mixture of quasienantiomers (**89/89'**) a iminium intermediates were formed in perfect 50:50 ratio

Figure 84: ESI-MS screening of enantiopure and racemic organocatalyst **109**. Different approaches to impact the intermediate ratio that resulted all in the iminium ratio started from.

In preliminary tests the "naked" isoindoline core **119** was identified to form iminium intermediates in the back reaction after 15 min in acceptable intensities. Other frameworks such as dihydrobenzo[1,4]oxazines **132** previously successfully applied by EBNER and PFALTZ[113] as organocatalysts for transfer hydrogenations and the MacMillan catalyst **133*HCl** did not generate the iminium ions derived from the Michael product **89** under the established screening conditions (Scheme 63).[16]
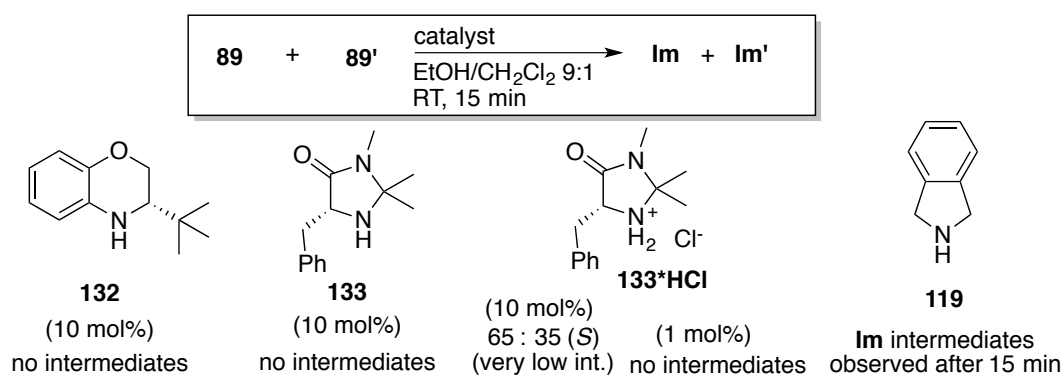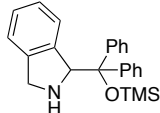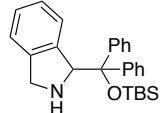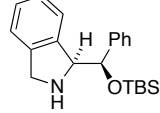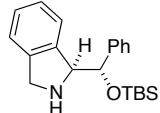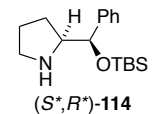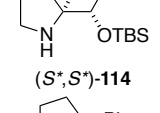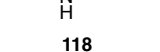
Scheme 63: Preliminary test experiments for other catalyst frameworks that might mediate the back reaction.

Besides isoindoline derivatives the diastereomeric monophenyl substituted prolinols **114** were not evaluated in the organocatalyzed Michael addition thus far and therefore became interesting structures for the ESI-MS screening of racemic catalysts. In addition α-phenyl substituted pyrrolidine **118** was tested in the racemate screening. For all catalysts investigated, the back reaction took place and the intermediates **Im** and **Im'** were detected in acceptable to excellent intensities. In general, iminium ions derived from pyrrolidine-based catalysts led to slightly better signal intensities than observed for the isoindoline derivatives. The determined iminium ratios were converted into the theoretical *ee* of the racemic catalyst applying **Eq. 2** (Table 9).[i] These values were then transformed into the proposed actual *ee* according to the correction function (**Eq. 3**) established with the Hayashi-Jørgensen type catalysts **77a-d** (see Figure 81). The results of the racemate screening were then validated with the corresponding enantiopure catalysts. When comparing these results it became obvious that the selectivity trend and therefore the most selective catalysts were again clearly identified by screening the racemic catalysts (Table 9, entry 1-5). Moreover, the corrected values are all in excellent agreement with the actual *ee*. This highlights, that the correction function is generally applicable to determine the actual enantioselectivity of racemic catalysts (with a selectivity of >50-60% *ee*). This was also demonstrated by the excellent linear correlation for all catalysts

---

[i] The depicted *ee* is the average value out of four independent measurements (see appendix).

>60% *ee* with a perfect R^2 value, that indicate the fitness of the trend line (Figure 85).

Table 9: ESI-MS screening results.

entry	catalyst	racemate screening theo. calc. *ee* [%][a]	corrected value *ee* [%][b]	enantiopure catalyst *ee* [%][c]
1	**128a**	47	78	79
2	**128b**	58	85	87
3	(*S**,*R**)-**129**	44	77	78[d]
4	(*S**,*S**)-**129**	23	65	66
5	(*S**,*R**)-**114**	33	71	70
6	(*S**,*S**)-**114**	0	-[e]	49
7	**118**	0	-[e]	2

a) For screening conditions see Figure 80. b) Values corrected using the correction function **Eq. 3** (y = 0.56x + 52.43). c) Determined by ESI-MS analysis of the back reaction applying 1 mol% of the enantiopure catalyst and an equimolar mixture of quasienantiomers (**89**/**89'**). d) 2 mol% of catalyst used. e) No correction due to low catalyst selectivities.
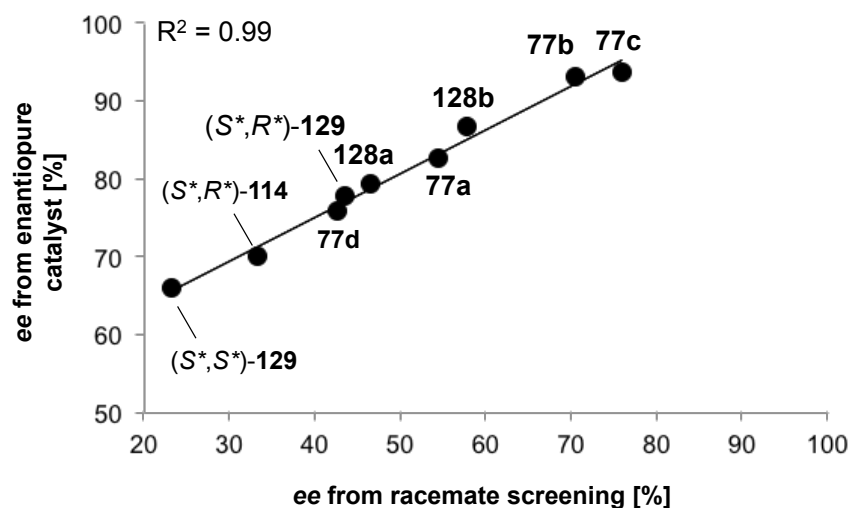
Figure 85: Linear correlation for all catalysts with an *ee* >60%.

For catalyst (*S*,S**)-**114** (Table 9, entry 6) a signal ratio (**Im/Im'**) of 24:76 and even 23:77 was found, although the quasienantiomers were applied in a 25:75 mixture. A signal ratio higher than the initially scalemic mixture should theoretically not be possible and demonstrates that other effects, more related to the measurement quality and maybe dependent on the iminium stability, led to a slight signal alteration as already proposed for cyclopentyl-based catalyst **109**. Nevertheless the observed iminium ratio indicated low selectivity for catalyst (*S*,S**)-**114** (<50-60% *ee*). Furthermore, commercially available racemic α-phenyl substituted pyrrolidine **118** (Table 9, entry 7) was tested as an example of a more varied catalyst structure. This catalyst was also revealed to be weakly selective when screening the racemate (ratio of 75:25; 0-5% calc. theo. *ee*). Indeed, an enantioselectivity less than 50% was found in both cases for the enantiopure catalysts (49% *ee* **114** and 2% *ee* **118**, respectively). Although it was not possible to distinguish between these two different selective catalysts by screening the racemate it was again clearly possible to differ between these two weakly selective catalysts (*S*,S**)-**114** and **118** and the higher selective ones on the basis of the signal ratios determined by the ESI-MS racemate screening.

The almost racemic product produced by the enantiopure α-phenyl substituted pyrrolidine catalyst **118** indicates an orientation of the phenyl group orthogonal to the pyrrolidine plane. Both sides are similarly shielded against an approach of the nucleophile and the aryl moiety is far away from the reaction center. Similar problems were also expected for more sterically demanding aryl groups. Therefore, α-aryl substituted pyrrolidines were not expected to be highly selective in organocatalyzed Michael additions and a synthesis of racemic derivatives (Negishi approach) was not further investigated.
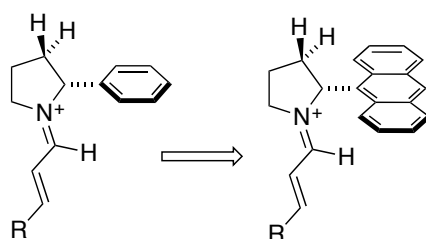
Figure 86: Potential orthogonal arrangement leading to low induced selectivities.

Initially, the ESI-MS screening of diastereomeric isoindoline-based catalysts **129** revealed some problems. With catalyst (*S*,S**)-**129** the calculated selectivities obtained from the signal ratios led to a corrected value of 77% *ee* (according to **Eq. 3**), which was about 10% higher than the selectivity determined with the enantiopure catalyst of 67% and 68% *ee*. Moreover, when using the enantiomeric catalyst, where the iminium ion **Im** derived from the ethyl-

substituted (*S*)-quasienantiomer (*S*)-**89** was the minor peak a lower theoretic *ee* of 61% was determined in the enantiopure catalyst screening. However, the ESI-MS spectra revealed for both, the racemic and the enantiopure catalyst screening an overlay of the first isotope peak of the sodium adduct of quasienantiomer (*R*)-**89'** with the iminium signal derived from the ethyl-substituted quasienantiomer (Figure 87, left). For other catalysts such a problem did not occur due to higher signal intensities. These "false" ratios were corrected by reducing the absolute intensity of the iminium signal by the theoretically calculated intensity of the 1st isotope peak of the **89'**+Na$^+$ signal (intensity of 1st isotope peak = 31% of the major isotopomer according to ChemDraw calculations). With the corrected iminium ratios in hand the corresponding calculated selectivities were considerably lower (41%→26% *ee* and 47%→28% *ee*). Another approach to avoid the signal overlay was the application of the inversely labeled mixture of quasienantiomers (Figure 87, right). When the ethyl-substituted derivative **89** was used as the major quasienantiomer, the derived iminium ion was the major signal, which minimizes an overlay. In addition, the corresponding sodium adduct of quasienantiomer **89'** was of lower intensity as it was present in the reaction mixture in reduced quantities. With this combination of quasienantiomers the overlay was negligible and the calculated theoretical selectivities of 13% *ee* and 26% *ee* were in excellent agreement within the measurement accuracy with the corrected values discussed above (Figure 87, right). Although it had a minor impact on the enantiopure catalyst screening, this overlay was also corrected here as described above. Applying the combination of quasienantiomers and catalyst enantiomer, which provides the ethyl-derived iminium ion (**Im**) as the major signal further reduced the signal alteration. By doing so, an actual *ee* of 65-67% was determined, which is in perfect agreement with 65% *ee* determined from the racemate screening after correction and minimizing of the overlay and transformation of the theoretically calculated selectivity into the actual *ee* applying **Eq. 3** (page 154). It should be noted that due to low signal intensities of the iminium ions derived from catalyst (*S*,R**)-**129**, even with the inversely labeled mixture of quasienantiomers an overlay still occurred and a correction as described above was necessary. Moreover, to validate the results of the racemate screening 2 mol% of enantiopure catalyst was required in order to improve the intensity and stability of the minor peak.
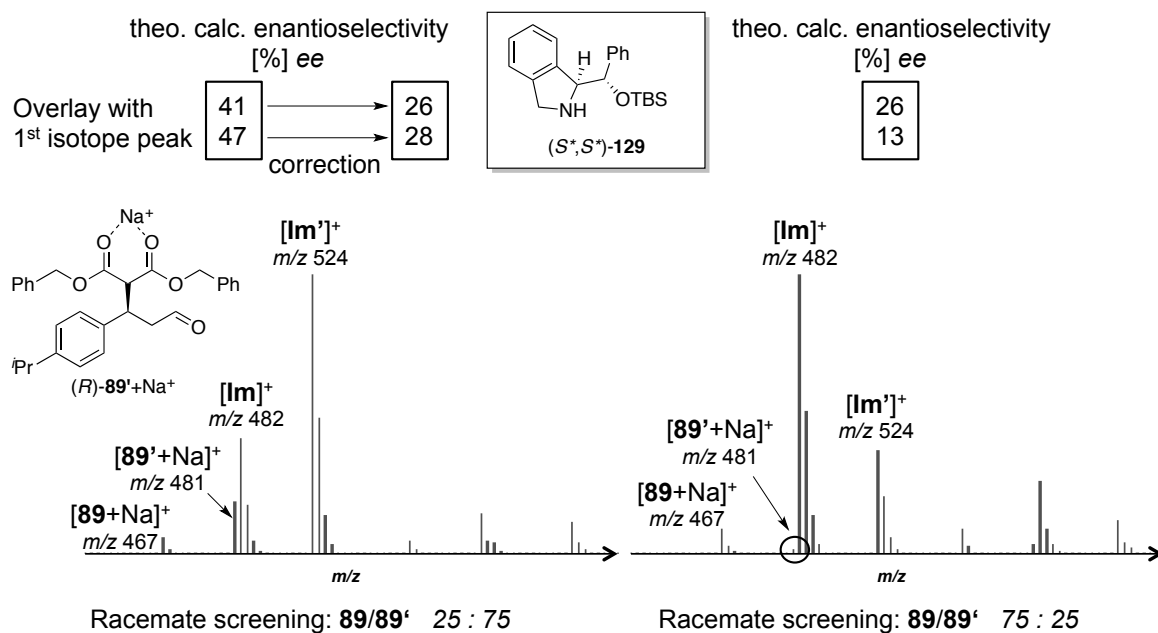
Figure 87: Signal overlay observed in the racemate screening of catalyst **129** leading to a prediction of "false" higher selectivities.

The selectivities obtained for the investigated catalysts allowed for some conclusions about the influence of the protecting group, the annulated phenyl ring, the number of phenyl substituents at the side chain and the relative configuration of catalysts possessing a second stereogenic center. The selectivities were found to increase with the bulk of the oxygen protecting groups for pyrrolidine and isoindoline derivatives (TIPS **77c** > TBS **77b** > TMS **77a** > Me **77d** and TBS **128b** > TMS **128a**). The new cyclopentyl-substituted catalyst **109** and the pyrrolidine-derived diastereomers ((S^*,S^*)-**114** and (S^*,R^*)-**114**) were considerably less selective than the corresponding TBS-protected diphenyl substituted catalyst **77b**. This demonstrates, that two phenyl groups are essential for a perfect orientation of the bulky silyl protecting group to induce high selectivities. Catalyst (S^*,R^*)-**114** where the C–N bond at the pyrrolidine moiety and at the OTBS group both formally point in the same direction was more selective than its diastereomer ((S^*,S^*)-**114**. The same trend was observed for the diastereomeric isoindoline catalysts (S^*,S^*)- and (S^*,R^*)-**129**. Nevertheless, the annulated phenyl ring of the isoindoline catalysts has an influence on the conformation of the molecule, mainly due to a steric interaction between the aromatic hydrogen of the isoindoline and the phenyl groups of the side chain and a planar conformation of the pyrrolidine ring due to the rigid backbone. Unfortunately, the induced selectivity of isoindoline catalysts **128a** and **128b** was lower than the selectivity of the corresponding pyrrolidine catalysts **77a** and **77b**. In contrast, the monophenyl substituted isoindoline catalysts (S^*,S^*)- and (S^*,R^*)-**129** are both more selective than their pyrrolidine derived counterparts **114**, yet of considerably lower

162

selectivity than all diphenyl-substituted catalysts. Therefore, diastereomeric isoindoline catalysts **129** are likely more fixed in their conformation than the corresponding pyrrolidine derivatives **114** due to the additional interaction of the aromatic H-atom of the isoindoline moiety with the side chain phenyl group. This led to the assumption, that this interaction has the primary influence on the conformation of the stereocontrolling element of the catalyst.

5.5 Summary

In summary, the application of the ESI-MS monitoring of mass-labeled catalytic intermediates as a tool to determine the enantioselectivity of racemic catalysts was demonstrated. After a successful ESI-MS screenings of the Pd-catalyzed allylic substitution previously reported,[17] the methodology was successfully extended to organocatalyzed reactions screening the Michael addition as a benchmark process, illustrating the more general applicability of this concept. A screening protocol was established using 1 mol% catalyst loading, which provides acceptable to excellent signal intensities of the desired iminium intermediates and on the other hand allowed for an, at least partial, pseudo zero-order regime. New catalysts were synthesized, four of them derived from an isoindoline core. These catalysts were not available from the chiral pool and were therefore more challenging to obtain in an enantiomerically pure form. By screening the racemic catalyst, out of a variety of different catalysts the most selective ones were clearly identified and the racemate screening allowed for a clear distinction between catalysts of moderate to excellent selectivities and catalysts of low selectivity. Although the selectivity trend of the catalysts (induced enantioselectivity >60% *ee*) was clearly reflected by the ESI-MS screening, the conditions did not provide a perfect pseudo zero-order kinetic regime leading to deviations of the theoretical enantioselectivity determined from the racemic catalyst and the actual *ee*. Thus, a correction function was established, which allowed for the prediction of a more reliable *ee* of the racemic catalyst (for catalysts >60% *ee*). This transformation into the actual *ee* provided values, which were in excellent agreement with the selectivities obtained from the enantiopure catalyst. Although, one example was identified, which did not fit with the selectivity trend, this catalyst (**109**) was still of lower selectivity, close to the 75:25 ratio were small errors in the signal ratio or signal alterations considerably influences the calculated selectivity.

CHAPTER 6

EXPERIMENTAL PART

6.1   General Remarks

6.1.1 Analytical Methods

Melting Points (m.p.): Melting points were determined on a Büchi B-545 apparatus and were not corrected.

Thin Layer Chromatography (TLC): TLC plates were obtained from Macherey-Nagel (Polygram SIL G/UV254, 0.2 mm silica with fluorescence indicator, 40 × 80 mm). For visualization UV light (254 nm), basic permanganate or ceric ammonium molybdate solutions were used. Preparative TLC was performed on Merck silica gel 60 F254 plates.

Nuclear Magnetic Resonance-Spectroscopy (NMR): NMR spectra were measured either on a Bruker DPX-NMR (400MHz) or a Bruker Avance DRX-NMR (500 MHz) spectrometer equipped with BBO broadband probe heads. Chemical shifts (δ) are reported in parts per million (ppm) and coupling constants (J) are reported in (Hz). Deuterated NMR solvents were obtained from Cambridge Isotope Laboratories, Inc. (Andover, MA, USA). The measurements were performed at 25 °C. The chemical shift δ values of ^{1}H spectra were referenced relative to the solvent residual peaks[114] (CDCl$_3$ 7.26 ppm, CD$_3$OD 3.31 ppm, (CD$_3$)$_2$SO 2.50 ppm, CD$_3$CN 1.94) and the signals of the ^{13}C spectra relative to the signals of the deuterated solvents[114] (CDCl$_3$ 77.16 ppm, CD$_3$OD 49.00 ppm, (CD$_3$)$_2$SO 39.52 ppm). The assignment of ^{1}H and ^{13}C signals was partly made by DEPT and 2D-NMR (COSY, HMQC, HMBC and NOSY). Multiplicities are reported as follows: s = singlet, d = doublet, t = triplet, q = quartet, sept = septet, m = multiplet, br = broad signal shape. ^{13}C NMR signals are reported as singlet if not otherwise noted.

Infrared Spectroscopy (FTIR): IR spectra were recorded on a Varian 800 FT-IR ATR Spectrometer. The absorption bands are reported cm^{-1}. The peak intensity is assigned with s (strong), m (medium) and w (weak). The note br stands for a broad peak shape.

Mass Spectrometry (MS): Mass spectra were measured by Dr. H. Nadig (Department of Chemistry, University of Basel) on a VG70-250 (electron ionization (EI)) mass spectrometer or a Finnigan MAR 312 (fast atom bombardment (FAB)) mass spectrometer with 3-nitrobenzyl alcohol (NBA) as matrix. ESI-MS spectra were measured on a Varian 1200L Triple Quad MS/MS spectrometer using mild desolvation conditions (39 psi nebulizing gas,

4.9 kV spray voltage, 19 psi drying gas at 100-200 °C, 1300 V detector voltage, 50-110 V capillary voltage). The samples were diluted with MeOH, if not otherwise noted, prior to their analysis and measured using direct injection. The spectra were acquired in the centroid mode. The data are reported as mass units per charge (*m/z*) and relative intensities of the signals are given in brackets.

High Resolution Mass Spectrometry (HRMS-ESI): Mass spectra were measured by Dr. H. Nadig (Department of Chemistry, University of Basel) on a Bruker maXis 4G.

Gas Chromatography-Mass Spectrometry (GC-MS): The GC-MS spectra were recorded on A Shimadzu GCMS-QP2010 SE equipped with a *Restek* Rtx®-5MS column (30 m × 0.2 mm × 0.2 μm) and He as carrier gas.

Gas Chromatography (GC): Gas chromatograms were collected on Shimadzu GC 2010-Plus or Carlo Erba HRGC Mega2 Series 800 (HRGS Mega2) instruments.

Elemental Analysis (EA): Elemental analyses were measured by Mr. W. Kirsch or Sylvie Mittelheiser (Department of Chemistry, University of Basel) on a Leco CHN-900 analyzer or on a Vario Micro Cube by C-, H-, N detection. The data are indicated in mass percent.

High Performance Liquid Chromatography (HPLC): HPLC analysis was measured on Shimadzu Class-VP Version 5.0 systems with SCL-10A system controller, LC-10AD pump system, SIL-10AD auto injector, CTO-10AC column oven, DGU-14A degasser and SPDM10A diode array- or UV/VIS detector or on Shimadzu LC-20A prominence with LC-20AD pump system, SIL-20AHT auto injector, CTO-10AS column oven, SPD-M20A diode array, DGU-20A3 degasser. Chiral columns (4.6 mm × 250 mm) from Daicel Chemical Industries were used

Semi-preparative High Performance Liquid Chromatography (semi-preparative HPLC): Separations by semi-preparative HPLC were performed on a Shimadzu system with SIL 10 Advp autosampler, CTO 10 ASVP column oven, LC 10 Atvp pump system, FCV 10 Alvp degasser and SPD M10 Acp diode array detector. Columns (2 cm × 25 cm) and precolumns (20 mm x 50 mm) from Daicel Chemical Industries and Reprosphere silica columns (2 cm × 25 cm) from Reprosil Industries were used.

Optical Rotation ($[\alpha]_D^{20}$): Optical rotations were measured on a Perkin Elmer Polarimeter 341 in a 1 dm cuvette at 20 °C at 589 nm (sodium lamp). Concentration (c) is given in g/100 mL.

6.1.2 Reagents and Working Techniques

Commercially available reagents were purchased from Acros, Aldrich, Alfa-Aesar, Bachem, Cambridge Isotope Laboratories, Fluka, Fluorochem, Frontier Scientific, Merck or TCI and used as received without further purification unless otherwise noted. The solvents were collected from a purification column system (PureSolv, Innovative Technology Inc.) or purchased from Aldrich or Fluka in sure/sealedTM bottles over molecular sieves.

Column chromatographic purifications were performed on Fluka silica gel 60 (particle size 40-63 nm) or Merck silica gel 60 (particle size 40-63 nm) according to the procedure published by Still and Mitra[115] under 0.1-0.5 bar nitrogen pressure. Column dimensions are given in height x diameter. Eluents of technical grade were distilled prior to use. As far as not mentioned external temperature data was assigned. A high vacuum (HV) of 0.08-0.10 mbar was applied. Concentration under reduced pressure was performed by rotary evaporation at 30-40 °C. Air and moisture sensitive reactions were carried out in heat gun or flame dried glassware applying standard Schlenk techniques. DIPEA was distilled over CaH_2 and stored over molecular sieves. Anhydrous Et_3N was purchased from Aldrich in a sure/sealedTM bottle and used as received. Further amine bases were distilled prior to use by Dieckmann distillation. Preparative organocatalyzed aldol reactions were performed in culture tubes with screw-cap under air.

6.2 ESI-MS Screening of Organocatalyzed Aldol Reactions

6.2.1 Synthesis of the Mass-Labeled Aldol Products

(*R*)-4-Hydroxy-4-(4-nitrophenyl)butan-2-one (*R*)-(7)
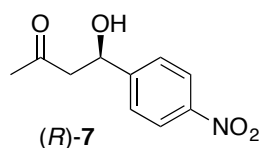
In a round bottom flask *para*-nitrobenzaldehyde (456 mg, 3.00 mmol, 1.00 eq.) and *N*-toluenesulfonyl-L-proline amide (*S*)-**31** (82.0 mg, 0.30 mmol, 10 mol%) were dissolved in dry acetone and stirred until TLC monitoring showed complete conversion (48-72 h). The yellow solution was directly subjected to flash column chromatography (SiO$_2$, 15 cm x 6.5 cm, cyclohexane/EtOAc 1:1) to give (*R*)-4-Hydroxy-4-(4-nitrophenyl)butan-2-one as a pale yellow solid in 86% *ee*. The product was recrystallized from hexane/EtOAc (4:1, 10 mL) at 55 °C followed by storage for 48-72 h in the fridge. The resulting precipitated crystals were recrystallized once more under identical conditions to afford aldol product (*R*)-**7** (259 mg, 41%, >99.5% *ee*) as colorless needles. Analytical data are in accordance with literature data.[43]

C$_{10}$H$_{11}$NO$_4$ (209.20 g/mol)

m.**p**.: 68-69 °C.

***R**$_f$* = 0.25 (cyclohexane/EtOAc 1:1).

^{1}H NMR (CDCl$_3$, 400 MHz) δ/ppm: 8.18 (d, $^3J_{HH}$ = 8.8 Hz, 2 H, Ar-*H*), 7.52 (d, $^3J_{HH}$ = 8.8 Hz, 2 H, Ar-*H*), 5.23-5.27 (m, 1 H, C*H*OH), 3.65 (d, $^3J_{HH}$ = 3.3 Hz, 1 H, O*H*), 2.79-2.90 (m, 2 H, C*H*$_2$), 2.21 (s, 3 H, C*H*$_3$).

^{13}C{^{1}H} NMR (CDCl$_3$, 101 MHz) δ/ppm: 208.6 (*C*O), 150.1, 147.4 (2 x Ar-*C*), 126.5, 123.8 (2 x Ar-*C*H), 69.0 (*C*HOH), 51.6 (*C*H$_2$), 30.8 (*C*H$_3$).

HPLC (*Daicel* Chiralpak AS-H, heptane/*i*PrOH 70:30, 0.8 mL/min, 20 °C, 266 nm): t_R((*R*)-**7**) = 15.9 min, t_R((*S*)-**7**) = 19.0 min.

Optical rotation: $[\alpha]_D^{20}$ = +68.8° (c = 1.00, CHCl$_3$, >99.5% *ee*) (Lit.[43] $[\alpha]_D^{22}$ = +66.2°, c = 0.5, CHCl$_3$, 99% *ee*).

(*S*)-4-Hydroxy-4-(4-nitrophenyl)butan-2-one (*S*)-7
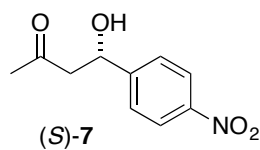
The (*S*)-enantiomer was synthesized according to procedure described for the (*R*)-enantiomer (*R*)-7 using *N*-toluenesulfonyl-D-proline amide (*R*)-31 as catalyst. The (*S*)-aldol product (*S*)-7 was obtained in >99.5% *ee*. Analytical data are in accordance with data of (*R*)-7.

Optical rotation: $[\alpha]_D^{20}$ = –68.2° (c = 0.57, CHCl$_3$).

(1,2,3-^{13}C$_3$)-4-Hydroxy-4-(4-nitrophenyl)butan-2-one 29
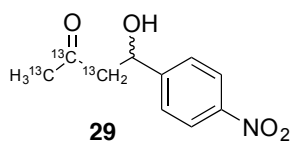
Under an argon atmosphere, a heat gun dried Schlenk tube was charged with activated molecular sieves (4 Å, 400 mg) and (1,2,3)-^{13}C$_3$-acetone (229 mg, 290 μL, 3.94 mmol, 1.00 eq.). CH$_2$Cl$_2$ (20 mL) was added and the solution cooled to 0 °C. After 5 min *para*-nitrobenzaldehyde (834 mg, 5.52 mmol, 1.40 eq.) was added to the solution. After 15 min DIPEA (765 mg, 1.03 mL, 5.92 mmol, 1.50 eq.) and TMSOTf (1.05 g, 856 μL, 4.73 mmol, 1.20 eq.) were added subsequently. The reaction mixture was stirred for 1 h at 0 °C, slowly allowed to warm to room temperature and stirred for additional 17 h. The mixture was filtered over a plug of silica gel (12 cm x 2.5 cm) and eluted with Et$_2$O (100 mL). The solvent was evaporated and the resulting yellow oil dissolved in THF (24 mL) and 1 N HCl (8 mL). After 1.5 h TLC monitoring indicated complete consumption of the TMS-protected intermediate (*R*$_f$ = 0.52, cyclohexane/EtOAc 1:1). The mixture was diluted with Et$_2$O (80 mL) and washed with H$_2$O (80 mL), NaHCO$_3$ (40 mL) and brine (40 mL). The combined aqueous layers were extracted with Et$_2$O (40 mL). The combined organic layers were dried over MgSO$_4$, filtered and concentrated under reduced pressure. The crude product was subjected to flash column chromatography (SiO$_2$, 17 cm x 3.5 cm, EtOAc/cyclohexane 1:1) to afford racemic aldol product 29 (766 mg, 92%) as a pale yellow solid.

C$_7$^{13}C$_3$H$_{11}$NO$_4$ (212.18 g/mol)

m.p.: 60-62 °C.

R$_f$ = 0.25 (cyclohexane/EtOAc 1:1).

^{1}H NMR (CDCl$_3$, 400 MHz) δ/ppm: 8.20 (d, $^3J_{HH}$ = 8.7 Hz, 2 H, Ar-*H*), 7.53 (d, $^3J_{HH}$ = 8.7 Hz, 2 H, Ar-*H*), 5.28-5.23 (m, 1 H, C*H*OH), 3.61-3.59 (m, 1 H, O*H*), 3.06-2.63 (m, $^1J_{H\text{-}13C}$ = 126.8 Hz, 2 H, ^{13}C*H*$_2$), 2.21 (ddd, $^1J_{H\text{-}13C}$ = 127.7 Hz, $^2J_{H\text{-}13C}$ = 5.9 Hz, $^3J_{H\text{-}13C}$ = 1.6 Hz, 3H,

CH$_3$).

^{13}C{^{1}H} NMR (CDCl$_3$, 101 MHz) δ/ppm: 208.6 (dd, $^1J_{13C-13C}$ = 41 Hz, $^1J_{13C-13C}$ = 38 Hz, ^{13}CO), 150.1 (d, $^2J_{13C-13C}$ = 4 Hz, Ar-*C*), 147.5 (Ar-*C*), 126.5, 123.9 (2 x Ar-*CH*), 69.0 (d, $^1J_{13C-13C}$ = 38 Hz, *CHOH*), 51.6 (dd, $^1J_{13C-13C}$ = 38 Hz, $^2J_{13C-13C}$ = 13 Hz, $^{13}CH_2$), 30.8 (dd, $^1J_{13C-13C}$ = 41 Hz, $^2J_{13C-13C}$ = 13 Hz, $^{13}CH_3$).

FTIR (ATR): 3455s, 2909w, 1667s, 1600m, 1513s, 1418m, 1338s, 1286s, 1238m, 1183m, 1106m, 1071s, 1045m, 856m, 745m, 697m cm^{-1}.

HRMS (ESI, 4500 V, 180 °C, MeOH+NaOAc (10^{-3} M)): calc. *m/z* for C$_{13}$^{13}C$_3$H$_{22}$NNaO$_4$: 235.0681, found: 235.0682 [M+Na]$^+$.

(1,2,3-^{13}C$_3$)-4-(*tert*-Butyldimethylsilyloxy)-4-(4-nitrophenyl)butan-2-one 38
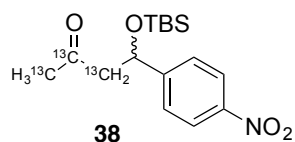
Under an argon atmosphere in a heat gun dried Schlenk tube racemic (1,2,3-^{13}C$_3$)-4-hydroxy-4-(4-nitrophenyl)butan-2-one **29** (830 mg, 3.91 mmol 1.00 eq.) was dissolved in DMF (13 mL). Pyridine (3.10 g, 3.16 mL, 39.2 mmol, 10.00 eq.) and AgNO$_3$ (2.66 g, 15.6 mmol, 4.00 eq.) were added subsequently. When AgNO$_3$ was completely dissolved, TBSCl (2.36 g, 15.6 mmol, 4.00 eq.) was added and a white precipitate was formed immediately. The reaction mixture was stirred overnight at room temperature and the precipitate was filtered-off through a plug of Celite. The filtrate was diluted with Et$_2$O (80 mL) and washed with H$_2$O (50 mL). The aqueous layer was extracted with Et$_2$O (50 mL) and the combined organic layers were washed with aqueous CuSO$_4$ solution (30 mL). The organic layer was washed with brine (2 x 40 mL) and the combined aqueous layers were re-extracted with Et$_2$O (2 x 40 mL). The combined organic layers were dried over MgSO$_4$, filtered and concentrated under reduced pressure. The resulting crude oil was subjected to flash column chromatography (SiO$_2$, 13 cm x 6 cm, cyclohexane/EtOAc 6:1) to afford TBS-protected aldol product **38** (1.07 g, 84%) as a pale yellow solid.

C$_{13}$^{13}C$_3$H$_{25}$NO$_4$Si (326.44 g/mol)

m.**p**.: 37-38 °C.

R$_f$ = 0.39 (cyclohexane/EtOAc 6:1).

^{1}H NMR (CDCl$_3$, 400 MHz) δ/ppm: 8.19 (d, $^3J_{HH}$ = 8.7 Hz, 2 H, Ar-*H*), 7.52 (d, $^3J_{HH}$ = 8.7 Hz, 2 H, Ar-*H*), 5.30-5.25 (m, 1 H, C*H*OSi), 3.13-2.74 (m, $^1J_{H-13C}$ = 129.2 Hz, 1 H, $^{13}CH_2$), 2.76-2.70 (m, $^1J_{H-13C}$ = 126.1 Hz, 1 H, $^{13}CH_2$), 2.15 (ddd, $^1J_{H-13C}$ = 127.4 Hz, $^2J_{H-13C}$ = 5.9 Hz, $^3J_{H-13C}$ = 1.5 Hz, 3H, $^{13}CH_3$), 0.86 (s, 9 H, C(C*H$_3$*)), 0.04 (s, 3 H, Si(C*H$_3$*)), −0.15 (s, 3 H,

Si(C*H*$_3$)).

^{13}C{^{1}H} NMR (CDCl$_3$, 101 MHz) δ/ppm: 206.1 (dd, $^1J_{13C\text{-}13C}$ = 41 Hz, $^1J_{13C\text{-}13C}$ = 39 Hz, ^{13}C*O*), 152.1 (d, $^2J_{13C\text{-}13C}$ = 3 Hz, Ar-*C*), 147.4 (Ar-*C*), 126.8, 123.9 (2 x Ar-*C*H), 70.9 (d, $^1J_{13C\text{-}13C}$ = 39 Hz, *C*HOSi), 54.0 (dd, $^1J_{13C\text{-}13C}$ = 39 Hz, $^2J_{13C\text{-}13C}$ = 14 Hz, ^{13}*C*H$_2$), 31.9 (dd, $^1J_{13C\text{-}13C}$ = 41 Hz, $^2J_{13C\text{-}13C}$ = 14 Hz, ^{13}*C*H$_3$), 25.8 (C(*C*H$_3$)), –4.6, –5.1 (Si*C*H$_3$).

FTIR (ATR): 2956m, 2930m, 2859w, 2857m, 1678s, 1608w, 1519s, 1468m, 1289m, 1341s, 1247m, 1136m, 1088s, 1049m, 989m, 938w, 836s, 283s, 694m cm^{-1}.

HRMS (ESI, 4500 V, 180 °C, MeOH+NaOAc (10^{-3} M)): calc. *m/z* for C$_{13}$^{13}C$_3$H$_{25}$NNaO$_4$Si$^+$: 349.1545, found: 349.1548 [M+Na]$^+$; calc. *m/z* for C$_{26}$^{13}C$_6$H$_{50}$N$_2$NaO$_8$Si$_2$$^+$: 675.3198, found: 675.3204 [2M+Na]$^+$.

(*R*)-(1,2,3-^{13}C$_3$)-4-(*tert*-Butyldimethylsilyloxy)-4-(4-nitrophenyl)butan-2-one (*R*)-38 and (*S*)-(1,2,3-^{13}C$_3$)-4-(*tert*-butyldimethylsilyloxy)-4-(4-nitrophenyl)butan-2-one (*S*)-38

(1,2,3-^{13}C$_3$)-4-(*tert*-Butyldimethylsilyloxy)-4-(4-nitrophenyl)butan-2-one **38** (1.07 g) was separated into its enantiomers by semi-preparative HPLC on a chiral stationary phase (*Daicel* Chiralpak IC with achiral precolumn SiO$_2$, hexane/*i*PrOH 98:2, 6 mL/min, 25 °C, 40 mg/200 µL, t_R((*R*)-**38**) = 49 min, t_R((*S*)-**38**) = 56 min) to afford (*R*)-**38** (453 mg, 36%, >99.5% *ee*) and (*S*)-**38** (447 mg, 35%, 99% *ee*) as colorless oils that solidified in the fridge. Analytical data are in accordance with data of the racemic compound (*rac*)-**38**.

HPLC (*Daicel*, Chiralpak IC, heptane/*i*PrOH 98:2, 0.5 mL/min, 25 °C, 265 nm): t_R((*R*)-**38**) = 21.0 min, t_R((*S*)-**38**) = 23.7 min.

Optical rotation: $[\alpha]_D^{20}$ = –78.1° (c = 1.0, CHCl$_3$, >99.5% *ee* (*R*)); $[\alpha]_D^{20}$ = +71.8° (c = 1.0, CHCl$_3$, 99% *ee* (*S*)).

An alternative semi-preparative HPLC separation afforded the enantiomers in >99.5% *ee* and 94% *ee* (*Daicel* Chiralcel OD with precolumn OD, hexane/*i*PrOH 99:1, 6 mL/min, 20 °C, 40 mg/200 µL): t_R((*R*)-**38**) = 30 min, t_R((*S*)-**38**) = 34 min.

(R)-(1,2,3-^{13}C$_3$)-4-Hydroxy-4-(4-nitrophenyl)butan-2-one (R)-29

(R)-(1,2,3-^{13}C$_3$)-4-(*tert*-Butyldimethylsilyloxy)-4-(4-nitrophenyl)butan-2-one (R)-**38** (420 mg, 1.29 mmol, 1.00 eq.) was dissolved in mixture of CH$_3$CN/CH$_2$Cl$_2$ (4:1, 26 mL) and cooled to 0 °C with an ice bath (Dewar). HF (50% in H$_2$O, 0.18 mL, 5.08 mmol, 4.00 eq.) was added and the reaction mixture stirred overnight while slowly warming to room temperature in the ice bath. The reaction mixture was added to an aqueous NaHCO$_3$ solution (60 mL) and the aqueous phase was extracted with CH$_2$Cl$_2$ (4 x 90 mL). The combined organic layers were dried over MgSO$_4$, filtered, and concentrated under reduced pressure. The crude product was suspended in hot hexane (6 mL, 55 °C) and EtOAc was added dropwise until the product was completely dissolved. Slow crystallization at room temperature and in the fridge for 24 h afforded the product as colorless needles (189 mg, >99.5% *ee*). The mother lye was concentrated under reduced pressure und subjected to flash column chromatography (SiO$_2$, 15 cm x 2.5 cm, EtOAc/cyclohexane 1:1). The purified product was recrystallized under identical conditions and the colorless crystals were combined to afford the aldol product (R)-**29** (258 mg, 94%, >99.5% *ee*). Analytical data are in accordance with data of the racemic compound **29**.

m.p.: 70-71 °C.

HPLC (*Daicel*, Chiralpak AS-H, heptane/*i*PrOH 70:30, 0.8 mL/min, 20°C, 268 nm): t_R((*S*)-**29**) = 17.0 min, t_R((*R*)-**29**) = 19.8 min).

Optical rotation: $[\alpha]_D^{20}$ = –67.0° (c = 1.0, CHCl$_3$, >99.5% *ee* (R)).

(S)-(1,2,3-^{13}C$_3$)-4-Hydroxy-4-(4-nitrophenyl)butan-2-one (S)-29

Aldol product (S)-**29** was synthesized according to the procedure described for (R)-**29** using (S)-(1,2,3-^{13}C$_3$)-4-(*tert*-butyldimethylsilyloxy)-4-(4-nitrophenyl)butan-2-one (S)-**38** (424 mg, 1.30 mmol, 1.00 eq.). After recrystallization, flash column chromatography of the mother lye and additional recrystallization aldol product (S)-**29** (239 mg, 87%, >99.5% *ee*) was obtained as colorless needles. Analytical data are in accordance with data of the racemic compound (*rac*)-**29**.

Optical rotation: $[\alpha]_D^{20}$ = +66.7° (c = 1.0, CHCl$_3$, >99.5% *ee* (S)).

6.2.2 Synthesis of Test Substrates for the ESI-MS Back Reaction Screening

d^5-(*S*)-4-Hydroxy-4-(4-nitrophenyl)butan-2-one (*S*)-28

Under an argon atmosphere, in a heat gun dried Schlenk tube *para*-nitrobenzaldehyde (151 mg, 1.00 mmol, 1.00 eq.) and *N*-toluenesulfonyl-D-proline amide (*R*)-**31** (26.8 mg, 0.10 mmol, 10 mol%) were dissolved in deuterated acetone (5 mL) and stirred until TLC monitoring showed complete conversion (72 h). The yellow solution was directly subjected to flash column chromatography (SiO$_2$, 30 cm x 3.5 cm, cyclohexane/EtOAc 1:1) to give d^5-(*S*)-4-hydroxy-4-(4-nitrophenyl)butan-2-one as a pale yellow solid (85% *ee*). The product was recrystallized from a mixture of hexane/EtOAc (2:1, 6 mL) at 55 °C followed by storage for 24 h in the freezer (–25 °C). The precipitated crystals were recrystallized once more from hexane/EtOAc (4:1, 6 mL) at 55 °C. Precipitation over the weekend at room temperature afforded deuterated aldol product (*S*)-**28** (80 mg, 37%, >99.5% *ee*) as colorless needles.

C$_{10}$H$_6$D$_5$NO$_4$ (214.23 g/mol)

m.**p**.: 69-70 °C.

R$_f$ = 0.25 (cyclohexane/EtOAc 1:1).

^{1}H NMR (CDCl$_3$, 400 MHz) δ/ppm: 8.23-8.20 (m, 2 H, Ar-*H*), 7.56-7.52 (m, 2 H, Ar-*H*), 5.26 (d, $^3J_{HH}$ = 3.3 Hz, 1 H, C*H*OH), 3.54 (d, $^3J_{HH}$ = 3.3 Hz, 1 H, O*H*).

^{13}C{^{1}H,^{2}H} NMR (CDCl$_3$, 151 MHz) δ/ppm: 208.9 (*C*O), 150.1, 147.5 (2 x Ar-*C*), 126.5, 123.9 (2 x Ar-*C*H), 69.0 (*C*HOH), 50.9 (*C*D$_2$), 30.2 (*C*D$_3$).

FTIR (ATR): 3439s, 2903w, 1699s, 1597m, 1513s, 1397w, 1346s, 1310m, 1267s, 1228m, 1194w, 1112w, 1075s, 1023w, 977w, 847s, 807m, 750m, 693m cm^{-1}.

HRMS (ESI, 4500 V, 180 °C, MeOH+NaOAc (10^{-3} M)): calc. *m/z* for C$_{10}$H$_6$D$_5$NNaO$_4^+$: 237.0894, found: 237.0895 [M+Na]$^+$.

HPLC (*Daicel* Chiralcel OJ, heptane/*i*PrOH 90:10, 1.0 mL/min, 25 °C, 265 nm): *t*$_R$((*R*)-**28**) = 34.8 min, *t*$_R$((*S*)-**28**) = 39.4 min.

Optical rotation: $[\alpha]_D^{20}$ = –60.8° (c = 0.31, CHCl$_3$, >99.5% *ee*).

General Procedure 1 (GP1): Racemic Mukaiyama Aldol Reaction

A round-bottomed flask was dried with a heat-gun and flushed with argon. The enolate precursor (1.00 eq.) was dissolved in dry CH_2Cl_2 (5 mL/mmol) at 0 °C. DIPEA (1.50 eq.), aldehyde (1.40 eq.) and TMSOTf (1.20 eq.) were added subsequently. The reaction mixture was allowed to warm to room temperature and stirred overnight. The reaction mixture was directly filtered through a plug of silica gel (5-10 cm x 2.5 cm) and eluted with Et_2O (50-100 mL). The solvent was concentrated under reduced pressure and the crude product dissolved in THF (6 mL/mmol) and stirred for 1-2 h at room temperature. The reaction mixture was diluted with H_2O (20 mL/mmol) and Et_2O (20 mL/mmol). The layers were separated and the organic layer washed with sat. $NaHCO_3$ solution (20 mL/mmol) and brine (20 mL/mmol). The organic layer was dried over $MgSO_4$, filtered and the solvent concentrated under reduced pressure. The crude product was purified by flash column chromatography and recrystallization to afford the aldol product.

4-Hydroxy-4-(4-nitrophenyl)butan-2-one 7

Aldol product **7** was synthesized according to **GP1** with acetone (116 mg, 147 µL, 2.00 mmol, 1.00 eq.), DIPEA (388 mg, 496 µL, 3.00 mmol, 1.50 eq.), *para*-nitrobenzaldehyde (423 mg, 2.80 mmol, 1.40 eq.) and TMSOTf (539 mg, 435 µL, 2.40 mmol, 1.20 eq.). Flash column chromatography (SiO_2, 10 cm x 3.5 cm, cyclohexane/EtOAc 1:1) afforded aldol product **7** (400 mg, 96%) as a pale yellow solid. Analytical data are in accordance with the enantiopure compound (*R*)-**7**.

HPLC data of the TMS protected intermediate:

HPLC (*Daicel* Chiralcel OD, heptane/*i*PrOH 99:1, 0.7 mL/min, 20 °C, 265 nm): t_R = 16.6 min and 17.9 min.

4-(*tert*-Butyldimethylsilyloxy)-4-(4-nitrophenyl)butan-2-one 37

The TBS-protected alcohol was synthesized according to the procedure described for its ^{13}C-labeled analog **38** with racemic 4-hydroxy-4-(4-nitrophenyl)butan-2-one **7** (704 mg, 3.37 mmol, 1.00 eq.), pyridine (3.10 g, 3.16 mL, 33.7 mmol, 10.00 eq.), $AgNO_3$ (2.27 g, 13.5 mmol, 4.00 eq.) and TBSCl

(2.03 g, 13.5 mmol, 4.00 eq.) in DMF (11 mL). Stirring overnight, workup and purification by flash column chromatography (SiO$_2$, 11 cm x 6 cm, cyclohexane/EtOAc 6:1) afforded TBS-protected alcohol **37** (897 mg, 82%) as a pale yellow solid. Analytical data are in accordance with literature data.[57]

C$_{16}$H$_{25}$NO$_4$Si (323.46 g/mol)

R$_f$ = 0.39 (cyclohexane/EtOAc 6:1).

m.**p**.: 36-38 °C.

¹H NMR (CDCl$_3$, 400 MHz) δ/ppm: 8.18 (d, $^3J_{HH}$ = 8.7 Hz, 2 H, Ar-*H*), 7.51 (d, $^3J_{HH}$ = 8.7 Hz, 2 H, Ar-*H*), 5.27 (dd, $^3J_{HH}$ = 8.2 Hz, $^3J_{HH}$ = 4.4 Hz, 1 H, C*H*OH), 2.93 (dd, $^2J_{HH}$ = 15.7 Hz, $^3J_{HH}$ = 8.2 Hz, 1 H, C*H*aHb), 2.57 (dd, $^2J_{HH}$ = 15.7 Hz, $^3J_{HH}$ = 4.4 Hz, 1 H, CHa*H*b), 2.15 (s, 3 H, C*H*$_3$CO), 0.86 (s, 9 H, C(C*H*$_3$)$_3$), 0.03 (s, 3 H, SiC*H*$_3$), −0.16 (s, 3 H, SiC*H*$_3$).

¹³C{¹H} NMR (CDCl$_3$, 101 MHz) δ/ppm: 206.1 (CH$_3$*C*O), 152.1, 147.4 (2 x Ar-*C*), 126.7, 123.8 (2 x Ar-*C*), 70.8 (*C*HOH), 54.0 (*C*H$_2$), 31.8 (*C*H$_3$CO), 25.8 (SiC(*C*H$_3$)$_3$), 18.2 (Si*C*(CH$_3$)$_3$), −4.6, −5.1 (2 x Si*C*H$_3$).

MS (FAB, NBA) *m/z* (%): 324.2 ([M+H]$^+$, 52), 266.0 (100), 192.1 (22), 115.0 (63), 73.0 (79).

HPLC (*Daicel* Chiralcel OD, heptane/*i*PrOH 99:1, 0.5 mL/min, 20 °C, 265 nm): t_R = 18.5 min and 20.8 min.

4-Hydroxy-4-(2-nitrophenyl)butan-2-one 32

Aldol product **32** was synthesized according to **GP1** with acetone (116 mg, 147 µL, 2.00 mmol, 1.00 eq.), DIPEA (388 mg, 496 µL, 3.00 mmol, 1.50 eq.), *o*-nitrobenzaldehyde (423 mg, 2.80 mmol, 1.40 eq.) and TMSOTf (539 mg, 435 µL, 2.40 mmol, 1.20 eq.). Flash column chromatography (SiO$_2$, 17 cm x 3.5 cm, cyclohexane/EtOAc 2:1) afforded aldol product **32** (93 mg, 0.44 mmol, 22%) as a pale yellow solid and unreacted *o*-nitrobenzaldehyde (356 mg, 2.36 mmol, **R**$_f$ = 0.34, cyclohexane/EtOAc 2:1). Analytical data are in accordance with literature data.[116]

C$_{10}$H$_{11}$NO$_4$ (209.20 g/mol)

m.p.: 54-55 °C (Lit.[116] 52-55 °C).

**R**$_f$ = 0.13 (cyclohexane/EtOAc 2:1).

¹H NMR (CDCl$_3$, 400 MHz) δ/ppm: 7.97 (dd, $^3J_{HH}$ = 8.2 Hz, $^4J_{HH}$ = 1.2 Hz, 1 H, Ar-*H*), 7.90 (dd, $^3J_{HH}$ = 8.0 Hz, $^4J_{HH}$ = 1.2 Hz, 1 H, Ar-*H*), 7.67 (td, $^3J_{HH}$ = 8.0 Hz, $^4J_{HH}$ = 1.2 Hz, 1 H, Ar-*H*), 7.46-7.42 (m, 1 H, Ar-*H*), 5.68 (ddd, $^3J_{HH}$ = 9.6 Hz, $^3J_{HH}$ = 3.0 Hz, $^3J_{HH}$ = 2.2 Hz, C*H*OH), 3.73

(d, $^3J_{HH}$ = 3.0 Hz, 1 H, OH), 3.15 (dd, $^2J_{HH}$ = 17.8 Hz, $^3J_{HH}$ = 2.2 Hz, 1 H, CH_aH$_b$), 2.72 (dd, $^2J_{HH}$ = 17.8 Hz, $^3J_{HH}$ = 9.4 Hz, 1 H, CH$_a$$H_b$), 2.24 (s, 3 H, C$H_3$).
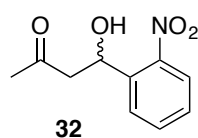
^{13}**C{^{1}H} NMR** (CDCl$_3$, 101 MHz) δ/ppm: 209.0 (*C*O), 147.2, 138.5 (2 x Ar-*C*), 134.0, 128.4, 128.3, 124.6 (4 x Ar-*C*H), 65.8 (*C*HOH), 51.2 (*C*H$_2$), 30.6 (*C*H$_3$).

HPLC (*Daicel* Chiralcel OD, heptane/*i*PrOH 90:10, 1.0 mL/min, 20 °C, 210 nm): t_R = 11.5 min and 13.5 min.

4-Hydroxy-4-(4-methoxyphenyl)butan-2-one 19
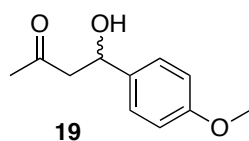
Aldol product **19** was synthesized according to **GP1** with acetone (116 mg, 147 µL, 2.00 mmol, 1.00 eq.), DIPEA (388 mg, 496 µL, 3.00 mmol, 1.50 eq.), *p*-anisaldehyde (381 mg, 340 µL, 2.80 mmol, 1.40 eq.) and TMSOTf (539 mg, 435 µL, 2.40 mmol, 1.20 eq.). Flash column chromatography (SiO$_2$, 10 cm x 3.5 cm, cyclohexane/EtOAc 3:1) afforded aldol product **19** (375 mg, 96%) as a yellow oil that solidified upon standing. Analytical data are in accordance with literature data.[116]

C$_{11}$H$_{14}$O$_3$ (194.23 g/mol)

m.p.: 39-40 °C (Lit.[116] 36-38 °C).

R_f = 0.09 (cyclohexane/EtOAc 3:1).

^{1}**H NMR** (CDCl$_3$, 400 MHz) δ/ppm: 7.28 (d, $^3J_{HH}$ = 8.6 Hz, 2 H, Ar-*H*), 6.88 (d, $^3J_{HH}$ = 8.6 Hz, 2 H, Ar-*H*), 5.10 (dt, $^3J_{HH}$ = 9.2 Hz, $^3J_{HH}$ = 3.2 Hz, C*H*OH), 3.80 (s, 3 H, OCH_3), 3.21 (d, $^3J_{HH}$ = 3.2 Hz, 1 H, O*H*), 2.89 (dd, $^2J_{HH}$ = 17.4 Hz, $^3J_{HH}$ = 9.2 Hz, 1 H, CH_aH$_b$), 2.79 (dd, $^2J_{HH}$ = 17.4 Hz, $^3J_{HH}$ = 3.2 Hz, 1 H, CH$_a$$H_b$), 2.19 (s, 3 H, C$H_3$).

^{13}**C{^{1}H} NMR** (CDCl$_3$, 101 MHz) δ/ppm: 209.2 (*C*O), 159.2, 135.1 (2 x Ar-*C*), 127.0, 114.0 (2 x Ar-*C*H), 69.6 (*C*HOH), 55.4 (O*C*H$_3$), 52.1 (*C*H$_2$), 30.9 (*C*H$_3$).

4-(4-Chlorophenyl)-4-hydroxybutan-2-one 33
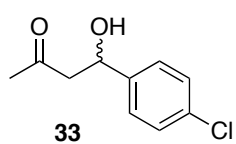
Aldol product **33** was synthesized according to **GP1** with acetone (58.1 mg, 73.5 µL, 1.00 mmol, 1.00 eq.), DIPEA (194 mg, 248 µL, 1.50 mmol, 1.50 eq.), *p*-chlorobenzaldehyde (197 mg, 165 µL, 1.40 mmol, 1.40 eq.) and TMSOTf (269 mg, 220 µL, 1.20 mmol, 1.20 eq.). Flash column chromatography (SiO$_2$, 10 cm x 3.5 cm, cyclohexane/EtOAc 2:1) afforded aldol product **33** (196 mg, 99%) as a colorless solid. Analytical data are in accordance with literature data.[117]

178

$C_{10}H_{11}ClO_2$ (198.65 g/mol)

m.p.: 44-45 °C (Lit.[116] 47-50 °C).

R_f = 0.19 (cyclohexane/EtOAc 2:1).

¹H NMR (CDCl₃, 400 MHz) δ/ppm: 7.33-7.27 (m, 4 H, Ar-*H*), 5.12 (dd, $^3J_{HH}$ = 8.1 Hz, $^3J_{HH}$ = 3.4 Hz, C*H*OH), 3.40 (br s, 1 H, O*H*), 2.87-2.75 (m, 2 H, C*H₂*), 2.19 (s, 3 H, C*H₃*).

¹³C{¹H} NMR (CDCl₃, 101 MHz) δ/ppm: 209.1 (*C*O), 141.3, 133.4 (2 x Ar-*C*), 128.8, 127.2 (2 x Ar-*C*H), 69.3 (*C*HOH), 51.9 (*C*H₂), 30.9 (*C*H₃).

HPLC (*Daicel* Chiralpak AD, heptane/*i*PrOH 90:10, 1.0 mL/min, 20 °C, 220 nm): t_R = 8.7 min and 9.3 min.

4-(2-Chlorophenyl)-4-hydroxybutan-2-one 34
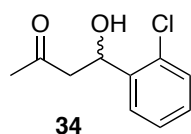
Aldol product **34** was synthesized according to **GP1** with acetone (116 mg, 147 µL, 2.00 mmol, 1.00 eq.), DIPEA (388 mg, 496 µL, 3.00 mmol, 1.50 eq.), *o*-chlorobenzaldehyde (394 mg, 315 µL, 2.80 mmol, 1.40 eq.) and TMSOTf (539 mg, 435 µL, 2.40 mmol, 1.20 eq.). Flash column chromatography (SiO₂, 20 cm x 3.5 cm, cyclohexane/EtOAc 2:1) afforded aldol product **34** (396 mg, quant.) as a pale yellow oil that solidified in the fridge. Analytical data are in accordance with literature data.[116]

$C_{10}H_{11}ClO_2$ (198.65 g/mol)

R_f = 0.28 (cyclohexane/EtOAc 2:1).

¹H NMR (CDCl₃, 400 MHz) δ/ppm: 7.62 (dd, $^3J_{HH}$ = 7.7 Hz, $^4J_{HH}$ = 1.7 Hz, 1 H, Ar-*H*), 7.33-7.28 (m, 2 H, Ar-*H*), 7.21 (td, $^3J_{HH}$ = 7.6 Hz, $^4J_{HH}$ = 1.7 Hz, 1 H, Ar-*H*), 5.50 (dt, $^3J_{HH}$ = 9.7 Hz, $^3J_{HH}$ = 3.0 Hz, C*H*OH), 3.56 (d, $^3J_{HH}$ = 3.0 Hz, 1 H, O*H*), 2.99 (dd, $^2J_{HH}$ = 17.8 Hz, $^3J_{HH}$ = 2.3 Hz, 1 H, CH*ₐ*H*ᵦ*), 2.67 (dd, $^2J_{HH}$ = 17.8 Hz, $^3J_{HH}$ = 9.7 Hz, 1 H, CH*ₐ*H*ᵦ*), 2.21 (s, 3 H, C*H₃*).

¹³C{¹H} NMR (CDCl₃, 101 MHz) δ/ppm: 209.4 (*C*O), 140.2, 131.2 (2 x Ar-*C*), 129.4, 128.7, 127.4, 127.2 (4 x Ar-*C*H), 66.7 (*C*HOH), 50.1 (*C*H₂), 30.7 (*C*H₃).

HPLC (*Daicel* Chiralcel OD, heptane/*i*PrOH 90:10, 1.0 mL/min, 20 °C, 210 nm): t_R = 8.1 min and 8.5 min.

HPLC (*Daicel* Chiralpak AD, heptane/*i*PrOH 95:5, 1.0 mL/min, 20 °C, 210 nm): t_R = 10.3 min and 11.8 min.

anti- And *syn*-2-(hydroxy(4-methoxyphenyl)methyl)cyclohexan-1-one 22

anti-22
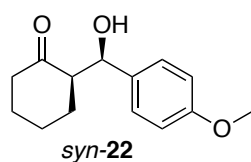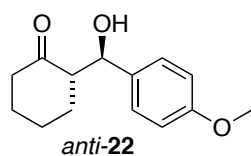
syn-22

Aldol products *anti-* and *syn*-**22** were synthesized according to **GP1** with cyclohexanone (393 mg, 415 µL, 4.00 mmol, 1.00 eq.), DIPEA (776 mg, 992 µL, 6.00 mmol, 1.50 eq.), *p*-anisaldehyde (762 mg, 680 µL, 5.60 mmol, 1.40 eq.) and TMSOTf (1.07 g, 871 µL, 4.80 mmol, 1.20 eq.). ^{1}H NMR analysis of the crude product indicated a mixture of diastereoisomers of 56:44 in favor for the *anti* isomer (according to the integration of the C*H*OH signals). Flash column chromatography (SiO$_2$, 22 cm x 3.5 cm, cyclohexane/EtOAc 5:1) afforded aldol products **22** (*anti*: 477 mg, 51%; *syn*: 360 mg, 38%) as colorless and pale yellow solid. Recrystallization from EtOH afforded the diastereomerically pure aldol products **22** (*anti*: 140 mg, *syn*: 280 mg) as colorless needles. Analytical data are in accordance with literature data.[118]

C$_{14}$H$_{18}$O$_3$ (234.30 g/mol)

Analytical data of *anti*-**22**:[118a]

m.p.: 80-81 °C.

R_f = 0.05 (cyclohexane/EtOAc 5:1).

^{1}H NMR (CDCl$_3$, 400 MHz) δ/ppm: 7.24 (d, $^3J_{HH}$ = 8.7 Hz, 1 H, Ar-*H*), 6.88 (d, $^3J_{HH}$ = 8.7 Hz, 1 H, Ar-*H*), 4.74 (dd, $^3J_{HH}$ = 8.9 Hz, $^3J_{HH}$ = 2.7 Hz, 1 H, C*H*OH), 3.91 (d, $^3J_{HH}$ = 2.7 Hz, 1 H, O*H*), 3.80 (s, 3 H, OC*H*$_3$), 2.59 (dddd, $^3J_{HH}$ = 12.9 Hz, $^3J_{HH}$ = 8.9 Hz , $^3J_{HH}$ = 5.5 Hz, $^4J_{HH}$ = 1.2 Hz, 1 H, C*H*), 2.48 (dddd, $^2J_{HH}$ = 13.6 Hz, $^3J_{HH}$ = 4.5 Hz , $^3J_{HH}$ = 3.0 Hz, $^4J_{HH}$ = 1.7 Hz, 1 H, (CO)C*H*$_a$H$_b$), 2.36 (tdd, $^2J_{HH}$ = 13.6 Hz, $^3J_{HH}$ = 6.1 Hz, $^4J_{HH}$ = 1.3 Hz, 1 H, (CO)CH$_a$*H*$_b$), 2.12-2.05 (m, 1 H, C*H*$_2$), 1.83-1.75 (m, 1 H, C*H*$_2$), 1.72-1.49 (m, 3 H, C*H*$_2$), 1.32-1.21 (m, 1 H, C*H*$_2$).

^{13}C{^{1}H} NMR (CDCl$_3$, 101 MHz) δ/ppm: 215.8 (*C*O), 159.4, 133.3 (2 x Ar-*C*), 128.3, 113.9 (2 x Ar-*C*H), 74.4 (*C*HOH), 57.6, 55.4 (*C*H and O*C*H$_3$), 42.8, 31.0, 27.9, 24.9 (4 x *C*H$_2$).

Analytical data of *syn*-**22**:[118b]

R_f = 0.07 (cyclohexane/EtOAc 5:1).

^{1}H NMR (CDCl$_3$, 400 MHz) δ/ppm: 7.22 (d, $^3J_{HH}$ = 8.7 Hz, 1 H, Ar-*H*), 6.88 (d, $^3J_{HH}$ = 8.7 Hz, 1 H, Ar-*H*), 5.33 (t, $^3J_{HH}$ = 3.3 Hz, 1 H, C*H*OH), 3.80 (s, 3 H, OC*H*$_3$), 2.95 (d, $^3J_{HH}$ = 3.3 Hz, 1 H, O*H*), 2.56 (dddd, $^3J_{HH}$ = 12.5 Hz, $^3J_{HH}$ = 5.8 Hz , $^3J_{HH}$ = 2.7 Hz, $^4J_{HH}$ = 1.2 Hz, 1 H, C*H*), 2.42-2.32 (m, 2 H, (CO)C*H*$_2$), 2.12-2.04 (m, 1 H, C*H*$_2$), 1.89-1.61 (m, 4 H, C*H*$_2$), 1.58-1.49 (m, 1 H, C*H*$_2$).

3-Hydroxy-3-(4-nitrophenyl)-1-phenylpropan-1-one 23
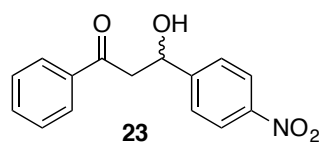
Aldol product **23** was synthesized according to **GP1** with acetophenone (120 mg, 117 µL, 1.00 mmol, 1.00 eq.), DIPEA (194 mg, 248 µL, 1.50 mmol, 1.50 eq.), *para*-nitrobenzaldehyde (212 mg, 1.40 mmol, 1.40 eq.) and TMSOTf (269 mg, 220 µL, 1.20 mmol, 1.20 eq.). Flash column chromatography (SiO$_2$, 10 cm x 3.5 cm, cyclohexane/EtOAc 6:1) followed by a second flash column chromatography (SiO$_2$, 10 cm x 3.5 cm, cyclohexane/EtOAc 10:1) afforded aldol product **23** (175 mg, 70%) as a pale yellow solid. Analytical data are in accordance with literature data.[56]

C$_{15}$H$_{13}$O$_4$ (271.27 g/mol)

m.p.: 111-112 °C (Lit.[56] 113-114 °C).

R_f = 0.07 (cyclohexane/EtOAc 10:1).

^{1}H NMR (CDCl$_3$, 400 MHz) δ/ppm: 8.24-8.20 (m, 2 H, Ar-*H*), 7.96-7.93 (m, 2 H, Ar-*H*), 7.63-7.59 (m, 3 H, Ar-*H*), 7.50-7.46 (m, 2 H, Ar-*H*), 5.45 (dt, $^3J_{HH}$ = 8.7 Hz, $^3J_{HH}$ = 3.2 Hz, 1 H, C*H*OH), 3.88 (d, $^3J_{HH}$ = 3.2 Hz, 1 H, O*H*), 3.41 (dd, $^2J_{HH}$ = 17.9 Hz, $^3J_{HH}$ = 3.2 Hz, 1 H, C*H*$_a$H$_b$), 3.34 (dd, $^2J_{HH}$ = 17.9 Hz, $^3J_{HH}$ = 8.7 Hz, 1 H, CH$_a$*H*$_b$).

^{13}C{^{1}H} NMR (CDCl$_3$, 101 MHz) δ/ppm: 199.6 (*C*O), 150.4, 147.4, 136.3 (3 x Ar-*C*), 134.1, 129.0, 128.3, 126.7, 123.9 (5 x Ar-*C*H), 69.3 (*C*H), 47.1 (*C*H$_2$).

3-Hydroxy-3-(4-methoxyphenyl)-1-phenylpropan-1-one 24
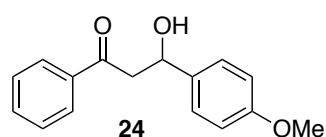
Aldol product **24** was synthesized according to **GP1** with acetophenone (120 mg, 117 µL, 1.00 mmol, 1.00 eq.), DIPEA (194 mg, 248 µL, 1.50 mmol, 1.50 eq.), *p*-anisaldehyde (191 mg, 170 µL, 1.40 mmol, 1.40 eq.) and TMSOTf (269 mg, 220 µL, 1.20 mmol, 1.20 eq.). Flash column chromatography (SiO$_2$, 10 cm x 3.5 cm, cyclohexane/EtOAc 5:1) afforded aldol product **24** (257 mg, quant.) as a yellow oil. Analytical data are in accordance with literature data.[56]

C$_{16}$H$_{16}$O$_3$ (256.30 g/mol)

R_f = 0.12 (cyclohexane/EtOAc 5:1).

^{1}H NMR (CDCl$_3$, 400 MHz) δ/ppm: 7.97-7.95 (m, 2 H, Ar-*H*), 7.61-7.57 (m, 1 H, Ar-*H*), 7.49-7.45 (m, 2 H, Ar-*H*), 7.39-7.35 (m, 2 H, Ar-*H*), 6.93-6.90 (m, 2 H, Ar-*H*), 5.32-5.28 (m, 1 H, C*H*OH), 3.82 (s, 3 H, OC*H*$_3$), 3.53 (d, $^3J_{HH}$ = 2.8 Hz, 1 H, O*H*), 3.38-3.35 (m, 2 H, C*H*$_2$).

^{13}C{^{1}H} NMR (CDCl$_3$, 101 MHz) δ/ppm: 200.3 (CO), 159.2, 136.7, 135.3 (3 x Ar-C), 133.7, 128.8, 128.3, 127.1, 114.0 (5 x Ar-CH), 69.8 (CH), 55.4 (OCH$_3$), 47.5 (CH$_2$)

4-Hydroxy-4-phenyl-butan-2-one 18
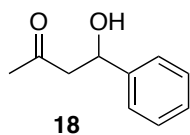
A mixture of pyrrolidine (28.4 mg, 32.8 µL, 0.40 mmol, 20 mol%), *para*-nitrophenol (111 mg, 0.80 mmol, 40 mol%) and benzaldehyde (212 mg, 202 µL, 2.00 mmol) in acetone (20 mL) was stirred for 3.5 h at room temperature. The reaction mixture was diluted with CH$_2$Cl$_2$ (30 mL) and H$_2$O (30 mL). The aqueous layer was extracted with CH$_2$Cl$_2$ (20 mL) and the combined organic layers were dried over MgSO$_4$, filtered and the solvent concentrated under reduced pressure. The residue was purified by flash column chromatography (SiO$_2$, 20 cm x 3.5 cm, cyclohexane/EtOAc 3:1) to afford aldol product **18** (194 mg, 59%) as a pale yellow solid. Analytical data are in accordance with literature data.[119]

C$_{10}$H$_{12}$O$_2$ (164.20 g/mol)

m.p.: 35-36 °C (Lit.[119] 36-37 °C (hexane)).

R_f = 0.13 (cyclohexane/EtOAc 3:1).

^{1}H NMR (CDCl$_3$, 400 MHz) δ/ppm: 7.36-7.27 (m, 5 H, Ar-H), 5.16 (dd, $^3J_{HH}$ = 9.1 Hz, $^3J_{HH}$ = 3.3 Hz, CHOH), 3.42 (br s, 1 H, OH), 2.91 (dd, $^2J_{HH}$ = 17.6 Hz, $^3J_{HH}$ = 9.1 Hz, CH$_a$H$_b$), 2.91 (dd, $^2J_{HH}$ = 17.6 Hz, $^3J_{HH}$ = 3.3 Hz, CH$_a$H$_b$), 2.20 (s, 3 H, CH$_3$).

^{13}C{^{1}H} NMR (CDCl$_3$, 101 MHz) δ/ppm: 209.2 (CO), 142.8 (Ar-C), 128.7, 127.8, 125.7 (3 x Ar-CH), 70.0 (CHOH), 52.1 (CH$_2$), 30.9 (CH$_3$).

HPLC (*Daicel* Chiralcel OD, heptane/*i*PrOH 90:10, 1.0 mL/min, 20 °C, 210 nm): t_R = 10.7 min and 11.5 min.

HPLC (*Daicel* Chiralpak AD, heptane/*i*PrOH 90:10, 1.0 mL/min, 20 °C, 210 nm): t_R = 8.5 min and 9.2 min.

anti- And *syn-*2-(hydroxy(4-nitrophenyl)methyl)cyclohexan-1-one 20

anti-20

syn-20
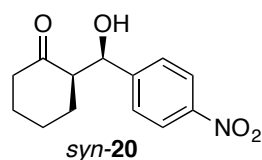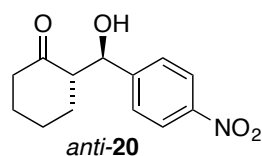
A mixture of cyclohexanone (1.47 g, 1.55 mL, 15.0 mmol, 3.00 eq.), *para*-nitrobenzaldehyde (756 mg, 5.00 mmol, 1.00 eq.), L-proline (173 mg, 1.50 mmol, 0.30 eq.) and H_2O (270 mg, 270 µL, 15.0 mmol, 3.00 eq.) was stirred at room temperature for 6 d. The reaction mixture was diluted with CH_2Cl_2 (40 mL), the organic layer was washed with H_2O (20 mL), dried over $MgSO_4$, filtered and the solvent concentrated under reduced pressure. The orange crude product was recrystallized from cyclohexane (9 mL) to afford aldol products **20** (1.11 g, 89%) as yellow solid as a mixture of diastereoisomers. ^1H NMR analysis of the crude product indicated a ratio of 77:23 in favor for the *anti* isomer (according to the integration of the C*H*OH signals). The diastereoisomers were partially separated by flash column chromatography (SiO_2, 20 cm x 6 cm, cyclohexane/EtOAc 6:1) to afford *anti-***20** (198 mg, 16%) and *syn-***20** (135 mg, 11%) as pale yellow solids. Analytical data are in accordance with literature data.[118]

$C_{13}H_{15}NO_4$ (249.27 g/mol)

Analytical data of *anti-***20**:[118a]

R_f = 0.13 (cyclohexane/EtOAc 3:1).

^1H NMR (CDCl$_3$, 400 MHz) δ/ppm: 8.21 (d, $^3J_{HH}$ = 8.7 Hz, 1 H, Ar-*H*), 7.52 (d, $^3J_{HH}$ = 8.7 Hz, 1 H, Ar-*H*), 4.90 (d, $^3J_{HH}$ = 8.4 Hz, 1 H, C*H*OH), 4.04 (br s, 1 H, O*H*), 2.62-2.55 (m, 1 H, C*H*), 2.53-2.47 (m, 1 H, (CO)C*H*$_a$H$_b$), 2.36 (tdd, $^2J_{HH}$ = 13.6 Hz, $^3J_{HH}$ = 6.1 Hz, $^4J_{HH}$ = 1.2 Hz, 1 H, (CO)CH$_a$*H*$_b$), 2.15-2.08 (m, 1 H, C*H*$_2$), 1.88-1.81 (m, 1 H, C*H*$_2$), 1.73-1.50 (m, 3 H, C*H*$_2$), 1.43-1.32 (m, 1 H, C*H*$_2$).

$^{13}C\{^1H\}$ NMR (CDCl$_3$, 101 MHz) δ/ppm: 214.9 (*C*O), 148.5, 147.7 (2 x Ar-*C*), 128.0, 123.7 (2 x Ar-*C*H), 74.2 (*C*HOH), 57.3 (*C*H), 42.8, 30.9, 27.8, 24.8 (4 x *C*H$_2$).

Analytical data of *syn-***20**:[118b]

R_f = 0.18 (cyclohexane/EtOAc 3:1).

^1H NMR (CDCl$_3$, 400 MHz) δ/ppm: 8.18 (d, $^3J_{HH}$ = 8.7 Hz, 1 H, Ar-*H*), 7.47 (d, $^3J_{HH}$ = 8.7 Hz, 1 H, Ar-*H*), 5.47 (d, $^3J_{HH}$ = 2.4 Hz, 1 H, C*H*OH), 3.20 (br s, 1 H, O*H*), 2.62 (dddd, $^3J_{HH}$ = 12.7 Hz, $^3J_{HH}$ = 5.7 Hz , $^3J_{HH}$ = 2.4 Hz, $^4J_{HH}$ = 1.1 Hz, 1 H, C*H*), 2.49-2.34 (m, 2 H, C*H*$_2$), 2.13-2.05 (m, 1 H, C*H*$_2$), 1.87-1.81 (m, 1 H, C*H*$_2$), 1.77-1.46 (m, 4 H, C*H*$_2$).

$^{13}C\{^1H\}$ NMR (CDCl$_3$, 101 MHz) δ/ppm: 214.1 (*C*O), 149.3, 147.1 (2 x Ar-*C*), 126.7, 123.4 (2 x Ar-*C*H), 70.2 (*C*HOH), 56.9 (*C*H), 42.7, 27.9, 26.0, 24.8 (4 x *C*H$_2$).

anti-2-(Hydroxy(phenyl)methyl)cyclohexan-1-one 21

*anti-***21**
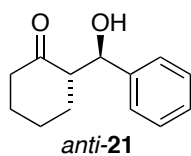
n-BuLi (1.6 M in hexane, 2.50 mL, 4.00 mmol, 1.00 eq.) was added to a solution of TMP (565 mg, 681 µL, 4.00 mmol, 1.00 eq.) in dry THF (12 mL) at 0 °C. The solution was stirred for 15 min and cooled to −78 °C. Cyclohexanone (393 mg, 415 µL, 4.00 mmol, 1.00 eq.) was added to the solution. After 30 min benzaldehyde (424 mg, 406 µL, 4.00 mmol, 1.00 eq.) was added. After 5 min the reaction mixture was quenched with sat. NH_4Cl solution (20 mL) at −78 °C. The mixture was allowed to warm to room temperature and was extracted with Et_2O (40 mL). The organic layer was dried over $MgSO_4$, filtered and the solvent concentrated under reduced pressure. ^{1}H NMR analysis out of the crude product indicated a mixture of diastereoisomers of 86:14 in favor for the *anti* isomer (according to the integration of the C*H*OH signals). The crude product was purified by flash column chromatography (SiO_2, 20 cm x 3.5 cm, cyclohexane/EtOAc 5:1) to afford aldol product **21** (586 mg, 72%) as yellow solid. Pure *anti* diastereoisomer (122 mg) was obtained by recrystallization from EtOAc (3 mL) as colorless needles. Addition of pentane to the mother lye afforded further *anti* diastereoisomer (145 mg, combined yield: 267 mg, 33%) as a colorless solid. Analytical data are in accordance with literature data.[118a]

$C_{13}H_{16}O_2$ (204.27 g/mol)

R_f = 0.07 (cyclohexane/EtOAc 5:1).

^{1}H NMR (CDCl$_3$, 400 MHz) δ/ppm: 7.37-7.27 (m, 5 H, Ar-*H*), 4.79 (dd, $^3J_{HH}$ = 8.8 Hz, $^3J_{HH}$ = 2.8 Hz, 1 H, C*H*OH), 3.94 (d, $^3J_{HH}$ = 2.8 Hz, 1 H, O*H*), 2.62 (dddd, $^3J_{HH}$ = 12.9 Hz, $^3J_{HH}$ = 8.9 Hz, $^3J_{HH}$ = 5.5 Hz, $^4J_{HH}$ = 1.3 Hz, 1 H, C*H*), 2.48 (dddd, $^2J_{HH}$ = 13.6 Hz, $^3J_{HH}$ = 4.6 Hz, $^3J_{HH}$ = 2.9 Hz, $^4J_{HH}$ = 1.8 Hz, 1 H, (CO)C*H*$_a$H$_b$), 2.36 (tdd, $^2J_{HH}$ = 13.6 Hz, $^3J_{HH}$ = 6.1 Hz, $^4J_{HH}$ = 1.2 Hz, 1 H, (CO)CH$_a$*H*$_b$), 2.13-2.04 (m, 1 H, C*H*$_2$), 1.82-1.49 (m, 4 H, C*H*$_2$), 1.35-1.24 (m, 1 H, C*H*$_2$).

^{13}C{^{1}H} NMR (CDCl$_3$, 101 MHz) δ/ppm: 215.7 (*C*O), 141.1 (Ar-*C*), 128.5, 128.1, 127.2 (3 x Ar-*C*H), 74.9 (*C*HOH), 57.6 (*C*H), 42.8, 31.0, 27.9, 24.9 (4 x *C*H$_2$).

1-Hydroxy-1-phenylheptan-3-one 25
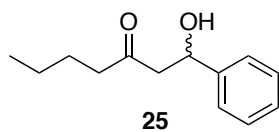
n-BuLi (1.6 M in hexane, 2.06 mL, 3.30 mmol, 1.10 eq.) was added to a solution of TMP (509 mg, 613 µL, 3.60 mmol, 1.20 eq.) in dry THF (6 mL) at 0 °C. The solution was stirred for 5 min and cooled to −78 °C. 2-Hexanone (307 mg, 415 µL, 3.00 mmol, 1.00 eq.) dissolved in dry THF (6 mL) was added dropwise over 10 min. After 30 min benzaldehyde (318 mg, 305 µL, 3.00 mmol, 1.00 eq.) dissolved in dry THF (3 mL) was added over 5 min. After 3 h the reaction mixture was quenched with sat. NH$_4$Cl solution (15 mL) at −78 °C. The mixture was allowed to warm to room temperature and was extracted with EtOAc (3 x 20 mL). The organic layer was dried over MgSO$_4$, filtered and the solvent concentrated under reduced pressure. The crude product was purified by flash column chromatography (SiO$_2$, 30 cm x 3.5 cm, cyclohexane/EtOAc 7:1) to afford the linear aldol product **25** (250 mg, 40%) as a pale yellow oil and the hexanone homo aldol product (91 mg, 30%) as a yellow oil. Analytical data are in accordance with literature data.[119]

C$_{13}$H$_{18}$O$_2$ (206.28 g/mol)

***R**$_f$* = 0.08 (cyclohexane/EtOAc 7:1).

^{1}H NMR (CDCl$_3$, 400 MHz) δ/ppm: 7.37-7.26 (m, 5 H, Ar-*H*), 5.16 (dt, $^3J_{HH}$ = 8.6 Hz, $^3J_{HH}$ = 3.2 Hz, 1 H, C*H*OH), 3.35 (d, $^3J_{HH}$ = 3.2 Hz, 1 H, O*H*), 2.89-2.76 (m, 2 H, C*H*$_2$), 2.43 (t, $^3J_{HH}$ = 7.4 Hz, 2 H, C*H*$_2$), 1.61-1.53 (m, 2 H, C*H*$_2$), 1.36-1.24 (m, 2 H, C*H*$_2$), 0.90 (t, $^3J_{HH}$ = 7.3 Hz, 3 H, C*H*$_3$).

^{13}C{^{1}H} NMR (CDCl$_3$, 101 MHz) δ/ppm: 211.8 (*C*O), 143.0 (Ar-*C*), 128.6, 127.7, 125.7 (3 x Ar-*C*H), 70.1 (*C*HOH), 51.1, 43.5, 25.7, 22.4 (4 x *C*H$_2$), 13.9 (*C*H$_3$).

Analytical data of the homo aldol side product:
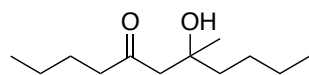
C$_{12}$H$_{24}$O$_2$ (200.32 g/mol)

***R**$_f$* = 0.16 (cyclohexane/EtOAc 7:1).

^{1}H NMR (CDCl$_3$, 400 MHz) δ/ppm: 3.87 (s, 1 H O*H*), 2.60 (d, $^2J_{HH}$ = 17.0 Hz, 1 H, C*H*$_a$H$_b$COH), 2.54 (d, $^2J_{HH}$ = 17.0 Hz, 1 H, CH$_a$*H*$_b$COH), 2.41 (t, $^3J_{HH}$ = 7.4 Hz, 2 H, COC*H*$_2$), 1.59-1.46 (m, 4 H, C*H*$_2$), 1.36-1.25 (m, 6 H, C*H*$_2$), 1.19 (s, 3 H, COHC*H*$_3$), 0.93-0.88 (m, 6 H, C*H*$_3$).

1-Hydroxy-1-phenyloctan-3-one 26
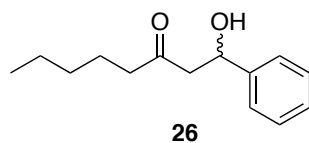
n-BuLi (1.6 M in hexane, 2.75 mL, 4.40 mmol, 1.10 eq.) was added to a solution of TMP (678 mg, 817 μL, 4.80 mmol, 1.20 eq.) in dry THF (8 mL) at 0 °C. The solution was stirred for 5 min and cooled to –78 °C. 2-Heptanone (457 mg, 557 μL, 4.00 mmol, 1.00 eq.) dissolved in dry THF (8 mL) was added dropwise over 15 min. After 30 min benzaldehyde (424 mg, 406 μL, 4.00 mmol, 1.00 eq.) dissolved in dry THF (4 mL) was added over 5 min. After 3 h the reaction mixture was quenched with sat. NH$_4$Cl solution (20 mL) at –78 °C. The mixture was allowed to warm to room temperature and was extracted with EtOAc (3 x 25 mL). The organic layer was dried over MgSO$_4$, filtered and the solvent concentrated under reduced pressure. The crude product was purified by flash column chromatography (SiO$_2$, 20 cm x 3.5 cm, cyclohexane/EtOAc 8:1) to afford the linear aldol product **26** (662 mg, 75%) as a colorless oil. Analytical data are in accordance with literature data.[120]

C$_{14}$H$_{20}$O$_2$ (220.31 g/mol)

R_f = 0.14 (cyclohexane/EtOAc 8:1).

^{1}H NMR (CDCl$_3$, 400 MHz) δ/ppm: 7.36-7.26 (m, 5 H, Ar-*H*), 5.15 (dd, $^3J_{HH}$ = 8.9 Hz, $^3J_{HH}$ = 3.5 Hz, 1 H, C*H*OH), 3.25 (br s, 1 H, O*H*), 2.85 (dd, $^2J_{HH}$ = 17.4 Hz, $^3J_{HH}$ = 8.9 Hz, 1 H, COC*H*$_a$H$_b$), 2.77 (dd, $^2J_{HH}$ = 17.4 Hz, $^3J_{HH}$ = 3.5 Hz, 1 H, COCH$_a$*H*$_b$), 2.42 (t, $^3J_{HH}$ = 7.4 Hz, 2 H, C*H*$_2$), 1.61-1.54 (m, 2 H, C*H*$_2$), 1.35-1.19 (m, 4 H, C*H*$_2$), 0.89 (t, $^3J_{HH}$ = 7.0 Hz, 3 H, C*H*$_3$).

^{13}C{^{1}H} NMR (CDCl$_3$, 101 MHz) δ/ppm: 211.8 (*C*O), 143.0 (Ar-*C*), 128.6, 127.7, 125.7 (3 x Ar-*C*H), 70.1 (*C*HOH), 51.1, 43.8, 31.4, 23.3, 22.5 (4 x *C*H$_2$), 14.0 (*C*H$_3$).

3-Hydroxy-2,2-dimethyl-3-(4-nitrophenyl)propanal 27
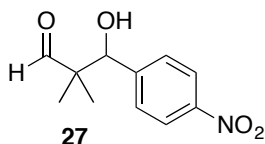
A mixture of *para*-nitrobenzaldehyde (756 mg, 5.00 mmol, 1.00 eq.), isobutyraldehyde (433 mg, 548 μL, 6.00 mmol, 1.20 eq.), pyrrolidine (17.8 mg, 20.5 μL, 0.25 mmol, 5 mol%) and AcOH (75.1 mg, 71.6 μL, 1.25 mmol, 25 mol%) in DMSO (5 mL) was stirred at room temperature for 1.5 h until TLC monitoring indicate complete consumption of the starting material. The volatiles were removed in HV, the residue was diluted with Et$_2$O (50 mL) and the organic layer was washed with brine (2 x 10 mL) and dried over MgSO$_4$, filtered and the solvent concentrated under reduced pressure. The yellow residue was purified by flash column chromatography (SiO$_2$,

10 cm x 3.5 cm, cyclohexane/EtOAc 7:3) and recrystallization from EtOAc to afford aldehyde **27** (389 mg, 35%) as a colorless solid. Analytical data are in accordance with literature data.[121]

$C_{11}H_{13}NO_4$ (223.23 g/mol)

R_f = 0.19 (cyclohexane/EtOAc 7:3).

¹H NMR (CDCl₃, 400 MHz) δ/ppm: 9.61 (s, 2 H, *H*CO), 8.22 (d, ${}^3J_{HH}$ = 8.8 Hz, 2 H, Ar-*H*), 7.51 (d, ${}^3J_{HH}$ = 8.8 Hz, 1 H, Ar-*H*), 5.05 (d, ${}^3J_{HH}$ = 3.3 Hz, 1 H, C*H*OH), 2.83 (d, ${}^3J_{HH}$ = 3.3 Hz, 1 H, O*H*), 1.07 (s, 3 H, C*H₃*), 0.99 (s, 3 H, C*H₃*).

¹³C{¹H} NMR (CDCl₃, 101 MHz) δ/ppm: 206.0 (*H*CO), 147.7, 147.1 (2 x Ar-*C*), 128.5, 123.2 (2 x Ar-*C*H), 76.3 (*C*HOH), 50.9 (*C*(CH₃)₂), 20.0, 15.7 (C(*C*H₃)₂).

1-(4-Nitrophenyl)-3-oxobutyl camphanic acid 35
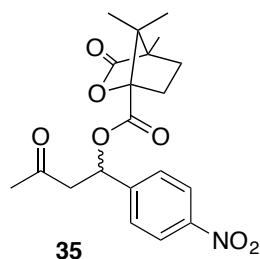
Racemic 4-hydroxy-4-(4-nitrophenyl)butan-2-one **7** (72.0 mg, 0.34 mmol, 1.00 eq.), pyridine (38.1 mg, 38.9 µL, 0.48 mmol, 1.40 eq.) and (−)-camphanic acid chloride (82.0 mg, 0.38 mmol, 1.10 eq.) were dissolved in CH₂Cl₂ (3.5 mL) at 0 °C. The mixture was allowed to warm to room temperature and stirred for 15 h. The reaction mixture was diluted with CH₂Cl₂ (20 mL) and washed with sat. NH₄Cl solution (10 mL) and brine (10 mL). The organic layer was dried over MgSO₄, filtered and the solvent concentrated under reduced pressure. The crude product was purified by flash column chromatography (SiO₂, 10 cm x 5.5 cm, cyclohexane/EtOAc 3:1) to afford ester **35** (92 mg, 69%) as a colorless solid as 1:1 mixture of diastereoisomers.

$C_{20}H_{23}NO_7$ (389.40 g/mol)

m.p.: 118-120 °C.

R_f = 0.07 (cyclohexane/EtOAc 3:1).

¹H NMR (CDCl₃, 400 MHz) δ/ppm: 8.22 (2 x d, 2 x ${}^3J_{HH}$ = 8.8 Hz, 2 H, Ar-*H*), 7.56 (2 x d, 2 x ${}^3J_{HH}$ = 8.9 Hz, 2 H, Ar-*H*), 6.38 (dd, ${}^3J_{HH}$ = 8.9 Hz, ${}^3J_{HH}$ = 4.4 Hz, 1 H, CH₂C*H*), 3.29-3.22 (m, 2 x 0.5 H, C*H*₂CH), 2.89 (dd, ${}^2J_{HH}$ = 17.8 Hz, ${}^3J_{HH}$ = 4.4 Hz, 0.5 H, C*H*₂CHO), 2.83 (dd, ${}^2J_{HH}$ = 17.8 Hz, ${}^3J_{HH}$ = 4.4 Hz, 0.5 H, C*H*₂CHO), 2.44-2.31 (m, 1 H, C*H*₂), 2.19 and 2.18 (2 x s, 3 H, COC*H₃*), 2.06-1.99 (m, 0.5 H, C*H*₂), 1.97-1.87 (m, 1.5 H, C*H*₂), 1.72-1.63 (m, 1 H, C*H*₂), 1.11, 1.09, 1.04, 0.98, 0.93, 0.82 (6 x s, 9 H, 3 x C*H₃*), (*1:1 mixture of diastereoisomers*).

^{13}C{^{1}H} NMR (CDCl$_3$, 125 MHz) δ/ppm: 2 x 203.4 (CO), 178.4 and 178.2 (CO$_2$), 166.7 and 166.6 (CO$_2$), 148.0, 2 x 146.3 (2 x Ar-C), 127.6 and 127.4, 124.2 and 124.1 (2 x Ar-CH), 90.9 and 90.7 (C$_q$), 71.7 and 71.6 (CH$_2$CHO), 55.0 and 54.9, 54.7 and 54.7 (2 x C$_q$), 49.2 (CH$_2$CHO), 31.0, 30.8, 30.6, 29.0, 28.9 (COCH$_3$, 2 x CH$_2$), 2 x 16.7, 9.8, 9.7 (3 x CH$_3$), (1:1 mixture of diastereoisomers).

Side product formation:
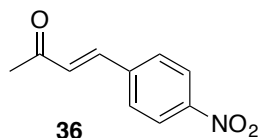
Applying DMAP instead of pyridine or longer reaction times as well as purification by flash column chromatography and HPLC analysis let to the formation of the aldol condensation product 36.

Analytical data of the condensation product 36:[122]

C$_{10}$H$_9$NO$_3$ (191.19 g/mol)

R_f = 0.18 (cyclohexane/EtOAc 3:1).

^{1}H NMR (CDCl$_3$, 400 MHz) δ/ppm: 8.26 (d, $^3J_{HH}$ = 8.7 Hz, 2 H, Ar-H), 7.70 (d, $^3J_{HH}$ = 8.7 Hz, 2 H, Ar-H), 7.54 (d, $^3J_{HH,trans}$ = 16.2 Hz, 1 H, CH), 6.82 (d, $^3J_{HH,trans}$ = 16.2 Hz, 1 H, CH), 2.42 (s, 3 H, CH$_3$).

6.2.3 Synthesis of Aminoalcohols

(S)-2-Amino-4-methyl-1,1-diphenylpentan-1-ol 30
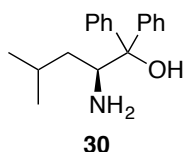
A two-necked flask was charged with magnesium turnings (0.67 g, 27.5 mmol, 5.00 eq.) and flame-dried under vacuum. The flask was flushed with argon and the magnesium suspended in dry Et$_2$O (6 mL). Bromobenzene (4.37 g, 2.91 mL, 27.8 mmol, 5.05 eq.) dissolved in dry Et$_2$O (12 mL) was added dropwise to the mixture. After stirring for 30 min at room temperature L-Leucine methyl ester hydrochloride (1.00 g, 5.51 mmol, 1.00 eq.) was added in small portions to the Grignard reagent. The brown solution was stirred for 4 h at room temperature. The reaction mixture was poured onto ice cooled sat. NH$_4$Cl solution (70 mL) and diluted with EtOAc (100 mL). The layers were separated and the aqueous layer was extracted with EtOAc (3 x 50 mL). The combined organic layers were washed with NaHCO$_3$ (50 mL), H$_2$O (50 mL), brine (50 mL), dried over MgSO$_4$, filtered and the solvent was concentrated under reduced pressure. The yellow crude product was recrystallized from hot EtOAc. The residual mother lye was

recrystallized again from EtOAc/cyclohexane and the precipitates were combined to afford aminoalcohol **30** (596 mg, 41%) as a colorless solid. Analytical data are in accordance with literature data.[52]

$C_{18}H_{23}NO$ (269.39 g/mol)

m.p.: 131-133 °C (EtOAc) (Lit.[52] 126.5-128.5 °C).

^{1}H NMR (CDCl$_3$, 400 MHz) δ/ppm: 7.63-7.60 (m, 2 H, Ar-*H*), 7.49-7.47 (m, 2 H, Ar-*H*), 7.34-7.25 (m, 4 H, Ar-*H*), 7.21-7.14 (m, 2 H, Ar-*H*), 3.99 (dd, $^3J_{HH}$ = 10.2 Hz, $^3J_{HH}$ = 2.1 Hz, 1 H, NC*H*), 1.65-1.53 (m, 1 H, C*H*), 1.27 (ddd, $^2J_{HH}$ = 14.1 Hz, $^3J_{HH}$ = 10.2 Hz, $^3J_{HH}$ = 3.8 Hz, 1 H, C*H*$_a$H$_b$), 1.09 (ddd, $^2J_{HH}$ = 14.1 Hz, $^3J_{HH}$ = 10.6 Hz, $^3J_{HH}$ = 2.1 Hz, 1 H, CH$_a$*H*$_b$), 0.90 (d, $^3J_{HH}$ = 6.6 Hz, C*H*$_3$), 0.87 (d, $^3J_{HH}$ = 6.6 Hz, C*H*$_3$). *NH and OH protons are not visible.*

^{13}C{^{1}H} NMR (CDCl$_3$, 101 MHz) δ/ppm: 147.3, 144.6 (2 x Ar-*C*), 128.6, 128.2, 126.8, 126.5, 126.0, 125.7 (6 x Ar-*C*H), 79.2 (*C*OH), 54.6 (N*C*H), 39.6 (*C*H$_2$), 25.5 (*C*H), 24.2, 21.4 (2 x *C*H$_3$).

Optical rotation: $[\alpha]_D^{20}$ = –97.3° (c = 0.99, CHCl$_3$) (Lit.[52] $[\alpha]_D^{20}$ = –97.7° (c = 1.0, CHCl$_3$)).

L-*tert*-Butyl-leucine methyl ester hydrochloride 42
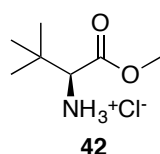
Under an argon atmosphere, a heat gun dried 250 mL two-necked flask, equipped with a dropping funnel and connected to a gas wash bottle with aqueous NaOH solution, was charged with L-*tert*-leucine (10.0 g, 76.2 mmol, 1.00 eq.). The amino acid was dissolved in MeOH (100 mL) and thionyl chloride (90.7 g, 55.4 mL, 762 mmol, 10.0 eq.) was added over 2 h at 0 °C. The resulting solution was allowed to warm to room temperature and stirred under reflux overnight. The mixture was allowed to cool to approximately 30 °C and additional thionyl chloride (10 mL) was added and stirred under reflux until gas evolution ceased when another 10 mL thionyl chloride was added and stirred at reflux. When gas evolution ceased, the volatiles were removed under high vacuum to yield hydrochloride **42** (13.8 g, quant., purity ≈ 93-94% (^{1}H NMR)) as a colorless solid. The crude product showed traces of unreacted acid and was used as it for the next reaction step.

$C_7H_{16}ClNO_2$ (181.66 g/mol)

^{1}H NMR (CDCl$_3$, 400 MHz) δ/ppm: 8.74 (s, 3 H, N*H*$_3$), 3.82 (s, 3 H, OC*H*$_3$), 3.75 (s, 1 H, C*H*), 1.17 (s, 9 H, C(C*H*$_3$)$_3$).

MS (ESI, 100°C, 50 V, MeOH) *m/z* (%): 146.0 [M–Cl]$^+$, 291.2 [2M–2Cl–H]$^+$.

(*S*)-2-Amino-3,3-dimethyl-1,1-diphenylbutan-1-ol 43
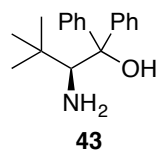
A two-necked flask was charged with magnesium turnings (1.28 g, 52.5 mmol, 10.5 eq.) and flame-dried under vacuum. The flask was flushed with argon, the magnesium suspended in Et_2O (20 mL) and an iodine crystall was added. A dropping funnel was charged with bromobenzene (7.85 g, 5.27 mL, 50.0 mmol, 10.0 eq.) and bromobenzene was added dropwise in several portions to avoid tremendous reflux. After stirring for 30 min at room temperature the crude L-*tert*-butyl-leucine methyl ester hydrochloride **42** (903 mg, 5.00 mmol, 1.00 eq.) was added in small portions. The solution was stirred at room temperature overnight and then poured onto ice water under vigorous stirring. The mixture was acidified using 1 M aqueous HCl. The resulting colorless precipitate was removed by filtration and washed with Et_2O (10 mL) and water (10 mL). To the colorless solid Et_2O (100 mL) was added and the suspension was basified with 1 M NaOH and stirred until the solid was dissolved. The layers were separated and the aqueous layer extracted with Et_2O (3 x 150 mL). The combined organic layers were dried over $MgSO_4$, filtered and the solvent evaporated to afford 970 mg of a pale grey solid. The gray solid was recrystallized from EtOAc (8 mL) to afford aminoalcohol **43** (622 mg, 46%) as colorless needles.

The separated aqueous layer obtained after filtration of the precipitated hydrochloride was washed with Et_2O (200 mL) and basified with 4 M aqueous NaOH solution and extracted with EtOAc (3 x 100 mL), the combined organic layers were dried over $MgSO_4$, filtered and the solvent evaporated under reduced pressure to give another 245 mg of the product as a colorless solid. The residue was combined with the mother lye of the first recrystallization and purified by flash column chromatography (SiO_2, 20 cm x 3.5 cm, cyclohexane/EtOAc 6:1 (350 mL) then EtOAc/MeOH 50:1). Aminoalcohol **43** (320 mg, 24%, overall yield 70%) was isolated as a colorless solid.

$C_{18}H_{23}NO$ (269.39 g/mol)

m.p.: 128-130 (EtOAc) (Lit.[123] 131.5-132 °C).

R_f = 0.20-0.33 (EtOAc/MeOH 50:1).

¹H NMR ($CDCl_3$, 400 MHz) δ/ppm: 7.69-7.67 (m, 2 H, Ar-*H*), 7.58-7.55 (m, 2 H, Ar-*H*), 7.34-7.30 (m, 2 H, Ar-*H*), 7.24-7.09 (m, 4 H, Ar-*H*), 4.42 (br s, O*H*), 3.83, (s, 1 H, C*H*), 1.39 (br s, 2 H, N*H₂*), 0.80 (s, 9 H, C(C*H₃*)₃).

¹³C{¹H} NMR ($CDCl_3$, 101 MHz) δ/ppm: 150.0, 145.4 (2 x Ar-*C*), 128.6, 127.8, 126.6, 126.3, 126.3, 125.7 (6 x Ar-*C*H), 80.0 (*C*OH), 63.8 (*C*H), 35.7 (*C*(CH₃)₃), 29.2 (C(*C*H₃)₃).

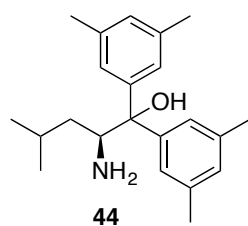**FTIR** (ATR): 3376w, 3347w, 3288w, 2997w, 2951w, 2906w, 2872w, 1584m, 1491m,

1448m, 1372w, 1190w, 1186w, 1058w, 967m, 898m, 741s, 696s cm^{-1}.

MS (FAB, NBA) *m/z* (%): 270.1 ([M+H]$^+$, 76), 196.1 (100), 86.1 (81).

EA calc. (%) for C$_{18}$H$_{23}$NO: C 80.26, H 8.61, N 5.20; found: C 80.13, H 8.39, N 5.07.

Optical rotation: $[\alpha]_D^{20}$ = −167.9° (c = 1.01, CHCl$_3$) (Lit.[123] $[\alpha]_D^{20}$ = +166.6° (c = 0.318, CHCl$_3$, (*R*)).

(*S*)-2-Amino-1,1-bis(3,5-dimethylphenyl)-4-methylpentan-1-ol 44

A two-necked flask was charged with magnesium turnings (438 mg, 18.0 mmol, 6.00 eq.) and flame-dried under vacuum. The flask was flushed with argon and the magnesium suspended in dry THF (5.5 mL). 5-Bromo-*m*-xylene (3.33 g, 2.44 mL, 18.0 mmol, 6.00 eq.) dissolved in dry THF (2.5 mL) was added dropwise to the mixture. The resulting black solution was stirred for 15 min at room temperature and cooled to 0 °C. L-Leucine methyl ester hydrochloride (544 mg, 3.00 mmol, 1.00 eq.) was added in small portion to the Grignard reagent and the reaction mixture was stirred for 3 h under reflux. The reaction mixture was poured onto ice cooled sat. NH$_4$Cl solution (100 mL) and the aqueous layer extracted with EtOAc (3 x 100 mL). The combined organic layers were washed with 1 M NaOH (50 mL) and brine (50 mL), dried over MgSO$_4$, filtered and the solvent concentrated under reduced pressure. The residue was dissolved in Et$_2$O (1 mL) and HCl (1 mL, 4 M in dioxane) was added dropwise whereupon a colorless precipitate was formed. The suspension was stored at −25 °C for 1 h and the precipitate was filtered off. The colorless solid was dissolved in CH$_2$Cl$_2$ (50 mL) and the organic layer washed with 1 M NaOH (3 x 20 mL) The combined aqueous layers were re-extracted with CH$_2$Cl$_2$ (20 mL) and the combined organic layers were washed with brine (20 mL), dried over MgSO$_4$, filtered and the solvent concentrated under reduced pressure to afford aminoalcohol **44** (512 mg, 52%) as a colorless solid.

C$_{22}$H$_{31}$NO (325.49 g/mol)

m.p.: 88-90 °C.

^{1}H NMR (CDCl$_3$, 400 MHz) δ/ppm: 7.20 (s, 2 H, Ar-*H*), 7.08 (s, 2 H, Ar-*H*), 6.81 (s, 1 H, Ar-*H*), 6.79 (s, 1 H, Ar-*H*), 3.93 (dd, $^3J_{HH}$ = 10.1 Hz, $^3J_{HH}$ = 2.1 Hz, 1 H, NC*H*), 2.30 (s, 6 H, C*H*$_{3(Ar)}$), 2.28 (s, 6 H, C*H*$_{3(Ar)}$), 1.68-1.55 (m, 1 H, C*H*$_{(iBu)}$), 1.24 (ddd, $^2J_{HH}$ = 14.0 Hz, $^3J_{HH}$ = 10.1 Hz, $^3J_{HH}$ = 2.1 Hz, 1 H, C*H*$_a$H$_b$), 1.12 (ddd, $^2J_{HH}$ = 14.0 Hz, $^3J_{HH}$ = 10.5 Hz, $^3J_{HH}$ = 2.1

Hz, 1 H, CH$_a$H$_b$), 0.93 (d, $^3J_{HH}$ = 6.6 Hz, 3 H, CH$_{3(iBu)}$), 0.88 (d, $^3J_{HH}$ = 6.6 Hz, 3 H, CH$_{3(iBu)}$). *NH and OH protons were not observed.*

^{13}C{^{1}H} NMR (CDCl$_3$, 101 MHz) δ/ppm: 147.3, 144.7 (2 x Ar-*C*), 137.9, 137.4 (2 x Ar-*C*– *C*H$_3$), 128.4, 128.1, 123.6, 123.4 (4 x Ar-*C*H), 79.1 (*C*OH), 54.7 (N*C*H), 39.6 (*C*H$_2$), 25.6 (*C*H$_{(iBu)}$), 24.2, 21.8, 21.7, 21.5 (4 x *C*H$_3$).

FTIR (ATR): 3409w, 3399w, 3340w, 3329w, 2953m, 2930m, 2869m, 1606 m, 1595m, 1464m, 1364m, 1256w, 1157m, 1080w, 1036w, 961w, 903m, 869m, 847m, 820m, 797m, 747s, 727s, 686m cm^{-1}.

MS (ESI) *m/z* (%): 326.2 [M+H]$^+$, 651.5 [2M+H]$^+$.

EA calc. (%) for C$_{22}$H$_{31}$NO: C 81.18, H 9.60, N 4.30; found: C 81.05, H 9.47, N 4.27.

Optical rotation: $[\alpha]_D^{20}$ = –76.2° (c = 0.97, CHCl$_3$).

(*S*)-2-Amino-4-methyl-1,1-bis(4-(trifluoromethyl)phenyl)pentan-1-ol (*S*)-45
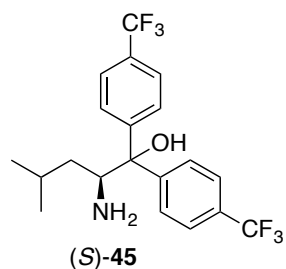
A two-necked flask was charged with magnesium turnings (438 mg, 18.0 mmol, 6.00 eq.) and flame-dried under vacuum. The flask was flushed with argon and the magnesium suspended in dry THF (8 mL). 4-Bromobenzotrifluoride (4.05 g, 2.53 mL, 18.0 mmol, 6.00 eq.) was added dropwise to the mixture. The color turned immediately into red within addition of aryl halide. The dark red solution was stirred for 30 min at room temperature and cooled to 0 °C. L-Leucine methyl ester hydrochloride (544 mg, 3.00 mmol, 1.00 eq.) was added in small portions to the Grignard reagent and the reaction mixture was stirred for 4 h at room temperature. The reaction mixture was poured onto ice cooled H$_2$O whereupon a white precipitate was formed. Aqueous NH$_4$Cl solution (50 mL) was added to dissolve the precipitate and the aqueous layer was extracted with EtOAc (3 x 100 mL). The combined organic layers were washed with 1 M NaOH (50 mL) and brine (50 mL), dried over MgSO$_4$, filtered and the solvent concentrated under reduced pressure. The red viscous oil was adsorbed onto celite and purified by flash column chromatography (SiO$_2$, 15 cm x 6 cm, cyclohexane/EtOAc 6:1 + 1% Et$_3$N) to afford aminoalcohol (*S*)-45 (828 mg, 68%, 73% *ee*) as a pale yellow solid.

$C_{20}H_{21}F_6NO$ (405.38 g/mol)

m.p.: 90-92 °C.

R_f = 0.41-0.49 (EtOAc).

^{1}H NMR (CDCl$_3$, 400 MHz) δ/ppm: 7.75 (d, $^3J_{HH}$ = 8.3 Hz, 2 H, Ar-*H*), 7.61-7.54 (m, 6 H, Ar-*H*), 4.57 (br s, 1 H, O*H*), 4.04 (dd, $^3J_{HH}$ = 10.4 Hz, $^3J_{HH}$ = 2.1 Hz, 1 H, NC*H*), 1.66-1.54 (m, 1 H, C*H*$_{(iBu)}$), 1.30 (ddd, $^2J_{HH}$ = 14.2 Hz, $^3J_{HH}$ = 10.4 Hz, $^3J_{HH}$ = 3.8 Hz, 1 H, C*H*$_a$H$_b$), 1.20 (br s, 2 H, N*H*$_2$), 0.97 (ddd, $^2J_{HH}$ = 14.2 Hz, $^3J_{HH}$ = 10.4 Hz, $^3J_{HH}$ = 2.1 Hz, 1 H, CH$_a$*H*$_b$), 0.90 (d, $^3J_{HH}$ = 6.6 Hz, 3 H, C*H*$_3$), 0.88 (d, $^3J_{HH}$ = 6.6 Hz, 3 H, C*H*$_3$).

^{13}C{^{1}H} NMR (CD$_3$OD, 101 MHz) δ/ppm: 151.4, 150.6 (2 x Ar-*C*), 130.2, 130.0 (2 x q, $^2J_{CF}$ = 32 Hz, Ar-*C*), 128.1, 127.7 (2 x Ar-*C*H), 126.4, 126.1 (2 x q, $^3J_{CF}$ = 4 Hz, Ar-C*H*), 125.6 (q, $^1J_{CF}$ = 271 Hz, *C*F$_3$), 81.3 (*C*OH), 56.1 (N*C*H), 41.2 (*C*H$_2$), 26.0 (*C*H$_{(iBu)}$), 24.6, 21.7 (2 x *C*H$_3$).

^{19}F NMR (CDCl$_3$, 376 MHz) δ/ppm: –62.5, –62.6 (2 x C*F*$_3$).

FTIR (ATR): 3092w, 2965w, 2945w, 1618m, 1467w, 1415m, 1325s, 1161s, 1118s, 1068s, 1024m, 1007m, 988m, 962m, 840s, 829m, 771w, 730w, 678w cm^{-1}.

MS (ESI) *m/z* (%): 406.1 [M+H]$^+$.

EA calc. (%) for $C_{20}H_{21}F_6NO$: C 59.26, H 5.22, N 3.46; found: C 59.15, H 5.38, N 3.42.

HPLC (*Daicel* Chiralpak IA, heptane/*i*PrOH 99:1, 0.5 mL/min, 25 °C, 223 nm): t_R((*R*)-**45**) = 23.4 min, t_R((*S*)-**45**) = 25.6 min.

Optical rotation: $[\alpha]_D^{20}$ = –59.2° (c = 0.54, CHCl$_3$, 73% *ee*).

(*R*)-2-Amino-4-methyl-1,1-bis(4-(trifluoromethyl)phenyl)pentan-1-ol (*R*)-45
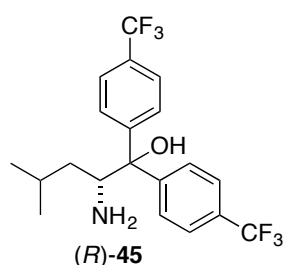
(*R*)-**45** was synthesized according to the procedure described for the (*S*)-enantiomer (*S*)-**45** with magnesium turnings (320 mg, 13.2 mmol, 6.00 eq.), 4-bromobenzotrifluoride (2.97 g, 1.85 mL, 13.2 mmol, 6.00 eq.) and dry THF (6.5 mL). D-Leucine methyl ester hydrochloride (400 mg, 2.20 mmol, 1.00 eq.) was added in small portions to the Grignard reagent at –78 °C. The reaction mixture was allowed to warm to room temperature over 1.5 h and stirred at ambient temperature for additional 3 h. Reaction workup and purification as described for (*S*)-**45** afforded aminoalcohol (*R*)-**45** (589 mg, 66%, 65% *ee*) as pale yellow solid. Analytical data are in accordance with data of the (*S*)-enantiomer.

Optical rotation: $[\alpha]_D^{20}$ = +55.4° (c = 0.52, CHCl$_3$, 65% *ee*).

For further transformations enantiomerically enriched (*R*)-**45** (>98% *ee*) was obtained by separation of the enantiomers by semi-preparative HPLC on a chiral stationary phase (Chiralpak AD with precolumn Chiralpak AD, hexane/*i*PrOH 98:2, 6.0 mL/min, 25 °C, 205 nm, $t_R(R)$ = 35 min, $t_R(S)$ = 41 min) as colorless solid.

Optical rotation: $[\alpha]_D^{20}$ = +79.3° (c = 0.99, CHCl$_3$, >98% *ee*).

2-Amino-1,1-diphenylethanol 46
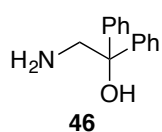
A flame dried three-necked flask was flushed with argon and phenylmagnesium bromide solution (3.33 mL, 3 M in Et$_2$O, 10 mmol, 4.00 eq.) was dissolved in dry THF (100 mL). 2-Aminoacetophenone hydrochloride (429 mg, 2.50 mmol, 1.00 eq.) was added in small portions. The resulting orange solution was stirred at 50 °C for 3 h. The reaction mixture was quenched with H$_2$O (20 mL) and diluted with Et$_2$O (50 mL). The organic layer was washed with brine (40 mL) and the combined aqueous layers were extracted with Et$_2$O/THF (3:2, 2 x 50 mL). The combined organic layers were dried over MgSO$_4$, filtered and the solvent concentrated under reduced pressure. The orange oil was purified by flash column chromatography (SiO$_2$, 20 cm x 3.5 cm, CHCl$_3$/MeOH 9:1) to afford aminoalcohol **46** (414 mg, 77%) as off-white solid. Analytical data are in accordance with literature data.[124]

C$_{14}$H$_{15}$NO (213.28 g/mol)
m.p.: 104-105 °C (Lit.[124] 102-104 °C).
R$_f$ = 0.25-0.32 (CHCl$_3$/MeOH 9:1).
^{1}H NMR (CDCl$_3$, 400 MHz) δ/ppm: 7.45-7.42 (m, 4 H, Ar-*H*), 7.33-7.30 (m, 4 H, Ar-*H*), 7.24-7.20 (m, 2 H, Ar-*H*), 3.42 (s, 2 H, C*H*$_2$), 2.64 (br s, 3 H, N*H*$_2$, O*H*).
^{13}C{^{1}H} NMR (CDCl$_3$, 101 MHz) δ/ppm: 145.3 (Ar-*C*), 129.4, 127.2, 126.3 (3 x Ar-*C*H), 77.1 (*C*OH), 50.9 (*C*H$_2$).

6.2.4 Catalyst Synthesis

N-Toluenesulfonyl-D-proline amide (R)-31

(R)-**31**
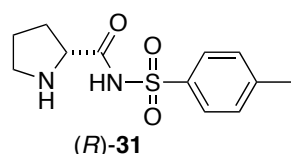
Under an argon atmosphere, a heat gun dried two-necked flask was charged with activated 4 Å molecular sieves (800 mg). N-Boc-D-proline (1,08 g, 5.03 mmol, 1.00 eq.) and EtOAc (15 mL) were added and the mixture stirred for 5 min at room temperature. The reaction mixture was cooled to 0 °C and pyridine (0.40 mL, 4.96 mmol, 1.00 eq.), *para*-nitrophenol (0.77 g, 5.50 mmol, 1.10 eq.) and DCC (1.08 g, 5.22 mmol. 1.05 eq.) were added subsequently. A colorless precipitate was formed and the resulting suspension was allowed to warm to room temperature overnight. The precipitate was removed by filtration over celite. The filtrate was concentrated under reduced pressure to afford the activated ester (1.69 g) as yellow oil.

Under an argon atmosphere, a heat gun dried flask was charged with NaH (0.31 g, 7.65 mmol, 60% in mineral oil, 1.50 eq.) and dry DMF (22 mL). *para*-Toluenesulfonamide (1.13 g, 6.60 mmol, 1.30 eq.) was added in small portions. The reaction mixture was stirred for 30 min until gas evolution ceased. The activated ester (1.69 g) was dissolved in dry DMF (12 mL) and added to the suspension under formation of a yellow solution. The mixture was stirred overnight and poured onto ice water. The aqueous phase was acidified using citric acid and extracted with EtOAc (4 x 40 mL). The combined organic layers were washed with H_2O (3 x 20 mL), brine (60 mL) and dried over Na_2SO_4. The solvent was removed under reduced pressure to afford a pale yellow solid. The solid was suspended in Et_2O (ca. 10 mL) and stored in the freezer for 45 min. The colorless Boc-protected sulfonamide (1.45 g) was removed by filtration and dried in HV.

The Boc-protected sulfonamide (1.45 g) was dissolved in CH_2Cl_2 (17 mL). TFA (7.00 mL, 91.5 mmol, 23.2 eq.) was added and the reaction mixture stirred for 3 h at room temperature. The solvent and excess TFA were removed in HV. The oily residue was treated with toluene (8 mL) in an ultrasonic bath and then removed in HV. To the crude oil ammonia in MeOH (ca. 7 N, 15 mL) was added, the mixture treated with an ultrasonic bath whereupon a pale yellow solid precipitated. Recrystallization from MeOH afforded sulfonamide (R)-**31** (730 mg, 69%) as colorless crystals. Analytical data are in accordance with literature data.[54]

$C_{12}H_{16}N_2O_3S$ (268.33 g/mol)

m.p.: 220-221 °C (MeOH) (Lit.[54] 217 °C).

^{1}H NMR (d^6-DMSO, 400 MHz) δ/ppm: 8.49 (br s, 1 H, N*H*), 7.66 (d, $^3J_{HH}$ = 8.2 Hz, Ar-*H*), 7.19 (d, $^3J_{HH}$ = 8.2 Hz, Ar-*H*), 3.80 (dd, $^3J_{HH}$ = 8.5 Hz, $^3J_{HH}$ = 8.5 Hz, 1 H, NC*H*), 3.18-3.12

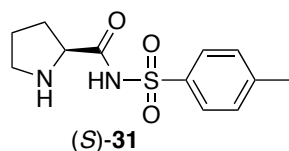(m, 1 H, NCH_2), 3.06-3.00 (m, 1 H, NCH_2), 2.32 (s, 3 H, CH_3), 2.15-2.06 (m, 1 H, CH_2), 1.85-1.65 (m, 3 H, CH_2).

^{13}C{^{1}H} NMR (d^6-DMSO, 101 MHz) δ/ppm: 171.1 (CO), 142.5, 139.9 (2 x Ar-C), 128.1, 126.9 (2 x Ar-CH), 61.8 (NCH), 45.2 (NCH_2), 29.0, 23.3 (2 x CH_2), 20.9 (CH_3).

Elemental analysis calc. (%) for C$_{12}$H$_{16}$N$_2$O$_3$S: C 53.71, H 6.01, N 10.44; found: C 53.57, H 5.97, N 10.40.

Optical rotation: $[\alpha]_D^{20}$ = +20.9° (c = 1.07, DMSO, (R)) (Lit.[125] $[\alpha]_D^{20}$ = +5.8° (c = 1.9, MeOH, (S)).[i]

N-Toluenesulfonyl-L-proline amide (S)-31

Sulfonamide (S)-31 was synthesized according to the procedure described for (R)-31.

Optical rotation: $[\alpha]_D^{20}$ = –21.1° (c = 0.83, DMSO).[i]

(S)-N-((S)-1-Benzyl-2-hydroxy-ethyl)pyrrolidine-2-carboxamide 9
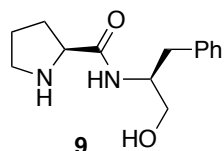
N-Cbz-L-proline (499 mg, 2.00 mmol, 1.00 eq.) was dissolved in dry THF (7.5 mL) and the solution was cooled to 0 °C. Et$_3$N (202 mg, 281 μL, 2.00 mmol, 1.00 eq.) was added dropwise whereupon a colorless precipitate was formed. The suspension was stirred for 30 min, followed by addition of (S)-2-amino-3-phenylpropan-1-ol (302 mg, 2.00 mmol, 1.00 eq.). The reaction mixture was stirred at elevated temperature (50 °C) for 3 h, followed by additional 16 h at room temperature. The reaction mixture was diluted with EtOAc (20 mL) and filtered over a plug of celite. The crude product was purified by flash column chromatography (SiO$_2$, 10 cm x 3.5 cm, cyclohexane/EtOAc 2:1) to afford the protected amine (456 mg).

The protected amine and Pd/C (10 wt.%, 50 mg) were dissolved in MeOH (12 mL) and stirred under H$_2$ atmosphere (1 bar) for 3 h until TLC indicate complete consumption of the protected amine. The reaction mixture was filtered through plug of celite and the solvent was removed under reduced pressure. The crude product was purified by recrystallization from EtOAc to afford organocatalyst 9 (196 mg, 40%) as colorless needles. Analytical data are in accordance

---

[i] In MeOH and in DMSO an optical rotation with opposite sign as published in the literature was observed. In addition, even in lower concentrations as applied in the reference the sulfonamide was not completely soluble in MeOH. Purity of the catalyst was confirmed by elemental analysis and optical rotations determined for both enantiomers were in agreement.

with literature data.[42a]

$C_{14}H_{20}N_2O_2$ (248.32 g/mol)

m.p.: 100-101 °C (EtOAc) (Lit.[42a] 104.4-105.9 °C).

^{1}H NMR (CDCl$_3$, 500 MHz) δ/ppm: 7.86 (d, $^3J_{HH}$ = 6.9 Hz, 1 H, N*H*CO), 7.32-7.26 (m, 2 H, Ar-*H*), 7.25-7.18 (m, 3 H, Ar-*H*), 4.15-4.09 (m, 1 H, C*H*CH$_2$Ph), 3.72 (dd, $^2J_{HH}$ = 11.1 Hz, $^3J_{HH}$ = 3.6 Hz, 1 H, C*H*$_a$H$_b$OH), 3.68 (dd, $^3J_{HH}$ = 9.3 Hz, $^3J_{HH}$ = 5.0 Hz, 1 H, NC*H*), 3.60 (dd, $^2J_{HH}$ = 11.1 Hz, $^3J_{HH}$ = 6.2 Hz, 1 H, CH$_a$*H$_b$*OH), 2.95 (dd, $^2J_{HH}$ = 13.9 Hz, $^3J_{HH}$ = 6.0 Hz, 1 H, CHC*H$_a$*H$_b$Ph), 2.91-2.87 (m, 1 H, NC*H*$_2$), 2.75 (dd, $^2J_{HH}$ = 13.9 Hz, $^3J_{HH}$ = 8.9 Hz, 1 H, CHCH$_a$*H$_b$*Ph), 2.66-2.60 (m, 1 H, NC*H*$_2$), 2.04-1.95 (m, 1 H, C*H*$_{2(Pyr)}$), 1.72-1.66 (m, 1 H, C*H*$_{2(Pyr)}$), 1.61-1.51 (m, 1 H, C*H*$_{2(Pyr)}$), 1.45-1.31 (m, 1 H, C*H*$_{2(Pyr)}$).

^{13}C{^{1}H} NMR (CDCl$_3$, 101 MHz) δ/ppm: 176.5 (*C*O), 137.9 (Ar-*C*), 129.3, 128.6, 126.7 (3 x Ar-*C*H), 65.7 (*C*H$_2$OH), 60.5 (N*C*H), 53.1 (CH*C*H$_2$Ph), 47.2 (N*C*H$_2$), 37.2 (CH*C*H$_2$Ph), 30.7 (*C*H$_{2(Pyr)}$), 26.1 (*C*H$_{2(Pyr)}$).

Optical rotation: $[\alpha]_D^{20}$ = –44.5° (c = 0.60, EtOH) (Lit.[42a] $[\alpha]_D^{25}$ = –63.0° (c = 0.50, EtOH).

(*S*)-*N*-((*S*)-1-Hydroxy-4-methyl-1,1-diphenylpentan-2-yl)pyrrolidine-2-carboxamide (Singh's catalyst) 13
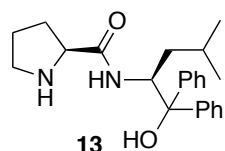
N-Cbz-L-proline (1.02 g, 4.08 mmol, 1.1 eq.) was dissolved in dry CH$_2$Cl$_2$. DIPEA (0.67 g, 0.86 mL, 5.20 mmol, 1.40 eq.) was added and the solution was cooled to 0 °C. EDCCl (0.99 g, 5.20 mmol, 1.40 eq.) and HOBt (0.80 g, 5.20 mmol, 1.40 eq.) were added simultaneously to the stirred solution. After 15 min (*S*)-2-amino-4-methyl-1,1-diphenylpentan-1-ol **30** (1.01 g, 3.71 mmol, 1.0 eq.) was added at 0 °C. The solution was allowed to warm to room temperature and stirred overnight. The reaction mixture was diluted with EtOAc (100 mL) and the organic layer washed with 1 M aqueous HCl (2 x 45 mL), saturated aqueous NaHCO$_3$ (60 mL) and brine (60 mL). The organic layer was dried over MgSO$_4$, filtered and the solvent evaporated to afford the Cbz-protected amine as colorless solid (1.56 g).

Cbz-protected amine (1.56 g), Pd/C (10 wt.%, 150 mg) were dissolved in MeOH/CH$_2$Cl$_2$ (3:1, 18 mL) and stirred under H$_2$ atmosphere (1 bar) overnight. The reaction mixture was filtered through a plug of celite and the filtrate was concentrated under reduced pressure. The crude product was purified by flash column chromatography (SiO$_2$ (deactivated with 100 mL EtOAc/cyclohexane 9:1 + 1% Et$_3$N before loading), 15 cm x 6 cm, EtOAc/cyclohexane 9:1)

to afford Singh's catalyst **13** (641 mg, 47%) as a colorless solid. An aliquot (300 mg) was further purified by recrystallization from EtOAc (7 mL) to afford highly analytically pure product (245 mg). Analytical data are in accordance with literature data.[44b]

$C_{23}H_{30}N_2O_2$ (366.50 g/mol)

**m**.**p**.: 190-192 °C (EtOAc) (Lit.[44b] 184-187 °C).

^{1}H NMR (CDCl$_3$, 500 MHz) δ/ppm: 7.94 (d, $^3J_{HH}$ = 8.4 Hz, 1 H, CON*H*), 7.57-7.54 (m, 4 H, Ar-*H*), 7.31-7.28 (m, 2 H, Ar-*H*), 7.26-7.23 (m, 2 H, Ar-*H*), 7.20-7.17 (m, 1 H, Ar-*H*), 7.14-7.11 (m, 1 H, Ar-*H*), 5.45 (br s, 1 H, O*H*), 4.59 (ddd, $^3J_{HH}$ = 11.1 Hz, $^3J_{HH}$ = 8.4 Hz, $^3J_{HH}$ = 2.1 Hz, C*H*COH), 3.48 (dd, $^3J_{HH}$ = 9.4 Hz, $^3J_{HH}$ = 4.7 Hz, 1 H, NC*H*), 2.84-2.79 (m, 1 H, NC*H*$_2$), 2.59-2.54 (m, 1 H, NC*H*$_2$), 1.90-1.84 (m, 2 H, C*H*$_{2(Pyr)}$, C*H*$_{2(iBu)}$), 1.80 (br s, 1 H, N*H*), 1.60-1.52 (m, 1 H, C*H*$_{(iBu)}$), 1.49-1.41 (m, 2 H, C*H*$_{2(Pyr)}$, C*H*$_{2(Pyr)}$), 1.27-1.19 (m, 2 H, C*H*$_{2(iBu)}$, C*H*$_{2(Pyr)}$), 0.92 (d, $^3J_{HH}$ = 6.7 Hz, 3 H, C*H*$_3$), 0.86 (d, $^3J_{HH}$ = 6.7 Hz, 3 H, C*H*$_3$).

^{13}C{^{1}H} NMR (CDCl$_3$, 101 MHz) δ/ppm: 176.3 (*C*O), 146.8, 145.3 (2 x Ar-*C*), 128.4, 128.0, 126.8, 126.6, 125.9, 125.8 (6 x Ar-*C*H), 81.0 (*C*HCOH), 60.4 (N*C*H), 57.0 (*C*HCOH), 47.2 (N*C*H$_2$), 37.5 (*C*H$_{2(iBu)}$), 30.6, 25.9 (2 x *C*H$_{2(Pyr)}$), 25.5 (*C*H$_{(iBu)}$), 24.0, 21.6 (2 x *C*H$_3$).

Elemental analysis calc. (%) for $C_{23}H_{30}N_2O_2$: C 75.37, H 8.25, N 7.64; found: C 75.08, H 8.15, N 7.71.

Optical rotation: $[\alpha]_D^{20}$ = –46.2° (c = 1.54, CHCl$_3$) (Lit.[44b] $[\alpha]_D^{25}$ = –45.9° (c = 1.2, CHCl$_3$).

(2*S*,4*R*)-4-Hydroxy-*N*-[(*S*)-1-hydroxy-4-methyl-1,1-diphenylpentan-2-yl]pyrrolidine-2-carboxamide 40
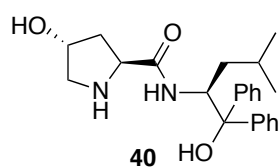
Hydroxy-proline derived organocatalyst **40** was synthesized according to the procedure described for Singh's catalyst **13** with *N*-Cbz-hydroxy-L-proline (265 mg, 1.00 mmol, 1.00 eq.), (*S*)-2-amino-4-methyl-1,1-diphenylpentan-1-ol **30** (269 mg, 1.00 mmol, 1.00 eq.), DIPEA (181 mg, 231 μL, 1.40 mmol, 1.40 eq.), EDCCl (268 mg, 1.40 mmol, 1.40 eq.) and HOBt (214 mg, 1.40 mmol, 1.40 eq.) in CH$_2$Cl$_2$ (6 mL). After stirring overnight and workup the protected crude (575 mg) was isolated as colorless solid.

The protected crude (575 mg) and Pd/C (10 wt.%, 58 mg) dissolved in MeOH (6 mL) were stirred under H$_2$ atmosphere (1 bar) overnight. Filtration through a plug of celite and purification by flash column chromatography (SiO$_2$, 20 cm x 3.5 cm, EtOAc/MeOH 5:1) afforded the organocatalyst **40** (273 mg, 71%) as colorless solid. Analytical data are in

accordance with literature data.[53]

C$_{23}$H$_{30}$N$_2$O$_3$ (382.50 g/mol)

m.p.: 189-191 °C (Lit.[53] 187-188 °C).

***R**$_f$* = 0.33 (EtOAc/MeOH 5:1).

^{1}H NMR (CD$_3$OD, 500 MHz) δ/ppm: 7.56-7.53 (m, 4 H, Ar-*H*), 7.32-7.26 (m. 2 H, Ar-*H*), 7.23-7.17 (m, 3 H, Ar-*H*), 7.12-7.09 (m, 1 H, Ar-*H*), 5.03 (dd, $^3J_{HH}$ = 11.1 Hz, 2.0 Hz, 1 H, C*H*COH), 4.18-4.16 (m, 1 H, C*H*OH), 3.67 (t, $^3J_{HH}$ = 8.2 Hz, 1 H, NC*H*), 2.89 (dd, $^2J_{HH}$ = 12.0 Hz, $^3J_{HH}$ = 4.1 Hz, 1 H, NC*H*$_a$H$_b$), 2.82 (ddd, $^2J_{HH}$ = 12.0 Hz, $^3J_{HH}$ = 1.9 Hz, $^4J_{HH}$ = 1.9 Hz, 1 H, NCH$_a$*H*$_b$), 1.83 ("ddt", $^2J_{HH}$ = 13.6 Hz, $^3J_{HH}$ = 8.2 Hz, $^3J_{HH}$ = 1.9 Hz, $^4J_{HH}$ = 1.9 Hz, 1 H, C*H*$_{2(Pyr)}$), 1.59-1.50 (m, 2 H, C*H*$_{2(iBu)}$, C*H*$_{(iBu)}$), 1.30 (ddd, $^2J_{HH}$ = 13.6 Hz, $^3J_{HH}$ = 8.2 Hz, $^3J_{HH}$ = 5.0 Hz, CH$_a$*H*$_{b(Pyr)}$), 1.22-1.17 (m, 1 H, C*H*$_{2(iBu)}$), 0.95 (d, $^3J_{HH}$ = 6.6 Hz, 3 H, C*H*$_3$), 0.84 (d, $^3J_{HH}$ = 6.6 Hz, 3 H, C*H*$_3$).

^{13}C{^{1}H} NMR (CD$_3$OD, 101 MHz) δ/ppm: 175.3 (*C*O), 147.5, 147.0 (2 x Ar-*C*), 129.2, 128.7, 127.7, 127.4, 127.0, 126.8 (6 x Ar-*C*H), 81.8 (Ph$_2$*C*OH), 73.0 (*C*HOH), 60.5 (N*C*H), 55.7 (N*C*H$_2$), 55.2 (*C*HCOH), 40.7 (*C*H$_{2(Pyr)}$), 40.3 (*C*H$_{2(iBu)}$), 26.3 (*C*H$_{(iBu)}$), 24.4, 22.1 (2 x *C*H$_3$).

Optical rotation: $[\alpha]_D^{20}$ = –29.2° (c = 0.43, MeOH) (Lit.[53] $[\alpha]_D^{20}$ = –31.61° (c = 1.55, MeOH).

(2*S*,4*R*)-4-*tert*-Butyldimethylsilyloxy-*N*-[(*S*)-1-hydroxy-4-methyl-1,1-diphenylpentan-2-yl]pyrrolidine-2-carboxamide 47
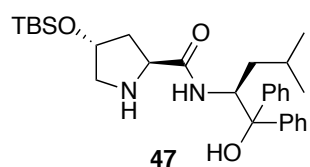
(2*S*,4*R*)-4-Hydroxy-*N*-[(*S*)-1-hydroxy-4-methyl-1,1-diphenylpentan-2-yl]pyrrolidine-2-carboxamide **40** (50.0 mg, 131 µmol, 1.00 eq.) and imidazole (44.5 mg, 654 µmol, 5.00 eq.) were dissolved in dry CH$_2$Cl$_2$ (0.5 mL). The solution was cooled to 0 °C and TBSCl (49.3 mg, 327 µmol. 2.50 eq.) was added in several portions. The solution was stirred at room temperature overnight. The reaction mixture was diluted with CH$_2$Cl$_2$ (20 mL), washed with H$_2$O (20 mL) and brine (20 mL). The combined organic layers were dried over MgSO$_4$, filtered and the solvent concentrated under reduced pressure. The crude product was purified by flash column chromatography (SiO$_2$, 9 cm x 2 cm, cyclohexane/EtOAc 1:1) to afford TBS-protected catalyst **47** (52.1 mg, 80%) as a colorless solid.

$C_{29}H_{44}N_2O_3Si$ (496.76 g/mol)

m.**p**.: 141-142 °C.

R_f = 0.17-0.30 (cyclohexane/EtOAc 1:1)

^{1}H NMR (CDCl$_3$, 400 MHz) δ/ppm: 8.05 (d, $^3J_{HH}$ = 8.5 Hz, 1 H, CONH), 7.62-7.49 (m, 4 H, Ar-H), 7.32-7.28 (m, 2 H, Ar-H), 7.26-7.10 (m, 4 H, Ar-H), 5.40 (br s, 1 H, OH), 4.58 (ddd, $^3J_{HH}$ = 10.9 Hz, $^3J_{HH}$ = 8.5 Hz, $^3J_{HH}$ = 2.1 Hz, 1 H, CHCOH), 4.09-4.06 (m, 1 H, CHOTBS), 3.74 (t, $^3J_{HH}$ = 8.3 Hz, 1 H, NCH), 2.71 (dt, $^2J_{HH}$ = 11.8 Hz, $^3J_{HH}$ = 1.8 Hz, 1 H, NCH_aH$_b$), 2.29 (dd, $^2J_{HH}$ = 11.8 Hz, $^3J_{HH}$ = 3.2 Hz, 1 H, NCH$_a$$H_b$), 2.14 (br s, 1 H, N$H$), 2.00-1.86 (m, 2 H, C$H_{2(Pyr)}$, C$H_{2(iBu)}$), 1.61-1.51 (m, 1 H, C$H_{(iBu)}$), 1.30 (ddd, $^2J_{HH}$ = 13.5 Hz, $^3J_{HH}$ = 7.8 Hz, $^3J_{HH}$ = 4.5 Hz, 1 H, C$H_{2(Pyr)}$), 1.22 (ddd, $^2J_{HH}$ = 14.2 Hz, $^3J_{HH}$ = 10.2 Hz, $^3J_{HH}$ = 2.1 Hz, 1 H, C$H_{2(iBu)}$), 0.91 (d, $^3J_{HH}$ = 6.7 Hz, 3 H, CH$_{3(iBu)}$), 0.85 (d, $^3J_{HH}$ = 6.7 Hz, 3 H, CH$_{3(iBu)}$), 0.83 (s, 9 H, C(CH_3)$_3$).

^{13}C{^{1}H} NMR (CDCl$_3$, 101 MHz) δ/ppm: 175.6 (CO), 146.7, 145.1 (2 x Ar-C), 128.2, 127.9, 126.7, 126.4, 125.7, 125.6 (6 x Ar-CH), 80.9 (Ph$_2$$C$OH), 73.4 ($C$HOTBS), 59.5 (N$C$H), 56.9 ($C$HCOH), 55.4 (N$CH_2$), 39.8 ($CH_{2(Pyr)}$), 37.3 ($CH_{2(iBu)}$), 25.7 (C($CH_3$)$_3$), 25.4 ($CH_{(iBu)}$), 23.8, 21.5 (2 x CH$_3$), 18.0 (C(CH$_3$)$_3$).

FTIR (ATR): 3385w, 3261w, 2950m, 2927m, 2856m, 1640m, 1535s, 1491w, 1450m, 1382w, 1361w, 1287m, 1119s, 941m, 839s, 773s, 745s, 731s, 704s, 637m cm^{-1}.

MS (ESI) *m/z* (%): 497.4 [M+H]$^+$.

EA calc. (%) for $C_{29}H_{44}N_2O_3Si$: C 70.12, H 8.93, N 5.64; found: C 69.95, H 8.78, N 5.62.

Optical rotation: $[\alpha]_D^{20}$ = –28.4° (c = 0.96, CHCl$_3$).

(2*S*,4*R*)-4-*tert*-Butyldiphenylsilyloxy-*N*-[(*S*)-1-hydroxy-4-methyl-1,1-diphenylpentan-2-yl]pyrrolidine-2-carboxamide 48
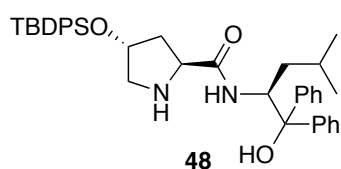
(2*S*,4*R*)-4-Hydroxy-*N*-[(*S*)-1-hydroxy-4-methyl-1,1-diphenylpentan-2-yl]pyrrolidine-2-carboxamide **40** (53.0 mg, 139 µmol, 1.00 eq.) and imidazole (47.2 mg, 693 µmol, 5.00 eq.) were dissolved in dry CH$_2$Cl$_2$ (500 µL) and cooled to 0 °C. TBDPSCl (98.2 mg, 91.4 µL, 346 µmol, 2.50 eq.) was added and the solution allowed to warm to room temperature and stirred overnight. The reaction mixture was directly subjected to flash column chromatography (SiO$_2$, 20 cm x 2.5 cm, cyclohexane (100 mL), then cyclohexane/EtOAc 1:1) to afford the TBDPS-protected catalyst **48** (79 mg, < 92%, spectra contained signals of the silyl ether) as a pale yellow foam. An aliquot was purified by semi-

preparative HPLC (Reprospher silica, hexane/*i*PrOH 95:5, 6.0 mL/min, 25 °C, 205 nm, t_R = 20 min) for analytical purposes.

$C_{39}H_{48}N_2O_3Si$ (496.76 g/mol)

$\boldsymbol{R_f}$ = 0.42 (SiO_2, cyclohexane/EtOAc 1:1).

^{1}H NMR (CDCl$_3$, 500 MHz) δ/ppm: 8.01 (d, $^3J_{HH}$ = 8.5 Hz, 1 H, CON*H*), 7.62-7.59 (m, 4 H, Ar-*H*), 7.56 (dd, $^3J_{HH}$ = 8.5 Hz, $^4J_{HH}$ = 1.1 Hz, 2 H, Ar-*H*), 7.52 (dd, $^3J_{HH}$ = 8.5 Hz, $^4J_{HH}$ = 1.2 Hz, 2 H, Ar-*H*), 7.48-7.44 (m, 2 H, Ar-*H*), 7.41-7.38 (m, 4 H, Ar-*H*), 7.33-7.28 (m, 2 H, Ar-*H*), 7.22-7.17 (m, 3 H, Ar-*H*), 7.07-7.03 (m, 1 H, Ar-*H*), 5.38 (br s, 1 H, O*H*), 4.56 (ddd, $^3J_{HH}$ = 11.0 Hz, $^3J_{HH}$ = 8.5 Hz, $^3J_{HH}$ = 2.1 Hz, 1 H, C*H*COH), 4.17-4.16 (m, 1 H, C*H*OTBDPS), 3.82 (t, $^3J_{HH}$ = 8.4 Hz, 1 H, NC*H*), 2.76 (ddd, $^2J_{HH}$ = 12.1 Hz, $^3J_{HH}$ = 2.3 Hz, $^4J_{HH}$ = 1.2 Hz, 1 H, NC*H*$_a$H$_b$), 2.15 (dd, $^2J_{HH}$ = 12.1 Hz, $^3J_{HH}$ = 3.1 Hz, 1 H, NCH$_a$*H*$_b$), 2.12-2.07 (m, 2 H, C*H*$_{2(Pyr)}$, N*H*), 1.88 (ddd, $^2J_{HH}$ = 14.4 Hz, $^3J_{HH}$ = 11.0 Hz, $^3J_{HH}$ = 3.6 Hz, 1 H, C*H*$_{2(iBu)}$), 1.58-1.50 (m, 1 H, C*H*$_{(iBu)}$), 1.34-1.16 (m, 2 H, C*H*$_{2(Pyr)}$, C*H*$_{2(iBu)}$), 1.04 (s, 9 H, C(C*H*$_3$)$_3$), 0.91 (d, $^3J_{HH}$ = 6.6 Hz, 3 H, C*H*$_{3(iBu)}$), 0.85 (d, $^3J_{HH}$ = 6.6 Hz, 3 H, C*H*$_{3(iBu)}$).

^{13}C{^{1}H} NMR (CDCl$_3$, 101 MHz) δ/ppm: 175.9 (*C*O), 146.7, 145.2 (2 x Ar-*C*), 135.8, 135.7 (2 x Ar-*C*H), 134.1, 133.8 (2 x Ar-*C*), 129.9, 129.7, 128.4, 128.0, 127.9, 127.6, 126.8, 126.6, 125.8, 125.7 (10 x Ar-*C*H), 81.0 (Ph$_2$*C*OH), 74.8 (*C*HOTBDPS), 59.8 (N*C*H), 56.9 (*C*HCOH), 55.5 (N*C*H$_2$), 39.9 (*C*H$_{2(Pyr)}$), 37.5 (*C*H$_{2(iBu)}$), 27.0 (C(*C*H$_3$)$_3$), 25.5 (*C*H$_{(iBu)}$), 24.0, 21.6 (2 x *C*H$_3$), 19.2 (*C*(CH$_3$)$_3$).

FTIR (ATR): 3329w (br), 2955w, 2934w, 2858w, 1645m, 1526m, 1450m, 1432m, 1634w, 1264w, 1175w, 1107m, 1063m, 1004m, 900w, 822m, 741m, 699s, 613m cm^{-1}.

HRMS (ESI, 4500 V, 180 °C) calc. *m/z* for $C_{39}H_{49}N_3O_3Si$: 621.3507, found: 621.3514 [M+H]$^+$.

Optical rotation: $[\alpha]_D^{20}$ = –20.8° (c = 0.31, CHCl$_3$).

(*S*)-*N*-((*S*)-1-Hydroxy-3,3-dimethyl-1,1-diphenylbutan-2-yl)pyrrolidine-2-carboxamide 41
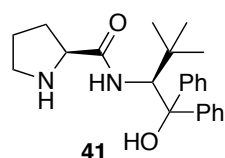
Under an argon atmosphere, *N*-Cbz-L-proline (137 mg, 0.55 mmol, 1.10 eq.) was dissolved in dry DMF (2.5 mL) and DIPEA (71.1 mg, 90.9 µL, 0.55 mmol, 1.10 eq.) was added. The solution was cooled to 0 °C and HATU (209 mg, 0.55 mmol, 1.10 eq.) was added. The resulting pale yellow solution was stirred for 15 min at 0 °C followed by addition of (*S*)-2-amino-3,3-dimethyl-1,1-diphenylbutan-1-ol **43** (135 mg, 0.50 mmol, 1.00 eq.). The solution was allowed to warm to

room temperature and stirred for 5 h. The reaction mixture was diluted with EtOAc (30 mL) washed with 1 M HCl solution (10 mL), saturated NaHCO$_3$ solution (10 mL) and brine (3 x 10 mL). The organic layer was dried over MgSO$_4$, filtered and the solvent concentrated under reduced pressure. The crude product was adsorbed onto silica, filtered through a plug of silica gel (2 cm x 3.5 cm) and eluted with cyclohexane/EtOAc (1:1, ca. 200 mL). Evaporation of the solvent afforded a colorless solid (217 mg), which appeared to be quite insoluble in the eluent. The protected amine (217 mg) and Pd/C (10 wt.%, 22 mg) dissolved in a mixture of MeOH/CH$_2$Cl$_2$ (3:1, 4 mL) were stirred under H$_2$ atmosphere (1 bar) for 4 h until TLC indicate complete consumption of the starting material (R_f = 0.47, cyclohexane/EtOAc 1:1). The reaction mixture was filtered through a syringe filter and the solvent concentrated under reduced pressure. The colorless crude product was purified by flash column chromatography (SiO$_2$, 10 cm x 3.5 cm, cyclohexane/EtOAc 1:1 (150 mL) then EtOAc + 1% Et$_3$N) to afford organocatalyst **41** (138 mg, 75%) as colorless solid. An aliquot was further purified by recrystallization from EtOAc for analytical purposes.

C$_{23}$H$_{30}$N$_2$O$_2$ (366.50 g/mol)

m.**p**.: 214-215 °C.

R$_f$ = 0.05-0.15 (EtOAc + 1% Et$_3$N).

^{1}H NMR (CD$_3$OD, 500 MHz) δ/ppm: 7.65 ("d", $^3J_{HH}$ = 7.8 Hz, 2 H, Ar-*H*), 7.56 ("d", $^3J_{HH}$ = 7.7 Hz, 2 H, Ar-*H*), 7.25-7.17 (m, 4 H, Ar-*H*), 7.12-7.05 (m, 2 H, Ar-*H*), 4.96 (br s, 1 H, C*H*tBu), 3.29-3.25 (m, 1 H, NC*H*), 2.91-2.86 (m, 1 H, NC*H*$_2$), 2.78 (dt, $^2J_{HH}$ = 10.5 Hz, $^3J_{HH}$ = 7.0 Hz, 1 H, NC*H*$_2$), 1.75-1.67 (m, 1 H, C*H*$_{2(Pyr)}$), 1.59-1.49 (m, 2 H, C*H*$_{2(Pyr)}$), 1.24 (br s, 1 H, C*H*$_{2(Pyr)}$)).

^{13}C{^{1}H} NMR (CD$_3$OD, 126 MHz) δ/ppm: 176.1(*C*O), 150.2, 148.1 (2 x Ar-*C*), 128.8, 127.2, 127.1, 126.7, 126.2 (5 x Ar-*C*H), 83.1 (br s, *C*HCOH), 62.2 (br s, *C*HCOH), 61.6 (N*C*H), 48.0 (N*C*H$_2$), 38.6 (br s, *C*(CH$_3$)$_3$), 31.6 (*C*H$_{2(Pyr)}$), 30.0 (C(*C*H$_3$)$_3$), 27.0 (*C*H$_{2(Pyr)}$).

FTIR (ATR): 3299w (br), 2958w, 2870w, 1642s, 1524s, 1448m, 1365m, 1298w, 1240w, 1206w, 1165w, 1107m, 1067m, 1036w, 895w, 738s, 707s, 695s, 665s cm^{-1}.

MS (ESI) *m/z* (%): 367.1 [M+H]$^+$, 733.5 [2M+H]$^+$.

EA calc. (%) for C$_{23}$H$_{23}$N$_2$O$_2$: C 75.37, H 8.25, N 7.64; found: C 75.30, H 8.14, N 7.73.

Optical rotation: $[\alpha]_D^{20}$ = −106.9° (c = 0.70, CHCl$_3$).

(S)-N-(2-Hydroxy-2,2-diphenylethyl)pyrrolidine-2-carboxamide 14
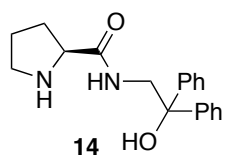
Organocatalyst **14** was synthesized according to the procedure described for organocatalyst **41** with N-Cbz-L-proline (137 mg, 0.55 mmol, 1.10 eq.), DIPEA (75.1 mg, 90.0 µL, 0.55 mmol, 1.10 eq.), HATU (209 mg, 0.55 mmol, 1.10 eq.) and 2-amino-1,1-diphenylethanol **46** (107 mg, 0.50 mmol, 1.00 eq.) in dry DMF (2.5 mL). The yellow solution was stirred for 3 h. Workup and filtration through a plug of silica gel (5 cm x 2 cm, cyclohexane/EtOAc 1:1, 120 mL) afforded the protected catalyst as colorless solid (ca. 185 mg).

The protected catalyst (185 mg) and Pd/C (10 wt.%, 19 mg) were dissolved in MeOH (4 mL) and stirred under H_2 atmosphere (1 bar) for 4 h until TLC indicate complete consumption of the starting material (R_f = 0.28, cyclohexane/EtOAc 1:1). The reaction mixture was filtered through a plug of celite and the solvent concentrated under reduced pressure. The colorless crude product was purified by flash column chromatography (SiO_2, 19 cm x 3.5 cm, EtOAc/MeOH 50:1 + 1% Et_3N) to afford organocatalyst **14** (104 mg) as colorless solid. The product was further purified by recrystallization from EtOAc (2 mL) to yield 72.4 mg of colorless solid. The mother lye was recrystallized from EtOAc/hexane (2:1) to give another 17.5 mg of pure organocatalyst **14** (overall yield: 89.9 mg, 58%).

$C_{19}H_{22}N_2O_2$ (310.40 g/mol)[44b]i

m.p.: 159-160 °C.

R_f = 0.20 (EtOAc/MeOH 50:1 + 1% Et_3N).

^{1}H NMR (CD$_3$OD, 400 MHz) δ/ppm: 7.45-7.42 (m, 4 H, Ar-H), 7.31-7.27 (m, 4 H, Ar-H), 7.23-7.18 (m, 2 H, Ar-H), 4.13 (d, $^2J_{HH}$ = 13.6 Hz, 1 H, CONHCH$_a$H$_b$), 3.91 (d, $^2J_{HH}$ = 13.6 Hz, 1 H, CONHCH$_a$H$_b$), 3.53 (dd, $^3J_{HH}$ = 9.0, $^3J_{HH}$ = 5.0, 1 H, NCH), 2.84-2.78 (m, 1 H, NCH$_2$), 2.70-2.64 (m, 1 H, NCH$_2$), 1.95-1.86 (m, 1 H, CH$_{2(Pyr)}$), 1.57-1.33 (m, 3 H, CH$_{2(Pyr)}$).

^{13}C{^{1}H} NMR (CD$_3$OD, 101 MHz) δ/ppm: 177.8 (CO), 146.7, 146.4 (2 x Ar-C), 129.1, 129.0, 128.1, 128.0, 127.3, 127.3 (6 x Ar-CH), 78.8 (COH), 61.4 (NCH), 49.6 (CONHCH$_2$), 47.8 (NCH$_2$), 31.8 (CH$_{2(Pyr)}$), 26.8 (CH$_{2(Pyr)}$).

FTIR (ATR): 3283m (br), 2970w, 2923w, 2872w, 1635s, 1529s, 1491m, 1448m, 1393w, 1254w, 1203w, 1177w, 1132w, 1104w, 1065m, 1026w, 954w, 917w, 751s, 696s, 596s cm^{-1}.

MS (ESI) m/z (%): 311.2 [M+H]$^+$.

EA calc. (%) for $C_{19}H_{22}N_2O_2$: C 73.52, H 7.14, N 9.03; found: C 73.21, H 7.10, N 8.76.

Optical rotation: $[\alpha]_D^{20}$ = –20.2° (c = 0.45, MeOH).

---

i Analytical data were not consistent with data from the literature.

(*S*)-*N*-((*S*)-1,1-Bis(3,5-dimethylphenyl)-1-hydroxy-4-methylpentan-2-yl)pyrrolidine-2-carboxamide 49
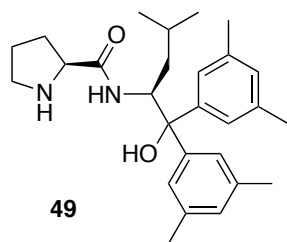
Organocatalyst **49** was synthesized according to the procedure described for organocatalyst **41** with *N*-Cbz-L-proline (82.3 mg, 0.33 mmol, 1.10 eq.), DIPEA (42.7 mg, 54.5 μL, 0.33 mmol, 1.10 eq.), HATU (125 mg, 0.33 mmol, 1.10 eq.) and (*S*)-2-amino-1,1-bis(3,5-dimethylphenyl)-4-methylpentan-1-ol **44** (97.6 mg, 0.30 mmol, 1.00 eq.) in dry DMF (1.5 mL). The pale yellow solution was stirred for 5 h. Workup and filtration through a plug of silica gel (3 cm x 2 cm, cyclohexane/EtOAc 1:1, 100 mL) afforded the protected catalyst as colorless glue (ca. 180 mg).

The viscous solid and Pd/C (10 wt.%, 18 mg) were dissolved in MeOH/CH$_2$Cl$_2$ (4:1, 2.5 mL) and stirred under H$_2$ atmosphere (1 bar) for 3 h until TLC indicate complete consumption of the starting material (R_f = 0.62, cyclohexane/EtOAc 1:1). The reaction mixture was filtered through a syringe filter and the solvent concentrated under reduced pressure. The resulting colorless foam was purified by flash column chromatography (SiO$_2$, 10 cm x 2 cm, cyclohexane/EtOAc 1:1 (120 mL) then EtOAc + 1% Et$_3$N) to afford organocatalyst **49** (114 mg (corr. yield[i]), 90%) as colorless foam. The foam was treated with hexane in an ultrasonic bath to yield a colorless solid after removal of the solvent in HV. An aliquot was purified by semi-preparative HPLC (Reprospher silica, hexane/*i*PrOH 60:40, 9.0 mL/min, 25 °C, 210 nm, t_R = 17.5-22.5 min) for analytical purposes.

C$_{27}$H$_{38}$N$_2$O$_2$ (422.60 g/mol)

m.**p**.: 164-166 °C.

***R**$_f$* = 0.25 (EtOAc + 3% Et$_3$N).

^{1}H NMR (CDCl$_3$, 400 MHz) δ/ppm: 7.89 (d, $^3J_{HH}$ = 8.6 Hz, 1 H, CON*H*), 7.15 (s, 2 H, Ar-*H*), 7.14 (s, 2 H, Ar-*H*), 6.81 (s, 1 H, Ar-*H*), 6.75 (s, 1 H, Ar-*H*), 5.20 (br s, 1 H, O*H*), 4.61-4.55 (m, 1 H, C*H*COH), 3.56 (dd, $^3J_{HH}$ = 9.3 Hz, $^3J_{HH}$ = 4.7 Hz, 1 H, NC*H*), 2.86 ("dt", $^2J_{HH}$ = 10.2 Hz, $^3J_{HH}$ = 6.8 Hz, 1 H, NC*H*$_2$), 2.78 (br s, 1 H, N*H*), 2.62-2.57 (m, 1 H, NC*H*$_2$), 2.28 (s, 6 H, C*H*$_{3(Ar)}$), 2.25 (s, 6 H, C*H*$_{3(Ar)}$), 1.94-1.79 (m, 2 H, C*H*$_{2(Pyr)}$, C*H*$_{2(iBu)}$), 1.61-1.38 (m, 3 H, C*H*$_{(iBu)}$, C*H*$_{2(Pyr)}$), 1.31-1.18 (m, 2 H, C*H*$_{2(Pyr)}$, C*H*$_{2(iBu)}$), 0.95 (d, $^3J_{HH}$ = 6.7 Hz, C*H*$_{3(iBu)}$), 0.86 (d, $^3J_{HH}$ = 6.5 Hz, C*H*$_{3(iBu)}$).

^{13}C{^{1}H} NMR (CDCl$_3$, 101 MHz) δ/ppm: 175.4 (*C*O), 146.7, 145.2 (2 x Ar-*C*), 137.6, 137.3 (2 x Ar-*C*–*C*H$_3$) 128.4, 128.1, 123.5, 123.4 (4 x Ar-*C*H), 80.9 (*C*HCOH), 60.4 (N*C*H), 56.9

---

[i] Product still contained EtOAc as solvent impurity after drying in HV.

($CHCOH$), 47.2 (NCH_2), 37.7 ($CH_{2(iBu)}$), 30.6, 25.7 (2 x $CH_{2(Pyr)}$), 25.5 ($CH_{(iBu)}$), 24.0 ($CH_{3(iBu)}$), 21.7, 21.7 ($CH_{3(iBu)}$, 2 x $CH_{3(Ar)}$)).

FTIR (ATR): 3319w (br), 2954m, 2925m, 2869m, 1638s, 1605m, 1522s, 1461s, 1376m, 1263m, 1151m, 1102m, 1037m, 852s, 734s, 696m, 602m cm^{-1}.

HRMS (ESI, 4500 V, 180 °C) calc. *m/z* for $C_{27}H_{39}N_2O_2$: 423.3006, found: 423.3010 [M+H]$^+$.

EA calc. (%) for $C_{27}H_{38}N_2O_2$: C 76.74, H 9.06, N 6.63; found: C 75.61, H 9.16, N 6.20.[i]

Optical rotation: $[\alpha]_D^{20} = -21.2°$ (c = 0,91, CHCl$_3$).

(S)-N-((S)-1-Hydroxy-4-methyl-1,1-bis(4-(trifluoromethyl)phenyl)pentan-2-yl)pyrrolidine-2-carboxamide (S,S)-50

(S,S)-50
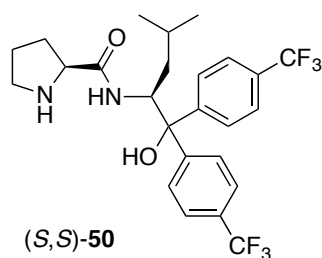
CF$_3$-substituted catalyst **50** was synthesized according to the procedure described for Singh's catalyst **13** with *N*-Cbz-hydroxy-L-proline (203 mg, 0.81 mmol, 1.10 eq.), (*S*)-2-amino-4-methyl-1,1-bis(4-(trifluoromethyl)phenyl)pentan-1-ol (*S*)-**45** (300 mg, 0.74 mmol, 1.00 eq., 73% *ee*), DIPEA (134 mg, 171 μL, 1.04 mmol, 1.40 eq.), EDCCl (199 mg, 1.04 mmol, 1.40 eq.) and HOBt (159 mg, 1.04 mmol, 1.40 eq.) in dry CH$_2$Cl$_2$ (5 mL). After stirring overnight and workup the protected crude (450 mg) was isolated as colorless solid.

The protected crude (450 mg) and Pd/C (10 wt.%, 45 mg) were dissolved in MeOH/CH$_2$Cl$_2$ (3:1, 6 mL) and stirred under H$_2$ atmosphere (1 bar) overnight. The reaction mixture was filtered and the solvent concentrated under reduced pressure to give a mixture of diastereoisomers as colorless solid. Purification by flash column chromatography (SiO$_2$ (two column lengths cyclohexane/EtOAc 1:9 + 1% Et$_3$N before loading), 20 cm x 3.5 cm, cyclohexane/EtOAc 1:9) afforded minor diastereoisomer (*S,R*)-**50** (14 mg, >20:1) and two fractions of the major diastereoisomer (*S,S*)-**50** (148 mg, ca. 6:1; 110 mg, >13:1; overall yield: 272 mg, 73%). The mixed fraction (148 mg) was recrystallized by dropwise addition of EtOAc to a suspension of (*S,S*)-**50** in hot hexane to afford CF$_3$-catalyst (*S,S*)-**50** (93 mg) as pure diastereoisomer (>20:1).

$C_{25}H_{28}F_6N_2O_2$ (502.49 g/mol)

m.**p**.: 173-175 °C.

R$_f$ = 0.10 (cyclohexane/EtOAc 1:9 + 1% Et$_3$N).

---

[i] Product contained hexane applied for semi-preparative HPLC purification.

¹H NMR (CDCl₃, 400 MHz) δ/ppm: 8.19 (d, $^3J_{HH}$ = 7.7 Hz, 1 H, CON*H*), 7.71 (d, $^3J_{HH}$ = 8.3 Hz, 4 H, Ar-*H*), 7.57 (d, $^3J_{HH}$ = 8.3 Hz, 2 H, Ar-*H*), 7.53 (d, $^3J_{HH}$ = 8.3 Hz, 2 H, Ar-*H*), 6.70 (br s, 1 H, O*H*), 4.43 (ddd, $^3J_{HH}$ = 11.2 Hz, $^3J_{HH}$ = 7.7 Hz, $^3J_{HH}$ = 2.1 Hz, C*H*COH), 3.53 (dd, $^3J_{HH}$ = 9.4 Hz, $^3J_{HH}$ = 4.6 Hz, 1 H, NC*H*), 2.82 (dt, $^2J_{HH}$ = 10.2 Hz, $^3J_{HH}$ = 6.9 Hz, 1 H, NC*H*ₐH_b), 2.46 (dt, $^2J_{HH}$ = 10.2 Hz, $^3J_{HH}$ = 6.2 Hz, 1 H, NCHₐ*H*_b), 2.07 (ddd, $^2J_{HH}$ = 14.5 Hz, $^3J_{HH}$ = 11.2 Hz, $^3J_{HH}$ = 3.7 Hz, C*H*ₐH_b(*i*Bu)), 1.91-1.82 (m, 1 H, C*H*₂(Pyr)), 1.68 (br s, 1 H, N*H*), 1.62-1.52 (m, 1 H, C*H*(*i*Bu)), 1.48-1.38 (m, 1 H, C*H*₂(Pyr)), 1.32-1.25 (m, 1 H, C*H*₂(Pyr)), 1.12 (ddd, $^2J_{HH}$ = 14.5 Hz, $^3J_{HH}$ = 10.2 Hz, $^3J_{HH}$ = 2.1 Hz, CHₐ*H*_b(*i*Bu)), 1.06-0.96 (m, 1 H, C*H*₂(Pyr)), 0.89 (d, $^3J_{HH}$ = 6.1 Hz, C*H*₃), 0.88 (d, $^3J_{HH}$ = 6.1 Hz, C*H*₃).

¹³C{¹H} NMR (CD₃OD, 101 MHz) δ/ppm: 176.7 (*C*O), 151.3, 150.8 (2 x Ar-*C*), 130.3, 129.9 (2 x q, $^2J_{CF}$ = 32 Hz, Ar-*C*), 127.7, 127.6 (2 x Ar-*C*H), 126.3, 125.7 (2 x q, $^3J_{CF}$ = 4 Hz, Ar-*C*H), 125.7, 125.6 (2 x q, $^1J_{CF}$ = 271 Hz, *C*F₃), 81.5 (*C*HCOH), 61.3 (N*C*H), 55.0 (*C*HCOH), 48.0 (N*C*H₂), 40.1 (*C*H₂(*i*Bu)), 32.1, 26.8 (2 x *C*H₂(Pyr)), 26.3 (*C*H(*i*Bu)), 24.3, 22.1 (2 x *C*H₃).

¹⁹F NMR (CDCl₃, 376 MHz) δ/ppm: –62.5, –62.6 (2 x C*F*₃).

FTIR (ATR): 3313w (br), 2956w, 2873w, 1646m, 1523m, 1413m, 1324s, 1162m, 1117s, 1070s, 1016m, 836m, 789w, 771m, 604m cm⁻¹.

MS (ESI) *m/z* (%): 503.2 [M+H]⁺.

EA calc. (%) for C₂₅H₂₈F₆N₂O₂: C 59.76, H 5.62, N 5.57; found: C 59.60, H 5.76, N 5.35.

Optical rotation: $[\alpha]_D^{20}$ = –40.3 (c = 0.50, CHCl₃).

(*S*)-*N*-((*R*)-1-Hydroxy-4-methyl-1,1-bis(4-(trifluoromethyl)phenyl)pentan-2-yl)pyrrolidine-2-carboxamide (*S,R*)-50

(*S,R*)-**50**
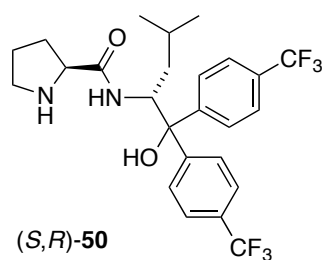
Under an argon atmosphere, Boc-proline (63.9 mg, 297 μmol, 1.20 eq.) were dissolved in dry CH₂Cl₂ (4 mL) and cooled to 0 °C. Et₃N (30.1 mg, 41.2 μL, 297 μmol, 1.20 eq.) and ethyl chloroformate (32.2 mg, 28.3 μL, 297 μmol, 1.20 eq.) were added and stirred for 30 min when a colorless precipitate was formed. (*R*)-2-Amino-4-methyl-1,1-bis(4-(trifluoromethyl)phenyl)pentan-1-ol (*R*)-**45** (100 mg, 247 μmol, 1.00 eq., >98% *ee*) dissolved in dry CH₂Cl₂ (4 mL) was added over 5 min at 0 °C and the resulting solution was allowed to warm to room temperature overnight. HCl in MeOH[i] (1.20 mL, 1.25 M, ca. 6.00 eq.) was directly added into the reaction mixture and stirred at

---

[i] Freshly prepared by dropwise addition of AcCl into dry MeOH and stirred for 1 h at room temperature.

ambient temperature overnight. The solvent was concentrated under reduced pressure, the colorless residue was suspended in EtOAc (20 mL) and 1 M KOH (10 mL) was added under vigorous stirring. The solution was transferred into a separation funnel and the aqueous layer extracted with EtOAc (3 x 10 mL). The combined organic layers were washed with 1 M KOH (10 mL), H_2O (10 mL) and brine (10 mL). The organic layer was dried over $MgSO_4$, filtered and the solvent concentrated under reduced pressure. The crude product was purified by flash column chromatography (SiO_2, 13 cm x 2 cm, cyclohexane/EtOAc 1:9 + 1% Et_3N) to afford catalyst (*S,R*)-**50** (105 mg, 85%) as colorless solid.

$C_{25}H_{28}F_6N_2O_2$ (502.49 g/mol)

m.p.: 197-199 °C.

R_f = 0.18 (cyclohexane/EtOAc 1:9 + 1% Et_3N).

^{1}H NMR (CDCl$_3$, 400 MHz) δ/ppm: 8.02 (d, $^3J_{HH}$ = 8.7 Hz, 1 H, CON*H*), 7.68 (d, $^3J_{HH}$ = 8.3 Hz, 4 H, Ar-*H*), 7.58 (d, $^3J_{HH}$ = 8.4 Hz, 2 H, Ar-*H*), 7.52 (d, $^3J_{HH}$ = 8.3 Hz, 2 H, Ar-*H*), 4.96 (br s, 1 H, O*H*), 4.80 (ddd, $^3J_{HH}$ = 11.0 Hz, $^3J_{HH}$ = 8.7 Hz, $^3J_{HH}$ = 1.9 Hz, C*H*COH), 3.54 (dd, $^3J_{HH}$ = 9.2 Hz, $^3J_{HH}$ = 4.8 Hz, 1 H, NC*H*), 2.87 (dt, $^2J_{HH}$ = 10.3 Hz, $^3J_{HH}$ = 6.5 Hz, 1 H, NC*H*$_a$H$_b$), 2.54 (dt, $^2J_{HH}$ = 10.3 Hz, $^3J_{HH}$ = 6.1 Hz, 1 H, NCH$_a$*H*$_b$), 1.97-1.90 (m, 1 H, C*H*$_{2(Pyr)}$), 1.85 (br s, 1 H, N*H*), 1.73 (ddd, $^2J_{HH}$ = 14.2 Hz, $^3J_{HH}$ = 11.3 Hz, $^3J_{HH}$ = 3.4 Hz, C*H*$_a$H$_{b(iBu)}$), 1.62-1.42 (m, 3 H, C*H*$_{(iBu)}$, C*H*$_{2(Pyr)}$), 1.32-1.23 (m, 1 H, C*H*$_{2(Pyr)}$), 1.12 (ddd, $^2J_{HH}$ = 14.2 Hz, $^3J_{HH}$ = 10.4 Hz, $^3J_{HH}$ = 2.0 Hz, CH$_a$*H*$_{b(iBu)}$), 0.95 (d, $^3J_{HH}$ = 6.5 Hz, C*H*$_3$), 0.87 (d, $^3J_{HH}$ = 6.7 Hz, C*H*$_3$).

^{13}C{^{1}H} NMR (CD$_3$OD, 101 MHz) δ/ppm: 177.3 (*C*O), 151.3, 150.7 (2 x Ar-*C*), 130.3, 129.9 (2 x q, $^2J_{CF}$ = 32 Hz, Ar-*C*), 127.6, 127.5 (2 x Ar-*C*H), 126.3, 125.8 (2 x q, $^3J_{CF}$ = 4 Hz, Ar-*C*H), 125.6, 125.6 (2 x q, $^1J_{CF}$ = 271 Hz, *C*F$_3$), 81.5 (CH*C*OH), 61.3 (N*C*H), 54.4 (*C*HCOH), 47.8 (N*C*H$_2$), 40.4 (*C*H$_{2(iBu)}$), 31.6, 26.7 (2 x *C*H$_{2(Pyr)}$), 26.2 (*C*H$_{(iBu)}$), 24.3, 22.1 (2 x *C*H$_3$).
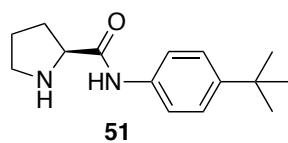
^{19}F NMR (CDCl$_3$, 376 MHz) δ/ppm: –62.6, –62.6 (2 x CF$_3$).

FTIR (ATR): 3299w (br), 2959w, 2876w, 1644m, 1523m, 1414w, 1322s, 1164m, 1122s, 1069s, 1017m, 828m, 774w, 734m, 604m cm^{-1}.

MS (ESI) *m/z* (%): 503.3 [M+H]$^+$.

EA calc. (%) for $C_{25}H_{28}F_6N_2O_2$: C 59.76, H 5.62, N 5.57; found: C 59.99, H 6.07, N 5.60.

Optical rotation: $[\alpha]_D^{20}$ = +2.6° (c = 0.65, CHCl$_3$).

(*S*)-*N*-(4-*tert*-Butylphenyl)pyrrolidine-2-carboxamide 51

Organocatalyst **51** was synthesized according to the procedure described for organocatalyst (*S,R*)-**50** with Boc-proline (258 mg, 1.20 mmol, 1.20 eq.), Et$_3$N (121 mg, 169 µL, 1.20 mmol, 1.20 eq.), ethyl chloroformate (130 mg, 115 µL, 1.20 mmol, 1.20 eq.) and *tert*-butylaniline (151 mg, 1.00 mmol, 1.00 eq.) in dry CH$_2$Cl$_2$ (2 x 5 mL). After 3 h stirring at room temperature HCl in MeOH (4.80 mL, 1.25 M, ca. 6.00 eq.) was directly added into the reaction mixture and stirred at ambient temperature overnight. Workup afforded the crude product (261 mg) as pale yellow foam. The foam was treated with hexane and the resulting precipitate recrystallized from hexane/EtOAc to afford organocatalyst **51** (158 mg, 64%).

C$_{15}$H$_{22}$N$_2$O (246.35 g/mol)

m.**p**.: 93-95 °C.

^{1}H NMR (CDCl$_3$, 400 MHz) δ/ppm: 9.66 (s, 1 H, CON*H*) 7.54-7.50 (m, 2 H, Ar-*H*), 7.35-7.32 (m, 2 H, Ar-*H*), 3.86 (dd, $^3J_{HH}$ = 9.2 Hz, $^3J_{HH}$ = 5.2 Hz, 1 H, NC*H*), 3.08 (dt, $^2J_{HH}$ = 10.3 Hz, $^3J_{HH}$ = 6.8 Hz, 1 H, NC*H*$_a$H$_b$), 2.97 (dt, $^2J_{HH}$ = 10.3 Hz, $^3J_{HH}$ = 6.3 Hz, 1 H, NCH$_a$*H*$_b$), 2.21 (ddt, $^2J_{HH}$ = 12.9 Hz, $^3J_{HH}$ = 9.2 Hz, $^3J_{HH}$ = 7.5 Hz, C*H*$_2$), 2.10 (br s, 1 H, N*H*), 2.10-1.99 (m, 1 H, C*H*$_2$), 1.82-1.68 (m, 2 H, C*H*$_2$), 1.30 (s, 9 H, C(C*H*$_3$)$_3$).

^{13}C{^{1}H} NMR (CDCl$_3$, 101 MHz) δ/ppm: 173.0 (*C*O), 147.1, 135.4 (2 x Ar-*C*), 125.9, 119.3 (2 x Ar-*C*H), 61.1 (N*C*H), 47.5 (N*C*H$_2$), 34.5 (*C*(CH$_3$)$_3$), 31.5 (C(*C*H$_3$)$_3$), 30.9, 26.3 (2 x *C*H$_2$).

FTIR (ATR): 3362w, 3217w, 2959m, 2868w, 1671m, 1612w, 1583m, 1523s, 1404m, 1317w, 1296m, 1243w, 1148w, 1106m, 879w, 835m, 825s, 740m, 626m, 550s cm^{-1}.

MS (ESI) *m/z* (%): 247.2 [M+H]$^+$, 493.5 [2M+H]$^+$.

EA calc. (%) for C$_{15}$H$_{22}$N$_2$O: C 73.13, H 9.00, N 11.37; found: C 73.04, H 8.97, N 11.35.

Optical rotation: $[\alpha]_D^{20}$ = −55.7 (c = 1.00, CHCl$_3$).

(2*R*)-*N*-((1*R*,2*R*)-1,2-Diphenyl-2-((trimethylsilyl)oxy)ethyl)pyrrolidine-2-carboxamide 52
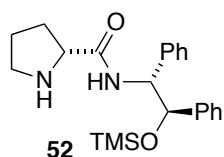
(2*R*)-*N*-((1*R*,2*R*)-2-Hydroxy-1,2-diphenylethyl)pyrrolidine-2-carboxamide **10** (51.9 mg, 167 µmol, 1.00 eq.) and Et$_3$N (23.7 mg, 32.9 µL, 234 µmol, 1.40 eq.) were dissolved in dry CH$_2$Cl$_2$ at −78 °C. Trimethylsilyl trifluoromethanesulfonate (48.8 mg, 39.8 µL, 217 µmol, 1.30 eq.) was added and the solution allowed to warm to room temperature. The reaction mixture was quenched

with water (5 mL) and extracted with CH_2Cl_2 (3 x 10 mL). The crude product was purified by flash column chromatography (7 cm x 3.5 cm, EtOAc + 1% Et_3N) to afford TMS-protected catalyst **52** (55.8 mg, 87%) as pale yellow solid.

$C_{22}H_{30}N_2O_2Si$ (382.58 g/mol)

m.p.: 74-75 °C.

R_f = 0.12 (EtOAc + 1% Et_3N).

^{1}H NMR (CDCl$_3$, 400 MHz) δ/ppm: 8.40 (d, $^3J_{HH}$ = 8.8 Hz, 1 H, CON*H*), 7.33-7.22 (m, 10 H, Ar-*H*), 5.08 (dd, $^3J_{HH}$ = 8.9 Hz, $^3J_{HH}$ = 2.6 Hz, 1 H, NC*H*Ph), 4.91 (d, $^3J_{HH}$ = 2.6 Hz, 1 H, C*H*OSi), 3.58 (dd, $^3J_{HH}$ = 9.1 Hz, $^3J_{HH}$ = 5.0 Hz, 1 H, NC*H*), 3.07-2.97 (m, 2 H, NC*H*$_2$), 2.28 (br s, 1 H, N*H*), 2.05-1.96 (m, 1 H, C*H*$_2$), 1.80-1.64 (m, 3 H, C*H*$_2$, C*H*$_2$), –0.20 (s, 9 H, Si(C*H*$_3$)$_3$).

^{13}C{^{1}H} NMR (CDCl$_3$, 101 MHz) δ/ppm: 174.3 (*C*O), 147.1, 135.4 (2 x Ar-*C*), 128.2, 128.0, 127.5, 127.4, 127.2, 127.0 (6 x Ar-*C*H), 77.9 (*C*HOSi), 60.7, 59.2 (N*C*H and N*C*HPh), 47.4 (N*C*H$_2$), 30.8, 26.2 (*C*H$_2$), –0.34 (Si(*C*H$_3$)$_3$).

FTIR (ATR): 3317w, 2958w, 2867w, 1667s, 1496s, 1450m, 1366w, 1290w, 1251m, 1202w, 1092m, 1063m, 1030w, 964w, 871s, 838s, 755s, 698s, 614m cm^{-1}.

HRMS (ESI, 4500 V, 180 °C) calc. (*m/z*) for $C_{22}H_{31}N_2O_2Si^+$: 383.2149, found: 383.2150 [M+H]$^+$.

Optical rotation: $[\alpha]_D^{20}$ = +9.8° (c = 0.37, CHCl$_3$).

(*S,S*)-2-Amino-*N*-(1-hydroxy-4-methyl-1,1-diphenylpentan-2-yl)-4-methylpentanamide 53
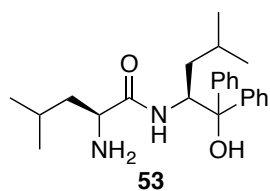
N-Cbz-L-leucine (220 mg, 721 μmol, 1.10 eq.) and Et_3N (73.0 mg, 101 μL, 721 μmol, 1.10 eq.) were dissolved in dry THF (300 μL) and cooled to 0 °C. Ethyl chloroformate (78.3 mg, 69 μL, 721 μmol, 1.10 eq.) was added dropwise whereupon a white precipitate was formed. The reaction mixture was stirred for 30 min at 0 °C followed by addition of (*S*)-2-amino-4-methyl-1,1-diphenylpentan-1-ol **30** (177 mg, 656 μmol, 1.00 eq.). The reaction mixture was stirred for 16 h at room temperature and additional 3 h under reflux. The reaction mixture was diluted with EtOAc and filtered over a plug of celite. The solvent was removed under reduced pressure to afford colorless foam, which was purified by flash column chromatography (SiO$_2$, 20 cm x 3.5 cm, cyclohexane/EtOAc 5:1, R_f = 0.17) to give the Cbz-protected catalyst (240 mg).

The protected catalyst (240 mg) and Pd/C (5 wt.%, 12 mg) were dissolved in MeOH (7 mL) and stirred under H_2 atmosphere (1 bar) for 4 h until TLC indicate complete consumption of the starting material. The reaction mixture was filtered through a plug of celite and the solvent concentrated under reduced pressure. The resulting foam was purified by recrystallization from hexane/EtOAc (dropwise addition of EtOAc into hot hexane) to afford primary amine **53** (98 mg, 39%) as a colorless solid. Analytical data are in accordance with literature data.[61, 126]

$C_{24}H_{34}N_2O_2$ (382.54 g/mol)

m.p.: 179-181 °C (Lit.[61] 180-182 °C).

R_f = 0.69 (EtOAc/MeOH 20:1).

^{1}H NMR (CDCl$_3$, 400 MHz) δ/ppm: 7.55-7.52 (m, 4 H, Ar-*H*), 7.38 (d, $^3J_{HH}$ = 8.9 Hz, 1 H, N*H*), 7.31 (t, $^3J_{HH}$ = 7.7 Hz, 2 H, Ar-*H*), 7.27-7.18 (m, 3 H, Ar-*H*), 7.16-7.11 (m, 1 H, Ar-*H*), 4.80 (ddd, $^3J_{HH}$ = 11.2 Hz, $^3J_{HH}$ = 8.9 Hz, $^3J_{HH}$ = 2.0 Hz, 1 H, NHC*H*), 4.47 (br s, 1 H, O*H*), 3.15 (dd, $^3J_{HH}$ = 9.7 Hz, $^3J_{HH}$ = 4.4 Hz, 1 H, NH$_2$C*H*), 1.69 (ddd, $^2J_{HH}$ = 14.2 Hz, $^3J_{HH}$ = 11.2 Hz, $^3J_{HH}$ = 3.5 Hz, 1 H, C*H*$_2$), 1.62-1.53 (m, 1 H, C*H*), 1.51-1.20 (m, 5 H, N*H*$_2$, C*H*, C*H*$_2$), 0.97-0.90 (m, 4 H, C*H*$_3$, C*H*$_2$), 0.86 (d, $^3J_{HH}$ = 6.7 Hz, 3 H, CH$_3$), 0.84 (d, $^3J_{HH}$ = 6.7 Hz, 3 H, C*H*$_3$), 0.84 (d, $^3J_{HH}$ = 6.5 Hz, 3 H, C*H*$_3$).

^{13}C{^{1}H} NMR (CDCl$_3$, 101 MHz) δ/ppm: 176.3 (*C*O), 146.3, 145.2 (2 x Ar-*C*), 128.5, 128.1, 127.0, 126.7, 125.8, 125.8 (6 x Ar-*C*H), 81.2 (*C*OH), 55.6, 53.7 (2 x *C*H), 44.0, 38.5 (2 x *C*H$_2$), 25.4, 24.9, 24.1, 23.4, 21.7, 21.5 (2 x *C*H, 4 x *C*H$_3$).

Optical rotation: $[\alpha]_D^{20}$ = –46.2° (c = 0.60, DMSO) (Lit.[61] $[\alpha]_D^{20}$ = –44° (c = 1.00, DMSO)).

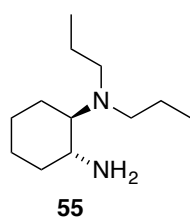### *N*-((1*R*,2*R*)-2-aminocyclohexyl)acetamide 54
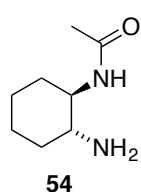
Ethyl acetimidate hydrochloride (687 mg, 5.56 mmol, 2.00 eq.) and (1*R*,2*R*)-1,2-diaminocyclohexane (317 mg, 2.78 mmol, 1.00 eq.) were dissolved in dry EtOH (6 mL) at 0 °C. The colorless solution was allowed to warm to room temperature and stirred overnight. 1 M NaOH (15 mL) was added and the mixture extracted with 5% MeOH in CH$_2$Cl$_2$ (3 x 20 mL). The combined organic layers were dried over MgSO$_4$, filtered and the solvent concentrated under reduced pressure. The residue was dissolved in a mixture of EtOH/H$_2$O (1:1, 28 mL) and stirred under reflux for 8 h. The solvent was evaporated to afford amide **54** (390 mg, 90%) as colorless solid, which was used for the next step without further purification. Analytical data are in accordance with literature data.[127]

$C_8H_{16}N_2O$ (156.23 g/mol)

¹H NMR (CDCl₃, 400 MHz) δ/ppm: 5.62 (d, $^3J_{HH}$ = 7.9 Hz, 1 H, N*H*), 3.55-3.47 (m, 1 H, C*H*), 2.41-2.34 (m, 1 H, C*H*), 2.00 (s, 3 H, C*H₃*), 2.00-1.93 (m, 2 H, C*H₂*), 1.80 (br s, 2 H, N*H₂*), 1.74-1.67 (m, 2 H, C*H₂*), 1.38-1.05 (m, 4 H, C*H₂*).

(1*R*,2*R*)-*N*,*N*-Dipropylcyclohexane-1,2-diamine 55

N-((1*R*,2*R*)-2-Aminocyclohexyl)acetamide **54** (280 mg, 1.79 mmol, 1.00 eq.) and propionaldehyde (520 mg, 0.65 mL, 8.96 mmol, 5.00 eq.) were dissolved in CH₃CN (10 mL) and H₂O (0.5 mL). The colorless solution was stirred for 15 min followed by slow addition of sodium cyanoborohydride (237 mg, 3.76 mmol, 2.10 eq.). After additional 15 min AcOH (0.5 mL) was added dropwise. After 2 h, the volatiles were removed in HV and the residue was dissolved in EtOAc (10 mL) and 1 M NaOH (2 mL). The layers were separated and the organic layer was washed with 1 M NaOH (2 mL) and brine (2 mL). The organic layer was dried over MgSO₄, filtered and the solvent concentrated under reduced pressure.

The residue was taken up in 4 M aqueous HCl (8 mL) and stirred under reflux for 15 h. After cooling to room temperature, the resulting solution was basified with 4 M NaOH (pH ≈ 13). The basic layer was extracted with CH₂Cl₂ (3 x 20 mL) and the combined organic layers were dried over MgSO₄, filtered and the solvent concentrated under reduced pressure to afford a black oil. The crude product was purified by bulb-to-bulb distillation (160 °C, 0.4 mbar) to afford the diamine **55** (261 mg, 73%) as colorless oil. Analytical data are in accordance with literature data.[128]

$C_{12}H_{26}N_2$ (198.35 g/mol)

¹H NMR (CDCl₃, 400 MHz) δ/ppm: 2.54 (td, $^3J_{HH}$ = 10.3 Hz, $^3J_{HH}$ = 4.2 Hz, 1 H, C*H*), 2.42-2.34 (m, 2 H, NC*H₂*), 2.28 (ddd, $^2J_{HH}$ = 12.8 Hz, $^3J_{HH}$ = 8.1 Hz, $^3J_{HH}$ = 4.7 Hz, 2 H, NC*H₂*), 2.08-1.95 (m, 2 H, C*H₂*), 1.76-1.63 (m, 5 H, C*H*, C*H₂*, N*H₂*), 1.49-1.33 (m, 4 H, C*H₂*), 1.24-1.00 (m, 4 H, C*H₂*), 0.86 (t, $^3J_{HH}$ = 7.3 Hz, 6 H, C*H₃*).

¹³C{¹H} NMR (CDCl₃, 101 MHz) δ/ppm: 67.1, 52.2, 51.5, 35.3, 26.2, 25.3, 23.0, 22.6, 12.1.

MS (ESI) *m/z* (%): 199.2 [M+H]⁺.ⁱ

ⁱ Impurity at *m/z* 241 detected by ESI-MS, which was not completely removed by several purification methods.

6.2.5 Synthesis of Catalyst Mixtures

General Procedure 2 (GP2)

Under an argon atmosphere, *N*-cbz-L-proline (27.4 mg, 0.11 mmol, 1.10 eq.) was dissolved in dry DMF (0.5 mL) and DIPEA (14.2 mg, 18.2 µL, 0.11 mmol, 1.10 eq.) was added. The solution was cooled to 0 °C and HATU (41.8 mg, 0.11 mmol, 1.10 eq.) was added. The resulting pale yellow solution was stirred for 15 min at 0 °C followed by addition of a mixture of the corresponding aminoalcohols (0.10 mmol, 1.00 eq.). The solution was allowed to warm to room temperature and stirred for 5 h. The reaction mixture was diluted with EtOAc (10 mL) washed with 0.1 M HCl (5 mL), saturated $NaHCO_3$ solution (5 mL) and brine (3 x 5 mL). The organic layer was dried over $MgSO_4$, filtered and the solvent concentrated under reduced pressure. The crude product was adsorbed onto silica, filtered through a plug of silica gel (2 cm x 2 cm) and eluted with cyclohexane/EtOAc (1:1, 100 mL). Evaporation of the solvent afforded a colorless solid or foam.

The protected crude product and Pd/C (10 wt.%, ca. 5 mg) were dissolved in MeOH (2 mL) and stirred under H_2 atmosphere (1 bar) overnight. The reaction mixture was filtered through a syringe filter and the solvent concentrated under reduced pressure. The crude product was subjected without further purifications to ESI-MS back reaction analysis.

General Procedure 3 (GP3)

Under an argon atmosphere, Boc-proline (25.8 mg, 0.12 mmol, 1.20 eq.) was dissolved in dry CH_2Cl_2 (0.5 mL) and cooled to 0 °C. Et_3N (12.1 mg, 16.6 µL, 0.12 mmol, 1.20 eq.) and ethyl chloroformate (13.0 mg, 11.4 µL, 0.12 mmol, 1.20 eq.) were added subsequently and the solution stirred for 30 min. An equimolar mixture of aminoalcohols (0.10 mmol, 1.00 eq.) dissolved in dry CH_2Cl_2 (0.5 mL) was added over 5 min at 0 °C and the resulting solution was allowed to warm to room temperature overnight. HCl in MeOH[i] (0.5 mL, 1.25 M, ca. 6.00 eq.) was directly added into the reaction mixture and stirred at ambient temperature overnight. The solvent was concentrated under reduced pressure, the colorless residue was suspended in EtOAc (20 mL) and 1 M KOH (10 mL) was added under vigorous stirring. The solution was transferred into a separation funnel and the aqueous layer extracted with EtOAc (3 x 10 mL). The combined organic layers were washed with 1 M KOH (10 mL), H_2O (10 mL) and brine

---

[i] Freshly prepared by dropwise addition of AcCl into dry MeOH and stirred for 1 h at room temperature.

(10 mL). The organic layer was dried over MgSO$_4$, filtered and the solvent concentrated under reduced pressure. The crude product was subjected without further purifications to ESI-MS back reaction analysis.

(*S*)-*N*-(2-Hydroxy-2,2-diphenylethyl)pyrrolidine-2-carboxamide 14
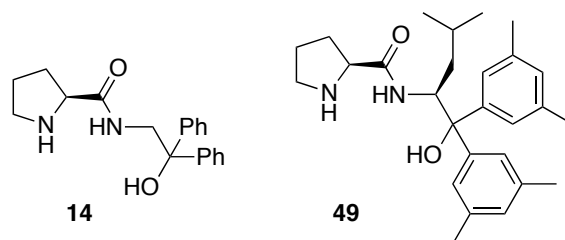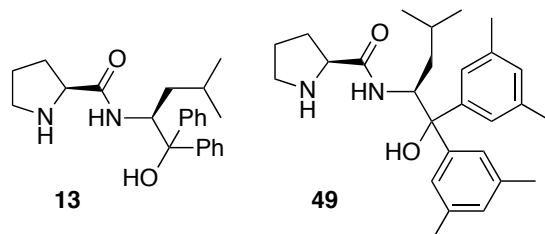**(*S*)-*N*-((*S*)-1,1-Bis(3,5-dimethylphenyl)-1-hydroxy-4-methylpentan-2-yl)pyrrolidine-2-carboxamide 49**
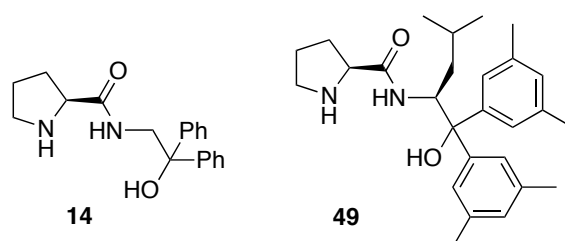
The crude mixture of catalysts was synthesized according to **GP2** with an equimolar mixture of 2-amino-1,1-diphenylethanol **46** (10.6 mg, 50.0 µmol, 0.50 eq.) and (*S*)-2-amino-1,1-bis(3,5-dimethylphenyl)-4-methylpentan-1-ol **44** (16.3 mg, 50.0 µmol, 0.50 eq.).

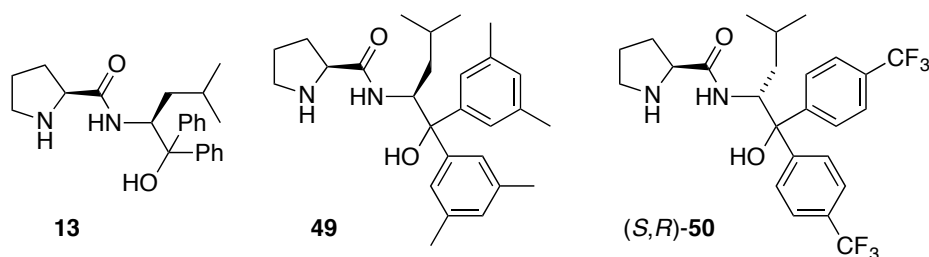C$_{27}$H$_{38}$N$_2$O$_2$ (422.60 g/mol) and C$_{19}$H$_{22}$N$_2$O$_2$ (310.40 g/mol)
MS (ESI) *m/z* (%): 311.2 [**14**-M+H]$^+$, 423.4 [**49**-M+H]$^+$.

(*S*)-*N*-(2-Hydroxy-2,2-diphenylethyl)pyrrolidine-2-carboxamide 14
(*S*)-*N*-((*S*)-1,1-Bis(3,5-dimethylphenyl)-1-hydroxy-4-methylpentan-2-yl)pyrrolidine-2-carboxamide 49

The crude mixture of catalysts was synthesized according to **GP2** with an mixture of 2-amino-1,1-diphenylethanol **46** (12.8 mg, 60.0 µmol, 0.60 eq.) and (*S*)-2-amino-1,1-bis(3,5-dimethylphenyl)-4-methylpentan-1-ol **44** (13.0 mg, 40.0 µmol, 0.40 eq.).

C$_{27}$H$_{38}$N$_2$O$_2$ (422.60 g/mol) and C$_{19}$H$_{22}$N$_2$O$_2$ (310.40 g/mol)
MS (ESI) *m/z* (%): 311.2 [**14**-M+H]$^+$, 333.2 [**14**-M+Na]$^+$, 423.4 [**49**-M+H]$^+$.

(*S*)-*N*-((*S*)-1-Hydroxy-4-methyl-1,1-diphenylpentan-2-yl)pyrrolidine-2-carboxamide (Singh's catalyst) 13

(*S*)-*N*-((*S*)-1,1-Bis(3,5-dimethylphenyl)-1-hydroxy-4-methylpentan-2-yl)pyrrolidine-2-carboxamide 49
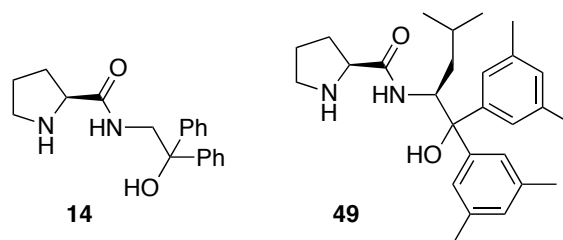

The crude mixture of catalysts was synthesized according to **GP2** with an equimolar mixture of (*S*)-2-amino-4-methyl-1,1-diphenylpentan-1-ol **30** (13.5 mg, 50.0 µmol, 0.50 eq.) and (*S*)-2-amino-1,1-bis(3,5-dimethylphenyl)-4-methylpentan-1-ol **44** (16.3 mg, 50.0 µmol, 0.50 eq.).

$C_{23}H_{30}N_2O_2$ (366.50 g/mol) and $C_{27}H_{38}N_2O_2$ (422.60 g/mol)
MS (ESI) *m/z* (%): 367.2 [**13**-M+H]$^+$, 423.2 [**49**-M+H]$^+$.

(*S*)-*N*-((*S*)-1-Hydroxy-4-methyl-1,1-diphenylpentan-2-yl)pyrrolidine-2-carboxamide (Singh's catalyst) 13

(*S*)-*N*-((*S*)-1,1-Bis(3,5-dimethylphenyl)-1-hydroxy-4-methylpentan-2-yl)pyrrolidine-2-carboxamide 49

(*S*)-*N*-((*R*)-1-Hydroxy-4-methyl-1,1-bis(4-(trifluoromethyl)phenyl)pentan-2-yl)pyrrolidine-2-carboxamide (*S*,*R*)-50

The crude mixture of catalysts was synthesized according to **GP2** with an equimolar mixture of (*S*)-2-amino-4-methyl-1,1-diphenylpentan-1-ol **30** (8.9 mg, 33.3 µmol, 0.33 eq.), (*S*)-2-amino-1,1-bis(3,5-dimethylphenyl)-4-methylpentan-1-ol **44** (10.7 mg, 33.3 µmol, 0.33 eq.) and (*R*)-2-amino-4-methyl-1,1-bis(4-(trifluoromethyl)phenyl)pentan-1-ol (*R*)-**45** (13.4 mg, 33.3 µmol, 0.33 eq.).

$C_{23}H_{30}N_2O_2$ (366.50 g/mol), $C_{27}H_{38}N_2O_2$ (422.60 g/mol) and $C_{25}H_{28}F_6N_2O_2$ (502.49 g/mol)

MS (ESI) *m/z* (%): 367.2 [**13**-M+H]$^+$, 423.2 [**49**-M+H]$^+$, 503.2 [**50**-M+H]$^+$.

(*S*)-*N*-(2-Hydroxy-2,2-diphenylethyl)pyrrolidine-2-carboxamide 14

(*S*)-*N*-((*S*)-1,1-Bis(3,5-dimethylphenyl)-1-hydroxy-4-methylpentan-2-yl)pyrrolidine-2-carboxamide 49
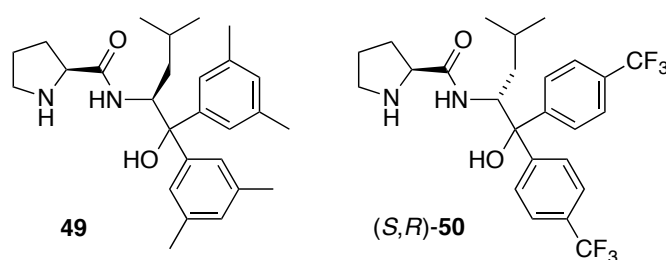

The crude mixture of catalysts was synthesized according to **GP3** with an equimolar mixture of 2-amino-1,1-diphenylethanol **46** (10.7 mg, 0.05 mmol, 0.50 eq.) and (*S*)-2-amino-1,1-bis(3,5-dimethylphenyl)-4-methylpentan-1-ol **44** (16.3 mg, 0.05 mmol, 0.50 eq.).

$C_{27}H_{38}N_2O_2$ (422.60 g/mol) and $C_{19}H_{22}N_2O_2$ (310.40 g/mol)

MS (ESI) *m/z* (%): 311.2 [**14**-M+H]$^+$, 405.2 [**49**-M–OH]$^+$, 423.4 [**49**-M+H]$^+$.

(*S*)-*N*-((*S*)-1,1-Bis(3,5-dimethylphenyl)-1-hydroxy-4-methylpentan-2-yl)pyrrolidine-2-carboxamide 49

(*S*)-*N*-((*R*)-1-Hydroxy-4-methyl-1,1-bis(4-(trifluoromethyl)phenyl)pentan-2-yl)pyrrolidine-2-carboxamide (*S*,*R*)-50

The crude mixture of catalysts was synthesized according to **GP3** with an equimolar mixture of (*S*)-2-amino-1,1-bis(3,5-dimethylphenyl)-4-methylpentan-1-ol **44** (16.3 mg, 50.0 μmol, 0.50 eq.) and (*R*)-2-amino-4-methyl-1,1-bis(4-(trifluoromethyl)phenyl)pentan-1-ol (*R*)-**45** (20.3 mg, 50.0 μmol, 0.50 eq.).

215

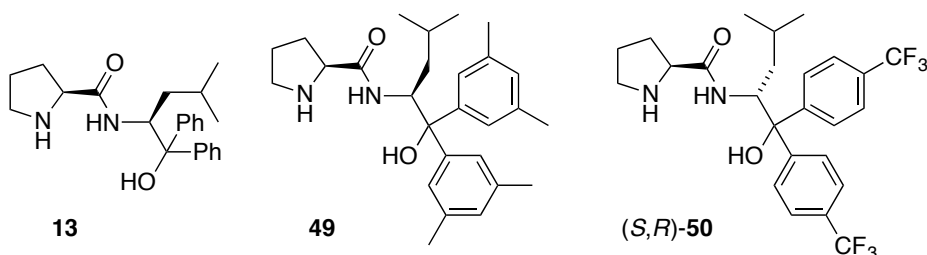C$_{27}$H$_{38}$N$_2$O$_2$ (422.60 g/mol) and C$_{25}$H$_{28}$F$_6$N$_2$O$_2$ (502.49 g/mol)

MS (ESI) *m/z* (%): 405.2 [**49**-M–OH]$^+$, 423.4 [**49**-M+H]$^+$, 503.2 [**50**-M+H]$^+$.

(*S*)-*N*-((*S*)-1-Hydroxy-4-methyl-1,1-diphenylpentan-2-yl)pyrrolidine-2-carboxamide (Singh's catalyst) 13

(*S*)-*N*-((*S*)-1,1-Bis(3,5-dimethylphenyl)-1-hydroxy-4-methylpentan-2-yl)pyrrolidine-2-carboxamide 49

(*S*)-*N*-((*R*)-1-Hydroxy-4-methyl-1,1-bis(4-(trifluoromethyl)phenyl)pentan-2-yl)pyrrolidine-2-carboxamide (*S,R*)-50

The crude mixture of catalysts was synthesized according to **GP3** with an equimolar mixture of (*S*)-2-amino-4-methyl-1,1-diphenylpentan-1-ol **30** (8.9 mg, 33.3 μmol, 0.33 eq.), (*S*)-2-amino-1,1-bis(3,5-dimethylphenyl)-4-methylpentan-1-ol **44** (10.7 mg, 33.3 μmol, 0.33 eq.) and (*R*)-2-amino-4-methyl-1,1-bis(4-(trifluoromethyl)phenyl)pentan-1-ol (*R*)-**45** (13.4 mg, 33.3 μmol, 0.33 eq.).

C$_{23}$H$_{30}$N$_2$O$_2$ (366.50 g/mol), C$_{27}$H$_{38}$N$_2$O$_2$ (422.60 g/mol) and C$_{25}$H$_{28}$F$_6$N$_2$O$_2$ (502.49 g/mol)

MS (ESI) *m/z* (%): 367.2 [**13**-M+H]$^+$, 405.2 [**49**-M–OH]$^+$, 423.2 [**49**-M+H]$^+$, 503.2 [**50**-M+H]$^+$.

6.2.6 Preparative Organocatalyzed Aldol Reactions

General procedure for the preparative forward reaction under ESI-MS screening conditions without additive
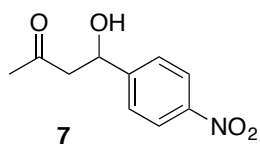
para-Nitrobenzaldehyde (15.1 mg, 0.10 mmol, 1.00 eq.) and the corresponding catalyst (0.01 mmol, 10 mol%) were dissolved in the reaction solvent (0.92 mL) and acetone (73.5 μL, 1.00 mmol, 10 eq.) was added. The solution was stirred for 24 h at room temperature. An aliquot of the reaction mixture was either directly filtered through a pipette column of silica (cyclohexane/EtOAc 1:1) or purified by preparative TLC (glass plate coated with silica, cyclohexane/EtOAc 3:2). The crude product was analyzed by HPLC to determine the enantioselectivity.

General procedure for the preparative forward reaction under ESI-MS screening conditions with solid additives

para-Nitrobenzaldehyde (15.1 mg, 0.10 mmol, 1.00 eq.), the corresponding catalyst (0.01 mmol, 10 mol%) and the corresponding additive (0.01-0.03 mmol, 10-30 mol%) were dissolved in the reaction solvent (0.92 mL) and acetone (73.5 μL, 1.00 mmol, 10 eq.) was added. The solution was stirred for 24 h at room temperature. An aliquot of the reaction mixture was either directly filtered through a pipette column of silica (eluent cyclohexane/EtOAc 1:1) or purified by preparative TLC (glass plate coated with silica, cyclohexane/EtOAc 3:2). The crude product was analyzed by HPLC to determine the enantioselectivity.

General procedure for the preparative forward reaction under ESI-MS screening conditions with acetic acid as additive

para-Nitrobenzaldehyde (15.1 mg, 0.10 mmol, 1.00 eq.) and the corresponding catalyst (0.01 mmol, 10 mol%) were dissolved in the reaction solvent (0.92 mL). AcOH (6.0 mg, 5.7 μL, 0.10 mmol, 100 mol%) and acetone (73.5 μL, 1.00 mmol, 10 eq.) were added subsequently. The solution was stirred for 24 h at room temperature. An aliquot of the reaction mixture was either directly filtered through a pipette column of silica (eluent cyclohexane/EtOAc 1:1) or purified by preparative TLC (glass plate coated with silica,

cyclohexane/EtOAc 3:2). The crude product was analyzed by HPLC to determine the enantioselectivity.

**General procedure for the preparative forward reaction under ESI-MS screening conditions at 0 °C in CH₃CN with *tert*-butyl-*para*-nitrophenol or without additive**

para-Nitrobenzaldehyde (15.1 mg, 0.10 mmol, 1.00 eq.), the corresponding catalyst (0.01 mmol, 10 mol%) (and *tert*-BNP (2.5 mg, 0.01 mmol, 10 mol%)) were dissolved in CH₃CN (0.92 mL) and cooled to 0 °C. Acetone (73.5 µL, 1.00 mmol, 10 eq.) was added. The solution was stirred for 24-48 h at 0 °C. An aliquot of the reaction mixture was directly filtered through a pipette column of silica (eluent cyclohexane/EtOAc 1:1). The crude product was analyzed by HPLC to determine the enantioselectivity.

General procedure for the preparative forward reaction (Singh's protocol)[44b]

The corresponding catalyst (10 mol%) was dissolved in dry acetone (1 M) at the indicated reaction temperature. The mixture was stirred for 30 min and *para*-nitrobenzaldehyde (0.50 mmol or 1.00 mmol, 1.00 eq.) was added. The reaction mixture was stirred for the indicated time and quenched with NH₄Cl. The aqueous layer was extracted three times with EtOAc and the combined organic layers were washed with brine. The organic layer was dried over MgSO₄, filtered and the solvent concentrated under reduced pressure. The crude product was analyzed by ¹H NMR and HPLC. Purification by flash column chromatography (SiO₂, cyclohexane/EtOAc 3:2) afforded product **7**. Alternatively, an aliquot of the reaction mixture was directly purified by preparative TLC (glass plate coated with silica, cyclohexane/EtOAc 3:2) and analyzed by HPLC.

$C_{10}H_{11}NO_4$ (209.20 g/mol)

HPLC (*Daicel* Chiralcel AS-H, heptane/*i*PrOH 70:30, 0.8 mL/min, 20 °C, 266 nm): $t_R((R)$-**7**) = 15.9 min, $t_R((S)$-**7**) = 19.0 min.

General Procedure for the aldol reaction in water (Berkessel's protocol):[52] (*R*)-4-(3-Chlorophenyl)-4-hydroxybutan-2-one 17
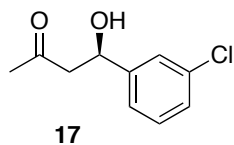
A mixture of 3-chlorobenzaldehyde (70.3 mg, 56.6 µL, 500 µmol, 1.00 eq.), Singh's catalyst **13** (916 µg, 2.5 µmol, 0.5 mol%) or organocatalyst **13** (916 µg, 2.5 µmol, 0.5 mol%) and acetone (262 mg, 331 µL, 4.50 mmol, 9.00 eq.) in brine (0.33 mL) was stirred at room temperature for 26 h. The reaction mixture was extracted with CH_2Cl_2 (3 x 2 mL). The combined organic layers were dried over $MgSO_4$, filtered and the solvent concentrated under reduced pressure. The pale red oil was directly subjected to HPLC analysis on a chiral stationary phase on a chiral stationary phase. Analytical data are in accordance with literature data.[44b]

$C_{10}H_{11}ClO_2$ (198.65 g/mol)

^{1}H NMR (CDCl$_3$, 400 MHz) δ/ppm: 7.38-7.36 (m, 1 H, Ar-*H*), 7.29-7.21 (m, 3 H, Ar-*H*), 5.13 (dd, $^3J_{HH}$ = 7.9 Hz, $^3J_{HH}$ = 4.5 Hz, 1 H, C*H*OH), 3.37 (br s, 1 H, O*H*), 2.85-2.82 (m, 2 H, C*H*$_2$), 2.20 (s, 3 H, C*H*$_3$).

^{13}C{^{1}H} NMR (CDCl$_3$, 101 MHz) δ/ppm: 208.8 (*C*O), 145.0, 134.4 (Ar-*C*), 129.9, 127.8, 125.9, 123.6 (Ar-*C*H), 69.2 (*C*OH), 51.8 (*C*H$_2$), 30.8 (*C*H$_3$).

HPLC (*Daicel*, Chiralpak AD-H, heptane/*i*PrOH 95:5, 1.0 mL/min, 25 °C, 220 nm): t_R((*R*)-**17**) = 14.5 min, t_R((*S*)-**17**) = 16.7 min.

6.2.7 ESI-MS Back Reaction Screening

General remarks

ESI-MS spectra were measured on a Varian 1200L Quadrupol MS/MS spectrometer using mild desolvation conditions (50 V capillary voltage, 100 °C drying gas temperature). The samples were diluted immediately with MeOH or CH_3CN prior to their analysis. Every spectrum consisted of at least 30 scans and the selectivity was calculated from the ratios of the peak heights of the major isotopomers of the [12]C- and ^{13}C-enamines.

General procedure for the ESI-MS back reaction screening in MeOH or CH₃CN without additive

A GC-vial was charged with the corresponding organocatalyst (1.00 µmol or 2.00 µmol, 10 mol%) and an equimolar mixture of (*R*)-(+)-**7** (1.05 mg, 5.00 µmol or 2.09 mg, 10.0 µmol, 0.50 eq.) and (*R*)-(−)-**29** (1.06 mg, 5.00 µmol or 2.12 mg, 10.0 µmol, 0.50 eq.) or with the inversed labeled combination ((*S*)-(−)-**7** and (*S*)-(+)-**29**), respectively. This mixture was dissolved in the corresponding solvent (100 µL or 200 µL, 0.1 M) and stirred for 5-30 min at room temperature. The reaction mixture was directly diluted with the corresponding reaction solvent (1 mL) and some drops of AcOH (3-10 µL) were added. This mixture was subjected to ESI-MS analysis.

General procedure for the ESI-MS back reaction screening in CH₃CN with additive

A GC-vial was charged with the corresponding organocatalyst (1.00 µmol or 2.00 µmol, 10 mol%), the additive (10-30 mol%) and an equimolar mixture of (*R*)-(+)-**7** (1.05 mg, 5.00 µmol or 2.09 mg, 10.0 µmol, 0.50 eq.) and (*R*)-(−)-**29** (1.06 mg, 5.00 µmol or 2.12 mg, 10.0 µmol, 0.50 eq.) or with the inversed labeled combination ((*S*)-(−)-**7** and (*S*)-(+)-**29**), respectively. This mixture was dissolved in CH₃CN (100 µL or 200 µL, 0.1 M) and stirred for 5-30 min at room temperature. The reaction mixture was directly diluted with CH₃CN (1 mL) and subjected to ESI-MS analysis.

General procedure for the ESI-MS back reaction screening in MeOH or CH₃CN with AcOH as additive

A GC-vial was charged with the corresponding organocatalyst (2.00 µmol, 10 mol%) and an equimolar mixture of (*R*)-(+)-**7** (2.09 mg, 10.0 µmol, 0.50 eq.) and (*R*)-(−)-**29** (1.06 mg or 2.12 mg, 10.0 µmol, 0.50 eq.) or with the inversed labeled combination ((*S*)-(−)-**7** and (*S*)-(+)-**29**), respectively. This mixture was dissolved in the corresponding solvent (200 µL, 0.1 M) and AcOH (10 mol% or 100 mol%) and stirred for 5-30 min at room temperature. The reaction mixture was directly diluted with the corresponding reaction solvent (1 mL) and subjected to ESI-MS analysis.

General procedure for the ESI-MS back reaction screening in CH$_3$CN at 0 °C with or without additive

A GC-vial was charged with the corresponding organocatalyst (2.00 µmol, 10 mol%), (*tert*-BNP (503 µg, 2.00 µmol, 10 mol%)) and an equimolar mixture of (*R*)-(+)-**7** (2.09 mg, 10.0 µmol, 0.50 eq.) and (*R*)-(−)-**29** (2.12 mg, 10.0 µmol, 0.50 eq.) or with the inversed labeled combination ((*S*)-(−)-**7** and (*S*)-(+)-**29**), respectively. This mixture was dissolved in CH$_3$CN (200 µL, 0.1 M) and stirred for 30 min at 0 °C. The reaction mixture was frozen in N$_{2(l)}$ and diluted with precooled CH$_3$CN (1 mL, ca. −30 °C) (without additive some drops of AcOH (3-10 µL) were added). This mixture was subjected to ESI-MS analysis.

Procedure for the ESI-MS back reaction screening with low substrate amounts

A GC-vial was charged with an equimolar mixture of (*S*)-(+)-**7** (209 µg, 1.0 µmol, 0.50 eq.) and (*S*)-(−)-**29** (212 µg, 1.0 µmol, 0.50 eq.). A 0.01 M solution of *tert*-BNP (10 µL, 5 mol%) and a 0.01 M solution Singh's catalyst **13** (10 µL, 5 mol%), both in CH$_3$CN, were added subsequently. The reaction mixture was shaken for 5 min, diluted with CH$_3$CN (1 mL) and subjected to ESI-MS analysis.

General procedure for the ESI-MS back reaction screening in CH$_3$CN with catalyst mixtures

A GC-vial was charged with the crude mixture of catalysts (average molecular weight of all catalysts) or an equimolar mixture of organocatalysts (1.00 µmol or 2.00 µmol, 10 mol%), *tert*-BNP (251 µg, 1.00 µmol or 503 µg, 2.00 µmol, 10 mol%) and an equimolar mixture of (*R*)-(+)-**7** (1.05 mg, 5.00 µmol or 2.09 mg, 10.0 µmol, 0.50 eq.) and (*R*)-(−)-**29** (1.06 mg, 5.00 µmol or 2.12 mg, 10.0 µmol, 0.50 eq.) or the inversed labeled combination ((*S*)-(−)-**7** and (*S*)-(+)-**29**), respectively. This mixture was dissolved in CH$_3$CN (100 µL or 200 µL, 0.1 M) and stirred for 5-10 min at room temperature. The reaction mixture was directly diluted with CH$_3$CN (1 mL) and subjected to ESI-MS analysis.

6.3 Morita-Baylis-Hillman Reaction

6.3.1 Synthesis of Acryloyl Esters

General Procedure 4 (GP4)

A round bottom flask was charged with the corresponding alcohol (1.00 eq.), Et$_3$N (1.10-1.30 eq.) and dry CH$_2$Cl$_2$ (ca. 7 mL). To the resulting solution, acryloyl chloride (1.10-1.30 eq.) was added dropwise at 0 °C. The mixture was stirred for 30 minutes at 0 °C and allowed to warm to room temperature and stirred for the appropriate reaction time. The reaction mixture was quenched with water (1 mL/mmol) and extracted with CH$_2$Cl$_2$ (2 x 1 mL/mmol). The combined organic layers were washed with sat. NH$_4$Cl solution (1 mL/mmol), brine (1 mL/mmol), dried over MgSO$_4$ and concentrated under reduced pressure. The crude product was purified by fractional distillation or flash column chromatography.
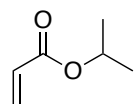
Isopropyl acrylate 64

According to **GP4**, isopropyl alcohol (1.00 g, 0.85 mL, 11.1 mmol, 1.00 eq.), Et$_3$N (1.23 g, 1.69 mL, 12.2 mmol, 1.10 eq.) and acryloyl chloride (1.10 g, 0.99 mL, 12.2 mmol, 1.10 eq.) were stirred for 8 h and purified by distillation (66 °C, 231 mbar) to afford acrylate **64** (869 mg, 69%) as a colorless liquid. Analytical data are in accordance with literature data.[129]

C$_6$H$_{10}$O$_2$ (114.14 g/mol)

^{1}H NMR (CDCl$_3$, 400 MHz) δ/ppm: 6.37 (dd, $^3J_{HH}$ = 17.3 Hz, $^2J_{HH}$ = 1.6 Hz, 1 H, CH$_a$H$_b$), 6.09 (dd, $^3J_{HH}$ = 17.3 Hz, $^3J_{HH}$ = 10.4 Hz, 1 H, CH), 5.78 (dd, $^3J_{HH}$ = 10.4 Hz, $^2J_{HH}$ = 1.6 Hz, 1 H, CH$_a$H$_b$), 5.08 (sept, $^3J_{HH}$ = 6.3 Hz, 1 H, CH$_{(iPr)}$), 1.27 (d, $^3J_{HH}$ = 6.3 Hz, 6 H, CH$_3$).

^{13}C{^{1}H} NMR (CDCl$_3$, 101 MHz) δ/ppm: 165.9 (CO$_2$), 130.3 (CH$_2$), 129.3 (CH), 68.0 (CH$_{(iPr)}$), 22.0 (2 x CH$_3$).

### *tert*-Butyl acrylate 65
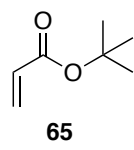
According to **GP4**, *tert*-butyl alcohol (1.00 g, 1.29 mL, 13.5 mmol, 1.00 eq.), Et$_3$N (1.50 g, 2.05 mL, 14.8 mmol, 1.10 eq.) and acryloyl chloride (1.40 g, 1.20 mL, 14.8 mmol, 1.10 eq.) were stirred for 16 h and purified by distillation (67 °C, 200 mbar) to afford acrylate **65** (416 mg, 24%) as a colorless liquid. Analytical data are in accordance with literature data.[130]

C$_7$H$_{12}$O$_2$ (128.17 g/mol)

^{1}H NMR (CDCl$_3$, 400 MHz) δ/ppm: 6.30 (dd, $^3J_{HH}$ = 17.3 Hz, $^2J_{HH}$ = 1.6 Hz, 1 H, C*H*$_a$H$_b$), 6.03 (dd, $^3J_{HH}$ = 17.3 Hz, $^3J_{HH}$ = 10.3 Hz, 1 H, C*H*), 5.72 (dd, $^3J_{HH}$ = 10.3 Hz, $^2J_{HH}$ = 1.6 Hz, 1 H, CH$_a$*H*$_b$), 1.49 (s, 9 H, C(C*H*$_3$)$_3$).

^{13}C{^{1}H} NMR (CDCl$_3$, 101 MHz) δ/ppm: 165.7 (*C*O$_2$), 130.5 (*C*H$_2$), 129.4 (*C*H), 80.7 (*C*(CH$_3$)$_3$), 28.2 (C(*C*H$_3$)$_3$).

tert-Pentyl acrylate 66
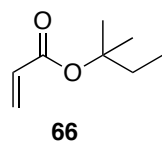
According to **GP4**, 2-methyl-2-butanol (1.00 g, 1.24 mL, 11.4 mmol, 1.00 eq.), Et$_3$N (1.27 g, 1.73 mL, 12.5 mmol, 1.10 eq.) and acryloyl chloride (1.13 g, 1.01 mL, 12.5 mmol, 1.10 eq.) were stirred for 8 h and purified by distillation (82 °C, 140 mbar) to afford acrylate **66** (382 mg, 24%) as a colorless liquid.

C$_8$H$_{14}$O$_2$ (142.20 g/mol)

^{1}H NMR (CDCl$_3$, 400 MHz) δ/ppm: 6.30 (dd, $^3J_{HH}$ = 17.3 Hz, $^2J_{HH}$ = 1.6 Hz, 1 H, C*H*$_a$H$_b$), 6.04 (dd, $^3J_{HH}$ = 17.3 Hz, $^3J_{HH}$ = 10.3 Hz, 1 H, C*H*), 5.72 (dd, $^3J_{HH}$ = 10.3 Hz, $^2J_{HH}$ = 1.6 Hz, 1 H, CH$_a$*H*$_b$), 1.81 (q, $^3J_{HH}$ = 7.5 Hz, 2 H, C*H*$_2$CH$_3$), 1.46 (s, 6 H, C*H*$_3$), 0.89 (t, $^3J_{HH}$ = 7.5 Hz, 3 H, CH$_2$C*H*$_3$).

^{13}C{^{1}H} NMR (CDCl$_3$, 101 MHz) δ/ppm: 165.7 (*C*O$_2$), 130.5 (*C*H$_2$), 129.4 (*C*H), 83.1 (*C*(CH$_3$)$_2$), 33.6 (*C*H$_2$CH$_3$), 25.7 (C(*C*H$_3$)$_2$), 8.3 (CH$_2$*C*H$_3$).

FTIR (ATR): 2977m, 2939w, 2885w, 1720s, 1636w, 1462w, 1402m, 1285m, 1207s, 1154s, 1047m, 985m, 840m, 680m, 628m cm^{-1}.

MS (EI, 70 eV, 150 °C) *m/z* (%): 127.1 (5), 113.1 (11), 70.1 (31), 55.0 ([M-O^{tert}Pent]$^+$, 100), 43.0 (23).
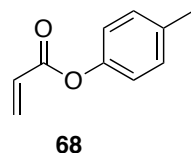
Octyl acrylate 67
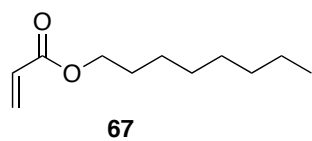
According to **GP4**, octanol (1.00 g, 1.20 mL, 7.71 mmol, 1.00 eq.), Et$_3$N (0.94 g, 1.30 mL, 9.25 mmol, 1.20 eq.) and acryloyl chloride (0.84 g, 0.75 mL, 9.25 mmol, 1.20 eq.) were stirred for 16 h and purified by flash column chromatography (SiO$_2$, 15 cm x 3.5 cm, CH$_2$Cl$_2$/pentane 1:1) to afford acrylate **67** (739 mg, 52%) as a colorless liquid. Analytical data are in accordance with literature data.[131]

C$_{11}$H$_{20}$O$_2$ (184.28 g/mol)

R_f = 0.50 (SiO$_2$, CH$_2$Cl$_2$/pentane 1:1).

^{1}H NMR (CDCl$_3$, 400 MHz) δ/ppm: 6.35 (dd, $^3J_{HH}$ = 17.3 Hz, $^2J_{HH}$ = 1.9 Hz, 1 H, CH_aH$_b$), 6.10 (dd, $^3J_{HH}$ = 17.4 Hz, $^3J_{HH}$ = 10.1 Hz, 1 H, CH), 5.72 (dd, $^3J_{HH}$ = 10.1 Hz, $^2J_{HH}$ = 1.9 Hz, 1 H, CH$_a$$H_b$), 4.13 (t, $^3J_{HH}$ = 6.6 Hz, 2 H, OCH_2), 1.70-1.60 (m, 2 H, CH_2), 1.27 (br s, 10 H, CH_2), 0.86 (t, $^3J_{HH}$ = 6.4 Hz, 3 H, CH_3).

^{13}C{^{1}H} NMR (CDCl$_3$, 101 MHz) δ/ppm: 166.4 (CO_2), 130.5 (CH_2), 128.8 (CH), 64.8 (OCH_2), 31.9, 29.3, 29.3, 28.7, 26.0, 22.7 (6 x CH_2), 14.2 (CH_3).

$para$-Tolyl acrylate 68

According to **GP4**, p-cresol (1.00 g, 0.98 mL, 9.3 mmol, 1.00 eq.), Et$_3$N (1.22 g, 1.68 mL, 12.1 mmol, 1.30 eq.) and acryloyl chloride (1.10 g, 0.98 mL, 12.1 mmol, 1.30 eq.) were stirred for 16 h and purified by flash column chromatography (SiO$_2$, 15 cm x 3.5 cm, CH$_2$Cl$_2$/pentane 1:1) to afford acrylate **68** (1.1 g, 74%) as a colorless liquid.

C$_{10}$H$_{10}$O$_2$ (162.19 g/mol)

R_f = 0.67 (SiO$_2$, CH$_2$Cl$_2$/pentane 1:1).

^{1}H NMR (CDCl$_3$, 400 MHz) δ/ppm: 7.19 (d, $^3J_{HH}$ = 8.3 Hz, 2 H, Ar-H), 7.01 (d, $^3J_{HH}$ = 8.3 Hz, 2 H, Ar-H), 6.60 (dd, $^3J_{HH}$ = 17.3 Hz, $^2J_{HH}$ = 1.3 Hz, 1 H, CH_aH$_b$), 6.32 (dd, $^3J_{HH}$ = 17.3 Hz, $^3J_{HH}$ = 10.4 Hz, 1 H, CH), 6.00 (dd, $^3J_{HH}$ = 10.4 Hz, $^2J_{HH}$ = 1.3 Hz, 1 H, CH$_a$$H_b$), 2.35 (s, 3 H, C$H_3$).

^{13}C{^{1}H} NMR (CDCl$_3$, 101 MHz) δ/ppm: 164.9 (CO_2), 148.5, 135.7 (2 x Ar-C), 132.5 (CH_2), 130.1 (Ar-CH), 128.2 (CH), 121.3 (Ar-CH), 21.0 (CH_3).

6.3.2 Synthesis of Morita-Baylis-Hillman Products

General Procedure 5 (GP5)

A round bottom flask was charged with the corresponding acryloyl ester (1.00-1.10 eq.), 4-nitrobenzaldehyde (1.00-1.20 eq.) and dry THF. To the resulting solution DABCO (1.00 eq.), La(OTf)$_3$ (5 mol%) and triethanolamine (50 mol%) were added. The reaction mixture was stirred at room temperature for the appropriate reaction time and was diluted with ether (1 mL/mmol). The organic layer was washed with 1 M HCl solution (1 mL/mmol), water (1 mL/mmol), dried over MgSO$_4$, filtered and concentrated under reduced pressure. The crude product was purified by flash column chromatography.

Methyl 3-hydroxy-2-methylene-3-(4-nitrophenyl) propanoate 69
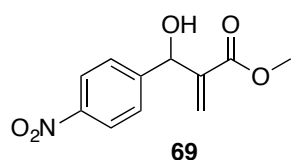
According to **GP5**, methyl acrylate (114 mg, 120 μL, 1.32 mmol, 1.00 eq.), *para*-nitrobenzaldehyde (200 mg, 1.32 mmol, 1.00 eq.), dry THF (100 μL), DABCO (148 mg, 1.32 mmol, 1.00 eq.), La(OTf)$_3$ (39.8 mg, 0.07 mmol, 5 mol%) and triethanolamine (98.5 mg, 87.1 μL, 0.66 mmol, 50 mol%) were stirred for 3 h and purified by flash column chromatography (15 cm x 3.5 cm, cyclohexane/EtOAc 2:1) to afford MBH product **69** (234 mg, 75%) as a pale yellow solid. Analytical data are in accordance with literature data.[132]

C$_{11}$H$_{11}$NO$_5$ (237.21 g/mol)

R_f = 0.42 (cyclohexane/EtOAc 2:1).

^{1}H NMR (CDCl$_3$, 400 MHz) δ/ppm: 8.21 (d, $^3J_{HH}$ = 8.7 Hz, 2 H, Ar-*H*), 7.58 (d, $^3J_{HH}$ = 8.7 Hz, 2 H, Ar-*H*), 6.40 (s, 1 H, C*H*$_2$), 5.87 (s, 1 H, C*H*$_2$), 5.63 (br s, 1 H, C*H*), 3.75 (s, 3 H, C*H*$_3$), 3.30 (br s, 1 H, O*H*).

^{13}C{^{1}H} NMR (CDCl$_3$, 101 MHz) δ/ppm: 166.6 (*C*O$_2$), 148.7, 147.7 (2 x Ar-*C*), 141.1 (*C*CH$_2$), 127.5 (Ar-*C*H, C*C*H$_2$), 123.8 (Ar-*C*H), 73.0 (*C*OH), 52.4 (*C*H$_3$).

HPLC (*Daicel*, Chiralcel OD-H, heptane/*i*PrOH 96:4, 0.5 mL/min, 25 °C, 266 nm): t_R = 46.4 min and 50.7 min.

**Ethyl 3-hydroxy-2-methylene-3-(4-nitrophenyl) propanoate 70**
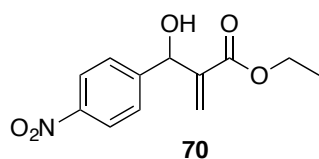
According to **GP5**, ethyl acrylate (160 mg, 170 µL, 1.60 mmol, 1.00 eq.), *para*-nitrobenzaldehyde (241 mg, 1.60 mmol, 1.00 eq.), dry THF (200 µL), DABCO (179 mg, 1.60 mmol, 1.00 eq.), La(OTf)$_3$ (46.9 mg, 0.08 mmol, 5 mol%) and triethanolamine (119 mg, 106 µL, 0.80 mmol, 50 mol%) were stirred for 3 h and purified by flash column chromatography (15 cm x 3.5 cm, cyclohexane/EtOAc 2:1) to afford MBH product **70** (227 mg, 69%) as a pale yellow solid. Analytical data are in accordance with literature data.[133]

$C_{12}H_{13}NO_5$ (237.21 g/mol)

R_f = 0.29 (cyclohexane/EtOAc 2:1).

^{1}H NMR (CDCl$_3$, 400 MHz) δ/ppm: 8.22-8.20 (m, 2 H, Ar-*H*), 7.59-7.56 (m, 2 H, Ar-*H*), 6.40 (s, 1 H, C*H*$_2$), 5.84 (s, 1 H, C*H*$_2$), 5.62 (d, $^3J_{HH}$ = 6.3 Hz, 1 H, C*H*), 4.19 (q, $^3J_{HH}$ = 7.1 Hz, 2 H, C*H*$_2$CH$_3$), 3.34 (d, $^3J_{HH}$ = 6.3 Hz, 1 H, O*H*), 1.27 (t, $^3J_{HH}$ = 7.1 Hz, 3 H, CH$_2$C*H*$_3$).

^{13}C{^{1}H} NMR (CDCl$_3$, 101 MHz) δ/ppm: 166.1 (*C*O$_2$), 148.8, 147.6 (2 x Ar-*C*), 141.1 (*C*CH$_2$), 127.5 (Ar-*C*H), 127.3 (C*C*H$_2$), 123.8 (Ar-*C*H), 73.1 (*C*OH), 61.5 (*C*H$_2$CH$_3$), 14.2 (CH$_2$*C*H$_3$).

Isopropyl 3-hydroxy-2-methylene-3-(4-nitrophenyl) propanoate 71
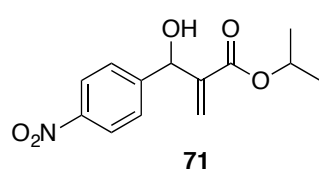
According to **GP5**, isopropyl acrylate **64** (205 mg, 230 µL, 1.80 mmol, 1.00 eq.), *para*-nitrobenzaldehyde (326 mg, 2.16 mmol, 1.20 eq.), dry THF (200 µL), DABCO (196 mg, 1.80 mmol, 1.00 eq.), La(OTf)$_3$ (52.7 mg, 0.09 mmol, 5 mol%) and triethanolamine (134 mg, 119 µL, 0.90 mmol, 50 mol%) were stirred for 5 h and purified by flash column chromatography (SiO$_2$, 15 cm x 3.5 cm, cyclohexane/EtOAc 2:1) to afford MBH product **71** (93 mg, 20%) as a pale yellow solid. Analytical data are in accordance with literature data.[134]

$C_{13}H_{15}NO_5$ (265.26 g/mol)

R_f = 0.44 (cyclohexane/EtOAc 2:1).

^{1}H NMR (CDCl$_3$, 400 MHz) δ/ppm: 8.21 (d, $^3J_{HH}$ = 8.9 Hz, 2 H, Ar-*H*), 7.57 (d, $^3J_{HH}$ = 8.9 Hz, 2 H, Ar-*H*), 6.37 (s, 1 H, C*H*$_2$), 5.81 (s, 1 H, C*H*$_2$), 5.61 (d, $^3J_{HH}$ = 6.4 Hz, 1 H, C*H*), 5.04 (sept, $^3J_{HH}$ = 6.2 Hz, 1 H, C*H*(CH$_3$)$_2$), 3.37 (d, $^3J_{HH}$ = 6.4 Hz, 1 H, O*H*), 1.23 (d, $^3J_{HH}$ =

6.2 Hz, 3 H, CH(CH_3)$_2$), 1.22 (d, $^3J_{HH}$ = 6.2 Hz, 3 H, CH(CH_3)$_2$).

^{13}C{^{1}H} NMR (CDCl$_3$, 101 MHz) δ/ppm: 165.6 (CO$_2$), 148.9, 147.6 (2 x Ar-C), 141.6 (CCH$_2$), 127.5 (Ar-CH), 127.1 (CCH$_2$), 123.7 (Ar-CH), 73.1 (COH), 69.3 (CH(CH$_3$)$_2$), 21.8 (CH(CH$_3$)$_2$).

tert-Butyl 3-hydroxy-2-methylene-3-(4-nitrophenyl) propanoate 72
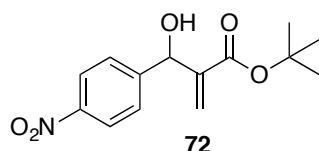
According to **GP5**, *tert*-butyl acrylate **65** (96.1 mg, 0.78 mmol, 1.00 eq.), *para*-nitrobenzaldehyde (134 mg, 0.94 mmol, 1.20 eq.), dry THF (200 μL), DABCO (87.5 mg, 0.78 mmol, 1.00 eq.), La(OTf)$_3$ (22.9 mg, 0.04 mmol, 5 mol%) and triethanolamine (58.2 mg, 51.5 μL, 0.39 mmol, 50 mol%) were stirred for 6 h and purified by flash column chromatography (15 cm x 3.5 cm, CH$_2$Cl$_2$/EtOAc 50:1) to afford MBH product **72** (23 mg, 10%) as a pale yellow solid. Analytical data are in accordance with literature data.[135]

C$_{14}$H$_{17}$NO$_5$ (279.29 g/mol)

R_f = 0.25 (CH$_2$Cl$_2$/EtOAc 50:1).

^{1}H NMR (CDCl$_3$, 400 MHz) δ/ppm: 8.21 (d, $^3J_{HH}$ = 8.7 Hz, 2 H, Ar-H), 7.57 (d, $^3J_{HH}$ = 8.7 Hz, 2 H, Ar-H), 6.30 (s, 1 H, CH_2), 5.74 (s, 1 H, CH_2), 5.56 (d, $^3J_{HH}$ = 6.4 Hz, 1 H, CH), 3.41 (d, $^3J_{HH}$ = 6.4 Hz, 1 H, OH), 1.43 (s, 9 H, C(CH_3)$_3$).

^{13}C{^{1}H} NMR (CDCl$_3$, 101 MHz) δ/ppm: 165.4 (CO$_2$), 149.1, 147.5 (2 x Ar-C), 142.4 (CCH$_2$), 127.4 (Ar-CH), 126.8 (CCH$_2$), 123.7 (Ar-CH), 82.6 (C(CH$_3$)$_3$), 73.3 (COH), 28.1 (C(CH$_3$)$_3$).

tert-Pentyl 3-hydroxy-2-methylene-3-(4-nitrophenyl) propanoate 73
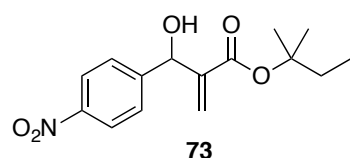
According to **GP5**, *tert*-pentyl acrylate **66** (70.0 mg, 0.49 mmol, 1.00 eq.), *para*-nitrobenzaldehyde (75.0 mg, 0.50 mmol, 1.00 eq.), dry THF (200 μL), DABCO (55.0 mg, 0.49 mmol, 1.00 eq.), La(OTf)$_3$ (15.0 mg, 0.02 mmol, 5 mol%) and triethanolamine (37.3 mg, 33.0 μL, 0.25 mmol, 50 mol%) were stirred overnight and purified by flash column chromatography (SiO$_2$, 15 cm x 3.5 cm, CH$_2$Cl$_2$/EtOAc 50:1) to afford MBH product **73** (65 mg, 45%) as a pale yellow solid.

$C_{15}H_{19}NO_5$ (293.32 g/mol)

m.p.: 48-49 °C.

$\boldsymbol{R}_f$ = 0.36 (CH_2Cl_2/EtOAc 50:1).

^{1}H NMR (CDCl$_3$, 400 MHz) δ/ppm: 8.21-8.18 (m, 2 H, Ar-*H*), 7.58 -7.54 (m, 2 H, Ar-*H*), 6.30 (s, 1 H, C*H*$_2$), 5.74 (dd, $^2J_{HH}$ = 0.9 Hz, $^4J_{HH}$ = 0.9 Hz, 1 H, C*H*$_2$), 5.56 (d, $^3J_{HH}$ = 6.7 Hz, 1 H, C*H*), 3.47 (d, $^3J_{HH}$ = 6.7 Hz, 1 H, O*H*), 1.75 (q, $^3J_{HH}$ = 7.5 Hz, 2 H, C*H*$_2$CH$_3$) 1.39 (s, 6 H, C(C*H*$_3$)$_2$), 0.79 (t, $^3J_{HH}$ = 7.5 Hz, 3 H, CH$_2$C*H*$_3$).

^{13}C{^{1}H} NMR (CDCl$_3$, 101 MHz) δ/ppm: 165.4 (*C*O$_2$), 149.1, 147.5 (2 x Ar-*C*), 142.4 (*C*CH$_2$), 127.4 (Ar-*C*H), 126.6 (C*C*H$_2$), 123.7 (Ar-*C*H), 85.1 (*C*(CH$_3$)$_2$), 73.3 (*C*OH), 33.4 (*C*H$_2$CH$_3$), 25.7, 25.6 (C(*C*H$_3$)$_2$), 8.2 (CH$_2$*C*H$_3$).

FTIR (ATR): 3330m (br), 2982w, 2944w, 1708s, 1607w, 1522s, 1461w, 1350s, 1269s, 1147s, 1018s, 961m, 830s, 757m, 699s, 652m cm^{-1}.

MS (FAB, NBA) *m/z* (%): 294.1 ([M+H]$^+$, 1), 224.0 (27), 296.0 (19), 160.0 (22), 71.1 (100) 43.1 (86).

Octyl 3-hydroxy-2-methylene-3-(4-nitrophenyl) propanoate 74
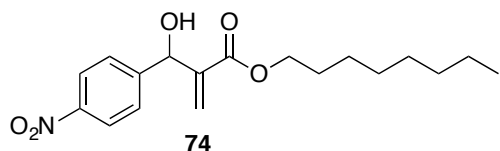
According to **GP5**, octyl acrylate **67** (242 mg, 1.46 mmol, 1.10 eq.), *para*-nitrobenzaldehyde (200 mg, 1.32 mmol, 1.00 eq.), dry THF (500 μL), DABCO (142 mg, 1.32 mmol, 1.00 eq.), La(OTf)$_3$ (38.7 mg, 0.07 mmol, 5 mol%) and triethanolamine (98.5 mg, 87.1 μL, 0.66 mmol, 50 mol%) were stirred for 48 h and purified by flash column chromatography (SiO$_2$, 15 cm x 3.5 cm, CH_2Cl_2/EtOAc 50:1) to afford MBH product **74** (380 mg, 86%) as a yellow oil.

$C_{18}H_{25}NO_5$ (335.40 g/mol)

$\boldsymbol{R}_f$ = 0.40 (CH_2Cl_2/EtOAc 50:1).

^{1}H NMR (CDCl$_3$, 400 MHz) δ/ppm: 8.20 (d, $^3J_{HH}$ = 8.8 Hz, 2 H, Ar-*H*), 7.57 (d, $^3J_{HH}$ = 8.8 Hz, 2 H, Ar-*H*), 6.39 (s, 1 H, C*H*$_2$), 5.85 (s, 1 H, C*H*$_2$), 5.62 (d, $^3J_{HH}$ = 6.4 Hz, 1 H, C*H*), 4.12 (t, $^3J_{HH}$ = 6.8 Hz, 1 H, OC*H*$_2$), 3.34 (d, $^3J_{HH}$ = 6.4 Hz, 1 H, O*H*), 1.63-1.59 (m, 2 H, C*H*$_2$), 1.30-1.22 (m, 10 H, C*H*$_2$), 0.87 (t, $^3J_{HH}$ = 7.2 Hz, 3 H, C*H*$_3$).

^{13}C{^{1}H} NMR (CDCl$_3$, 101 MHz) δ/ppm: 166.2 (*C*O$_2$), 148.8, 147.6 (2 x Ar-*C*), 141.3 (*C*CH$_2$), 127.4 (Ar-*C*H), 127.2 (C*C*H$_2$), 123.7 (Ar-*C*H), 73.1 (*C*OH), 65.6 (O*C*H$_2$), 32.0, 29.6, 293, 28.6, 26.0, 22.8 (6 x *C*H$_2$), 14.2 (*C*H$_3$).
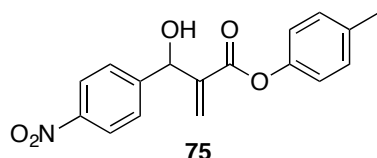
FTIR (ATR): 3483w (br), 2955w, 2927m, 2857w, 1711m, 1630w, 1523m, 1466w, 1402w,

1347m, 1278w, 1156w, 1050w, 962w, 828w, 723w, 631s cm^{-1}.

MS (FAB, NBA) *m/z* (%): 336.2 ([M+H]$^+$, 74), 319.2 (40), 318.2 (92), 272.2 (100), 206.0 (22), 190.0 (38), 161.0 (26), 160.1 (98), 116.1 (35), 111.1 (24), 71.1 (46), 69.1 (35), 57.1 (66), 55.1 (31), 43.1 (59), 41.0 (38).

para-Tolyl 3-hydroxy-2-methylene-3-(4-nitrophenyl) propanoate 75

According to **GP5**, *para*-tolyl acrylate **68** (225 mg, 1.46 mmol, 1.10 eq.), *para*-nitrobenzaldehyde (200 mg, 1.32 mmol, 1.00 eq.), dry THF (200 μL), DABCO (142 mg, 1.32 mmol, 1.00 eq.), La(OTf)$_3$ (38.7 mg, 0.07 mmol, 5 mol%) and triethanolamine (98.5 mg, 87.1 μL, 0.66 mmol, 50 mol%) were stirred overnight and purified by flash column chromatography (SiO$_2$, 15 cm x 3.5 cm, CH$_2$Cl$_2$/EtOAc 50:1) to afford MBH product **75** (29 mg, 7%) as a pale yellow solid.

C$_{17}$H$_{15}$NO$_5$ (313.31 g/mol)

m.p.: 93-94 °C.

R_f = 0.49 (CH$_2$Cl$_2$/EtOAc 100:1).

^{1}H NMR (CDCl$_3$, 400 MHz) δ/ppm: 8.22 (d, $^3J_{HH}$ = 8.7 Hz, 2 H, Ar-*H*), 7.63 (d, $^3J_{HH}$ = 8.7 Hz, 2 H, Ar-*H*), 7.16 (d, $^3J_{HH}$ = 8.4 Hz, 2 H, Ar-*H*), 6.90 (d, $^3J_{HH}$ = 8.4 Hz, 2 H, Ar-*H*), 6.65 (s, 1 H, C*H*$_2$), 6.08 (s, 1 H, C*H*$_2$), 5.74 (d, $^3J_{HH}$ = 5.8 Hz, 1 H, C*H*), 3.16 (d, $^3J_{HH}$ = 5.8 Hz, 1 H, O*H*), 2.34 (s, 3 H, C*H*$_3$).

^{13}C{^{1}H} NMR (CDCl$_3$, 101 MHz) δ/ppm: 164.8 (*C*O$_2$), 148.7, 148.0, 147.7 (3 x Ar-*C*), 141.0 (*C*CH$_2$), 136.2 (Ar-*C*), 130.2 (Ar-*C*H), 128.6 (C*C*H$_2$), 127.6, 123.8, 121.1 (3 x Ar-*C*H), 72.7 (*C*OH), 21.0 (*C*H$_3$).

FTIR (ATR): 3467m (br), 2923w, 1701s, 1603w, 1509s, 1347s, 1302m, 1265m, 1193s, 1120s, 1039s, 820m, 745m, 635w cm^{-1}.

MS (FAB, NBA) *m/z* (%): 314.1 ([M+H]$^+$, 31), 296.1 (73), 143.0 (37), 136.0 (24), 116.0 (21), 109.0 (24), 108.0 (100), 107.0 (30), 91.1 (25), 77.1 (25), 73.0 (24), 69.1 (33), 57.1 (31), 55.1 (34), 43.1 (27), 41.0 (23).

6.4 ESI-MS Back Reaction Screening as Tool for Mechanistic Investigations

General remarks

ESI-MS spectra were measured on a Varian 1200L Quadrupol MS/MS spectrometer using mild desolvation conditions (110 V capillary voltage for the peptide catalysts **78a-e** and 50 V capillary voltage for the Hayashi-Jørgensen catalyst **77a**, 200 °C drying gas temperature). The samples were diluted immediately with MeOH prior to their analysis. Every spectrum consisted of at least 30 scans and the selectivity was calculated from the ratios of the peak heights of the major isotopomers of **En** and **En'**.

General procedure for the ESI-MS screening of the back-reaction without acid additive

A 0.1 M solution (10-20 µL) of the organocatalyst in the corresponding solvent was mixed with a 1 M solution (10-20 µL) of an equimolar mixture of (2*S*,3*R*)-2-(4-methylbenzyl)-4-nitro-3-phenylbutanal **79** and (2*R*,3*S*)-2-(4-ethylbenzyl)-4-nitro-3-phenylbutanal ***ent*-79'** in the same solvent. The mixture was stirred for 10 min and then diluted with 1 mL of MeOH. This mixture was analyzed by ESI-MS under mild desolvation conditions.

Alternative procedure for the ESI-MS screening of the back-reaction without acid additive

An equimolar mixture of (2*S*,3*R*)-2-(4-methylbenzyl)-4-nitro-3-phenylbutanal **79** (5 µmol) and (2*R*,3*S*)-2-(4-ethylbenzyl)-4-nitro-3-phenylbutanal ***ent*-79'** (5 µmol) were dissolved in DMSO (10 µL). A 0.1 M solution (10 µL) of the organocatalyst in DMSO was added and the mixture was stirred for 10 min and then diluted with 1 mL of MeOH. This mixture was analyzed by ESI-MS under mild desolvation conditions.

General procedure for the ESI-MS screening of the back-reaction with acid additive

An equimolar mixture of (2*S*,3*R*)-2-(4-methylbenzyl)-4-nitro-3-phenylbutanal **79** (5 µmol) and (2*R*,3*S*)-2-(4-ethylbenzyl)-4-nitro-3-phenylbutanal ***ent*-79'** (5 µmol) and the corresponding acid (10 mol% or 100 mol%) were dissolved in DMSO (10 µL). A 0.1 M solution (10 µL) of the organocatalyst **78d** or **77a** in DMSO was added and the mixture was stirred for 2 min and then diluted with 1 mL of MeOH. This mixture was analyzed by ESI-MS under mild desolvation conditions.
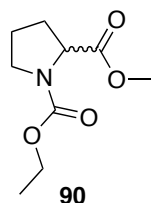
6.5 ESI-MS Screening of Racemic Catalysts

6.5.1 1st Generation Catalyst Synthesis

1-(Ethoxycarbonyl)proline methyl ester 90

DL-Proline (1.15 g, 10.0 mmol, 1.00 eq.) and K$_2$CO$_3$ (1.38 g, 10.0 mmol, 1.00 eq.) were dissolved in dry MeOH (20 mL) and stirred for 10 min. The reaction mixture was cooled to 0 °C and ethyl chloroformate (2.31 g, 2.10 mL, 22.0 mmol, 2.20 eq.) was added dropwise. The mixture was stirred for 45 min and allowed to warm to room temperature. After stirring overnight TLC monitoring indicate incomplete conversion. Additional ethyl chloroformate (0.4 mL) was added and the mixture stirred for 1 h when the solvent was removed under reduced pressure. The white residue was dissolved in H$_2$O (20 mL) and extracted with CHCl$_3$ (3 x 50 mL). The combined organic layers were dried over MgSO$_4$, filtered and the solvent concentrated under reduced pressure to afford methyl ester **90** (1.97 g, 98%) as a colorless oil, which was used without further purification. Analytical data are in accordance with literature data.[102]

C$_9$H$_{15}$NO$_4$ (201.22 g/mol)

R_f = 0.26 (cyclohexane/EtOAc 3:1).

^{1}H NMR (CDCl$_3$, 400 MHz) δ/ppm: 4.34 and 4.28 (2 x dd, $^3J_{HH}$ = 8.6 Hz, $^3J_{HH}$ = 3.8 Hz, 1 H, NC*H*, rotamers), 4.19-4.02 (m, 2 H, C*H$_2$*CH$_3$), 3.71 and 3.70 (2 x s, 3 H, CO$_2$C*H$_3$*, rotamers), 3.61-3.37 (m, 2 H, NC*H$_2$*), 2.28-2.10 (m, 1 H, C*H$_2$*), 2.03-1.82 (m, 3 H, 4-H, C*H$_2$*), 1.24 and 1.17 (2 x t, $^3J_{HH}$ = 7.1 Hz, 3 H, CH$_2$C*H$_3$*, rotamers).

^{13}C{^{1}H} NMR (CDCl$_3$, 101 MHz) δ/ppm: 173.5 and 173.4 (*C*O$_2$CH$_3$, rotamers), 155.3 and 154.7 (*C*O$_2$Et, rotamers), 61.4 and 61.3 (*C*H$_2$CH$_3$, rotamers), 59.1 and 58.9 (N*C*H, rotamers), 52.3 and 52.32 (O*C*H$_3$, rotamers), 46.8 and 46.4 (N*C*H$_2$, rotamers), 31.0 and 30.0 (*C*H$_{2(Pyr)}$, rotamers), 24.5 and 23.6 (*C*H$_{2(Pyr)}$, rotamers), 14.8 and 14.7 (CH$_2$*C*H$_3$, rotamers).

MS (EI, 70 eV, 300°C) *m/z* (%): 201.1 (M$^+$, 2), 142.1 (100), 114.1 (10), 98.1 (18), 70.1 (56).

Ethyl 2-(hydroxydiphenylmethyl)pyrrolidine-1-carboxylate 91
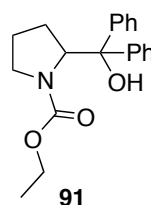
A 25 mL two-necked flask was charged with magnesium turnings (0.38 g, 15.7 mmol, 2.40 eq.). The flask was flame-dried and flushed with argon. The magnesium was suspended in dry THF (7 mL) and an iodine crystal was added. Bromobenzene (2.25 g, 1.50 mL, 14.3 mmol, 2.20 eq.) was added dropwise

avoiding tremendous reflux. The cloudy suspension was stirred 20 min at room temperature and refluxed for additional 30 min. The Grignard reagent was transferred into an ice cooled solution of 1-(ethoxycarbonyl)proline methyl ester **90** (1.31 g, 6.50 mmol, 1.00 eq.) in dry THF (6.5 mL). The resulting mixture was stirred for 30 min at 0 °C followed by 2.5 h at room temperature. The reaction mixture was quenched with sat. NH_4Cl solution (10 mL). The organic layer was separated and the aqueous layer extracted with $CHCl_3$ (2 x 10 mL). The combined organic layers were dried over Na_2SO_4, filtered and the solvent concentrated under reduced pressure. The crude product was purified by flash column chromatography (SiO_2, 20 cm x 6 cm, cyclohexane/EtOAc 4:1) to afford alcohol **91** (1.59 g, 75%) as a colorless solid. Analytical data are in accordance with literature data.[102]
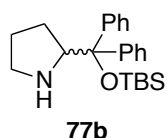
$C_{20}H_{23}NO_3$ (325.40 g/mol)

m.p.: 108-109 °C (Lit.[102] 112-113 °C).

R_f = 0.29 (cyclohexane/EtOAc 4:1).

^{1}H NMR (CDCl$_3$, 400 MHz) δ/ppm: 7.42-7.35 (m, 4 H, Ar-*H*), 7.35-7.22 (m, 6 H, Ar-*H*), 4.93 (dd, $^3J_{HH}$ = 8.9 Hz, $^3J_{HH}$ = 3.6 Hz, 1 H, NC*H*), 4.19-4.02 (m, 2 H, C*H*$_2$CH$_3$), 3.42 (m, 1 H, NC*H*$_2$), 2.99-2.89 (m, 1 H, NC*H*$_2$), 2.15-2.03 (m, 1 H, C*H*$_2$), 1.98-1.89 (m, 1 H, C*H*$_2$), 1.54-1.43 (m, 1 H, C*H*$_2$), 1.22 (t, $^3J_{HH}$ = 7.0 Hz, 3 H, CH$_2$C*H*$_3$), 0.81 (br s, 1 H, C*H*$_2$).

^{13}C{^{1}H} NMR (CDCl$_3$, 101 MHz) δ/ppm: 158.4 (N*C*O$_2$)*, 146.4, 143.7 (2 x Ar-*C*), 128.2, 127.9, 127.6, 127.5, 127.2, 127.2 (6 x Ar-*C*H), 81.6 (*C*OH), 66.0 (N*C*H), 61.9 (*C*H$_2$CH$_3$), 47.7 (N*C*H$_2$), 29.7 (*C*H$_2$), 23.0 (*C*H$_2$), 14.7 (CH$_2$*C*H$_3$). *Deduced from HMBC*.

[(*tert*-Butyldimethylsiloxy)-diphenylmethyl]-pyrrolidine 77b

Under an argon atmosphere, ethyl 2-(hydroxydiphenylmethyl)pyrrolidine-1-carboxylate **91** (204 mg, 627 μmol, 1.00 eq.) and KOH (368 mg, 6.56 mmol, 10.5 eq.) were dissolved in dry MeOH (2 mL). The suspension was refluxed for 2.5 h until TLC indicate complete consumption of the starting material. The solvent was removed under reduced pressure, the residue dissolved in H_2O (5 mL) and extracted with CH_2Cl_2 (3 x 10 mL). The combined organic layers were dried over Na_2SO_4, filtered and the solvent concentrated under reduced pressure to afford the deprotected aminoalcohol as yellow solid, which was used without further purification.

The yellow solid was dissolved in dry CH_2Cl_2 (0.6 mL) and cooled to 0 °C. To this mixture 2,6-lutidine (417 mg, 0.45 mL, 3.89 mmol, 7.30 eq.) and TBSOTf (563 mg, 0.49 mL, 2.13 mmol, 4.00 eq.) were added subsequently. The reaction mixture was stirred overnight,

quenched with MeOH (2 mL) and sat. NH_4Cl solution (2 mL) and the aqueous layer was extracted with $CHCl_3$ (3 x 5 mL). The combined organic layers were washed with 1 M NaOH (2 mL) and H_2O (2 mL). The organic layer was dried over Na_2SO_4, filtered and the solvent concentrated under reduced pressure to give the crude product as yellow oil. The excess 2,6-lutidine was removed by bulb-to-bulb distillation (ca. 200 °C, 0.1 mbar). The residue was purified by flash column chromatography (SiO_2, 15 cm x 3.5 cm, cyclohexane/EtOAc 99:1 (50 mL) to 10:1 (50 mL) to 1:1) to afford organocatalyst **77b** (114 mg, 58%) as pale yellow solid. Analytical data are in accordance with literature data.[80]
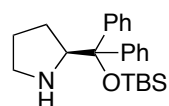
$C_{23}H_{33}NOSi$ (367.60 g/mol)

m.**p**.: 62-64 °C.

R_f = 0.08 (cyclohexane/EtOAc 1:1).

^{1}H NMR (CDCl_3, 400 MHz) δ/ppm: 7.53-7.50 (m, 2 H, Ar-*H*), 7.37-7.35 (m, 2 H, Ar-*H*), 7.29-7.23 (m, 6 H, Ar-*H*), 4.01 (t, $^3J_{HH}$ = 7.3 Hz, 1 H, NC*H*), 2.87-2.78 (m, 1 H, N C*H*$_2$), 2.72-2.66 (m, 1 H, N C*H*$_2$), 1.72 (br s, 1 H, N*H*), 1.62-1.48 (m, 3 H, CH_2, C*H*$_2$), 1.25-1.17 (m, 1 H, C*H*$_2$), 0.95 (s, 9 H, C(C*H*$_3$)$_3$), −0.21 (s, 3 H, SiC*H*$_3$), −0.46 (s, 3 H, SiC*H*$_3$).

^{13}C{^{1}H} NMR (CDCl_3, 101 MHz) δ/ppm: 146.6, 145.4 (2 x Ar-*C*), 129.4, 128.4, 127.7, 127.4, 127.2, 127.1 (6 x Ar-*C*H), 83.2 (*C*OSi), 65.8 (N*C*H), 47.3 (N*C*H_2), 28.0 (*C*H_2), 26.5 (C(*C*H_3)$_3$), 25.1 (*C*H_2), 19.2 (*C*(CH_3)$_3$), −2.6 (Si*C*H_3), −3.2 (Si*C*H_3).

(*S*)-[(*tert*-Butyldimethylsiloxy)-diphenylmethyl]-pyrrolidine (*S*)-77b

Enantiopure organocatalyst (*S*)-**77b** was synthesized according to the racemic compound starting from commercial available (*S*)-diphenylprolinol. Analytical data are in accordance with data of the racemic compound.

m.**p**.: 66-68 °C.

Optical rotation: $[\alpha]_D^{20}$ = −33.4 (c = 0.36, CHCl_3) (Lit.[80] $[\alpha]_D^{32}$ = −34.4 (c = 0.198, CHCl_3)).

6.5.2   2nd Generation Catalyst Synthesis

tert-**Butyl 2-(hydroxydiphenylmethyl)pyrrolidine-1-carboxylate 94**
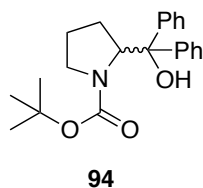
 Under an argon atmosphere, a flame-dried Schlenk tube was charged with *N-tert*-butyloxycarbonyl-pyrrolidine **93** (171 mg, 175 µL, 1.00 mmol, 1.00 eq.), freshly distilled TMEDA (153 mg, 198 µL, 1.30 mmol, 1.30 eq.) and Et$_2$O (3 mL) at −78 °C using a dry ice/acetone bath. *sec*-BuLi (1.4 M in cyclohexane, 0.93 mL, 1.30 mmol, 1.30 eq.) was added dropwise and the solution was kept at −78 °C for 4 h. Benzophenone (273 mg, 1.50 mmol, 1.50 eq.) was added in small portions and the mixture was slowly allowed to warm to room temperature in the dry ice bath overnight. The yellow solution was quenched with H$_2$O (5 mL), the phases were separated and the aqueous layer was extracted with Et$_2$O (2 x 20 mL). The combined organic layers were washed with 5% aqueous H$_3$PO$_4$ (5 mL), dried over MgSO$_4$, filtered and the solvent concentrated under reduced pressure. The crude product contained a mixture of alcohol **94** and oxazolidinone **95** (9:1, determined by ^{1}H NMR analysis out of the crude product, according to the integrals of the corresponding NC*H* protons at 4.87 and 4.55 ppm). The crude product was purified by flash column chromatography (SiO$_2$, 20 cm x 3.5 cm, cyclohexane/EtOAc 10:1) to afford pure alcohol **94** (210 mg, 59%) as colorless solid. Analytical data are in accordance with literature data.[136]

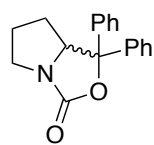C$_{22}$H$_{27}$NO$_3$ (353.45 g/mol)

m.**p**.: 116-117 °C.

R$_f$ = 0.20 (cyclohexane/EtOAc 10:1).

^{1}H NMR (CDCl$_3$, 400 MHz) δ/ppm: 7.39-7.34 (m, 4 H, Ar-*H*), 7.31-7.21 (m, 6 H, Ar-*H*), 6.43 (br s, 1 H, O*H*), 4.87 (dd, $^3J_{HH}$ = 9.0 Hz, $^3J_{HH}$ = 3.7 Hz, 1 H, NC*H*), 3.36-3.30 (m, 1 H, NC*H*$_2$), 2.87-2.81 (m, 1 H, N C*H*$_2$), 2.12-2.02 (m, 1 H, C*H*$_2$), 1.93-1.86 (m, 1 H, C*H*$_2$), 1.46-1.40 (m, 10 H, C*H*$_2$, C(C*H*$_3$)$_3$), 0.76 (br s, 1 H, C*H*$_2$).

^{13}C{^{1}H} NMR (CDCl$_3$, 101 MHz) δ/ppm: 146.6, 143.9 (2 x Ar-*C*), 128.4, 128.0, 127.8, 127.5, 127.2, 127.1 (6 x Ar-*C*H), 81.8 (*C*OH), 80.8 (*C*(CH$_3$)$_3$), 65.8 (N*C*H), 48.0 (N*C*H$_2$), 29.9 (*C*H$_2$), 28.5 C(*C*H$_3$)$_3$, 23.1 (*C*H$_2$). *NCO$_2$ signal was not detected.*

MS (FAB, NBA) *m/z* (%): 354.2 ([M+H]$^+$, 15), 280.0 (100), 236.1 (30), 170.1 (29), 114.0 (49), 70.0 (28), 57.0 (28).

Analytical data of oxazolidinone **95**:
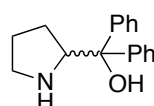
C$_{18}$H$_{17}$NO$_2$ (279.34 g/mol)

R$_f$ = 0.10 (cyclohexane/EtOAc 10:1).

^{1}H NMR (CDCl$_3$, 400 MHz) δ/ppm: 7.54-7.49 (m, 2 H, Ar-*H*), 7.40-7.25 (m, 8 H, Ar-*H*), 4.55 (dd, $^3J_{HH}$ = 10.5 Hz, $^3J_{HH}$ = 5.6 Hz, 1 H, NC*H*), 3.77-3.69 (m, 1 H, NC*H*$_2$), 3.28-3.21 (m, 1 H, NC*H*$_2$), 2.03-1.91 (m, 1 H, C*H*$_2$), 1.91-1.79 (m, 1 H, C*H*$_2$), 1.76-1.67 (m, 1 H, C*H*$_2$), 1.18-1.07 (m, 1 H, C*H*$_2$).

^{13}C{^{1}H} NMR (CDCl$_3$, 101 MHz) δ/ppm: 160.4 (N*C*O), 143.6, 140.3 (2 x Ar-*C*), 128.6, 128.3, 128.3, 127.7, 126.0, 125.5 (6 x Ar-*C*H), 85.9 (Ph$_2$*C*O), 69.3 (N*C*H), 46.1 (N*C*H$_2$), 29.0 (*C*H$_2$), 24.9 (*C*H$_2$).

Alternative synthesis without purification of the Boc-protected intermediate: Diphenyl-pyrrolidin-2-yl-methanol 92

A flame-dried Schlenk tube was flushed with argon and charged with *N-tert*-butyloxycarbonyl-pyrrolidine **93** (342 mg, 351 µL, 2.00 mmol, 1.00 eq.), TMEDA (306 mg, 396 µL, 2.60 mmol, 1.30 eq., distilled over 4 Å molecular sieves) and Et$_2$O (6 mL) at –78 °C using a dry ice/acetone bath. *sec*-BuLi (1.4 M in cyclohexane, 1.86 mL, 2.60 mmol, 1.30 eq.) was added dropwise and the solution was kept at –78 °C for 2 h. Benzophenone (728 mg, 4.00 mmol, 2.00 eq.) was added in several portions and the mixture was slowly allowed to warm to room temperature in the dry ice bath overnight. The yellow solution was quenched with H$_2$O (10 mL), the phases were separated and the aqueous layer was extracted with Et$_2$O (2 x 40 mL). The combined organic layers were washed with 5% aqueous H$_3$PO$_4$ (10 mL), dried over MgSO$_4$, filtered and the solvent concentrated under reduced pressure. The resulting colorless oil was dissolved in dry MeOH (10 mL). KOH (1.68 g, 30.0 mmol, 15.0 eq.) was added and the suspension was stirred for 5 h under reflux and additional 14 h at room temperature until TLC monitoring indicate complete consumption of the protected aminoalcohol **94** and oxazolidinone **95**. The reaction mixture was diluted with H$_2$O (10 mL) and extracted with CHCl$_3$ (2 x 20 mL). The combined organic layers were washed with brine (10 mL), dried over MgSO$_4$, filtered and the solvent evaporated. The crude product was purified by flash column chromatography (SiO$_2$, 20 cm x 3.5 cm, EtOAc + 1% Et$_3$N) to afford 300 mg of product, which was further purified by recrystallization from pentane/Et$_2$O. Storage at –25 °C afforded prolinol **92** (286 mg, 56%) as a colorless solid. Analytical data are in accordance with literature data.[110]

C$_{17}$H$_{19}$NO (253.34 g/mol)

m.**p**.: 78-80 °C (Lit.[110] 80-81°C).

***R**$_f$* = 0.31 (EtOAc + 1% Et$_3$N).

^{1}H NMR (CDCl$_3$, 400 MHz) δ/ppm: 7.59-7.56 (m, 2 H, Ar-*H*), 7.51-7.49 (m, 2 H, Ar-*H*), 7.31-7.25 (m, 4 H, Ar-*H*), 7.19-7.14 (m, 2 H, Ar-*H*), 4.61 (br s, 1 H, O*H*), 4.25 (t, $^3J_{HH}$ = 7.6 Hz, 1 H, C*H*N), 3.06-3.01 (m, 1 H, NC*H*$_2$), 2.97-2.91 (m, 1 H, NC*H*$_2$), 1.78-1.53 (m, 5 H, 2 x C*H*$_2$, N*H*).

^{13}C{^{1}H} NMR (CDCl$_3$, 101 MHz) δ/ppm: 148.3, 145.5 (2 x Ar-*C*), 128.4, 128.1, 126.6, 126.5, 126.0, 125.6 (6 x Ar-*C*H), 77.2 (*C*OH), 64.6 (*C*HN), 46.9 (N*C*H$_2$), 26.4, 25.6 (2 x *C*H$_2$).

2-(Diphenyl((trimethylsilyl)oxy)methyl)pyrrolidine 77a
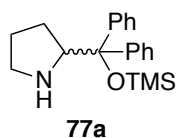
Under an argon atmosphere, a two-necked flask was charged with diphenyl-pyrrolidin-2-yl-methanol **92** (100 mg, 395 μmol, 1.00 eq.), Et$_3$N (52.0 mg, 71.2 μL, 514 μmol, 1.30 eq.) and dry CH$_2$Cl$_2$ (2 mL). The solution was cooled to 0 °C and TMSOTf (114 mg, 93.0 μL, 514 μmol, 1.30 eq.) was added dropwise. The reaction mixture was slowly allowed to warm to room temperature and was further stirred for 1 h. The mixture was quenched with H$_2$O (5 mL) and was extracted with CH$_2$Cl$_2$ (3 x 10 mL). The combined organic layers were dried over MgSO$_4$, filtered and the solvent concentrated under reduced pressure. The crude product was purified by flash column chromatography (SiO$_2$, 20 cm x 3.5 cm, cyclohexane/EtOAc 1:1 + 1% Et$_3$N) to afford racemic Hayashi-Jørgensen catalyst **77a** (107 mg, 83%) as an off-white solid. Analytical data are in accordance with literature data.[81]

C$_{20}$H$_{27}$NOSi (325.52 g/mol)

m.**p**.: 56-58 °C.

***R**$_f$* = 0.60 (cyclohexane/EtOAc 1:1 + 1% Et$_3$N).

^{1}H NMR (CDCl$_3$, 400 MHz) δ/ppm: 7.53-7.51 (m, 2 H, Ar-*H*), 7.43-7.41 (m, 2 H, Ar-*H*), 7.36-7.25 (m, 6 H, Ar-*H*), 4.09 (t, $^3J_{HH}$ = 7.3 Hz, 1 H, C*H*N), 2.94-2.83 (m, 2 H, NC*H*$_2$), 1.74 (br s, 1 H, N*H*), 1.68-1.58 (m, 3 H, C*H*$_2$), 1.49-1.39 (m, 1 H, C*H*$_2$), –0.03 (s, 9 H, Si(C*H*$_3$)$_3$).

^{13}C{^{1}H} NMR (CDCl$_3$, 101 MHz) δ/ppm: 147.0, 145.9 (2 x Ar-*C*), 126.6, 127.7, 127.6, 127.6, 127.0, 126.9 (6 x Ar-*C*H), 83.3 (*C*OSi), 65.5 (*C*HN), 47.3 (N*C*H$_2$), 27.6, 25.2 (2 x *C*H$_2$), 2.3 (Si(*C*H$_3$)$_3$).

(*S*)-2-(Diphenyl((triisopropylsilyl)oxy)methyl)pyrrolidine (*S*)-77c
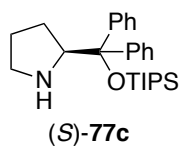
Under an argon atmosphere, a two-necked flask was charged with (*S*)-diphenyl-pyrrolidin-2-yl-methanol (*S*)-**92** (201 mg, 0.79 mmol, 1.00 eq.), 2,6-lutidine (595 mg, 647 µL, 5.55 mmol, 7.00 eq.) and dry CH_2Cl_2 (2 mL). The solution was cooled to 0 °C and TIPSOTf (1.25 g, 1.10 mL, 3.97 mmol, 5.00 eq.) was added dropwise. The reaction mixture was allowed to warm to room temperature and was stirred for 72 h. The mixture was quenched with sat. NH_4Cl solution (10 mL) and was extracted with $CHCl_3$ (3 x 20 mL). The combined organic layers were washed with 1 M KOH solution (10 mL) and brine (10 mL). The aqueous layers were re-extracted with $CHCl_3$ (20 mL) and the combined organic layers were dried over $MgSO_4$, filtered and the solvent concentrated under reduced pressure. The crude product was purified by flash column chromatography (SiO_2, 30 cm x 3.5 cm, CH_2Cl_2/MeOH 20:1) to afford organocatalyst **77c** (84 mg, 26%) as yellow oil and recovered starting material **92** (101 mg, 50%) as a colorless solid.

$C_{26}H_{39}NOSi$ (409.69 g/mol)

R_f = 0.22 (CH_2Cl_2/MeOH 20:1).

^{1}H NMR (CDCl$_3$, 400 MHz) δ/ppm: 7.52-7.49 (m, 2 H, Ar-*H*), 7.45-7.42 (m, 2 H, Ar-*H*), 7.31-7.25 (m, 6 H, Ar-*H*), 4.27 (t, $^3J_{HH}$ = 7.4 Hz, 1 H, C*H*N), 2.84 (dt, $^2J_{HH}$ = 10.1 Hz, $^3J_{HH}$ = 7.2 Hz, 1 H, NC*H*$_a$H$_b$), 2.41 (dt, $^2J_{HH}$ = 10.1 Hz, $^3J_{HH}$ = 6.9 Hz, 1 H, NCH$_a$*H*$_b$), 1.89-1.81 (m, 1 H, C*H*$_2$), 1.73-1.65 (m, 1 H, C*H*$_2$), 1.59-1.49 (m, 1 H, C*H*$_2$), 1.12-1.03 (m, 1 H, C*H*$_2$), 0.94, 0.93 (2 x d, $^3J_{HH}$ = 7.3 Hz, 18 H, Si(CH(C*H*$_3$)$_2$)$_3$), 0.87-0.78 (m, 3 H, Si(C*H*(CH$_3$)$_2$)$_3$). *NH* was *not detected.*

^{13}C{^{1}H} NMR (CDCl$_3$, 101 MHz) δ/ppm: 145.4, 144.4 (2 x Ar-*C*), 129.4, 129.2, 127.7, 127.6, 127.3 (5 x Ar-*C*H), 83.5 (*C*OSi), 65.6 (*C*HN), 47.2 (N*C*H$_2$), 28.0, 25.1 (2 x *C*H$_2$), 18.7, 18.6 (2 x Si*C*H(*C*H$_3$)$_2$), 13.9 (Si*C*H(CH$_3$)$_2$).

FTIR (ATR): 2944m, 2866m, 1490w, 1463w, 1445w, 1103m, 1062m, 1015w, 882w, 704m, 676m, 633s, 531s cm^{-1}.

**HRMS** (ESI, 4500 V, 180 °C) calc. (*m/z*) for $C_{26}H_{40}NOSi^+$: 410.2874, found: 410.2875 [M+H]$^+$; calc. (*m/z*) for $C_{17}H_{18}N^+$: 236.1434, found: 236.1435 [M-OTIPS]$^+$.

Optical rotation: $[\alpha]_D^{20}$ = –7.6 (c = 0.61, CHCl$_3$).

2-(Diphenyl((triisopropylsilyl)oxy)methyl)pyrrolidine 77c
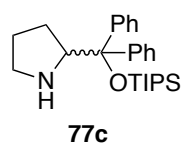
The racemic catalyst **77c** was synthesized according to the procedure described for the enantiopure catalyst (*S*)-**77c**. After stirring overnight at room temperature the racemic catalyst **77c** was isolated in 2% yield. Analytical data are in accordance with data of (*S*)-**77c**.

1-Benzyl-2-(1-hydroxy-1,1-diphenylmethyl)-pyrrolidine 98
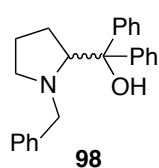
Diphenylpyrrolidin-2-yl-methanol **92** (250 mg, 987 µmol, 1.00 eq.) and K_2CO_3 (136 mg, 987 µmol, 1.00 eq.) were dissolved in dry EtOH (5 mL). Benzyl bromide was added (177 mg, 1.04 mmol, 1.05 eq.) and the mixture was heated to reflux for 3 h. The solvent was evaporated, the residue was dissolved in H_2O (20 mL) and the aqueous layer was extracted with Et_2O (3 x 20 mL). The combined organic layers were dried over $MgSO_4$, filtered and the solvent evaporated. The residue was purified by flash column chromatography (SiO_2, 15 cm x 2.5 cm, cyclohexane/EtOAc 1:1) to afford alcohol **98** (329 mg, 97%) as a colorless solid. Analytical data are in accordance with literature data.[105]

$C_{24}H_{25}NO$ (343.46 g/mol)

m.**p**.: 108-110 °C.

R_f = 0.22 (cyclohexane/EtOAc 1:1).

¹H NMR (CDCl₃, 400 MHz) δ/ppm: 7.72 (dd, $^3J_{HH}$ = 8.5 Hz, $^4J_{HH}$ = 1.1 Hz, 2 H, Ar-*H*), 7.58 (dd, $^3J_{HH}$ = 8.5 Hz, $^4J_{HH}$ = 1.1 Hz, 2 H, Ar-*H*), 7.32-7.00 (m, 11 H, Ar-*H*), 4.93 (br s, 1 H, O*H*), 3.97 (dd, $^3J_{HH}$ = 9.4 Hz, $^3J_{HH}$ = 4.6 Hz, 1 H, C*H*N), 3.22 (d, $^2J_{HH}$ = 12.6 Hz, 1 H, PhC*H*ₐHᵦ), 3.02 (d, $^2J_{HH}$ = 12.6 Hz, 1 H, PhCHₐ*H*ᵦ), 2.94-2.87 (m, 1 H, NC*H₂*), 2.38-2.30 (m, 1 H, NC*H₂*), 2.01-1.89 (m, 1 H, C*H₂*), 1.80-1.71 (m, 1 H, C*H₂*), 1.68-1.56 (m, 2 H, C*H₂*).

¹³C{¹H} NMR (CDCl₃, 101 MHz) δ/ppm: 148.2, 146.8, 139.8 (3 x Ar-*C*), 128.7, 128.3, 128.2, 128.2, 126.9, 126.5, 126.3, 125.7, 125.7 (9 x Ar-*C*H), 78.0 (*C*OH), 70.8 (*C*HN), 60.7 (Ph*C*H₂N), 55.6 (N*C*H₂), 29.9 (*C*H₂), 24.3 (*C*H₂).

1-Benzyl-2-(1-methoxy-1,1-diphenylmethyl)pyrrolidine 99
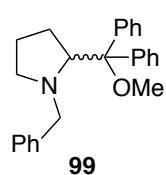
Under an argon atmosphere, 1-benzyl-2-(1-hydroxy-1,1-diphenylmethyl)-pyrrolidine **98** (312 mg, 620 µmol, 1.00 eq.) was dissolved in dry THF (1.2 mL) and cooled to −30 °C. Iodomethane (889 mg, 390 µL, 6.20 mmol, 10.0 eq.) and NaH (60% in mineral oil, 62.0 mg, 1.55 mmol, 2.50 eq.) were added subsequently. The mixture was further stirred for 30 min at this temperature followed by 2.5 h at reflux upon TLC monitoring indicated complete conversion. The reaction mixture was quenched with some drops of sat. NH₄Cl solution and the volatiles were removed under HV. The residue was suspended in H_2O (10 mL) and the aqueous layer was extracted with CH_2Cl_2 (3 x 20 mL). The combined organic layers were dried over $MgSO_4$, filtered and the solvent concentrated under reduced pressure to yield an orange oil, which was purified by flash column chromatography (SiO₂, 15 cm x 3.5 cm, cyclohexane/EtOAc 5:1). Methyl ether **99** (188 mg, 85%) was isolated as a yellow solid. Analytical data are in accordance with literature data.[105]

$C_{25}H_{27}NO$ (343.46 g/mol)

R_f = 0.55 (cyclohexane/EtOAc 4:1 + 1% Et₃N).

¹H NMR (CDCl₃, 400 MHz) δ/ppm: 7.64-7.60 (m, 4 H, Ar-*H*), 7.37-7.12 (m, 11 H, Ar-*H*), 4.19 (d, $^2J_{HH}$ = 12.8 Hz, 1 H, PhC*H*ₐHᵦ), 3.81 (dd, $^3J_{HH}$ = 9.7 Hz, $^3J_{HH}$ = 3.4 Hz, 1 H, C*H*N), 3.28 (d, $^2J_{HH}$ = 12.8 Hz, 1 H, PhCHₐ*H*ᵦ), 2.93 (s, 3 H, OC*H₃*), 2.45 (ddd, $^2J_{HH}$ = 9.4 Hz, $^3J_{HH}$ = 6.9 Hz, $^3J_{HH}$ = 2.3 Hz, 1 H, NC*H*ₐHᵦ), 2.08 (ddd, $^2J_{HH}$ = 9.4 Hz, $^3J_{HH}$ = 9.7 Hz, $^3J_{HH}$ = 6.0 Hz, 1 H, NCHₐ*H*ᵦ), 1.97-1.87 (m, 1 H, C*H₂*), 1.79-1.74 (m, 1 H, C*H₂*), 1.26-1.19 (m, 1 H, C*H₂*), 0.38-0.27 (m, 1 H, C*H₂*).

¹³C{¹H} NMR (CDCl₃, 101 MHz) δ/ppm: 141.2, 140.8, 139.4 (3 x Ar-*C*), 130.5, 130.3, 128.7, 128.1, 127.4, 127.2, 127.2, 127.1, 126.5 (9 x Ar-*C*H), 87.8 (*C*OCH₃), 70.4 (*C*HN), 62.0 (Ph*C*H₂), 54.9 (N*C*H₂), 52.0 (COC*H₃*), 29.0 (*C*H₂), 23.7 (*C*H₂).

2-(1-Methoxy-1,1-diphenylmethyl)pyrrolidine 77d
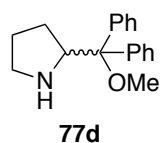
An autoclave was charged with 1-benzyl-2-(1-methoxy-1,1-diphenylmethyl)pyrrolidine **99** (93.0 mg, 260 µmol, 1.00 eq.), Pd/C (9.3 mg, 10 wt.%) and EtOH (1.5 mL). The mixture was stirred overnight under H_2 atmosphere (30 bar). Pd/C was filtered off and the solvent concentrated under reduced pressure. The crude product was purified by flash column chromatography (SiO₂, 17 cm x 2

cm, EtOAc/MeOH 20:1) to give a yellow oil that solidified upon storage in the fridge. The yellow solid was washed with cold Et_2O to afford organocatalyst **77d** (54 mg, 78%) as pale yellow solid. Analytical data are in accordance with literature data.[105]

$C_{18}H_{21}NO$ (267.37 g/mol)

m.p.: 218-220 °C.

R_f = 0.01-0.20 (EtOAc/MeOH 20:1).

^{1}H NMR (CDCl$_3$, 400 MHz) δ/ppm: 7.44-7.39 (m, 4 H, Ar-*H*), 7.33-7.24 (m, 6 H, Ar-*H*), 3.81 (t, $^3J_{HH}$ = 7.4 Hz, 1 H, C*H*N), 3.08 (s, 3 H, C*H*$_3$), 2.77-2.70 ("td", $^2J_{HH}$ = 10.3 Hz, $^3J_{HH}$ = 7.0 Hz, 1 H, NC*H*$_a$H$_b$), 2.59-2.53 (ddd, $^2J_{HH}$ = 10.3 Hz, $^3J_{HH}$ = 7.3 Hz, $^3J_{HH}$ = 5.5 Hz, 1 H, NCH$_a$*H*$_b$), 2.01 (br s, 1 H, N*H*) 1.91-1.83 (m, 1 H, C*H*$_2$), 1.68-1.48 (m, 2 H, C*H*$_2$), 1.13-1.03 (m, 1 H, C*H*$_2$).

^{13}C{^{1}H} NMR (CDCl$_3$, 101 MHz) δ/ppm: 142.9, 141.9 (2 x Ar-*C*), 129.3, 129.1, 127.7, 127.6, 127.3, 127.3 (6 x Ar-*C*H), 85.4 (*C*OCH$_3$), 62.3 (*C*HN), 51.5 (COC*H*$_3$), 47.0 (N*C*H$_2$), 27.6 (*C*H$_2$), 25.5 (*C*H$_2$).

N-(*tert*-Butyloxycarbonyl)-1-pyrrolidine-2-yl-cyclopentanol 104
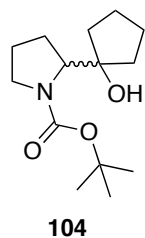
Under an argon atmosphere, a flame-dried two-necked flask equipped with a low temperature thermometer was charged with *N*-*tert*-butyloxycarbonyl-pyrrolidine **93** (342 mg, 351 μL, 2.00 mmol, 1.00 eq.), TMEDA (349 mg, 453 μL, 3.00 mmol, 1.50 eq., distilled over 4 Å molecular sieves) and dry THF (8 mL) at −78 °C using a dry ice/acetone bath. *sec*-BuLi (1.4 M in cyclohexane, 2.14 mL, 3.00 mmol, 1.50 eq.) was added dropwise over a period of 30 min with a syringe pump. The solution was kept at −78 °C for 3 h. Cyclopentanone (673 mg, 708 μL, 8.00 mmol, 4.00 eq.) dissolved in dry THF (8 mL) was added dropwise over a period of 1h with a syringe pump keeping the internal temperature below −50 °C. The reaction mixture was allowed to warm to room temperature and stirred at ambient temperature for 1 h. As soon the internal temperature exceeds 0 °C the color turned into yellow. The solution was cooled to −10 °C and quenched with sat. NH$_4$Cl solution (10 mL), the phases were separated and the aqueous layer was extracted with Et$_2$O (3 x 20 mL). The combined organic layers were washed with brine (10 mL), dried over MgSO$_4$, filtered and the solvent concentrated under reduced pressure. The crude product was purified by flash column chromatography (SiO$_2$, 20 cm x 3.5 cm, cyclohexane/EtOAc 3:1) to afford alcohol **104** (126 mg, 35%) as a colorless solid. Analytical data are in accordance with literature data.[137]

$C_{14}H_{25}NO_3$ (255.35 g/mol)

m.p.: 105-106 °C.

R_f = 0.22 (cyclohexane/EtOAc 3:1).

^{1}H NMR (CDCl$_3$, 400 MHz) δ/ppm: 5.00 (br s, 1 H, O*H*), 4.07-4.01 (m, 1 H, C*H*N), 3.66 (br s, 1 H, NC*H*$_a$H$_b$), 3.21 (dt, $^2J_{HH}$ = 11.2 Hz, $^3J_{HH}$ = 7.7 Hz, 1H, NCH$_a$*H*$_b$), 2.07-1.98 (m, 1 H, C*H*$_2$), 1.91-1.85 (m, 3 H, C*H*$_2$), 1.68-1.52 (m, 8 H, C*H*$_2$), 1.45 (s, 9 H, C(C*H*$_3$)$_3$).

^{13}C{^{1}H} NMR (CDCl$_3$, 101 MHz) δ/ppm: 157.1 (N*C*O$_2$), 85.7 (*C*OH), 80.2, (*C*(CH$_3$)$_3$), 65.2 (N*C*H), 48.4 (N*C*H$_2$), 38.7, 35.5, 28.9 (3 x *C*H$_2$), 28.6 (C(*C*H$_3$)$_3$), 24.6 (br s, *C*H$_2$), 24.5, 23.6 (2 x *C*H$_2$).

MS (EI, 70 eV, 250 °C) *m/z* (%): 114.1 (100), 70.1 (89), 57.1 (38), 41.1 (17).

(*S*)-*N*-(Ethoxycarbonyl)-1-pyrrolidine-2-yl-cyclopentanol 107
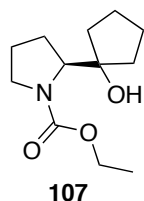
A two-necked flask was charged with magnesium turnings (0.86 g, 35.3 mmol, 7.10 eq.) and was flame-dried in HV. The flask was flushed with argon and 1,4-dibromobutane (2.71 g, 1.50 mL, 12.4 mmol, 7.10 eq.) dissolved in dry THF (3.5 mL) was added dropwise over 20 min with a syringe pump. To avoid tremendous reflux the flask was cooled with an external water bath. The mixture was stirred for 1 h at ambient temperature. The grey slurry was cooled to 0 °C and (*S*)-1-(ethoxycarbonyl)proline methyl ester (*S*)-**90** (1.00 g, 4.97 mmol, 1.00 eq.) dissolved in dry THF (90 mL) was added over 45 min. The reaction mixture was stirred for 90 min until GC/MS indicate complete consumption of the starting material. The reaction mixture was quenched with NH$_4$Cl solution (15 mL) and the precipitate was dissolved with H$_2$O (5 mL). The excess magnesium was filtered off and the organic layer was diluted with EtOAc. The phases were separated, the aqueous layer was extracted with EtOAc (2 x 50 mL) and the combined organic layers were washed with brine (20 mL) dried over MgSO$_4$, filtered and the solvent concentrated under reduced pressure. The crude product was purified by flash column chromatography (SiO$_2$, 15 cm x 6 cm, cyclohexane/EtOAc 3:1) to afford alcohol **107** (432 mg, 38%) as a pale yellow oil. Analytical data are in accordance with literature data.[138]

$C_{12}H_{21}NO_3$ (227.30 g/mol)

R_f = 0.10 (cyclohexane/EtOAc 3:1).

^{1}H NMR (CDCl$_3$, 400 MHz) δ/ppm: 4.14 (q, $^3J_{HH}$ = 7.1 Hz, 2 H, C*H*$_2$CH$_3$), 4.06 (t, $^3J_{HH}$ = 6.9 Hz, 1 H, C*H*N), 3.74-3.69 (m, 1 H, NC*H*$_a$H$_b$), 3.24 (dt, $^2J_{HH}$ = 11.0 Hz, $^3J_{HH}$ = 7.9 Hz, 1 H, NCH$_a$*H*$_b$), 2.08-1.98 (m, 1 H, C*H*$_2$), 1.98-1.76 (m, 3 H, C*H*$_2$), 1.74-1.66 (m, 3 H, C*H*$_2$),
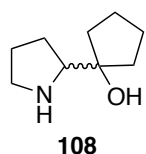
1.61-1.47 (m, 5 H, CH$_2$), 1.26 (t, $^3J_{HH}$ = 7.1 Hz, 3 H, CH$_2$CH$_3$).

^{13}C{^{1}H} NMR (CDCl$_3$, 101 MHz) δ/ppm: 157.7 (NCO$_2$)*, 85.6 (COH), 61.7 (CH$_2$CH$_3$), 48.3 (NCH$_2$), 38.7, 35.6, 28.9, 24.6, 23.6 (5 x CH$_2$), 14.8 (CH$_2$CH$_3$). *Deduced from HMBC.

MS (EI, 70 eV, 200 °C) m/z (%): 142.1 (66), 114.1 (100), 98.1 (11), 70.1 (69), 41.1 (11).

Optical rotation: $[\alpha]_D^{20}$ = –68.2° (c = 0.97, toluene) (Lit.[138] $[\alpha]_D^{20}$ = –60.8° (c = 0.4, toluene).

1-Pyrrolidine-2-yl-cyclopentanol 108

A solution of N-(tert-butyloxycarbonyl)-1-pyrrolidine-2-yl-cyclopentanol 104 (66.0 mg, 258 µmol, 1.00 eq.) in a 1:1 mixture of AcOH (2.5 mL) and 3 M HCl (2.5 mL) was stirred for 3 h at room temperature. The volatiles were removed in HV. The residue was diluted with H$_2$O (10 mL) and extracted with Et$_2$O (2 x 10 mL). The aqueous layer was basified with 4 M NaOH (10 mL) and extracted with CH$_2$Cl$_2$ (4 x 10 mL). The combined organic layers were dried over MgSO$_4$, filtered and the solvent concentrated under reduced pressure to afford aminoalcohol 108 (41 mg, quant.) as a colorless solid, which was used without further purification. Analytical data are in accordance with literature data.[138]

C$_6$H$_{17}$NO (155.24 g/mol)

m.p.: 50-51 °C.

^{1}H NMR (CDCl$_3$, 400 MHz) δ/ppm: 3.13-3.09 (m, 1 H, NCH), 3.03-2.93 (m, 2 H, NCH$_2$), 2.70 (br s, 2 H, NH, OH), 1.85-1.57 (m, 10 H, CH$_2$), 1.49-1.46 (m, 2 H, CH$_2$),

^{13}C{^{1}H} NMR (CDCl$_3$, 101 MHz) δ/ppm: 81.8 (COH), 66.5 (NCH), 46.9 (NCH$_2$), 39.9, 36.5, 26.4, 25.9, 24.2, 24.1 (6 x CH$_2$).

(S)-1-Pyrrolidine-2-yl-cyclopentanol (S)-108
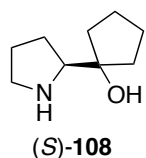
A mixture of (S)-N-(ethoxycarbonyl)-1-pyrrolidine-2-yl-cyclopentanol 107 (123 mg, 541 µmol, 1.00 eq.) and KOH (608 mg, 10.8 mmol, 20.0 eq.) in dry MeOH (2 mL) was stirred for 7 h at reflux and 14 h at room temperature under an argon atmosphere. MeOH was evaporated in HV and the residue was taken up in H$_2$O (10 mL) and extracted with CHCl$_3$ (3 x 20 mL). The combined organic layers were dried over MgSO$_4$, filtered and the solvent concentrated under reduced pressure to afford a yellow oil. The crude product was purified by flash column chromatography (SiO$_2$, 15 cm x 2.5 cm,

CH$_2$Cl$_2$/MeOH 5:1 + 1% Et$_3$N) to afford aminoalcohol (*S*)-**108** (55 mg, 66%) as a pale yellow semi-solid. Analytical data are in accordance with data of the racemic compound **108**.

R_f = 0.21 (CH$_2$Cl$_2$/MeOH 5:1 + 1% Et$_3$N).

Optical rotation: $[\alpha]_D^{20}$ = –33.8° (c = 0.60, CH$_2$Cl$_2$) (Lit.[138] $[\alpha]_D^{20}$ = –35.4° (c = 0.3, CH$_2$Cl$_2$).

(*S*)-2-(1-((*tert*-Butyldimethylsilyl)oxy)cyclopentyl)pyrrolidine (*S*)-109
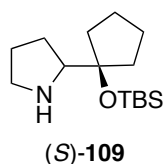
A flask was charged with (*S*)-1-pyrrolidine-2-yl-cyclopentanol (*S*)-108 (40.0 mg, 258 µmol, 1.00 eq.) and purged with argon. CH$_2$Cl$_2$ (400 µL) was added and the mixture cooled to 0 °C. 2,6-Lutidine (193 mg, 210 µL, 1.80 mmol, 7.00 eq.) and TBSOTf (341 mg, 296 µL, 1.29 mmol, 5.00 eq.) were added subsequently and stirred at room temperature overnight. The reaction mixture was quenched with NH$_4$Cl solution (1 mL) and extracted with CH$_2$Cl$_2$ (10 mL). The organic layer was washed with 1 M NaOH (5 mL), dried over MgSO$_4$, filtered and the solvent concentrated under reduced pressure. The residue was purified by flash column chromatography (SiO$_2$, 10 cm x 2.5 cm, CH$_2$Cl$_2$ (30 mL), then CH$_2$Cl$_2$/MeOH 10:1) to afford organocatalyst (*S*)-**109** (33 mg, 48%) as a pale yellow oil.

C$_{15}$H$_{31}$NOSi (269.50 g/mol)

R_f = 0.04-0.22 (CH$_2$Cl$_2$/MeOH 20:1).

^{1}H NMR (CDCl$_3$, 400 MHz) δ/ppm: 3.06-2.94 (m, 2 H, NC*H*, NC*H$_2$*), 2.79-2.73 (m, 1 H, NC*H$_2$*), 2.05 (br s, 1 H, N*H*), 1.90-1.85 (m, 1 H, C*H$_2$*), 1.77-1.47 (m, 11 H, C*H$_2$*), 0.85 (s, 9H, SiC(C*H$_3$*)$_3$), 0.10 (s, 3 H, SiC*H$_3$*), 0.09 (s, 3 H, SiC*H$_3$*).

^{13}C{^{1}H} NMR (CDCl$_3$, 101 MHz) δ/ppm: 86.5 (*C*OSi), 67.7 (N*C*H), 47.7 (N*C*H$_2$), 28.3, 38.1, 27.1, 26.5 (4 x *C*H$_2$), 26.1 (SiC(*C*H$_3$)$_3$), 24.4, 24.3 (2 x *C*H$_2$), 18.5 (Si*C*(CH$_3$)$_3$), –2.3, –2.3 (2 x Si*C*H$_3$).

FTIR (ATR): 2954m, 2930m, 2856w, 1472w, 1252w, 1066m (br), 833m, 771m, 676w, 632s, 535s cm^{-1}.

HRMS (ESI, 4500 V, 180 °C) calc. (*m/z*) for C$_{15}$H$_{32}$NOSi$^+$: 270.2248, found: 270.2250 [M+H]$^+$.

2-(1-((*tert*-Butyldimethylsilyl)oxy)cyclopentyl)pyrrolidine 109
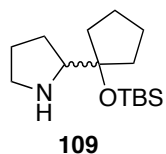
The racemic catalyst was synthesized according to the procedure described for the (*S*)-enantiomer. Analytical data are in accordance with data of the enantiopure compound (*S*)-**109**.

(2*S*)-*N*-(*tert*-Butoxycarbonyl)pyrrolidine-2-carboxaldehyde 111
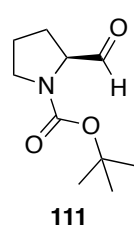
Under an argon atmosphere, a solution of oxalyl chloride (378 mg, 2.98 mmol, 1.20 eq.) in CH$_2$Cl$_2$ (1.5 mL) was cooled to –78 °C with a dry ice/acetone bath. DMSO (427 mg, 388 μL, 5.47 mmol, 2.20 eq.) dissolved in CH$_2$Cl$_2$ (6.0 mL) was added dropwise over 5 min and the mixture stirred for 10 min. *N*-Boc-L-prolinol **132** (500 mg, 2.58 mmol, 1.00 eq.) dissolved in CH$_2$Cl$_2$ (2.5 mL) was added dropwise over 5 min and the mixture was stirred for 30 min whereupon a white solid precipitated. DIPEA (1.28 g, 1.64 mL, 9.94 mmol, 4.00 eq.) was added over 1 min and the resulting solution was allowed to warm to room temperature over 30 min. The reaction mixture was diluted with CH$_2$Cl$_2$ (50 mL) and washed with 5% aqueous HCl solution (3 x 20 mL) and with brine (20 mL). The organic layer was dried over MgSO$_4$, filtered and the solvent evaporated at 30 °C. Aldehyde **111** (493 mg, quant.) was isolated as a yellow liquid and used without further purification. Analytical data are in accordance with literature data.[139]

C$_{10}$H$_{17}$NO$_3$ (199.25 g/mol)

^{1}H NMR (CDCl$_3$, 400 MHz) δ/ppm: 9.54 and 9.45 (2 x s, 1 H, C*H*O, rotamers), 4.20-4.17 and 4.05-4.02 (2 x m, 1 H, NC*H*, rotamers), 3.57-3.43 (m, 2 H, NC*H$_2$*), 2.14-1.85 (m, 4 H, C*H$_2$*), 1.46 and 1.42 (2 x s, 9 H, C(C*H$_3$*)$_3$, rotamers).

^{13}C{^{1}H} NMR (CDCl$_3$, 101 MHz) δ/ppm: 200.6 and 200.5 (*C*HO, rotamers), 155.1 and 154.1 (*N*CO$_2$, rotamers), 80.8 and 80.4 (*C*(CH$_3$)$_3$, rotamers), 65.2 and 65.0 (N*C*H, rotamers), 47.0 and 46.9 (N*C*H$_2$, rotamers), 28.5 and 28.4 (C(*C*H$_3$)$_3$, rotamers), 28.1 and 26.9 (*C*H$_2$, rotamers), 24.8 and 24.1 (*C*H$_2$, rotamers).

Optical rotation: $[\alpha]_D^{20}$ = –98.2° (c = 0.61, CHCl$_3$) (Lit.[139] $[\alpha]_D^{20}$ = –98.4° (c = 0.66, CHCl$_3$)).

(1S*,2S*)- and (1R*,2S*)-2-(Hydroxyphenylmethyl)pyrrolidine-1-carboxylic acid *tert*-butyl ester (S*,S*)-112 and (R*,S*)-112
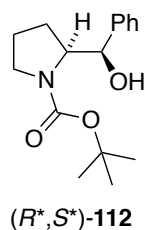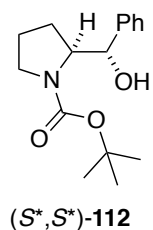
A flame dried Schlenk tube was flushed with argon and charged with TMEDA (353 mg, 458 µL, 3.05 mmol, 1.30 eq., distilled over 4 Å molecular sieves) and dry Et_2O (5 mL) at −78 °C using a dry ice/acetone bath. *sec*-BuLi (1.4 M in cyclohexane, 2.17 mL, 3.04 mmol, 1.30 eq.) was added dropwise and stirred for 10 min. *N-tert*-butyloxycarbonyl-pyrrolidine **93** (400 mg, 409 µL, 2.34 mmol, 1.00 eq.) dissolved in dry Et_2O (1.5 mL) was added dropwise and the solution was stirred for additional 3 h at −78 °C. Benzaldehyde (496 mg, 475 µL, 4.67 mmol, 2.00 eq.) in Et_2O (1 mL) was added dropwise and the mixture was allowed to warm to room temperature and stirred overnight. The reaction mixture was quenched with sat. NH_4Cl solution (30 mL) and diluted with Et_2O (30 mL). The layers were separated and the aqueous layer extracted with Et_2O (30 mL). The combined organic layers were washed with 5% aqueous H_3PO_4 solution (10 mL) and dried over $MgSO_4$, filtered and the solvent evaporated. ^{1}H NMR analysis out of the crude product indicated a mixture of diastereoisomers ((S*,S*)-112/(R*,S*)-112 ≈ 2:1). The crude mixture was purified by flash column chromatography (SiO_2, 17 cm x 6 cm, CH_2Cl_2/acetone 20:1 (1 L), then CH_2Cl_2/acetone 10:1) to afford 2-(hydroxyphenylmethyl)pyrrolidine-1-carboxylic acid *tert*-butyl ester **112** (371 mg (S*,S*); 103 mg (S*,S*)/(R*,S*) ≈ 1:1.2; 154 mg (R*,S*); combined yield: 628 mg, 98%) as pale yellow oils and the pure (R*,S*)-diastereoisomer as colorless solid. Analytical data are in accordance with literature data. The relative configuration was assigned based on the corresponding ^{1}H NMR spectra.[107]

$C_{16}H_{23}NO_3$ (277.36 g/mol)

Analytical data of diastereoisomer (S*,S*)-**112**

R_f = 0.30 (CH_2Cl_2:acetone 98:2).

^{1}H NMR (CDCl$_3$, 400 MHz) δ/ppm: 7.37-7.25 (m, 5 H, Ar-*H*), 5.85 (br s, 1 H, O*H*), 4.52 (br d, $^3J_{HH}$ = 8.4 Hz, 1 H, C*H*OH), 4.09 (td, $^3J_{HH}$ = 8.4 Hz, $^3J_{HH}$ = 3.8 Hz, 1 H, C*H*N), 3.50-3.42 (m, 1 H, NC*H*$_2$), 3.40-3.33 (m, 1 H, NC*H*$_2$), 1.78-1.50 (m, 4 H, C*H*$_2$), 1.52 (s, 9 H, C(C*H*$_3$)$_3$).

^{13}C{^{1}H} NMR (CDCl$_3$, 101 MHz) δ/ppm: 158.3 (N*C*O$_2$), 142.7 (Ar-*C*), 128.3, 127.8 (2 x Ar-*C*H), 127.2 (br, Ar-*C*H), 80.8 (*C*(CH$_3$)$_3$), 79.3 (*C*HOH), 64.2 (N*C*H), 47.7 (N*C*H$_2$), 28.7 (*C*H$_2$), 28.5 (C(*C*H$_3$)$_3$), 23.8 (*C*H$_2$).

Analytical data of diastereoisomer (*R**,*S**)-**112**

R_f = 0.20 (CH$_2$Cl$_2$:acetone 98:2).

^{1}H NMR (CDCl$_3$, 400 MHz) δ/ppm: 7.33-7.23 (m, 5 H, Ar-*H*), 4.94 (d, $^3J_{HH}$ = 1.8 Hz, 1 H, C*H*OH), 4.24-4,16 (m, 1 H, C*H*N), 3.93 (br s, 1 H, OH), 3.40-3.33 (m, 1 H, NC*H*$_2$), 2.99-2.92 (m, 1 H, NC*H*$_2$), 1.86-1.72 (m, 2 H, C*H*$_2$), 1.59-1.52 (m, 10 H, C*H*$_2$, C(C*H*$_3$)$_3$), 1.38-1.29 (m, 1 H, C*H*$_2$).

^{13}C{^{1}H} NMR (CDCl$_3$, 101 MHz) δ/ppm: 141.4 (Ar-*C*), 128.2, 127.4, 126.8 (3 x Ar-*C*H), 80.4 (*C*HOH), 63.5 (N*C*H), 47.9 (N*C*H$_2$), 28.6 (C(*C*H$_3$)$_3$), 27.0, 23.7 (2 x *C*H$_2$). *Quaternary signals of the Boc-group were not detected.*

(1*S*,2*S*)- and (1*R*,2*S*)-2-(Hydroxyphenylmethyl)pyrrolidine-1-carboxylic acid *tert*-butyl ester (*S*,*S*)-112 and (*R*,*S*)-112
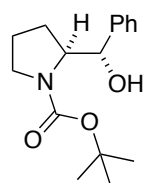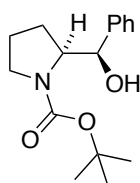
(*S*,*S*)-**112**   (*R*,*S*)-**112**

Under an argon atmosphere, (2*S*)-*N*-(*tert*-butoxycarbonyl)pyrrolidine-2-carboxaldehyde (200 mg, 1.00 mmol, 1.00 eq.) was dissolved in dry THF (3.0 mL). The solution was cooled to −78 °C and phenylmagnesiumbromide solution (3 M in Et$_2$O, 0.67 mL, 2.00 mmol, 2.00 eq.) was added dropwise. The reaction mixture was stirred at room temperature for 4 h, was quenched with sat. NH$_4$Cl solution (10 mL) and extracted with CH$_2$Cl$_2$ (2 x 20 mL). The combined organic layers were washed with brine (20 mL) and the aqueous layer was re-extracted with CH$_2$Cl$_2$ (20 mL). The combined organic layers were dried over MgSO$_4$, filtered and the solvent evaporated under reduced pressure. ^{1}H NMR analysis out of the crude product indicated a mixture of diastereoisomers ((*S*,*S*)-112/(*R*,*S*)-112 ≈ 1:1.2). The crude mixture was purified by flash column chromatography (SiO$_2$, 20 cm x 3.5 cm, CH$_2$Cl$_2$/acetone 20:1) to afford 2-(hydroxyphenylmethyl)pyrrolidine-1-carboxylic acid *tert*-butyl ester **112** (83 mg , 30% (*S*,*S*), 97 mg, 35% (*R*,*S*)) as pale yellow oils.

Optical rotation (*S*,*S*)-**112**: $[\alpha]_D^{20}$ = +1.9° (c = 0.65, CHCl$_3$) (Lit.[107] $[\alpha]_D^{20}$ = +2.3° (c = 1.0, CHCl$_3$, 94% *ee*).

Optical rotation (*R*,*S*)-**112**: $[\alpha]_D^{20}$ = −116.4° (c = 0.53, CHCl$_3$) (Lit.[107] $[\alpha]_D^{20}$ = −105.1° (c = 1.00, CHCl$_3$, 94% *ee*).

Additional analytical data are in accordance with data of the racemic compounds (*S**,*S**)-**112** and (*R**,*S**)-**112**.

(1*S*,2*S*)-1-Phenyl-2-pyrrolidinemethanol (*S*,*S*)-113
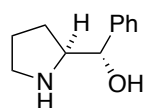
A solution of (1*S*,2*S*)-2-(hydroxyphenylmethyl)pyrrolidine-1-carboxylic acid *tert*-butyl ester (67.3 mg, 243 µmol, 1.00 eq.) in a 1:1 mixture of AcOH (2.5 mL) and 3 M HCl (2.5 mL) was stirred for 16 h at room temperature. The volatiles were removed in HV and the resulting colorless solid was dissolved in H_2O (10 mL). The aqueous layer was washed with Et_2O (2 x 10 mL), basified with a 4 M aqueous NaOH solution (10 mL) and extracted with CH_2Cl_2 (4 x 10 mL). The combined organic layers were dried over $MgSO_4$, filtered and the solvent was concentrated under reduced pressure to afford aminoalcohol (*S*,*S*)-113 (36.0 mg, 84%) as a colorless solid, which was used without further purification. Analytical data are in accordance with literature data.[139]

$C_{11}H_{15}NO$ (177.25 g/mol)

^{1}H NMR (CDCl$_3$, 400 MHz) δ/ppm: 7.37-7.24 (m, 5 H, Ar-*H*), 4.31 (br d, $^3J_{HH}$ = 7.0 Hz, 1 H, C*H*OH), 3.70 (br s, 2 H, N*H*, O*H*), 3.35 (ddd, $^3J_{HH}$ = 7.0 Hz, 2 x $^3J_{HH}$ = 6.8 Hz, 1 H, C*H*N), 3.02-2.93 (m, 2 H, NC*H*$_2$), 3.40-3.33 (m, 1 H, NC*H*$_2$), 1.90-1.79 (m, 1 H, C*H*$_2$), 1.76-1.54 (m, 3 H, C*H*$_2$).

^{13}C{^{1}H} NMR (CDCl$_3$, 101 MHz) δ/ppm: 143.1 (Ar-*C*), 128.4, 127.6, 126.7 (3 x Ar-*C*H), 75.5 (*C*HOH), 65.0 (N*C*H), 46.4 (N*C*H$_2$), 28.5, 26.2 (2 x *C*H$_2$).

(*S*)-2-(((*S*)-*tert*-Butyldimethylsilyloxy(phenyl)methyl)pyrrolidine (*S*,*S*)-114

A flask was charged with (1*S*,2*S*)-1-Phenyl-2-pyrrolidinemethanol (*S*,*S*)-113 (32.1 mg, 181 µmol, 1.00 eq.) and purged with argon. Dry CH_2Cl_2 (300 µL) was added and the solution cooled to 0 °C. Dry Et_3N (32.9 mg, 45.7 µL, 325 µmol, 1.80 eq.) and TBSOTf (76.4 mg, 66.4 µL, 289 µmol, 1.60 eq.) were added subsequently and the solution was allowed to warm to room temperature and stirred for 5 h. The reaction mixture was quenched with sat. NH_4Cl solution (10 mL) and extracted with $CHCl_3$ (3 x 10 mL). The combined organic layers were washed with 1 M aqueous KOH solution (5 mL) and brine (5 mL). The organic layer was dried over $MgSO_4$, filtered and the solvent evaporated under reduced pressure. The crude product was adsorbed onto silica and purified by flash column chromatography (SiO_2, 5 cm x 2.5 cm, CH_2Cl_2/MeOH 20:1) to afford organocatalyst (*S*,*S*)-114 (32 mg, 61%) as pale yellow oil.

247

$C_{17}H_{29}NOSi$ (291.51 g/mol)

$\mathbf{\mathit{R}_f}$ = 0.20 (CH$_2$Cl$_2$/MeOH 20:1).

^{1}H NMR (CDCl$_3$, 400 MHz) δ/ppm: 7.31-7.22 (m, 5 H, Ar-*H*), 4.60 (d, $^3J_{HH}$ = 7.2 Hz, C*H*OSi), 3.23 ("q", $^3J_{HH}$ = 7.2 Hz, 1 H, C*H*N), 3.05 (ddd, $^2J_{HH}$ = 9.8 Hz, $^3J_{HH}$ = 7.8 Hz, $^3J_{HH}$ = 5.7 Hz, 1 H, NC*H*$_a$H$_b$), 2.93-2.87 (m, 1 H, NCH$_a$*H*$_b$), 1.80-1.65 (m, 2 H, C*H*$_2$), 1.52-1.36 (m, 2 H, C*H*$_2$), 0.87 (s, 9 H, SiC(C*H*$_3$)$_3$), 0.04 (s, 3 H, SiC*H*$_3$), −0.22 (s, 3 H, SiC*H*$_3$). *NH proton was not detected.*

^{13}C{^{1}H} NMR (CDCl$_3$, 101 MHz) δ/ppm: 143.1 (Ar-*C*), 128.2, 127.6, 126.9 (3 x Ar-*C*H), 78.3 (*C*HOSi), 66.1 (N*C*H), 46.0 (N*C*H$_2$), 27.3 (*C*H$_2$), 26.0 (SiC(*C*H$_3$)$_3$), 24.6 (*C*H$_2$), 18.3 (Si*C*(CH$_3$)$_3$), −4.4, −4.8 (2 x Si*C*H$_3$).

FTIR (ATR): 2952m, 2928m, 2856m, 1471w, 1390w, 1251m, 1086s, 1061s, 1005w, 835s, 776s, 700s, 623s cm^{-1}.

HRMS (ESI, 4500 V, 180 °C) calc. (*m/z*) for C$_{17}$H$_{30}$NOSi$^+$: 292.2091, found: 292.2095 [M+H]$^+$; calc. (*m/z*) for C$_{11}$H$_{14}$N$^+$: 160.1121, found: 160.1121 [M-OTBS]$^+$.

Optical rotation: $[\alpha]_D^{20}$ = +52.9° (c = 0.53, CHCl$_3$).

(*S**)-2-((*S**)-*tert*-Butyldimethylsilyloxy(phenyl)methyl)pyrrolidine (*S**,*S**)-114
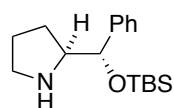
The racemic organocatalyst was synthesized according to the procedures described for the enantiopure aminoalcohol (*S*,*S*)-**113** and organocatalyst (*S*,*S*)-**114** over two steps. Analytical data are in accordance with data of the enantiopure compounds.
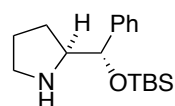
(1*R*,2*S*)-1-Phenyl-2-pyrrolidinemethanol (*R*,*S*)-113
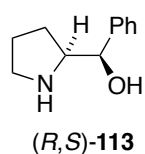
A solution of (1*R*,2*S*)-2-(hydroxyphenylmethyl)pyrrolidine-1-carboxylic acid *tert*-butyl ester (53.0 mg, 191 μmol, 1.00 eq.) in a 1:1 mixture of AcOH (2 mL) and 3 M HCl (2 mL) was stirred for 14 h at room temperature. The volatiles were removed in HV and the resulting colorless solid was dissolved in H$_2$O (10 mL). The aqueous layer was washed with Et$_2$O (2 x 10 mL), basified with a 4 M aqueous NaOH solution (10 mL) and extracted with CH$_2$Cl$_2$ (4 x 10 mL). The combined organic layers were dried over MgSO$_4$, filtered and the solvent was concentrated under reduced pressure to afford aminoalcohol (*R*,*S*)-**113** (30.0 mg, 89%) as a colorless glue, which was used without further

purification. Analytical data are in accordance with literature data.[139]

$C_{11}H_{15}NO$ (177.25 g/mol)

^{1}H NMR (CDCl$_3$, 400 MHz) δ/ppm: 7.38-7.31 (m, 4 H, Ar-*H*), 7.27-7.23 (m, 1 H, Ar-*H*), 4.76 (d, $^3J_{HH}$ = 4.4 Hz, 1 H, C*H*OH), 3.45 (td, $^3J_{HH}$ = 7.6 Hz, $^3J_{HH}$ = 4.4 Hz, 1 H, C*H*N), 3.06-2.92 (m, 2 H, NC*H*$_2$), 2.84 (br s, 2 H, N*H*, O*H*), 1.80-1.61 (m, 3 H, C*H*$_2$), 1.50-1.41 (m, 1 H, C*H*$_2$).

^{13}C{^{1}H} NMR (CDCl$_3$, 101 MHz) δ/ppm: 142.2 (Ar-*C*), 128.3, 127.3, 126.0 (3 x Ar-*C*H), 73.7 (*C*HOH), 64.2 (N*C*H), 46.8 (N*C*H$_2$), 25.6, 24.9 (2 x *C*H$_2$).

(*S*)-2-((*R*)-*tert*-Butyldimethylsilyloxy(phenyl)methyl)pyrrolidine (*S,R*)-114
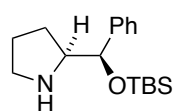
A flask was charged with (1*R*,2*S*)-1-phenyl-2-pyrrolidinemethanol (*R,S*)-**113** (30.0 mg, 169 µmol, 1.00 eq.) and purged with argon. Dry CH$_2$Cl$_2$ (340 µL) was added and the solution cooled to 0 °C. Dry Et$_3$N (42.8 mg, 59.5 µL, 423 µmol, 2.50 eq.) and TBSOTf (94.0 mg, 81.7 µL, 355 µmol, 2.10 eq.) were added subsequently and the solution was allowed to warm to room temperature and stirred for 3 h. The reaction mixture was quenched with sat. NH$_4$Cl solution (10 mL) and extracted with CHCl$_3$ (3 x 10 mL). The combined organic layers were washed with 1 M aqueous KOH solution (5 mL) and brine (5 mL). The organic layer was dried over MgSO$_4$, filtered and the solvent evaporated. The crude product was adsorbed onto silica and purified by flash column chromatography (SiO$_2$, 5 cm x 2.5 cm, CH$_2$Cl$_2$/MeOH 20:1) to afford organocatalyst (*S,R*)-**114** (36 mg, 73%) as a pale yellow oil.

$C_{17}H_{29}NOSi$ (291.51 g/mol)

R$_f$ = 0.16 (CH$_2$Cl$_2$/MeOH 20:1).

^{1}H NMR (CDCl$_3$, 400 MHz) δ/ppm: 7.35-7.29 (m, 4 H, Ar-*H*), 7.26-7.22 (m, 1 H, Ar-*H*), 4.60 (d, $^3J_{HH}$ = 5.9 Hz, C*H*OSi), 3.13-3.09 (m, 1 H, C*H*N), 3.04-2.98 (m, 1 H, NC*H*$_2$), 2.96 (br s, 1 H, N*H*), 2.80-2.73 (m, 1 H, NC*H*$_2$), 1.77-1.62 (m, 4 H, C*H*$_2$), 0.88 (s, 9 H, C(C*H*$_3$)$_3$), 0.03 (s, 3 H, SiC*H*$_3$), −0.21 (s, 3 H, SiC*H*$_3$).

^{13}C{^{1}H} NMR (CDCl$_3$, 101 MHz) δ/ppm: 144.0 (Ar-*C*), 128.2, 127.3, 126.6 (3 x Ar-*C*H), 76.6 (*C*HOSi), 66.4 (*C*HN), 46.9 (N*C*H$_2$), 27.3 (*C*H$_2$), 26.0 (C(*C*H$_3$)$_3$), 25.3 (*C*H$_2$), 18.3 (Si*C*(CH$_3$)$_3$), −4.3, −4.9 (2 x Si*C*H$_3$).

FTIR (ATR): 2955m, 2929m, 2857m, 1471w, 1405w, 1361w, 1251m, 1086s, 1061s, 1026w, 1005w, 861s, 835s, 775s, 700s, 623s cm^{-1}.

HRMS (ESI, 4500 V, 180 °C) calc. (*m/z*) for $C_{17}H_{30}NOSi^+$: 292.2091, found: 292.2090 [M+H]$^+$; calc. (*m/z*) for $C_{11}H_{14}N^+$: 160.1121, found: 160.1120 [M-OTBS]$^+$.

Optical rotation: $[\alpha]_D^{20} = -72.8°$ (c = 0.48, CHCl$_3$).

(*S**)-2-((*R**)-*tert*-Butyldimethylsilyloxy(phenyl)methyl)pyrrolidine (*S***,*R**)-114
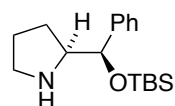
The racemic organocatalyst was synthesized according to the procedures described for the enantiopure aminoalcohol (*R*,*S*)-**113** and organocatalyst (*S*,*R*)-**114** over two steps. Analytical data are in accordance with the data of the enantiopure compounds.

6.5.3 Synthesis of Further Pyrrolidine-based Organocatalysts

2-[(*tert*-Butyldimethylsilyloxy)methyl]pyrrolidine 116
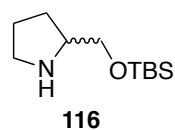
Under an argon atmosphere, TBSCl (328 mg, 2.18 mmol, 1.10 eq.) dissolved in dry CH$_2$Cl$_2$ (6 mL) was added to a mixture of D/L-prolinol (200 mg, 1.98 mmol, 1.00 eq.) and Et$_3$N (202 mg, 2.97 mmol, 3.00 eq.) in dry CH$_2$Cl$_2$ (10 mL) at room temperature. The solution was stirred for 8 h at room temperature. The reaction mixture was diluted with CH$_2$Cl$_2$ (35 mL) and washed with brine (50 mL). The aqueous layer was extracted with CH$_2$Cl$_2$ (50 mL) and the combined organic layers were washed with 1 M NaOH solution (10 mL), dried over MgSO$_4$, filtered and the solvent concentrated under reduced pressure. The crude product was purified by bulb-to-bulb distillation (120 °C, 0.15 mbar) to afford a colorless oil which was further purified by filtration through a plug of alox (basic, 3 cm x 1 cm, pentane 30 mL, then Et$_2$O 40 mL) to afford amine **116** (165 mg, 39%) as colorless oil. Analytical data are in accordance with literature data.[140]

$C_{11}H_{25}NOSi$ (215.41 g/mol)

R_f = 0.10-0.20 (CH$_2$Cl$_2$/MeOH 10:1).

¹H NMR (CDCl$_3$, 400 MHz) δ/ppm: 3.59 (dd, $^2J_{HH}$ = 10.1 Hz, $^3J_{HH}$ = 4.8 Hz, 1 H, C*H*$_a$H$_b$OSi), 3.52 (dd, $^2J_{HH}$ = 10.1 Hz, $^3J_{HH}$ = 6.0 Hz, 1 H, CH$_a$*H*$_b$OSi), 3.20-3.14 (m, 1 H, NC*H*), 3.02-2.96 (m, 1 H, NC*H*$_2$), 2.88-2.82 (m, 1 H, NC*H*$_2$), 2.24 (br s, 1 H, N*H*), 1.80-1.69 (m, 3 H, C*H*$_2$), 1.48-1.42 (m, 1 H, C*H*$_2$), 0.89 (s, 9 H, SiC(C*H*$_3$)$_3$), 0.05 (s, 6 H, SiC*H*$_3$).

$^{13}C\{^1H\}$ **NMR** (CDCl$_3$, 101 MHz) δ/ppm: 65.8 (CH_2OSi), 60.2 (NCH), 46.6 (NCH_2), 27.6 (CH_2), 26.1 (SiC(CH_3)$_3$), 25.5 (CH_2), 18.5 (SiC(CH$_3$)$_3$), −5.2 (SiCH_3)

(*S*)-2-[(*tert*-Butyldimethylsilyloxy)methyl]pyrrolidine (*S*)-116
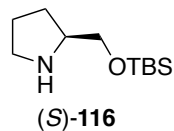
The enantiopure compound was synthesized according to the procedure described for racemic organocatalyst **116**. Analytical data are in accordance with data of the racemic organocatalyst **116**.

Optical rotation: $[\alpha]_D^{20} = -2.9°$ (c = 1.09, CHCl$_3$).

(*R*)-2-Phenylpyrrolidine (*R*)-118
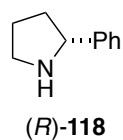
Commercial available 2-phenylpyrrolidine was partially separated into its enantiomers by semi-preparative HPLC on a chiral stationary phase (*Daicel* Chiralpak AD with chiral precolumn AD, hexane/*i*PrOH 96:4, 7 ml/min, 40 °C, 55 mg/500 µL, $t_R(R)$ = 29 min, $t_R(S)$ = 34 min). The (*R*)-enantiomer was subjected again to HPLC separation under identical conditions to afford amine (*R*)-**118** (15 mg) in 99% *ee.* The amine and an excess of TFAO$_2$ and Et$_3$N in CH$_2$Cl$_2$ were shaken for 1 min and filtrated over a plug of silica gel using Et$_2$O as eluent. The resulting trifluoroacetamide (CF$_3$CO-**118**) was subjected to GC analysis for a determination of the enantiomeric excess. The absolute configuration of the stereogenic center was assigned according to its optical rotation value.[109]

C$_{10}$H$_{13}$N (147.22 g/mol)

MS (EI, 70 eV, 250 °C) *m/z* (%) for (*R*)-**118**: 147.1 ([M]$^+$, 28), 146.1 (54), 118.1 (100), 91.1 (12), 104.1 (12), 70.1 (35), 41.1 (10); for CF$_3$CO-**118**: 243.1 ([M]$^+$, 100), 242.1 (86), 215.1 (40), 174.1 (27), 166.1 (25), 146.1 (48), 131.1 (18), 130.1 (23), 129.1 (15), 117.1 (19), 115.1 (15), 104.1 (40), 103.1 (15), 91.1 (59), 77.1 (20), 69.0 (24), 51.0 (11), 41.1 (12).

Chiral GC (β-Cyclodextrin, DEtTButSil (Brechbühler, SE54, 25 m × 0.25 mm × 0.25 µm), 60 kPa He, (100 °C – 2 min – 1 °C/min -150 °C – 0 min - 10 °C/min - 180 °C – 10 min): t_R((*S*)-CF$_3$CO-**118**) = 26.3 min, t_R((*R*)-CF$_3$CO-**118**) = 27.9 min.

Optical rotation: $[\alpha]_D^{20}$ = +58.3° (c = 0.95, CH$_2$Cl$_2$, 99% *ee*) (Lit.[109] $[\alpha]_D^{20}$ = +57.47° (c = 0.132, CH$_2$Cl$_2$, 98% *ee*).

6.5.4 Synthesis of Isoindoline-Derived Organocatalysts

N-*tert*-Butyloxycarbonyl-isoindoline 120
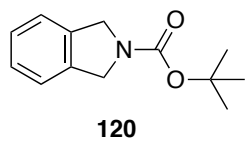
Di-*tert*-butylcarbonat (714 mg, 700 µL, 3.27 mmol, 1.30 eq.) was added to a solution of isoindoline (300 mg, 286 µL, 2.52 mmol, 1.00 eq.) and dry Et$_3$N (382 mg, 531 µL, 3.78 mmol, 1.50 eq.) in dry CH$_2$Cl$_2$ (5 mL) at 0 °C. The mixture was allowed to warm to room temperature and stirred for 3 h. Sat. NH$_4$Cl solution (10 mL) and CH$_2$Cl$_2$ (30 mL) were added and the phases separated. The organic layer was washed with brine (10 mL), dried over MgSO$_4$, filtered and the solvent concentrated under reduced pressure. The crude product was purified by flash column chromatography (SiO$_2$, 18 cm x 3.5 cm, cyclohexane/EtOAc 10:1) to afford product **120** (510 mg, 92%) as a colorless solid.

C$_{13}$H$_{17}$NO$_2$ (219.28 g/mol)

m.**p**.: 64-66 °C.

R$_f$ = 0.23 (cyclohexane/EtOAc 10:1).

^{1}H NMR (CDCl$_3$, 400 MHz) δ/ppm: 7.25 (br s, 4 H, Ar-*H*), 4.69 (s, 2 H, C*H*$_2$, rotamers), 4.66 (s, 2 H, C*H*$_2$, rotamers), 1.52 (br s, 9 H, C(C*H*$_3$)$_3$).

^{13}C{^{1}H} NMR (CDCl$_3$, 101 MHz) δ/ppm: 154.7 (NCO$_2$), 137.5, 137.1 (2 x Ar-*C*), 127.4, 122.9, 122.7 (3 x Ar-*CH*), 79.8 (*C*(CH$_3$)$_3$), 52.4, 52.2 (2 x *CH*$_2$), 28.7 (C(*CH*$_3$)$_3$).

FTIR (ATR): 2979w, 2936w, 2900w, 2865w, 1688s, 1477m, 1393s, 1288m, 1256m, 1170m, 1108s, 873m, 747s, 605m cm^{-1}.

MS (EI, 70 eV, 200°C) *m/z* (%): 219.1 ([M]$^+$, 1), 162.1 ([M-C(CH$_3$)$_3$]$^+$, 100), 146.1 (49), 118.1 (83), 91.1 (15), 57.1 (81), 41.1 (11).

EA calc. (%) for C$_{13}$H$_{17}$NO$_2$: C 71.21, H 7.81, N 6.39; found: C 70.83, H 7.67, N 6.33.

N-Benzylisoindoline 122
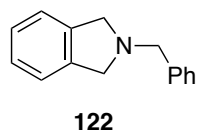
Benzylamine (3.20 g, 3.26 ml, 29.80 mmol, 1.05 eq.) dissolved in CHCl$_3$ (12 ml) was added over 5 min to a solution of 1,2-dibromo-*o*-xylene (7.50 g, 28.4 mmol, 1.00 eq.) and Et$_3$N (6.33 g, 8.79 ml, 62.5 mmol, 2.20 eq.) in CHCl$_3$ (20 ml) at 0°C. The mixture was stirred under reflux for 13 h. The reaction mixture was washed with NaHCO$_3$ (3 x 40 ml) and brine (40 ml). The aqueous layers were re-extracted with CHCl$_3$ (80 ml). The combined organic layers were dried over MgSO$_4$, filtered and the solvent concentrated under reduced pressure. The yellow oil was purified by bulb-to-

bulb distillation (130 °C, 0.3 mbar) to afford amine **122** (4.07 g, 68%) as a colorless solid. Analytical data are in accordance with literature data.[141]

$C_{15}H_{15}NO$ (209.29 g/mol)

m.**p**.: 35-36 °C.

^{1}H NMR (CDCl$_3$, 400 MHz) δ/ppm: 7.46-7.42 (m, 2 H, Ar-*H*), 7.39-7.35 (m, 2 H, Ar-*H*), 7.32-7.29 (m, 1 H, Ar-*H*), 7.20 (s, 4 H, Ar-*H*), 3.96 (s, 4 H, NC*H*$_2$), 3.94 (s, 2 H, PhC*H*$_2$).

^{13}C{^{1}H} NMR (CDCl$_3$, 101 MHz) δ/ppm: 140.3, 139.2 (2 x Ar-*C*), 128.9, 128.5, 127.3, 126.8, 122.5 (5 x Ar-*C*H), 60.4 (Ph*C*H$_2$), 59.1 (N*C*H$_2$).

(*N*)-(*tert*-Butyliminomethyl)isoindoline 123

123
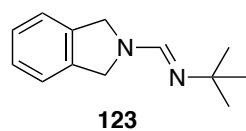
A suspension of freshly distilled isoindoline (1.06 g, 8.91 mmol, 1.00 eq.), *N'*-*tert*-butyl-*N*,*N*-dimethylformamidine (2.14 g, 2.61 mL, 16.7 mmol, 1.90 eq.) and ammonium sulfate (0.12 g, 0.89 mmol, 10 mol%) in toluene (50 mL) was stirred under reflux for 20 h under an argon atmosphere. The solvent was evaporated under reduced pressure and the crude product (1.68 g) was purified by flash column chromatography (SiO$_2$, 20 cm x 3.5 cm, cyclohexane/EtOAc 5:1 + 5% Et$_3$N (200 mL), cyclohexane/EtOAc 1:1 + 5 % Et$_3$N (200 mL) then EtOAc + 5% Et$_3$N). Subsequent bulb-to-bulb distillation (0.2 mbar, 160 °C) afforded imim **123** (1.28 g, 71%) as a colorless solid.

$C_{13}H_{18}N_2$ (202.30 g/mol)

m.**p**.: 59-60 °C.

R_f = 0.42 (EtOAc + 5% Et$_3$N).

^{1}H NMR (CDCl$_3$, 400 MHz) δ/ppm: 7.70 (s, 1 H, NC*H*N), 7.25 (br s, 4 H, Ar-*H*), 4.70 (s, 4 H, C*H*$_2$), 1.22 (s, 9 H, C(C*H*$_3$)$_3$).

^{13}C{^{1}H} NMR (CDCl$_3$, 101 MHz) δ/ppm: 147.9 (N*C*HN), 137.6 (Ar-*C*), 127.3, 122.8 (2 x Ar-*C*H), 53.6 (*C*(CH$_3$)), 53.1 (*C*H$_2$), 31.5 (C(*C*H$_3$)).

FTIR (ATR): 3049w, 2963m, 2897w, 2866w 1643s, 1464m, 1400m, 1368s, 1358s, 1320m, 1279w, 1207s, 1163m, 1092w, 1028w, 937m, 876w, 813w, 738s cm^{-1}.

MS (EI, 70 eV, 200°C) *m/z* (%): 202.2 ([M]$^+$, 17), 145.1 (34), 130.1 (10), 118.1 ([M-HCNC(CH$_3$)$_3$]$^+$, 100), 117.1 (11).

MS (ESI) *m/z*: 203.1 [M+H]$^+$.

EA calc. (%) for $C_{13}H_{18}N_2$: C 77.18, H 9.97, N 13.85; found: C 77.00, H 8.67, N 13.59.

(2-((*tert*-Butylimino)methyl)isoindolin-1-yl)diphenylmethanol 124
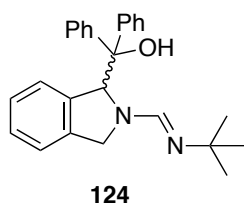
124

A heat gun dried Schlenk tube was flushed with argon and charged with (*N*)-(*tert*-butyliminomethyl)isoindoline **123** (225 mg, 1.11 mmol, 1.00 eq.) and dry THF (5 ml). The mixture was cooled to -78 °C with a dry ice/acetone bath. *sec*-BuLi (0.79 ml (1.4 M), 1.11 mmol, 1.00 eq.) was added dropwise. The mixture was stirred for 1 h at −78 °C and benzophenone (304 mg, 1.67 mmol, 1.50 eq.) was added slowly in small portions. The reaction mixture was allowed to warm to room temperature in the cooling bath overnight. The dark red to black solution was cooled to 0 °C, quenched with H_2O (10 mL) and diluted with Et_2O (30 mL). The layers were separated and the organic layer was washed with brine (10 mL). The combined aqueous phases were re-extracted with Et_2O (20 mL). The combined organic layers were dried over $MgSO_4$, filtered and the solvent evaporated. The crude product was purified by flash column chromatography (SiO_2, 20 cm x 3.5 cm, cyclohexane/EtOAc 10:1 (200 ml), cyclohexane/EtOAc 5:1 (100 ml) then EtOAc + 5% Et_3N) to afford alcohol **124** (351 mg, 82%) as a brownish solid. For analytical purposes, an aliquot was further purified by recrystallization from Et_2O/pentane to afford a colorless solid.

$C_{26}H_{28}N_2O$ (384.51 g/mol)

m.**p**.: 145-146 °C.

R_f = 0.61 (EtOAc + 5% Et_3N).

^{1}H NMR (CDCl$_3$, 400 MHz) δ/ppm: 10.69 (br s, 1 H, O*H*), 7.55 (dd, $^3J_{HH}$ = 8.0 Hz, $^4J_{HH}$ = 1.8 Hz, 2 H, Ar-*H*), 7.36 (s, 1 H, NC*H*N), 7.35-7.29 (m, 3 H, Ar-*H*), 7.21-7.09 (m, 7 H, Ar-*H*), 6.90 (t, $^3J_{HH}$ = 7.6 Hz, 1 H, Ar-*H*), 5.87 (d, $^3J_{HH}$ = 7.8 Hz, 1 H, Ar-*H*), 5.84 (d, $^4J_{HH}$ = 2.7 Hz, 1 H, C*H*N), 4.45 (d, $^2J_{HH}$ = 13.3 Hz, 1 H, C*H*$_a$H$_b$), 3.98 (dd, $^2J_{HH}$ = 13.3 Hz, $^4J_{HH}$ = 2.7 Hz, 1 H, CH$_a$*H*$_b$), 1.23 (s, 9 H, C(C*H*$_3$)$_3$).

^{13}C{^{1}H} NMR (CDCl$_3$, 101 MHz) δ/ppm: 149.4 (N*C*HN), 144.6, 143.2, 138.8, 138.2 (4 x Ar-*C*), 128.5, 128.0, 127.7, 127.6, 127.5, 127.0, 126.9, 126.6, 124.8, 121.7 (10 x Ar-*C*H), 83.0 (*C*OH), 76.2 (*C*HN), 55.1 (*C*H$_2$), 53.5 (*C*(CH$_3$)$_3$), 31.0 (C(*C*H$_3$)$_3$).

FTIR (ATR): 3064w, 2964w, 2857w, 1635m, 1491w, 1463m, 1371m, 1317w, 1212m, 1179m, 1095w, 1049m, 867w, 788m, 757m, 725s, 698s cm^{-1}.

MS (ESI) *m/z*: 385.1 [M+H]$^+$.

EA calc. (%) for $C_{26}H_{28}N_2O$: C 81.21, H 7.34, N 7.29; found: C 81.09, H 7.30, N 7.17.

1-(Diphenyl((trimethylsilyl)oxy)methyl)isoindoline 128a
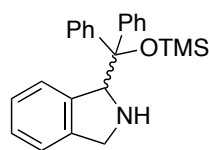
(2-((*tert*-Butylimino)methyl)isoindolin-1-yl)diphenylmethanol (138 mg, 360 µmol, 1.00 eq.) and $LiAlH_4$ (41.0 mg, 1.08 mmol, 3.00 eq.) were suspended in dry THF (3.5 mL) under an argon atmosphere. The suspension was stirred under reflux for 16 h. The reaction mixture was cooled to 0 °C diluted with Et_2O (1 mL) and treated with H_2O (41 µL), 4 M NaOH solution (41 µL) and H_2O (123 µL) subsequently. After 15 minutes Na_2SO_4 was added, the suspension filtered and the solvent evaporated under reduced pressure and the residue dried in HV to afford the deprotected aminoalcohol **126** (108 mg) as a black foam.

The crude product was dissolved in dry CH_2Cl_2 (1.8 mL) and cooled to 0 °C. Dry Et_3N (109 mg, 150 µL, 1.08 mmol, 3.00 eq.) and TMSOTf (160 mg, 130 µL, 720 µL, 2.00 eq.) were added dropwise and the reaction mixture stirred overnight. The black solution was treated with sat. $NaHCO_3$ solution (10 mL) and H_2O (5 mL) and the aqueous layers were extracted with CH_2Cl_2 (3 x 20 mL). The combined organic layers were washed with brine (10 mL), dried over $MgSO_4$, filtered and the solvent evaporated. The crude product was purified by flash column chromatography (SiO_2, 20 cm x 3.5 cm, CH_2Cl_2/MeOH 20:1) to afford the racemic organocatalyst **128a** (98 mg, 73%) as a black oil. For analytical purposes, an aliquot was purified by semi-preparative HPLC (*Reprospher* SiO_2, hexane/*i*PrOH 90:10, 6.0 mL/min, 25 °C, 195 nm, t_R = 16 min) to afford **128a** as a pale red solid,[i] which became dark red upon drying in HV overnight and in solution.

Analytical data of aminoalcohol intermediate **126**

$C_{21}H_{19}NO$ (301.39 g/mol)

^{1}H NMR (CDCl$_3$, 400 MHz) δ/ppm: 7.71-7.67 (m, 2 H, Ar-*H*), 7.61-7.57 (m, 2 H, Ar-*H*), 7.38-7.32 (m, 4 H, Ar-*H*), 7.28-7.15 (m, 4 H, Ar-*H*), 6.93-6.89 (m, 1 H, Ar-*H*), 5.94 (d, $^3J_{HH}$ = 7.8 Hz, 1 H, Ar-*H*), 5.75 (t, $^4J_{HH}$ = 2.4 Hz, 1 H, NC*H*), 4.29-4.20 (m, 2 H, C*H*$_2$), 2.87 (br s, 2 H, N*H*, O*H*).

^{13}C{^{1}H} NMR (CDCl$_3$, 101 MHz) δ/ppm: 147.6, 144.1, 142.1, 138.6 (4 x Ar-*C*), 128.6, 128.3, 127.6, 127.0, 126.9, 126.5, 126.2, 126.2, 124.5, 122.5 (10 x Ar-*C*H), 79.0 (*C*OH), 69.9 (N*C*H), 51.2 (*C*H$_2$).

---

[i] The solvent was concentrated under reduced pressure at room temperature.

Analytical data of organocatalyst **128a**

$C_{24}H_{27}NOSi$ (373.57 g/mol)

m.p.: >100 °C (decomposition).

$\boldsymbol{R_f}$ = 0.32 (CH$_2$Cl$_2$/MeOH 20:1).

^{1}H NMR (CDCl$_3$, 400 MHz) δ/ppm: 7.39-7.35 (m, 2 H, Ar-*H*), 7.29-7.25 (m, 5 H, Ar-*H*), 7.19-7.13 (m, 4 H, Ar-*H*), 7.10-7.03 (m, 2 H, Ar-*H*), 6.88 (d, $^3J_{HH}$ = 7.0 Hz, 1 H, Ar-*H*), 5.59 (d, $^4J_{HH}$ = 2.8 Hz, 1 H, NC*H*), 3.89 (d, $^3J_{HH}$ = 13.3 Hz, 1 H, C*H*$_a$H$_b$), 3.35 (dd, $^3J_{HH}$ = 13.3 Hz, $^4J_{HH}$ = 2.8, 1 H, CH$_a$*H*$_b$), 2.37 (br s, 1 H, N*H*), –0.11 (s, 9H, Si(C*H*$_3$)$_3$).

^{13}C{^{1}H} NMR (CDCl$_3$, 101 MHz) δ/ppm: 143.2, 143.2, 142.8, 140.2 (4 x Ar-*C*), 129.3, 129.2, 127.6, 127.5, 127.2, 127.2, 126.0, 125.2, 122.0 (9 x Ar-*C*H), 84.7 (*C*OSi), 71.1 (N*C*H), 51.6 (*C*H$_2$), 2.0 (Si(*C*H$_3$)$_3$).

FTIR (ATR): 3057w, 2953w, 2838w, 1492w, 1445m, 1248s, 1096m, 1085m, 1068s, 887m, 861m, 834s, 743m, 701s, 651m cm^{-1}.

HRMS (ESI, 4500 V, 180 °C) calc. *m/z* for $C_{24}H_{28}NOSi^+$: 374.1935, found: 374.1932 [M+H]$^+$; calc. *m/z* for $C_{21}H_{18}N^+$: 284.1434, found: 284.1434 [M-OTMS]$^+$.

Racemic Organocatalyst **128a** was separated into its enantiomers by semi-preparative HPLC on a chiral stationary phase (*Daicel* Chiralpak AD with precolumn AD, hexane/*i*PrOH 97:3, 8.0 mL/min, 25 °C, 210 nm, t_R(–) = 33 min, t_R(+) = 40 min). Both enantiomers were obtained in > 99.5% *ee.*

HPLC (*Daicel* Chiralpak AD, heptane/*i*PrOH 97:3, 0.5 mL/min, 25 °C, 210 nm): t_R((–)-**128a**) = 14.1 min, t_R((+)-**128a**= 17.7 min.

Optical rotation: $[\alpha]_D^{20}$ = –51.5° (c = 0.33, CHCl$_3$) and $[\alpha]_D^{20}$ = +50.2° (c = 0.35, CHCl$_3$).

1-(((*tert*-Butyldimethylsilyl)oxy)diphenylmethyl)isoindoline 128b
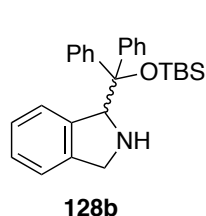
(2-((*tert*-Butylimino)methyl)isoindolin-1-yl)diphenylmethanol **124** (126 mg, 328 μmol, 1.00 eq.) and LiAlH$_4$ (37.3 mg, 1.08 mmol, 3.00 eq.) were suspended in dry THF (3 mL) under an argon atmosphere. The suspension was stirred under reflux for 16 h. The reaction mixture was cooled to 0 °C diluted with Et$_2$O (1 mL) and treated with H$_2$O (37 μL), 4 M NaOH solution (37 μL) and H$_2$O (111 μL) subsequently. MgSO$_4$ was added after 15 min, the suspension filtered and the solvent evaporated under reduced pressure and the residue dried in HV to afford the deprotected aminoalcohol **126** (99.3 mg) as a black foam.

The crude product was dissolved in dry CH$_2$Cl$_2$ (0.7 mL) and cooled to 0 °C. Dry Et$_3$N (233 mg, 324 µL, 2.30 mmol, 7.00 eq.) and TBSOTf (435 mg, 377 µL, 1.64 mmol, 5.00 eq.) were added dropwise and the reaction mixture stirred overnight. The black solution was treated with sat. NH$_4$Cl solution (10 mL) and the aqueous layer was extracted with CH$_2$Cl$_2$ (3 x 20 mL). The combined organic layers were washed with 1 M KOH (10 mL), brine (10 mL), dried over MgSO$_4$, filtered and the solvent evaporated under reduced pressure. The crude product was purified by flash column chromatography (SiO$_2$, 20 cm x 3.5 cm, CH$_2$Cl$_2$/MeOH 20:1) to afford the racemic organocatalyst **128b** (110 mg, 80%) as a black glue. For analytical purposes, an aliquot was purified by semi-preparative HPLC (*Reprospher* SiO$_2$, hexane/iPrOH 95:5, 6.0 mL/min, 25 °C, 205 nm, t_R = 19 min) to afford **128b** as a colorless foam,[i] which became dark red upon drying in HV overnight.

C$_{27}$H$_{33}$NOSi (415.65 g/mol)

R_f = 0.29 (CH$_2$Cl$_2$/MeOH 20:1).

^{1}H NMR (CDCl$_3$, 400 MHz) δ/ppm: 7.48-7.45 (m, 2 H, Ar-*H*), 7.26-7.20 (m, 5 H, Ar-*H*), 7.19-7.12 (m, 4 H, Ar-*H*), 7.09-7.01 (m, 2 H, Ar-*H*), 6.85 (d, $^3J_{HH}$ = 7.1 Hz, 1 H, Ar-*H*), 5.66 (d, $^4J_{HH}$ = 2.7 Hz, 1 H, NC*H*), 3.82 (d, $^2J_{HH}$ = 13.2 Hz, 1 H, C*H*$_a$H$_b$), 3.17 (d, $^2J_{HH}$ = 13.2 Hz, 1 H, CH$_a$*H*$_b$), 2.15 (br s, 1 H, N*H*), 0.99 (s, 9 H, C(C*H*$_3$)$_3$), –0.31 (s, 3 H, SiC*H*$_3$), –0.39 (s, 3 H, SiC*H*$_3$).

^{13}C{^{1}H} NMR (CDCl$_3$, 101 MHz) δ/ppm: 143.0, 142.9, 142.8, 139.6 (4 x Ar-*C*), 129.8, 129.1, 127.8, 127.5, 127.3, 127.1, 126.0, 125.2, 122.0 (9 x Ar-*C*H), 84.8 (*C*OSi), 70.9 (N*C*H), 51.3 (*C*H$_2$), 26.5 (C(*C*H$_3$)$_3$), 19.1 (*C*(CH$_3$)$_3$), –3.0, –3.1 (2 x Si*C*H$_3$).

FTIR (ATR): 3060w, 3033w, 2952m, 2928m, 2855m, 1465m, 1462m, 1446m, 1393w, 1185w, 1056s, 932w, 834s, 775s, 744m, 702s, 668m cm^{-1}.

HRMS (ESI, 4500 V, 180 °C) calc. *m/z* for C$_{27}$H$_{34}$NOSi$^+$: 416.2404, found: 416.2406 [M+H]$^+$; calc. *m/z* for C$_{21}$H$_{18}$N$^+$: 284.1434, found: 284.1436 [M-OTBS]$^+$.

Racemic Organocatalyst **128b** was separated into its enantiomers by semi-preparative HPLC on a chiral stationary phase (*Daicel* Chiralpak AD with precolumn AD, hexane/iPrOH 95:5, 6.0 mL/min, 25 °C, 205 nm, t_R(–) = 27 min, t_R(+) = 49 min). Both enantiomers were obtained in > 99.5% *ee*.

HPLC (*Daicel* Chiralpak AD, heptane/iPrOH 95:5, 0.5 mL/min, 25 °C, 205 nm): t_R((–)-**128b**) = 9.5 min, t_R((+)-**128b**= 15.1 min.

---

[i] The solvent was concentrated under reduced pressure at room temperature.

Optical rotation: $[\alpha]_D^{20} = -12.7°$ (c = 0.35, CHCl$_3$) and $[\alpha]_D^{20} = +13.9°$ (c = 0.28, CHCl$_3$).

1-(((*tert*-Butyldimethylsilyl)oxy)diphenylmethyl)isoindolinium tetrafluoroborate 128b

128b*HBF$_4$
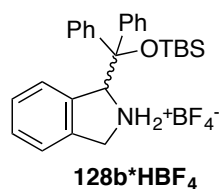
1-(((*tert*-Butyldimethylsilyl)oxy)diphenylmethyl)isoindoline **128b** (100 mg, 241 µmol, 1.00 eq.) was dissolved in Et$_2$O (1 mL) cooled to 0 °C and tetrafluoroboric acid diethyl ether complex (42.7 mg, 35.9 µL, 264 µmol, 1.10 eq.) was added. The BF$_4$-salt (109 mg) precipitated as a

black solid. The product was recrystallized from CHCl$_3$ to afford the BF$_4$-salt **128b** (73 mg, 60%) as a pale grey solid.

C$_{27}$H$_{34}$BF$_4$NOSi (503.46 g/mol)

m.**p**.: >216 °C (decomposition).

¹H NMR (CDCl$_3$, 400 MHz) δ/ppm: 8.67 (br s, 1 H, N*H*$_2$), 7.57-7.44 (m, 5 H, Ar-*H*), 7.31-7.24 (m, 2 H, Ar-*H*), 7.16 (t, J_{HH} = 7.4 Hz, 3 H, Ar-*H*), 7.04 (d, J_{HH} = 7.7 Hz, 1 H, Ar-*H*), 6.99 (br s, 2 H, Ar-*H*), 6.93 (d, J_{HH} = 7.7 Hz, 1 H, Ar-*H*), 6.72 (br s, 1 H, N*H*$_2$), 6.21 (d, J_{HH} = 6.2 Hz, 1 H, NC*H*), 4.41 (dd, J_{HH} = 14.7 Hz, J_{HH} = 6.7 Hz, 1 H, C*H*$_a$H$_b$), 3.11-3.04 (m, 1 H, CH$_a$*H*$_b$), 2.15 (br s, 1 H, N*H*), 0.98 (s, 9 H, C(C*H*$_3$)$_3$), –0.32 (s, 3 H, SiC*H*$_3$), –0.36 (s, 3 H, SiC*H*$_3$).

¹³C{¹H} NMR (CDCl$_3$, 101 MHz) δ/ppm: 138.5, 137.2, 136.4, 133.1 (4 x Ar-*C*), 130.5, 130.0, 129.8, 128.9, 128.8, 128.5, 128.4, 127.9, 125.0, 122.6 (10 x Ar-*C*H), 82.78 (*C*OSi), 73.0 (N*C*H), 51.4 (*C*H$_2$), 26.3 (C(*C*H$_3$)$_3$), 18.8 (*C*(CH$_3$)$_3$), –3.0, –3.2 (2 x Si*C*H$_3$).

¹⁹F NMR (CDCl$_3$, 376 MHz) δ/ppm: –150.7 (¹¹B*F*$_4$), –150.6 (¹⁰B*F*$_4$).

¹¹B NMR (CDCl$_3$, 128 MHz) δ/ppm: –1.0.

FTIR (ATR): 3234w, 3101w, 2955w, 2929w, 2857w, 1588w, 1488w, 1467w, 1447w, 1401w, 1254w, 1133m, 1094m, 1056s, 1003 m, 968s, 836s, 779s, 700s cm⁻¹.

HRMS (ESI, 4500 V, 180 °C) calc. *m/z* for C$_{27}$H$_{34}$NOSi⁺: 416.2404, found: 416.2406 [M+H]⁺; calc. *m/z* for C$_{21}$H$_{18}$N⁺: 284.1434, found: 284.1435 [M-OTBS]⁺.

EA calc. (%) for C$_{27}$H$_{34}$BF$_4$NOSi: C 64.41, H 6.81, N 2.78; found: C 63.34, H 6.79, N 2.89.

(*S*)-((*S***)-2-((*tert*-Butylimino)methyl)isoindolin-1-yl)(phenyl)methanol (*S**,*S**)-125 and (*S**)-((*R**)-2-((*tert*-Butylimino)methyl)isoindolin-1-yl)(phenyl)methanol (*S**,*R**)-125**
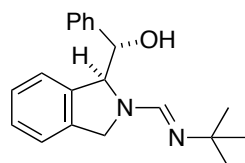
(*S**,*S**)-**125**
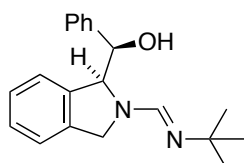
(*S**,*R**)-**125**

A heat gun dried Schlenk tube was flushed with argon and charged with (*N*)-(*tert*-butyliminomethyl)isoindoline **123** (203 mg, 1.00 mmol, 1.00 eq.) and dry THF (4 ml). The mixture was cooled to –78 °C with a dry ice/acetone bath. *sec*-BuLi (0.78 ml (1.4 M in cyclohexane), 1.00 mmol, 1.00 eq.) was added dropwise. The mixture was stirred for 1 h at –78 °C and benzaldehyde (160 mg, 152 μL, 1.51 mmol, 1.50 eq.) was added dropwise. The reaction mixture was allowed to warm to room temperature in the cooling bath overnight. The solution was cooled to 0 °C, quenched with H_2O (10 mL) and diluted with Et_2O (40 mL). The layers were separated and the organic layer was washed with brine (10 mL). The combined aqueous phases were re-extracted with Et_2O (2 x 10 mL). The combined organic layers were dried over $MgSO_4$, filtered and the solvent evaporated under reduced pressure. The crude product was purified by flash column chromatography (SiO_2, 20 cm x 3.5 cm, cyclohexane/EtOAc 1:1 + 5% Et_3N). The upper spot (R_f = 0.35) was further purified by a second flash column chromatography (SiO_2, 20 cm x 3.5 cm, cyclohexane/EtOAc 10:1 (200 mL) then 1:1 cyclohexane/EtOAc + 5% Et_3N) to afford the (*R**,*S**)-diastereoisomer (90 mg, 29%) as a brownish solid. The lower spot of the first column (R_f = 0.18) was further purified by a second flash column chromatography (SiO_2, 20 cm x 3.5 cm, cyclohexane/EtOAc 1:1 + 5% Et_3N) to afford the (*S**,*S**)-diastereoisomer (113 mg, 37%) as a pale yellow solid.

Analytical data of diastereoisomer (*S**,*S**)-**125**

$C_{20}H_{24}N_2O$ (308.43 g/mol)

m.p.: 103-104 °C.

R_f = 0.18 (cyclohexane/EtOAc 1:1 + 5% Et_3N).

¹H NMR (CDCl₃, 400 MHz) δ/ppm: 8.98 (br s, 1 H, O*H*), 7.73 (s, 1 H, NC*H*N), 7.36-7.29 (m, 5 H, Ar-*H*), 7.21-7.13 (m, 2 H, Ar-*H*), 6.87 (t, $^3J_{HH}$ = 7.6 Hz, 1 H, Ar-*H*), 5.73 (d, $^3J_{HH}$ = 7.6 Hz, 1 H, Ar-*H*), 5.35 (dd, $^3J_{HH}$ = 8.4 Hz, $^4J_{HH}$ = 2.0 Hz, 1 H, NC*H*), 4.89 (dd, $^2J_{HH}$ = 13.6 Hz, $^4J_{HH}$ = 2.0 Hz, 1 H, C*H*ₐHᵦ), 4.72 (d, $^2J_{HH}$ = 13.6 Hz, 1 H, CHₐ*H*ᵦ), 4.63 (d, $^3J_{HH}$ = 8.4 Hz, 1 H, C*H*OH), 1.26 (s, 9 H, C(C*H*₃)₃).

¹³C{¹H} NMR (CDCl₃, 101 MHz) δ/ppm: 150.9 (N*C*HN), 142.1, 137.5, 137.1 (3 x Ar-*C*), 128.3, 128.2, 128.0, 127.6, 126.5, 125.1, 122.0 (7 x Ar-*C*H), 81.1 (*C*HOH), 71.6 (N*C*H), 54.4

(CH_2), 53.4 ($C(CH_3)_3$), 31.1 (C($CH_3)_3$).

FTIR (ATR): 3028w, 2959w, 2900w, 2861w, 1633s, 1590m, 1450w, 1410m, 1377m, 1356m, 1312m, 1202m, 1061m, 1028m, 966w; 764s, 743s, 719s, 698s, 671m cm^{-1}.

HRMS (ESI, 4500 V, 180 °C) calc. (m/z) for $C_{20}H_{25}N_2O^+$: 309.1961, found: 309.1962 [M+H]$^+$.

Analytical data of diastereoisomer (S^*,R^*)-**125**

$C_{20}H_{24}N_2O$ (308.43 g/mol)

m.p.: 118-119 °C.

R_f = 0.35 (cyclohexane/EtOAc 1:1 + 5% Et$_3$N).

^{1}H NMR (CDCl$_3$, 400 MHz) δ/ppm: 7.53 (s, 1 H, NCHN), 7.47 (d, $^3J_{HH}$ = 7.5 Hz, 1 H, Ar-H), 7.36 (t, $^3J_{HH}$ = 7.5 Hz, 1 H, Ar-H), 7.24 (t, $^3J_{HH}$ = 7.5 Hz, 1 H, Ar-H), 7.10-6.98 (m. 4 H, Ar-H), 6.85-6.80 (m, 2 H, Ar-H), 5.62 (br s, 1 H, CHN), 5.13 (br s, 1 H, CHOH), 4.40 (d, $^2J_{HH}$ = 13.2 Hz, 1 H, CH_aH$_b$), 3.73 (dd, $^2J_{HH}$ = 13.2 Hz, $^4J_{HH}$ = 2.4 Hz, 1 H, CH$_a$$H_b$), 1.31 (s, 9 H, C(C$H_3)_3$). *OH proton was not detected.*

^{13}C{^{1}H} NMR (CDCl$_3$, 101 MHz) δ/ppm: 149.1 (NCHN), 141.3, 138.6, 137.2 (3 x Ar-C), 127.8, 127.7, 127.1, 126.7, 126.4, 123.6, 122.3 (7 x Ar-CH), 78.8 (CHOH), 71.6 (CHN), 54.2 (CH$_2$), 53.5 (C(CH$_3)_3$), 31.3 (C(CH$_3)_3$).

FTIR (ATR): 2964w, 2858w, 1631s, 1489m, 1450m, 1400m, 1361s, 1262w, 1209m, 1156w, 1091w, 1055m, 1026w, 890w, 741s, 716s, 702s cm^{-1}.

HRMS (ESI, 4500 V, 180 °C) calc. (m/z) for $C_{20}H_{25}N_2O^+$: 309.1961, found: 309.1964 [M+H]$^+$.

(S^*)-1-((S^*)-((*tert*-Butyldimethylsilyl)oxy)(phenyl)methyl)isoindoline (S^*,S^*)-129
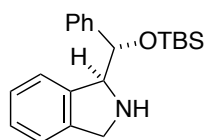
(S^*,S^*)-**129**

(S^*)-((S^*)-2-((*tert*-Butylimino)methyl)isoindolin-1-yl)(phenyl)methanol (S^*,S^*)-**125** (63.0 mg, 204 μmol, 1.00 eq.) and LiAlH$_4$ (23.3 mg, 613 μmol, 3.00 eq.) were suspended in dry THF (2.5 mL) under an argon atmosphere. The suspension was stirred under reflux for 16 h. The reaction mixture was cooled to 0 °C diluted with Et$_2$O (1 mL) and treated with H$_2$O (23 μL), 4 M NaOH solution (23 μL) and H$_2$O (69 μL) subsequently. MgSO$_4$ was added after 15 min, the suspension filtered and the solvent evaporated and dried in HV to afford the deprotected aminoalcohol **127** (46 mg) as a red glue.

The crude product was dissolved in dry CH$_2$Cl$_2$ (0.5 mL) and cooled to −78 °C. Dry Et$_3$N (103

mg, 144 µL, 1.02 mmol, 5.00 eq.) and TBSOTf (162 mg, 141 µL, 613 µmol, 3.00 eq.) were added dropwise, the reaction mixture was stirred for 4 h at −78 °C and additional 4 h at ambient temperature. The dark red solution was treated with sat. NH$_4$Cl solution (10 mL) and the aqueous layer was extracted with CHCl$_3$ (3 x 20 mL). The combined organic layers were washed with 1 M KOH (10 mL), brine (10 mL), dried over MgSO$_4$, filtered and the solvent evaporated. The crude product was purified by flash column chromatography (SiO$_2$, 15 cm x 2.5 cm, CH$_2$Cl$_2$ (100 mL), CH$_2$Cl$_2$/MeOH 99:1 (100 mL), then CH$_2$Cl$_2$/MeOH 50:1) to afford the racemic organocatalyst (S*,S*)-**129** (55 mg, 79%) as black oil. For analytical purposes, an aliquot was purified by semi-preparative HPLC (*Reprospher* SiO$_2$, hexane/iPrOH 96:4, 6.0 mL/min, 25 °C, 205 nm, t_R = 40 min) to afford (S*,S*)-**129** as a pale red oil.[i] An aliquot (ca. 10 mg) was dissolved in Et$_2$O (300 µL) and HCl solution (4 M in dioxane, 20 µL) was added. The solution was layered with pentane and the biphasic mixture stored at room temperature whereupon the HCl-salt of amine (S*,S*)-**129** precipitated as x-ray suitable crystals.

Analytical data of aminoalcohol intermediate (S*,S*)-**127**
C$_{15}$H$_{15}$NO (225.29 g/mol)
^{1}H NMR (CDCl$_3$, 400 MHz) δ/ppm: 7.40-7.29 (m, 5 H, Ar-*H*), 7.24-7.22 (m, 2 H, Ar-*H*), 7.15-7.11 (m, 1 H, Ar-*H*), 6.75 (d, $^3J_{HH}$ = 7.3 Hz, 1 H, Ar-*H*), 4.60-4.57 (m, 2 H, NC*H*, C*H*OH or C*H*$_2$), 4.314.23 (m, 2 H, NC*H*, C*H*OH or C*H*$_2$), 3.12 (br s, 2 H, N*H*, O*H*).

Analytical data of organocatalyst (S*,S*)-**129**
C$_{21}$H$_{29}$NOSi (339.55 g/mol)
R_f = 0.22 (CH$_2$Cl$_2$/MeOH 20:1).
^{1}H NMR (CDCl$_3$, 400 MHz) δ/ppm: 7.32-7.23 (m, 5 H, Ar-*H*), 7.21-7.10 (m, 2 H, Ar-*H*), 7.10-7.06 (m, 1 H, Ar-*H*), 6.76 (d, $^3J_{HH}$ = 7.6 Hz, 1 H, Ar-*H*), 4.72 (d, $^3J_{HH}$ = 5.4 Hz, C*H*OSi), 4.52 (dd, $^3J_{HH}$ = 5.4 Hz, $^4J_{HH}$ = 2.2 Hz, 1 H, C*H*N), 4.23 (d, $^2J_{HH}$ = 13.4 Hz, $^4J_{HH}$ = 2.2 Hz, 1 H, C*H*$_a$H$_b$), 4.10 (d, $^2J_{HH}$ = 13.4 Hz, 1 H, CH$_a$*H*$_b$), 2.28 (br s, 1 H, N*H*), 0.81 (s, 9 H, C(C*H*$_3$)$_3$), −0.13 (s, 3 H, SiC*H*$_3$), −0.23 (s, 3 H, SiC*H*$_3$).
^{13}C{^{1}H} NMR (CDCl$_3$, 101 MHz) δ/ppm: 142.5, 142.3, 141.0 (3 x Ar-*C*), 128.1, 127.6, 127.3, 127.3, 126.2, 124.0, 122.4 (7 x Ar-*C*H), 78.0 (*C*HOSi), 70.9 (*C*HN), 51.7 (*C*H$_2$), 25.9 (C(*C*H$_3$)$_3$)), 19.2 (*C*(CH$_3$)$_3$), −4.5, −5.1 (2 x Si*C*H$_3$).
FTIR (ATR): 3073w, 3032w, 2952m, 2928m, 2902w, 2856m, 1477m, 1462m, 1398w,

---
[i] The solvent was concentrated under reduced pressure at room temperature.

1253m, 1099m, 1066s, 905w, 837s, 701s, 633s cm^{-1}.

HRMS (ESI, 4500 V, 180 °C) calc. (*m/z*) for C$_{21}$H$_{30}$NOSi$^+$: 340.2091, found: 340.2096 [M+H]$^+$; calc. (*m/z*) for C$_{15}$H$_{14}$N$^+$: 208.1121, found: 208.1122 [M-OTBS]$^+$.

Racemic Organocatalyst (*S**,*S**)-**129** was separated into its enantiomers by semi-preparative HPLC on a chiral stationary phase (*Daicel* Chiralpak AD with precolumn AD, hexane/*i*PrOH 96:4, 6 mL/min, 25 °C, 205 nm, t_R(–) = 30 min, t_R(+) = 46 min). Both enantiomers were obtained in > 99.5% *ee*.

HPLC (*Daicel* Chiralpak AD, heptane/*i*PrOH 95:5, 0.5 mL/min, 25 °C, 205 nm): t_R((–)-**129**) = 10.9 min, t_R((+)-**129**)= 14.5 min.

Optical rotation: $[\alpha]_D^{20}$ = –39.5° (c = 0.34, CHCl$_3$) and $[\alpha]_D^{20}$ = +40.9° (c = 0.88, CHCl$_3$).

(*S**)-1-((*R**)-((*tert*-Butyldimethylsilyl)oxy)(phenyl)methyl)isoindoline (*S**,*R**)-129
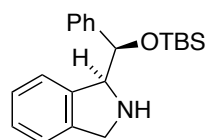
(*S**,*R**)-**129**

(*S**)-((*R**)-2-((*tert*-Butylimino)methyl)isoindolin-1-yl)(phenyl)methanol (*S**,*R**)-**125** (61.5 mg, 199 µmol, 1.00 eq.) and LiAlH$_4$ (22.7 mg, 598 µmol, 3.00 eq.) were suspended in dry THF (2.5 mL) under an argon atmosphere. The suspension was stirred under reflux for 16 h whereupon additional LiAlH$_4$ (22.7 mg, 598 µmol, 3.00 eq.) was added at room temperature and the reaction mixture stirred for 4 h under reflux. The reaction mixture was cooled to 0 °C diluted with Et$_2$O (1 mL) and treated with H$_2$O (46 µL), 4 M NaOH solution (46 µL) and H$_2$O (138 µL) subsequently. MgSO$_4$ was added after 15 minutes, the suspension filtered and the solvent evaporated under reduced pressure and the residue dried in HV to afford the deprotected aminoalcohol **127** (49 mg) as a red oil.

The crude product was dissolved in dry CH$_2$Cl$_2$ (0.5 mL) and cooled to −78 °C. Dry Et$_3$N (101 mg, 140 µL, 997 µmol, 5.00 eq.) and TBSOTf (158 mg, 138 µL, 598 µmol, 3.00 eq.) were added dropwise, the reaction mixture was stirred for 4 h at −78 °C and additional 4 h at ambient temperature. The dark red solution was treated with sat. NH$_4$Cl solution (10 mL) and the aqueous layer was extracted with CHCl$_3$ (3 x 20 mL). The combined organic layers were washed with 1 M KOH (10 mL), brine (10 mL), dried over MgSO$_4$, filtered and the solvent evaporated. The crude product was purified by flash column chromatography (SiO$_2$, 15 cm x 2.5 cm, CH$_2$Cl$_2$ (100 mL), CH$_2$Cl$_2$/MeOH 99:1 (100 mL), then CH$_2$Cl$_2$/MeOH 50:1) to afford the racemic organocatalyst (*S**,*R**)-**129** (41 mg, 61%) as a black oil. For analytical purposes, an aliquot was purified by semi-preparative HPLC (*Reprospher* SiO$_2$, hexane/*i*PrOH 95:5,

6.0 mL/min, 25 °C, 205 nm, t_R = 33 min) to afford (S*,R*)-**129** as a pale red oil.[i]

Analytical data of aminoalcohol intermediate (S*,R*)-**127**

$C_{15}H_{15}NO$ (225.29 g/mol)

1H NMR (CDCl$_3$, 400 MHz) δ/ppm: 7.38-7.28 (m, 5 H, Ar-*H*), 7.21-7.14 (m, 2 H, Ar-*H*), 7.10-7.06 (m, 1 H, Ar-*H*), 6.77 (d, $^3J_{HH}$ = 7.3 Hz, 1 H, Ar-*H*), 4.88 (d, $^3J_{HH}$ = 5.0 Hz, 1 H, NC*H* or C*H*OH), 4.83 (d, $^3J_{HH}$ = 5.0 Hz, 1 H, NC*H* or C*H*OH), 4.19 (d, $^2J_{HH}$ = 13.6 Hz, 1 H, C*H*$_a$H$_b$), 4.10 (dd, $^2J_{HH}$ = 13.6 Hz, $^4J_{HH}$ = 2.1 Hz, 1 H, CH$_a$*H*$_b$). *Acidic protons (NH and OH) were not detected*.

Analytical data of organocatalyst (S*,R*)-**129**

$C_{21}H_{29}NOSi$ (339.55 g/mol)

R_f = 0.27 (CH$_2$Cl$_2$/MeOH 20:1).

1H NMR (CDCl$_3$, 400 MHz) δ/ppm: 7.38-7.26 (m, 1 H, Ar-*H*), 7.26-7.19 (m, 7 H, Ar-*H*), 7.13-7.11 (m, 1 H, Ar-*H*), 4.67 (d, $^3J_{HH}$ = 6.0 Hz, C*H*OSi), 4.58 (dd, $^3J_{HH}$ = 6.0 Hz, $^4J_{HH}$ = 2.2 Hz, 1 H, NC*H*), 4.02 (d, $^2J_{HH}$ = 13.5 Hz, 1 H, C*H*$_a$H$_b$), 3.90 (d, $^2J_{HH}$ = 13.5 Hz, $^4J_{HH}$ = 2.2 Hz, 1 H, CH$_a$*H*$_b$), 2.00 (br s, 1 H, N*H*), 0.88 (s, 9 H, C(C*H*$_3$)$_3$), –0.02 (s, 3 H, SiC*H*$_3$), –0.22 (s, 3 H, SiC*H*$_3$).

13C{1H} NMR (CDCl$_3$, 101 MHz) δ/ppm: 142.2, 142.0, 141.7 (3 x Ar-*C*), 127.9, 127.5, 127.3, 127.2, 126.3, 124.6, 122.4 (7 x Ar-*C*H), 78.6 (*C*HOSi), 70.4 (N*C*H), 51.6 (*C*H$_2$), 26.1 (*C*(CH$_3$)$_3$)), 18.4 (*C*(CH$_3$)$_3$), –4.5, –4.7 (2 x Si*C*H$_3$).

FTIR (ATR): 3066w, 3031w, 2953m, 2928m, 2888w, 2856m, 1462m, 1405w, 1361w, 1252s, 1079s, 1069s, 903w, 836s, 776s, 716s, 701s, 670s cm^{-1}.

HRMS (ESI, 4500 V, 180 °C) calc. (*m/z*) for $C_{21}H_{30}NOSi^+$: 340.2091, found: 340.2095 [M+H]$^+$; calc. (*m/z*) for $C_{15}H_{14}N^+$: 208.1121, found: 208.1121 [M-OTBS]$^+$.

Racemic Organocatalyst (S*,R*)-**129** was separated into its enantiomers by semi-preparative HPLC on a chiral stationary phase (*Daicel* Chiralpak AD with precolumn AD, hexane/*i*PrOH 96:4, 6 mL/min, 25 °C, 205 nm, t_R = 32 min and 38 min). The earlier enantiomer was isolated in > 99.5% *ee*, the later enantiomer in 98% *ee*.

HPLC (*Daicel* Chiralpak AD, heptane/*i*PrOH 95:5, 0.5 mL/min, 25 °C, 205 nm): t_R = 10.5 min and 12.5 min.

Optical rotation: Unstable values <1° were observed. Assignment of the sign to the

---

[i] The solvent was concentrated under reduced pressure at room temperature.

enantiomers was not possible.

6.5.5 ESI-MS Screening of Racemic Catalysts

General remarks

ESI-MS spectra were measured on a Varian 1200L Quadrupol MS/MS spectrometer using mild desolvation conditions (50 V capillary voltage, 200 °C drying gas). The samples were diluted immediately with CH_3CN prior to their analysis. Every spectrum consisted of at least 30 scans and the selectivity was calculated from the ratios of the peak heights of the major isotopomers of **Im** and **Im'**.

General procedure for the ESI-MS screening of racemic organocatalysts

A GC-vial was charged with a scalemic 3:1 mixture of (*R*)-**89'** (4.30 mg 9.38 µmol, 0.75 eq.) and (*S*)-**89** (1.39 mg, 3.13 µmol, 0.25 eq.). The mixture was dissolved in $EtOH/CH_2Cl_2$ (85 µL/10 µL) and a solution of corresponding racemic organocatalyst in EtOH (5 µL, 0.025 M, 1 mol%) was added. The mixture was stirred for 15 min at room temperature. The reaction mixture was diluted with CH_3CN (1 mL) and subjected to ESI-MS analysis.

General procedure for the ESI-MS screening of enantiopure organocatalysts

A GC-vial was charged with an equimolar mixture of (*R*)-**89'** (2.87 mg 6.25 µmol, 0.50 eq.) and (*S*)-**89** (2.78 mg, 6.25 µmol, 0.50 eq.). The mixture was dissolved in $EtOH/CH_2Cl_2$ (85 µL/10 µL) and a solution of corresponding racemic organocatalyst in EtOH (5 µL, 0.025 M, 1 mol%) was added. The mixture was stirred for 15 min at room temperature. The reaction mixture was diluted with CH_3CN (1 mL) and subjected to ESI-MS analysis.

CHAPTER 7

APPENDIX

7.1 ESI-MS Signal Ratios Determined in the Aldol Reaction

Table 10: Summary of ESI-MS screening results in MeOH (Figure 31).

entry	catalyst	ESI-MS screening (En-7/En-29)	
		(+)-**7**/(−)-**29**	(−)-**7**/(+)-**29**
1	L-**Pro**	63 : 37	38 : 62
2	**9**	59 : 41	46 : 54
3	**10**	59 : 41	41 : 59
4	**13**	66 : 34	34 : 66
5	**14**	60 : 40	43 : 57
6	**40**	65 : 35	35 : 65
7	**41**	68 : 32	31 : 69
8	**47**	65 : 35	34 : 66
9	**49**	68 : 32	32 : 68
10	(*S,S*)-**50**	59 : 41	40 : 60
11	(*S,R*)-**50**	54 : 46	47 : 53
12	**52**	48 : 52	63 : 37

Table 11: Summary of ESI-MS screening results in CH$_3$CN/*tert*-BNP (Figure 34).

entry	catalyst	ESI-MS screening (En-7/En-29)	
		(+)-**7**/(−)-**29**	(−)-**7**/(+)-**29**
1	**13**	87 : 13	12 : 88
2	**41**	88 : 12	11 : 89
3	**49**	88 : 12	13 : 87
4	(*S,S*)-**50**	83 : 17	19 : 81
5	(*S,R*)-**50**	31 : 69	70 : 30
6	**14**	65 : 35	35 : 65
7	**40**	82 : 18	19 : 81
8	**47**	87 : 13	13 : 87
9	**10**	59 : 41	40 : 60
10	**52**	n.d.	68 : 32
11	**9**	52 : 48	49 : 51
12	**51**	77 : 23	n.d.

7.2 ESI-MS Results Determined in the Michael Addition

Table 12: Calculated enantioselectivity determined from the intermediate ratio by ESI-MS screening of the racemate and selectivity determined from the enantio-pure catalyst.

entry	catalyst	ESI-MS screening racemic cat. theo. *ee* [%]	ESI-MS screening enantiopure cat. theo. *ee* [%]
1		62	84.6
2	77a	52	86.2
3		53	77.8
4		50	82.2
	average	**54.3**	**82.7**
5		72	92.4
6	77b	70	93.0
7		69	92.6
8		71	94.2
	average	**70.5**	**93.1**
9		74	93.6
10	77c	76	93.8
11		76	93.4
12		77	94.0
	average	**75.8**	**93.7**
13		46	72.2
14		46	76.8
15	77d	43	79.4
16		35	73.6
17			77.8
	average	**42.5**	**76.0**
18		39	65.8
19	(S*,R*)-114	33	70.2
20		35	69.8
21		26	74.4
	average	**33.3**	**70.1**

22		46	79.4
23	**128a**	47	81.0
24		46	75.8
25		47	81.6
	average	**46.5**	**79.5**
26		55	87.8
27	**128b**	57	89.6
28		61	83.8
29		58	85.5
	average	**57.8**	**86.7**
30		46	81.0
31	(*S**,*R**)-**129**	44	77.6
32		46	77.2
33		38	75.4
	average	**43.5**	**77.8**
34		26	67.0
35	(*S**,*S**)-**129**	28	66.0
36		13	65.6
37		26	65.4
	average	**23.1**	**66.0**

7.3   Crystallographic Data

Crystal   data   for   (*S**)-1-((*S**)-((*tert*-Butyldimethylsilyl)oxy)(phenyl)methyl)isoindoline hydrochloride **(*S**,*S**)-129•HCl**:

The crystal was measured on a Bruker Kappa Apex2 diffractometer at 123 K using graphite-monochromated Cu K_α-radiation with λ = 1.54178 Å, Θmax = 68.572°. Minimal/maximal transmission 0.94/0.94, μ = 2.116 mm^{-1}. The Apex2 suite has been used for data collection and integration. From a total of 67168 reflections, 8034 were independent (merging r = 0.045). From these, 7264 were considered as observed (I>2.0σ(I)) and were used to refine 506 parameters. The structure was solved by other methods using the program Superflip. Least-squares refinement against F was carried out on all non-hydrogen atoms using the program CRYSTALS. Chebychev polynomial weights were used to complete the refinement. Plots were produced using CAMERON.

molecular formula	$C_{44}H_{64}Cl_2N_2O_3Si_2$
molecular weight	796.08 g/mol^{-1}
description and size of crystal	colorless plate, 0.030·0.110·0.230 mm^3
crystal system, space group	triclinic, P-1
Z	2
F(000)	856
a	13.7887(11) Å
b	13.8031(11) Å
c	14.9665(12) Å
α	113.532(3)°
β	114.902(3)°
γ	95.978(4)°
V	2238.3(3) Å^3
$D_{calc.}$	1.181 Mg · m^{-3}
R (observed data)	0.0403
wR (all data)	0.0497
GOF	1.0220
Minimal/maximal residual electron density	-0.33/0.63 e Å^{-3}

7.4 List of Abbreviations

Å	Angstrom (1 Å = 10^{-10} m)
AcOH	acetic acid
aq.	aqueous
Ar	aryl
Asp	aspartic acid
Bn	benzyl
tert-BNP	3,5-di-*tert*-butyl-*para*-nitrophenol
Boc	*tert*-butoxycarbonyl
b.p.	boiling point
br	broad
Bu	butyl
BuLi	butyl lithium
°C	degree centigrade
c	concentration
calc.	calculated
Cbz	benzyloxycarbonyl
conv.	conversion
d	day(s)
D	sodium D line
δ	chemical shift
DCC	*N,N'*-dicyclohexylcarbodiimide
DIPEA	*N,N*-diisopropylethylamine
DMAP	*N,N*-4-(dimethylamino)pyridine
DMF	dimethylformamide
DMSO	dimethyl sulfoxide
d.r.	diastereomeric ratio
EA	elemental analysis
EDCCl	1-ethyl-3-(3-dimethylaminopropyl)carbodiimide hydrochloride
ee	enantiomeric excess
EI	electron-impact ionization
En	enamine
ent	enantiomeric
e.r.	enantiomeric ratio
ESI	electrospray ionization
Et	ethyl
EtOH	ethanol
Eq.	equation
eq.	equivalent(s)
eV	electron Volt
FAB	fast atom bombardment
FT	Fourier transformation
GC	gas chromatography
Gln	glutamine

Glu	glutamic acid
h	hour(s)
HATU	1-[bis(dimethylamino)methylene]-1H-1,2,3-triazolo[4,5-b] pyridinium 3-oxid hexafluorophosphate
HMBC	heteronuclear multiple bond coherence
HOBt	1-Hydroxybenzotriazole
HPLC	high performance liquid chromatography
HV	high vacuum
Hz	Hertz
i	iso
I	intensity
Im	iminium
IR	infrared spectroscopy
J	coupling constant
k	rate constant
K	Kelvin
L	ligand
LDA	lithium diisopropylamide
Leu	leucine
M	molarity [mol/L]
m	medium (IR)
MBH	Morita-Baylis-Hillman
Me	methyl
MeOH	methanol
min	minute(s)
mL	milliliter
m.p.	melting point
MS	mass spectrometry
m/z	mass-to-charge ratio
n.d.	not determined
NMM	*N*-methylmorpholine
NMR	nuclear magnetic resonance
NOESY	nuclear Overhauser enhancement spectroscopy
Nu	nucleophile
Ph	phenyl
PHOX	phosphino-oxazoline
ppm	parts per million
Pr	propyl
prep.	Preparative
Pro	proline
rac	racemic
rec.	recrystallized
$\boldsymbol{R_f}$	retention factor
RT	room temperature
s	selectivity factor

s	second(s)
s	strong (IR)
sat.	saturated
sec	secondary
SM	starting material
T	temperature
t	time
tert	*tertiary*
TBAF	tetrabutylammonium fluoride
TBS	*tert*-butyldimethylsilyl
TBDPS	*tert*-butyldiphenylsilyl
theo.	theoretical
TFA	trifluoro acetate
THF	tetrahydrofurane
TIPS	triisopropylsilyl
TLC	thin layer chromatography
TMEDA	*N,N,N',N'*-tetramethyl ethylenediamine
TMP	2,2,6,6-tetramethyl piperidine
TMS	trimethylsilyl
para-TsOH	*para*-toluenesulfonic acid
t_R	retention time
Val	valine
w	weak (IR)

CHAPTER 8

REFERENCES

[1]   a) *Comprehensive Chirality* (Eds.: E. M. Carreira, H. Yamamoto)*, Vol. 3-6*, Elsevier, Amsterdam, **2012**; b) *Catalytic Asymmetric Synthesis* (Ed.: I. Ojima)*, 3rd ed., John Wiley, New York, **2010**.

[2]   For selected reviews see: a) S. Mignani, M. Patek, in *Comprehensive Chirality* (Eds.: E. M. Carreira, H. Yamamoto), Elsevier, Amsterdam, **2012**, pp. 217-245; b) P. T. Corbett, J. Leclaire, L. Vial, K. R. West, J.-L. Wietor, J. K. M. Sanders, S. Otto, *Chem. Rev.* **2006**, *106*, 3652-3711; c) J. G. de Vries, L. Lefort, *Chem. Eur. J.* **2006**, *12*, 4722-4734; d) M. B. Francis, T. F. Jamison, E. N. Jacobsen, *Curr. Opin. Chem. Biol.* **1998**, *2*, 422-428; e) *Chem. Rev.* **1997**, *97*, 347-510.

[3]   For selected reviews see: a) D. Leung, S. O. Kang, E. V. Anslyn, *Chem. Soc. Rev.* **2012**, *41*, 448-479; b) J. Revell, H. Wennemers, in *Creative Chemical Sensor Systems, Vol. 277* (Ed.: T. Schrader), Springer Berlin Heidelberg, **2007**, pp. 251-266; c) M. H. Fonseca, B. List, *Curr. Opin. Chem. Biol.* **2004**, *8*, 319-326; d) P. Chen, *Angew. Chem. Int. Ed.* **2003**, *42*, 2832-2847; e) J. F. Traverse, M. L. Snapper, *Drug Discovery Today* **2002**, *7*, 1002-1012; f) M. T. Reetz, *Angew. Chem. Int. Ed.* **2001**, *40*, 284-310.

[4]   M. T. Reetz, M. H. Becker, K. M. Kühling, A. Holzwarth, *Angew. Chem. Int. Ed.* **1998**, *37*, 2647-2650.

[5]   N. Millot, P. Borman, M. S. Anson, I. B. Campbell, S. J. F. Macdonald, M. Mahmoudian, *Org. Process Res. Dev.* **2002**, *6*, 463-470.

[6]   For selected reviews see: a) C. A. Mueller, C. Markert, A. M. Teichert, A. Pfaltz, *Chem. Commun.* **2009**, 1607-1618; b) K. A. Schug, W. Lindner, *J. Sep. Sci.* **2005**, *28*, 1932-1955.

[7]   A. Horeau, A. Nouaille, *Tetrahedron Lett.* **1990**, *31*, 2707-2710.

[8]   For a review see: Q. Zhang, D. P. Curran, *Chem. Eur. J.* **2005**, *11*, 4866-4880.

[9]   J. Guo, J. Wu, G. Siuzdak, M. G. Finn, *Angew. Chem. In. Ed.* **1999**, *38*, 1755-1758.

[10]   M. T. Reetz, M. H. Becker, H.-W. Klein, D. Stöckigt, *Angew. Chem. Int. Ed.* **1999**, *38*, 1758-1761.

[11]   C. Fraschetti, A. Filippi, M. Crestoni, T. Ema, M. Speranza, *J. Am. Soc. Mass Spectrom.* **2013**, *24*, 573-578.

[12]   C. Hinderling, P. Chen, *Angew. Chem. Int. Ed.* **1999**, *38*, 2253-2256.

[13]   J. Wassenaar, E. Jansen, Z.-J. van, F. M. Bickelhaupt, M. A. Siegler, A. L. Spek, J. N. H. Reek, *Nat. Chem.* **2010**, *2*, 417-421.

[14]   a) C. A. Müller, A. Pfaltz, *Angew. Chem. Int. Ed.* **2008**, *47*, 3363-3366; b) C. Markert, P. Rösel, A. Pfaltz, *J. Am. Chem. Soc.* **2008**, *130*, 3234-3235; c) C. Markert, A. Pfaltz, *Angew. Chem. In. Ed.* **2004**, *43*, 2498-2500.

[15]   A. Teichert, A. Pfaltz, *Angew. Chem. Int. Ed.* **2008**, *47*, 3360-3362.

[16]   I. Fleischer, A. Pfaltz, *Chem. Eur. J.* **2010**, *16*, 95-99.

[17]   C. Ebner, C. A. Müller, C. Markert, A. Pfaltz, *J. Am. Chem. Soc.* **2011**, *133*, 4710-4713.

[18]   a) *Enantioselective Organocatalysis* (Ed.: P. I. Dalko)*, Wiley-VCH, Weinheim, **2007**; b) K. L. Jensen, G. Dickmeiss, H. Jiang, Ł. Albrecht, K. A. Jørgensen, *Acc. Chem. Res.* **2012**, *45*, 248-264; c) S. Mukherjee, J. W. Yang, S. Hoffmann, B. List, *Chem. Rev.* **2007**, *107*, 5471-5569.

[19]   A. Wurtz, *J. Prakt. Chem.* **1872**, *5*, 457-464.

[20]   A. Borodin, *J. Prakt. Chem.* **1864**, *93*, 413-425.

[21]   For a recent review about the impact of the Mukaiyama aldol reaction see: S. B. J. Kan, K. K. H. Ng, I. Paterson, *Angew. Chem. Int. Ed.* **2013**, *52*, 9097-9108.

[22]   a) G. L. Beutner, S. E. Denmark, *Angew. Chem. Int. Ed.* **2013**, *52*, 9086-9096; b) J. Matsuo, M. Murakami, *Angew. Chem. Int. Ed.* **2013**, *52*, 9109-9118; c) E. M. Carreira, *Comprehensive Asymmetric Catalysis* (Eds.: E. N. Jacobsen, A. Pfaltz, H. Yamamoto)*, Vol. III*, Springer, Heidelberg, **1999**.

[23]   T. Yanagimoto, T. Toyota, N. Matsuki, Y. Makino, S. Uchiyama, T. Ohwada, *J. Am. Chem. Soc.* **2007**, *129*, 736-737.

[24]   a) N. Mase, in *Comprehensive Chirality* (Eds.: E. M. Carreira, H. Yamamoto), Elsevier, Amsterdam, **2012**, pp. 97-124; b) H. Gotoh, Y. Hayashi, in *Comprehensive Chirality* (Eds.: E. M. Carreira, H. Yamamoto), Elsevier, Amsterdam, **2012**, pp. 125-156; c) V. Bisai, A. Bisai, V. K. Singh, *Tetrahedron* **2012**, *68*, 4541-4580; d) B. M. Trost, C. S. Brindle, *Chem. Soc. Rev.* **2010**, *39*, 1600-1632; e) P. Melchiorre, M. Marigo, A. Carlone, G. Bartoli, *Angew. Chem. Int. Ed.* **2008**, *47*, 6138-6171; f) B. List, *Tetrahedron* **2002**, *58*, 5573-5590.

[25]   B. List, R. A. Lerner, C. F. Barbas, *J. Am. Chem. Soc.* **2000**, *122*, 2395-2396.

[26]   K. A. Ahrendt, C. J. Borths, D. W. C. MacMillan, *J. Am. Chem. Soc.* **2000**, *122*, 4243-4244.

[27]   D. W. C. MacMillan, *Nature* **2008**, *455*, 304-308.

[28]   Z. G. Hajos, D. R. Parrish, *J. Org. Chem.* **1974**, *39*, 1615-1621.

[29]   B. List, L. Hoang, H. J. Martin, *Proc. Natl. Acad. Sci. U. S. A.* **2004**, *101*, 5839-5842.

[30]   L. Hoang, S. Bahmanyar, K. N. Houk, B. List, *J. Am. Chem. Soc.* **2003**, *125*, 16-17.

[31]   F. R. Clemente, K. N. Houk, *Angew. Chem. Int. Ed.* **2004**, *43*, 5766-5768.

[32]   A. Heine, G. DeSantis, J. G. Luz, M. Mitchell, C.-H. Wong, I. A. Wilson, *Science* **2001**, *294*, 369-374.

[33]   X. Zhu, F. Tanaka, R. A. Lerner, C. F. Barbas III, I. A. Wilson, *J. Am. Chem. Soc.* **2009**, *131*, 18206-18207.

[34]   S. Bahmanyar, K. N. Houk, H. J. Martin, B. List, *J. Am. Chem. Soc.* **2003**, *125*, 2475-2479.

[35]   C. Marquez, J. O. Metzger, *Chem. Commun.* **2006**, 1539-1541.

[36]   a) Markus B. Schmid, K. Zeitler, Ruth M. Gschwind, *Angew. Chem. Int. Ed.* **2010**, *49*, 4997-5003; b) D. Seebach, A. K. Beck, D. M. Badine, M. Limbach, A. Eschenmoser, A. M. Treasurywala, R. Hobi, W. Prikoszovich, B. Linder, *Helv. Chim. Acta* **2007**, *90*, 425-471.

[37]   N. Zotova, L. J. Broadbelt, A. Armstrong, D. G. Blackmond, *Bioorg. Med. Chem. Lett.* **2009**, *19*, 3934-3937.

[38]   A. K. Sharma, R. B. Sunoj, *Angew. Chem. Int. Ed.* **2010**, *49*, 6373-6377.

[39]   M. M. Heravi, S. Asadi, *Tetrahedron: Asymmetry* **2012**, *23*, 1431-1465.

[40]   For pka scales of proline amides in DMSO: X.-Y. Huang, H.-J. Wang, J. Shi, *J. Phys. Chem. A* **2010**, *114*, 1068-1081.

[41]   A. El-Faham, F. Albericio, *Chem. Rev.* **2011**, *111*, 6557-6602.

[42]   a) Z. Tang, F. Jiang, L.-T. Yu, X. Cui, L.-Z. Gong, A.-Q. Mi, Y.-Z. Jiang, Y.-D. Wu, *J. Am. Chem. Soc.* **2003**, *125*, 5262-5263; b) Z. Tang, F. Jiang, X. Cui, L.-Z. Gong, A.-Q. Mi, Y.-Z. Jiang, Y.-D. Wu, *Proc. Natl. Acad. Sci. USA* **2004**, *101*, 5755-5760.

[43]   Z. Tang, Z.-H. Yang, X.-H. Chen, L.-F. Cun, A.-Q. Mi, Y.-Z. Jiang, L.-Z. Gong, *J. Am. Chem. Soc.* **2005**, *127*, 9285-9289.

[44]   a) M. R. Vishnumaya, V. K. Singh, *J. Org. Chem.* **2009**, *74*, 4289-4297; b) M. Raj, Vishnumaya, S. K. Ginotra, V. K. Singh, *Org. Lett.* **2006**, *8*, 4097-4099.

[45]   H. Zhang, S. Zhang, L. Liu, G. Luo, W. Duan, W. Wang, *J. Org. Chem.* **2009**, *75*, 368-374.

[46]   K. Baer, M. Kraußer, E. Burda, W. Hummel, A. Berkessel, H. Gröger, *Angew. Chem. Int. Ed.* **2009**, *48*, 9355-9358.

[47]   V. Maya, M. Raj, V. K. Singh, *Org. Lett.* **2007**, *9*, 2593-2595.

[48]   a) G. Rulli, K. A. Fredriksen, N. Duangdee, T. Bonge-Hansen, A. Berkessel, H. Gröger, *Synthesis* **2013**, *45*, 2512-2519; b) G. Rulli, N. Duangdee, K. Baer, W. Hummel, A. Berkessel, H. Gröger, *Angew. Chem. Int. Ed.* **2011**, *50*, 7944-7947.

[49]   N. Duangdee, W. Harnying, G. Rulli, J.-M. Neudörfl, H. Gröger, A. Berkessel, *J. Am. Chem. Soc.* **2012**, *134*, 11196-11205.

[50]   R. C. Tolman, *Proc. Natl. Acad. Sci. USA* **1925**, *11*, 436-439.

[51]   a) K. Mei, S. Zhang, S. He, P. Li, M. Jin, F. Xue, G. Luo, H. Zhang, L. Song, W. Duan, W.

Wang, *Tetrahedron Lett.* **2008**, *49*, 2681-2684; b) Richard D. Carpenter, James C. Fettinger, Kit S. Lam, Mark J. Kurth, *Angew. Chem. Int. Ed.* **2008**, *47*, 6407-6410; c) H. Torii, M. Nakadai, K. Ishihara, S. Saito, H. Yamamoto, *Angew. Chem. Int. Ed.* **2004**, *43*, 1983-1986.

[52]   A. Berkessel, W. Harnying, N. Duangdee, J.-M. Neudörfl, H. Gröger, *Org. Process Res. Dev.* **2012**, *16*, 123-128.

[53]   Y. Okuyama, H. Nakano, Y. Watanabe, M. Makabe, M. Takeshita, K. Uwai, C. Kabuto, E. Kwon, *Tetrahedron Lett.* **2009**, *50*, 193-197.

[54]   A. Berkessel, B. Koch, J. Lex, *Adv. Synth. Catal.* **2004**, *346*, 1141-1146.

[55]   a) W. Henderson, S. McIndoe, *Mass spectrometry of inorganic and organometallic compounds*, John Wiley, New York, **2005**; b) R. Saf, C. Mirtl, K. Hummel, *Tetrahedron Lett.* **1994**, *35*, 6653-6656.

[56]   C. W. Downey, M. W. Johnson, *Tetrahedron Lett.* **2007**, *48*, 3559-3562.

[57]   L. C. Dias, A. A. de Marchi, M. A. B. Ferreira, A. M. Aguilar, *Org. Lett.* **2007**, *9*, 4869-4872.

[58]   A. T. Khan, E. Mondal, *Synlett* **2003**, *2003*, 694-698.

[59]   K. Alexander (nee Gillon), S. Cook, C. L. Gibson, A. R. Kennedy, *J. Chem. Soc., Perkin Trans. 1* **2001**, 1538-1549.

[60]   A. Krasovskiy, F. Kopp, P. Knochel, *Angew. Chem. Int. Ed.* **2006**, *45*, 497-500.

[61]   C.-S. Da, L.-P. Che, Q.-P. Guo, F.-C. Wu, M. Xiao, Y.-N. Jia, *J. Org. Chem.* **2009**, *74*, 2541-2546.

[62]   S. Luo, P. Zhou, J. Li, J.-P. Cheng, *Chem. Eur. J.* **2010**, *16*, 4457-4461.

[63]   A. Fuentes, Angel L., L. Simon, C. Raposo, V. Alcazar, F. Sanz, F. M. Muniz, J. R. Moran, *Org. Biomol. Chem.* **2010**, *8*, 2979-2985.

[64]   S. Hu, T. Jiang, Z. Zhang, A. Zhu, B. Han, J. Song, Y. Xie, W. Li, *Tetrahedron Lett.* **2007**, *48*, 5613-5617.

[65]   *Privileged Chiral Ligands and Catalysts* (Ed.: Q.-L. Zhou)*, Wiley-VCH, Weinheim, **2011**.

[66]   Y. C. Fan, O. Kwon, *Chem. Commun.* **2013**, *49*, 11588-11619.

[67]   D. Basavaiah, G. Veeraraghavaiah, *Chem. Soc. Rev.* **2012**, *41*, 68-78.

[68]   a) Y. Wei, M. Shi, *Chem. Rev.* **2013**, *113*, 6659-6690; b) D. Basavaiah, B. S. Reddy, S. S. Badsara, *Chem. Rev.* **2010**, *110*, 5447-5674; c) J. Mansilla, S. J. M., *Molecules* **2010**, *15*, 709-734; d) D. Basavaiah, A. J. Rao, T. Satyanarayana, *Chem. Rev.* **2003**, *103*, 811-892.

[69]   T.-Y. Liu, M. Xie, Y.-C. Chen, *Chem. Soc. Rev.* **2012**, *41*, 4101-4112.

[70]   Y. Wei, M. Shi, *Acc. Chem. Res.* **2010**, *43*, 1005-1018.

[71]   K. Yuan, H.-L. Song, Y. Hu, X.-Y. Wu, *Tetrahedron* **2009**, *65*, 8185-8190.

[72]   D. Rageot, D. H. Woodmansee, B. Pugin, A. Pfaltz, *Angew. Chem. Int. Ed.* **2011**, *50*, 9598-9601.

[73]   L. S. Santos, C. H. Pavam, W. P. Almeida, F. Coelho, M. N. Eberlin, *Angew. Chem. Int. Ed.* **2004**, *43*, 4330-4333.

[74]   a) V. K. Aggarwal, S. Y. Fulford, G. C. Lloyd-Jones, *Angew. Chem. Int. Ed.* **2005**, *44*, 1706-1708; b) K. E. Price, S. J. Broadwater, H. M. Jung, D. T. McQuade, *Org. Lett.* **2005**, *7*, 147-150.

[75]   E. Ciganek, *Organic Reactions* **1997**, *51*, 201-350.

[76]   V. K. Aggarwal, A. Mereu, G. J. Tarver, R. McCague, *J. Org. Chem.* **1998**, *63*, 7183-7189.

[77]   P. Isenegger, Master thesis, University of Basel **2012**.

[78]   D. Roca-Lopez, D. Sadaba, I. Delso, R. P. Herrera, T. Tejero, P. Merino, *Tetrahedron: Asymmetry* **2010**, *21*, 2561-2601.

[79]   J. M. Betancort, C. F. Barbas, *Org. Lett.* **2001**, *3*, 3737-3740.

[80]   Y. Hayashi, H. Gotoh, T. Hayashi, M. Shoji, *Angew. Chem. Int. Ed.* **2005**, *44*, 4212-4215.

[81]   M. Marigo, T. C. Wabnitz, D. Fielenbach, K. A. K. A. Jørgensen, *Angew. Chem. Int. Ed.* **2005**, *44*, 794-797.

[82]   K. L. Jensen, G. Dickmeiss, H. Jiang, Å. u. Albrecht, K. A. JÃ¸rgensen, *Acc. Chem. Res.* **2011**.

[83]   a) M. Wiesner, H. Wennemers, *Synthesis* **2010**, *2010*, 1568-1571; b) M. Wiesner, G. Upert, G. Angelici, H. Wennemers, *J. Am. Chem. Soc.* **2009**, *132*, 6-7; c) M. Wiesner, M. Neuburger, H. Wennemers, *Chem. Eur. J.* **2009**, *15*, 10103-10109; d) M. Wiesner, J. D. Revell, H. Wennemers, *Angew. Chem. Int. Ed.* **2008**, *47*, 1871-1874.

[84]   a) R. Kastl, H. Wennemers, *Angew. Chem. Int. Ed.* **2013**, *52*, 7228-7232; b) J. Duschmalé, H. Wennemers, *Chem. Eur. J.* **2012**, *18*, 1111-1120.

[85]   M. B. Schmid, K. Zeitler, R. M. Gschwind, *J. Am. Chem. Soc.* **2011**, *133*, 7065-7074.

[86]   Cesar A. Marquez, F. Fabbretti, Jürgen O. Metzger, *Angew. Chem. Int. Ed.* **2007**, *46*, 6915-6917.

[87]   D. A. Yalalov, S. B. Tsogoeva, T. E. Shubina, I. M. Martynova, T. Clark, *Angew. Chem. Int. Ed.* **2008**, *47*, 6624-6628.

[88]   a) C. T. Wong, *Tetrahedron Lett.* **2009**, *50*, 811-813; b) C. Teck Wong, *Tetrahedron* **2009**, *65*, 7491-7497.

[89]   S. Belot, A. Quintard, N. Krause, A. Alexakis, *Adv. Synth. Catal.* **2010**, *352*, 667-695.

[90]   *Reactive Intermediates* (Ed.: L. S. Santos)*,* Wiley-VCH, Weinheim, **2010**.

[91]   a) J. Duschmalé, J. Wiest, M. Wiesner, H. Wennemers, *Chem. Sci.* **2013**, *4*, 1312-1318; b) D. Seebach, X. Sun, M.-O. Ebert, W. B. Schweizer, N. Purkayastha, A. K. Beck, J. Duschmalé, H. Wennemers, T. Mukaiyama, M. Benohoud, Y. Hayashi, M. Reiher, *Helv. Chim. Acta* **2013**, *96*, 799-852; c) J. Bures, A. Armstrong, D. G. Blackmond, *J. Am. Chem. Soc.* **2012**, *134*, 6741-6750; d) J. Burés, A. Armstrong, D. G. Blackmond, *J. Am. Chem. Soc.* **2012**, *134*, 14264-14264 (Referendum); e) G. Sahoo, H. Rahaman, A. Madarasz, I. Papai, M. Melarto, A. Valkonen, P. M. Pihko, *Angew. Chem. Int. Ed.* **2012**, *51*, 13144-13148; f) J. Bures, A. Armstrong, D. G. Blackmond, *J. Am. Chem. Soc.* **2011**, *133*, 8822-8825; g) K. Patora-Komisarska, M. Benohoud, H. Ishikawa, D. Seebach, Y. Hayashi, *Helv. Chim. Acta* **2011**, *94*, 719-745.

[92]   F. Bächle, J. Duschmalé, C. Ebner, A. Pfaltz, H. Wennemers, *Angew. Chem. Int. Ed.* **2013**, *52*, 12619-12623.

[93]   C. Ebner, Ph.D. thesis, University of Basel **2012**.

[94]   For a review about the application of chiral racemic catalysts see: L. A. Evans, N. S. Hodnett, G. C. Lloyd-Jones, *Angew. Chem. Int. Ed.* **2012**, *51*, 1526-1533.

[95]   For a review see: J. W. Faller, A. R. Lavoie, J. Parr, *Chem. Rev.* **2003**, *103*, 3345-3368.

[96]   K. Maruoka, H. Yamamoto, *J. Am. Chem. Soc.* **1989**, *111*, 789-790.

[97]   K. Mikami, T. Korenaga, T. Ohkuma, R. Noyori, *Angew. Chem. Int. Ed.* **2000**, *39*, 3707-3710.

[98]   F. Lagasse, M. Tsukamoto, C. J. Welch, H. B. Kagan, *J. Am. Chem. Soc.* **2003**, *125*, 7490-7491.

[99]   B. Dominguez, N. S. Hodnett, G. C. Lloyd-Jones, *Angew. Chem. Int. Ed.* **2001**, *40*, 4289-4291.

[100] C. Ebner, PhD thesis, University of Basel **2012**.

[101] I. Fleischer, PhD thesis, University of Basel **2010**.

[102] F. M. Gautier, S. Jones, S. J. Martin, *Org. Biomol. Chem.* **2009**, *7*, 229-231.

[103] a) R. R. Knowles, S. Lin, E. N. Jacobsen, *J. Am. Chem. Soc.* **2010**, *132*, 5030-5032; b) G. Barker, P. O'Brien, K. R. Campos, *Org. Lett.* **2010**, *12*, 4176-4179; c) K. M. B. Gross, P. Beak, *J. Am. Chem. Soc.* **2001**, *123*, 315-321; d) S. T. Kerrick, P. Beak, *J. Am. Chem. Soc.* **1991**, *113*, 9708-9710.

[104] Y. Chi, S. H. Gellman, *Org. Lett.* **2005**, *7*, 4253-4256.

[105] D. Enders, H. Kipphardt, P. Gerdes, L. Breña-Valle, V. Bhushan, *Bull. Soc. Chim. Belg.* **1988**, *97*, 691.

[106] D. Seebach, U. Grošelj, D. M. Badine, W. B. Schweizer, A. K. Beck, *Helv. Chim. Acta* **2008**,

91, 1999-2034.

[107] J. L. Bilke, S. P. Moore, P. O'Brien, J. Gilday, *Org. Lett.* **2009**, *11*, 1935-1938.

[108] F. Liu, S. Wang, N. Wang, Y. Peng, *Synlett* **2007**, 2415.

[109] D. S. Matteson, G. Y. Kim, *Org. Lett.* **2002**, *4*, 2153-2155.

[110] O. N. Burchak, C. Philouze, P. Y. Chavant, S. Py, *Org. Lett.* **2008**, *10*, 3021-3023.

[111] a) C. Quin, J. Trnka, A. Hay, M. P. Murphy, R. C. Hartley, *Tetrahedron* **2009**, *65*, 8154-8160; b) R. Braslau, V. Chaplinski, P. Goodson, *J. Org. Chem.* **1998**, *63*, 9857-9864.

[112] L. J. Beeley, C. J. M. Rockell, *Tetrahedron Lett.* **1990**, *31*, 417-420.

[113] C. Ebner, A. Pfaltz, *Tetrahedron* **2011**, *67*, 10287-10290.

[114] G. R. Fulmer, A. J. M. Miller, N. H. Sherden, H. E. Gottlieb, A. Nudelman, B. M. Stoltz, J. E. Bercaw, K. I. Goldberg, *Organometallics* **2010**.

[115] W. C. Still, M. Kahn, A. Mitra, *J. Org. Chem.* **1978**, *43*, 2923-2925.

[116] S. S. Chimni, D. Mahajan, *Tetrahedron* **2005**, *61*, 5019-5025.

[117] J.-R. Chen, X.-L. An, X.-Y. Zhu, X.-F. Wang, W.-J. Xiao, *J. Org. Chem.* **2008**, *73*, 6006-6009.

[118] a) J. G. Hernández, E. Juaristi, *J. Org. Chem.* **2011**, *76*, 1464-1467; b) P. Zhou, S. Luo, J.-P. Cheng, *Org. Biomol. Chem.* **2011**, *9*, 1784-1790.

[119] S. E. Denmark, R. A. Stavenger, *J. Am. Chem. Soc.* **2000**, *122*, 8837-8847.

[120] J. F. Hayes, M. Shipman, H. Twin, *J. Org. Chem.* **2002**, *67*, 935-942.

[121] N. Mase, F. Tanaka, C. F. Barbas, *Org. Lett.* **2003**, *5*, 4369-4372.

[122] J. Dambacher, W. Zhao, A. El-Batta, R. Anness, C. Jiang, M. Bergdahl, *Tetrahedron Lett.* **2005**, *46*, 4473-4477.

[123] A. K. Mills, A. E. W. Smith, *Helv. Chim. Acta* **1960**, *43*, 1915-1927.

[124] S. J. Pike, M. De Poli, W. Zawodny, J. Raftery, S. J. Webb, J. Clayden, *Org. Biomol. Chem.* **2013**, *11*, 3168-3176.

[125] Y. Wu, Y. Zhang, M. Yu, G. Zhao, S. Wang, *Org. Lett.* **2006**, *8*, 4417-4420.

[126] X.-Y. Xu, Y.-Z. Wang, L.-Z. Gong, *Org. Lett.* **2007**, *9*, 4247-4249.

[127] R. Baran, E. Veverkova, A. Skvorcova, R. Sebesta, *Org. Biomol. Chem.* **2013**, *11*, 7705-7711.

[128] S. Luo, H. Xu, J. Li, L. Zhang, J.-P. Cheng, *J. Am. Chem. Soc.* **2007**, *129*, 3074-3075.

[129] T. Miura, Y. Mikano, M. Murakami, *Org. Lett.* **2011**, *13*, 3560-3563.

[130] M. Helms, H. Füllbier, *J. Prakt. Chem.* **1986**, *328*, 643-647.

[131] Y. Ishii, M. Takeno, Y. Kawasaki, A. Muromachi, Y. Nishiyama, S. Sakaguchi, *J. Org. Chem.* **1996**, *61*, 3088-3092.

[132] B. Zhu, L. Yan, Y. Pan, R. Lee, H. Liu, Z. Han, K.-W. Huang, C.-H. Tan, Z. Jiang, *J. Org. Chem.* **2011**, *76*, 6894-6900.

[133] B. R. V. Ferreira, R. V. Pirovani, L. G. Souza-Filho, F. Coelho, *Tetrahedron* **2009**, *65*, 7712-7717.

[134] T. Kataoka, T. Iwama, H. Kinoshita, Y. Tsurukami, S. Tsujiyama, M. Fujita, E. Honda, T. Iwamura, S.-i. Watanabe, *J. Organomet. Chem.* **2000**, *611*, 455-462.

[135] D. Sabatino, C. Proulx, P. Pohankova, H. Ong, W. D. Lubell, *J. Am. Chem. Soc.* **2011**, *133*, 12493-12506.

[136] M. D. Price, M. J. Kurth, N. E. Schore, *J. Org. Chem.* **2002**, *67*, 7769-7773.

[137] I. Reiners, J. Wilken, J. Martens, *Tetrahedron: Asymmetry* **1995**, *6*, 3063-3070.

[138] A. S. Demir, I. Mecitoglu, C. Tanyeli, V. Gülbeyaz, *Tetrahedron: Asymmetry* **1996**, *7*, 3359-3364.

[139] P. E. Reed, J. A. Katzenellenbogen, *J. Org. Chem.* **1991**, *56*, 2624-2634.

[140] E. Vedejs, N. Lee, *J. Am. Chem. Soc.* **1995**, *117*, 891-900.

[141] K. Fujita, T. Fujii, R. Yamaguchi, *Org. Lett.* **2004**, *6*, 3525-3528.

SUMMARY

This thesis is focused on the application of ESI-MS as a screening method and mechanistic tool for organocatalyzed reactions. Monitoring mass-labeled reaction intermediates, which are formed in the back reaction of an equimolar mixture of quasienantiomeric substrates in the presence of a catalyst, allows for determination of the enantioselectivity that this catalyst induces in the corresponding forward reaction (Figure 88). This screening method is operationally simple, extraordinarily fast, avoids reaction workup and consumes only very small quantities of substrates and catalysts.
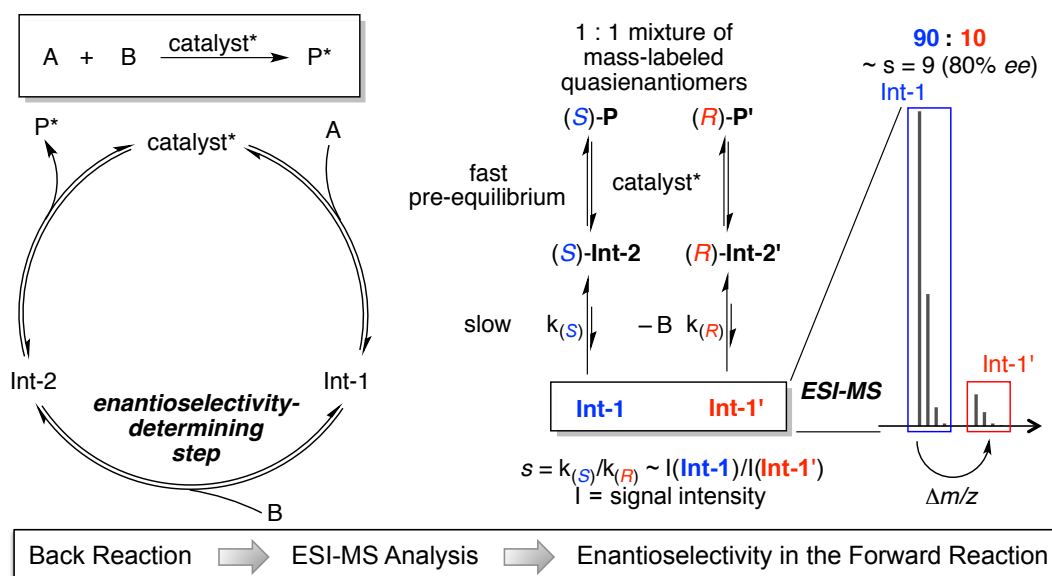
Figure 88: Generalized concept of the ESI-MS back reaction screening to determine the enantioselectivity of chiral catalysts theoretically induced in the forward reaction.

As discussed in CHAPTER 2, this concept was successfully applied to organocatalyzed aldol reactions, which proceed *via* neutral enamine species as key intermediates for ESI-MS analysis. The combination of acetone- and $^{13}C_3$-acetone-based aldol products (**P** and **P'**) was identified as a suitable pair of quasienantiomers providing the enamine intermediates (**Int-1** and **Int-1'**) in excellent signal intensities. With MeOH as a reaction solvent excellent agreements between the ESI-MS results and the *ee* determined from the corresponding forward reaction were found. However, in CH_3CN a correct prediction of the *ee* by ESI-MS back reaction analysis was shown to be more problematic due to signal alteration after dilution and an insufficiently fast pre-equilibrium between the quasienantiomeric reaction product and the iminium intermediate. These limitations were overcome by the addition of acidic reaction additives. Furthermore, when using a bulky nitrophenol as additive, the most selective catalysts under optimized screening conditions proved also to be the most selective species under preparative conditions in the absence of the additive. In addition, effects of solvents, additives and temperature could also be screened by ESI-MS. Finally, the screening

285

protocol was successfully extended to a simultaneous multi-catalyst screening by applying crude mixtures of several catalysts obtained in a one-pot synthesis with Boc-proline and various aminoalcohols (Figure 89).
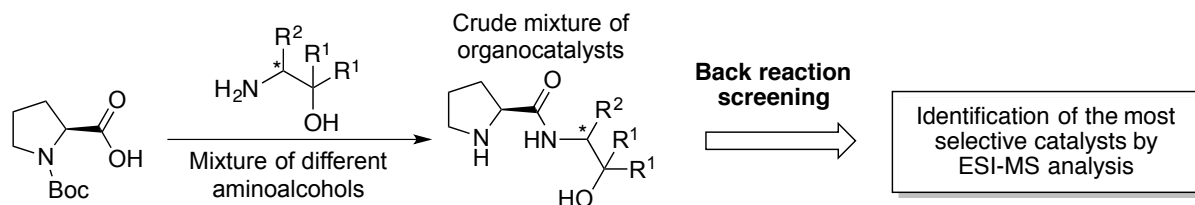
Figure 89: Identification of the catalysts' selectivity applying crude mixtures containing several catalysts in the back reaction screening.

The organocatalyzed Morita-Baylis-Hillman (MBH) reaction was another transformation, which was considered for the application of the screening concept illustrated in Figure 88 (CHAPTER 3). For the first time, phosphorus species were monitored as key intermediates by ESI-MS analysis. Preliminary experiments for the identification of a suitable screening protocol were highly promising as the intermediates were easily visualized in the back reaction using MBH-products based on *para*-nitrobenzaldehyde and acrylates (Scheme 64). This work was continued by P. ISENEGGER during his master thesis and is currently an ongoing research project within the PFALTZ group.
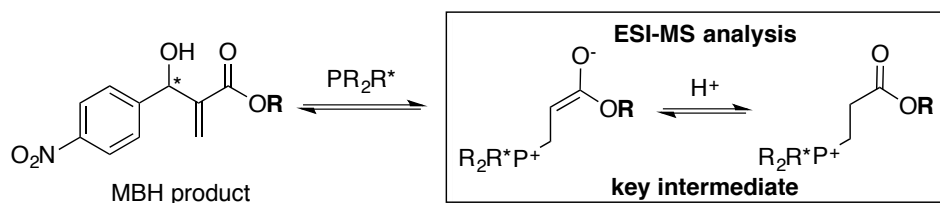
**Scheme 64:** MBH back reaction and intermediates for ESI-MS analysis involved herein.

In CHAPTER 4, the application of the ESI-MS back reaction screening concept (Figure 88) as a mechanistic tool is demonstrated in terms of the organocatalyzed conjugate addition of aldehydes to nitroolefins. Conventional ESI-MS investigations of reaction mixtures only provide information about intermediates present in the reaction mixture. However, this does not provide clear evidence that these intermediates are actively involved in the catalytic cycle. In contrast, the combination of ESI-MS analysis with the back reaction screening using quasienantiomeric substrates, affords information about the enantioselectivity-determining step and the intermediates involved therein. Therefore, ratios of intermediates determined in the back reaction, which match the enantioselectivity of the corresponding catalyst in the forward reaction, clearly identify these intermediates as being involved in the catalytic cycle and even more in the enantioselectivity-determining step of the reaction (Figure 90). This was demonstrated for the conjugate addition reaction catalyzed by tripeptides bearing an acidic

side chain, where excellent agreements between the enamine ratios and the *ee* determined from the forward reaction were found. Therefore, clear evidence was obtained that such reactions proceed *via* an enamine rather than an enol intermediate and that C–C bond formation occurring between enamine and nitroolefine is the enantioselectivity-determining step of the reaction. Furthermore, we found that with non-acidic catalysts, such as the Hayashi–Jørgensen catalyst, a different step determines the stereoselectivity.
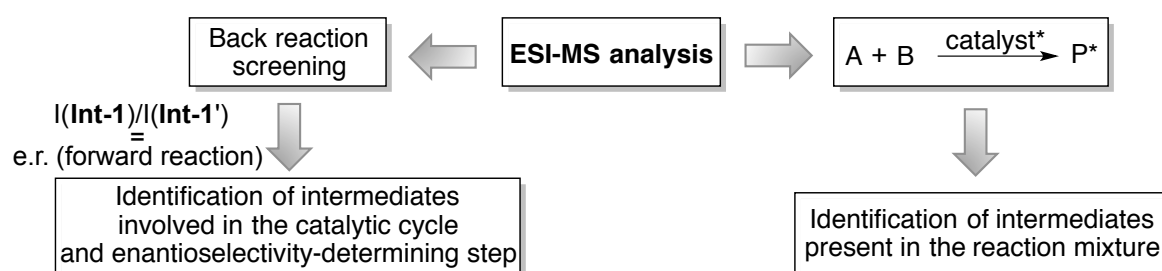
Figure 90: ESI-MS back reaction screening as mechanistic tool *vs.* conventional ESI-MS analysis of reaction mixtures.

Finally, in CHAPTER 5 an extension of the ESI-MS screening is described, which allows determination of the enantioselectivity of a chiral organocatalyst in the Michael addition by testing its racemic form. In contrast to the ESI-MS screening of enantiopure catalysts, the mass-labeled quasienantiomeric substrates were applied in a scalemic, instead of an equimolar ratio, under reaction conditions providing a pseudo-zero order regime. By monitoring the signal ratio of the iminium ions derived from the quasienantiomeric substrates, the most selective catalysts were clearly identified by screening their racemic form and the same selectivity trend was observed as for the corresponding enantiopure catalysts. Furthermore, the selectivity factor *s* and therefore the theoretical *ee* was calculated from these signal ratios (Figure 91). However, the values determined for racemic catalysts were consistently lower than the values obtained from the enantiopure catalyst, due to deviation from a perfect pseudo-zero kinetic regime. A linear correlation was identified allowing for a correction of this deviation and a more precise prediction of the actual *ee* of the catalyst. The determination of the selectivity-trend by screening racemic catalysts significantly broadens the scope of possible catalyst candidates. Structures, which are not available from the chiral pool but easily accessible in the racemic form, such as the isoindoline derivatives were easily tested and their selectivity trend correctly predicted by the ESI-MS racemate screening.
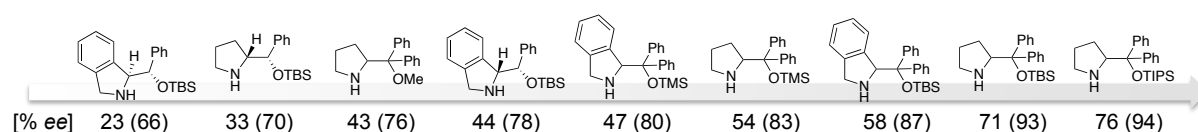
Figure 91: Selectivity trend and theoretical *ee* determined from the racemate. The *ee* determined from the corresponding enantiopure catalyst is given in brackets.

287